

UNCLASSIFIED

AD NUMBER

AD350590

CLASSIFICATION CHANGES

TO: UNCLASSIFIED

FROM: SECRET//RESTRICTED DATA

LIMITATION CHANGES

TO:  
Approved for public release; distribution is unlimited.

FROM:  
Distribution authorized to U.S. Gov't. agencies and their contractors;  
Administrative/Operational Use; FEB 1963. Other requests shall be referred to Aeronautical Systems Division, ATTN: Propulsion Laboratory, Wright-Patterson AFB, OH 45433. Restricted Data.

AUTHORITY

OSD/WHS memo dtd 17 Mar 2016; OSD/WHS memo dtd 17 Mar 2016

THIS PAGE IS UNCLASSIFIED



DEPARTMENT OF DEFENSE  
WASHINGTON HEADQUARTERS SERVICES  
1155 DEFENSE PENTAGON  
WASHINGTON, DC 20301-1155



MAR 17 2016

MEMORANDUM FOR DEFENSE TECHNICAL INFORMATION CENTER  
(ATTN: DTIC-OQ INFORMATION SECURITY)  
8725 JOHN J. KINGMAN ROAD, SUITE 0944  
FORT BELVOIR, VA 22060-6218

SUBJECT: OSD MDR Case 13-M-3701

We have reviewed the attached document in consultation with the Department of Energy, Department of the Navy, and Department of the Air Force and have declassified it in full. If you have any questions please contact Mr. John D. Smith by phone at 571-372-0482 or by email at [john.d.smith887.civ@mail.mil](mailto:john.d.smith887.civ@mail.mil), [john.d.smith887.civ@mail.smil.mil](mailto:john.d.smith887.civ@mail.smil.mil), or [john.smith@osdj.ic.gov](mailto:john.smith@osdj.ic.gov).

George R. Sturgis  
Deputy Chief, Records and Declassification  
Division

Attachments:

1. MDR request w/ document list
2. Document 2



~~SECRET~~  
~~RESTRICTED DATA~~

AD 3 5 0 5 9 0

DEFENSE DOCUMENTATION CENTER

FOR

SCIENTIFIC AND TECHNICAL INFORMATION

CAMERON STATION, ALEXANDRIA, VIRGINIA

Office of the Secretary of Defense <sup>5 US\$552</sup>  
Chief, RDD, ESD, WHS +  
Date: 02 Oct 2015 Authority: EO 13526  
Declassify: X Deny in Full: \_\_\_\_\_  
Declassify in Part: \_\_\_\_\_  
Reason: \_\_\_\_\_  
MDR: 13 -M- 3701

Department of the Navy DON/AA DRMD Date: <u>10 Oct 2015</u> Authority: EO 13526 Declassify: <u>X</u> Deny in Full: _____ Declassify in Part: _____ Reason: _____ MDR <u>2015 -M- 0001</u>
---

**DECLASSIFIED IN FULL**  
Authority: EO 13526  
Chief, Records & Declass Div, WHS  
Date: OCT 02 2015



DEPARTMENT OF ENERGY DECLASSIFICATION REVIEW	
1 <sup>st</sup> Review Date: <u>10/17/13</u>	DETERMINATION (CIRCLE NUMBER(S))
Authority: <input type="checkbox"/> DC <input checked="" type="checkbox"/> DD	1. CLASSIFICATION RETAINED
Name: <u>R.L. Shankle</u>	2. CLASSIFICATION CHANGED TO: <u>NSI</u>
2 <sup>nd</sup> Review Date: <u>10/30/2013</u>	3. CONTAINS NO DOE CLASSIFIED INFO
Authority: <u>DD</u>	4. COORDINATE WITH:
Name: <u>S. Fivozinsky</u>	5. CLASSIFICATION CANCELED
	6. CLASSIFIED INFO BRACKETED
	7. OTHER (SPECIFY):

~~RESTRICTED DATA~~  
~~SECRET~~

RI

13-M-3701

NOTICE: When government or other drawings, specifications or other data are used for any purpose other than in connection with a definitely related government procurement operation, the U. S. Government thereby incurs no responsibility, nor any obligation whatsoever; and the fact that the Government may have formulated, furnished, or in any way supplied the said drawings, specifications, or other data is not to be regarded by implication or otherwise as in any manner licensing the holder or any other person or corporation, or conveying any rights or permission to manufacture, use or sell any patented invention that may in any way be related thereto.

NOTICE:

THIS DOCUMENT CONTAINS INFORMATION  
AFFECTING THE NATIONAL DEFENSE OF  
THE UNITED STATES WITHIN THE MEAN-  
ING OF THE ESPIONAGE LAWS, TITLE 18,  
U.S.C., SECTIONS 793 and 794. THE  
TRANSMISSION OR THE REVELATION OF  
ITS CONTENTS IN ANY MANNER TO AN  
UNAUTHORIZED PERSON IS PROHIBITED  
BY LAW.

Page determined to be Unclassified  
Reviewed Chief, RDD, WNS  
IAW EO 13526, Section 3.5  
Date: OCT 02 2015

CATALOGED BY DDC 350590

AS AD 100

~~SECRET RESTRICTED DATA~~  
~~ATOMIC ENERGY ACT OF 1954~~

ASD-TDR-63-277  
Volume IV

**3 5 0 5 9 0**

(UNCLASSIFIED TITLE)  
NUCLEAR RAMJET PROPULSION SYSTEM  
APPLIED RESEARCH AND ADVANCED TECHNOLOGY  
(PROJECT PLUTO)

VOLUME IV  
PROPULSION SYSTEM DESIGN AND STRUCTURAL ANALYSIS

TECHNICAL DOCUMENTARY REPORT ASD-TDR-63-277, VOLUME V

15 February 1963

Directorate of Aeromechanics  
Propulsion Laboratory  
Aeronautical Systems Division  
Air Force Systems Command  
Wright-Patterson Air Force Base, Ohio

**DECLASSIFIED IN FULL**  
Authority: EO 13526  
Chief, Records & Declass Div, WHS  
Date: OCT 02 2015

Project No. 655A, Tasks Nos. 1 and 5

(Prepared under Contract AF 33(657)-8123  
by The Marquardt Corporation, Van Nuys, California  
Author: R. D. Grossman)

JUN 6 1964

~~EXCLUDED FROM AUTOMATIC  
REGRADING; DOD DIR 5200.10  
DOES NOT APPLY~~

~~SECRET RESTRICTED DATA~~  
~~ATOMIC ENERGY ACT OF 1954~~

63 ASRM-36

MAC 487

1005 88

## NOTICES

~~RESTRICTED DATA~~

~~This document contains restricted data as defined in the Atomic Energy Act of 1954. Its transmittal or the disclosure of its contents in any manner to an unauthorized person is prohibited by law.~~

When US Government drawings, specifications, or other data are used for any purpose other than a definitely related government procurement operation, the government thereby incurs no responsibility nor any obligation whatsoever; and the fact that the government may have formulated, furnished, or in any way supplied the said drawings, specifications, or other data is not to be regarded by implication or otherwise, as in any manner licensing the holder or any other person or corporation, or conveying any rights or permission to manufacture, use, or sell any patented invention that may in any way be related thereto.

Copies of this report should not be returned to the Aeronautical Systems Division unless return is required by security considerations, contractual obligation, or notice on a specific document.

**DECLASSIFIED IN FULL**  
**Authority: EO 13526**  
**Chief, Records & Declass Div, WHS**  
**Date: OCT 02 2015**

UNCLASSIFIED

2

REPORT 6003

ASD-TDR-63-277, Vol. IV

FOREWORD

This report was prepared by The Marquardt Corporation, Van Nuys, California, on Air Force Contract AF 33(657)-8123, under Task Order No. 1 and No. 5 of Project No. 655A, "Nuclear Ramjet Propulsion Systems Research and Technology". The work was administered under the direction of the Propulsion Laboratory (Directorate of Aeromechanics), Aeronautical Systems Division. R. F. Latham was Project Engineer for the Laboratory.

The studies presented here were performed during the contract period 1 January-31 December 1962. The Marquardt Corporation activities were under the direction of A. O. Mooneyham, Senior Project Engineer. Chief contributors were J. G. Bendot, Aerothermodynamics; R. D. Grossman, Design and Development; R. K. Nuno, Controls.

This report is the final technical summary report and concludes the work on Contract AF 33(657)-8123. The contractor's report number is Marquardt Report 6003. The volumes of this report are as follows:

- Volume I: Summary
- Volume II: Propulsion System Performance and Aerothermodynamics
- Volume III: Propulsion System Controls
- Volume IV: Propulsion System Design and Structural Analysis
- Volume V: Propulsion System Test Planning and Ground Test Facility Studies
- Volume VI: Structural Materials Investigations

This report is ~~classified Secret-Restricted Data~~ in conformance with requirements contained in AF-provided security guidance (Form 151) and OC DOC 75.

DECLASSIFIED IN FULL  
Authority: EO 13526  
Chief, Records & Declass Div, WHS  
Date: OCT 02 2015

S	marquardt	C
E		O
C		N
R		T
E		R
T		O
		L

- 11 -  
MAC 4872

UNCLASSIFIED

~~SECRET RESTRICTED DATA~~

ASD-TDR-63-277, Vol. IV

~~ATOMIC ENERGY ACT OF 1954~~

PORT 6003

ABSTRACT

(This abstract is ~~classified SECRET~~)

This volume contains the results of design, structures and materials studies and structures component testing of a nuclear propulsion system in support of the Pluto reactor program. These studies include design concepts, structural analysis of steady state and dynamic loads, material evaluation, and recommended dynamic and structural test programs. The methods of analysis used have been outlined in each case for reference.

**DECLASSIFIED IN FULL**  
**Authority: EO 13526**  
**Chief, Records & Declass Div, WHS**  
**Date: OCT 02 2015**

~~SECRET RESTRICTED DATA~~

~~ATOMIC ENERGY ACT OF 1954~~

MAC 463

## SUMMARY

The mechanical and structural design effort during this contract period (1 January 1962 through 31 December 1962) has been directed towards the design of a flight type propulsion system, designated the MA50-1B, which incorporates a reactor reflecting Tery IIC reactor technology. Effort has also been expended in design and fabrication of development test hardware for component testing.

Design layouts have been completed for the MA50-XC Propulsion System in addition to the major components that make up the entire system; namely, the inlet and diffuser duct, ejector exhaust nozzle, reactor control rods support system, reactor lateral and axial support structure, inlet spike translation and bypass door mechanism and exhaust nozzle attachment.

Design and fabrication have been completed for the direct-connect and free jet aerodynamic coupling test hardware, engine airframe lateral attachment test hardware, and reactor lateral support spring test hardware.

Test outlines and test results for the aerodynamic coupling tests are reported in Volume II of this report.

**DECLASSIFIED IN FULL**  
**Authority: EO 13526**  
**Chief, Records & Declass Div, WHS**  
**Date: OCT 02 2015**

UNCLASSIFIED

NET 6003

ASD-TDR-63-277, Vol. IV

CONTENTS

<u>Section</u>	<u>Page</u>
1.0 INTRODUCTION . . . . .	1
2.0 PROPULSION SYSTEM DESIGN CRITERIA . . . . .	3
2.1 General Discussion . . . . .	3
2.2 Mission Parameters . . . . .	3
2.2.1 Contractual Requirements . . . . .	3
2.2.2 Flight Capability . . . . .	3
2.3 Typical Mission Profiles . . . . .	4
2.4 Flight Envelopes . . . . .	4
2.5 Nomenclature . . . . .	5
2.5.1 Operational Phases . . . . .	5
2.5.2 Reference Axes . . . . .	5
2.6 Basic Operational Factors . . . . .	6
2.6.1 Inertial Load Factors . . . . .	6
2.6.2 Vibration Environment . . . . .	6
2.7 Analytical Factors . . . . .	6
2.7.1 Design Factors and Factors of Safety . . . . .	6
2.8 Margins of Safety . . . . .	7
2.9 Limits of Structural Deformation . . . . .	7
2.10 Materials and Material Properties . . . . .	8
2.10.1 Choice of Material . . . . .	8
2.10.2 Over Aging and Cyclic Loading . . . . .	8
2.11 Design Parameters . . . . .	8
3.0 INLET . . . . .	9
3.1 Design . . . . .	9
3.1.1 Discussion . . . . .	9
3.1.2 Boundary Layer Air Bleed . . . . .	9
3.1.3 Bypass Doors . . . . .	9
3.1.4 Spike Transition . . . . .	9
3.1.5 Weights and Centers of Gravity . . . . .	10
3.2 Structural Analysis . . . . .	10
3.2.1 Discussion . . . . .	10
3.2.2 Cowl Lip . . . . .	11
3.2.3 Diffuser Skin . . . . .	15

UNCLASSIFIED

MAC 4672

UNCLASSIFIED

REPORT 6003

ASD-TDR-63-277, Vol. IV

CONTENTS (Continued)

<u>Section</u>	<u>Page</u>
3.2.4 Load Paths of Unsymmetrical Airloads. . . . .	15
3.2.5 Strut . . . . .	19
3.2.6 Innerbody Ring at Section (F-F) . . . . .	22
3.2.7 Innerbody Skin. . . . .	24
3.2.8 Thrust Fitting. . . . .	27
4.0 SUBSONIC DIFFUSER AND REACTOR CONTROL SUPPORT STRUCTURE . . . . .	29
4.1 Design. . . . .	29
4.1.1 Discussion. . . . .	29
4.1.2 Weights and Centers of Gravity. . . . .	30
4.2 Preliminary Analysis of Control Rod Support Structure . . . . .	30
4.2.1 Loads . . . . .	30
4.2.2 Deflection Check of Strut . . . . .	32
5.0 REACTOR SUPPORT SYSTEM. . . . .	35
5.1 Side Support System Design. . . . .	35
5.1.1 Side Support System Function. . . . .	35
5.1.2 Side Support Annulus Thickness to Vehicle Drag Comparison . . . . .	36
5.1.3 Reduction in Annulus Width. . . . .	36
5.1.4 Design Side Support System. . . . .	37
5.1.5 Operating and Installation Requirements . . . . .	37
5.2 Side Support System Analysis. . . . .	38
5.2.1 Nomenclature. . . . .	38
5.2.2 Dynamics Model and Optimum Spring Rate. . . . .	40
5.2.3 Structural. . . . .	43
5.3 Front Support Structural Criteria . . . . .	51
5.3.1 Discussion of Axial Support System. . . . .	51
5.3.2 Dynamic Analysis. . . . .	54
5.3.3 Structural Summary. . . . .	60
5.3.4 Conclusions and Recommendations . . . . .	61
5.4 Side Support System Test. . . . .	61
5.4.1 Discussion. . . . .	61
5.4.2 High Temperature Springs. . . . .	62
5.4.3 Engine-Airframe Lateral Attachment Tests Phases I and II . . . . .	67

SAC 4678

UNCLASSIFIED

## CONTENTS (Continued)

<u>Section</u>	<u>Page</u>
6.0 EXIT NOZZLE . . . . .	73
6.1 Design. . . . .	73
6.1.1 Discussion. . . . .	73
6.1.2 Weights and Centers of Gravity. . . . .	73
6.1.3 Design Data . . . . .	73
6.2 Structural Analysis . . . . .	74
6.2.1 Nozzle Forward Cylinder and Convergent Cone (PPrimary Shell) . . . . .	74
6.2.2 Cone-Cylinder and Cone-Cone Intersection. . . . .	78
6.2.3 Divergent Exit Cone . . . . .	82
6.2.4 Ejector Shroud (Nozzle Inner Liner) . . . . .	96
6.2.5 Analysis of Exit Nozzle Attach Joint. . . . .	100
7.0 MODELS. . . . .	107
7.1 Direct-Connect Aerodynamic Coupling . . . . .	107
7.1.1 Design. . . . .	107
7.2 One-Third Scale Free Jet Model. . . . .	107
7.2.1 Design. . . . .	107
8.0 REFERENCES. . . . .	109
-- APPENDIX A--Classified Materials Studies. . . . .	300
-- DISTRIBUTION. . . . .	311

Page determined to be Unclassified  
Reviewed Chief, RDD, WMS  
IAW EO 13526, Section 3.5  
Date: OCT 02 2015

MAC 4673

UNCLASSIFIED

- vii -

~~SECRET RESTRICTED DATA~~  
~~ATOMIC ENERGY ACT OF 1954~~

ASD-TDR-63-277, Vol. IV

REPORT 6003

ILLUSTRATIONS

<u>Figure</u>		<u>Page</u>
1.	Master Layout - Pluto Propulsion System - MA50-XCB. . . . .	141
2.	Installation - Pluto Propulsion System - MA50-XCB . . . . .	143
3.	Typical Mission Profile for 11,000 Nautical Miles (ICAO Standard Day) . . . . .	145
4.	Typical Mission Profile for 11,000 Nautical Miles (ANA Hot Day) . . . . .	146
5.	Typical Mission Profile for 11,000 Nautical Miles (ANA Cold Day) . . . . .	147
6.	Estimated Operating Envelope for Marquardt Model MA50- B Ramjet (ICAO Standard Day) . . . . .	148
7.	Estimated Operating Envelope for Marquardt Model MA50- B Ramjet (ANA Hot Day) . . . . .	149
8.	Estimated Operating Envelope for Marquardt Model MA50- B Ramjet (ANA Cold Day) . . . . .	150
9.	Typical Pluto Boost Trajectory. . . . .	151
10.	MA50-XCB Propulsion System Net Flow Areas . . . . .	153
11.	Internal Engine Parameters for Design Point Operation . . . . .	155
12.	MA50-XCB Propulsion System Auxiliary Air Requirements . . . . .	157
13.	Design Layout - Inlet and Duct Lines. . . . .	159
14.	Design Layout - Inlet and Duct Lines. . . . .	161
15.	Design Layout - Axisymmetric Inlet. . . . .	163
16.	Design Layout - Axisymmetric Inlet. . . . .	165
17.	Design Layout - Axisymmetric Inlet. . . . .	167
18.	Sketch of Inlet Assembly for Inlet Structural Analysis . . . . .	169
19.	Sketch of Spike and Inner-Body for Inlet Structural Analysis . . . . .	170
20.	MA50-XCA Inlet-Diffuser Static Pressure . . . . .	171
21.	Varying Pressures on Inside and Outside Lip and Cowl Surface . . . . .	172

MAC A672

~~SECRET RESTRICTED DATA~~  
~~ATOMIC ENERGY ACT OF 1954~~

~~SECRET RESTRICTED DATA~~  
~~ATOMIC ENERGY ACT OF 1954~~

ASD-TDR-63-277, Vol. IV

OFF 6003

ILLUSTRATIONS (Continued)

<u>Figure</u>		<u>Page</u>
22.	Throc Loadings for Analysis Structure . . . . .	173
23.	Sketch of Cowl Lip for Inlet Structural Analysis. . . . .	174
24.	Spike Geometry. . . . .	175
25.	Cowl and Innerbody Unsymmetrical Loadings . . . . .	176
26.	Cowl and Innerbody Load Paths (Unsymmetrical Loadings). . . . .	177
27.	Unsymmetrical Air Load Distribution . . . . .	178
28.	Shears, Moments, and Torques from Y Direction . . . . .	179
29.	Shears and Moments from Z Direction Components. . . . .	180
30.	Geometry and Pressures for Inlet Structural Analysis. . . . .	181
31.	Derived Load Distribution on Fittings . . . . .	182
32.	Longitudinal Section Through Typical Strut. . . . .	183
33.	Load on Struts from Supporting Rings. . . . .	184
34.	Loads on Strut Spars from Unsymmetrical Loads . . . . .	185
35.	Vertical and Horizontal Loads on Strut Spars. . . . .	186
36.	Load Paths from Spike and Drive Mechanism to Fixed Innerho . . . . .	187
37.	Innerbody Ring Loads. . . . .	188
38.	Symmetrical and Unsymmetrical Loadings. . . . .	189
39.	Ring Section Properties . . . . .	190
40.	Ring Section Properties . . . . .	191
41.	Thrust Fitting Loads. . . . .	192
42.	Struts. . . . .	193
43.	Strut Cross Section . . . . .	194
44.	Design Progress on Reactor Side Support Structure . . . . .	195
45.	Design Layout - Reactor Installation. . . . .	197

AMC 672

~~SECRET RESTRICTED DATA~~  
~~ATOMIC ENERGY ACT OF 1954~~

~~SECRET RESTRICTED DATA~~  
~~ATOMIC ENERGY ACT OF 1954~~

REPORT 6003

ASD-TDR-63-277, Vol. IV

ILLUSTRATIONS (Continued)

<u>Figure</u>		<u>Page</u>
46.	Assumed Side Support Temperatures (ANA Hot Day) . . . . .	199
47.	Assumed Side Reflector Temperature Distribution . . . . .	200
48.	Schematic of Radial and Tangential Support Structure . . . . .	201
49.	Dynamic System Model. . . . .	202
50.	Pressure Distribution . . . . .	203
51.	Required Energy Storage for Lateral Support System. . . . .	204
52.	Typical Section of Web-Shell Combination. . . . .	205
53.	Estimated Full Scale Reactor Drag Load Variation During Unstart Transient Flight Operation. . . . .	206
54.	Estimated Pressure Transient on Full Scale Reactor During Unstart . . . . .	207
55.	Estimated Differential Pressure Variation on Full Scale Reactor During Unstart. . . . .	208
56.	Reactor Drag, 1,000-Ft Altitude . . . . .	209
57.	Estimated Full Scale Reactor Drag Load Variation During Unstart Transient Ground Test Only. . . . .	210
58.	Estimated Reactor Displacement During Unstart Transient Ground Test Only--Mach 3, 1000-Ft Altitude, ANA Hot Day . . . . .	211
59.	Estimated Reactor Velocity During Unstart Transient Ground Test Only--Mach 3, 1000-Ft Altitude, ANA Hot Day. . . . .	212
60.	Estimated Reactor Displacement During Unstart Transient Flight Operation with 3 g Vehicle Deceleration - Mach 3, 1000-Ft Altitude, ANA Hot Day . . . . .	213
61.	Estimated Reactor Velocity During Unstart Transient Flight Operation with 3g Vehicle Deceleration - Mach 3, 1000-Ft Altitude, ANA Hot Day . . . . .	214
62.	Belleville Springs--R-235 Material. . . . .	215
63.	Belleville Spring--R-235 Material (1/16-in. Full Radial I.D. Edges) . . . . .	216

~~SECRET RESTRICTED DATA~~  
~~ATOMIC ENERGY ACT OF 1954~~

MAC 4628

~~SECRET RESTRICTED DATA~~  
~~ATOMIC ENERGY ACT OF 1954~~

ASD-TDR-63-277, Vol. IV

ORR 6003

ILLUSTRATIONS (Continued)

<u>Figure</u>		<u>Page</u>
64.	Test Setup for Single Belleville Spring--R-235 Material . . .	217
65.	Strain Gages Installed on Inner and Outer Radius of Modified Belleville Spring (1/16-in. Full Radius Both I.D. Edges)-- R-235 Material. . . . .	218
66.	Setup for Test of Single Belleville Spring with Strain Gage Installed . . . . .	219
67.	Test Setup for Strain Gaged Belleville Springs (R-235 Material). . . . .	220
68.	Test Setup for 10-Spring Series Stack of Belleville Springs R-235 Material. . . . .	221
69.	Partial Setup for 1400°F Test of 10-Spring Series Stack of Belleville Springs--R-235 Material. . . . .	222
70.	Permanent Set vs. Deflection During Presetting of Single Belleville Springs (R-235 Alloy). . . . .	223
71.	Load vs. Deflection: No. 11, No. 109, and No. 111 Single Belleville Springs (R-235 Alloy). . . . .	224
72.	Permanent Set vs. Deflection During Presetting of Single Belleville Springs. . . . .	225
73.	Load vs. Deflection for Single Belleville Springs (R-235 Alloy) . . . . .	226
74.	Load vs. Deflection for Single Belleville Springs (R-235 Alloy)--Ambient Temperature . . . . .	227
75.	Load vs. Deflection: No. 95 Belleville Spring--1/16-in. Full Radius Both I.D. Edges (R-235 Alloy). . . . .	228
76.	Stress vs. Spring Radial Width -Belleville Springs No. 29 a No. 25 (R-235 Material, Ambient Temperature; Flat Plate Loading). . . . .	229
77.	Load vs. Deflection: No. 1 and No. 4 10-Spring Series Stack of Belleville Springs (R-235 Alloy) . . . . .	230
78.	Load Loss vs. Time at Constant Spring Deflection: No. 4 10- Spring Series Stack of Belleville Springs (R-235 Alloy) . . . . .	231
79.	Tapered Curved Plate Springs--Renard Alloy. . . . .	232

~~SECRET RESTRICTED DATA~~  
~~ATOMIC ENERGY ACT OF 1954~~

MAC 202

~~SECRET RESTRICTED DATA~~  
~~ATOMIC ENERGY ACT OF 1954~~

ASD-TDR-63-277, Vol. IV

MT 6003

ILLUSTRATIONS (Continued)

<u>Figure</u>		<u>Page</u>
99.	Core Dynamic Response (Run No. 10) . . . . .	252
100.	Lateral Attach Assembly-Engine-Airframe . . . . .	253
101.	Test Item for Engine-Airframe Lateral Attachment Test (Phase II) . . . . .	255
102.	Vibration Test Sctup for Engine-Airframe Lateral Attachment Test (Phase II) . . . . .	256
103.	Instrumentation Requirements for Engine-Airframe Lateral Attachment Test (Phase II) . . . . .	257
104.	Spring Displacement vs. Frequency (15 psi Core Preload) . . . . .	258
105.	Core Deflection Pattern, Run 4. . . . .	259
106.	Spring Displacement vs. Frequency (6g Force Input). . . . .	260
107.	Design Layout - Propulsion System Exit Nozzle . . . . .	261
108.	Wall Pressure Distribution for MA50-XCB Ejector Nozzle (Altitude = 10,000 Feet). . . . .	263
109.	Wall Pressure Distribution for MA50-XCB Ejector Nozzle (Altitude = 35,000 Feet). . . . .	264
110.	Local Wall Pressure Distribution in Exhaust Region of Airfra Cooling Flow: MA50-XCB Ejector Nozzle . . . . .	265
111.	MA50-XCB Ejector Nozzle Axial Loads (Drag). . . . .	266
112.	Estimated Temperature Distribution for MA50-XCB Ejector Nozzle (3.22 M ) . . . . .	267
113.	Estimated Temperature Distribution for MA50-XCB Ejector Nozzle (3.90 M ) . . . . .	268
114.	MA50-XCB Ejector Nozzle Contours (Based on 0.125 in. Nozzle Liner Thickness). . . . .	269
115.	MA50-XCB Ejector Nozzle Liner Exit Details. . . . .	270
116.	Nozzle Load Parameters. . . . .	271
117.	Doubler Ring. . . . .	272

MAC 6073

~~SECRET RESTRICTED DATA~~  
~~ATOMIC ENERGY ACT OF 1954~~

~~SECRET RESTRICTED DATA~~  
~~ATOMIC ENERGY ACT OF 1954~~

ASD-TDR-63-277, Vol. IV

REPORT 6003

ILLUSTRATIONS (Continued)

<u>Figure</u>		<u>Page</u>
118.	Liner Load Parameters . . . . .	273
119.	Assumed Coupling Geometry . . . . .	274
120.	Retaining Ring Geometry . . . . .	275
121.	Airframe Fitting Shell. . . . .	276
122.	Lock Ring . . . . .	277
123.	Exit Nozzle Attach Ring . . . . .	278
124.	Testing of Aerodynamic Coupling with 1/3 Scale Engine (Phase I - Direct Connect Test) . . . . .	279
125.	Aft Transition Section for Aerodynamic Coupling Test. . . . .	280
126.	Buildup of Simulated Reactor Segment for Aerodynamic Coupling Test (Closeup). . . . .	281
127.	Front Support Section of Aerodynamic Coupling (Looking Forward). . . . .	282
128.	Aft End of Simulated Reactor Segment (Viewed Up Exit Nozzle). . . . .	283
129.	Engine Assembly Aerodynamic Coupling Free Jet Test. . . . .	285
130.	Cowl Assembly for Free Jet Aerodynamic Coupling Test. . . . .	287
131.	Spike Adapter for Free Jet Aerodynamic Coupling Test. . . . .	288
132.	Display of Components for Free Jet Aerodynamic Coupling Test. . . . .	289
133.	Closeup of Components for Free Jet Aerodynamic Coupling Test. . . . .	290
134.	Spike Actuator and Housing Details for Free Jet Aerodynamic Coupling Test . . . . .	291
135.	Spike Actuator and Housing Assembly for Free Jet Aerodynamic Coupling Test . . . . .	292
136.	Simulated Reactor and Housing for Free Jet Aerodynamic Coupling Test . . . . .	293
137.	Test Item Assembly (Axial Load Spring Retention) for Free Jet Aerodynamic Coupling Test . . . . .	294

MAC 1677

~~SECRET RESTRICTED DATA~~  
~~ATOMIC ENERGY ACT OF 1954~~

ILLUSTRATIONS (Continued)

<u>Figure</u>		<u>Page</u>
138.	Centerbody and Inlet Duct for Free Jet Aerodynamic Coupling Test . . . . .	295
139.	Centerbody and Inlet Duct Assembly for Free Jet Aerodynamic Coupling Test . . . . .	296
140.	Exposed Inlet Assembly for Free Jet Aerodynamic Coupling Test . . . . .	297
141.	Inlet Assembly for Free Jet Aerodynamic Coupling Test (Three Quarter View) . . . . .	298
142.	Setup of Pluto Propulsion System Model for Free Jet Aerodynamic Coupling Test . . . . .	299
A-1.	Stress-Time Profile for Rene' 41. . . . .	305
A-2.	Creep of Rene' 41 Sheet (1400°F; 52 Ksi). . . . .	306
A-3.	Ultimate Tensile Strength and Yield Strength of Rene' 41 Sheet at Selected Strain Rates. . . . .	307
A-4.	Young's Modulus and Percent Elongation of Rene' 41 Sheet at Selected Strain Rates . . . . .	308

DECLASSIFIED IN FULL  
Authority: EO 13526  
Chief, Records & Declass Div, WHS  
Date: OCT 02 2015

MAC 467

UNCLASSIFIED

ASD-TDR-63-277, Vol. IV

REPORT 6003

TABLES

<u>Table</u>		<u>Page</u>
I	Table of Weights and Centers of Gravity for MA50-XCB Propulsion System . . . . .	111
II	Margins of Safety . . . . .	112
III	Inertial Load Factors . . . . .	114
IV	Inertia Load Factors Flight Maneuver Conditions . . . . .	115
V	Vertical Load Factors . . . . .	116
VI	Ground Handling Load Factors. . . . .	117
VII	Analytical Design Factors and Factors of Safety . . . . .	118
VIII	Weights and Centers of Gravity for Axisymmetric Inlet . . . . .	119
IX	Section Properties and Locations for Calculation of Stress. . . . .	120
X	Moments from Air Load . . . . .	121
XI	Torque Loads at Various Sections. . . . .	122
XII	Shears, Moments, and Torques from Z Direction Components. . . . .	123
XIII	Pressure Calculations . . . . .	124
XIV	Joint Loads . . . . .	125
XV	Attachment Reactions from Airloads for the Unsymmetrical Condition . . . . .	126
XVI	Symmetrical Load Portion of Steady State Flight Condition Ring Moments. . . . .	128
XVII	Steady State Flight Condition Ring Moments. . . . .	129
XVIII	Ring Moments from Short Time Maneuver Loads . . . . .	130
XIX	Weight and Centers of Gravity for Control Rod Support Structure and Actuator Mechanism. . . . .	131
XX	Weights and Centers of Gravity for Reactor and Support System . . . . .	132
XXI	Thermal Expansion of Tangentially and Radially Oriented Springs . . . . .	133
XXII	Summary of Criteria . . . . .	134
XXIII	Table of Dynamic Test Runs, "Nominal Conditions". . . . .	135

MAC 4673

UNCLASSIFIED

TABLES (Continued)

<u>Table</u>		<u>Page</u>
XXIV	Accelerometer Response, Run No. 4 . . . . .	136
XXV	Accelerometer Response, Run No. 10. . . . .	137
XXVI	Weights and Centers of Gravity for Ejector Exhaust Nozzle . . .	138
XXVII	Required Material Thickness . . . . .	139
XXVIII	Shroud Pressure and Temperature Data. . . . .	140
A-I	Creep of Rene' 41 During Cyclic Testing . . . . .	301
A-II	Tensile Properties of Rene' 41 Sheet After Cyclic Testing . .	302
A-III	Creep-Rupture of Rene' 41 Sheet Control Specimens . . . .	303
A-IV	Tensile Properties of Rene' 41 Sheet at Selected Strain Ra: s .	304

Page determined to be Unclassified  
 Reviewed Chief, RDD, WHS  
 IAW EO 13526, Section 3.5  
 Date: OCT 02 2015

MAC A03

~~SECRET RESTRICTED DATA~~  
~~ATOMIC ENERGY ACT OF 1954~~

ASD-TDR-63-277, Vol. IV

REPORT 6003

## 1.0 INTRODUCTION

The model MA50-XCB nuclear ramjet propulsion system as shown in Figures 1 and 2 consists of a variable geometry supersonic inlet with a modified isentropic spike, a subsonic diffuser incorporating a variable area bypass, a nuclear reactor similar in construction to the Tory II reactor with integrated control system, and a convergent-divergent ejector type exhaust nozzle.

The inlet, which is an underslung, axisymmetric, internal-internal compression type, has a translating centerbody spike with a maximum travel of seven inches. The spike actuation mechanism is housed within the centerbody structure and is air-operated. Air is supplied to the actuator through a slot located in the centerbody structure. The bypass doors are located in the vicinity of the aft centerbody structure and are an integral part of the supersonic inlet structure.

The subsonic diffuser duct, from aft of the supersonic inlet to the front face of the reactor, is an integral part of the missile airframe structure.

The nuclear reactor is composed of a series of individual ceramic elements that make up the fueled core and front rear and radial reflectors. The reactor is maintained in the form of a right circular cylinder by a series of spring-loaded expansion shell pads. A series of axial tie tubes (which pass through the reactor) collect all aft directional loads through rear bearing plates and transfer them to a front support structure. All axial loads imposed upon the reactor are transferred to the airframe through a shear ring located in the vicinity of the front support structure.

The reactor control rod translating mechanisms are mounted forward of the front support structure and housed within the inlet duct. Control rod actuators are mounted in the annulus between the diffuser duct and the missile airframe.

The exhaust nozzle, is a convergent-divergent ejector type with fixed primary and secondary nozzle flow areas. This design employs a convergent-divergent outer shell with an inner shell in the convergent section only. The annulus between the inner and outer shell is sized such that the engine cooling air (secondary flow) cools the convergent portion of the nozzle by forced convection. The divergent portion of the nozzle is then film-cooled by the air issuing from the annular passage just aft of the throat.

The weights and centers of gravity for the MA50-XCB and its components are shown in Table I. Margins of safety are presented in Table II.

Manuscript released by The Marquardt Corporation on 15 February 1963 for publication as an ASD Technical Documentary Report.

~~SECRET RESTRICTED DATA~~  
~~ATOMIC ENERGY ACT OF 1954~~

MAC A57

~~SECRET RESTRICTED DATA~~  
~~ATOMIC ENERGY ACT OF 1954~~

ASD-TDR-63-277, Vol. IV

REPORT 6003

## 2.0 PROPULSION SYSTEM DESIGN CRITERIA

### 2.1 General Discussion

Particular emphasis for efficient operation of any propulsion system designed for high speed flight must be placed on lightweight and reliable structure, which will provide the necessary performance. Structural design will determine the shape and size of individual structural members to obtain the minimum weight of these structures. Design criteria are concerned with the data associated with the operational life, the associated loads, temperatures, and times at load and temperature. Also included will be nomenclature and design factors for use in analysis together with the physical properties of the materials used in fabrication. Such data are presented in the pages following.

### 2.2 Mission Parameters

#### 2.2.1 Contractual Requirements

The following typical mission parameters are specified in Reference 1, Paragraph 1.1, to be used as a basis for propulsion system design:

Minimum range 11,000 nautical miles

Maximum payload 10,000 pounds

#### 2.2.2 Flight Capability

High altitude cruise at 35,000 feet at Mach 3.5 to 4.0:

Minimum time 4.0 hours

Maximum time 7.0 hours

Penetration at 500 to 1000 feet at Mach 2.8 to 3.0:

Minimum time 2.0 hours

Maximum time 3.0 hours

Component design lifetime to be adequate for high reliability in performing above maximum requirements.

The Pluto propulsion system is designated the Arquardt Model MA50-XCA Nuclear Ramjet Engine. Operating envelopes for this engine are presented in Reference 2. The envelope limits are associated with control and actuator requirements and structural limitations of materials. Due to the establishment of temperature and pressure limitations (inlet air total temperature of 1070°F and diffuser exit pressure of 420 psia), the system would operate at Mach 3.2, Sea Level, on an ICAO Standard Day. This point places the system in the most severe steady state operating condition (exceeding the requirements stated above) and should be taken as the structural design point.

MAC A671

~~SECRET RESTRICTED DATA~~  
~~ATOMIC ENERGY ACT OF 1954~~

PRECEDING PAGE BLANK

~~SECRET RESTRICTED DATA~~  
~~ATOMIC ENERGY ACT OF 1954~~

ASD-TDR-63-277, Vol. IV

6003

2.3 Typical Mission Profiles

Vehicle total mission flight profiles used by Marquardt or ICAO Standard and ANA 421 Hot and Cold Days, and presented in Figures 3, 4 and 5, are reproduced for reference from Ling-Temco-Vought data presented in Reference 3, and again in Reference 4. Critical Mach number vs. altitude combinations from these curves are as follows:

Day Condition	Operational Phase	Altitude (feet)	Mach No
ANA 421	High Altitude Cruise	32,000	3.55
	Low Altitude Cruise	1,000	2.92
ANA 421	High Altitude Cruise	35,000	4.0
	Low Altitude Cruise	1,000	3.1
ICAO	High Altitude Cruise	35,000	3.8
	Low Altitude Cruise	1,000	3.1

A typical regime represents a flight of 11,000 nautical miles in approximately 310 minutes. These regimes consist of launch and rocket boost to high altitude, steady state cruise at high altitude for approximately 1-2/3 hours, letdown to low altitude in approximately 2.0 minutes, and steady state cruise to target for the balance of flight, approximately 1-1/3 hours. During cruise phases intermittent maneuver and gust loadings will occur.

Contractual requirements of Section 2.2.0 specify a more critical design life of 10 hours. The flight envelope (Figure 6) for ICAO Standard Day specifies a more severe low altitude cruise combination of Mach 3.2 at Sea Level.

2.4 Flight Envelopes

The preliminary Pluto propulsion system operating envelopes for the Model MA50-XCB Nuclear Ramjet for ICAO Standard and ANA 421 Hot and Cold days were presented in Reference 2 and are reproduced in Figures 6, 7, and 8. A typical boost trajectory is shown in Figure 9. Limits for these envelopes are as follows:

1. Mach 2.0 lower limit is established by operation requirements on pneumatic components.
2. Upper altitude limit is established as the line of constant diffuser exit pressure of 45 psia (assures required to 1 pneumatic pressure ratio) up to 50,000 feet.
3. Mach number and altitude requirement is set either by ram air total temperature of 1070°F or a diffuser duct total pressure of 420 psia.

~~SECRET RESTRICTED DATA~~  
~~ATOMIC ENERGY ACT OF 1954~~

MAC 4673

~~SECRET RESTRICTED DATA~~  
~~ATOMIC ENERGY ACT OF 1954~~

ASD-TDR-63-277, Vol. IV

REPORT 6003

2.5 Nomenclature

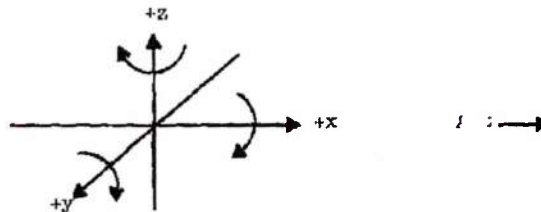
2.5.1 Operational Phases

As an aid to systematic analyses, proposed typical missile mission profiles are divided into a series of operational phases. These phases which are studied separately for individual maximum loadings and collectively for lifetime loading effects, are the following:

1. Ground handling
2. Boost
  - a. Burnout (launch to burnout)
  - b. Separation (booster separation to high altitude cruise)
3. High altitude cruise
4. Letdown
5. Low altitude (penetration) cruise
6. Weapons delivery (ejection of multiple stores during final phase of low altitude flight)

2.5.2 Reference Axes

The following reference axes notations were used in the analyses: (1) loads, linear accelerations, and dimensions positive when acting aft, up, and to the left (viewed from aft); (2) moments, angular accelerations, and angular velocities about reference axes follow the "left hand" rule:



MAC AEB

~~SECRET RESTRICTED DATA~~  
~~ATOMIC ENERGY ACT OF 1954~~

~~SECRET RESTRICTED DATA~~

ASD-TDR-63-277, Vol. IV

~~ATOMIC ENERGY ACT OF 1954~~

FORM 6003

2.6 Basic Operational Factors

2.6.1 Inertial Load Factors

2.6.1.1 Flight Maneuver Factors at Missile Center of Gravity

The inertial load factors presented in Table I represent the translational acceleration at the vehicle center of gravity and are reproduced from data presented by Ling-Temco-Vought in Reference 3. Rotational accelerations  $\dot{W}_y$  and  $\dot{W}_z$  are referenced to the vehicle center of gravity.

Dynamic load shears and moments for ejection of multiple warheads must be added to the static rigid body shears and moments derived from these load factors.

2.6.1.2 Flight Maneuver Translational Inertial Load Factors at Centers of Gravity of Individual Components

The component inertial loads shown in Table IV were calculated from data presented in Reference 3 (Figure 18).

2.6.1.3 Design Limit Load Factors for Reactor

The following inertial factors (Figure 19 of Reference 3) represent the combined inertial effects of both translational and rotational acceleration acting at the reactor center of gravity at vehicle Fuselage Station 842.48. The vertical load factors for the case of weapons ejection are presented in Table V for the reactor end stations.

2.6.1.4 Design Limit Ground Handling Inertial Factors

The following factors (Table VI) are in terms of translational acceleration at the missile center of gravity (refer to Reference 3, Figure 20).

2.6.2 Vibration Environment

- |                                  |  |               |
|----------------------------------|--|---------------|
| 1. Launch-Boost                  | Average 3.0g RMS in all directions (180db) | 5 to 2000 cps |
| 2. Cruise (Boundary Layer Noise) | Average 2.25 g in all directions (164db)   | 5 to 2000 cps |

2.7 Analytical Factors

2.7.1 Design Factors and Factors of Safety

Multiplying numerical factors used in the structural analysis design of structural components are classed as "Design Factor" and "Factors of Safety" (Table VII).

~~SECRET RESTRICTED DATA~~

~~ATOMIC ENERGY ACT OF 1954~~

MAC 4873

~~SECRET RESTRICTED DATA~~  
~~ATOMIC ENERGY ACT OF 1954~~

ASD-TDR-63-277. Vol. IV

REPORT 6003

2.7.1.1 Design Factors

Structural deformations alter propulsion system performance and, if excessive, may result in functional failure. Design factors are utilized to provide greater assurance against deformations that are difficult to predict with confidence.

2.7.1.2 Factors of Safety

Factors of Safety are utilized to reduce the possibility of catastrophic structural failure, such as buckling or rupture

2.7.1.3 Limit Loads

A limit load is defined as the maximum value of the load to which a structural member will be subjected during a critical design condition.

2.7.1.4 Design Load

A design load is a limit load increased by a specified Design Factor or Factor of Safety.

2.7.1.5 Use of Factors

To avoid confusion, the limit values of loads and/or stresses shall be utilized in all calculations and design factors or factors of safety applied only in the calculation of margins of safety.

2.8 Margins of Safety

Calculated values of limit stresses increased by the appropriate multiplying design or safety factor are compared to the pertinent allowable mechanical strength properties and margins of safety derived as follows:

$$\text{Margin of Safety} = \left( \frac{\text{Allowable Stresses}}{\text{Limit Stresses} \times \text{factor}} \right) - .00$$

2.9 Limits of Structural Deformation

Material strain within the elastic action range rarely affects end product function, but additional progressive deformation associated with time and temperature will progressively alter propulsion system performance and may result in system malfunction.

For a given functional design the object of structural design, then, is to determine the amounts of deformation that can be tolerated without excessive functional loss and then to provide the minimum weight structure that will accomplish these requirements.

~~SECRET RESTRICTED DATA~~  
~~ATOMIC ENERGY ACT OF 1954~~

MAC 4477

~~SECRET RESTRICTED DATA~~

~~ATOMIC ENERGY ACT OF 1954~~

ASD-TDR-63-277, Vol. IV

CONF 6003

Deformation limits vary between individual structural components, depending upon their function in the system and the interaction between components.

Allowable limits of deformation are specified in the separate analyses of individual components presented in later sections of this report.

## 2.10 Materials and Material Properties

### 2.10.1 Choice of Material

A study of available materials suitable for high temperature operation indicates that nickel base alloys are the most suitable for the current load, time, and environment operational requirements of the turbo propulsion system.

Rene' 41, a precipitation-hardened type of nickel base alloy, the strength of which is developed by various solution and aging heat treatments, appears to be more attractive for use in the present thermal environment. However, if the thermal environment should become less severe, then 15-7PH may be considered.

### 2.10.2 Over Aging and Cyclic Loading

Long life at temperatures approaching the precipitation heat treatment range may result in excessive overaging and lower stress rupture life. In addition, the low cycle-high stress level fatigue life decreases rapidly at temperatures near the precipitation treatment range.

Since the operational temperatures of the inlet structures are in the 1000°F range, the chosen material should be investigated for cyclic loading.

## 2.11 Design Parameters

Engine design parameters are shown in Figures 10, 11, and 12 presenting net flow areas, Mach numbers, temperatures, pressures, and auxiliary air requirements.

DECLASSIFIED IN FULL  
Authority: EO 13526  
Chief, Records & Declass Div, WHS  
Date: OCT 02 2015

~~SECRET RESTRICTED DATA~~

~~ATOMIC ENERGY ACT OF 1954~~

MAC 6027

~~SECRET RESTRICTED DATA~~

ASD-TDR-63-277, Vol. IV

REPORT 6003

### 3.0 INLET

#### 3.1 Design

##### 3.1.1 Discussion

Design layouts have been completed for the basic inlet. Basic lines are shown in Figures 13 and 14, and structural framing, the spike translation mechanism, and the bypass door actuation mechanism are shown in Figures 15, 16, and 17, respectively.

The inlet is a complete, self-contained assembly starting at Engine Station 49.348 (at tip of spike) and terminating at Engine Station 286.936. The inlet assembly is attached to the underside of the vehicle by bolts through oversized holes for vertical loads only and by shear pin connections for forward and aft loads. Side loads are resisted by the shear pin connection and six shear pins equally spaced around the structural ring at Engine Station 286.936.

##### 3.1.2 Boundary Layer Air Bleed

Provision for efficiently discharging inlet boundary layer bleed air is made by ducting the air through the two lower outlets into the annulus between the inner and outer shells of the inlet diffuser such that the boundary layer bleed exits axially downstream through a stepped outlet.

##### 3.1.3 Bypass Doors

Bypass doors are used to control the airflow to the reactor. Due to the control package, the doors are located in the subsonic section of the supersonic inlet diffuser where the nuclear heat generation rates are low and space restriction for the actuator mechanism is less severe. The doors are of the vertically hinged, counterbalanced shutter type, mounted on both sides of the inlet on the inlet horizontal centerline. The doors are designed to operate at a maximum pressure differential of 420 psi at design point, and are capable of opening and reclosing within three seconds when required. The inlet restart during low altitude cruise. The doors are rotated by means of a top crank operated from a single pneumatic actuator, thereby insuring synchronization.

##### 3.1.4 Spike Translation

The inlet must be capable of start, restart, and shock positioning at Mach numbers below and above design point. The spike must move forward to start or restart the inlet and must retract for operation at higher Mach number. At reduced Mach numbers the intersection point of the two compression shocks moves forward, and it is necessary to extend the spike forward to keep these shocks positioned properly on the centerbody and boundary layer bleed. The translating spike is designed to retract as determined by critical operation at Mach 2.8. Also, the spike is designed to translate, at one inch per second with the capability of translating 7.00 inches in three seconds.

~~SECRET RESTRICTED DATA~~

~~ATOMIC ENERGY ACT OF 1954~~

MAC 2477

~~SECRET RESTRICTED DATA~~  
~~ATOMIC ENERGY ACT OF 1954~~

ASD-TDR-63-277, Vol. IV

ORT 6003

The spike translation mechanism is designed to operate against a maximum spike load of 58,000 pounds. A modified pneumatic motor with servo valve (input speed: 1200 rpm; output speed: 8.2 rpm) drives a cone drive worm gear (30:1 reduction), which drives a 19-tooth pinion which drives two racks (3 1/2 diametral pitch teeth with effective face width of four inches) that are attached to the inlet spike, thereby providing for spike translation.

The centerbody spike is mounted to a guide system, which consists of four one-inch rods (equally spaced circumferentially about and radially located 5.25 inches from the inlet horizontal centerline) and roller guide bushings affixed to the internal centerbody structure. Axial loads are resisted by the actuation mechanism, and the side loads are resisted by the guide system.

### 3.1.5 Weights and Centers of Gravity

Weights and centers of gravity for the inlet spike are listed in Table VIII.

## 3.2 Structural Analysis

### 3.2.1 Discussion

The following preliminary structural analysis of the inlet is concerned primarily with major structural items, (Figures 18 and 19). It has been found that in most cases the inertia forces counteract the primary air loads and are small in magnitude. It has therefore been considered sufficiently accurate to omit them from this analysis.

It has been assumed that the structure has been subjected to three possible conditions:

1. A steady state, long time (10 hours) flight regime near sea level with air entering the inlet at 1.0° pitch angle.
2. A short time flight regime (3 minutes) near sea level with air entering the inlet at 6.0° pitch angle and 3.6° yaw angle; this regime represents a "pull-up" condition.
3. A short time flight regime similar to (2) but with shock outside the cowl producing abnormal axial loads on the spike itself.

The following nomenclature is used in the structural analysis:

- F = Stress, psi  
 $\Delta p$  = Pressure differential, psi  
I = Moment of inertia, in<sup>4</sup>

~~SECRET RESTRICTED DATA~~  
~~ATOMIC ENERGY ACT OF 1954~~

~~SECRET RESTRICTED DATA~~

~~ATOMIC ENERGY ACT OF 1954~~

ASD-TDR-63-277, Vol. IV

REPORT 6003

- b = Width of section, in.
- t = Thickness, in.
- F<sub>cr</sub> = Allowable crippling stress, psi
- M.S. = Margin-of-safety

3.2.2 Cowl Lip

The pressures for a condition of Mach 3.0 . 1000 feet from data given in Figure 20 are combined as follows to determin cowl stresses and deflections, as these were the only data available at the ti of this analysis.

Pressures on inside and outside lip surfac for an axial length of 4.8 inches are shown in Figure 21 (Sketch A).

Pressures on inside and outside cowl surfa s for an additional axial length of 8.4 inches are shown in Figure 21 (Sket : B).

These pressures are averaged as follows to find the average pressure on the whole 13.2 inches of axial length and a to l loading per inch of circumference as shown in Figure 21 (Sketch C).

$\Delta P$ (psi)	Length (inches)	Loading Per Inch of Circumference (lb/inch)	
-37	(4.8)	- 177.5	Sketch .
-96	(8.4)	- 806.0	Sketch
-74.5	(13.2)	- 985.5	

The foregoing loading of Figure 21 (Sketch ) is now broken into three portions to represent unsymmetrical loading cc itions that could result from pitch or yaw angles of attack at the same alti de and speed.

It is assumed in this analysis that the ou ard loading on the windward side drops to one-half its original value, that e outward loading on the leeward side could increase to twice its original alne and that the loadings on the neutral sides would remain unchanged. The t ec loadings which will be superimposed one on another for analysis of the st cture then appear in Figure 22.

Stresses due to hoop tension and bending a combined at the 0° and the 90° locations. Section properties and locations which stress- es are calculated are shown in Table IX and Figure 23. Moments e from Table X.

~~SECRET RESTRICTED DATA~~

~~ATOMIC ENERGY ACT OF 1954~~

MAC 6073

~~SECRET RESTRICTED DATA~~  
~~ATOMIC ENERGY ACT OF 1954~~

ASD-TDR-63-277, Vol. IV

ORT 6003

3.2.2.1 Circumferential Location 0°

$$f("e", "g", \text{ or } "n") = F_{H.T.} + \frac{M\bar{a}}{I} = + \frac{984 \times 20}{3.94} + \frac{-17,500(-0.522)}{0.631}$$

$$= 5000 + 11,000 = 16,000 \text{ psi}$$

$$f("s") = + \frac{984 \times 20}{3.94} + \frac{-13,250(0.50)}{0.631} = 5000 - 10,500 = -5500 \text{ psi}$$

$$f("a") = + \frac{984 \times 20}{3.94} + \frac{-13,250(0.147)}{0.631} = 5000 - 3080 = +1920 \text{ psi}$$

$$f("l") = + \frac{984 \times 20}{3.94} + \frac{-13,250(1.067)}{0.631} = 5000 - 22,400 = -17,400 \text{ psi}$$

3.2.2.2 Circumferential Location 90°

$$f("e", "g", \text{ or } "n") = F_{H.T.} + \frac{M\bar{a}}{I} = + \frac{984 \times 20}{3.94} + \frac{14,500(-0.522)}{0.631}$$

$$= +5000 - 12,000 = -7000 \text{ psi}$$

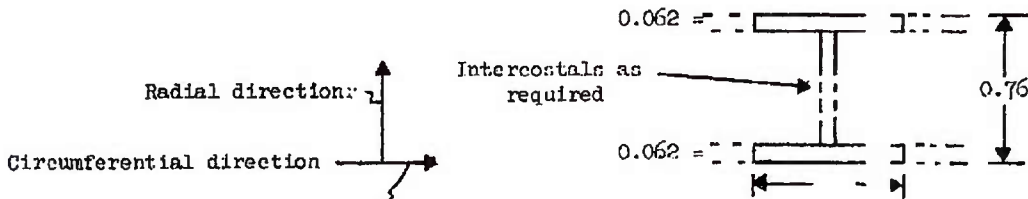
$$f("s") = + \frac{984 \times 20}{3.94} + \frac{14,500(0.50)}{0.631} = +5000 + 11,500 = +16,500 \text{ psi}$$

$$f("a") = + \frac{984 \times 20}{3.94} + \frac{14,500(0.147)}{0.631} = +5000 + 3370 = +8370 \text{ psi}$$

$$f("l") = + \frac{984 \times 20}{3.94} + \frac{14,500(1.067)}{0.631} = +5000 + 24,500 = +29,500 \text{ psi}$$

3.2.2.3 Longitudinal Lip Bending at Station 6.92 (Hollow Section)

Bending Moment: 1989 inch-pounds



~~SECRET RESTRICTED DATA~~  
~~ATOMIC ENERGY ACT OF 1954~~

MAC 4873

~~SECRET RESTRICTED DATA~~  
~~ATOMIC ENERGY ACT OF 1954~~

ASD-TDR-63-277, Vol. IV

REPORT 6003

$$I = (0.062 \times 1.0 \times 0.349^2)2 = 0.01512 \text{ in}^4$$

$$f_b = \frac{M\bar{d}}{I} = \frac{1989 \times 0.349}{0.01512} = 45,800 \text{ psi}$$

(longitudinal tension on inside surface and longitudinal compression on outside surface)

3.2.2.4 Longitudinal Lip Bending at Station 5.0 (Solid Section)

Depth is 0.40 inch. Take circumferential dimension as 1.00 inch, moment as 925 inch-pounds:

$$f_b = \frac{M\bar{d}}{I} = \frac{925 \times 6}{1.0 \times 0.40^2} = 34,700 \text{ psi}$$

3.2.2.5 Margins of Safety

The stresses of Para. 3.2.2.1, 3.2.2.2, and 3.2.2.3 are all considered as "short time" stresses occurring during a gust. For the purpose of design conservatism, the above stresses are raised by the factor of 1.25 and compared with material yield stresses for short times. At local points where buckling is not a problem, the operating stresses are raised by the factor of 1.10 and compared with the material yield stresses-- short time.

3.2.2.6 Circumferential Bending and Tension, Location 0°

Temperature taken as 1100°F; material yield stress 141,000 psi

$$\text{Tension on outside: MS} = \frac{+105,000}{+16,000 \times 1.25} = 4.25$$

$$\text{Tension at splice: MS} = \frac{+105,000 \times 0.75}{+16,000 \times 1.1} = 4.06$$

$$\text{Compression on inside: MS} = \frac{-105,000}{-17,400 \times 1.1} = 3.82$$

MAC 1427

~~SECRET RESTRICTED DATA~~  
~~ATOMIC ENERGY ACT OF 1954~~

~~SECRET RESTRICTED DATA~~

ASD-TDR-63-277, Vol. IV

~~ATOMIC ENERGY ACT OF 1954~~

INT 6003

Compression on leading edge (tangential direct stress):

Take  $b = 2.00$  in., take  $t_{\text{effective}}$  as  $0.057 + 143$   
 $(0.25 - 0.057) = 0.0846$  in.

$$b/t = \frac{200}{0.0846} = 23.6$$

$$F_{cr} = 0.452 E \left(\frac{t}{b}\right)^2 = 0.452 \times 22.7 \times 10^6 \left(\frac{1}{23.6}\right)^2 = 8,400 \text{ psi}$$

(Reference 6, Table B 5.2)

$$MS = \frac{-18,400}{-1.25 \times 5500} - 1 = 1.67$$

### 3.2.2.7 Circumferential Bending and Tension, Location 1

Temperature taken as  $1100^\circ\text{F}$ ; material Rene' 41

$$\text{Tension on inside surface: } MS = \frac{+105,000}{+1.25 \times 29,500} - 1 = 1.85$$

$$\text{Tension at splice: } MS = \frac{+105,000 \times 0.8}{+1.10 \times 29,500} - 1 = 1.75$$

### 3.2.2.8 Longitudinal Bending Stress at Location 0

Temperature taken as  $1100^\circ\text{F}$ ; material Rene' 41

Compression on outside surface from Para. 3.2.1.3

There is a weld splice, so efficiency of joint taken as 0.85:

$$MS = \frac{105,000 \times 0.85}{45,800 \times 1.25} - 1 = +0.56$$

### 3.2.2.9 Summary Note

Since the above calculations were made there has been a slight modification of skin gages; however, it is believed that changes in gages will not appreciably affect the above analysis.

~~SECRET RESTRICTED DATA~~

~~ATOMIC ENERGY ACT OF 1954~~

MAC 1573

~~SECRET RESTRICTED DATA~~  
~~ATOMIC ENERGY ACT OF 1954~~

ASD-TDR-63-277, Vol. IV

REPORT 6003

3.2.3 Diffuser Skin

3.2.3.1 Bursting Effects

This applies to the inner of double skin

R = 17.88 inches; design pressure inside 400 psi  
(maximum which would occur locally between frames)

Pressure outside = 15 psi; P = 385 psi

By conventional formula for bursting of cylinder,

$$f_{HT} = \frac{P \times R}{t} = \frac{385 \times 17.88}{0.10} = 68,750 \text{ psi}$$

Material: Rene' 41

Joint Allowable:

10 hours, 0.2% creep = 0.85 x 92,000 = 78,100 psi

$$MS = \frac{78,100}{1.1 \times 68,750} - 1 = + 0.03$$

3.2.4 Load Paths of Unsymmetrical Airloads

3.2.4.1 Loads Normal to Centerline of Spike

The spike geometry and loads normal to the center are shown in Figure 24.

The relation of cone length to diameter:

$$f_n = \frac{l}{d} = \frac{46.1}{30.48} = 1.51$$

Although data are not available for values of  $f_n$  down to 1.51 (Reference 7, Tables I and II), it is conservative to use the shortest cone  $f_n = 3.0$ , to arrive at normal force derivatives and centers of pressure. The value of  $f_n$ , the ratio of length to diameter for the cylinder downstream of the cone, is conservatively assumed to be zero.

MAC 452

~~SECRET RESTRICTED DATA~~  
~~ATOMIC ENERGY ACT OF 1954~~

~~SECRET RESTRICTED DATA~~

~~ATOMIC ENERGY ACT OF 1954~~

ASD-TDR-63-277, Vol. IV

NY 6003

From Reference 7 (Table I), with  $f_n = 3.0$  and  $f_a = 0$ , the change in normal force coefficient,  $C_n$ , with angle of attack,  $\alpha$  using the second order expansion method, is

$$\frac{dC_n}{d\alpha} = 1.83 \text{ rad}^{-1}$$

From Table II,  $f_n = 3.0$ ,  $f_a = 0$ ,  $X_{cp}/d = 2.00$  (second order expansion method). This places Center of Pressure at  $2/3$  the distance from the tip to the base of the  $f_n = 3.0$  cone.

At sea level and Mach 3 conditions, the dynamic pressure,  $q$ , is

$$q = \frac{\rho}{2} P_o M_o^2 = \frac{1.11}{2} \times 14.7 \times 3.0^2 = 93.4 \text{ lb/ft}^2$$

The normal force on the cone =  $C_n q S \alpha$ , where  $S$  is the cross-sectional area of the cone base, and  $\alpha$  is the angle of attack in radians.

$$\text{Take } S = (\pi) (30.48^2) / 4 = 731 \text{ in}^2$$

Using the coefficient  $C_n$  of the preceding page multiplied by 1.25 to cover discrepancies that may exist between the theoretical cone and the actual spike, the normal force per degree angle of attack is estimated to be:

$$F_N = 1.25 \times 1.83 \times 93.4 \times 731 \times \frac{1}{57.3^\circ/\text{rad}} = 2730 \text{ lbs/deg}$$

The fore and aft center-of-pressure location for this load will be taken at 60 percent of the distance from the tip to the base compared to the 67 percent for an  $f_n = 3.0$  cone.

#### 3.2.4.2 Cowl and Innerbody Unsymmetrical Loadings

The loads of Figure 25 appear in plan view in Figure 26 along with moment load calculations.

Design conditions selected (see Figure 27) are  $6^\circ$  pitch angle of attack for the inlet relative to entering air and  $3.6^\circ$  angle of yaw for the inlet relative to entering air.

~~SECRET RESTRICTED DATA~~

~~ATOMIC ENERGY ACT OF 1954~~

ASD TDR

~~SECRET RESTRICTED DATA~~  
~~ATOMIC ENERGY ACT OF 1954~~

ASD-TDR-63-277, Vol. IV

ONT 6003

$$R_{EE} = \frac{37,600 (127.86 + 32.60 + 39.06 - 10.4) - 10,840 (127.86 + 32.60) - 87,200}{127.86}$$

$$= (7,500,000 - 1,740,000 - 87,200) / 127.86 = 44,400 \text{ lbs.}$$

Shears, moments, and torques from Y direction components only are shown in Figure 28.

The torques are considered as reacted by the pile in proportion to the distance from the centerline to the fitting squared at any one station. Such reaction distributions are tabulated in Table XI.

Shears, moments, and torques from Z direction components only are calculated below, and the results are shown in Figure 29.

Distance from (A-A) to centroid of group is

$$\frac{\sum x}{6} = \frac{464.22}{6} = -77.3 \text{ inches} = \text{centroid P of vertical reactions}$$

Loads of Figure 29 are transposed to the centroid and the moment distributed out to the various reaction points as

$$P_z = \frac{mx'}{\sum (x')^2} \text{ where minus below indicates compression at joint}$$

$$\sum (\text{vertical load}) = 62,800 - 18,080 = 44,720 \text{ lbs}$$

$$\begin{aligned} \sum (\text{moment about P}) &= 62,800 (199.52 - 77.3 - 10.4) \\ &\quad - 145,200 - 18,080 (199.52 - 77.3 - 39.06) \end{aligned}$$

$$\sum M_p = + 7,020,000 - 145,200 - 1,502,000 = 5,372,200 \text{ in-lbs}$$

Load at any station (from moment) is then

$$p = \frac{5,372,200 x'}{18,867} = 285 x'$$

The calculation for this load is summarized in Table XII.

~~SECRET RESTRICTED DATA~~  
~~ATOMIC ENERGY ACT OF 1954~~

MAC 4073

The vertical load is divided equally among six stations.

$$\frac{44,720}{6} = 7452 \text{ lbs/each}$$

To determine fore and aft loads, the structure is broken into segments and the radii and pressures of Figure 30 are applied. The pressures given in Figure 30 represent the symmetrical portion of the asymmetrical load system used for analysis of the cowl lip.

The inside pressure of the innerbody is taken as 62 instead of 110 to obtain conservative panel pressures. The pressure calculations appear in Table XIII.

Loads of Table XIII are now summarized (a positive load is one acting aft):

Spike less skirt:

$$+7540 + 2400 - 3350 - 6580 = +10 \text{ lbs}$$

Spike including skirt attached to it:

$$+10 - 4370 = -4360 \text{ lbs}$$

Fixed part of innerbody complete:

$$-3500 - 28,100 - 56,600 - 56,300 = 144,000 \text{ lbs}$$

Complete innerbody, including spike:

$$-144,400 - 4360 = 148,760 \text{ lbs}$$

There will also be a drag on the wedge structure between the inlet and the vehicle. The half angle is 8°, and the average height is 5.0 inches. The base width at Section A-A of Figure 18 is 50 inches.

From Reference 8, the pressure ratio across two-dimensional shock at Mach 3.0 for a half angle of 8° is  $p/p_0 = 1.80$ , so that at sea level conditions the pressure behind the shock is  $1.80 \times 14.7 = 26.5$  psia. This pressure is considered constant from the entering edge back to Section A-A (Figure 18). The inside pressure will be considered as ambient, 14.7 psia, for the present such that total drag for the wedge structure aft to Section A-A becomes

$$(50 \text{ in.} \times 5 \text{ in.}) (26.5 - 14.7) = (250) (11.8) = 2950 \text{ lbs}$$

$$\left[ q \text{ (ref. only)} = \frac{\rho C}{2} P_0 M_0^2 - \frac{1.41}{2} \times 14.7 \times 3.0 = 93.4 \text{ psi} \right]$$

MAC 427

~~SECRET RESTRICTED DATA~~  
~~Atomic Energy Act of 1954~~

ASD-TDR-63-277, Vol. IV.

REPORT 6003

Axial load from the inlet and wedge structure is then:

$$= 148,760 + 2950 = 151,710 \text{ lbs (acting forward)}$$

The effect of inlet forward load on the vertical fitting at the inlet vehicle joint is now considered. The analysis is similar to that presented in Figure 29. However, in this case, the couple which is reacted vertically at the six fittings, results from axial loading on the vertical fitting at the vertical centerline of Section E-E.

Figure 31 shows the fitting. Calculations are presented below.

The couple resulting from forward load on the inlet is:

$$151,710 \times 25.08 = 3,804,888 \text{ in./lbs}$$

Point P is the centroid of the vertical reactions (Figure 29 and Table XII) that must resist this moment.

The load at any station due to the applied moment is then

$$P = \frac{3,804,888 \text{ x'}}{18.867} = 201,730 \text{ x'}$$

This example is evaluated in Table XIV.

#### 3.2.4.3 Summary Tables of Attachment Reactions

Following the nomenclature of Figure 18, the reactions from airloads of the unsymmetrical condition are listed in Table XV.

Loads marked with an asterisk would act on the aft portion of the split frame at Section (A-A), rather than directly on the fitting points (k) and (l).

#### 3.2.5 Strut

The forward load is 148,760 lbs from the aerodynamic body to the diffuser double wall for a normal cruising condition (Page

There are three struts to carry this shear load, so the load on each is:

$$\frac{148,760}{3} = 49,587 \text{ lbs}$$

MAC A572

~~SECRET RESTRICTED DATA~~  
~~Atomic Energy Act of 1954~~

~~SECRET RESTRICTED DATA~~  
~~ATOMIC ENERGY ACT OF 1954~~

ASD-TDR-63-277, Vol. IV:

PORT 6003

Radial reactions induced at spar stations (E-E and (F-F) are:

$$\frac{49,500 \times 6.6}{32.6} = 10,020 \text{ lbs total in radial direction}$$

These reactions are apportioned between inner and outer support rings in inverse proportion to the ring radii cubed for preliminary design purposes (see Figure 32). NOTE: Short time maneuver loads from the innerbody could produce loads of

$$\begin{array}{r} -204,400 \\ -148,760 \end{array}$$

or 1.38 times the above values (see Para. 3.2.5.2).

#### 3.2.5.1 Struts (Normal Symmetrical Loads Alone)

Load on struts from supporting rings are shown in Figure 33.

#### 3.2.5.2 Special Load Conditions Wherein Shock Has Moved Forward From Its Normal Location

With the shock moved well forward, the aft load on the spike is at 40,000 lbs. Using the normal cruising pressures for the fixed portion of the innerbody, the minimum forward load of the entire innerbody is now estimated as follows:

$$\text{Minimum Forward Load} = -148,760 + 4360 + 40,000 = -104,400 \text{ lbs (Reference Page)}$$

With the shock moved well aft, the spike forward load has been estimated at 60,000 lbs. Using the normal cruising pressures for the fixed portion of the innerbody, the maximum forward load of the innerbody is estimated as follows:

$$\text{Maximum Forward Load} = -148,760 + 4360 - 60,000 = -204,400 \text{ lbs}$$

The above may be compared with the normal cruising condition forward load:

$$\text{Normal Forward Load} = -144,400 - 4360 = -148,760 \text{ lbs (Reference Page)}$$

#### 3.2.5.3 Loads on Strut Spars from Unsymmetrical Loads Normal to the Centerline

The total loads from the spike and the fixed portion of the innerbody, as shown on Figure 26, are the resultant loads on a plane rotated 30° 58' from a vertical plane.

~~SECRET RESTRICTED DATA~~  
~~ATOMIC ENERGY ACT OF 1954~~

MAC 1603

~~SECRET RESTRICTED DATA~~  
~~ATOMIC ENERGY ACT OF 1954~~

ASD-TDR-63-277, Vol. IV.

REF ID: A6003

$$\begin{aligned} X - \text{Direction Reaction "R" + "S"} &= 600,000 \times \frac{2}{3} + \frac{564,000}{11.82} - \frac{18,100}{11.82} \quad (.06) \\ &= 40,000 + 47,700 - 59,800 = +27,900 \text{ lbs} \end{aligned}$$

$$\text{Load "R"} = \text{Load on "S"} = \frac{27,900}{2} = 13,950 \text{ lbs Tension on Joint}$$

### 3.2.6 Innerbody Ring at Section (F-F)

The innerbody rings, the diffuser ring, and the struts form a redundant system of load paths. However, a simplified and conservative set of loads on the innerbody ring of Section (F-F) has been employed to find the maximum bending moment. The ring is subjected to both transient short time and steady state long time loads.

#### 3.2.6.1 Steady State Long Time Loads

The innerbody forward load is taken as -148,760 lbs (Figures 32 and 33). The loads normal to the centerline of the innerbody are considered the same as those for the 1° angle of attack condition which is one sixth of those in Figure 36.

Steady State Flight Condition Ring Moments are calculated in Tables XVI and XVII.

For the unsymmetrical portion of moments, PR is 1,760 x 10.79 = 40,500 (see Figure 37). Moments for symmetrical portion of loads are carried over from preceding page.

#### 3.2.6.2 Short Time Maneuver Loads

The innerbody forward load is taken as -204,000 lbs, which is 1.38 times normal thrust (see Figure 32 and Paragraph 3.2.5.2). Thrust loadings then appear as shown in Figure 38.

The unsymmetrical load is taken as 7/6 times the vertical load shown in Figure 36.

Ring moments from short time maneuver loads are calculated in Table XVIII, and ring section properties are calculated in Figure 39.

#### 3.2.6.3 Stresses and Margins

Using the ring section properties and the two basic loading condition ring moments determined in the previous pages, the margins of safety of this ring are calculated as follows (Material is Rene' 41):

~~SECRET RESTRICTED DATA~~  
~~ATOMIC ENERGY ACT OF 1954~~

~~SECRET RESTRICTED DATA~~  
~~ATOMIC ENERGY ACT OF 1954~~

ASD-TDR-63-277, Vol. IV

REPORT 6003

Steady State - Long Time Loading:

$$\text{Free Flange } f_{b_i} = \frac{Mc}{I} = \frac{-27,100 \times 1.84}{3.27} = -15,250 \text{ psi (Compression)}$$

$$\text{I.B. Skin near Flange } f_{b_o} = \frac{-27,110 (-1.45)}{3.27} = +12,000 \text{ psi (Tension)}$$

It is proposed to maintain a 10 percent safety factor to material yield and a 25 percent safety factor to structural failure. The yield allowable is taken as the stress level to force a yield of 0.2 percent with 25-hour exposure at 1100°F. The ultimate allowable is taken as the short time 0.2 percent yield stress at 1100°F.

$$\text{MS on Yield} = \frac{-92,000}{1.10 (-15,250)} - 1 = \text{Ample}$$

$$\text{MS on Failure} = \frac{-105,000}{1.25 (-15,250)} - 1 = \text{Ample}$$

Short Time Maneuver Loading:

$$\text{Free Flange } f_{b_i} = \frac{Mc}{I} = \frac{-92,060 \times 1.84}{3.27} = 51,800 \text{ psi (Compression)}$$

$$\text{I.B. Skin near Flange } f_{b_o} = \frac{-92,060 (-1.45)}{3.27} = +40,800 \text{ psi (Tension)}$$

It is proposed to maintain a 10 percent safety factor to material yield and a 25 percent safety factor to structural failure. Short time yield is employed here for the allowable, because buckling could occur when yielding commences.

$$\text{MS on Yield} = \frac{-105,000}{1.10 (51,800)} - 1 = .85$$

$$\text{MS Against Failure} = \frac{-105,000}{1.25 (51,800)} - 1 = +0.62$$

MAC 4672

~~SECRET RESTRICTED DATA~~  
~~ATOMIC ENERGY ACT OF 1954~~

~~SECRET RESTRICTED DATA~~  
 ATOMIC ENERGY ACT OF 1954

ASD-TDR-63-277, Vol. IV

Item 6003

3.2.7 Innerbody Skin

At Section (F-F) of Figure 26, the following are the loads across the section:

Shear forward of section: 21,090 lbs (transverse)

Moment at section: 169,400 in.-lbs

Shear aft of section:  $169,400/32.6 = 5,200$  l (transverse)

Normal shear flow to each longeron from inner body thrust is  $49,500/32.6 = 1520$  lbs/in. (see Figure 32).

Normal shear flow to each longeron from short time thrust with shock in abnormal position on the spike is  $1.38 \times 1520 = 2100$  lbs/in. (see Figure 37).

Shear buckling forward of Section (F-F):

Panel width, 5.00 inches; radius, 12.5 inches  
 t, 0.125 in.

Maximum shear on side

$$\frac{V}{77Rt} = \frac{21,090}{77 \times 12.5 \times 0.125} = 4300 \text{ psi}$$

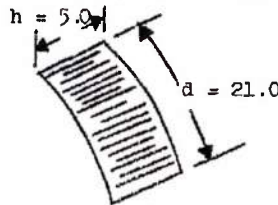
To estimate critical shear buckling, see Reference 10.

$$T_c = \left\{ (0.10 E \frac{t}{R}) + 5 E \left(\frac{t}{d}\right)^2 \left[ 1 + 0.8 \left(\frac{d}{h}\right)^2 \right] \right\} 0.75$$

$$= \left\{ (0.10 \times 22.5 \times 10^6 \times \frac{0.125}{12.5}) + 5 \times 22 \times 10^6 \left(\frac{0.125}{21}\right)^2 \left[ 1 + 0.8 \left(\frac{21}{5}\right)^2 \right] \right\} 0.75$$

$$= \left\{ (22,500) + 3980 [15.1] \right\} 0.75 = 62,000 \text{ psi}$$

The margin of safety against shear buckling is adequate.



~~SECRET RESTRICTED DATA~~  
 ATOMIC ENERGY ACT OF 1954

MAC 6071

~~SECRET RESTRICTED DATA~~  
 ATOMIC ENERGY ACT OF 1954

ASD-TDR-63-277, Vol. IV

REPORT 6003

3.2.7.1 Collapse of Skin between Frame Support at Forward of  
Section (F-F)

Normal pressures are 311 psia outside and 2 psi inside (Figure 30). However, to account for possible higher values of pressure introduced by angles of attack and yaw, a maximum outside pressure of 400 psia with 62 psia inside will be employed here. Therefore,  $\Delta P = 338$  (see Reference 11, Page 306, Table XVI, Cond. Q, Support 31):

$p'$  = pressure of collapse from external pressure

$$= 0.807 \frac{Et}{1r} \left[ \left( \frac{1}{1 - \nu^2} \right)^3 \frac{t^2}{r^2} \right]^{1/4} = 48 \text{ psia}$$

It is proposed to maintain a safety factor of 10 percent on the peak short time operating pressure:

$$MS = \frac{485}{1.10 \times 338} - 1 = +0.30$$

3.2.7.2 Shear Buckling of Skins between Sections (F-F) and (E-E)

Loading (short time maximum) from Paragraph 3.2.7 is 2100 lb/in. to allow for uneven distributions plus shear from transverse shear (skin shear to each side of strut is taken at 75 percent, or  $0.75 \times 2100 = 1575$  lb/in. To estimate critical shear buckling stress as in Paragraph 3.2.7 (except frame spacing is 7.7 and R is 11.50 in.):

$$T_o = \left\{ (0.10 E \frac{t}{R}) + 5E \left( \frac{t}{R} \right)^2 \left[ 1 + 0.8 \left( \frac{d}{R} \right) \right] \right\} 0.75$$

$$= 39,000 \text{ psi}$$

Since it is proposed to maintain a safety factor of 10 percent for this short time buckling shear stress, the margin of safety is:

$$MS = \frac{37,000}{1.10 \times \left( \frac{1575}{0.125} \right)} - 1 = \frac{37,000}{12,860} - 1 = 1.9$$

MAC 607

~~SECRET RESTRICTED DATA~~  
 ATOMIC ENERGY ACT OF 1954

~~SECRET RESTRICTED DATA~~

ASD-TDR-63-277, Vol. IV

INT. 6003

3.2.7.3 Collapse of Skin Between Frame Supports Aft of Section (F-F)

Design pressure, with some allowance for asymmetry at angles of attack, is taken as

$$1.15 \times 311 = 358$$

$$\Delta P = 358 - 62 = 296 \text{ psi}$$

$$p' * = 0.807 \times \frac{22.5 \times 10^6 \times 0.125^2}{7.7 \times 11.5} \left[ \left( \frac{1}{1 - 0.3^2} \right)^3 \frac{0.125^2}{11.5^2} \right]^{1/4} = 341 \text{ psi}$$

Proposed extra margin between operating load and buckling failure is 10 percent.

$$MS = \frac{341}{1.10 \times 296} - 1 = +0.05$$

3.2.7.4 Innerbody Intermediate Frames

Aft of Section (F-F) of Figure 19, the panel spacing is 7.7 inches. Maximum differential pressure is  $358 - 62 = 296$  psi. Loading on one ring per inch of its circumference is  $296 \times 7.7 = 2280$  lbs per inch. The elastic stability capacity of the ring is computed following Reference 11, Page 295, Table XV, Case 12. The section properties appear in Figure 10.

$$p' = \frac{3 EI}{R^3} = \frac{3 \times 22.5 \times 10^6 \times 0.0817}{11.28^3} = 3810 \text{ lbs per inch}$$

It is proposed to keep a 25 percent extra factor against such a collapse; therefore,

$$MS = \frac{3810}{1.25 \times 2280} - 1 = +0.34$$

\*Reference 5, Page 306, Table XVI, Cond. Q, Support 31

MAC AGZ

~~SECRET RESTRICTED DATA~~

~~ATOMIC ENERGY ACT OF 1954~~

~~SECRET RESTRICTED DATA~~

ASD-TDR-63-277, Vol. IV

REPORT 6003

3.2.8 Thrust Fitting

The critical loads (Figure 41) on this pin occur at the maximum forward load condition of the innerbody--Paragraph 3.2.2 (-204,400 lbs) and the lateral load of the yaw condition--Figure 27 (44,4 lbs). There will also be a wedge drag of 2950 lbs.

$$\text{Total load} = -204,400 + 2950 = -201,450 \text{ l}$$

ing and shear.

At Section (A-A) through the pin there will be both bend-

Bending is

$$206,000 \text{ lbs} \times 0.70 \text{ inches} = 144,000 \text{ -lbs}$$

Section (A-A) Moment of Inertia is

$$\frac{\pi D^4}{64} = \frac{\pi \times 2.75^4}{64} = 2.82^4 \text{ inches}$$

$$f_b = \frac{Mc}{I} = \frac{144,000 \times 1.375}{2.82} = 70,200 \text{ p}$$

$$f_{s(av)} = \frac{S}{A} = \frac{206,000 \times 4}{\pi \times 2.75^2} = 34,700 \text{ p}$$

Material: Rene' 41

Short time 0.2 percent yield at 1100°F is

105,000 psi

Short time ultimate stress at 1100°F is

152,000 psi

~~SECRET RESTRICTED DATA~~

~~SECRET RESTRICTED DATA~~

ASD-TDR-63-277, Vol. IV

6003

Long time (10 hours) 0.2 percent yield at 1100 psi  
92,000 psi

$$\text{MS (short time yield)} = \frac{105,000}{1.10 \times 70,200} - 1 = +0.36$$

$$\text{MS (short time ultimate)} = \frac{152,000}{1.25 \times 70,200} - 1 = +0.74$$

$$\text{MS (long time yield)} = \frac{92,000}{1.10 \times 70,200 \times \left(\frac{145,800}{206,000}\right)^*} - 1 = + 68$$

**DECLASSIFIED IN FULL**  
**Authority: EO 13526**  
**Chief, Records & Declass Div, WHS**  
**Date:**

OCT 02 2015

-----

$$*\left(\frac{145,800}{206,000}\right) = \text{Ratio } \frac{\text{Normal Operating Load}}{\text{Maximum Short Time Load}} \quad (\text{See Page } \quad )$$

~~SECRET RESTRICTED DATA~~

~~ATOMIC ENERGY ACT OF 1954~~

~~SECRET RESTRICTED DATA~~  
~~ATOMIC ENERGY ACT OF 1954~~

ASD-TDR-63-277, Vol. IV

REPORT 6003

#### 4.0 SUBSONIC DIFFUSER AND REACTOR CONTROL SUPPORT STRUCTURE

##### 4.1 Design

##### 4.1.1 Discussion

For purposes of this report, the subsonic diffuser is defined as that part of the propulsion system between Fuselage Station 1 and 2) and the front face of the reactor. The reactor control support structure is defined as the components within the subsonic diffuser that make up the mechanical linkage between the reactor control rods and the actuator as well as the structure needed to support this linkage and the rods.

Design of the subsonic diffuser, which (from the point of view of the propulsion system) is a pressure duct, is limited to defining aerodynamic lines. These lines are defined to permit optimum performance of the propulsion system with the smallest possible duct size. Mechanical design of the duct is the responsibility of the airframe manufacturer, inasmuch as the duct is an integral part of the airframe.

The design of the reactor control rod actuators, associated linkage, and support structure is a more complex problem for the engine manufacturer than is the subsonic diffuser. For the former, it is necessary to obtain requirements from the reactor company, geometric and environmental limitations from the airframe company, and inputs from the propulsion system contractor, and to integrate all these into a well-designed structural system.

Listed below are the factors that have been considered in this design:

1. Stroke: approximately 40 inches
2. Temperature: 1070°-1200°F
3. Rate of travel: Full stroke in 0.75 seconds
4. Minimum passage blockage
5. Maximum axial g load: 25 g
6. Maximum radial g load: 4.5-0.25g
7. Accessibility
8. Friction load between control rods and reactor tubes
9. Air drag loads in rods
10. Air drag loads in the support mechanism

~~SECRET RESTRICTED DATA~~  
~~ATOMIC ENERGY ACT OF 1954~~

~~SECRET RESTRICTED DATA~~  
~~ATOMIC ENERGY ACT OF 1954~~

ASD-TDR-63-277, Vol. IV

PORT 6003

11. Limiting deflections of supports, rods, and duct
12. Vibration of supports and control rods 0 to 36 inches D.A. Frequency, 0-3000 cps
13. Reliability
14. Number, types, and position of control rods: 12 shim and 2 vernier

In designing this portion of the system several approaches have been studied. The design as shown in Figure 2 has been considered most promising from the point of view that it presents the smallest blockage in the diffuser and provides the best accessibility to the actuator.

In the matter of mechanical and structural functions, the air motor, gear box, and control valve are positioned on the outside periphery of the duct to afford greater accessibility for maintenance and to reduce flow blockage in the duct.

A rack and pinion type drive unit is located on the main support strut. The unit is driven by the motor through a shaft that is located inside the strut. The rack is attached to a spider fitting, which picks up four control rods from the reactor, at the downstream end of the reactor. The attachment of the control rod to the spider fitting may be either fixed or a quick-disconnect type with manual or remote handling features. Movement of the rack translates the spider fitting along a guide shaft that is supported between the main support and the aft support. The guide shaft also serves as a housing for the feedback transducer, which is geared down and operates off the main rack. When moving upstream, the rack is housed and guided in a tube that is supported between the main support and the forward support.

Figure 2 does not reflect any method of attachment between the supports and the duct. Because of differential thermal expansion, these points will, of necessity, be a slip-fit type of connection.

A detailed design study and subsequent structural analysis of this area must be accomplished before a final decision can be made as to the best system. However, before this study can be accomplished an overall control system study must be made that will more accurately define the requirements of this structure.

#### 4.1.2 Weights and Centers of Gravity

Weights and centers of gravity for the reactor control rod support structure and actuation mechanism are shown in Table XII

#### 4.2 Preliminary Analysis of Control Rod Support Structure

##### 4.2.1 Loads

Weight of control rod = 5.7 lbs

~~SECRET RESTRICTED DATA~~  
~~ATOMIC ENERGY ACT OF 1954~~

~~SECRET RESTRICTED DATA~~

~~ATOMIC ENERGY ACT OF 1954~~

ASD-TDR-63-277, Vol. IV

REPORT 6003

Weight of rack (estimated) = 1 in.<sup>2</sup> x 50 in. long x 0.3 density = 15 lbs

Weight of spider fitting (estimated) = 1 6 in.<sup>2</sup> blockage

Estimated average thickness = 3 inches

Weight ≈ 13.6 x 3 x 0.3 = 12.25 lbs

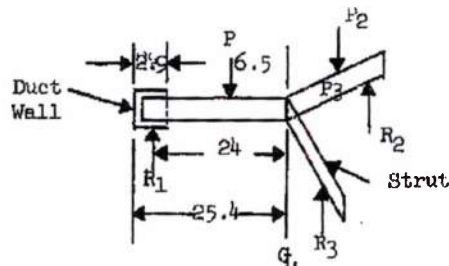
4.2.1.1 Aerodynamic Drag Load Per Strut = 422 lb

Total load per strut (inertia) = (4) (5) + 15 + 12.25 = 50 lbs

4.2.1.2 Strut Design Load

Load at the 6g boost condition = (6) (5) 422 = 722 lbs

The twelve coarse control rods are actuated in groups of four and are reacted by three struts as shown in Figure 42. To allow for thermal expansion, the struts are fixed at the center and have a sliding support at the duct wall.



$$P_1 = P_2 = P_3$$

$$R_1 = R_2 = R_3$$

Assume struts fixed at centerline.

Assume only shear load carried thru  $R_1, R_2, R_3$  at the duct wall

$$P_1 = R_1 \text{ etc}$$

$$P_1 = 722 \text{ lbs}$$

$$\text{Moment} = 722 (24 - 65) = 12,620 \text{ in-lbs (max)}$$

According to Reference 5 and Figure 43:

$$I_{xx} = ctL^3$$

$$C_1 = f \left( \frac{L_1}{D_1} \right)$$

$$D_1 = 1.50 - 0.05 = 1.45$$

$$\frac{L_1}{D_1} = \frac{5.20}{1.45} = 3.58$$

MAC ART

~~SECRET RESTRICTED DATA~~

~~ATOMIC ENERGY ACT OF 1954~~

~~SECRET RESTRICTED DATA~~  
~~ATOMIC ENERGY ACT OF 1954~~

ASD-TDR-63-277, Vol. IV

REPORT 6003

$$C_1 = 0.20$$

$$Y_1 = 49.09\% L_1$$

$$I = (0.2) (0.05) (5.20)^3 = 1.408 \text{ in.}^4$$

$$Y_1 = (0.4909) (5.20) = 2.55$$

$$C = 2.55 + 0.025 = 2.58$$

$$f_{bc} = (12,620)(2.58)/1.408 = 23,200 \text{ psi compression}$$

$$f_{bt} = (12,620)(2.67)/1.408 = 24,000 \text{ psi tension}$$

Using 19-9 DX material and assuming that buckling is not critical, then:

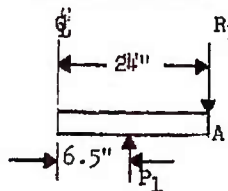
$$F_{TY} = 37,000 \text{ psi at } 1200^\circ\text{F}$$

$$F_{Tu} = 75,000 \text{ psi at } 1200^\circ\text{F}$$

$$E = 22 \times 10^6 \text{ at } 1200^\circ\text{F}$$

$$MS = (37,000/24,000) - 1 = + 0.54 \text{ tensile}$$

4.2.2 Deflection Check of Strut



$$R_1 = P_1 = 722 \text{ lbs}$$

$$l = 24$$

$$a = 6.5$$

$$I = 1.408$$

$$E = 22 \times 10^6$$

4.2.2.1 Deflection at PT A Due to R

$$y_1 = \frac{PL^3}{3EI}$$

4.2.2.2 Deflection at PT A Due to P1

$$y_1 = \frac{P}{6EI} (3a^2l - a^3)$$

MAC 1027

~~SECRET RESTRICTED DATA~~  
~~ATOMIC ENERGY ACT OF 1954~~

~~SECRET RESTRICTED DATA~~

ASD-TDR-63-277, Vol. IV

REPORT 6003

4.2.2.3 Total Deflection at PT A =  $y_1 - y_2$

$$y_1 - y_2 = \frac{P}{6EI} (2l^3 - 3a^2l + a^3)$$

$$= \frac{722}{(6)(22)(10)^6} 1.408 \quad (2)(24)^3 - (3)(6.5)^2 (24) \quad (6.5)^3$$

$$y_1 - y_2 = 0.097 \text{ in.} = \text{Max Deflection}$$

**DECLASSIFIED IN FULL**  
**Authority: EO 13526**  
**Chief, Records & Declass Div, WHS**  
**Date: OCT 0 2 2015**

MAC A87

~~SECRET RESTRICTED DATA~~

DECLASSIFIED IN FULL  
Authority: EO 13526  
Chief, Records & Declass Div, WHS  
Date: OCT 02 2015

5.0 REACTOR SUPPORT SYSTEM

5.1 Side Support System Design

During FY 1962 attention has been centered on the minimization of the lateral support annulus dimension in the interest of increasing the aerodynamic performance of the overall Pluto system.

The analytic optimization of the lateral support annulus is based on an assumed dynamic model (see Section 5.2.2) and consists of the optimization of both the radial spring rate and the support spring configuration. The spring rate is optimized to give a minimum required energy storage in the system for the specified design criteria. The spring configuration was selected to achieve a maximum of strain energy storage in the spring for a minimum volume of spring material. A detailed description of this work may be found in Section 5.2.3.

The nuclear reactor core and its reflectors consist of an assembly of approximately 450,000 hexagonal ceramic tubes measuring 0.297 inches across the flats and 2.0 to 4.0 inches in length. The tubes are stacked end to end to form continuous tubes approximately 62.0 inches in length, and these in turn are assembled side to side to form a right circular cylinder 53.25 inches in diameter. The reactor cylinder is aligned axially in the airframe duct.

The core assembly is clamped into the desired cylindrical shape and is supported to the airframe by the lateral support system. The present design concept consists of a series of close fitting, curved pressure pads, which form an expandable shell around the core. They are compressed against the core by radially orientated springs, which in turn bear against a monolithic cylindrical shell that encloses the entire core, pressure pad, and spring assembly.

The pressure pads are supported in radial planes by the springs and in tangential and meridional directions by radially oriented pin-and-socket connections to the pressure shell.

The pressure shell, in turn is supported tangentially by means of a longitudinal tongue and groove rail system, which allows radial growth of the shell with relation to the airframe.

The reactor tube matrix and spring support system are essentially a spring mass system, which is sensitive to vibration loading. The spring system must be so designed that response of the reactor to vibration loads from the airframe will not be excessive.

Weights and centers of gravity are shown in Table XX.

5.1.1 Side Support System Function

The reactor lateral support structure must be capable of (1) insuring an adequate clamping pressure on the reactor matrix, (2) accommodating severe relative thermal expansion between the matrix and the containing

MAC 4477

~~SECRET RESTRICTED DATA~~  
~~ATOMIC ENERGY ACT OF 1954~~

ASD-TDR-63-277, Vol. IV

INT 6003

shell, (3) limiting the transverse deflection of the core from inert and vibration loads, and (4) permitting the reactor to be handled as a complete assembly.

A compressive force must be exerted on the tube matrix at all times to prevent excessive distortion of the tube bundle or gross separation of tubes. The necessity for this compressive force arises from structural and aerodynamic considerations. Separation induces adverse load paths in the support system; and tube misalignment, with resulting flow blockage, could be caused by both distortion and separation.

A severe differential thermal expansion exists between the reactor and the surrounding structure; i.e., the reactor, at 2500°F, thermally expands into its supporting shell, which is at approximately 100°F.

The side support system must furnish adequate support to the reactor when it is subjected to lateral inertia loads. The reactor and the support springs, being essentially a spring-mass system, are sensitive to vibration loads. The support system must prevent the occurrence of excessive reactor response from this type of loads input.

The system should be designed in a way that permits the handling of the reactor as an entity. Such a design will ease ground handling and reactor-vehicle assembly problems.

The above requirements must be met while maintaining the structural integrity of the ceramic tubes. In addition, the structure of the side support system should be contained in as small an annulus as possible, thereby assuring as high a degree of performance as possible for the engine-vehicle system.

5.1.2 Side Support Annulus Thickness to Vehicle Drag Comparison

Since the drag of the vehicle is approximately proportional to the cross sectional area, a 1/8-inch reduction in radius will relieve a 1 percent reduction in drag; i.e., reducing the side support annulus to 1.0 inches will result in a 4 percent reduction in vehicle drag. Considering the low thrust-to-drag margins associated with nuclear ramjets (approximately 10 percent), it is extremely important to minimize the side support annulus dimension.

5.1.3 Reduction in Annulus Width

Considerable effort was expended in 1962 to minimize this annulus width, pointing toward a target of 1.0 inches. The results are illustrated in Figure 44, which depicts the reduction in annulus width versus time for the years 1961 and 1962. The reduction was achieved through optimization of the spring rate and the spring used in the side support system. Section 5.2 contains a detailed description of this work.

MAC 653

~~SECRET RESTRICTED DATA~~  
~~ATOMIC ENERGY ACT OF 1954~~

~~SECRET RESTRICTED DATA~~  
~~ATOMIC ENERGY ACT OF 1954~~

ASD-TDR-63-277, Vol. IV

REPORT 6003

#### 5.1.4 Design Side Support System

The resulting side support system is shown in Section (C-C), Figure 45. The system consists of four main components: spring pressure pad, (expansion pad) radial spring, pressure shell, and the support rails.

The spring pressure pad transmits radial loads between the reactor and the spring system. It aids in distributing the concentrated spring loads into the radial reflector. It also carries tangential shear loads due to friction between the pad and reactor, into the support rails.

The spring provides a compressive load during ground handling and flight, contains reactor thermal and inertial movement, and transfers resulting loads to the spring pressure shell.

The spring pressure shell reacts the thermal expansion loads and shears the reactor inertia loads to the support rails. This shell also helps isolate reactor axial movements from those of the airframe. This isolation is accomplished by slicing the shell into short axial sections so that a minimum of the friction load resulting from reactor movement will be transferred to the airframe structure. The support rails transfer reactor inertia loads from the spring pressure shell to the structure of the airframe.

#### 5.1.5 Operating and Installation Requirements

Assumed criteria are outlined for the side support system using either tangentially or radially oriented springs. Figures 46 and 47 show temperatures assumed for structural analysis. Table XXI presents the relative differential thermal expansion that occurs during the system's lifetime. Table XXII summarizes the thermal and inertial conditions used in design analysis. In addition to the above, the following general criteria must also be met.

1. Maximum permitted reactor lateral deflection = 0.100 inches. This requirement arises from considerations of tie rod-to-core interference.
2. No finite separation between the reactor and the support system is permitted for design condition; i.e., the support system must remain in contact with the reflector at all times.

##### 5.1.5.1 Assumptions

1. The structural shell surrounding the reactor remains circular.
2. The tube matrix behaves as a rigid cylinder.
3. The side support structure can be integrated into a single elastic constant or spring rate.

~~SECRET RESTRICTED DATA~~  
~~ATOMIC ENERGY ACT OF 1954~~

~~SECRET RESTRICTED DATA~~

~~ATOMIC ENERGY ACT OF 1954~~

ASD-TDR-63-277, Vol. IV

SI nr. 6003

4. Only the translational mode of the reactor is of interest.
5. Only friction-induced slip damping is present.
6. The dynamic input is a sinusoidal, undamped motion with a frequency of 9.5 cps and a peak load of 7g (see Note 1).
7. Average coefficient of friction on the reflector-support system interface is equal to 0.30.

Note 1. The major vibration loads input to the support system occur as a result of fuselage response, during the low altitude cruise phase of flight to free flight conditions. These conditions are terrain avoidance, atmospheric gusts, and stores ejection. Fuselage response to terrain avoidance is an approximate sinusoidal low frequency motion. That due to stores ejection is sinusoidal but highly damped (5-second duration), while that due to gust input is random. These three fuselage responses combine into a 7g peak load at a discrete frequency. The input used in analysis is conservatively assumed to be a 7g peak, sinusoidal, steady state vibration, occurring at the 9.5-cps fuselage frequency.

## 5.2 Side Support System Analysis

### 5.2.1 Nomenclature

- A = Amplification factor (dynamic deflection / static deflection)
- $P_o$  = Magnitude of driving load (lbs/in<sub>a</sub>)
- n = Inertia load factor (g)
- W = Reactor weight (185 lbs/in<sub>a</sub>)
- $V_z$  = Apparent load on springs (lbs/in<sub>a</sub>)
- F = Friction damping load (lbs/in<sub>a</sub>)
- $\mu$  = Reflector--support system interface friction coefficient
- R = Outer radius of reflector (in.)
- $p_o$  = Reactor preload pressure (psi)
- $\Delta p_T$  = Change in reactor pressure due to differential thermal expansion (psi)
- $\Delta p_I$  = Change in reactor maximum pressure due to inertia load (psi)

~~SECRET RESTRICTED DATA~~

~~ATOMIC ENERGY ACT OF 1954~~

MAC 4473

~~SECRET RESTRICTED DATA~~  
~~ATOMIC ENERGY ACT OF 1954~~

ASD-TDR-63-277, Vol. IV

REPORT 6003

- $P_s$  = Static reactor pressure after differential thermal expansion (psi)  
 $\Delta S_T$  = Differential thermal expansion (in)  
 $\Delta S_I$  = Reactor deflection from inertia load (in<sub>r</sub>)  
 $P_m$  = Reactor dynamic and static pressure (psi)  
 $f$  = Driving frequency (cps)  
 $f_n$  = Resonant frequency of reactor spring-mass system (cps)  
 $g$  = Gravity constant (386.4 in/sec<sup>2</sup>)  
 $K_z$  = Support system integrated spring rate (lbs/in<sub>a</sub>/in<sub>r</sub>)  
 $k_r$  = Support system radial spring rate (psi/in<sub>r</sub>)  
 $E$  = Spring material elastic moduli (psi)  
 $T_m$  = Maximum tensile load in tangential spring systems (lbs/in<sub>r<sub>a</sub></sub>)  
 $k_c$  = Circumferential spring rate (lbs/in<sub>r</sub>/in<sub>c</sub>)  
 $V_0$  = Volume of spring element (in<sup>3</sup>)  
 $l$  = Spring element length (in)  
 $\beta$  = Ratio of distance from end of spring to load point to spring length  
 $n_p$  = Number of springs in parallel  
 $n_s$  = Number of springs in series  
 $\eta$  = Surface efficiency of the spring  
 $\sigma$  = Allowable stress of the spring material (psi)  
 $b$  = Ratio of end thickness to center thickness of the spring  
 $\psi$  = Structural efficiency of the spring

Subscripts

- $r$  = Radial  
 $z$  = Transverse  
 $a$  = Axial

~~SECRET RESTRICTED DATA~~  
~~ATOMIC ENERGY ACT OF 1954~~

~~SECRET RESTRICTED DATA~~  
~~ATOMIC ENERGY ACT OF 1954~~

ASD-TDR-63-277, Vol. IV

6003

o = initial or preload conditions

c = circumferential direction

Superscripts

c = low altitude cruise conditions

b = boost-transition conditions

5.2.2 Dynamics Model and Optimum Spring Rate

5.2.2.1 Dynamics Model

A dynamic analysis of the reactor and support system, based on an idealized fluid cylinder vibrating in an elastic medium, reference 4, has shown that appreciable excitation of distortional modes of the tube matrix is unlikely in the frequency range of interest (5-30 cps). However, a low frequency resonance could exist corresponding to the rigid-body translation mode of the matrix. This mode occurs at the system fundamental frequency, which is determined by the mass of the reactor and the spring constant of the side support structure.

The result of the above dynamic analysis and consideration of the inertia load inputs suggests a simple dynamics model on which preliminary dynamic analysis of various lateral support structure configurations will be based. The model is a single-degree-of-freedom, slip-damped system.

The radial and tangential configurations are shown schematically in Figure 48. Figure 49 shows the idealized dynamics model with explanatory details.

Load on the reactor mass is

$$V_z = A n W \quad (1)$$

The solution to the amplification factor, A, is well known. Reference 12, page 437 gives

$$A = \frac{\sqrt{1 - \left(\frac{4}{\pi^2} \frac{F}{P_0}\right)^2}}{1 - f^2/f_n^2} \quad (2)$$

where

$$f_n = \frac{1}{2\pi} \sqrt{\frac{K_z}{M}} \quad (3)$$

~~SECRET RESTRICTED DATA~~  
~~ATOMIC ENERGY ACT OF 1954~~

MAC 4873

~~SECRET RESTRICTED DATA~~

~~ATOMIC ENERGY ACT OF 1954~~

ASD-TDR-63-277, Vol. IV

REPORT 6003

The above equation for amplification factor represents an approximate solution of the model. A plot of the exact solution of  $A$  vs.  $f/f_n$  with  $F/P_0$  as a parameter, may be found on page 438 of Reference 1.

The assumption that the tube matrix reflects as a rigid cylinder permits the solution of the reactor pressure distribution from a static balance of the load. A deflection of the cylindrical matrix of amount  $\Delta S_I$  (see Figure 50) results in a distribution of deflection given by

$$\Delta S_\theta = \Delta S_I \cos \theta \quad (4)$$

So

$$\Delta P_\theta = \Delta P_I \cos \theta \quad (5)$$

where

$$\Delta P_I = k_r \Delta S_I \quad (6)$$

$\Delta S_I$  defined in Figure 50

The differential force  $dV_z$  along the axis of displacement is given by

$$dV_z = \Delta P_I R \cos^2 \theta d\theta \quad (7)$$

Summing this force over the periphery gives

$$V_z = \int_0^{2\pi} \Delta P_I R \cos^2 \theta d\theta = \pi R \Delta P_I \quad (8)$$

or

$$\Delta P_I = \frac{V_z}{\pi R} \quad (9)$$

~~SECRET RESTRICTED DATA~~

~~ATOMIC ENERGY ACT OF 1954~~

MAC AEB3

~~SECRET RESTRICTED DATA~~  
~~ATOMIC ENERGY ACT OF 1954~~

The integrated spring rate,  $K_z$ , follows from this

$$K_z = \frac{V_z}{\Delta \delta_I} = \pi R k_r \quad (10)$$

The friction force is derived in a similar manner. The incremental friction force opposing the inertia force is

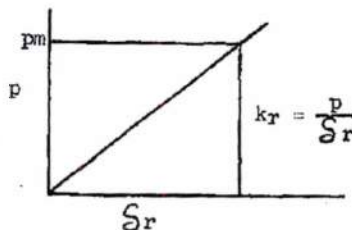
$$dF = \mu p_B \sin^2 \theta d\theta \quad (11)$$

Integration over the periphery gives

$$F = \int_0^{2\pi} \mu p_B R \sin^2 \theta d\theta = 4\mu R p_B \quad (12)$$

#### 5.2.2.2 Optimum Spring Rate

For the spring configurations suitable for the least support structure the volume of material required is directly proportional to the maximum value of elastic strain energy that the springs must absorb. For a spring with the following characteristic



the energy stored is

$$W_e = 1/2 p_m \delta_r = 1/2 p_m^2 / k_r \quad (13)$$

Thus, the volume of spring material required is proportional to the parameter  $p_m^2 / k_r$ . Since the springs constitute an appreciable portion of the side support structure, and since the volume of the remaining structural material is approximately proportional to the maximum spring load,

MAC 6272

~~SECRET RESTRICTED DATA~~  
~~ATOMIC ENERGY ACT OF 1954~~

~~SECRET RESTRICTED DATA~~  
~~ATOMIC ENERGY ACT OF 1954~~

ASD-TDR-63-277, Vol. IV

REPORT 6003

the least maximum value of  $p_m^2/k_r$  will also result in very nearly the minimum size of the entire support structure. The design procedure described below is based on this criterion.

The objective of the design is to limit the value of the reactor inertial deflection ( $\Delta \delta_T$ ) to a given magnitude by selection of the parameters that will result in the least value of  $p_m^2/k_r$ . This means that with a given spring rate the static pressure  $p_s$ , which is

$$P_B = P_O + \Delta P_T \quad (14)$$

is adjusted so that the friction damping force is of sufficient value to limit reactor deflection to 0.10 inches. By following the above procedure for different spring rates ( $k_r$ ), a minimum value of  $p_m^2/k_r$  is found. The spring rate associated with reactors may be used for design. The results of such a minimization procedure, for the design criteria used, are presented in Figure 51. This indicates that the optimum spring rates are 181 psi/in. (for radial systems) and 140,000 lbs/in.<sup>2</sup>/in.<sup>2</sup> (for tangential systems). These rates correspond to criteria based on the boost-transition design condition. The linear portion of each curve results from the satisfaction of the separation requirement (Paragraph 5.1.5.3) at initial boost condition.

### 5.2.3 Structural

#### 5.2.3.1 Spring Material Optimization

In the previous section, the spring rate was fixed, resulting in a minimum radial dimension for the side support structure. The spring that furnishes this rate must be as efficient as possible so that additional dimensional losses are minimized.

The strain energy capability of the spring can be expressed by

$$W_e = \frac{1}{2} \int_V \sigma \epsilon \, dV = \frac{\sigma_m^2}{2E} \int_V \left(\frac{\sigma}{\sigma_m}\right)^2 \, dV \quad (15)$$

where

$\sigma$  = bending stress

$\sigma_m$  = maximum allowable stress

\* This spring rate corresponds to 197 psi/inch in terms of an equivalent radial spring rate.

MAC ACT

~~SECRET RESTRICTED DATA~~  
~~ATOMIC ENERGY ACT OF 1954~~

~~SECRET RESTRICTED DATA~~  
~~ATOMIC ENERGY ACT OF 1954~~

ASD-TDR-63-277, Vol. IV

REF 6003

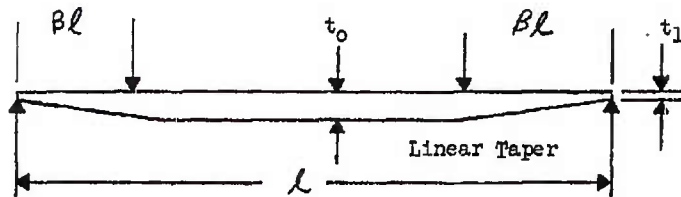
This may also be expressed by

$$W_c = \frac{\psi \sigma_m^2}{2E} \quad (16)$$

where

$$\psi = \frac{1}{V_0} \int_V \left(\frac{\sigma}{\sigma_m}\right)^2 dV \quad (17)$$

in which  $\psi$  is called the structural efficiency of the spring. It may be seen that if  $\sigma$  is equal to  $\sigma_m$  throughout the spring material, then 100 percent efficiency is realized. For bending beams, which have good spatial efficiency, the maximum efficiency is realized when the stress distribution over the length of the beam is constant. This stress distribution is approximately realized by a two-point loaded beam with tapered ends:



The moment distribution is



with the resulting stress distribution as



MAC 6078

~~SECRET RESTRICTED DATA~~  
~~ATOMIC ENERGY ACT OF 1954~~

~~SECRET RESTRICTED DATA~~  
 ATOMIC ENERGY ACT OF 1954

REPORT 6003

ASD-TDR-63-277 Vol. IV

The thickness variation, which results in a constant stress case, is actually parabolic. However, a parabolic taper is difficult to achieve practically in thin sheet, so a linear taper is used as an approximation. Using Equation 16, the volume of the spring material may be expressed as

$$V_0 = \frac{E \ell}{\eta \psi \sigma_m^2} P_m^2 / k_r \quad (18)$$

since  $W$  is proportional to  $P_m^2 / k_r$ . The parameter  $\eta$  is the surface efficiency of the spring; i.e., the spring reacts a load of  $\ell P / \eta$ . The volume of the spring is

$$V_0 = \beta \ell (t_0 + t_1) + t_0 \ell (1 - 2\beta) \quad (19)$$

The structural efficiency is evaluated from the integral in Equation 17 and is

$$\psi = \frac{1}{3} \frac{1 - 2\beta(1 - D)}{1 - \beta(1 - b)} \quad (20)$$

where

$$D = \frac{1}{(1 - b)^3} \left[ -\ln b - \frac{1}{2} (1 - b)(3 - b) \right] \quad (21)$$

With Equations 18, 19, and 20, the required total spring thickness is

$$t = \frac{E}{\eta \sigma_m^2} \frac{P_m^2}{k_r} \frac{1}{\psi [1 - \beta(1 - b)]} \quad (22)$$

The spring length,  $\ell$ , may be determined from the spring rate required and the spring beam dimensions, and is

$$\ell = \frac{t}{n_p n_b} \left( \frac{\eta n_p \sigma_m}{3\beta P_m} \right)^{1/2} \quad (23)$$

Thus, for given values of the parameters the minimum thickness of material required and its associated length can be determined from Equations 22 and 23.

The above design procedure was carried out and resulted in the spring presented in Figure 45. The spring has the following specifications:

~~SECRET RESTRICTED DATA~~  
 ATOMIC ENERGY ACT OF 1954

~~SECRET RESTRICTED DATA~~

~~ATOMIC ENERGY ACT OF 1954~~

ASD-TDR-63-277, Vol. IV

SPOT 6003

Radial free height = 0.857 inches  
Radial installed height = 0.807 inches  
Spring length = 4.450 inches  
Distance to load point = 1.556 inches  
Element maximum thickness = 0.092 inches  
End thickness (linear taper) = 0.046 inches  
Spring rate = 188 psi/in.<sub>r</sub> (cold)  
Spring rate = 181 psi/in.<sub>r</sub> (380°)  
Spring rate = 150 psi/in.<sub>r</sub> (1400°)  
Maximum stress = 109 ksi (boost-transition)  
Steady state stress = 37.3 ksi (cruise)  
Maximum reactor pressure = 70.7 psi (boost-transition)  
Steady state reactor pressure = 25.8 psi (cruise)  
Preload reactor pressure = 9.4 psi (cold)  
Preload spring deflection = 0.050 inches

#### 5.2.3.2 Component Analysis

##### 5.2.3.2.1 Spring Pressure Shell

Although it is desirable to hold this shell to the minimum thickness possible, the redundancy of the shell geometry makes this difficult to achieve analytically. The following analysis conservatively assumes that each circumferential web and a portion of the shell-in combination act as a ring (see Figure 52). If the web-shell combination is sufficiently stiff, the equivalent ring will be loaded in hoop tension.

Shell loads are critical at boost-transition condition:

Maximum pressure = 70.7 psi  
Shell temperature = 400°F  
Shell material = Rene' 41  
Material allowable = 120 Ksi

~~SECRET RESTRICTED DATA~~

~~ATOMIC ENERGY ACT OF 1954~~

~~SECRET RESTRICTED DATA~~  
~~ATOMIC ENERGY ACT OF 1954~~

ASD-TDR-63-277, Vol. IV

REPORT 6003

Shell point loads:

$$P = 1/4 \frac{22.5}{57.3} 27.4 (70.7) = 190 \text{ lbs/in}$$

Moment of inertia of Section (A-A):

$$I_{AA} = 0.00610 \text{ in}^4$$

Assume ring loaded at 32 equidistant points and determine deflection from Reference 5 (Case 9, page 158):

$$\delta_{\text{MAX}} = 0.0094 \text{ inches}$$

Deflection is small.

Hoop tension analysis:

$$\text{Diameter} = 55.19 \text{ in.}$$

$$\text{Reflector diameter} = 53.25 \text{ in.}$$

Equivalent ring pressure:

$$P_{EQ} = \frac{53.25}{55.19} 70.7 = 68.2 \text{ psi}$$

$$\text{Hoop Stress} = \frac{68.2 \times 27.50}{1.25} = 15 \text{ Ks}$$

$$MS (\text{Hoop Tension}) = \frac{120}{1.1 \times 15} - 1 = \frac{11}{15}$$

$$\text{Length between rails} = \frac{\pi \cdot 55.19}{16} = 10.6 \text{ in.}$$

$$\text{Rail width} = 1.25 \text{ in.}$$

$$\text{Beam length} = 10.6 + 1.25 = 9.35 \text{ in.}$$

$$\text{Load/section} = 68.2 \times 10.6 = 724 \text{ lbs/in}_a$$

$$\text{Load on web} = 68.2 \times 9.35 = 638 \text{ lbs/in}_a$$

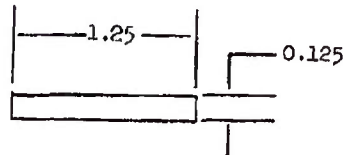
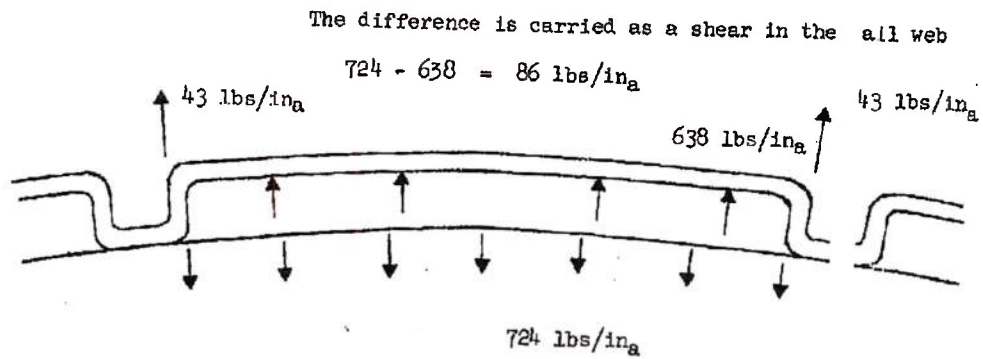
MAC 453

~~SECRET RESTRICTED DATA~~  
~~ATOMIC ENERGY ACT OF 1954~~

~~SECRET RESTRICTED DATA~~  
~~ATOMIC ENERGY ACT OF 1954~~

ASD-TDR-63-277, Vol. IV

part 6003



$$M = \frac{wL^2}{8} = \frac{68.2 (1.25)^2}{8} = 13.3 \text{ in-lb/ } a$$

Assume a stress concentration factor of 4:

$$f_b = 4 \frac{6M}{t^2} = \frac{24 \times 13.3}{(0.125)^2} = 20.4 \text{ Ksi}$$

$$f_t = \frac{4pr}{t} = \frac{4 \times 68.2 \times 27.59}{0.125} = 60.2 \text{ Ksi}$$

$$f_{\text{total}} = 20.4 + 60.2 = 80.6 \text{ Ksi}$$

$$MS (\text{Bending} + \text{Tension}) = \frac{120}{1.1 \times 80.6} = 1.35$$

MAC A673

~~SECRET RESTRICTED DATA~~  
~~ATOMIC ENERGY ACT OF 1954~~

~~SECRET RESTRICTED DATA~~  
~~ATOMIC ENERGY ACT OF 1954~~

ASD-TDR-63-277, Vol. IV

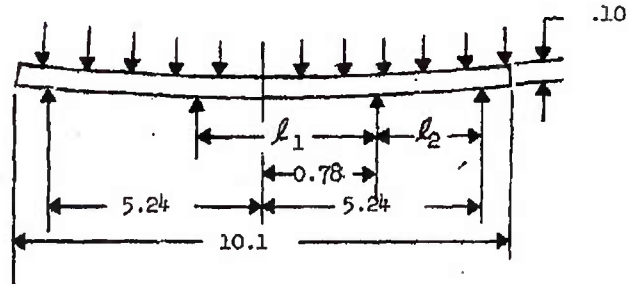
REPORT 6003

5.2.3.2.2 Spring Pressure Pad

5.2.3.2.2.1 Pad Lug Bending

Conservatively analyze the pad as a pressure loaded beam:

- Maximum Pressure = 70.7 psi
- Pad Temperature = 1400°F
- Pad Material = Rene' 41
- Allowable = 120 Ksi



$$M_{Max} = \frac{W}{12} \left( \frac{l_2^3}{2} - \frac{l_1^3}{2} \right) = 164 \text{ in-lbs. } n_a$$

$$\sigma = \frac{6M}{t^2} = \frac{6 \times 164}{(0.10)^2} = 98.5 \text{ Ksi}$$

$$MS (\text{Bend}) = \frac{120}{1.1 \times 98.5} - 1 = +0.$$

The pad lugs react the friction load that is produced by reactor movements and is a maximum on the side pads.

Pad lug bending is critical at the steady ejection condition.

Pressure = 23.6 psi

Lug Temperature = 1500°F (Assumed)

MAC 607

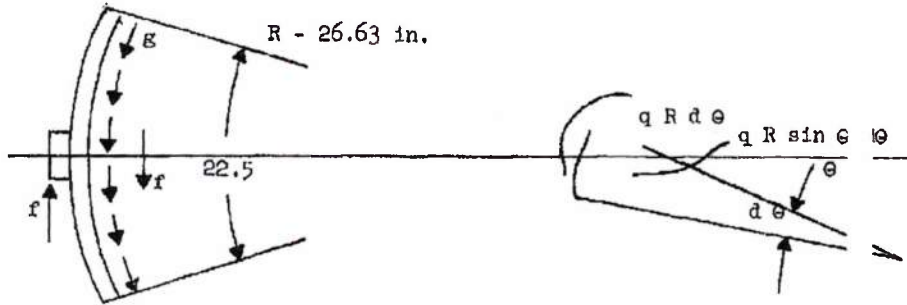
~~SECRET RESTRICTED DATA~~  
~~ATOMIC ENERGY ACT OF 1954~~

~~SECRET RESTRICTED DATA~~  
~~ATOMIC ENERGY ACT OF 1954~~

ASD-TDR-63-277, Vol. IV

REF 6003

Allowable = 95 Ksi  
 Lugs are 3.3 inches on center

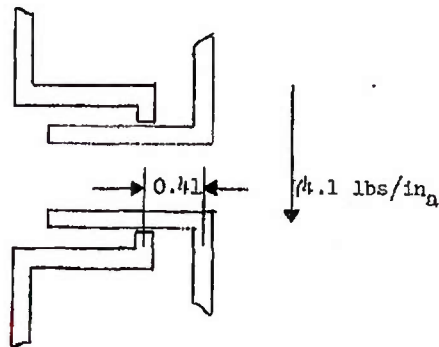


$$f = \int_{\theta_1}^{\theta_2} q R \sin \theta d \theta$$

$$q = \mu p \sin \theta$$

So:

$$\begin{aligned} f &= \int_{\theta_1}^{\theta_2} \mu p R \sin^2 \theta d \theta \\ &= (0.3)(23.6)(26.62) \int_{28.8^\circ}^{101.3^\circ} \sin^2 \theta d \theta \\ &= 189 \times 0.393 = 74.1 \text{ lbs/in}_n \end{aligned}$$



MAC 4872

~~SECRET RESTRICTED DATA~~  
~~ATOMIC ENERGY ACT OF 1954~~

~~SECRET RESTRICTED DATA~~  
~~ATOMIC ENERGY ACT OF 1954~~

ASD-TDR-63-777, Vol. IV

REPORT 6003

$$M = 0.41 \times 74.1 = 30.4 \text{ in-lbs/in}_a$$

$$M = 30.4 \text{ in-lbs/in}_a \times 3.3 \text{ in}_a/\text{lug} = 100 \text{ in-lbs/lug}$$

$$z = \frac{\pi}{64 \times 0.313} \left[ (0.625)^4 - (0.375)^4 \right] = 0.0208 \text{ in.}^3$$

$$f_b = \frac{M}{z} = \frac{100}{0.0208} = 4.8 \text{ Ksi}$$

$$MS (\text{Bend}) = \frac{95}{1.1 \times 4.8} - 1 = \text{High}$$

5.3 Front Support Structural Criteria

5.3.1 Discussion of Axial Support System

Axially directed air and inertial forces upon the assembly of hexagonal ceramic tubes comprising the reactor core are reacted by bearing on metal base plates that bear against flanges of tubes extending through the core. These tubes are attached to a structural grid located forward of the core and act as tension ties. The grid is connected to the airframe at its periphery.

This axial support system provides for a differential thermal expansion between the ceramic core and the metal structure by means of springs located on the tubes between the core and the grid.

During assembly, tube lengths are adjusted mechanically to clamp the core against the springs and the springs against the grid. The resulting spring deflection preload compresses the core against the airframe face plates and prevents forward movement.

Forward growth of the core due to differential thermal expansion further deflects the springs and increases the spring aft-directed preload. Elastic and plastic stress-induced elongations of the tie tubes partially relieve the spring deflection.

The net force exerted by the springs upon the core must exceed forward-directed core loads if core forward motion is to be prevented.

Forward-directed loading on the reactor core may occur momentarily during several flight phases.

Immediately after rocket booster burnout, an inertia factor of -0.32 g is attained. The net force, however, is less than that of the aft-directed air drag (Refer to Figure 53).

During unstart-restart conditions, the air drag on the reactor core becomes negligible while that on the airframe is unaffected. Inertia of the core will force it forward against the springs.

MAC 467

~~SECRET RESTRICTED DATA~~  
~~ATOMIC ENERGY ACT OF 1954~~

~~SECRET RESTRICTED DATA~~

ASD-TDR-63-277, Vol. IV

6003

### 5.3.1.2 Discussion of Axial Dynamic Loading Conditions

To obtain insight into the expected dynamic load on a full scale reactor, a one-third scale engine was tested during October 1962. Data from the tests were extrapolated to the full scale system at conditions of Mach 3, an altitude of 1,000 feet, and ANA Hot Day temperature.

Time response was corrected for full scale differences and temperature differences. Since the full scale diffuser is three times longer, the time for a pressure disturbance originating at the inlet to reactor is three times as great and, hence, pressure response data obtained with the one-third scale system should be reduced by a factor of one-third. However, since the test reactor was full length, the time for propagation of pressure disturbances through the reactor remains the same between the one-third scale and neglecting the effects of the nozzle. Both the fore and aft pressure response times were also corrected for sonic velocity differences between the full scale condition  $T_{T_0}$  of 1570°R and test data temperature of 900°R. The net result of the scale and temperature corrections was an expanding of the time scale of both front and rear response curves by a factor of:

$$\frac{\text{Full Scale}}{1/3 \text{ Scale}} \times \sqrt{\frac{T_{T_0} - 1/3 \text{ Scale}}{T_{T_0} - \text{Full Scale}}} = 2.3$$

but maintaining the relative lag through the core.

Equivalent full scale pressure levels were obtained by ratioing steady state values recorded for one-third scale system test just prior to inlet unstart to those given in Reference 13 for Mach 3.0, ANA Hot Day, and 1,000 feet. The pressure ratios from one-third scale to full scale were assumed to remain constant throughout the transient.

Typical one-third scale data corrected to full scale conditions are presented in Figure 54. The corrected data are also presented in Figure 55 in terms of  $\Delta P$  across the full scale core during unstart transient. The effect of such a  $\Delta P$  change on reactor drag load was evaluated assuming the steady state  $\Delta P$  was equivalent to the full scale steady state drag (Figure 56) and that drag remained proportional to  $\Delta P$  throughout the transient.

Based on these assumptions, Figure 57 was prepared and was considered representative of the change in full scale reactor drag loads throughout the unstart transient. The curve is presented as a series of straight lines as used to simplify the mathematical analysis. The effects of a hot day pressure response were not considered, and friction in the side support system was neglected. The loads of this curve were then incorporated into the differential equation of motion for the reactor to determine their effects. Section 5.3.2 presents the derivation of the equations used in this analysis, together with sample calculations. Figures 58 and 59 present the calculated displacements and velocities of the reactor over the time period of the unstart transient.

~~SECRET RESTRICTED DATA~~

~~SECRET RESTRICTED DATA~~  
~~ATOMIC ENERGY ACT OF 1954~~

ASD-TDR-63-777, Vol. IV

REPORT 6003

This analysis indicates that the reactor loads and then abrupt reloads during the unstart transient. F shown in Figure 57 for ground test operation, the forward load sufficient to cause separation from the base block in that el in the tie rods returns the reactor slightly past zero deflect

exceeds forward the load change are marginally ic energy stored n (Figure 58).

In flight, however, an unstarted inlet 1 drag sharply. Therefore, upon inlet unstart in flight, the re ject not only to forward forces arising from abrupt changes in the propulsion system, but also, since the reactor motion is u forward direction, to the relative deceleration of the vehicle the reactor. Figure 53 presents the estimated reactor drag lo ing an unstart transient that is accompanied by additive 3g ve A deceleration of 3g was selected as representative of a sever condition. In the preparation of Figure 53 it was assumed tha forward load was applied prior to time = 0 and displaced the t from that of Figure 57. The 3g load remained constant over th tion of the unstart transient (to t = 0.045) and did not affec dissipated as reload (and restart) occurred. The deceleration assumed to occur linearly over the flat portion at the bottom curve (time = 0.045 to time = 0.057). Offsetting the reload s that of Figure 57) was accomplished to compensate for pressure through the diffuser. The amount of offset and the rate of de decrease were arbitrarily selected to simplify the straight li the drag load curve.

reases vehicle tor becomes sub- ass flow through restricted in the ith respect to variation dur- cle deceleration. inflight drag the 3g additive e = 0 drag level unloading por- the rate, but oed decrease was the 0g drag rt time (from ulse travel time leration load construction of

In relation to the 0g drag load curve (F ure 57), Figure 53 is, therefore, lowered by a factor of 3 times the reactor m t = 0.045 seconds but with the same slope, and shows immediate stay time at minimum load. From time = 0.057 seconds on, Figu identical, since all deceleration loads are assumed to have di hicle reacceleration loads were not considered.

ure 57), Figure s from t = 0 to eload with no s 57 and 53 are ipated and ve-

A mathematical analysis similar to that ground test (0g) condition was conducted for the flight condit: 5.3.2 presents sample calculations of reactor motion under the of Figure 53. Figures 60 and 61 present the calculated result: and velocities of the reactor. As shown by these figures, the displacement and velocities increases considerably over that of ground test conditions. A maximum separation from the base bl: followed by rapid oscillatory separation at high velocities is indicated. Al- though these motion characteristics do not appear to overstres: appears probable that ceramic damage would result from such im;

nducted for the n. Section oad variation t displacements everity of the ined under k of 0.127 inches odicated. Al- the tie rods, it t load cycling.

It should be noted that the forward react r not considered in this analysis due to their relatively low sp: lbs/in./in. (Reference 13). Redesign of the forward spring sy: ably overcome the predicted forward deflection. It is recommen design be investigated.

r springs were ng constant (45 em could prob- ad that such re-

MAC AGS

~~SECRET RESTRICTED DATA~~  
~~ATOMIC ENERGY ACT OF 1954~~

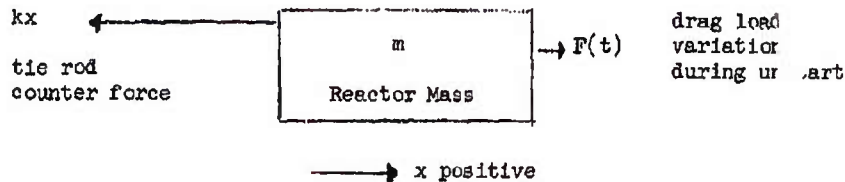
~~SECRET RESTRICTED DATA~~  
~~Atomic Energy Act of 1954~~

ASD-TDR-63-277, Vol. IV

RE # 6003

5.3.2 Dynamic Analysis

5.3.2.1 Derivation of Equations for Reactor Dynamic Load Analysis



For the above system

$$m \frac{dx^2}{dt^2} = F(t) - kx \quad (24)$$

or

$$\frac{d^2x}{dt^2} + \frac{k}{m} x = \frac{1}{m} F(t) \quad (25)$$

To solve per Reference 14 let

$$\frac{d^2x}{dt^2} + \frac{k}{m} x = 0 \quad (26)$$

Assume

$$x = e^{Rt} = x_1$$

then

$$\frac{dx}{dt} = R e^{Rt}$$

and

$$\frac{d^2x}{dt^2} = R^2 e^{Rt}$$

ASC 1637

~~SECRET RESTRICTED DATA~~  
~~Atomic Energy Act of 1954~~

~~SECRET RESTRICTED DATA~~

ASD-TDR-63-277, Vol. IV

REPORT 6003

Substituting in Equation (26)

$$R^2 e^{Rt} + \frac{k}{m} e^{Rt} = 0$$

$$\therefore R = \pm \left(-\frac{k}{m}\right)^{1/2}$$

and  $x_1$ , becomes

$$x_1 = c_1 e^{\left(\frac{k}{m}\right)^{1/2} i t} + c_2 e^{-\left(\frac{k}{m}\right)^{1/2} i t} \quad (27)$$

Assume  $1/m F(t)$  can be expressed as  $a + bt$

and let

$$x = A + Bt = x_2$$

then

$$\frac{dx}{dt} = B \quad \frac{dx^2}{dt^2} = 0$$

Then Equation (25) can be expressed as

$$\frac{k}{m} A + \frac{k}{m} Bt = a + bt$$

$$\therefore A = a/k/m \quad B = b/k/m$$

and

$$x = x_1 + x_2$$

$$x = c_1 e^{\left(\frac{k}{m}\right)^{1/2} i t} + c_2 e^{-\left(\frac{k}{m}\right)^{1/2} i t} + \frac{a}{k/m} + \frac{b}{k/m} t \quad (28)$$

which can also be expressed as

$$x = (c_1 + c_2) \cos \left(\frac{k}{m}\right)^{1/2} t + (c_1 - c_2) i \sin \left(\frac{k}{m}\right)^{1/2} t + \frac{a}{k} + \frac{b}{k/m} t \quad (29)$$

~~SECRET RESTRICTED DATA~~

~~ATOMIC ENERGY ACT OF 1954~~

MAC 14572

~~SECRET RESTRICTED DATA~~  
~~ATOMIC ENERGY ACT OF 1954~~

ASD-TDR-63-277, Vol. IV

6003

Differentiating Equation (28)

$$\frac{dx}{dt} = c_1 i \left(\frac{k}{m}\right)^{1/2} e^{\left(\frac{k}{m}\right)^{1/2} i t} - c_2 i \left(\frac{k}{m}\right)^{1/2} e^{-\left(\frac{k}{m}\right)^{1/2} i t} + \frac{b}{k/m} \quad (30)$$

or

$$\begin{aligned} \frac{dx}{dt} = & c_1 i \left(\frac{k}{m}\right)^{1/2} \left[ \cos \left(\frac{k}{m}\right)^{1/2} t + i \sin \left(\frac{k}{m}\right)^{1/2} t \right] \\ & - c_2 i \left(\frac{k}{m}\right)^{1/2} \left[ \cos \left(\frac{k}{m}\right)^{1/2} t - i \sin \left(\frac{k}{m}\right)^{1/2} t \right] + \frac{b}{k/m} \quad (31) \end{aligned}$$

Equations (29) and (30) define the displacement and velocity of the reactor during an unstart transient.  $c_1$  and  $c_2$  can be evaluated from known conditions at time = 0; however,  $x$  must be positive at  $t = 0$ . Values of  $a$  and  $b$  can be determined from test data by defining the unstart transient in terms of successive straight lines (Figure 57).

The value of  $m$  was taken as 11,400 lbs from Reference 13, and the steady state load, at Mach 3, 1000-foot altitude, ANA Hot Day, from Figure 56.

The tie rod strain under this load was computed from an effective area and weighted modulus of elasticity for the 81 Rene 41 and 40 R235 tie rods. A tie rod temperature of 1300°F was assumed (Reference 1). Rod length was taken as 80 inches. The initial steady state deflection was therefore:

$$x = \frac{L_F}{EA \text{ (no. of rods)}} = \frac{80 (263,000)}{24.5 \times 10^6 (0.095) (121)} = 0.075 \text{ in.}$$

The tie rod spring constant,  $k$ , was therefore

$$k = \frac{F}{x} = \frac{263,000}{0.075} = 3.5 \times 10^6 \text{ lbs/in.}$$

### 5.3.2.2 Sample Calculations of Reactor Displacement and Velocity Changes During Unstart-Ground Test

For conditions at  $t = 0$  (Figure 57)

$$x = 0.075 \quad \frac{dx}{dt} = 0$$

~~SECRET RESTRICTED DATA~~  
~~ATOMIC ENERGY ACT OF 1954~~

~~SECRET RESTRICTED DATA~~  
~~ATOMIC ENERGY ACT OF 1954~~

REPORT 6003

ASD-TDR-63-277, Vol. IV

the first straight line segment can be expressed as

$$\frac{a + bt}{m} = \frac{1}{m} F(t)$$

therefore,

$$a = 8,900 \quad b = -190,000$$

also,

$$\frac{k}{m} = 118,500$$

$$\left(\frac{k}{m}\right)^{1/2} = 344$$

at  $t = 0$ , Equation (28) and (30) become

$$x = c_1 + c_2 + \frac{a}{k/m}$$

$$\frac{dx}{dt} = c_1 \left(\frac{k}{m}\right)^{1/2} - c_2 \left(\frac{k}{m}\right)^{1/2} + \frac{b}{k/m}$$

Solving for  $c_1$  and  $c_2$  and substituting

$$c_1 = \frac{1.61}{6.881} \quad c_2 = \frac{1.61}{6.881}$$

Since all constants are now known,  $x$  and  $dx/dt$  can now be determined for times up to 0.045 seconds:

$$c_1 + c_2 = 0 \quad (c_1 - c_2) = 0.0047$$

$$x = 0.0047 \sin 344 t + 0.075 - 1.61 t$$

$$\frac{dx}{dt} = \frac{1.61}{6.881} (344) e^{344 t} - \frac{1.61}{6.881} (344) e^{-344 t} - 1.61$$

MAC 4472

~~SECRET RESTRICTED DATA~~  
~~ATOMIC ENERGY ACT OF 1954~~

~~SECRET RESTRICTED DATA~~  
~~ATOMIC ENERGY ACT OF 1954~~

ASD-TDR-63-277, Vol. IV

REPORT 6003

Solving at  $t = 0.045$ ,

$$x = 0.003 \text{ inches}$$

and

$$\frac{dx}{dt} = -3.20 \text{ inches/sec}$$

Thus, the tie rods have relaxed from 0.075 to 0.003 and the reactor is moving forward at 3.2 inches/sec. Each straight line segment of Figure 57 is treated similarly, and a, b,  $c_1$ , and  $c_2$  are reevaluated each time. For nose line segments where the velocity reverses direction, the time of zero velocity is determined and the maximum (or minimum) displacement is determined.

5.3.2.3 Sample Calculations for Reactor Displacement and Velocity Changes During Unstart-Flight Operation

It was assumed that the application of the 5g load prior to time = 0 (Figure 53) did not change the reactor motion characteristics at time = 0 from the characteristics under ground test conditions (i.e.,  $x = 0.075$  and  $dx/dt = 0$ ). This assumption was made to simplify the analysis and was justified because the change in initial drag load was relatively small, and its effect on initial displacement and velocity would also be relatively small.

Therefore, at  $t = 0$ ,

$$x = 0.075$$

and

$$\frac{dx}{dt} = 0$$

Solving for the constants a, b,  $c_1$ , and  $c_2$  as in Paragraph 5.3.2.1,

$$a = 7770$$

$$b = -190,000$$

$$c_1 = \frac{1.61 + 3.26 \text{ i}}{688 \text{ i}}$$

$$c_2 = \frac{-1.61 + 3.26 \text{ i}}{688 \text{ i}}$$

Solving Equations (29) and (31) with the known constants at  $t = 0.045$ ,

$$x = -0.016 \text{ inches}$$

and

$$\frac{dx}{dt} = -3.76 \text{ inches/sec}$$

~~SECRET RESTRICTED DATA~~  
~~ATOMIC ENERGY ACT OF 1954~~

MAC/STP

~~SECRET RESTRICTED DATA~~  
~~ATOMIC ENERGY ACT OF 1954~~

ASD-TDR-63-277, Vol. IV

REPORT 6003

Thus, the reactor has separated from the base plate and has forward momentum. To evaluate reactor motion over the next straight line segment new equations must be derived since the constants can not be evaluated for negative. Under a negative  $x$ ,  $k = 0$  and the equations are invalid. For  $x = 0$  and  $\dot{x} = 0$  at  $t = 0$ , Equation (25) becomes

$$\frac{d^2x}{dt^2} = \frac{1}{m} F(t)$$

Expressing  $1/m F(t)$  as  $a + bt$ ,

$$\frac{d^2x}{dt^2} = a + bt$$

Integrating for  $dx/dt$  and  $x$ ,

$$\frac{dx}{dt} = at + \frac{b}{2} t^2 + c_1 \quad (32)$$

$$x = \frac{a}{2} t^2 + \frac{b}{6} t^3 + c_1 t + c_2 \quad (33)$$

At  $t = 0$ ,

$$\frac{dx}{dt} = c_1 = -3.76$$

$$x = c_2 = -0.016$$

From Figure 52,

$$a = -834$$

$$c = 96,000$$

Equation (33) is solved for the time at which  $x$  returns to zero. Equations (32) and (33) are only valid up to this time after which Equations (31) through (31) must be used, since  $k$  is again the factor.

Setting Equation (33) equal to 0 and solving for  $t$ ,

$$0 = -417 t^2 + 16,000 t^3 - 3.76 t - 0.016$$

$$t = 0.033$$

MAC ABC

~~SECRET RESTRICTED DATA~~  
~~ATOMIC ENERGY ACT OF 1954~~

~~SECRET RESTRICTED DATA~~  
~~ATOMIC ENERGY ACT OF 1954~~

ASD-TDR-63-277, Vol. IV

6003

Therefore, after time  $0.045 + 0.033 = 0.078$  of Equations (32) and (33) no longer apply for the straight line segment from  $t = 0.045$  to  $t = 0.090$ . The segment from  $t = 0.078$  to  $t = 0.090$  is evaluated as before using Equations (28) through (31).

The remaining line segments of Figure 53 are evaluated similarly. Equations (32) and (33) are applied whenever  $x$  is negative at the start of a line segment. For all line segments times of maximum and minimum velocity are determined to define completely the behavior over the unsteady transient.

### 5.3.3 Structural Summary

According to Reference 13 (page III-29), data for the standard tie rod springs are as follows:

<u>Material Inconel X</u>	<u>Inconel X</u>
Number of springs	103
Outside Diameter, inches	1.75
Inside Diameter, inches	1.32
Spring constant, lbs/in. at 1100°F	45
Free length, inches	4.4
Bottom-out length, inches	2.9
Assembly pre-load, lbs	55.97

There are 121 tie rods, and the total reactor weight supported is approximately 11,500 lbs. Assuming the tubes are equally loaded,  $\frac{11,500}{121} = 95$  lbs/tube dead weight loading (1.0g).

Thus, a 1.0g forward inertia load would exceed the 55.97-lb preload by 39.03 lbs and would deflect the spring 0.87 inches. Such movement cannot be tolerated.

If loaded after the core and support structure have reached stabilized temperature levels and all differential expansion has occurred, the additional preload due to the core expansion spring deflection will be available. Total spring travel can be only  $4.4 - 2.9 = 1.5$  inches and spring load is then  $1.5 \times 45 = 67.5$  lbs. Since this value is less than the 95 lbs/tube load, forward movement would still occur.

The present spring system appears unsatisfactory for the unstart condition. Since the present load data are of a preliminary nature, spring redesign should be delayed until final load studies are available.

~~SECRET RESTRICTED DATA~~  
~~ATOMIC ENERGY ACT OF 1954~~

MAC A QZ

~~SECRET RESTRICTED DATA~~  
~~ATOMIC ENERGY ACT OF 1954~~

REPORT 6003

ASD-TDR-63-277, Vol. IV

5.3.4 Conclusions and Recommendations

1. Reactor damage due to forward loading may occur during ground testing of a full scale Pluto engine if inlet unstarts occurs. Full scale engine dynamic evaluations should be conducted with a dummy reactor prior to any hot core testing.
2. Definite forward loadings are predicted to accompany inlet unstart in flight due to the additional forward loads resulting from thrust loss and drag increase. Modifications to the existing Tory II front support system are indicated.
3. Additional dynamic load evaluations would be accomplished with the finalized one-third scale inlet configuration to ascertain the effects of inlet "hard start" (restart with bypass doors closed) and to determine possible change in the load characteristics with increasing inlet contraction Mach numbers.

5.4 Side Support System Test

5.4.1 Discussion

An extensive spring evaluation test program for the Pluto reactor side support system was continued during 1962. Seven spring configurations (Reference 15) were to be investigated to support earlier preliminary design studies:

1. Split cylindrical tube
2. Solid cylindrical tube
3. Modified Belleville
4. Buggy (elliptical)
5. Torsion bar
6. Corrugated
7. Plate

Test programs for evaluating the performance of Belleville corrugated and flat ribbed plate springs (all fabricated from no. 41 alloy material) were conducted in the past (Reference 16). Because in early 1962 the Belleville spring exhibited the most desirable high temperature characteristics at 1962 spring tests were directed toward the evaluation of Belleville spring incorporating increase load carrying capacity. Belleville springs of R-235 alloy material were on hand lending emphasis to this work. Subsequently, concerted analytical analysis of the other spring forms listed above indicated their potential was inferior to the Belleville spring regarding functional requirements.

~~SECRET RESTRICTED DATA~~  
~~ATOMIC ENERGY ACT OF 1954~~

~~SECRET RESTRICTED DATA~~  
~~ATOMIC ENERGY ACT OF 1954~~

ASD-TDR-63-277, Vol. IV

ONT 6003

Concurrent with the above work, analysis was begun on a new type of spring, embodying the aspects of a tapered curved beam specifically designed to minimize the lateral support annulus dimension. A detailed test program was formulated to evaluate the mechanical performance of this type of spring under expected operating conditions.

#### 5.4.2 High Temperature Springs

##### 5.4.2.1 Belleville Spring

A theoretical analysis of the stress profile of a Belleville spring (Reference 17) shows that very high stress concentrations occur at the inner diameter edges, the higher stress being at the convex edge. Consequently, the actual stresses occurring at both inner diameter edges usually exceed the allowable yield stress of the spring material and are responsible for the permanent set (local edge material plastic yield) during initial load-deflection operation.

It was assumed that, if the rather sharp inner diameter edges were modified, high stresses would be decreased resulting in reduced permanent set and a more uniform stress distribution across the spring. Particular attention was given to the alleviation of stress concentrations by employing full edge radii.

The test items were conventional form Belleville springs of R-235 material with an optimum solution heat treatment. Nominal dimensions were 0.100-inch material, 2.000-inch O.D., 0.875-inch I.D., and 0.05 inch coned height. These springs were designed with a linear load rate of approximately 85 percent of the spring deflection capability, and a load lift (flat position) of 1800 pounds (Reference 18). Several springs were modified by rounding the inside edges. Full edge radii of 1/64, 1/32, and 1/16 inch were used on either or both edges. Figure 62 shows some typical springs that were tested. A spring containing 1/16-inch full radii on both inner diameter edges is presented in Figure 63.

The spring research effort entailed compressive static load-deflection tests, which were conducted in a Baldwin Universal Test Machine at ambient and elevated temperatures. Appropriate spring holding fixtures, CHAL thermocouples, and Brown temperature recording equipment were used.

Single spring specimens of each of the conventional and modified configurations were tested with and without strain gages at ambient and elevated temperatures. A nonstrain gaged single spring setup is shown in Figure 64. The loading method shown in the figure is referred to as flat plate load. The nonstrain gaged springs were first preset by deflection to the flat position, and then subjected to a load-deflection test to 8570 of the maximum deflection for three cycles to establish the spring rate.

In order to determine the spring stress profile, one modified spring and one conventional spring (springs identical in physical dimension except inner diameter edge modification) were instrumented with strain gages and tested. SR-4 type A-19 gages were installed on both outside and in-

~~SECRET RESTRICTED DATA~~  
~~ATOMIC ENERGY ACT OF 1954~~

SECRET RESTRICTED DATA

~~ATOMIC ENERGY ACT OF 1954~~

ASD-TDR-63-277, Vol. IV

REPORT 6003

side spring surfaces at mirror view locations equally spaced (angle) in spiral fashion as shown in Figure 65. The spiral method of gage placement permitted average radial-wise strain coverage and also facilitated attachment of electrical leads. The actual test setup for these tests is shown in Figure 66, and details of the "house-of-cards" type of test arrangement are shown in Figure 67. A cone pointed ram was used to prevent damage to gages (as opposed to a flat plate) and yet produce effective flat plate loading. In general, the test load-deflection procedure for gaged springs duplicated the above procedure for non-gaged springs.

In addition to the single spring tests, compressive tests with 10-spring series stacks of conventional springs were conducted. Spring stack load-deflection rate was determined at ambient temperature and constant deflection-load relaxation characteristics at 85 percent of the stack deflection capability were evaluated at 1400°F. Setups of spring stacks for the ambient and elevated temperature tests are shown in Figures 68 and 69, respectively.

The average permanent set of a single conventional spring at initial deflection to flat position was approximately 32 percent of the original coned height (nominal, 0.030 inches). No differences in permanent set were observed between the conventional and any modified springs as shown in Figure 70.

The spring rate for the conventional for spring is linear up to 85 percent of deflection capability, and the load limit is approximately 1845 pounds as noted in Figure 71. These data verify the spring design (Reference 18).

For comparative purposes, one conventional R-235 alloy spring was tested at the same conditions as had been applied to the Rene' 41 alloy spring of near identical physical dimensions (tested in 1961). Figure 72 indicates that the Rene' 41 spring underwent a permanent set of only 42 percent of the R-235 spring set at the comparable deflection points. In Figure 73 the Rene' 41 spring exhibits approximately 12 percent greater load carrying capacity at 85 percent of the spring deflection capability.

An increase in load carrying capability is exhibited by springs tested with a radius on the outer I.D. edge (Figure 74). The spring that had the greatest increase was the one with a 1/16 inch radius. In the figure, a spring with the above outer edge conditions shows an increase of 12 percent in load capacity over that of the conventional spring at the 85 percent level of deflection capability. The increase in load capacity was predicted from the formulae in Reference 17 and is the result of permitting a shorter couple moment arm around the spring center as depicted schematically in Figure 75. Corresponding load-deflection data in the same figure verified this mechanical phenomenon. Also it will be noted in Figure 74 that no significant performance effects resulted from springs with a radius on only the inner I.D. edge as compared with the conventional spring data. In addition to increasing spring load capacity, rounded I.D. edges should also increase spring performance and integrity under a high temperature vibrational load environment.

SECRET RESTRICTED DATA

~~ATOMIC ENERGY ACT OF 1954~~

MAC 4872

SECRET RESTRICTED DATA  
~~ATOMIC ENERGY ACT OF 1954~~

ASD-TDR-63-777, Vol. IV

FORM 6005

Strain gages were installed on two nearly identical springs, on one conventional spring (No. 29), and on one modified spring (No. 25) having 1/16-inch full radius on both I.D. edges (Figure 65). All gages were positioned to record strains in the tangential direction. Identical loading point for both springs was accomplished by a cone pointed ram (Figure 67). Strain results were obtained for presetting and preset spring conditions during deflection to the flat position. These strain results were converted to stress values and are plotted in Figure 76.

In general, the rather consistent strain data indicate that high local compressive stress at the conventional spring outer I.D. edge was considerably reduced with a full rounded edge. The penalty for stress improvement was manifested in an increase of the remaining spring stress profile as compared to that of the conventional spring. Trend of the modified spring stress data here suggests that a "tear drop" form of edge rounding may reduce the developed stresses in the outer portion of the profile. Experimental stresses, although slightly lower, are in good agreement with the theoretical stresses calculated from the formulae in Reference 17.

The load-deflection rate for a preset 10-spring series stack of conventional form springs was found to be in close agreement with the rate of a single spring when tested at both ambient and elevated temperature; i.e., the deflection capability is ten times that of a single spring for the same load. At 1400°F the stack load is a maximum of 85 percent of the corresponding load at ambient temperature as shown in Figure 77. The rate change was predicted and is attributable to the reduction of material modulus of elasticity at elevated temperature.

Load loss of a preset 10-spring series stack due to constant deflection at 85 percent of the stack deflection capability at 1400°F is presented in Figure 78. The test data show an approximate linear load loss rate of 3 percent per hour.

#### 5.4.2.1.1 Conclusions

1. Of the modified Belleville springs tested the one with a 1/16-inch radius on the outer I.D. edge was found to have the greatest increase in load-carrying capability.
2. Creep test results indicate that a constant relaxation rate of approximately 3 percent per hour was obtained. Extrapolating this to 10 hours will give a total lifetime reduction of 30 percent, which is excessive. The results indicate that redesign of the Belleville spring is required to reduce the lifetime relaxation rate.
3. No future testing is contemplated for the Belleville spring at Marquardt. The curved plate spring appears more attractive from the standpoint of reducing the lateral support annulus.

SECRET RESTRICTED DATA  
~~ATOMIC ENERGY ACT OF 1954~~

~~SECRET RESTRICTED DATA~~  
~~ATOMIC ENERGY ACT OF 1954~~

ASD-TDR-63-277, Vol. IV

REPORT 6003

#### 5.4.2.2 Tapered Curved Plate Springs

The springs presently under development lateral side support of the Pluto reactor are linear rate, tapered plate spring stacks consisting of two sets of parallel spring leaves stacked in series. Single 1.0 inch wide spring leaves and an assembled stack are shown in Figure 79. The spring material is Rene' 41 with an optimum treatment.

Marquardt for ed, curved  
aves stacked  
stack are shown  
olution heat

The spring leaf is normally 4.450 inches widths of 1 inch, 2 inches, and 4 inches. The nominal height stack of any width is 0.750 inches. Each spring stack had a nominal deflection capability, with a rated load of 366 pounds per inch of spring width.

n length with  
a spring  
dinal 0.375-  
inch of spring

Spring tests at ambient temperature were Universal Tester as shown in Figure 80. A dial gage was used for spring deflection, and the readouts of multiple SR4 type A-18 strain gages on a spring leaf were monitored by an SR-4 strain indicator. Representative strain gage locations are shown schematically in Figure 81.

un on a Baldwin  
r recording  
rain gages on  
tentative

The setup used for high temperature test Temperature Test Machine is shown in Figure 82. This setup included a spring stack holding apparatus, 12-inch Hevi-Duty split tube furnace, thermocouples, Brown temperature recorder, Baldwin load cell, and automatic load programming equipment.

in an Elevated  
lved a special  
nace, CH-AL  
ring deflectom-

Spring stack load rate was established for width stacks under conditions of static compressive load-deflection at ambient and 1400°F. The magnitudes and effects of transverse deflection were determined for single spring leaves of each width. Dynamic performance was investigated under a cyclic load traverse over a simulated Pluto trajectory at 1400°F for a period in excess of 10 hours. A diagram of the load schedule is presented in Figure 83.

the various  
ion at both  
rains were de-  
mance was in-  
light trajec-  
the cyclic

#### 5.4.2.3 High Temperature Spring Test Results

Significant results of the spring tests are as follows:

1. Ambient temperature load-deflection tests for spring stacks 1 inch and 2 inches in width indicate an average load rate of 10 percent as shown in Figure 84. These spring stacks, in addition to the predicted rate based on nominal spring dimensions, exhibited an average of 24 percent greater spring rate. Stack permanent set averaged 4 percent of stack initial deflection capability. Strain gage data indicated that permanent sets were caused by stress concentrations near a mid-span load point. The test spring rate of a 1-inch stack was 3.4 percent greater than the calculated spring rate of the subject stack based on actual dimensions.

tes for spring  
ead of 10 per-  
a 4-inch  
an the predict-  
averaged 4  
a indicated  
a mid-span  
cent greater  
tual dimen-

MAC 4423

~~SECRET RESTRICTED DATA~~  
~~ATOMIC ENERGY ACT OF 1954~~

~~SECRET RESTRICTED DATA~~  
~~ATOMIC ENERGY ACT OF 1954~~

ASD-TDR-63-277, Vol. IV

SPORT 6003

2. Longitudinal material strains of single ring leaves verified the existence of stress concentrations around the 1-span load points as shown in Figures 85 and 86. Comparison of transverse strain data presented in Figures 87 and 88 shows that spring edge area stress increases with increased spring width (tendency of spring edge to turn inward spring side containing longitudinal tension strain).

3. Evaluation of spring rate for 1-inch and 2-inch spring stacks at 1400°F (Figure 84) produced data consistent with decreased material modulus of elasticity for the test temperature.

4. Spring stacks, 2 inches in width tested at 1400°F for 10 hours under cyclic load-deflection conditions (Figure 85) exhibited the following uniformly increasing material creep:

	Sector			Total Creep (in.)
	A (in.)	B (in.)	C	
Stack S/N 2	0.022	0.006	0	0.028
Stack S/N 4	0.024	0.011	0	0.035

These material deformations are attributed primarily to stress concentrations.

5. Ambient temperature recalibrations of spring stacks tested at elevated temperatures produced rates nearly identical to the initial ambient rates for respective stacks.

Conclusions from the significant test results listed above are as follows:

1. Tests indicate that springs can be designed with a 22 percent confidence in the predicted spring rate, based on nominal spring dimensions. This percentage should improve as spring tolerances are reduced.

2. Maximum deviation in the predicted vs. experimental strains was 25 percent. This deviation is probably due to the stress concentration caused by the spring loading bosses.

3. Cyclic, 10-hour creep testing indicated a total relaxation of 0.035 inches in spring-free height. This means a relaxation of 4.1 percent based on a nominal spring-free height of 0.857 inches. This value although based on only two spring tests, should be well within Pluto lateral support design requirements.

4. Future spring tests should be pointed toward increasing confidence in the total relaxation that the spring will undergo when subjected to the Pluto flight loads environment.

~~SECRET RESTRICTED DATA~~  
~~ATOMIC ENERGY ACT OF 1954~~

MAC 107

~~SECRET RESTRICTED DATA~~  
~~ATOMIC ENERGY ACT OF 1954~~

ASD-TDR-63-277, Vol. IV

REPORT 6003

5.4.3 Engine-Airframe Lateral Attachment Test -Phases I and II

5.4.3.1 Discussion

During the second quarter of 1962, experimental vibratory tests were conducted to evaluate the characteristics of a proposed engine-airframe lateral support system. The history and results of these tests are contained in Reference 19.

The objective of the tests was to evaluate the assembly integrity, the response modes, and the spring system characteristics of a 360° cross section of the engine-side support system in a vibratory loads and elevated temperature environment.

The full scale side support specimen tested consisted of a tangential (to core) corrugated spring array coupled to a track-rail system suspending a simulated core within an outer ring (see Figure 1).

Results of the above test were compared with the predicted dynamic responses as derived from a model analysis compiled in Reference 4. Inconclusive correlation was evident due to (1) the inflexibility of the core-side support assembly and (2) only one possible core preload (springs) magnitude. In addition, many difficulties occurred with the major instrumentation at elevated temperature. Analysis indicated the need for evaluation of a generalized test specimen at ambient temperature.

A second full scale engine-side support configuration, somewhat similar to the basic geometry of the first item, was designed and tested during the last quarter of 1962. The primary test objectives here were to bracket the dynamic test conditions used in the first test and to evaluate the basic dynamic response of the core matrix with variable spring preloads.

The results of the second test are reported in Reference 20.

5.4.3.2 Phase I Test

The test item consisted of a full scale 360° cross section of the side support system linking a simulated reactor core and outer ring. The core outside diameter was 53.25 inches, the outer ring inner diameter was 61.50 inches, and the thickness of the assembled unit was 10 inches.

The principal components of the side support system were expansion shells and tracks, curved linear rate corrugated springs, spring retainers, and rails (as shown in Figure 90). All support components were fabricated from Rene 41 alloy. On assembly, the nominal spring compressive load was approximately 900 pounds per spring, resulting in an average core pressure of 16 psi.

~~SECRET RESTRICTED DATA~~  
~~ATOMIC ENERGY ACT OF 1954~~

~~SECRET RESTRICTED DATA~~  
~~ATOMIC ENERGY ACT OF 1954~~

ASD-TDR-63-277, Vol. IV

REPORT 6003

5. Core resonant conditions in the range of 20 to 26 cps for two horizontal in-line accelerometers are indicated by the data plots in Figures 98 and 99, which are typical of all the data listed in Table XXIII. Apparently, these resonant data are in good agreement with the 21-cps resonant frequency determined from calculations (Reference 4) considered for a rigid body made for the core. Corresponding sine wave acceleration data for Figures 98 and 99) indicating core and outer ring dynamic responses are listed in Tables XXIV and XXV.

6. No change in amplification factor was indicated between ambient and 1300°F testing.

7. Phase angle and g level relationships between horizontal in-line accelerometers (Figure 98) indicated a core distortion mode (as opposed to rigid body mode) in the order of 0.02 inches for the 10 to 40 cps frequency band.

8. Flat random excitation data parallel to the sine wave data in that discrete resonant frequencies were not eminent at either ambient or high temperatures.

9. Post-test load-deflection calibration of springs showed no change from the pre-test calibrations.

10. Structural integrity of the side support system was maintained throughout the test.

Conclusions that may be drawn from the results are summarized as follows:

1. Apparently, binding of the rail-traction assemblies was primarily responsible for erratic dynamic response of the core relative to the ring (static tests provided an indication of irregular core peripheral friction distributions).

2. Results of the static g level tests indicate that, as predicted, a sinusoidal core pressure distribution was exhibited by the core matrix when the inertial loading exceeded the core friction.

3. Vertical response of the bottom of the core (Figure 98) compared with horizontal dynamic input indicates distortion of the core.

#### 5.4.3.3 Phase II Test

##### 5.4.3.3.1 Test Hardware Design and Description

Test hardware was designed and fabricated for the reaction airframe lateral support dynamic response test (slice test). The major components of this hardware are the reactor core matrix, support ring, and spring support assemblies. The configuration as shown in Figure 100 is 10 inches wide and simulates a section through the reactor airframe structure. The

MAC 4873

~~SECRET RESTRICTED DATA~~  
~~ATOMIC ENERGY ACT OF 1954~~

~~SECRET RESTRICTED DATA~~

~~ATOMIC ENERGY ACT OF 1954~~

ASD-TDR-63-277, Vol. IV

SR 6003

reactor core matrix consists of approximately 78,000 hexagonal steel tubes (0.3005 inches across flats), 36 peripheral shims, 107 tie rod tubes, and 14 control rod tubes. The outside diameter of the assembled core matrix is 53.250 inches. The core matrix is compressed radially by a series of 18 pad segments that form a cylindrical shell around the periphery. There is no physical connection between these pad segments; however, the compressive force is produced in the core matrix, through the pad segments, by a series of preloaded spring assemblies. Radially outward, the spring loads are reacted by a rigid support ring that simulates the airframe structure. A track and rail type connection is provided between each pad segment and the support ring to react the shear loads. Seventy-two spring assemblies are used for the entire test fixture, furnishing a spring rate of 150 psi/in. Four spring assemblies are mounted between each pad segment and the support ring. The spring assembly consists of a 3.00-inch O.D. primary coil spring, a 1.00-inch O.D. coil spring deflector, and a spring guide. Provisions are made for adjustment of the spring loads during various test setups. All metal parts are fabricated from mild steel except the ceramic hexagonal tubes and the springs, which are chrome-vanadium.

The assembled test item is presented in Figure 101. Total weight of this test item was approximately 3400 pounds.

#### 5.4.3.3.2 Dynamic Tests

Ambient temperature dynamic tests were conducted on a 28,000 force-pound MB Electrodynamics Shaker Model C210 at a facility outside Marquardt. Desired vertical vibration (Figure 102) was obtained in addition to imposed g loads on the test item at the expected flight magnitude (approximately 8g). The C210 control system is similar to that of the C100.

A typical instrumentation setup is shown in a schematic form in Figure 103. SR-4 Type A-7 strain gages on spring coils were utilized as prime instrumentation regarding core dynamic displacement. Accelerometers and linear motion transducers served as backup instrumentation to the strain gages.

All tests were performed at ambient temperature. Dynamic conditions for nine scheduled runs entailed sine wave sweeps of controlled discrete frequencies through the range of 5 to 300 to 5 cps at 0.5 to 8g. Three core preload pressures of 5, 15, and 30 psi were utilized through inputs as follows:

Preload (psi)	g Input
5	0.5, 2, 3
15	2, 4, 6
30	3, 6, 8

Results of the static and dynamic tests are summarized as follows:

~~SECRET RESTRICTED DATA~~

~~ATOMIC ENERGY ACT OF 1954~~

~~SECRET RESTRICTED DATA~~

~~ATOMIC ENERGY ACT OF 1954~~

RE AT 6003

ASD-TDR-63-277, Vol. IV

1. Information on dynamic responses of a simulated core matrix to vibration loads was obtained during the subject test program.

2. Displacement data indicated that the core matrix responded dynamically as a right-circular cylinder at the first resonant frequency. Examples of core displacements for several runs are shown in Figure 104.

3. At the second resonant frequency, the core responded dynamically in elliptical form. Core modes at the first and second resonant frequencies for Run 4 are presented in Figure 105.

4. These core mode shapes are in good agreement with theory as presented in Reference 4.

5. The frequencies at which the first and second modes occurred were higher than predicted by a factor of 2. This is thought to be due to an increase in the theoretical integrated spring rate caused by mechanical binding at the reactor periphery.

6. Maximum core displacements relative to the outer ring frame occurred at the 6g input force level and 15-psi core preload. The displacements were approximately 0.100 inches around the bottom vertical centerline and approximately 0.030 inches around each end of the horizontal centerline for the first and second mode conditions, respectively.

7. Apparent core separations observed during the 5 psi core preload and 3g input run were not reflected in the core displacement data.

8. The first resonant frequency of the core increases and displacement decreases with an increase in core preload pressure as shown in Figure 106.

9. Steatite hexagonal tube damage was slight and insignificant. No other apparent structural damage to the test item occurred during the test program.

Conclusions that may be drawn from the results are summarized as follows:

1. The analysis for the theoretical dynamic modes of core deformation as presented in Reference 4 were substantiated to a high degree by test results for first and second resonant frequencies.

2. At input frequencies above approximately 10 cps, core responses were negligible for all conditions tested.

3. Core separation can be prevented with proper values of core pressures during high g load inputs.

DECLASSIFIED IN FULL  
Authority: EO 13526  
Chief, Records & Classification Div, WHS  
Date: OCT 02 2015

~~SECRET RESTRICTED DATA~~

~~ATOMIC ENERGY ACT OF 1954~~

MAC 1070

~~SECRET RESTRICTED DATA~~  
~~ATOMIC ENERGY ACT OF 1954~~

ASD-TDR-63-277, Vol. IV

POST 6003

4. For any core preload, core displacement increases approximately in proportion to increases in input force levels.

5. Steatite tube damage was not detrimental to the operation aspects of the test item.

**DECLASSIFIED IN FULL**  
**Authority: EO 13526**  
**Chief, Records & Declass Div, WHS**  
**Date: OCT 02 2015**

~~SECRET RESTRICTED DATA~~  
~~ATOMIC ENERGY ACT OF 1954~~

MAC 4873

6.0 EXIT NOZZLE

DECLASSIFIED IN FULL  
Authority: EO 13526  
Chief, Records & Declass Div, WHS  
Date: OCT 02 2015

6.1 Design

6.1.1 Discussion

The exit nozzle is a convergent-divergent ejector type that extends from Engine Station 565.470 to Engine Station 668.070, as shown in Figure 107. The nozzle is cantilevered from and attached to the airframe near the aft face of the reactor. The nozzle-to-vehicle attach joint is a quick-disconnect type, which consists of the vehicle ring, exit nozzle ring, locking ring, and split ring retainer. The exit nozzle attach ring and locking ring are full-threaded, American Standard stub 29° Acme screw thread, with 24 inch lead and 1-inch pitch. The split ring retainer is assembled to the locking ring with a series of 3/8-inch diameter bolts. When fully assembled, a labyrinth type seal is made between the airframe ring and the exit nozzle attach ring. This joint design has the advantages of uniform distributed mass around the circumference to minimize thermal stress, thin sections to reduce gamma heat generation, uniform circumferential load distribution that increases joint structural efficiency, and a single joining member (lock ring) that has optimum quick-disconnect potential.

The nozzle is designed to provide for radial and axial thermal expansion between the nozzle outer shell, nozzle liner, and reactor expansion pads. The aft face of the aft series of reactor circumferential expansion pads is flanged to nest into a radial slip joint in a support ring, thereby allowing radial thermal expansion of the reactor. The nozzle liner forms a slip joint with the inside diameter of the support ring that allows the liner to expand axially. The liner is attached to the nozzle outer shell at the throat area by eight pylons, equally spaced about its circumference.

The exit area between the nozzle outer shell and the exit nozzle shroud is designed to provide a constant annular area in order that boattail drag may be minimized. The exit nozzle is designed to incorporate Rene' 41 material throughout.

6.1.2 Weights and Centers of Gravity

Weights and centers of gravity for the ejector exhaust nozzle are shown in Table XXVI.

6.1.3 Design Data

6.1.3.1 Operational Data

Critical operational phases for the exit nozzle system occur during high altitude cruise and low altitude cruise. Critical pressure loading and temperature environments occur during the following flight operations:

High Altitude Cruise: Mach 3.9 at 35,000 feet  
on an ICAO Standard Day

MAC 667

~~SECRET RESTRICTED DATA~~  
~~ATOMIC ENERGY ACT OF 1954~~

ASD-TDR-63-277, Vol. IV

REPORT 6003

Low Altitude Cruise: Mach 3.22 at 1000 feet on  
an ICAO Standard Day

Pressure and temperature profiles for these operational regimes are presented in Figures 108 to 113.

#### 6.1.3.2 Configuration

Radial and axial coordinates defining the configuration of the various components comprising the exit nozzle system are presented in Figures 114 and 115.

### 6.2 Structural Analysis

#### 6.2.1 Nozzle Forward Cylinder and Convergent Cone (Primary Shell)

##### 6.2.1.1 Discussion

The ring assembly by which the nozzle is attached to the airframe extends aft to Nozzle Station 11.7 (E.S. 577.170) and is essentially a right circular cylinder. The cylindrical shell portion of the throat extends to Nozzle Station 13.7 (E.S. 579.170) where a 3 1/2-inch radius transition knuckle joins the cylinder to a convergent circular cone. This cone is in turn connected to the small end of a diverging cone by a double curvature transition section which forms the nozzle throat.

From the nozzle forward station to approximately 10.0 inches aft of the minimum diameter section of the throat the net pressure differential between the nozzle inner and outer surfaces is internal, acting outward radially. This bursting pressure decreases with distance from the forward end.

Because hoop tension varies directly with both pressure and cylinder radius, the requirement for wall thickness also decreases with distance from the forward end.

Further, because joints are required at intersections of the cylinders, cones, and transition knuckles, a saving in structural weight may be achieved by progressively reducing gages at these points. Local stresses are small compared to hoop stresses.

##### 6.2.1.2 Operating Condition

Critical operation occurs during low altitude cruise at Mach 3.22 and 1000 feet on an ICAO Standard Day. Pressure and temperature profiles for this phase of operation are presented in Figures 108 and 112.

The shell temperature is nearly constant, varying from a high of 1225°F to a low of 1215°F.

~~SECRET RESTRICTED DATA~~  
~~ATOMIC ENERGY ACT OF 1954~~

MAC 4627

6.2.1.3 Material Properties

The nozzle material is Rene' 41 sheet, solution heat-treated at 1975°F for 30 minutes, water quenched, aged at 1650°F for 4 hours, and air cooled.

At 1225°F:

$$F_{t_y} \approx 106,000 \text{ psi (Yield Stress)}$$

$$F_{t_u} \approx 160,000 \text{ psi (Ultimate Stress)}$$

Stress Rupture: 1 hr > 100,000; 10 hrs > 100,000;  
100 hrs = 100,000 psi

6.2.1.4 Analytical Factors

Design Factor = 1.15

Factor of Safety = 1.25

Weld Efficiency = 85 percent

6.2.1.5 Analysis for Hoop Tension Loading

$$f = \frac{p R}{1.0 \times t} \quad \text{and} \quad t = \frac{p R}{f}$$

$$t \text{ required} = \frac{p R}{F_t}$$

Since the operating temperature is relatively low for this material creep and stress, rupture for the life involved is not critical. The design will be based upon yield stress which will be modified by a 1.15 design factor and an 85 percent weld efficiency factor.

$$F_{t_y} = 106,000 \text{ psi}$$

$$\text{Design Stress} = \frac{106,000 \times 0.85}{1.15} = 78,500$$

$$t_{\text{req.}} = \frac{p R}{78,500}$$

Required material thicknesses are shown in Tab. XXVII.

DECLASSIFIED IN FULL  
Authority: EO 13526  
Chief, Records & Classification Div, WHS  
Date: OCT 02 2015

~~SECRET RESTRICTED DATA~~  
~~ATOMIC ENERGY ACT OF 1954~~

ASD-TDR-63-277, Vol. IV

FORM 6003

Minimum Margin of Safety (see Figure 116):

At Station 24,  $t_{reqd} = 0.0765$  and  $t_{specified} = 0.08$

$$MS = \frac{0.08}{0.0765} - 1 = +0.05$$

#### 6.2.1.6 Analysis for Transverse and Axial Loading

##### 6.2.1.6.1 Discussion

Axial stresses resulting from axial drag and from transverse bending are rarely critical for an exit nozzle structure. Hoop tension or compression loading producing circumferential and radial stresses govern the gage requirements and are not additive to axial stresses.

##### 6.2.1.6.2 Axial Drag Force

Critical loading occurs at Mach 3.22 and 100 feet on an ICAO Standard Day.  $P = 367,438$ -lb limit (Reference: Figure 111)

##### 6.2.1.6.3 Inertia Factors

Referring to design criteria inertia factor specified in Table IV for weapons ejection in low altitude cruise,

$$\begin{aligned} \epsilon_z &= +8.50 \\ &= -1.17 \end{aligned}$$

and

$$\begin{aligned} \epsilon_x &= +0.3 \\ &= -0 \end{aligned}$$

##### 6.2.1.6.4 Weight and Center of Gravity

The total weight of the nozzle and shroud assembly is 1054 lb and the center of gravity is at Nozzle Station 28.75 (E.S. 4.22)

##### 6.2.1.6.5 Axial and Shear Stresses

Critical loadings are:

$$P_{axial} = 367,438 + 1100 \times 0.3 = 367,768$$

$$M_y = +8.5 \times 1100 \times 30 = 280,500$$

$$V_z = 8.5 \times 1100 = 9350 \text{ lb}$$

MAC ACTE

~~SECRET RESTRICTED DATA~~  
~~ATOMIC ENERGY ACT OF 1954~~

~~SECRET RESTRICTED DATA~~  
~~ATOMIC ENERGY ACT OF 1954~~

ASD-TDR-63-277, Vol. IV

REPORT 6003

Assume these loads act on the 0.093 in. gage shell.

$$R_1 = 28.06 \text{ in.}$$

$$R_m = 28.06 + \frac{0.093}{2} = 28.1065 \text{ in.}$$

$$f_b = \frac{M}{\pi r^2 t} \quad f_t = \frac{P_{\text{axial}}}{A}$$

$$f_s = \frac{V}{\pi r t}$$

$$f_b = \frac{280,500}{\pi \times 28.1065^2 \times 0.093} = 1220 \text{ psia}$$

$$f_s = \frac{9350}{\pi \times 28.1065 \times 0.093} = 1142 \text{ psi}$$

$$f_t = \frac{367,768}{\pi \times 2 \times 28.1065 \times 0.093} = 22,250 \text{ psi}$$

$$\text{Combined axial stress} = 22,250 + 220 = 23,470 \text{ psi}$$

$$\text{Shear} = 1142 \text{ psi}$$

#### 6.2.1.6.6 Analysis Factors

$$\text{Design} = 1.15$$

$$\text{Factor of safety} = 1.25$$

$$\text{Weld factor} = 0.85$$

MS (Combined Bending and Axial)

$$MS = \frac{106,000 \times 0.85}{23,470 \times 1.15} = + 2.33$$

MS (Ultimate Shear)

$$F_{su} = F_{tu} \times 0.6 = 0.6 \times 160,000 = 96,000 \text{ psi}$$

$$MS = \frac{96,000 \times 0.85}{1142 \times 1.25} - 1 = \text{High}$$

MAC AGS

~~SECRET RESTRICTED DATA~~  
~~ATOMIC ENERGY ACT OF 1954~~

6.2.2 Cone-Cylinder and Cone-Cone Intersections

6.2.2.1 General Discussion

The change of slope in the shell membranes at a cone-cylinder intersection produces large localized stresses.

The required thickness of the transition sections may be determined from Formula 3 of Para. UA-4(d), Page 111 of Reference 21:

$$t = \frac{PIM}{2SE - 0.2P}$$

or

$$P = \frac{2SEt}{IM + 0.2t}$$

where

$$M = 1/4 (3 + L/r)$$

P = Internal pressure, psi (use 100 psi as conservative average)

t = Material thickness

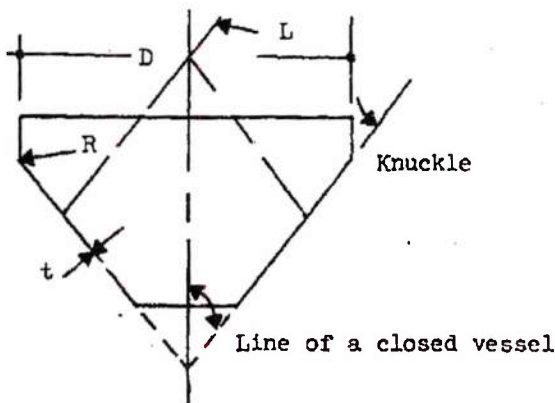
S = Maximum allowable working stress, psi

E = Lowest efficiency of joint: 80% (Refer to Para. UW-12, Reference 21)

L = Inside spherical or crown radius, inches (16.485 in.)

r = Inside knuckle radius, inches (21.48 in.)

DECLASSIFIED IN FULL  
Authority: EO 13526  
Chief, Records & Declass Div, WHS  
Date: OCT 02 2015



(Reference: Figure UA-4 (3), Page 110 of Reference 21)

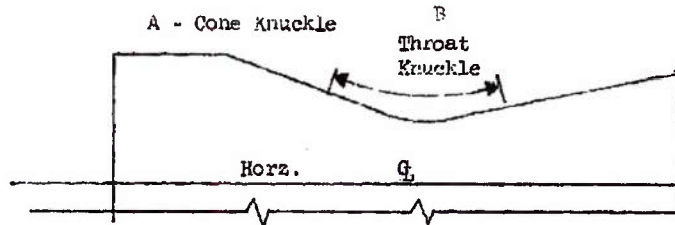
MAC 457

~~SECRET RESTRICTED DATA~~  
 ATOMIC ENERGY ACT OF 1954

ASD-TDR-63-277, Vol. IV

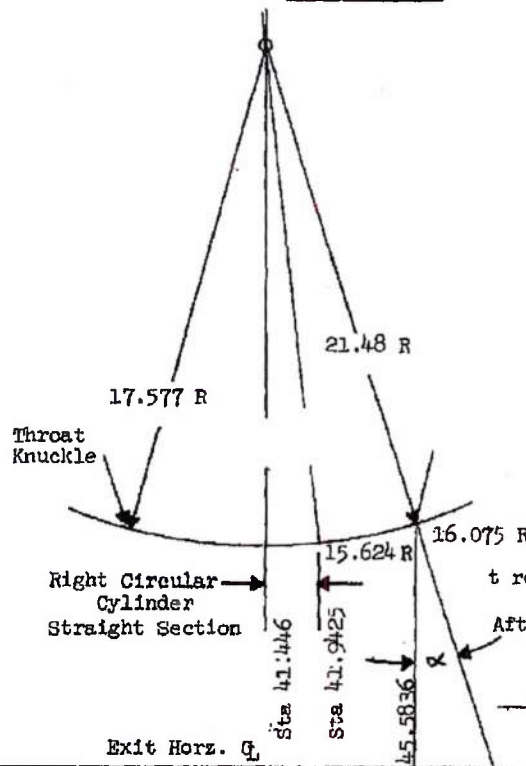
REPORT 6003

The actual exit shape is as follows:



Section A conforms to code shape, but Section B is reversed in that the section representing the head is smaller rather than larger than the cone. The theory still applies, however, since the cone angle is small and the transition fairly flat.

6.2.2.2 Nozzle Throat



$$M = \frac{1}{4} \left( 3 + \sqrt{\frac{L}{r}} \right)$$

$$= \frac{1}{4} \left( 3 + \sqrt{\frac{16.4}{21.4}} \right)$$

$$= \frac{1}{4} (3 + 0.875) = 0.97$$

$$t = \frac{PLM}{2SE + P(M - 2)}$$

$$= \frac{100 \times 16.4 \times 0.97}{(28 \times 0.80) + (0.97 - 0.2)}$$

$$= \frac{1598}{1.6S + 77}$$

S = 106,000 psi design factor of 1.15

$$S = \frac{106,000}{1.15} = 92,000$$

$$t_{req.} = \frac{1598}{1.6 \times 92,000 + 77}$$

$$= \frac{1598}{147,377} = 0.010 \text{ in.}$$

The gage chosen for the convergent cone and the throat is 0.005 inches. The divergent aft cone is 0.063 inches.

~~SECRET RESTRICTED DATA~~  
 ATOMIC ENERGY ACT OF 1954

By proportion,  $\frac{0.0108}{0.063} \times 147,372 = 25,200$  psi. At the throat where  $R_1 = 16.1$  inches, the bending moment is approximately  $225 \text{ lb} \times 8.5 \text{ gs} \times 32 \text{ in.} = 1,200$  in/lb (assume acting at joint with aft cone)

$$f_b = \frac{M}{\pi r^2 t} = \frac{61,200}{\pi \times (16.1)^2 \times 0.063} = 1,195 \text{ psi}$$

The axial drag is 33,650 lb.

$$\sum f_t = \frac{33,650}{2 \times 16.1 \times 0.063} = 16,600 \text{ psi}$$

$$\sum f_b + f_t = 17,800 \text{ psi}$$

$$\text{Transition stress} + f_b + f_t = 25,200 + 17,800 = 43,000 \text{ psi}$$

$$F_{t_y} = 106,000 \text{ psi and } \frac{106,000 \times 0.8}{1.15} = 73,700 \text{ psi}$$

$$MS = \frac{73,700}{43,000} - 1 = +0.71$$

Notes: 1. This analysis is conservative; the uniform pressure of 100 psi is greater than the actual average pressure, and the axial load effect was included in the original solution for  $t$  reqd.

2. For an analysis of bursting hoop stress refer to Para. 6.2.1.

### 6.2.2.3 Convergent Cone

The required thickness of the conical portion is determined by Formula 4 in Section UG-32-g of Reference 21:

$$t = \frac{PD_1}{2 \cos \alpha (SE - 0.6 P)}$$

$$\alpha = 30^\circ, \cos \alpha = 0.866 \text{ and } 2 \cot \alpha = 1.732$$

$$E = 0.80$$

$$P = 200 \text{ psi (assumed)}$$

$$D_1 = 18.0 \text{ inches}$$

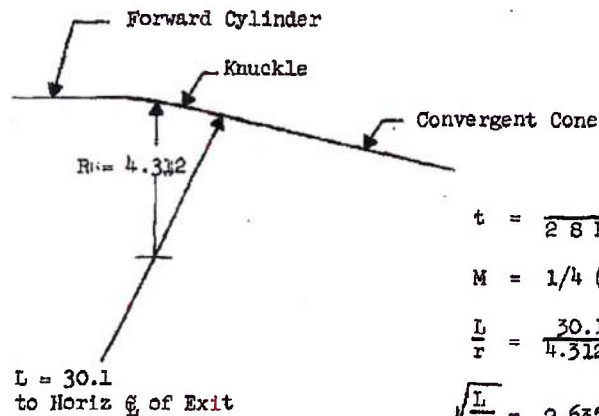
DECLASSIFIED IN FULL  
Authority: EO 13526  
Chief, Records & Declass Div, WHS  
Date: OCT 02 2015

$$s = 106,000 / 1.15 = 92,000$$
$$t_{req.} = \frac{200 \times 18}{1.732 (92,000 \times 0.8 - 0.6 \times 200)} = \frac{3600}{1.732 \times 73,480}$$
$$= 0.0284$$

$$MS = \frac{0.08}{0.0284} - 1 = +1.82$$

6.2.2.4 Forward Cylinder - Convergent Cone Intersection

Refer to Reference 21, Section UA-4-d, Equation 3.



$$t = \frac{PLM}{28E - 0. P}$$

$$M = 1/4 (3 + \sqrt{7r})$$

$$\frac{L}{r} = \frac{30.1}{4.3125} = 6.975$$

$$\sqrt{\frac{L}{r}} = 2.635$$

$$M = 1/4 (3 + 2.635)$$

$$= 1.409$$

$$P = 200 \text{ psi}$$

$$E = 0.8$$

$$s = 106,000 / 1.15 = 92,000$$

$$t = \frac{200 \times 30.1 \times 1.409}{(2 \times 92,000 \times 0.8) - (0.2 \times 200)} = \frac{8500}{147,000 - 40} = \frac{8500}{146,960} = 0.0578$$

$$MS = \frac{0.08}{0.0578} - 1 = +0.38$$

MAC 400

~~SECRET RESTRICTED DATA~~  
~~ATOMIC ENERGY ACT OF 1954~~

ASD-TDR-63-277, Vol. IV

REPORT 6003

6.2.3 Divergent Exit Cone

6.2.3.1 General Discussion

The exit internal pressure decreases rapidly aft of the forward cylinder, and approximately 10 inches aft of the nozzle throat becomes less than that of the annulus. Most of the divergent cone section is subjected to collapsing pressure.

6.2.3.2 Design of Cone

The weight of a cylinder subjected to an external collapsing pressure may be minimized by stiffening a thin shell with rings that hold the shell essentially round. The flexural rigidity of the combination must equal that of the minimum monolithic shell that will support the required pressure.

As the shell thickness decreases, the required weight of the rings increases. The optimum combination for minimum weight must be determined by trial. Preliminary calculations indicate that a 0.3 gage approaches the optimum requirement.

In the following analyses a 0.063 gage of Rene' 41 will be analyzed without stiffeners to determine the strength of the shell alone.

The material to be used is Rene' 41 sheet, solution heat-treated at the mill and solution heat-treated by Marquardt at 1975°F (30 minutes), water-quenched, aged at 1650°F (4 hours), and then air cooled.

6.2.3.3 Pressure and Temperature Data

Operation in low altitude cruise phase at Mach 3.22 and 1000 feet on an ICAO Standard Day produces critical pressure temperature loading (see Figures 108 and 112). Pressure and temperature data follow:

	Engine Station						
	613.412	623.416	633.416	643.416	653.416	662	668.070
Annulus Pressure (psia)	60.22	60.22	60.22	60.22	60.22	59	14.00
Nozzle Internal Pressure (psia)	109.00	60.22	37.75	28.50	23.90	20	19.75
Nozzle $\Delta p$ (psi)	+48.75	0	-22.49	-31.72	-36.72	-38	+5.75
Nozzle Internal Radius (in.)	15.656	17.80	20.41	22.75	24.46	26	27.259
Nozzle Temperature (°F)	1220	1225	1230	1245	1280	135	1450

The shell axial length is 39.05 inches.

~~SECRET RESTRICTED DATA~~  
~~ATOMIC ENERGY ACT OF 1954~~

MAC 463

~~SECRET RESTRICTED DATA~~  
~~ATOMIC ENERGY ACT OF 1954~~

ASD-TDR-63-277, Vol. IV

REPORT 6003

6.2.3.4 Analysis of Ring-Stiffened Cone for External Pressure

The methods employed in Reference 22 for determining the collapsing pressure of thin-walled cylinders with ring stiffeners will be employed to determine the size and location of rings required.

The shell is assumed to be divided into a series of short shells whose lengths are the distance between rings. This assumption applies well and is conservative for a conical shell.

6.2.3.4.1 Ring at Station 660.320

The height of the ring to be used must be limited or the ring will interfere with the cooling annulus airflow.

Shell inner radius = 26.18 inches

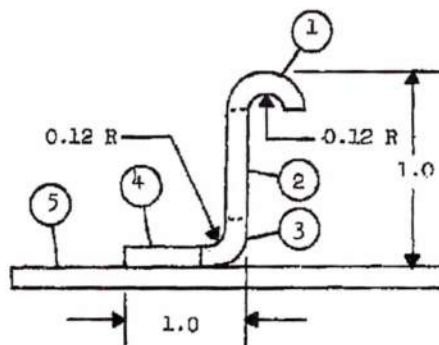
Differential pressure for Mach 3.22 at 6000 feet on ICAO Standard Day = -39.22 psi

Shell temperature = 1325°F

E of Rene' 41  $\approx 24.3 \times 10^6$

The height of a stiffening ring is limited to 1.0 inches by the annulus airflow requirements.

6.2.3.4.1.1 Ring Section Properties



~~SECRET RESTRICTED DATA~~  
~~ATOMIC ENERGY ACT OF 1954~~

~~SECRET RESTRICTED DATA~~  
~~ATOMIC ENERGY ACT OF 1954~~

ASD-TDR-63-277, Vol. IV

REPO 6003

30 t = 1.89 inches. Assume effective shell width acting with ring as

Item	Area	$y_1$	$AY_1$	$AY_1^2$	$I_{ox}$
1	0.0572	0.9426	0.0538	0.0507	0.0003
2	0.0422	0.532	0.02145	0.01142	0.000982
3	0.02106	0.10653	0.00224	0.0002385	0.00006
4	0.0636	0.103	0.00656	0.000676	0.000034
5	0.1190	0.0315	0.00376	0.0001182	0.0000396
	<u>0.30306</u>		<u>0.08781</u>	<u>0.0631527</u>	<u>0.0014156</u>

$$\bar{y} = 0.08781 / 0.30306 = 0.29 \text{ in.}$$

$$I = 0.0631527 + 0.0014156 - 0.29 \times 0.08781$$

$$0.0392 \text{ in}^4$$

6.2.3.4.1.2 Required Flexural Rigidity

For the case of a ring-stiffened cylinder, refer to Section IV, Page 36, of Reference 23. The shell is assumed divided into a series of short shells whose lengths are the distances between rings. The flexural rigidity,  $EI_s$ , of the combined ring stiffener and shell required to prevent collapsing from an external pressure is:

$$EI_s = \frac{w_s D^3 L_s}{24}$$

where

$I_s$  = Required moment of inertia of stiffener and effective width of shell

$E$  = Modulus of elasticity of material =  $24.3 \times 10^6$

$D$  = Cylinder outer diameter = 52.486 in.

$L_s$  = Ring spacing

$w_s$  = Maximum allowable unit pressure = 39.22 psi

For Station 660.320, the ring is placed close to the thickened throat section. The adjoining ring forward on the shell is spaced 6.0 inches away.

~~SECRET RESTRICTED DATA~~  
~~ATOMIC ENERGY ACT OF 1954~~

MAC A67

~~SECRET RESTRICTED DATA~~

~~ATOMIC ENERGY ACT OF 1954~~

ASD-TDR-63-277, Vol. IV

REPORT 6003

$$T_3 = 1350^\circ\text{F and } E = 24.3 \times 10^6$$

$$D^3 = 144,000$$

$$I_B = \frac{39.22 \times 144,000 L_B}{24 \times 24.3 \times 10^6} = 0.0392$$

$$L_{B_{\text{req}}} = 4.05 \text{ in.}$$

Since the shell width between the nozzle and the ring is small, the stiffening effect on the shell is greater than if an equal spacing were used on both sides. A ring spacing of six inches is therefore utilized to the next forward ring.

$$\begin{aligned} \text{Spacing to thickened aft section} &= 6.47 - 660.320 \\ &= 1.5 \end{aligned}$$

$$\text{Spacing to forward ring} = 6.00$$

$$\text{Average spacing} = 4.05 \text{ in.}$$

Since a high margin of safety was obtained on the thickened aft section, the shell is fully effective over the distance to the ring at Station 660.320, and the section is sufficient.

6.2.3.4.2 Ring at Shell Station 651.320

$$\text{Shell I.R.} = 25.20 \text{ in.}$$

$$\text{O.R.} = 25.263 \text{ in.}$$

$$\text{O.D.} = 50.526 \text{ in.}$$

$$\Delta P = 60.22 - 23.5 = 36.72 \text{ psi}$$

$$T = 1285^\circ\text{F (Use } 1300^\circ\text{F)}$$

$$E = 25 \times 10^6$$

$$L_B = 6.0$$

$$I_{B_{\text{req}}} = \frac{36.72 \times 50.526^3 \times 6.0}{24 \times 25 \times 10^6} = 0.0475 \text{ in.}^4$$

A ring section similar to that used at station 660.320 will be utilized with an over-all height of 1.5 inches and material gage of 0.063. An effective shell skin width of 2.5 inches is assumed.

MAC AGCZ

~~SECRET RESTRICTED DATA~~

~~ATOMIC ENERGY ACT OF 1954~~

~~SECRET RESTRICTED DATA~~  
~~ATOMIC ENERGY ACT OF 1954~~

ASD-TDR-63-277, Vol. IV

POST 6003

Item	Area	$y_1$	$A_{y_1}$	$A_{y_2}$	$I_{ox}$
1	0.0433	1.5469	0.0670	0.1033	0.0002
2	0.0668	0.7505	0.05025	0.0377	0.0062
3	0.01579	0.14967	0.00236	0.000354	0.0000
4	0.0512	0.0945	0.00483	0.000456	0.0000
5	0.1575	0.0315	0.00496	0.0001562	0.0000
	<u>0.33459</u>		<u>0.12940</u>	<u>0.1419666</u>	<u>0.0066</u>

$$\bar{y} = 0.1294 / 0.33459 = 0.3875 \text{ in.}$$

$$I_x = 0.1419666 + 0.00661915 - (0.3875 \times 0.1419666) = 0.11849 \text{ in.}^4$$

$I_x = 0.1185 > 0.0475$  required for 6.0 in. spacing; therefore, space 3rd ring at 8.0 inches from this (second) ring.

$$MS = \frac{0.1185}{0.0475 \times 1.25} - 1 = + 0.99$$

6.2.3.4.3 Ring at Shell Station 646.320

$$T = 1252^\circ\text{F}$$

$$\text{Inner radius} = 23.69; \text{ outer} = 23.75; \text{ O.D.} = 47.50$$

$$\text{Exit pressure} = + 27 \text{ psia}$$

$$\text{Annulus pressure} = - 60.22$$

$$\Delta p = - 33.22 \text{ psi}$$

$$E \text{ of Rene' 41} = 25.5 \times 10^6 \text{ at } 1250^\circ\text{F}$$

$$I = 0.1185 \text{ in.}^4$$

$$I_{s, \text{req}} = \frac{0.1185 \times 24 \times 25.5 \times 10^6}{33.22 \times 47.5^3} = 20.4$$

$$\text{For } L_s = 8.0 \text{ in.}$$

$$I_{s, \text{req}} = \frac{33.22 \times 47.5^3 \times 8}{24 \times 25.5 \times 10^6} = 0.0463 < 0.1184$$

$$MS = \frac{0.1184}{0.0463 \times 1.25} - 1 = + 1.0$$

Space next ring at 10 inches.

MAC AGZ

~~SECRET RESTRICTED DATA~~  
~~ATOMIC ENERGY ACT OF 1954~~

~~SECRET RESTRICTED DATA~~  
~~ATOMIC ENERGY ACT OF 1954~~

ASD-TDR-63-277, Vol. IV

REPORT 6003

6.2.3.4.4 Ring at Shell Station 636.320

Exit pressure = + 34 psia

Annulus Pressure = - 60.22 psia

$$\Delta p = - 26.22$$

Inner radius = 21.32; outer = 21.383; D = 42.766

T = 1235°F (Use 1250)

$$E = 25.5 \times 10^6$$

$$I_{req} = \frac{26.22 \times 42.77^3 \times 10}{24 \times 25.5 \times 10^6} = 0.0335 \text{ in.}^4$$

Section properties of 1 1/8 inch ring 0.063 gage:

I = 0.0453 in.<sup>4</sup> with 2.35 in. effect of shell

I = 0.0453 > 0.0335 req.

$$MS = \frac{0.0453}{0.0335 \times 1.25} - 1 = + 0.085$$

6.2.3.4.5 Shell Stations 623.416 to 636.320

At Station 623.416 10 inches aft of the throat, the annulus and exit pressures balance and the cylinder is subject to zero radial pressure.

At Station 633.416, 10 inches further a  $\Delta p$  of 23.22 psi exists. A ring is located at Station 636.320. The average shell pressure is  $\frac{0 + 23.33}{2} = 12.61$  psi. The average radius is  $\frac{16.096 + 20.6}{2} = 18.35$  in. The length is 10 inches.

By the method of Reference 22,

$$\frac{D}{t} = \frac{2(18.35 + 0.063)}{0.063} = \frac{36.826}{0.063} = 585$$

$$\frac{L}{R} = \frac{10}{18.143} = 0.55$$

K > 200

$$W_c = 25.5 \times 10^6 \times 200 \times \left(\frac{0.063}{36.823}\right)^3 = 12.61 \text{ psi} > 12.61 \text{ psi}$$

No rings are required in this area.

$$MS = \frac{12.61 \times 1.25}{25.5} - 1 = + 0.61$$

~~SECRET RESTRICTED DATA~~  
~~ATOMIC ENERGY ACT OF 1954~~

MAC 4603

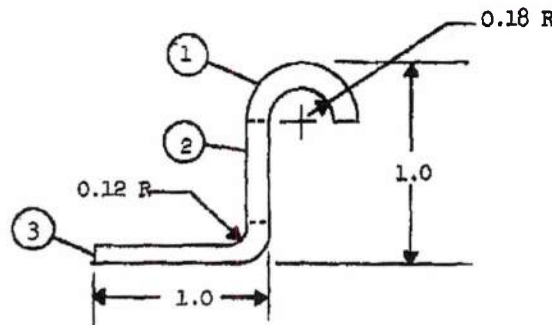
~~SECRET RESTRICTED DATA~~  
 SECURITY ENERGY ACT OF 1954

ASD-TDR-63-277, Vol. IV

on 6003

6.2.3.5 Stiffening Angles--Stiffening Crippling Stress:

Analysis by the methods given in Reference 23. Refer to Figure 11, page 228 of Reference 23 for equivalent sections.



Material is Rene' 41 sheet of 0.08 gage; temperature is 1400°F;  $E = 24.8 \times 10^6$ .

Material treatment is solution heat treat at 1575°F for 30 minutes, water quench, age at 1650°F for 4 hours AC.

$$F_{cy} = 118,000 \text{ psi}$$

$$F_{ce} = \frac{\sqrt{F_{cy} E}}{(b'/t)^{0.75}}$$

for individual angle sections  
 Equation 15, page 229 of Reference 23.

where

$F_{cy}$  = Compressive yield stress

$E$  = Young's modulus in compression

$b'/t$  = Equivalent  $b/t = \frac{a+b}{2t}$

$C_e$  = Edge support coefficient

$C_e = 0.316$  for 2 edges free

$= 0.342$  for 1 edge free

$= 0.366$  for no edge free

~~SECRET RESTRICTED DATA~~

~~SECRET RESTRICTED DATA~~  
 ATOMIC ENERGY ACT OF 1954

ASD-TDR-63-277, Vol. IV

REPORT 6003

The weighted crippling stress for stiffer ribs consisting of several equivalent angle sections is:

$$F_{cc} = \frac{\sum (\text{crippling loads of angles})}{\sum (\text{areas of angles})} \quad \text{Reference 23, page 229}$$

$$\begin{aligned} \sqrt{F_{cy} E} &= \sqrt{118,000 \times 24.8 \times 10^6} \\ &= \sqrt{2,820,000,000} = 530,000 \end{aligned}$$

$$\text{Item 1 } F_{cc} = \frac{0.316 \times 530,000}{(2.83) \cdot 0.75} = \frac{167,000}{2.18} = 76,700 \text{ psi}$$

$$\text{Item 2 } F_{cc} = \frac{0.366 \times 530,000}{(4.55) \cdot 0.75} = \frac{194,000}{3.6} = 54,000 \text{ psi}$$

$$\text{Item 3 } F_{cc} = \frac{194,000}{6.9 \cdot 0.75} = \frac{194,000}{4.5} = 43,000 \text{ psi}$$

$$\begin{aligned} F_{cc} \text{ combined} &= \frac{(76,700 \times 0.454) + (54,000 \times 0.727) + (43,000 \times 1.105)}{(0.454 + 0.727 + 1.105)} \\ &= \frac{34,800 + 39,300 + 47,500}{2.286} = \frac{121,600}{2.286} \\ &= 53,000 \text{ psi} \end{aligned}$$

Area of ring and skin at Station 660.320 0.303 in.<sup>2</sup>

$$p = -39.22 \text{ psi}$$

Ring spacing = 6.0 in.

$$p = p_{RS} = 39.22 \times 26.18 \times 6 = 6130 \text{ l}$$

$$P/A = \frac{6130}{0.303} = 20,200 \text{ psi}$$

$$MS = \frac{53,000}{20,200 \times 1.25} - 1 = +1.09$$

Rings at other stations are of smaller diameter and are less heavily loaded; they are, therefore, satisfactory by comparison.

MAC AGES

~~SECRET RESTRICTED DATA~~  
 ATOMIC ENERGY ACT OF 1954

~~SECRET RESTRICTED DATA~~  
~~ATOMIC ENERGY ACT OF 1954~~

ASD-TDR-63-277, Vol. IV

FORM 6003

6.2.3.6 Exit Nozzle Divergent Cone--Transverse and Axial Loading

The cone is loaded transversely and axially by inertia forces and axially by pressure forces. Since the cone acts as a cantilever beam with the reduced area forward, the critical section occurs at the forward end station where the shell gage changes from 0.08 inch (Station 623.416).

6.2.3.6.1 Axial Air Load

Maximum axial air load occurs in low altitude cruise at Mach 3.22 and 1000 feet on an ICAO Standard Day. The total axial load is 33,650 pounds.

6.2.3.6.2 Dead Weight and Center of Gravity

The weight of the divergent cone aft of the nozzle throat minimum diameter area at Engine Station 613.417 is approximately 223.6 lbs (total assembly weight). The assembly center of gravity is located 32.6 inches aft of the throat. The weight of the 0.08-inch section is approximately 38.1 lbs, and its CG is 5.8 inches aft of the throat.

6.2.3.6.3 Weight and CG of 0.063-in. Section Aft of Station 623.416

$$W = 223.6 - 38.1 = 185.5 \text{ lbs}$$

$$CG = \frac{(223.6 \times 32.6) - (38.1 \times 5.8)}{185.5} = \frac{7680 - 220.68}{185.5} = 40.21$$

$$\text{Arm to Station 520.412} = 40.2 - 10 = 30.2 \text{ inches}$$

$$M = 185.5 \times 30.2 = 5600 \text{ in.-lbs (dead weight)}$$

$$V = 185.5 \text{ lbs}$$

6.2.3.6.4 Inertia Load Factors

The critical combined y-z load factor acting at the missile center of gravity is approximately 5.0 g. A conservative value of 10 acting on the exit nozzle is assumed for this analysis.

6.2.3.6.5 Transverse Shear and Bending at Station 623.416

The bending stress at a section in a right circular cylinder is:

$$f_b = \frac{M}{\pi r^2 t}$$

~~SECRET RESTRICTED DATA~~  
~~ATOMIC ENERGY ACT OF 1954~~

MAC ANZ

~~SECRET RESTRICTED DATA~~

~~ATOMIC ENERGY ACT OF 1954~~

ASD-TDR-63-277, Vol. IV

REPORT 6003

For a truncated cone,  $f_{b1} = f_b \text{ Sec } \beta$  where  $\beta$  is the angle between the axial center line and meridional lines in the shell. Assuming a straight surface between throat and exit,

$$\beta = 10^\circ 55'$$

$$\text{Sec } \beta = \frac{1}{\cos \beta} = \frac{1}{0.98190} = 1.02$$

R at Station 623.416  $\approx$  17.5 inches

$$f_b = \frac{M}{77 \times 35^2 \times 0.063} = \frac{M}{242}$$

$$f_{b1} = 0.00422 M$$

For a 1.0 g inertia  $f_{b1} = 0.00422 \times 50 = 23.6 \text{ psi}$

$$10 \text{ g} = 236 \text{ psi}$$

The transverse shear stress at Station 623.416 is:

$$f_{s1} = \frac{V_1}{77 \times r t}$$

where

$$V_1 = v - \frac{M \tan \beta}{r}$$

for 1 g

$$V_1 = 185.5 - \frac{5600 \times 0.19287}{17.5} = 185.5 - 61.7 = 123.8 \text{ lbs}$$

$$f_b = \frac{123.8}{77 \times 17.5 \times 0.063} = 35.7 \text{ psi for 1.0 g}$$

$$= 357 \text{ psi for 10 g}$$

#### 6.2.3.6.6 Axial Air Load Stress

Total air load at throat - 33,650 lbs Since the section is obviously over strength, assume the same load at Station 623.416.

$$\text{Section area} = (2 \times 17.563) \times 0.063 = 7.05 \text{ in.}^2$$

$$P/A = \frac{33,650}{7.05} = 4780 \text{ psi}$$

~~SECRET RESTRICTED DATA~~

~~ATOMIC ENERGY ACT OF 1954~~

~~SECRET RESTRICTED DATA~~  
~~ATOMIC ENERGY ACT OF 1954~~

ASD-TDR-63-277, Vol. IV

REF 6003

6.2.3.6.7 Combined Axial Stress

Conservatively utilizing an inertia load factor of 10.0 g, the full cone drag load, and a design factor of 1.15, the design limit stress is:

$$f_t = (236 + 4780) (1.15) = 5770 \text{ psi}$$

6.2.3.6.8 Material Properties

The temperature at Shell Station 623.416 is 121 °F, and the  $F_{ty}$  of Rene' 41 sheet is 107,500 psi.

Assuming a weld joint efficiency of 85 percent

$$F_{tu} = 150,000 \text{ psi}$$

Assuming

$$F_{su} = 0.5 F_{tu}$$

$$F_{su} = 75,000 \text{ psi}$$

6.2.3.6.9 Margins of Safety

$$\text{MS Combined Tension Yield} = \frac{107,500 \times 0.85}{5770} - 1 \quad \text{High}$$

$$\text{MS Combined Tension Ultimate} = \frac{150,000 \times 0.85}{5016 \times 1.25} - 1 \quad \text{High}$$

$$\text{MS Ultimate Shear} = \frac{75,000 \times 0.85}{357 \times 1.25} - 1 \quad \text{High}$$

Note: Loads utilized in this analysis of combined axial-transverse, while not the true values, were obviously conservative, and in view of the high margins obtained are deemed sufficient.

6.2.3.7 Exit End Doublor Ring

6.2.3.7.1 Discussion

From Exit Station 662.470 to the aft end at Station 668.070, a 1/4-inch thick plate ring is utilized to stiffen the unsupported open end of the 0.063 gage conical shell (Figure 117). A similar ring is provided on the airframe shell that encloses the nozzle.

The annulus formed between these shells is utilized as a cooling air duct. The shells converge toward the open end, and by the end portions of the stiffening rings a convergent-divergent cooling air exhaust nozzle is formed.

~~SECRET RESTRICTED DATA~~  
~~ATOMIC ENERGY ACT OF 1954~~

MAC 102

~~SECRET RESTRICTED DATA~~  
~~ATOMIC ENERGY ACT OF 1954~~

ASD-TDR-63-277, Vol. IV

REPORT 6003

6.2.3.7.2 Pressure Loading

The divergent cone is subjected to a net external col-  
 lapsing pressure differential. The critical pressure-temper- ure combination  
 occurs during low altitude cruise on an ICAO Standard Day at Mach 3.22 and 1000  
 feet. Pressure profiles for the operation are presented in Figure 110. The  
 following are data from these curves:

	Exit Station			
	662.470	665.470	666.97	668.070
Annulus pressure, psia	-59.0	-54.7	-48.5	-14.00
Nozzle pressure, psia	+20.2	+20.0	+20.0	+19.75
$\Delta p$ on nozzle	-38.8	-34.7	-28.5	+ 5.75

The axial forces acting on this small section are negligible.

6.2.3.7.3 Temperature

The temperature through the shell thickness is assumed  
 uniform. The temperature profile for Mach 3.22 at 1000 feet in an ICAO Stand-  
 ard Day is presented as Figure 112. Values for the ring are as follows:

	Exit Station			
	662.470	665.470	666.97	668.070
Temperature, °F	1350	1392	1425	1450

6.2.3.7.4 Material

The material is Rene' 41 plate, mill annealed and proc-  
 ess-treated as follows:

Solution heat-treat at 1975°F (30 minutes); water  
 quench; age at 1650°F (4 hours); air cool.

6.2.3.7.5 Analysis by Method of Reference 24

In this report Donnell's equation for the equilibrium of  
 cylindrical shells in torsion is applied to find the critical stresses under  
 other loading conditions for cylinders with simply supported edges.

MAC A CTB

~~SECRET RESTRICTED DATA~~  
~~ATOMIC ENERGY ACT OF 1954~~

~~SECRET RESTRICTED DATA~~  
~~ATOMIC ENERGY ACT OF 1954~~

ASD-TDR-63-277, Vol. IV

REP 6003

6.2.3.7.6 Critical Buckling Stress for Uniform External Pressure

Pressure applied to entire outer surface radius  $r$ ; ends open; edges simply supported.

Solve for nondimensional buckling parameter,

$$z = \frac{L^2}{rt} \sqrt{1 - \mu^2}$$

Obtain buckling constant,

$$k_y = f_y \left( \frac{t L^2}{D \pi^2} \right)$$

Solve for  $f_y$  = critical compressive hoop stress

Values apply where  $n = 1 < 2$

$$D = \text{plate flexural stiffness/unit length} = \frac{t^3}{12 - 2}$$

Assume

$$\mu = 0.3$$

$$t = 0.25 \text{ in.}$$

$$L = 6.0 \text{ in.}$$

$$r = 26.9 \text{ in. (average)}$$

$$E = \text{at } 1375^\circ\text{F (average)} = 24.3 \times 10^6$$

$$D = \frac{24.3 \times 10^6 \times (0.25)^3}{12 (1 - 0.3^2)} = 34,700$$

$$z = \frac{(6^2)}{(26.9)(0.25)} \sqrt{(1 - 0.3^2)} = 5.09$$

$$r/t \sqrt{1 - \mu^2} = \frac{26.9}{0.25} \times 0.951 = 102.2$$

From Figure 1 of Reference 24:

$$k_y = 4.7$$

$$f_{y\text{cr}} = \left[ \frac{k_y}{\left( \frac{t L^2}{D \pi^2} \right)} \right] = \frac{4.7}{\left( \frac{0.25 \times 6^2}{34,700 \times \pi^2} \right)} = \frac{4.7 \times 34,700 \times \pi^2}{0.25 \times 6} = 178,000 \text{ psi}$$

~~SECRET RESTRICTED DATA~~  
~~ATOMIC ENERGY ACT OF 1954~~

MAC AGS

~~SECRET RESTRICTED DATA~~  
~~ATOMIC ENERGY ACT OF 1954~~

ASD-TDR-63-277, Vol. IV

REPORT 6003

For  $f_c$  (hoop compression), assume average pressure of 35 psi over ring width.

$$f_c = \frac{35 \times 26.9}{0.25} = 3770 \text{ psi}$$

$$\text{Design factor} = 1.15$$

$$\text{Factor of safety} = 1.25$$

$$\text{MS(Ultimate)} = \frac{178,000}{3770 \times 1.25} - 1 = \text{Hig}$$

6.2.3.7.7 Analysis by Method of Reference 5

Refer to Reference 5, page 270, Case 1 Table XIII. This theory applies to a more concentrated loading than the actual case involved. A conservative assumption will be used in which the entire pressure acting on the ring is concentrated at the end.

Then:

$$\text{Max } s_2 = \frac{-2 V_0}{t} \lambda R$$

$$V_0 = \text{transverse shear normal to wall (lbs/in.)}$$

$$\lambda = \sqrt[4]{\frac{3(1-\mu^2)}{R_2^2 t^2}}$$

$$R_2 = R = \text{mean radius of shell}$$

$$\mu = \text{Poisson's ratio} = 0.3$$

$$t = 0.25 \text{ in.}$$

$$s_2 = \text{hoop stress}$$

$$\begin{aligned} \lambda &= \sqrt[4]{\frac{3(1-0.3^2)}{26.9^2 \times 0.25^2}} \\ &= \left(\frac{2.71}{4.52}\right)^{1/4} = (0.6)^{1/4} \\ &= 0.88 \end{aligned}$$

$$V_0 = p \text{ (assume 35 psi average for 1.0 inch width)}$$

$$s_2 = \frac{-2 \times 35}{0.25} \times 0.88 \times 26.9 = 6620 \text{ psi}$$

$$\text{Station } 662.470 \text{ to } 668.070 = 5.6 \text{ inches}$$

~~SECRET RESTRICTED DATA~~  
~~ATOMIC ENERGY ACT OF 1954~~

MAC 407

~~SECRET RESTRICTED DATA~~  
~~ATOMIC ENERGY ACT OF 1954~~

ASD-TDR-63-277, Vol. IV

REPORT 6003

at the end:

If it is assumed that the entire load is concentrated

$$V_0 = 5.6 \times 35 \times 82 = 5.6 \times 6620 = 37,000 \text{ lb}$$

$F_{t_y}$  of Rene' 41 at 1450°F = 127,000 psi (sheet)

Design factor = 1.15

$$MS \text{ (Yield)} = \frac{127,000}{37,000 \times 1.15} - 1 = + 1.98$$

#### 6.2.4 Ejector Shroud (Nozzle Inner Liner)

##### 6.2.4.1 Discussion

The inner liner acts as a second nozzle and extends aft to the exit nozzle throat. It serves as a heat shield between the exhaust flow and the primary nozzle. Airflow from the lateral support annulus is ducted between these exit nozzle shells and used for nozzle cooling.

Exit nozzle exhaust flow pressure is less than that in the cooling annulus. The shroud is subjected to a collapsing pressure.

Radial components of pressure loadings are reacted within the shroud. Axial components are transferred to the exit nozzle throat by means of radially oriented pin and socket supports. Axial forces are reacted similarly. The shroud acts as a simply supported beam to transfer radial inertia loads to the exit throat and the airframe at the reactor aft end.

##### 6.2.4.1.1 Method of Analysis

Analysis of the cylindrical and conical shells is based on the methods of Reference 22 previously utilized in Section 6.2 for the divergent cone aft section of the exit nozzle.

##### 6.2.4.1.2 Operational Regimes, Pressure and Temperature

Critical pressure and temperature regimes occur during low altitude cruise operation at Mach 3.22 and 1,000 feet on an ISO Standard Day.

Data related to this operational phase of the regime are presented in Figure 108 and in Table XXVII.

##### 6.2.4.1.3 Materials

The material used is Rene' 41 sheet stock processed at 1650°F solution heat treated at 1975°F for 30 minutes, water quenched, and air cooled. The following strength values apply for 4 hours, and air cooled. The following strength values apply

~~SECRET RESTRICTED DATA~~  
~~ATOMIC ENERGY ACT OF 1954~~

MAC 457

~~SECRET RESTRICTED DATA~~

ASD-TDR-63-277, Vol. IV

~~ATOMIC ENERGY ACT OF 1954~~

REPORT 6003

Temperature (°F)	$F_{ty} \times 10^{-3}$	$E \times 10^{-6}$
1350	104.8	25
1400	102	24.3
1450	99	23
1500	96	21.5
1550	93	19.5

Assume

$$F_{cy} = F_{ty}$$

$$F_{su} = 0.6 F_{tu}$$

6.2.4.2 Analysis of Forward Cylinder

The forward 22.25 inches of the liner is a right circular cylinder with an I.D. of 53.5 inches. The open end is stiffened by a heavy doubler ring and is simply supported in the radial direction by the flange of the support ring attached to the airframe. The liner ring slides inside this ring and is unrestrained in the axial direction.

Critical operation occurs in low altitude cruise at Mach 3.22 and 1,000 feet on an ICAO Standard Day. The net differential pressure between the inner and outer shell surfaces is compressive and varies from 66 psi at the forward end to 26 psi at the aft end.

Utilizing the methods of Reference 22:

$$L = 22.25 \text{ in.}$$

$$R = 26.75 \text{ in.}$$

$$L/R = \frac{22.25}{26.75} = 0.833$$

$$D = 53.50 \text{ in.}$$

The average shell temperature is 1350°F and  $E$  is  $25 \times 10^6$  psi.

MAC 6073

~~SECRET RESTRICTED DATA~~

~~ATOMIC ENERGY ACT OF 1954~~

$t$	$D/t$	$K$	$t/D$	$(t/D)^3$	$W_c$ (psi)
0.063	850	220	0.001178	$1.63^{-9}$	8.95
0.080	667	190	0.001493	$3.34^{-9}$	15.85
0.093	576	175	0.001735	$5.23^{-9}$	22.95
0.109	490	160	0.00204	$9.45^{-9}$	37.80
0.125	428	140	0.00234	$1.285^{-8}$	45.10
0.156	343	135	0.00292	$2.5^{-8}$	84.2
0.1875	285	130	0.00351	$4.32^{-8}$	140.5

The forward edge of the shell aft to Station 568.47 is 0.1875 gage material. Ring grooves are machined in this area to provide a pressure seal, but the majority of the section is full thickness.

Maximum  $p = 66.0$  psi at the forward end

$$MS (t = 0.1875) = \frac{140.5}{66 \times 1.25} - 1 = 0.70$$

The shell is spin-formed and is assumed taper in thickness from 0.1875 at Station 568.47 to 0.125 at Station 580.47, here  $p = 31$  psi and  $W_c = 45.10$  psi

$$MS (t = 0.125) = \frac{45.10}{31 \times 1.25} - 1 = +0.16$$

6.2.4.3 Analysis of Aft Cone (Convergent)

Analysis methods are those utilized in the study of the exit shell (Refer to Paragraphs 6.2.1 and 6.2.3).

$L = 18.0$  inches

$R$  fwd = 27.5 inches;  $r$  aft = 18.25 inches; average  $r = 23.0$  inches

Average temperature = 1450°F

$E$  of Rene' 41 =  $23 \times 10^6$  psi

$$L/R = \frac{18}{23} = 0.782$$

~~SECRET RESTRICTED DATA~~  
~~ATOMIC ENERGY ACT OF 1954~~

ASD-TDR-63-277, Vol. IV

REPORT 6003

t	D/t	K	t/D	(t/D) <sup>3</sup>	W <sub>c</sub> (psi)
0.063	730	225	0.00137	2.58 <sup>-9</sup>	13.4
0.080	575	200	0.00173	5.17 <sup>-9</sup>	23.8
0.093	495	185	0.00202	8.22 <sup>-9</sup>	35.0
0.109	422	175	0.00237	1.33 <sup>-8</sup>	53.5
0.125	378	160	0.00272	2.01 <sup>-8</sup>	74

At the forward end, p = 27 psi and R = .75 inches.

At the aft end, p = 44.3 and R = 18.27 ches.

For a 23-inch average R, W<sub>c</sub> = 74 psi for a 1/8-inch gage.

W<sub>c</sub> for R = 27.75 on the forward cylinder = 45.10 psi.

$$MS \text{ (forward end)} = \frac{45.10}{27 \times 1.25} - 1 = +.333$$

At the aft end the radius of 18.25 will provide a higher W<sub>c</sub> than the 74.0 psi for the average R = 23.0 inches. The W<sub>c</sub> value for R = 16.0 inches in the throat area is greater than 100 psi. The 0.125 gage, therefore, is deemed satisfactory.

$$MS = \frac{74}{44.3 \times 1.25} - 1 = +0.33$$

#### 6.2.4.4 Analysis of Throat (Aft End)

The axial length from the point of tangency with the convergent conical shell to the open aft end is approximately 10 inches. The variation in shell radius is small, and the average radius is 16.4 inches. The maximum collapsing pressure is 140 psi at the throat mid-point and decreases to zero at the open end (see Figure 118).

Utilizing the method of Reference 22,

$$L/R = \frac{10}{16} = 0.625$$

Assume t = 0.109 in.,

$$D/t = \frac{32}{1109} = 293, K \approx 225$$

t = 1750°F maximum and E = 19.5 x 10<sup>6</sup> psi minimum

$$\begin{aligned} \left(\frac{t}{D}\right)^3 &= \left(\frac{0.109}{0.32}\right)^3 = 3.97 \times 10^{-8} \\ W_c &= 225 \times 18.5 \times 10^6 \times 3.97 \times 10^{-8} = 31.5 \text{ psi} > 140 \text{ psi} \end{aligned}$$

~~SECRET RESTRICTED DATA~~  
~~ATOMIC ENERGY ACT OF 1954~~

MAC 467

~~SECRET RESTRICTED DATA~~  
~~ATOMIC ENERGY ACT OF 1954~~

ASD-TDR-63-277, Vol. IV

1 027 6003

Using  $t = 0.125$ ,

$$D/t = \frac{32.0}{0.125} = 256, \quad K \approx 210$$

$$t/D^3 = 5.93 \times 10^{-8}$$

$$W_c = 210 \times 19.5 \times 10^6 \times 5.93 \times 10^{-8} = 243 \text{ p}$$

$$MS = \frac{243}{140 \times 1.25} - 1 = +0.39$$

#### 6.2.5 Analysis of Exit Nozzle Attach Joint

##### 6.2.5.1 General Discussion

The exit nozzle is cantilevered from the airframe at the aft face of the reactor where it is attached by a quick disconnecting ring joint consisting of an airframe ring, an exit nozzle ring, a locking ring, and a split ring retainer (see Figure 107).

The exit nozzle and locking ring are threaded. The retainer ring is fastened to the locking ring with 3/8-inch diameter steel bolts.

The attach ring is subjected to (1) the axial air load and inertia forces acting on the exit nozzle assembly, (2) a differential air pressure between its circumferential surfaces, and (3) the transverse shear and bending moments of the inertial loads on the nozzle.

##### 6.2.5.1.1 Design Loads

Critical pressures and temperatures occur during low altitude cruise operation at Mach 3.22 and 1000 feet on an ICAO Standard Day.

The net axial drag force acting on the nozzle assembly, nozzle and liner, at the attach joint is 367,438 pounds (limit).

The nozzle assembly weight is 1054 pounds, and the inertial load factors are  $g_x = 0$ ,  $g_z = 8.5$ ,  $g_y = 1.0$ .

The airframe annulus pressure is 60.22 psia, and the exit-liner annulus pressure is 320 psia at Station 565.47 and 305 psia at the joint of center line station. For analysis, a uniform differential of 250 psi and net axial load of 375,000 pounds are conservatively assumed.

##### 6.2.5.1.2 Temperatures

A uniform temperature of 1400°F is assumed for the entire attach structure with no variation throughout the length or radial thickness.

~~SECRET RESTRICTED DATA~~  
~~ATOMIC ENERGY ACT OF 1954~~

6.2.5.1.3 Material

The material is Rene' 41 fabrication, heat-treated at 1975°F for 1/2 hour, water quenched, aged at 1650°F for 4 hours and air cooled. The rings are machined from forged rings.

For 1400°F, the material properties are as follows:

$$F_{t_u} = 130,000 \text{ psi}$$

$$F_{t_y} = 100,000 \text{ psi}$$

$$E = 24 \times 10^6$$

$$0.2\% \text{ plastic creep in 10 hrs} = 68,000 \text{ psi}$$

$$1\% \text{ creep, 10 hrs} = 85,000 \text{ psi}$$

6.2.5.2 Analysis of Vehicle Coupling

The open end cylinder with its integral flange is subjected to a uniformly distributed axial load, applied in bearing to the flange, and to a uniform internal (bursting) pressure. The assumed coupling geometry is illustrated in Figure 119. A method for analyzing such a structure is presented in Reference 5, Case 16, Table XIII, page 263, and is applied in the calculations which follow:

$$V_o = \text{transverse shear normal to wall, linear in.}$$

$$M_o = \text{bending moment, uniform along circumference, in.-lb/linear in.}$$

$$p = \text{unit pressure, psi (250 psi)}$$

$$t = \text{wall thickness, in. (0.375 in.)}$$

$$a = \text{median diameter of vessel, in. (58.25 in.)}$$

$$b = \text{median diameter of flange, in. (59.75 in.)}$$

$$h = \text{flange thickness, in. (0.75 in.)}$$

$$P = \text{tensile force, lb. (375,000 lb.)}$$

$$f = \sqrt{at}, (4.688 \text{ in.})$$

$$d = \text{flange outer diameter, in. (59.50 in.)}$$

$$s_1 = \text{meridional membrane stress}$$

$$s_2 = \text{meridional bending stress}$$

~~SECRET RESTRICTED DATA~~  
~~ATOMIC ENERGY ACT OF 1954~~

ASD-TDR-63-277, Vol. IV

PT. 6003

$s_2$  = hoop membrane stress

$s_2^1$  = hoop bending stress

$$T_1 = \frac{t^3 (3a^2 + 5d^2)}{h^3 (d^2 - a^2)} = 33.864 \text{ lb/in.}$$

$$T_2 = \frac{3.58 t^3}{h^3 (d^2 - a^2)} \frac{d}{3} \log e \frac{b}{a} + 0.1 (b^2 - a^2) = 0.1033 \text{ /in.}$$

$$V_0 = \frac{(r^2 - \frac{h^3}{2t} t_1) (t + 0.2325 \text{ ft}) p - 2T_2 (h + 0.5377 f) P}{1.86 \text{ ft} + T, L^2 (2 + 0.116 \frac{f}{t} t_1) + 1.6103 fh + 0.866 r^2} = -12.31 \text{ lb/in.}$$

$$M_0 = \frac{(h^2 T_1 + 1.86 \text{ ft}) V_0 + ht_2 P - 0.5 t p (r^2 - \frac{h^3}{2t} t_1)}{1.5 T h - 3.464 t} = 710.93 \text{ --lb/in.}$$

The maximum axial stress in the cylinder is:

$$S (\text{cylinder}) = \frac{6M_0}{t^2} + \frac{P}{Tat} = 84,500 \text{ psi}$$

$$MS (\text{cylinder}) = \frac{100,000}{1.15 \times 84,500} - 1 = +0.03$$

The maximum radial stress in the flange is:

$$S_R (\text{flange}) = \frac{6}{h^2} (M_0 - 1/2 V_{oh}) + \frac{V_0}{h} + p = 816 \text{ psi}$$

The maximum tangential stress in the flange is

$$S_t (\text{flange}) = \frac{6}{h^2} (M_0 - \frac{1}{2} V_{oh}) + \frac{0.8}{h^2 (d^2 - a^2)} d^2 (-15 M + 7.5 h V_0 + 1. \dots \geq P \log e$$

$$\frac{b}{a} + 0.447 t P (b^2 - a^2) + \frac{h^2}{4t} T_1 (V_0 + hp) = 11,840 \text{ psi}$$

$$MS (\text{flange}) = \frac{100,000}{1.15 \times 11,840} - 1 = \text{High}$$

~~SECRET RESTRICTED DATA~~  
~~ATOMIC ENERGY ACT OF 1954~~

MAC 4573

~~SECRET RESTRICTED DATA~~  
~~ATOMIC ENERGY ACT OF 1954~~

ASD-TDR-63-277, Vol. IV

REPORT 6003

### 6.2.5.3 Retaining Ring and Bolts

The retaining ring is segmented and is bolted to the lock ring by 140 3/8-inch stud bolts. Retaining ring geometry is shown in Figure 120.

Total nozzle assembly axial load = 375,000 lbs

Load/bolt =  $375,000/140 = 2680$  lbs/lmt.

#### 6.2.5.3.1 Bolt Shear

$$A = 0.7854 (0.375)^2 = 0.1102 \text{ in.}^2$$

$$f_b = 2680/0.1102 = 24,300 \text{ psi}$$

$$F_{bu} = 0.6 \times 130,000 = 78,000 \text{ psi}$$

$$MS (\text{shear}) = \frac{7800}{24,300 \times 1.25} - 1 = + 1.56$$

#### 6.2.5.3.2 Bolt Bearing on Retainer

$$A = 0.15 \times 0.375 = 0.0563 \text{ in.}^2$$

$$f_{br} = 2680/0.0563 = 47,600 \text{ psi}$$

$$F_{bru} = F_{tu} (\text{conservative}) = 130,000 \text{ psi}$$

$$MS = \frac{130,000}{47,600 \times 1.25} - 1 = + 1.18$$

#### 6.2.5.3.3 Bolt Coupling Loading

The axial load transfers from the lock bolt, and thence through the retainer ring to the vehicle fitting shell (Figure 121). The moment occasioned by load transfer in the retainer ring is assumed to be reacted by a couple acting between the bolt centerline and the bearing of the retainer on the lock ring.

Moment Arm = 0.25 inches

Load/bolt = 2680 lbs; moment =  $2680 \times 0.25 = 670$  lbs;

$$\text{Couple} = \frac{670}{0.50} = 1340 \text{ in.-lbs}$$

Bolt inner dia. = 0.31179;  $A = 0.079 \text{ in.}^2$

$$F_t = 1340/0.079 = 17,000 \text{ psi}$$

$$MS = \frac{100,000}{17,000 \times 1.15} - 1 = \text{High}$$

~~SECRET RESTRICTED DATA~~  
~~ATOMIC ENERGY ACT OF 1954~~

~~SECRET RESTRICTED DATA~~  
~~ATOMIC ENERGY ACT OF 1954~~

ASD-TDR-63-277, Vol. IV

REPORT 6003

6.2.5.3.4 Bending of Retainer Ring

O.D. of lock ring = 60.9 in.; circumference = 193.5 in.;  
140 bolts are specified.

Perimeter of retainer ring at mid height = 36 in.;

$$\frac{186}{140} = 1.33 \text{ in./bolt.}$$

Assuming a cross sectional area 1.01 inches wide to act  
as a beam in simple bending,

$$f = \frac{6M}{bd^2} = \frac{6 \times 2680 \times 0.251}{1.0 \times (0.4)^2} = 25,300 \text{ psi}$$

$$MS = \frac{100,000}{25,300 \times 1.15} - 1 = + 2.44$$

6.2.5.3.5 Ring Shear-Out

Area =  $0.31 \times 0.4/2 = 0.124 \text{ in.}^2$

$P/A = 2680/0.124 = 21,620 \text{ psi}$

$F_{su} = 78,000 \text{ psi}$

$$MS = \frac{78,000}{21,620 \times 1.25} - 1 = + 1.9$$

6.2.5.4 Analysis of Lock Ring (Figure 122)

Assume each thread reacts one half of the 37,500-pound  
limit axial load. The load per inch of thread at the pitch diameter is:

$$P = \frac{375,000}{77 \times 59.6475 \times 2} = 1000 \text{ lb/in.}$$

At Section A-A, assuming a 1.0-inch circumferential width  
of shell and thread acting as a beam,

$$M = 1000 \times 0.4375 = 437.5 \text{ in.-lb}$$

$$I = \frac{1 \times (0.415)^3}{12} = 0.00595 \text{ in.}^4$$

$$f_b = \frac{437.5 \times 0.2075}{0.00595} = 15,250 \text{ psi}$$

~~SECRET RESTRICTED DATA~~  
~~ATOMIC ENERGY ACT OF 1954~~

~~SECRET RESTRICTED DATA~~  
~~ATOMIC ENERGY ACT OF 1954~~

ASD-TDR-63-277, Vol. IV

REPORT 6003

$$\text{Axial stress} = \frac{2 \times 1000}{1 \times 0.415} = 4820 \text{ psi}$$

$$\text{Total stress} = 15,250 + 4820 = 20,070 \text{ psi}$$

$$\text{MS (yield)} = \frac{100,000}{20,070 \times 1.15} - 1 = + 3.33$$

$$\text{MS (10-hr creep of 1\%)} = \frac{85,000}{20,070 \times 1.15} - 1 = 2.67$$

#### 6.2.5.4.1 Thread Shear at Pitch Diameter

$$\text{Area} = 0.50 \text{ in.}^2$$

$$F_{Bu} = 0.6 F_{tu} = 78,000 \text{ psi}$$

$$P = 1000 \text{ lbs; } F_s = \frac{1000}{0.5} = 2000 \text{ psi}$$

$$\text{MS} = \frac{78,000}{1.25 \times 2000} - 1 = \text{High}$$

#### 6.2.5.4.2 Analysis of Lock Ring as a Cylinder

Due to the high margins obtained in a similar analysis of the airframe portion of the attach assembly and the margins obtained in the preceding analyses of the lock ring, no further investigation is deemed necessary.

#### 6.2.5.4.3 Bending on Lock Ring--Section B-B

Assuming 1/140 x circumference-wide strip as a beam,

$$M = 0.54 \times 2680 = 1450 \text{ in.-lbs}$$

$$I = \frac{0.970 \times (0.55)^2}{12} = 0.0135 \text{ in.}^4$$

$$f = \frac{1450 \times 0.275}{0.0135} = 29,600 \text{ psi}$$

$$\text{Axial stress} = \frac{2680}{0.97 \times 0.55} = 5020 \text{ psi}$$

$$f_b + f_t = 29,600 + 5020 = 34,620 \text{ psi}$$

$$\text{MS (Yield)} = \frac{100,000}{34,620 \times 1.15} - 1 = + 1.5$$

$$\text{MS (10-hr. creep of 1.0\%)} = \frac{85,000}{34,620 \times 1.15} - 1 = + 1.14$$

~~SECRET RESTRICTED DATA~~  
~~ATOMIC ENERGY ACT OF 1954~~

~~SECRET RESTRICTED DATA~~

~~ATOMIC ENERGY ACT OF 1954~~

ASD-TDR-63-277, Vol. IV

REPORT 6003

6.2.5.4.4 Analysis--Exit Nozzle Attach Ring

A section of this ring is shown in Figure 3.

6.2.5.4.5 Stress at Section A-A

Load per inch on each thread is:

$$P = \frac{375,000}{(3.14) (59.647) (2)} = 995 \text{ lbs/in.}$$

$$M = (0.458) (995) = 450 \text{ in.-lbs/in.}$$

$$I = \frac{1.0 (0.437)^3}{12} = 0.00697 \text{ in.}^4 \text{ (assuming 1.0-in. wide section)}$$

$$f(\text{total}) = \frac{(450) (0.2185)}{0.00697} + \frac{375,000}{(3.14) (58.77) 0.437} = 1,720 \text{ psi}$$

$$MS = \frac{100,000}{1.15 \times 18,720} - 1 = \text{High}$$

DECLASSIFIED IN FULL  
Authority: EO 13526  
Chief, Records & Declass Div, WHS  
Date: OCT 02 2015

MAC 1427

~~SECRET RESTRICTED DATA~~

~~ATOMIC ENERGY ACT OF 1954~~

~~SECRET RESTRICTED DATA~~  
~~ATOMIC ENERGY ACT OF 1954~~

ASD-TDR-63-277, Vol. IV

REPORT 6003

## 7.0 MODELS

### 7.1 Direct-Connect Aerodynamic Coupling

#### 7.1.1 Design

The direct-connect aerodynamic coupling hardware for this contract period is a modification of the test hardware used in the 1961 aerodynamic coupling tests (see Figures 124-128).

To evaluate simulated reactor airflow distribution, a control rod and actuator assembly and front support assembly were designed to simulate geometrically the flight engine hardware and to create as nearly as possible the blockage and airflow distribution anticipated in a flight engine. A transition plate and exit plate were designed with approximately 50 static pressure pickups for use at the aft reactor face during testing. Test results are reported in Volume II.

### 7.2 One-Third Scale Free Jet Model

#### 7.2.1 Design

The 1/3 scale free jet model shown in Figure 129 utilizes the basic hardware from the direct-connect aerodynamic coupling test hardware; i.e., the reactor section, exit nozzle, exit nozzle spacers, and certain instrumentation sections.

Figures 130 to 142 show engine components in various stages of fabrication. The new hardware that was designed and fabricated included a free jet inlet with translating centerbody spike and bypass doors, subsonic diffuser section and translating exit nozzle plug. The geometric lines of the inlet nozzle and centerbody are reduced from the flight engine by a scaling factor of 0.3625, which produces an inlet cowl diameter of 4 inches. The inlet spike is translated by means of a hydraulic actuator that is mounted inside the centerbody structure. This actuator operates on 1000 psi supply pressure and is capable of translating the spike 2.5 inches at the rate of 0.25 inches per second working against a load of 3000 pounds.

Two by-pass doors are located on the external wall of the inlet structure near the aft end of the centerbody, one door on each side of the horizontal centerline. Each door has an open area of 18.8 square inches. A hydraulic actuator for each door is mounted externally and is capable of positioning the doors from full open to full closed within two seconds.

The exit nozzle plug is positioned at the center of the exit nozzle throat and is contoured for a linear area variation during translation. The plug is translated by means of a hydraulic actuator, which is capable of translating the plug 18 inches against a 2500-pound load at the rate of one inch per second.

~~SECRET RESTRICTED DATA~~  
~~ATOMIC ENERGY ACT OF 1954~~

~~SECRET RESTRICTED DATA~~

ASD-TDR-63-277, Vol. IV

REPORT 6003

The reactor section was modified to allow for thermal expansion of the reactor core when tested with 450°F inlet air. Axial thermal expansion was contained by use of a spring-loaded ring mounted at the forward face of the reactor. Radial thermal expansion was contained by use of spring-loaded straps around the periphery of the core matrix. All the basic components for this engine were fabricated from mild steel and 4130 steel. Test results are reported in Volume II.

**DECLASSIFIED IN FULL**  
Authority: EO 13526  
Chief, Records & Declass Div, WHS  
Date: OCT 02 2015

MAC 4637

~~SECRET RESTRICTED DATA~~

~~SECRET RESTRICTED DATA~~

~~ATOMIC ENERGY ACT OF 1954~~

ASD-TDR-63-277, Vol. IV

REPORT 6003

8.0 REFERENCES

1. "Letter Contract between Department of the Air Force and The Marquardt Corporation", Contract AF 33(657)-8125, 16 April 1962, ~~SECRET RESTRICTED DATA~~, Reg. 10,201.
2. "Performance Bulletin No. 5 for the Marquardt Nuclear Ramjet Engine", The Marquardt Corporation, 1 June 1962, Marquardt 5893, ~~SECRET RESTRICTED DATA~~, Reg. 22,593.
3. "Aerothermodynamics for Pluto", Part II, Volume 5, "Structural Design and Materials", Ling-Temco-Vought, April 1962, ASD-TDR-62-395, ~~SECRET RESTRICTED DATA~~, Reg. 22,718.
4. "Preliminary Analysis of Lateral Vibrations of the Pluto 1 Motor", The Marquardt Corporation, 15 December 1961, Marquardt Report 373, ~~SECRET RESTRICTED DATA~~, Reg. 22,350.
5. "Formulas for Stress and Strain", R. J. Roark, 1954, McGraw-Hill, New York.
6. "Analysis and Design of Aircraft Structures", E. F. Bruhn, 1949, Tri-State Offset Co., Cincinnati.
7. "A Second-Order Shock-Expansion Method Applicable to Bodies of Revolution Near Zero Lift", C. A. Syvertson and T. H. Dennis, National Advisory Committee for Aeronautics, 1957, NACA Technical Report 1328.
8. "Computation Curves for Compressible Fluid Problems", C. I. Dailey and F. C. Wood, 1949, John Wiley & Sons, New York.
9. "Statics of Circular-Ring Stiffeners for Monocoque Fuselages", W. Stieda, National Advisory Committee for Aeronautics, February 1942, NACA Technical Memorandum 1004.
10. "Loads Imposed upon Intermediate Frames of Stiffened Shells", Paul Kuhn, National Aeronautics and Space Administration, NASA Technical Note 687.
11. "Strength of Metal Aircraft Elements", Air Force, Navy, Commerce Departments, March 1955, ANC-5 Bulletin.
12. "Mechanical Vibrations", Den Hartog, 1947, McGraw-Hill, New York.
13. "Tory IIC Data Book", 16 October 1962, University of California, Lawrence Radiation Laboratory, ~~SECRET RESTRICTED DATA~~, Reg. 22,107.
14. "Elements of the Differential and Integral Calculus", Granville, Smith, and Longley, Ginn & Co.
15. "Nuclear Ramjet Propulsion System Research and Development Report for 1962", The Marquardt Corporation, 5 January 1962, Marquardt Proposal 3067A (Vol. I), ~~SECRET RESTRICTED DATA~~, Reg. 22,400.

~~SECRET RESTRICTED DATA~~

~~ATOMIC ENERGY ACT OF 1954~~

16. "Annual Report for 1961, Nuclear Ramjet Propulsion System, Final Report," The Marquardt Corporation, 30 January 1962, Marquardt Report 876, ~~SECRET RESTRICTED DATA~~, Reg. 22,395
17. "The Uniform-Section Disk Spring", American Society of Mechanical Engineers 1936. ASME, New York, Vol. 58, No. 6.
18. "Handbook of Mechanical Spring Design", Associated Spring Corporation, Bristol, Conn., 1951.
19. "Test Report, Reactor Side Support System", The Marquardt Corporation, 1 June 1962, Marquardt Report S-276, ~~SECRET RESTRICTED DATA~~, Reg. 22,625.
20. "Engine-Airframe Lateral Attachment Test (Phase II)", The Marquardt Corporation, 31 January 1962, Marquardt Report 5960, ~~CONFIDENTIAL RESTRICTED DATA~~, Reg. 23,066.
21. "Rules for Construction of Unfired Pressure Vessels", American Society of Mechanical Engineers, 1959, ASME Boiler and Pressure Vessel Code Section VIII.
22. "A Study of the Collapsing Pressures of Thin-Walled Cylinder", R. Sturm, Illinois Institute of Technology, Bulletin 329.
23. "The Ultimate Strength of Aluminum-Alloy Formed Structural Shapes in Compression", Robert A. Needham, Journal of Aeronautical Sciences 4-54, Vol. 21, No. 4, p. 217.
24. "A Simplified Method of Elastic-Stability Analysis for Thin Cylindrical Shells", S. B. Batdorf, National Advisory Committee for Aeronautics, 1947, NACA Technical Report 874.

DECLASSIFIED IN FULL  
Authority: EO 13526  
Chief, Records & Declass Div, WHS  
Date: OCT 02 2015

~~SECRET RESTRICTED DATA~~

~~ATOMIC ENERGY ACT OF 1954~~

ASD-TDR-63-277, Vol. IV

REPORT 6003

TABLE I

TABLE OF WEIGHTS AND CENTERS OF GRAVITY FOR MA50-XCB PROPULSION SYSTEM

Item	Weight (lb)	Eng: e Station C.G.
MA50-XCB Propulsion System	16,456	477
Inlet	2,717	170
Diffuser Duct*	919	405
Reactor Control Rod Support Mechanism	297	441
Reactor and Support System	11,468	333
Exhaust Nozzle	1,054	394

\* To be furnished by manufacturer

DECLASSIFIED IN FULL  
Authority: EO 13526  
Chief, Records & Declass Div, WHS  
Date: OCT 02 2015

~~SECRET RESTRICTED DATA~~  
~~ATOMIC ENERGY ACT OF 1954~~

MAC A 633

~~SECRET-RESTRICTED DATA~~  
~~ATOMIC ENERGY ACT OF 1954~~

ASD-TDR-63-277, Vol. IV

SPORT 6003

TABLE II  
 MARGINS OF SAFETY

Item	Type of Stress	Margin
<u>Cowl</u>		
Inside skin	Tension	1.75
Outside skin	Tension	4.06
Inside skin	Compression	3.82
Leading edge	Compression	1.67
Skin (near leading edge)	Bending	0.56
<u>Diffuser Skin</u>		
Long time "limit" load	Hoop tension	0.03
Short time "ultimate" load	Hoop tension	0.26
<u>Innerbody Support Ring</u>		
Long time "limit" load	Compression	ample
Long time "ultimate" load	Compression	ample
Short time "limit" load	Compression	0.85
Short time "ultimate" load	Compression	0.62
<u>Innerbody Skin</u>		
Short time "limit" load	Compression	0.30
Short time "limit" load	Shear	ample
Long time "ultimate" load	Compression	0.05
<u>Thrust Fitting (Pin)</u>		
Short time "limit" load	Bending	0.36
Long time "limit" load	Bending	0.68
Short time "ultimate" load	Bending	0.74
<u>Reactor Support</u>		
Pressure shell	Hoop tension	ample
Shell web	Bending	0.35
Pressure pad	Bending	0.11
Pressure pad lug	Bending	ample

~~SECRET-RESTRICTED DATA~~  
~~ATOMIC ENERGY ACT OF 1954~~

MAC 4873

DECLASSIFIED IN FULL  
 Authority: EO 13526  
 Chief, Records & Declass Div, WHS  
 Date: OCT 02 2015

~~SECRET RESTRICTED DATA~~  
~~ATOMIC ENERGY ACT OF 1954~~

REPORT 6003

ASO-TDR-63-277, Vol. IV

TABLE II (Continued)

Item	Type of Stress	Margin
<u>Exit Nozzle</u>		
Forward cylinder	Hoop tension	Mimum = + 0.05
Forward cylinder	Combined bending and axial	+ 2.33
Forward cylinder	Shear	High
Throat	Combined bending and axial	+ 1.32
Forward cone	Combined bending and axial	+ 1.82
Cone-Cylinder Intersection	Combined bending and axial	+ 0.38
<u>Aft Cone</u>		
Station 636.32	Collapsing	+ 0.085
Station 623.41 to 636.32	Collapsing	+ 0.61
	Bending and Axial	High
	Shear	High
Aft Doubler	Collapsing	High
<u>Shroud</u>		
Forward cylinder	Collapsing	+ 0.70
Station 15	Collapsing	+ 0.16
Cone	Collapsing	+ 0.33
Throat	Collapsing	+ 0.39

~~SECRET RESTRICTED DATA~~  
~~ATOMIC ENERGY ACT OF 1954~~

MAC 1628

TABLE III

INERTIAL LOAD FACTORS

Parameter	Launch Conditions		Low Level Maximum Cruise		War Head Ejection	High Altitude Cruise
	At Burnout	At Separation				
Altitude	12,500	21,500	1000	1000	10,000	30,000
Mach Number	2.25	2.95	2.90	3.0	2.9	3.5
Day Condition	Hot	Hot	Hot	Cold	Hot	Cold
$\epsilon_x$	+ 6.0 - 0	+ 0 - 0.32	+ 0 - 0.3	+ 0 - 0.3	+ 0 - 0.3	+ 0.10 -
$\epsilon_y$	± 1.0	± 1.0	± 1.0	± 1.0	± 0.25	± 1.0
$\epsilon_z$	0	0	+ 4.25 - 2.25	+ 4.25 - 2.25	+ 2.8 - 0.8	+ 1.5 - 0
$w_y$	± 0.12	0	± 0.50	± 0.50	± 0.50	± 0.50
$w_z$	± 0.25	± 0.25	± 0.50	± 0.25	0	± 0.50

DECLASSIFIED IN FULL  
 Authority: EO 13526  
 Chief, Records & Declass Div, WHS  
 Date: OCT 02 2015

MAC A/E/B

~~SECRET RESTRICTED DATA~~  
~~ATOMIC ENERGY ACT OF 1954~~

ASD-TDR-63-277, Vol. IV

REPORT 6003

TABLE IV  
 INERTIA LOAD FACTORS FLIGHT MANEUVER CONDITIONS  
 (Translational Accelerations ( $g=1/2$ ) at Centers of Gravity of Propulsion System Items)

Flight Phase	Inlet			Duct			Reactor Controls			Reactor			Exit		
	$\epsilon_x$	$\epsilon_y$	$\epsilon_z$	$\epsilon_x$	$\epsilon_y$	$\epsilon_z$	$\epsilon_x$	$\epsilon_y$	$\epsilon_z$	$\epsilon_x$	$\epsilon_y$	$\epsilon_z$	$\epsilon_x$	$\epsilon_y$	$\epsilon_z$
Boost at	+6.015	+1.144	+0	+6.0	+1.0	+0.005	+6.0	+1.058	+0.051	+6.0	+1.09	+0.042	+6.0	+1.06	+0.103
Burnout	-0	-0.856	-0.0672	-0	-1.0	-0.005	-0	-1.058	-0.051	-0	-1.09	-0	-0	-1.06	-0.103
Rocket	+0	+1.091	+0	+0	+1.06	+0	+0	+1.09	+0	+0	+1.14	+0	+0	+1.18	+0
Rejection	-0.32	-1.091	-0	-0.32	-1.06	-0	-0.32	-1.09	-0	-0.32	-1.14	-0	-0.32	-1.18	-0
High Altitude Cruise	+0.164	+1.182	+1.690	+0.10	+1.12	+1.62	+0.10	+1.17	+1.67	+0.10	+1.28	+1.78	+0.10	+1.37	+1.87
Low Altitude Cruise	-0.164	-1.182	-0.190	-0.10	-1.12	-0.12	-0.10	-1.17	-0.17	-0.10	-1.28	-0.28	-0.10	-1.37	-0.37
Weapons Ejection	+0.364	+1.182	+4.44	+0.3	+1.12	+4.37	+0.3	+1.17	+4.44	+0.3	+1.5	+4.53	+0.3	+1.37	+4.62
	-0.064	-1.182	-2.44	-0	-1.12	-2.37	-0	-1.17	-2.44	-0	-1.5	-2.53	-0	-1.37	-2.62
	+0.364	+0.25	+5.50	+0.3	+0.25	+4.50	+0.3	+0.25	+5.0	+0.3	+1.5	*	+0.3	+0.25	+8.50
	-0.064	-0.25	-0.99	-0.0	-0.25	-0.92	-0.0	-0.25	-0.97	-0	-1.5	-1.08	-0	-0.25	-1.17

\* +5.77 g at reactor forward end, Fuselage Station 882.4  
 +6.68 g at reactor aft end, Fuselage Station 938.5

~~SECRET RESTRICTED DATA~~  
~~ATOMIC ENERGY ACT OF 1954~~

TABLE V  
VERTICAL LOAD FACTORS

Parameters	Low Level Maximum Maneuver	Low Level Warhead Ejection
Altitude	1000	1000
Mach Number	2.9	2.9
Day Conditions	Hot	Hot
$g_x$	+ 0.3	+ 0.3
$g_y$	± 1.5	± 1.5
$g_z$	+ 4.5 - 2.5	*

\* Values of  $g_z$  for weapons ejection at the reactor ends are as follows:

<u>Forward End</u>	<u>Aft End</u>
F.S. 882.4	F.S. 938.5
$g_z = + 5.77$	$g_z = + 6.68$

DECLASSIFIED IN FULL  
Authority: EO 13526  
Chief, Records & Declass Div, WHS  
Date: OCT 02 2015

TABLE VI  
GROUND HANDLING LOAD FACTORS

Parameter	Hoist	Transport	Erection
$E_x$	$\pm 0.25$	$\pm 5.0$	$\pm 1.0$
$E_y$	$\pm 0.25$	$\pm 0.05$	$\pm 0$
$E_z$	+ 2.67 - 0	+ 2.0 - 1.0	+ 2.0 - 1.0

DECLASSIFIED IN FULL  
Authority: EO 13526  
Chief, Records & Declass Div, WHS  
Date: OCT 02 2015

MAC ACD

TABLE VII  
ANALYTICAL DESIGN FACTORS AND FACTORS OF SAFETY

A. For temperature regimes in which time and material creep are negligible factors			
Type of Limit Stress	Material Mechanical Strength Property	Multipl Design	ig Factor Safety
Single (uniaxial) (tension, compression, etc.)	Yield or proportional limit	1.10	--
Combined stresses biaxial, or triaxial	Yield or proportional limit	1.15	--
Single or combined	Short time ultimate	--	1.25
B. For temperature regimes in which time is a major factor			
Single	Uniaxial steady state creep	1.10	--
Combined	Uniaxial steady state creep for type of stress involved	1.15	--
Single or combined	Creep rupture for type of stress involved	--	1.25
Single or combined	Fatigue for type of stress and load-temperature pattern involved	--	1.25

DECLASSIFIED IN FULL  
Authority: EO 13526  
Chief, Records & Declass Div, WHS  
Date: OCT 02 2015

MAC ADS

TABLE VIII  
WEIGHTS AND CENTERS OF GRAVITY FOR AXISYMMETRIC LET

	Weight (lbs)	Center of Engine St avity ion
Inlet Assembly	2717.1	169.9
Nose Cone (Movable parts)	145.9	88.7
Innerbody - Rings	132.8	130.6
Innerbody - Skins	219.4	137.0
Outer Structure - Rings	333.7	192.1
Outer Structure - Skins	920.0	194.8
Longerons	251.1	146.4
Attach Struts	369.2	221.0
Actuating Mechanism	345.0	111.6

DECLASSIFIED IN FULL  
Authority: EO 13526  
Chief, Records & Declass Div, WHS  
Date: OCT 02 2015

MAC 1827

**TABLE IX**  
 SECTION PROPERTIES AND LOCATIONS FOR CALCULATION OF STRESS

Item	Thickness h (av)	w	Area h · w	d from * ref line	Ad	$\bar{d}$	$\bar{A}d$	$\bar{A}d^2$	$I_0$
a	0.228	3.28	0.74900	0.700	0.52400	+0.147	+0.10980	0.016120	0.000582
b	0.400	1.762	0.70500	0.480	0.33800	-0.073	-0.05150	0.003760	0.009400
c	0.600	1.920	1.15300	0.370	0.42700	-0.183	-0.21100	0.038600	0.020000 approx.
d	0.062	0.90	0.05570	0.800	0.04450	+0.247	+0.01375	0.003400	--
e	0.062	0.90	0.05570	0.031	0.00173	-0.522	-0.02905	0.015190	--
f	0.062	2.30	0.14250	1.250	0.17800	+0.697	+0.09940	0.069400	--
g	0.062	2.30	0.14250	0.031	0.00441	-0.522	-0.07450	0.038900	--
h	0.090	1.26	0.11320	1.120	0.12720	+0.567	+0.06430	0.036500	--
j.	0.090	1.26	0.11320	0.107	0.01212	-0.446	-0.05050	0.022520	--
k	1.000	0.09	0.09000	0.600	0.05400	+0.047	+0.00423	0.000199	0.007500
l	0.062	2.30	0.14280	1.620	0.23150	+1.067	+0.15220	0.162500	--
m	0.090	1.26	0.11320	1.520	0.17200	+0.967	+0.10940	0.105800	--
n	0.062	2.30	0.14280	0.031	0.00442	-0.522	-0.07460	0.039000	--
o	0.090	1.26	0.11320	0.107	0.01212	-0.446	-0.05050	0.022550	--
p	1.200	0.09	0.10800	0.800	0.08650	+0.247	+0.02670	0.006600	0.012930
			3.93980	0.553	2.21750		+0.57958 -0.54165 +0.03793	0.581039  0.631451 in. <sup>4</sup>	0.050412

\* Reference line is at 20.188 inch radius.  
 n to N.A. = 20.100-0.222 = 19.878 inch

MAC A672

~~SECRET RESTRICTED DATA~~  
~~ATOMIC ENERGY ACT OF 1954~~

REPORT 6003

ASD-TDR-63-277, Vol. IV

TABLE X  
 MOMENTS FROM AIR LOAD

1	2	3	4	5	6
x Location (degrees)	Moment from Loading I	Moment from Loading II	Combined Moment of I and II	sin	+20 sin x-M
Centerline					
0	+ 13250	- 26500	- 13250	0	0
10	+ 12650	- 25400	- 12750	0.17	- 44500
20	+ 10500	- 21000	- 10500	0.34	- 72000
30	+ 7350	- 14650	- 7300	0.50	- 73000
40	+ 2820	- 5610	- 2790	0.64	- 35900
50	- 1910	+ 3810	+ 1900	0.76	+ 29100
60	- 6650	+ 13320	+ 6580	0.86	+114000
70	- 10850	+ 21600	+ 10750	0.94	+202000
80	- 13640	+ 27200	+ 13560	0.98	+276000
Side					
90	- 14500	+ 29000	+ 14500	1.00	+290000
100	- 13640	+ 27200	+ 13560	0.98	+276000
110	- 10850	+ 21600	+ 10750	0.94	+202000
120	- 6650	+ 13320	+ 6580	0.86	+114000
130	- 1910	+ 3810	+ 1900	0.76	+ 29100
140	- 2820	- 5610	- 2790	0.64	- 35900
150	+ 7350	- 14650	- 7300	0.50	- 73000
160	+ 10500	- 21000	- 10500	0.34	- 72000
170	+ 12650	- 25400	- 12750	0.17	- 44500
Centerline					
180	+ 13250	- 26500	- 13250	0	0
					Σ 1,900,000 Units

Notes:

Columns 2 and 3 derived from Reference 5 (Case 27 data with = 77/2).

Column 2 based on + 492 lbs/in. maximum (inward)

Column 3 based on - 984 lbs/in. maximum (outward)

(+) moments place compression on outside of ring.

Columns 2 and 3 integrate to transverse loads of 30,900 lbs, 5,450 lbs or a total transverse load of 46,350. Radial deflection, Δ, of point at x = 0 relative to a line joining points at x = 90° and x = 270° is:

$$\Delta = \frac{1,900,000}{EI} = \frac{1,900,000}{22.7 \times 10^6 \times 0.631} = 0.132 \text{ in.}$$

AMC 483

~~SECRET RESTRICTED DATA~~  
~~ATOMIC ENERGY ACT OF 1954~~

TABLE XI

TORQUE LOADS AT VARIOUS SECTIONS

Section	Distance from Centerline to fitting y	y <sup>2</sup>	Ratio y <sup>2</sup> /1534	Torque (in.-lbs)	Σ Torq
A-A	22.5	506	0.330	370,000	370 00
B-B	21.76	472	0.308	345,000	715 00
C-C	18.24	333	0.217	243,000	958 00
D-D	12.40	154	0.100	112,000	1,070 00
E-E	8.30	69	0.045	50,000	1,120 00
		1534	1.000	1,120,000	See N e

Note: These values utilized for plot (Figure 27) of torques be sustained by inlet itself.

DECLASSIFIED IN FULL  
Authority: EO 13526  
Chief, Records & Declass Div, WHS  
Date: OCT 02 2015

MAC 1077

TABLE XII

SHEARS, MOMENTS, AND TORQUES FROM Z DIRECTION COMPONENTS

1	2	3	4		
Location	x to Section A-A	x' from Centroid to Section	(x') <sup>2</sup>	Load	Joint
A-A	0	+ 77.30	5,980	22,	0
B-B	- 26.90	+ 50.40	2,540	14,	0
C-C	- 53.50	+ 23.80	566	6,	0
D-D	- 95.50	- 18.20	331	- 5,	0
E-E	-127.86	- 50.56	2,550	- 14,	0
F-F	-160.46	- 83.16	6,900	- 23,	0
	-464.22	(+) is aft centroid	18,867	(+) t	s.

DECLASSIFIED IN FULL  
Authority: EO 13526  
Chief, Records & Declass Div, WHS  
Date: OCT 02 2015

MAC 4873

~~SECRET RESTRICTED DATA~~

~~ATOMIC ENERGY ACT OF 1954~~

REPORT 6003

ASD-TDR-63-277, Vol. IV

TABLE XIII

PRESSURE CALCULATIONS

Segment Station Location	Large Area (in. <sup>2</sup> )	Small Area (in. <sup>2</sup> )	Average Δ P (psi)	Forward Load (lb)	Aftward Load (lb)	Description
-37.7 to -15	124	0	35-62 = -27	3,350		pike ithout kirt
-15 to 0	453	124	42-62 = -20	6,580		
0 to 5	610	453	110-62 = +48		7,540	
5 to 8.4	660	610	110-62 = +48		2,400	
8.4 to 18.7 Outer	730	639	110-62 = +48	4,370		pike kirt
8.4 to 18.7 Inner	730	639	62-62 = 0		0	
18.7 to 22.4	639	566	110-62 = +48	3,500		ixed Part of nner Body
22.4 to 39.06	566	453	311-62 = 249	28,100		
39.06 to 71.66	453	226	311-62 = 249	56,500		
71.66 to 89.96	226	0	311-62 = 249	56,300		
0 to 5.0	1210	1150	110-62 = 48	2,880		nner Skin of cuble Wall owling
5 to 13.2	1210	1112	110-62 = 48		4,700	
13.2 to 22.4	1112	1010	110-62 = 48		4,900	
22.4 to 39.06	1010	966	311-62 = 249		10,940	
39.06 to 71.66	966	880	311-62 = 249		21,400	
71.66 to 89.96	880	855	311-62 = 249		6,220	
0 to 5.0	1278	1150	31-62 = -31	3,970		uter Surface of cuble Wall

NOTE: These symmetrical loads are base loads on which the loads 25 to 29 and Tables XI and XII are superposed to obtain an rical load pattern.

Figures  
naysymmet-

DECLASSIFIED IN FULL  
Authority: EO 13526  
Chief, Records & Declass Div, WHS  
Date: OCT 0 2 2015

~~SECRET RESTRICTED DATA~~

~~ATOMIC ENERGY ACT OF 1954~~

MAC 6827

TABLE XIV  
JOINT LOADS

1	2	3	4	5
Location	Section A-A	x' from Centroid to Section	(x') <sup>2</sup>	P at Joint
A-A	0	+77.30	5,980	15,000
B-B	-26.90	+50.40	2,540	9,790
C-C	-53.50	+23.80	566	4,610
D-D	-95.50	-18.20	331	3,530
E-E	-127.86	-50.56	2,550	9,800
F-F	-160.46	-83.16	6,900	16,120
	-464.22	(+) is aft of centroid	18,867	(- tension)

$$\frac{\sum x}{6} = \frac{-464.22}{6} = -77.3 \text{ inches}$$

DECLASSIFIED IN FULL  
Authority: EO 13526  
Chief, Records & Declass Div, WHS  
Date: OCT 02 2015

MAC AED

~~SECRET RESTRICTED DATA~~  
 ATOMIC ENERGY ACT OF 1954

ASD-TDR-63-277, Vol. IV

REPORT 6003

TABLE XV  
 ATTACHMENT REACTIONS FROM AIRLOADS FOR THE UNSYMMETRICAL CONDITION

Fitting Point	Description and References	X	Y	Z
a Center	Figure 29 Z = -31,173 Figure 31 Z = -16,120	0	0	- 47,273
b Left	Figure 29 Z = 0.5 (-21,853) = - 10,926 Figure 28 Z = 50,000 ÷ 16.6 = + 3010 Figure 31 Z = 0.05 (-9800) = - 4900	0	0	- 12,816
c Right	Figure 29 Z = 0.5 (-21,853) = - 10,926 Figure 28 Z = -(50,000 ÷ 16.6) = - 3010 Figure 31 Z = 0.5 (-9800) = - 4900	0	0	- 18,836
d Left	Figure 29 Z = 0.5 (-12,643) = - 6321 Figure 28 Z = 112,000 ÷ 24.8 = + 4520 Figure 31 Z = 0.5 (-3530) = - 1765	0	0	- 3,566
e Right	Figure 29 Z = 0.5 (-12,643) = - 6321 Figure 28 Z = -(112,000 ÷ 24.8) = - 4520 Figure 31 Z = 0.5 (-3530) = - 1765	0	0	- 16,606
f Left	Figure 29 Z = 0.5 (-673) = - 336 Figure 28 Z = 243,000 ÷ 36.48 = + 6670 Figure 31 Z = 0.5 (4610) = + 2305	0	0	+ 8,639
g Right	Figure 29 Z = 0.5 (-673) = - 336 Figure 28 Z = -(243,000 ÷ 36.48) = - 6670 Figure 31 Z = 0.5 (4610) = + 2305	0	0	- 4,701
h Left	Figure 29 Z = 0.5 (+6,927) = + 3464 Figure 28 Z = 345,000 ÷ 43.52 = + 7920 Figure 31 Z = 0.5 (+9790) = + 4895	0	0	+ 16,279

~~SECRET RESTRICTED DATA~~  
 ATOMIC ENERGY ACT OF 1954

~~SECRET RESTRICTED DATA~~  
~~ATOMIC ENERGY ACT OF 1954~~

ASD-TDR-63-277, Vol. IV

REPORT 6003

TABLE XV (Continued)

Fitting Point	Description and References	X	Y	Z
J Right	Figure 29 Z = $0.5 (+6,927) = + 3,464$ Figure 28 Z = $-(345,000 \div 43.52) = - 7920$ Figure 31 Z = $0.5 (+9790) = + 4895$			+ 439
K Left	Figure 29 Y = $0.5 (+17,640) = 8820$ (Aft of Section A-A Joint) Figure 29 Z = $0.5 (+14,547) = + 7,278$ Figure 31 Z = $0.5(15,000) = 75,000$ Figure 28 Z = $370,000 \div 45 = + 8,220$	0	* + 8,820	+ 22,998
L Right	Figure 27 Y = $0.5 (+17,640) = 8820$ (Aft of Section A-A Joint) Figure 29 Z = $0.5 (+14,547) = + 7,278$ Figure 31 Z = $0.5 (15,000) = + 7,500$ Figure 28 Z = $370,000 \div 45 = - 8,220$	0	* + 8,820	+ 6,558
t Center	Figure 27 Y = -44,400 Figure 31 X = +145,800	** +145,800	-44,400	0

\*\* For a short time, this load could rise to 204,400 lbs (See Paragraph 3.2.5)

~~SECRET RESTRICTED DATA~~  
~~ATOMIC ENERGY ACT OF 1954~~

~~SECRET RESTRICTED DATA~~  
~~ATOMIC ENERGY ACT OF 1954~~

ASD-TDR-63-277, Vol. IV

REPORT 6003

TABLE XVI  
 SYMMETRICAL LOAD PORTION OF STEADY STATE FLIGHT CONDITION RING MOMENTS

θ	Symmetrical Load Portion				MF C <sub>1</sub> (in-lbs)
	C <sub>1</sub> P at 0°	C <sub>1</sub> P at 120°	C <sub>1</sub> P at 240°	Total	
0	- 0.24	- 0.025	- 0.025	- 0.190	- 17 00
15	- 0.12	0.065	- 0.015	- 0.070	- 6 10
30	- 0.02	0.090	- 0.050	+ 0.020	
45	0.05	0.100	- 0.072	+ 0.078	
60	0.088	0.088	- 0.075	+ 0.101	+ 9 50
75	0.10	0.050	- 0.072	+ 0.078	
80	0.090	- 0.020	- 0.050	+ 0.020	
105	0.005	- 0.120	- 0.015	- 0.070	
120	0.025	- 0.240	+ 0.025	- 0.190	- 17 00
125	- 0.015	- 0.120	+ 0.065	- 0.070	
160	- 0.050	- 0.020	+ 0.090	+ 0.020	
165	- 0.072	0.050	+ 0.100	+ 0.078	
180	- 0.075	0.088	+ 0.088	+ 0.101	+ 9 50
195	- 0.072	0.100	+ 0.050	+ 0.078	
210	- 0.050	0.090	- 0.020	+ 0.020	
225	- 0.015	0.065	- 0.120	- 0.070	
240	0.025	0.025	- 0.24	- 0.190	- 17 00
255	0.065	- 0.015	- 0.12	- 0.070	
270	0.090	- 0.050	- 0.02	+ 0.020	
285	0.100	- 0.072	0.05	+ 0.078	
300	0.088	- 0.075	0.088	+ 0.101	+ 9 50
315	0.050	- 0.072	0.100	+ 0.078	
330	- 0.020	- 0.050	0.090	+ 0.020	
345	- 0.120	- 0.015	0.065	- 0.070	- 6 10
360	- 0.240	0.025	0.025	- 0.190	- 17 00

Notes:  
 Coefficient C<sub>1</sub> is from Reference 9; (+) moment is compression on outside; PR = 8500 x 10.79 = 91,600 (from Table XI)

~~SECRET RESTRICTED DATA~~  
~~ATOMIC ENERGY ACT OF 1954~~

MAC 102

~~SECRET RESTRICTED DATA~~  
 ATOMIC ENERGY ACT OF 1954

ASD-TDR-63-277, Vol. IV

REPORT 6003

TABLE XVII  
 STEADY STATE FLIGHT CONDITION RING MOMENTS

$\phi$	Unsymmetrical		Symmetrical	Combined
	$C_1$ P at $0^\circ$	$M_p =$ $C_1 PR$ (in-lbs)	$M_p$ (in-lbs)	$M_p$ (in-lbs)
0	- 0.24	- 9,710	- 17,400	27,110
15	- 0.12	- 4,860	- 6,410	11,270
30	- 0.02			
45	0.05			
60	0.088	+ 3,560	+ 9,250	12,810
75	0.100			
90	0.090			
105	0.065			
120	0.025	+ 1,012	- 17,400	16,388
135	- 0.015			
150	- 0.050			
165	- 0.072			
180	- 0.075	- 3,040	+ 9,250	6,210
195	- 0.072			
210	- 0.050			
225	- 0.015			
240	0.025	+ 1,012	- 17,400	16,388
255	0.065			
270	0.090			
285	0.100			
300	0.088	+ 3,560	+ 9,250	12,810
315	0.050			
330	- 0.020			
345	- 0.120	- 4,860	- 6,410	11,270
360	- 0.240	- 9,710	- 17,400	27,110

Notes: Coefficient  $C_1$  is from Reference 9; (+) moment is compression on outside. For unsymmetrical portion of moments, PR is  $3,760 \times 10.79 = 40,500$  (see Figure 37). Moments for symmetrical portion of moments are carried over from Table XVI.

~~SECRET RESTRICTED DATA~~  
 ATOMIC ENERGY ACT OF 1954

MAC 1603

~~SECRET RESTRICTED DATA~~  
~~ATOMIC ENERGY ACT OF 1954~~

ASD-TDR-63-277, Vol. IV

REPORT 6003

TABLE XVIII  
 RING MOMENTS FROM SHORT TIME MANEUVER LOADS

$\phi$	Symmetrical		Unsymmetrical		Combined
	Total Cl	Moment (in-lbs)	Total Cl	Moment (in-lbs)	
0	- 0.190	- 23,960	- 0.24	- 68,100	- 92, 0
15	- 0.070	- 8,810	- 0.12	- 34,050	- 42, 0
30	+ 0.020		- 0.02		
45	+ 0.078		0.05		
60	+ 0.101	+ 12,700	0.088	+ 25,000	+ 37, 0
75	+ 0.078		0.100		
80	+ 0.020		0.090		
105	- 0.070		0.065		
120	- 0.190	- 23,960	0.025	+ 7,100	- 16, 0
125	- 0.070		- 0.015		
160	+ 0.020		- 0.050		
165	+ 0.078		- 0.072		
180	+ 0.101	+ 12,700	- 0.075	- 21,300	- 8, 0
195	+ 0.078		- 0.072		
210	+ 0.020		- 0.050		
225	- 0.070		- 0.015		
240	- 0.190	- 23,960	0.025	+ 7,100	- 16, 0
255	- 0.070		0.065		
270	+ 0.020		0.090		
285	+ 0.078		0.100		
300	+ 0.101	+ 12,700	0.088	+ 25,000	+ 37, 0
315	+ 0.078		0.050		
330	+ 0.020		- 0.020		
345	- 0.070	+ 8,810	- 0.120	- 34,050	- 42, 0
360	- 0.190	- 23,960	- 0.240	- 68,100	- 92, 0

Notes: Data are from Table XVI; (+) moment is compression outside for symmetrical portion PR = 11,698 x 10. 126,000; for unsymmetrical portion PR = 26,320 x 10. 284,000.

~~SECRET RESTRICTED DATA~~  
~~ATOMIC ENERGY ACT OF 1954~~

MAC A073

TABLE XIX

WEIGHT AND CENTERS OF GRAVITY FOR CONTROL ROD SUPPORT STRUCTURE  
AND ACTUATION MECHANISM

Item	Weight	Engine Station C	
Assembly Total	297.7	422.4 Hot* 441.4 Cold	
(a) Front Support	9.7	393.4	
(b) Main Support Assembly	28.0	419.8	
(c) Vernier Rod Strut Assemblies	9.4	419.8	
(d) Motors and Servo Valves	90.0	419.8	
(e) Linear Transducers + Housing	10.0	419.8	
(f) Torque Drive Shaft + Gears	3.2	419.8	
(g) Rack Guide Tubes	24.0	422.6	
(h) Aft Support Structure	11.5	466.6	
(j) Drive Racks	75.0	396.6 Hot 436.6 old	
(k) Spider Fittings	36.9	423.6 Hot 463.6 old	

\* "Hot refers to an operating power reactor condition; "Cold" refers to a zero power reactor condition.

DECLASSIFIED IN FULL  
Authority: EO 13526  
Chief, Records & Declass Div, WHS  
Date: OCT 02 2015

MAC 467

TABLE XX

WEIGHTS AND CENTERS OF GRAVITY FOR REACTOR AND SUPPORT SYSTEM

Item	Weight (lbs)	Engine Station C
Reactor and Support System	11,468	533.940
Core and Reflector	7,569	537.046
Tie Rods	402	531.203
Retainer Assembly	228	509.563
Base Blocks	520	565.408
Grid	900	501.186
Lateral Support Structure	1,593	536.870
Axial Support Structure	256	501.186

DECLASSIFIED IN FULL  
Authority: EO 13526  
Chief, Records & Declass Div, WHS  
Date: OCT 02 2015

~~SECRET RESTRICTED DATA~~  
~~ATOMIC ENERGY ACT OF 1954~~

ASD-TDR-63-277, Vol. IV

REPORT 6003

TABLE XXI

THERMAL EXPANSION OF TANGENTIALLY AND RADIALY ORIENTED RINGS

Expansion (radial)  
 R (Core) = 23.625 in.  
 R (Reflector) = 26.625 in.  
 R (Pressure Shell) = 28.125 in

Reactor Component	Material	End of Boost (60 sec)			Steady Stat		Cruise (300 sec)	
		Temp. °F	Coef/Exp.	Δ R	Temp. °F	Co	/Exp	Δ R
Core	Fueled BeO	2570	$5.65 \times 10^{-6}$	0.3345	2570	5.	$\times 10^{-6}$	0.3345
Zone 1	Unfueled BeO	*		0.0046	1890	5.	$\times 10^{-6}$	0.0046
Zone 2	Unfueled BeO			0.0066	1490	4.	$\times 10^{-6}$	0.0066
Zone 3	Unfueled BeO			0.0091	1390	4.	$\times 10^{-6}$	0.0091
TOTAL				0.3548				0.3548
Tangential System								
Exp. Shell	Rene' 41	360	$6.8 \times 10^{-6}$	0.0525	1500	8.	$\times 10^{-6}$	0.322
Radial Diff.	Rene' 41	360	$6.8 \times 10^{-6}$	0.302	1500	8.	$\times 10^{-6}$	0.033
Diam. Diff	Rene' 41	360	$6.8 \times 10^{-6}$	0.604	1500	8.	$\times 10^{-6}$	0.066
Circ. Diff.	Rene' 41	360	$6.8 \times 10^{-6}$	1.895	1500	8.	$\times 10^{-6}$	0.207
Radial System								
Pressure Shell	Rene' 41	300	$6.8 \times 10^{-6}$	0.0439	1200	7.	$\times 10^{-6}$	0.248
Radial Diff.				0.311				0.107

\* Reflector expansion assumed the same as cruise.

MAC 633

~~SECRET RESTRICTED DATA~~  
~~ATOMIC ENERGY ACT OF 1954~~

TABLE XXII

SUMMARY OF CRITERIA

(Inertia Load Factors Taken from Section 2.0)

Condition	Spring Temperature (°F)	Relative Thermal Expansion		Inertia Load Factor (g)	Type of Load
		Radial System (in.)	Tangential System (in.)		
Ground Handling	70	0	0	3.75	Static *
Boost	70	0	0	3.00 (RMS)	Random vibration
Boost Transition	380	0.311	0.302	3.00 (RMS) 2.25	Random vibration Static*
High Altitude Cruise	1400	0.107	0.033	2.25 (RMS) 4.16	Random vibration Static*
Low Altitude Cruise	1400	0.107	0.033	2.25 (RMS) 5.95 7.0 (Peak)	Random vibration Static* Sinusoidal vibration at 9 cps

\* Conservatively assumed static.

DECLASSIFIED IN FULL  
Authority: EO 13526  
Chief, Records & Declass Div, WHS  
Date: OCT 02 2015

MAC 487

~~SECRET RESTRICTED DATA~~  
~~ATOMIC ENERGY ACT OF 1954~~

ASD-TDR-63-277, Vol. IV

OUT 6003

TABLE XXIII  
 TABLE OF DYNAMIC TEST RUNS "NOMINAL CONDITIONS"

Run No.	Temperature (°F)	Type of Test	Frequency Range	"g" Load	Duration of Run (min)	Comments
1	Ambient	Sine wave sweep	5-500	0.5 RMS	10	Check out } A-C noise interference
2	Ambient	Sine wave sweep	5-500	0.75 RMS	10	Check out }
3	Ambient	Sine wave sweep	5-2000	1 RMS	15	Low response
4	Ambient	Sine wave sweep	5-500	2 RMS	11	
5	Ambient	Sine wave sweep	5-500	3 RMS	11	
6	Ambient	Sine wave sweep	500-13	4 RMS	9	Broke shaker head support brace - repaired
7	Ambient	Flat random	20-500	3 RMS overall	10	
8	400-1130	Sine wave sweep	500-5	3 RMS	15	Lost 3 of 8 high temperature accelerometers
9	400-1130	Flat random	20-500	3 RMS overall	10	
10	1100-1380	Sine wave sweep	500-5	3 RMS	10	
11	1100-1380	Flat random	20-500	3 RMS overall	10	

MAC 4673

~~SECRET RESTRICTED DATA~~  
~~ATOMIC ENERGY ACT OF 1954~~

TABLE XXIV  
ACCELEROMETER RESPONSE  
(Run No. 4)

Input Frequency (cps)	Input gRMS	Response gRMS							
		A-10	A-3	A-4	A-5	A-6	A-7	A-8	A-9
12	0.55*	1.70*	0*	--	1.5*	--	0.3	0.8	0.8
15	0.65*	2.1	0.3*	0.26*	1.85*	--	0.9	1.1	1.8
20	0.75*	2.3	0.85*	0.60*	2.0*	--	1.6	1.1	1.3
25	0.85*	2.30*	0.85*	0.44*	2.0*	--	0.88	1.2	1.3
30	1.0*	2.05*	0.65*	0.52*	1.9*	--	1.0	1.6	1.2
35	1.20*	1.75*	0.40*	--	1.70*	--	1.0	1.2	2.0
40	1.25*	1.65*	0.30*	--	1.70*	--	0.75	1.0	1.2
80	1.5	2.0	1.2	1.5	2.0	1.6	1.0	2.0	2.0
140	1.7	3.0	0	1.8	2.5	2.4	2.0	2.0	2.5
200	2.5	3.2	4.0	2.0	3.5	3.0	--	3.8	2.5
250	2.3	4.0	3.6	2.0	3.0	3.5	--	3.5	--
320	2.2	3.8	1.2	2.0	2.5	2.5	--	2.4	1.0
400	2.2	2.5	0.80	1.0	1.0	0.80	2.5	1.0	1.50
440	1.7	3.0	0.80	0.70	1.2	0.50	1.0	1.0	1.60
500	1.5	2.6	1.8	0.60	1.0	0.70	0.50	2.0	)

\* Frequency analyzed.

DECLASSIFIED IN FULL  
Authority: EO 13526  
Chief, Records & Declass Div, WHS  
Date: OCT 0 2 2015

MAC 4873

TABLE XXV  
ACCELEROMETER RESPONSE.  
(Run No. 10)

Input Frequency (cps)	Input BRMS	Response BRMS					9
		A-10	A-3	A-4	A-5	A-8	
12	0.95*	2.2*	--	--	--		
15	1.0*	2.45*	0.5	0.2	0.8	6	
20	1.0*	2.65*	--	--	--		
25	1.0*	2.75*	2.0	0.8	0.5	4	
30	1.1*	2.70*	2.2	2.0	1.0	8	
35	1.2*	2.65*	--	--	--		
40	1.5*	2.50*	2.5	1.0	1.0	0	
80	3.0	--	3.0	1.0	1.5	0	
140	3.0	--	3.0	2.5	2.5	0	
200	3.1	5.5	3.0	2.5	--	7	
250	2.9	--	2.5	1.7	--	0	
320	2.7	--	3.0	1.0	0.5	5	
400	2.0	--	3.0	0.8	1.0	5	
440	1.7	--	1.0	1.0	1.0	5	
500	2.0	4.5	1.5	1.5	1.0	0	

\* Frequency analyzed.

DECLASSIFIED IN FULL  
Authority: EO 13526  
Chief, Records & Declass Div, WHS  
Date: OCT 02 2015

MAC 607

TABLE XXVI

WEIGHTS AND CENTERS OF GRAVITY FOR EJECTOR EXHAUST NOZZ

Item	Weight (lb)	Engine Station
Exhaust Nozzle Assembly	1054	594.2
Primary Shell	370.9	618.9
Secondary Shell	239.5	587.7
Lock Ring	178.4	568.1
Attach Ring	162.1	571.0
Ring Assembly - Expansion	41.0	565.8
Stiffener Ring - Aft	9.1	660.3
Stiffener Ring - Forward	8.4	654.3
Stiffener Ring - Intermediate	7.9	646.3
Stiffener Ring - Intermediate	6.1	636.3
Drag Brace (12 required)	8.7	573.9
Pylon (8 required)	9.0	613.3
Support Doubler (8 required)	11.8	613.9
Fitting - Inner (8 required)	1.1	663.4

DECLASSIFIED IN FULL  
Authority: EO 13526  
Chief, Records & Declass Div, WHS  
Date: OCT 02 2015

MAC A603

TABLE XXVII  
REQUIRED MATERIAL THICKNESS

Exit Station	Internal Radius (in.)	Nozzle Interior* (psia)	$\Delta p$ (psi)	$t_{reqd} \frac{(\Delta p)}{78,000}$ (in.)
0	28.06	320	260	0.093
5	28.06	300	240	0.086
10	28.06	292	232	0.083
15	28.06	288	228	0.081
20	28.06	286	226	0.080
22	27.80	284	224	0.079
24	26.70	283	223	0.076
26	25.50	282	222	0.075
28	24.40	280	220	0.068
30	23.20	279	219	0.064
32	22.10	277	217	0.061
34	21.00	275	215	0.057
36	19.90	273	213	0.054
38	18.70	270	210	0.050
40	17.70	266	206	0.046
42	16.90	262	202	0.043
44	16.40	258	198	0.041
46	16.20	254	194	0.040
48	16.10	248	188	0.036
52	16.40	77	17	0.003

\* Airframe cooling annulus pressure profile assumed uniform at 60 psia (Figure 110).

MAC ASST

~~SECRET RESTRICTED DATA~~

~~ATOMIC ENERGY ACT OF 1954~~

ASD-TDR-63-277, Vol. IV

6003

TABLE XXVIII

SHROUD PRESSURE AND TEMPERATURE DATA

(Low Altitude Cruise at Mach 3.22 and 1,000 ft, ICAO Standard D)

Engine Station	Inner Surface	Outer Surface	Pressure (psia)	Temperature (°F)
0	320	254	66	1350
570.470	300	254	46	1350
575.470	296	254	38	1350
585.470	286	258	28	1355
587.24	284	258	26	1360
590.470	283	256	27	1380
595.470	279	252	27	1420
600.470	274	241	33	1465
605.037	267	216	51	1520
611.289	254	126	128	1550
613.413	249	109	140	1550
615.87	160	90	70	1490
616.969	81	81	0	--

**DECLASSIFIED IN FULL**  
**Authority: EO 13526**  
**Chief, Records & Declass Div, WHS**  
**Date: OCT 02 2015**

~~SECRET RESTRICTED DATA~~

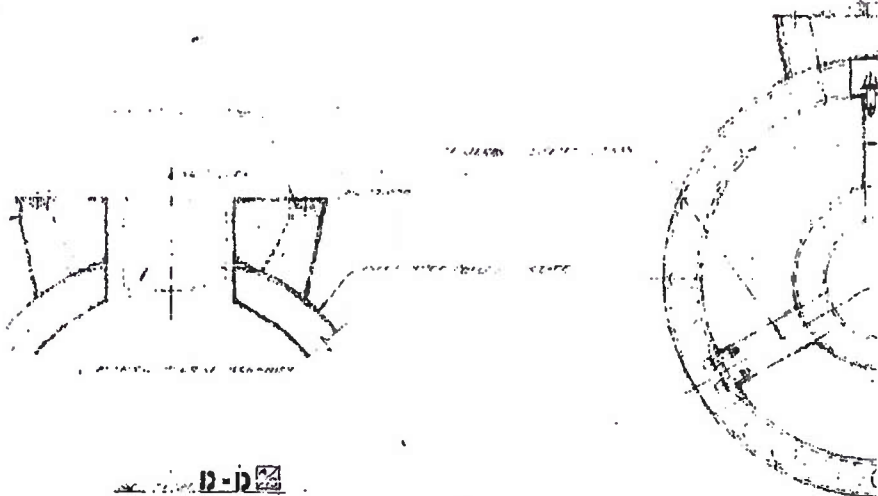
~~ATOMIC ENERGY ACT OF 1954~~

MAC 433

ASD-OR-63-277, Vol. IV  
~~SECRET RESTRICTED DATA~~  
~~ATOMIC ENERGY ACT OF 1954~~

DECLASSIFIED IN FULL  
Authority: EO 13526  
Chief, Records & Declass Div, WHS  
Date: OCT 02 2015

1

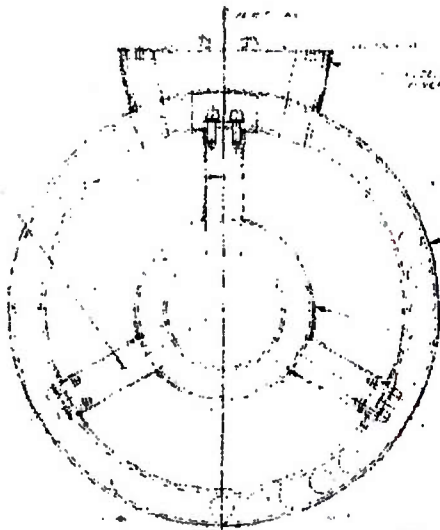


~~SECRET RESTRICTED DATA~~  
~~ATOMIC ENERGY ACT OF 1954~~

12-D

2

DECLASSIFIED IN FULL  
Authority: EO 13526  
Chief, Records & Declass Div, WHS  
Date: OCT 02 2015

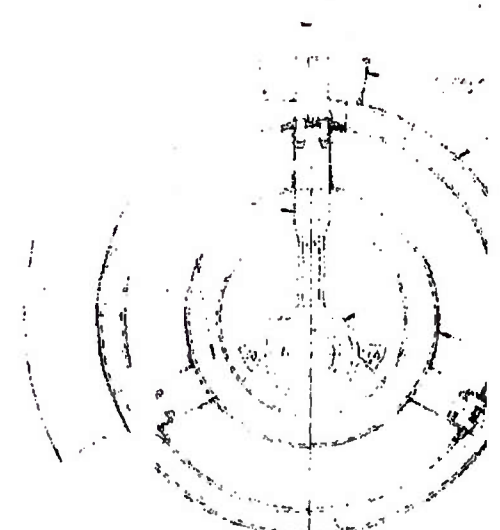


G-C

X81420

20

11



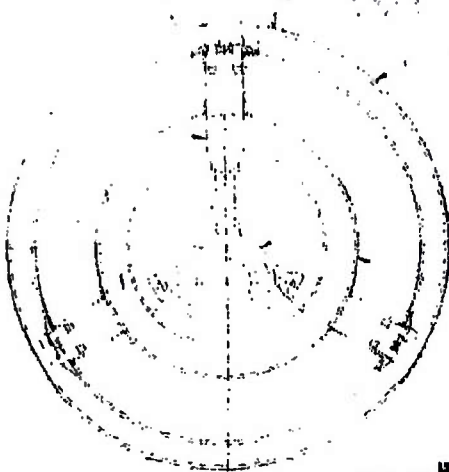
19

**3**

**DECLASSIFIED IN FULL**  
**Authority: EO 13526**  
**Chief, Records & Declass Div, WHS**  
**Date: OCT 02 2015**

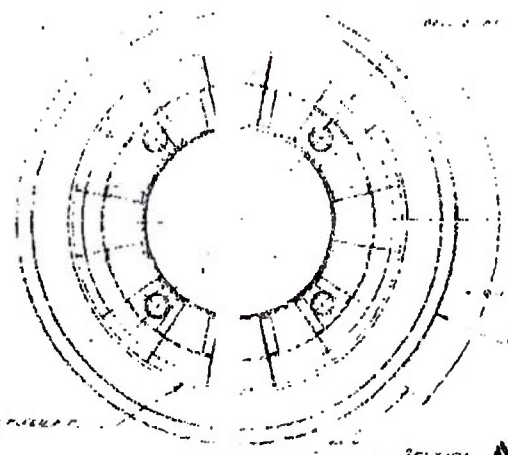
SECRET

E-12



B-B

19



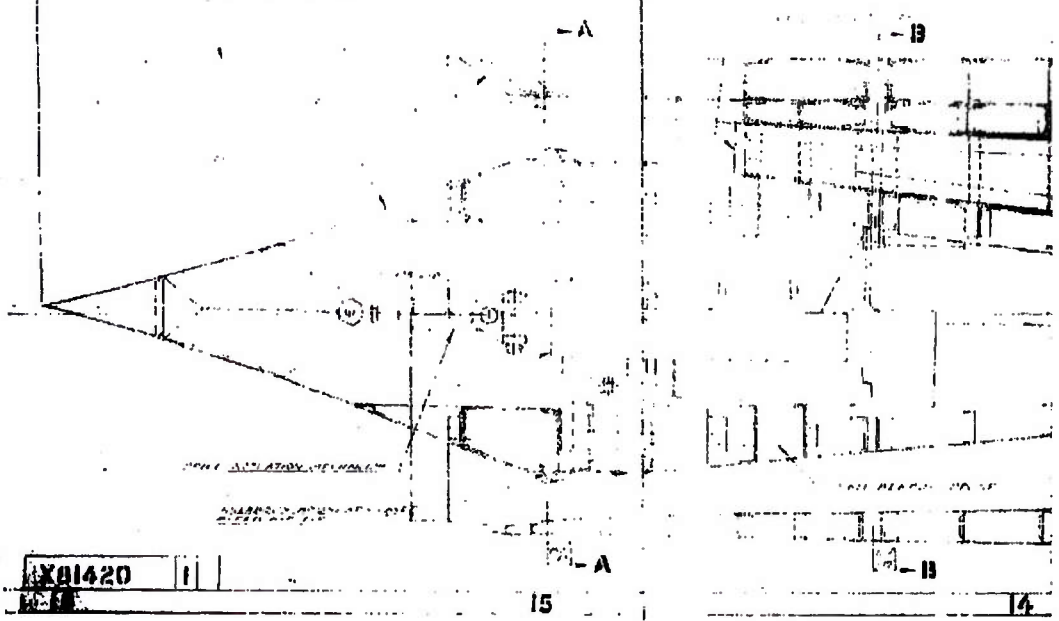
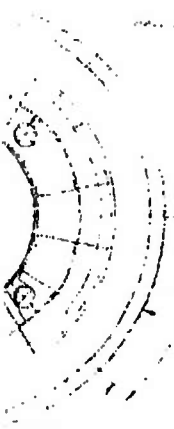
A-A

18

17

4

DECLASSIFIED IN FULL  
Authority: EO 13526  
Chief, Records & Declass Div, WHS  
Date: OCT 02 2015



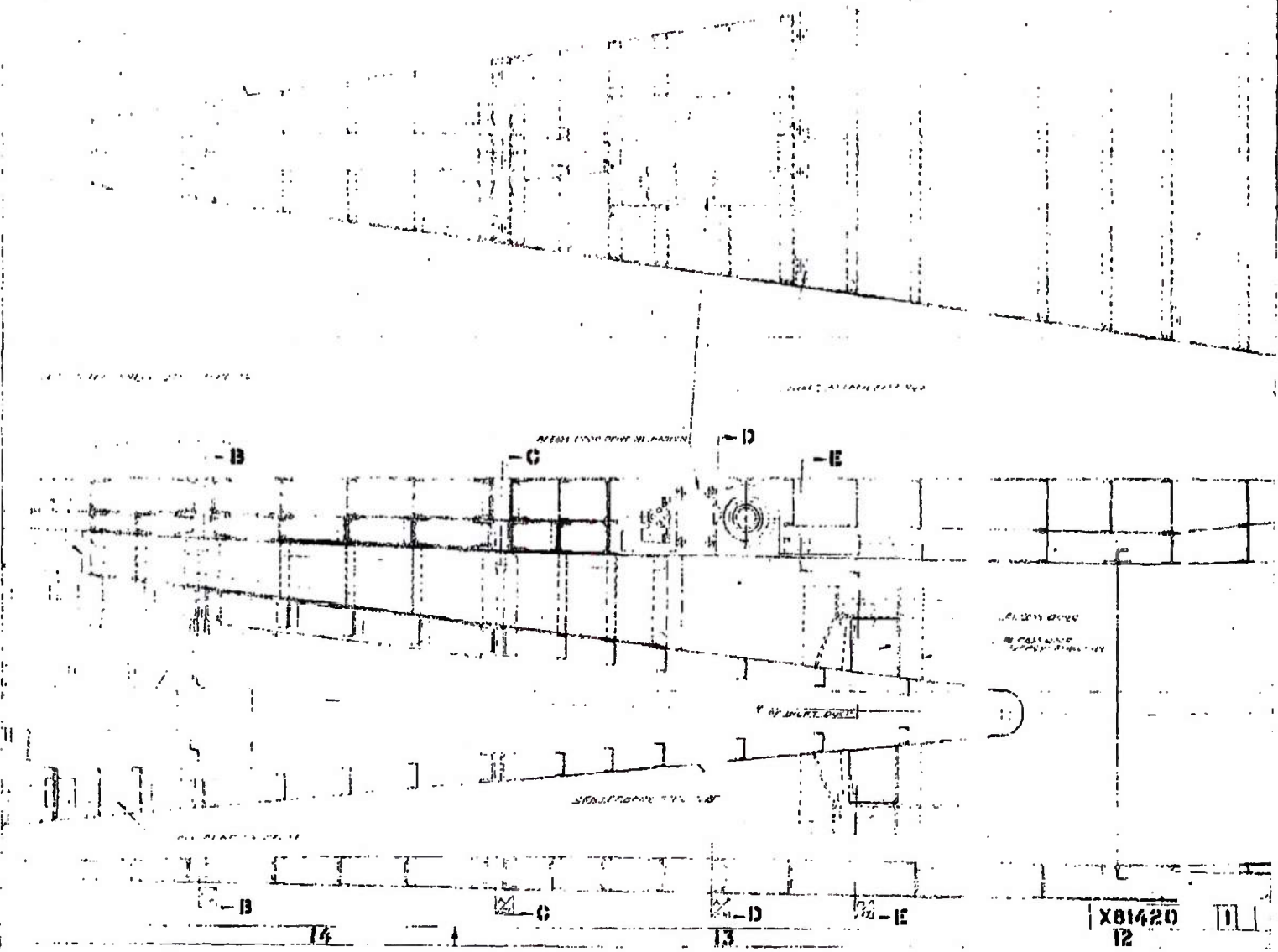
17

X81420

15

14

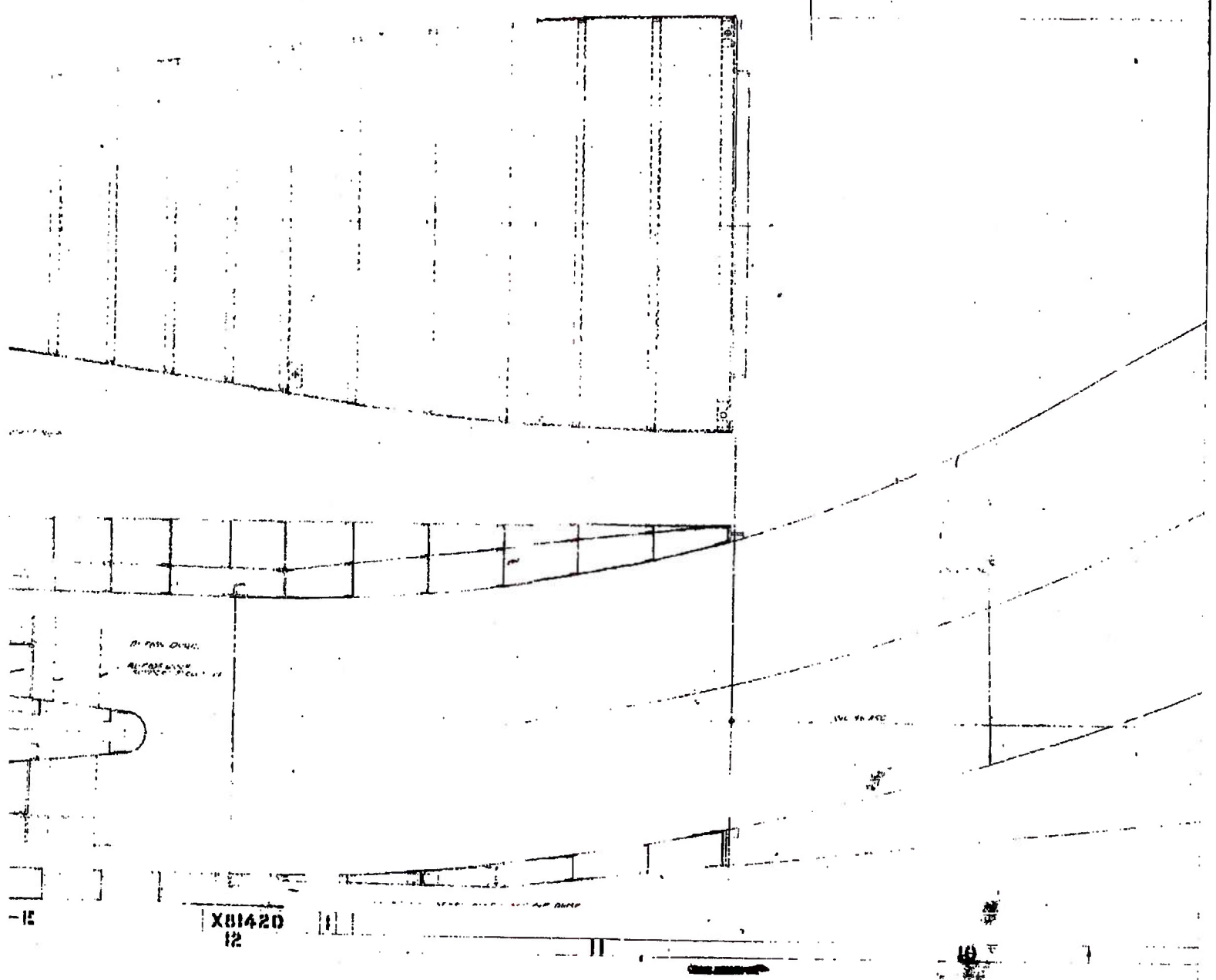
5



DECLASSIFIED IN FULL  
Authority: EO 13526  
Chief, Records & Declass Div, WHS  
Date: OCT 02 2015

X81420  
12

6



X81420  
12

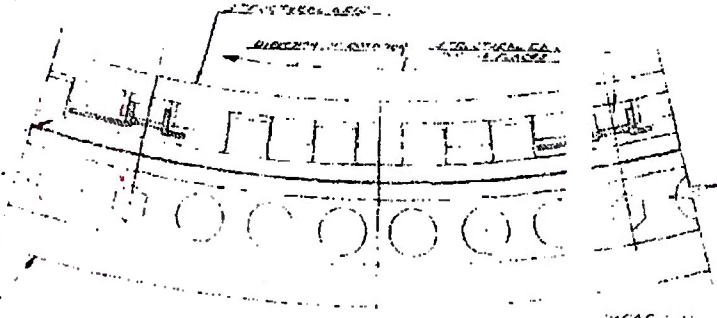
DECLASSIFIED IN FULL  
Authority: EO 13526  
Chief, Records & Declass Div, WHS  
Date: OCT 02 2015

7

P. 0002

SHEAR STRESS  
WASHER PLATE  
POSITION

0.0001000 11.0

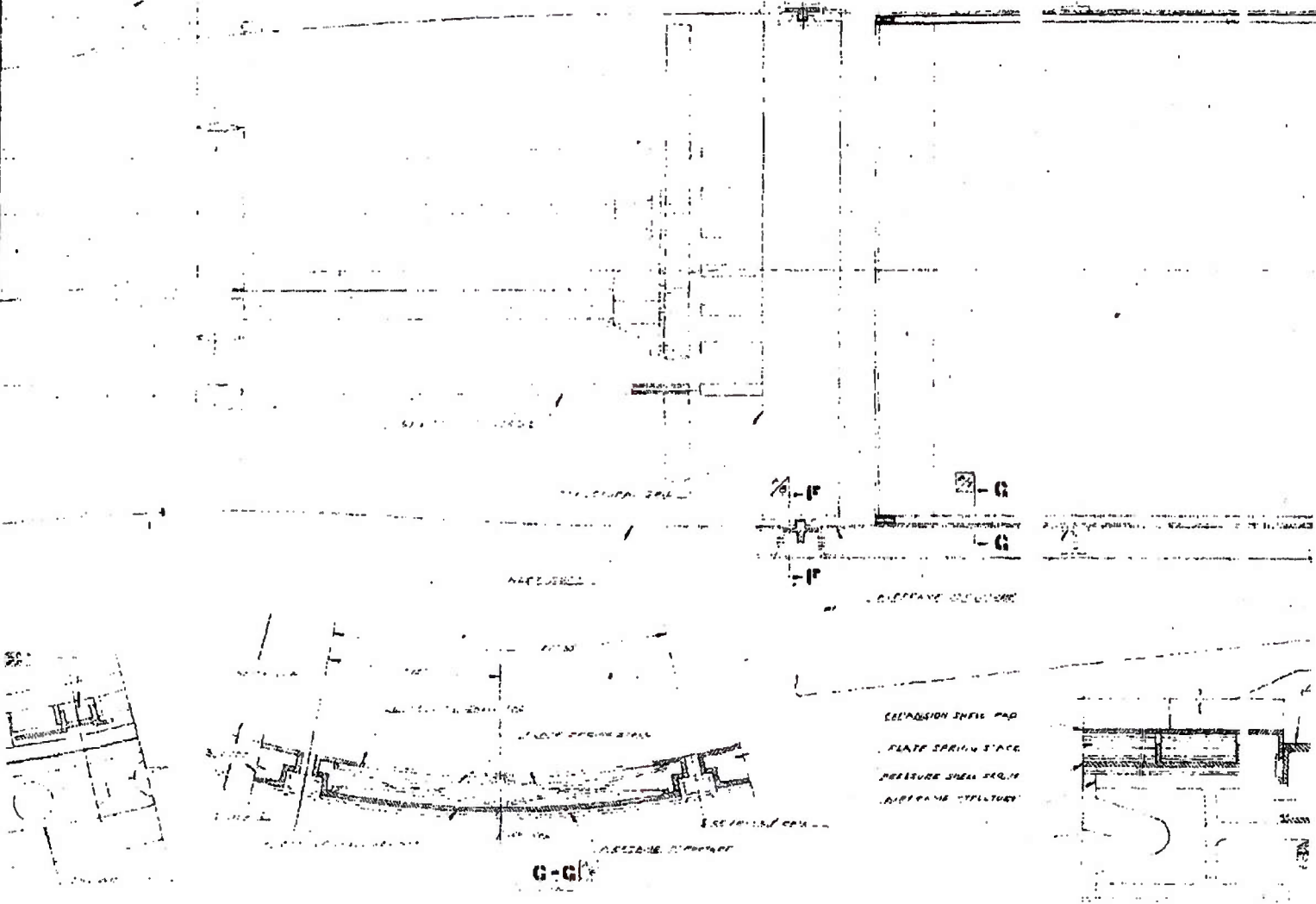


F-F

X01420

DECLASSIFIED IN FULL  
Authority: EO 13526  
Chief, Records & Declass Div, WHS  
Date: OCT 02 2015

8



7

6

5

DECLASSIFIED IN FULL  
Authority: EO 13526  
Chief, Records & Declass Div, WHS  
Date: OCT 02 2015



# 10

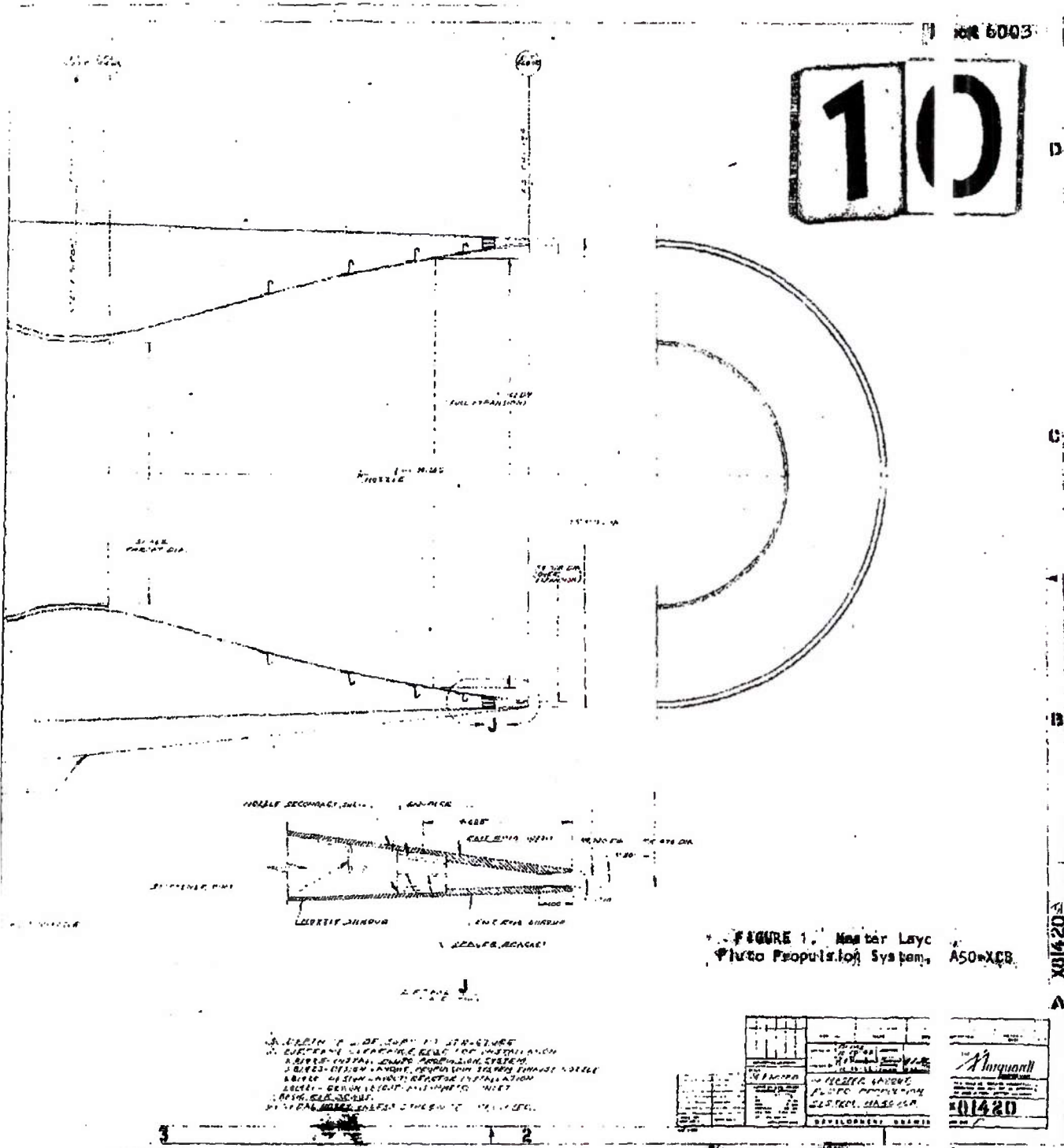


FIGURE 1. Moderator Layer  
Pilot Propulsion System, A50-XCB

1. DESIGN OF THE CORE STRUCTURE  
 2. DETERMINE THE REACTOR CRITICALITY  
 3. DETERMINE THE REACTOR PERIOD  
 4. DETERMINE THE REACTOR TEMPERATURE  
 5. DETERMINE THE REACTOR PRESSURE  
 6. DETERMINE THE REACTOR FLOW RATE  
 7. DETERMINE THE REACTOR CONTROL SYSTEM  
 8. DETERMINE THE REACTOR SAFETY SYSTEM  
 9. DETERMINE THE REACTOR MAINTENANCE SYSTEM  
 10. DETERMINE THE REACTOR OPERATING PROCEDURE

REV	DATE	BY	CHKD
1			
2			
3			
4			
5			
6			
7			
8			
9			
10			

DEVELOPMENT NUMBER  
 101420

~~SECRET RESTRICTED DATA~~  
~~ATOMIC ENERGY ACT OF 1954~~

HEADLINE  
(TERRAIN AVOIDANCE  
ANTENNA AREA)

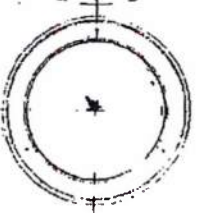
TERRAIN AVOIDANCE ANTENNA  
(AREA)

LONGITUDINAL STABILIZER

ELEVATOR AREA

PERSONAL AREA

REL. 48.850

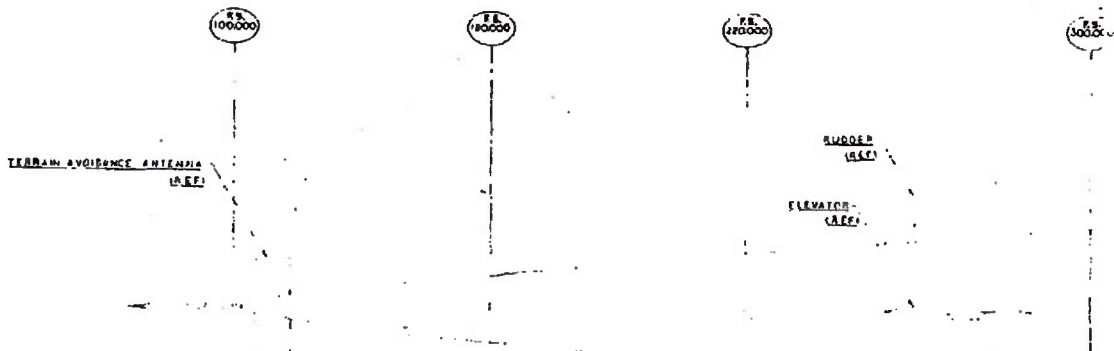


NEW LOOKING AREA

1

DECLASSIFIED IN FULL  
Authority: EO 13526  
Chief, Records & Declass Div, WHS  
Date: OCT 02 2015

~~SECRET RESTRICTED DATA~~  
~~ATOMIC ENERGY ACT OF 1954~~



**2**

**DECLASSIFIED IN FULL**  
 Authority: EO 13526  
 Chief, Records & Declass Div, WHS  
 Date: OCT 02 2015

X81425 1

13

12

11

CG. OF -MI J. ARSCHW  
ONISHIZ. IIT. PUMOR

F.S.  
168000

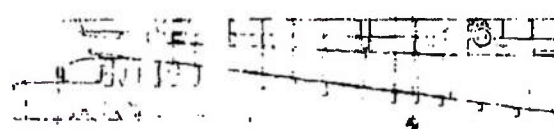
F.S.  
168000

F.S.  
168000

F.S.  
168000

F.S.  
168000

SHOULDER  
WHEEL  
ELEVATOR  
TRUCK



MULTI-PLATE

CRANK POSITION FULLY EXTENDED

SOME POSITION FULLY RETRACTED

SEE FIG. 108 AND MECHANISMS

91

**3**

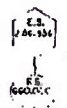
**DECLASSIFIED IN FULL**  
Authority: EO 13526  
Chief, Records & Declass Div, WHS  
Date: OCT 02 2015

10

9

C.O.P. PROJ  
25107112

C.G. OF INLET ASSEMBLY  
(WEIGHT: 1712.1 POUNDS)



C.G. OF  
DIFFUSER  
(WEIGHT: )

ISOLIC  
DUCT  
(WEIGHT: )

C.G. OF CONTROL  
SUPPORT STRUCTURE  
(WEIGHT: 121.000 POUNDS)



REACTION CONT.  
REACTION CONT.  
AND MECHANISM

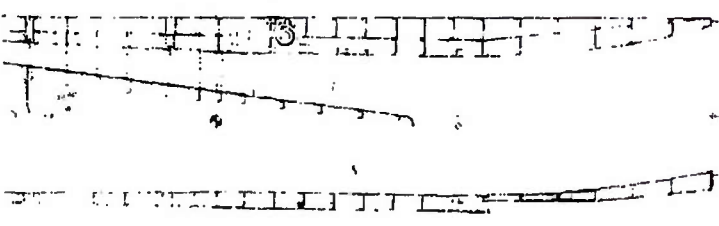
ACTUATOR

REACTIONAS (UNIT WEIGHT)

AIRFRAME, OUTER W.

INTERNAL STRUCTURE

DIFFUSER BODY  
ACTUATOR  
MECHANISM



W. # 153

DIFFUSER BODY  
ACTUATOR MECHANISM

AXIAL SUPPORT  
STRUCTURE MODEL OF C

DIFFUSER

BOUNDARY LAYER  
BASED RADIATION

4

DECLASSIFIED IN FULL  
Authority: EO 13526  
Chief, Records & Declass Div, WHS  
Date: OCT 02 2015

X81425

ALL INFORMATION CONTAINED  
HEREIN IS UNCLASSIFIED EXCEPT WHERE SHOWN  
OTHERWISE

CG. OF PROPELLION SYSTEM  
(WEIGHT: 16,455.8 POUNDS)



CG. OF SUBSONIC  
QUEEN'S DUCT  
(WEIGHT: 9,183 POUNDS)



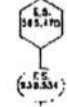
CG. OF CONTROL  
SUPPORT STRUCTURE  
(WEIGHT: 1,117 POUNDS)



CG. OF REACTOR AND  
ASSOCIATED SUPPORT STRUCTURE  
(WEIGHT: 11,835 POUNDS)



CG. OF EXIT NOZZLE  
(WEIGHT: 1,054.2 POUNDS)

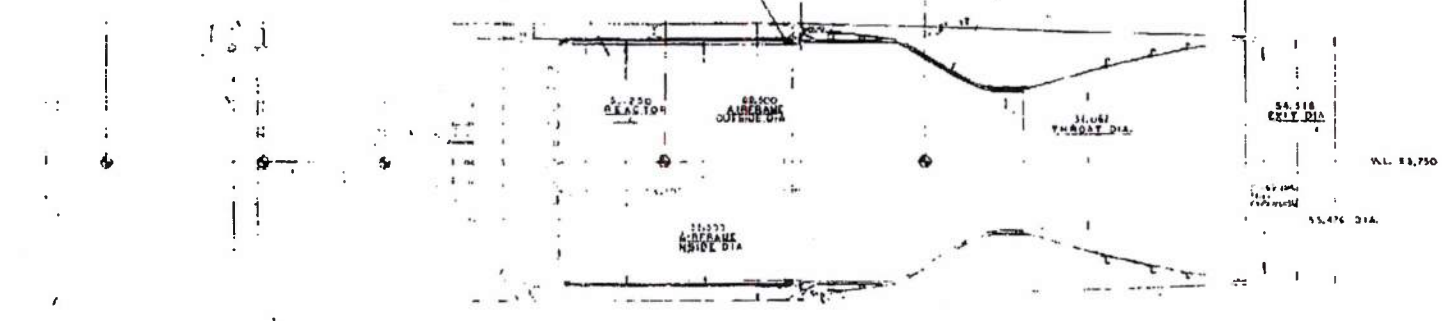


QUADRANTAL AIRVALVES  
ON CONTROL  
SYSTEM

REACTOR ASSEMBLY (MODIFIED FOR TEST)

REACTOR ASSEMBLY  
(MODIFIED FOR TEST)

EXIT NOZZLE (EJECTOR)  
REACTOR



SHEAR BOND, PINE #1  
SHEAR LIFTING BOND #1

EXHAUST NOZZLE ATTACH  
PINE #1 SHEAR BOND #1

SUPPORT SYSTEM  
TRACK AND RAIL, PINE #1

REA. SUPPORT  
STRUCTURE MODIFIED FOR TEST

5

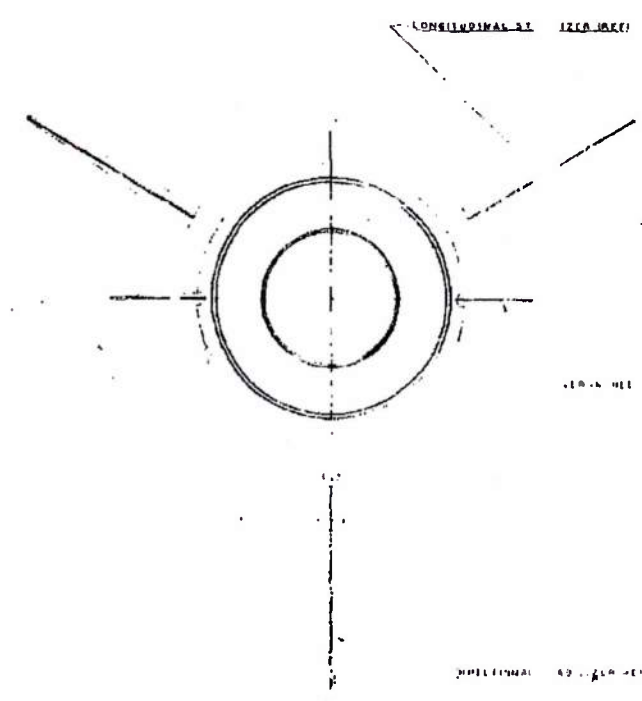
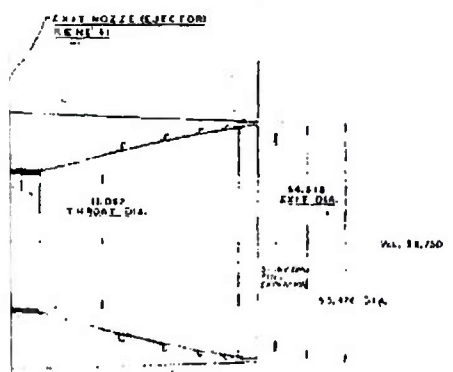
[REDACTED]

[REDACTED]

X 81425

DECLASSIFIED IN FULL  
Authority: EO 13526  
Chief, Records & Declass Div, WHS  
Date: OCT 02 2015

S.E.  
(N.R.S.)



ATTACH  
NE II  
STEM  
A. RING II

LOOKING FORWARD

6

Pluto

DECLASSIFIED IN FULL  
Authority: EO 13526  
Chief, Records & Declass Div, WHS  
Date: OCT 02 2015

X 81425

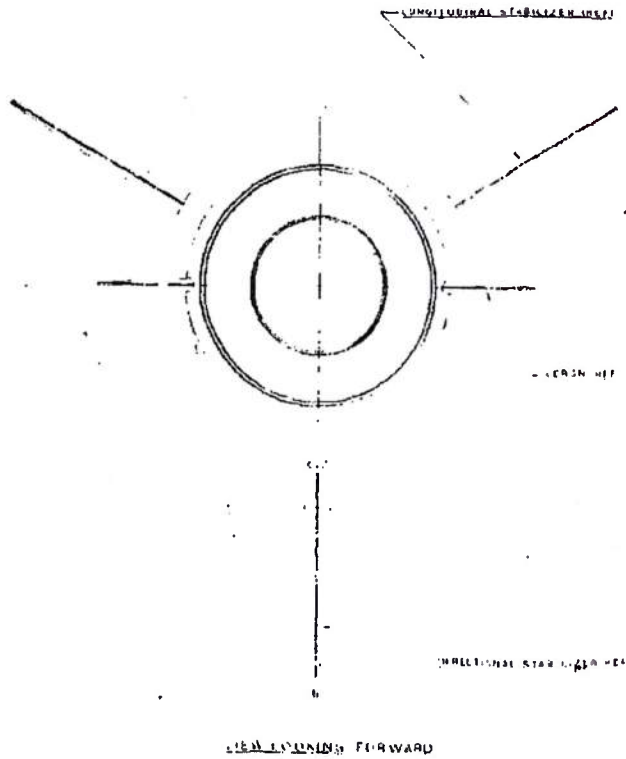
4

3

2

- 143-6-11-97

Report 6003



7

FIGURE 2. Installation  
Pluto Propulsion System, MA50-XCB

MA50-XCB PLUTO PROPULSION SYSTEM 666	X81425
--	--------

DECLASSIFIED IN FULL  
 Authority: EO 13526  
 Chief, Records & Declass Div, WHS  
 Date: OCT 02 2015

~~SECRET RESTRICTED DATA~~

~~ATOMIC ENERGY ACT OF 1954~~

ASD-TDR-63-277, Vol. IV

REPORT 6003

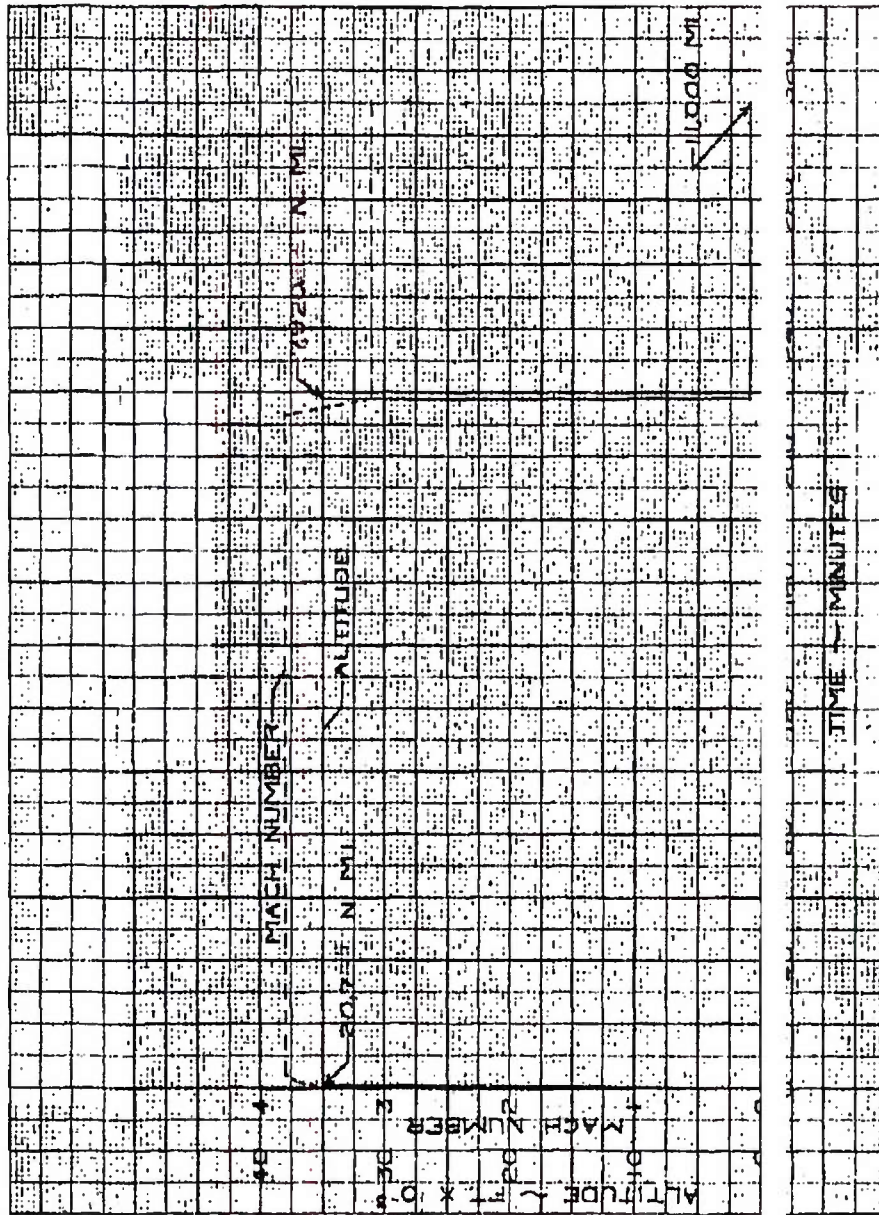


FIGURE 3. Typical Mission Profile for 11,000 Nautical Miles (ICAO Standard Day)

MAC 4622

~~SECRET RESTRICTED DATA~~

~~ATOMIC ENERGY ACT OF 1954~~

N22E643

- 145 -

DECLASSIFIED IN FULL  
Authority: EO 13526  
Chief, Records & Declass Div, WHS  
Date: OCT 02 2015

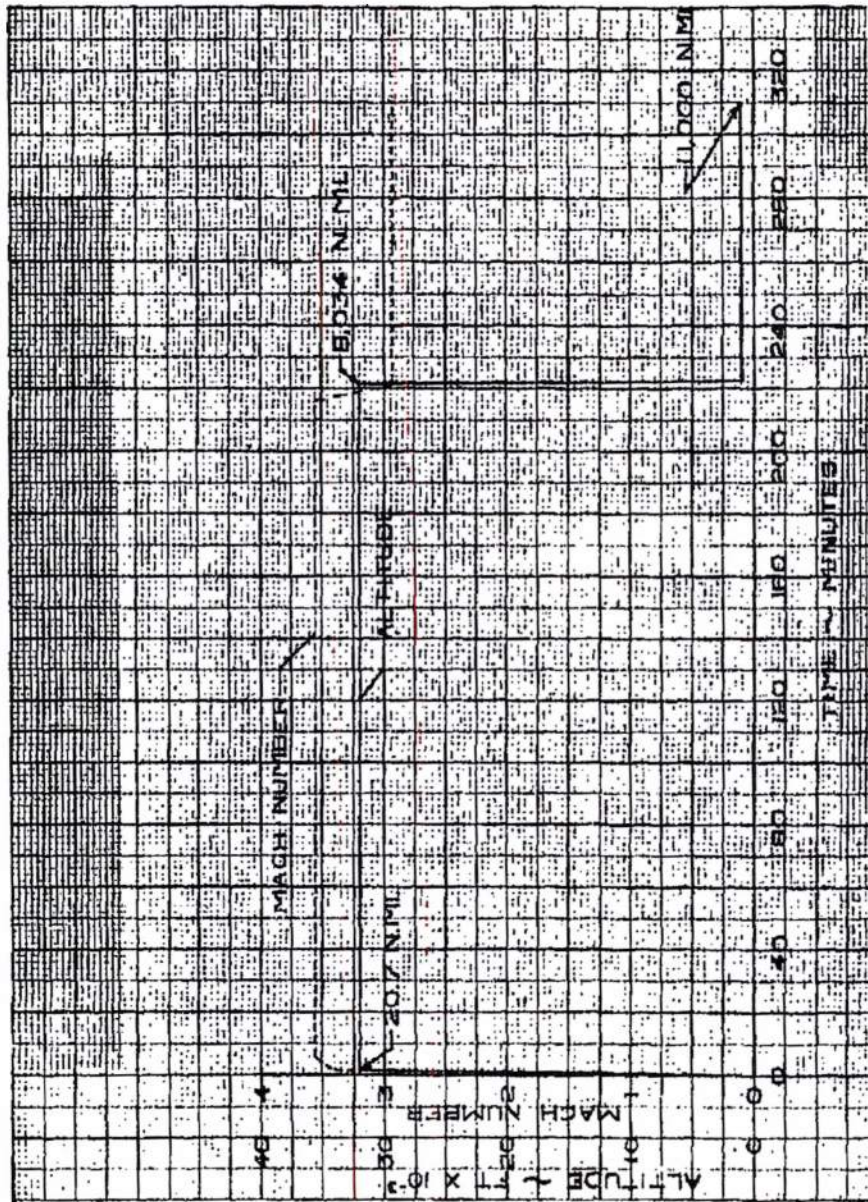


FIGURE 4. Typical Mission Profile for 11,000 Nautical Miles (ANA Hot Day)

MAC 407

~~SECRET RESTRICTED DATA~~  
~~ARMED SERVICES ACT OF 1954~~

REPORT 6003

ASD-TDR-63-277, Vol. IV

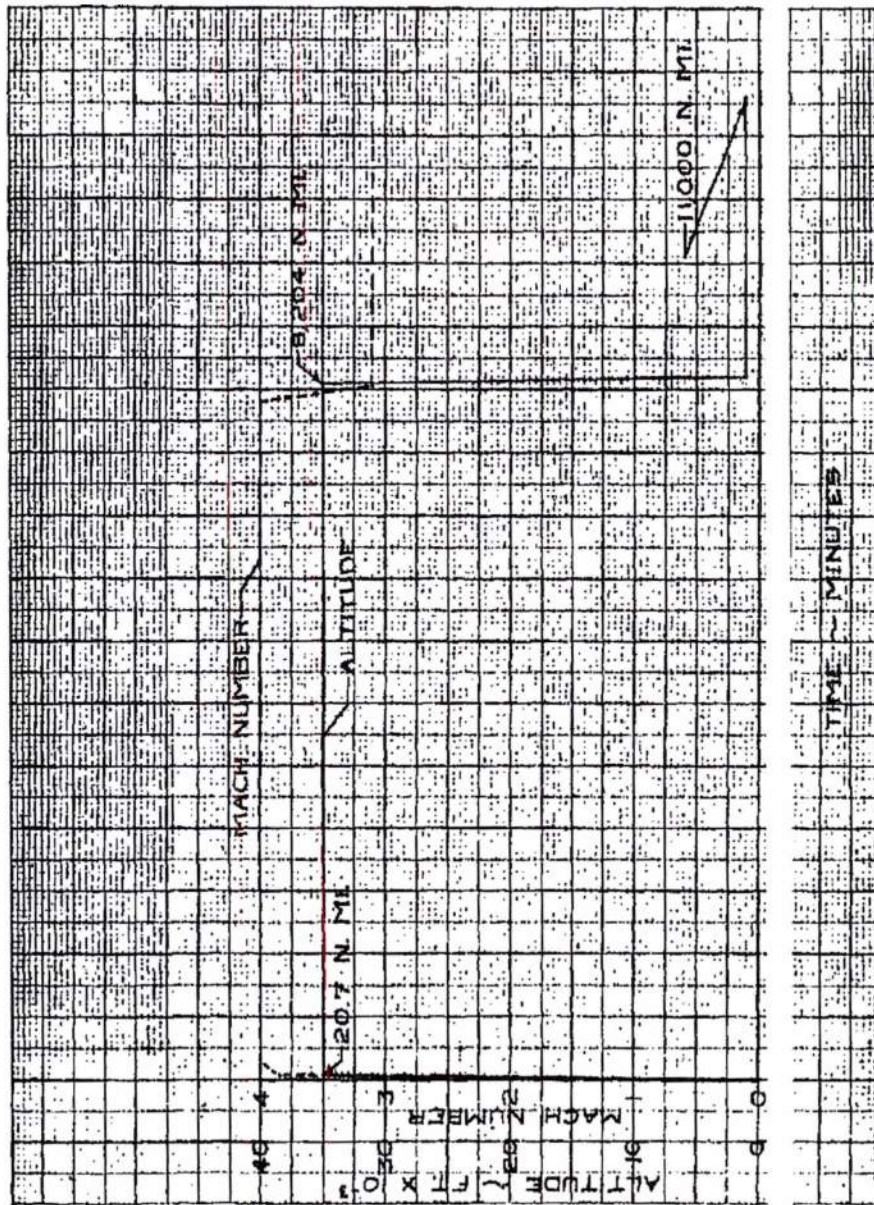


FIGURE 5. Typical Mission Profile for 11,000 Nautical Miles (ANA Cold Day)

MAC 4472

~~SECRET RESTRICTED DATA~~  
~~ARMED SERVICES ACT OF 1954~~

N22E645

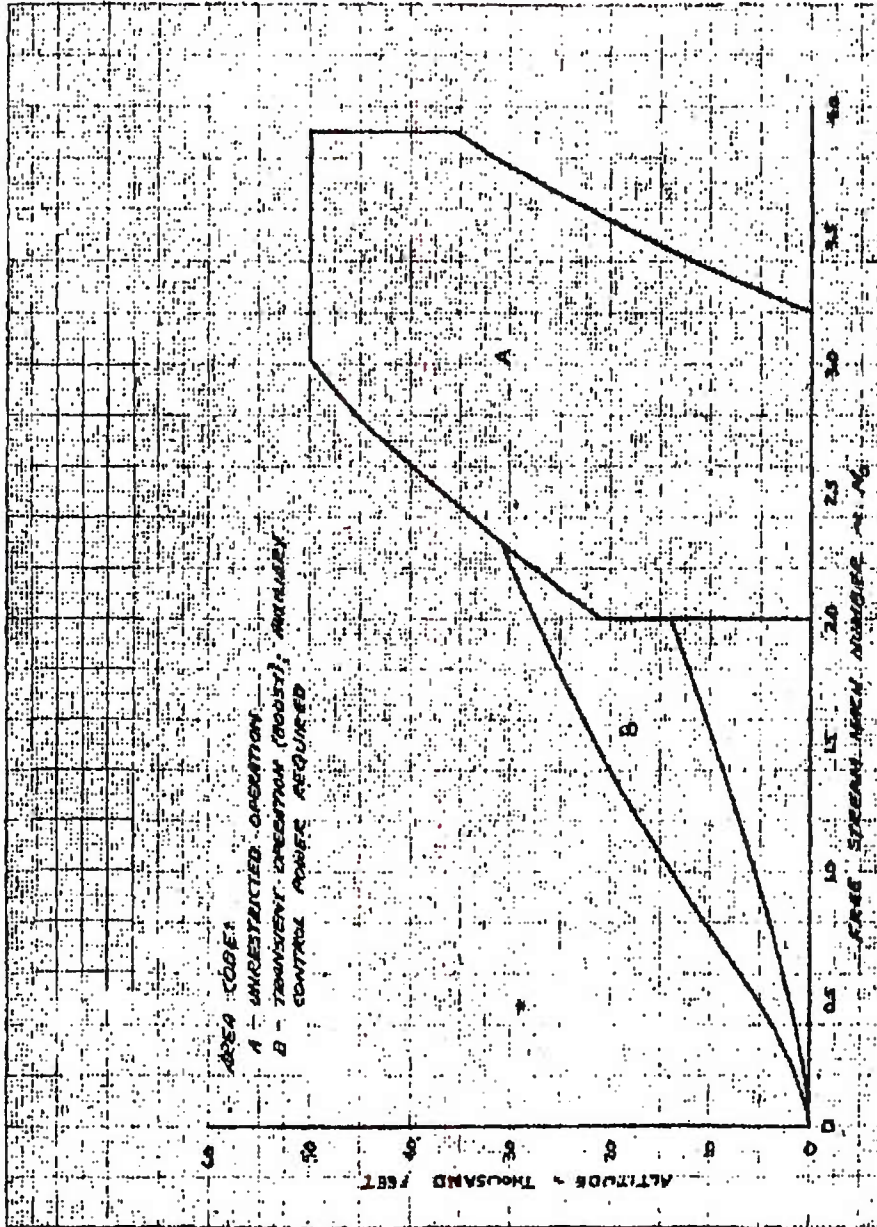


FIGURE 6. Estimated Operating Envelope for Marquardt Model MA50-XCB Ramjet (ICAO Standard Day)

MAC 402

DECLASSIFIED IN FULL  
Authority: EO 13526  
Chief, Records & Declass Div, WHS  
Date: OCT 02 2015

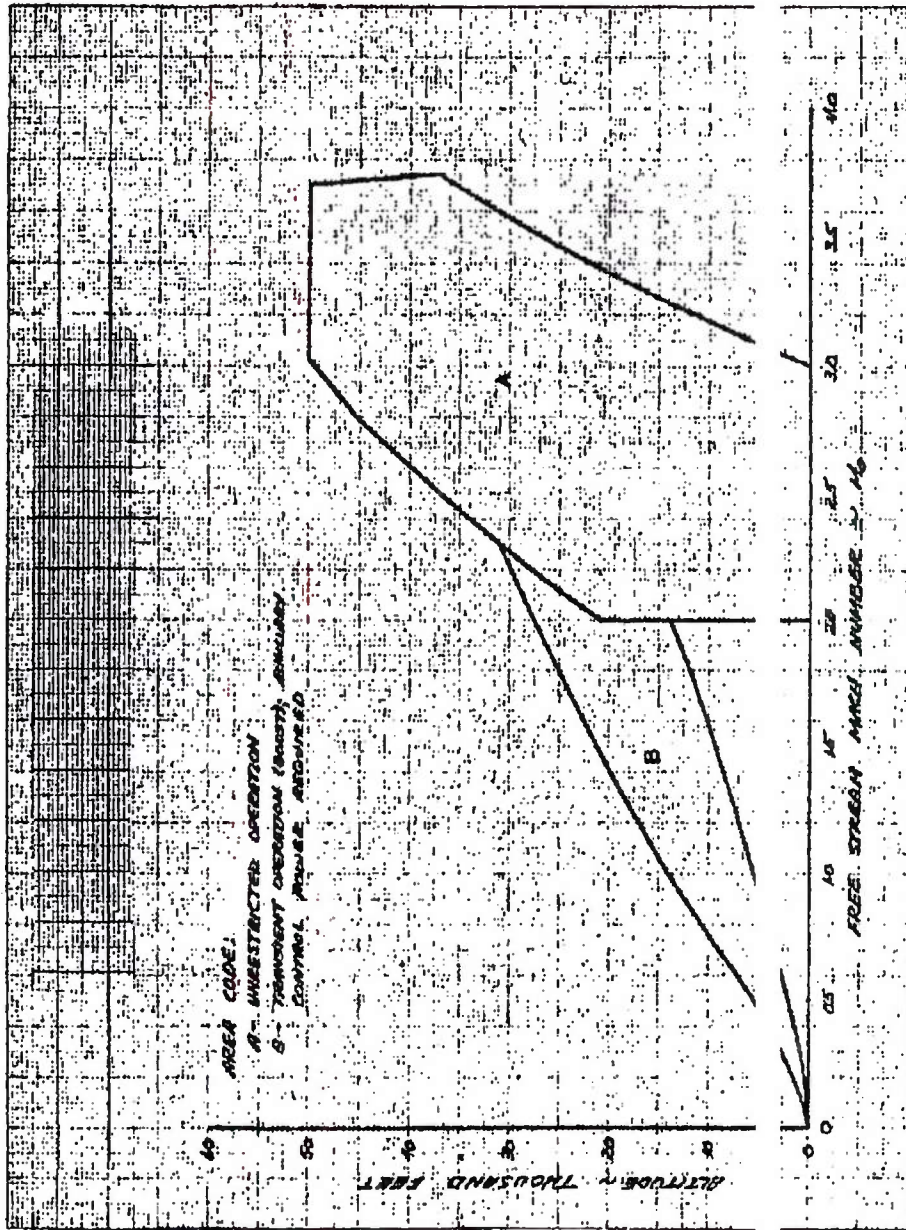


FIGURE 1. Estimated Operating Envelope for Marquardt Model MA50-XCB Ramjet (ANA Hot Day)

MAC A32

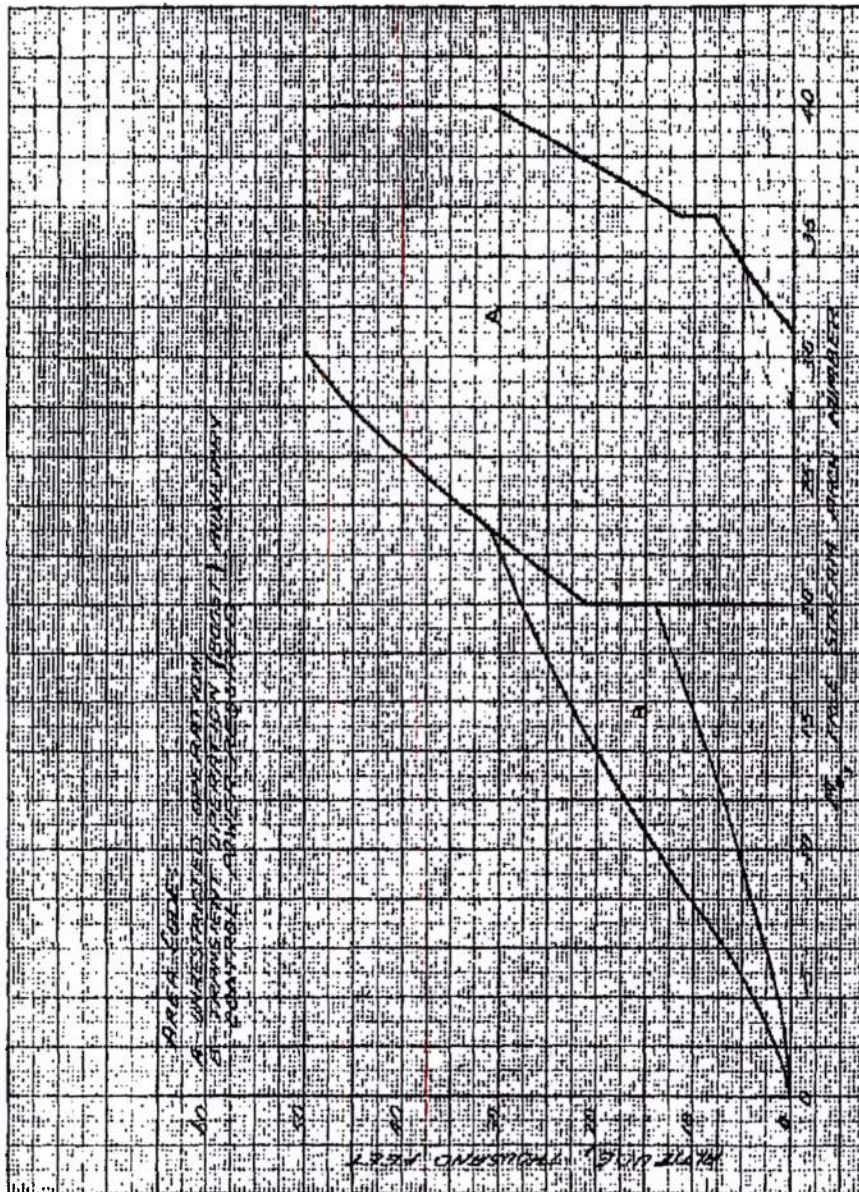


FIGURE 8. Estimated Operating Envelope for Marquardt Model MA50-XCB Ramjet (AWA Cold Day)

MAC 1473

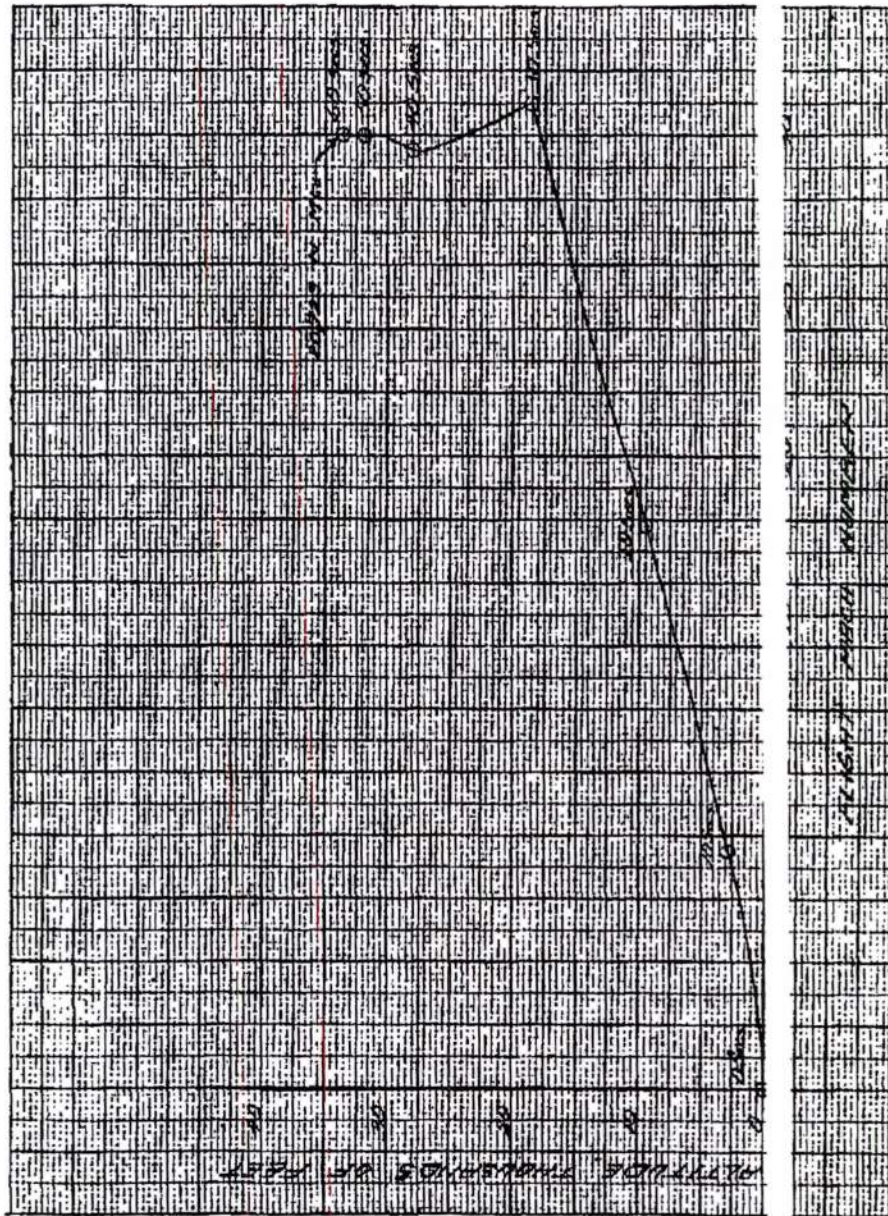


FIGURE 9. Typical Pluto Boost Trajectory

MAC 603

ASD-TDR-63-277, Vol. IV

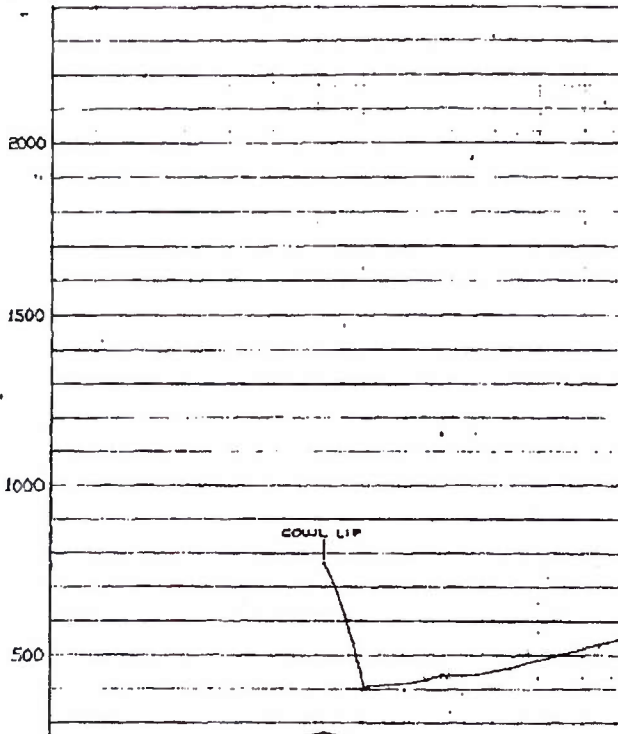
~~SECRET RESTRICTED DATA~~  
~~ATOMIC ENERGY ACT OF 1954~~

D

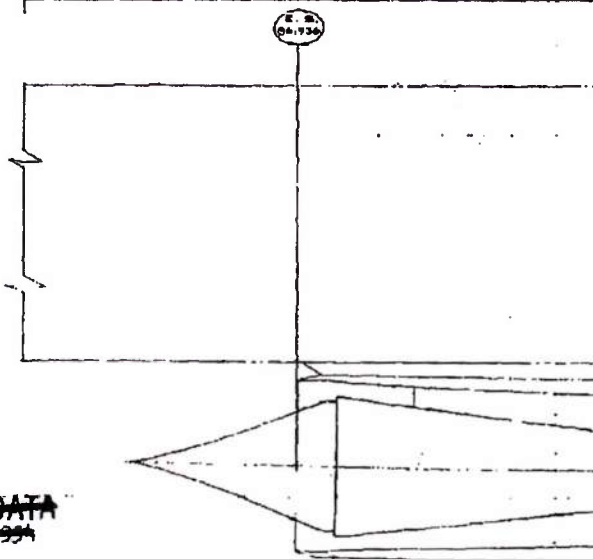
C

B

A



1



~~SECRET RESTRICTED DATA~~  
~~ATOMIC ENERGY ACT OF 1954~~

B

7

6

DECLASSIFIED IN FULL  
Authority: EO 13526  
Chief, Records & Declass Div, WHS  
Date: OCT 02 2015

2

COLL. LIP

E. D.  
08-734

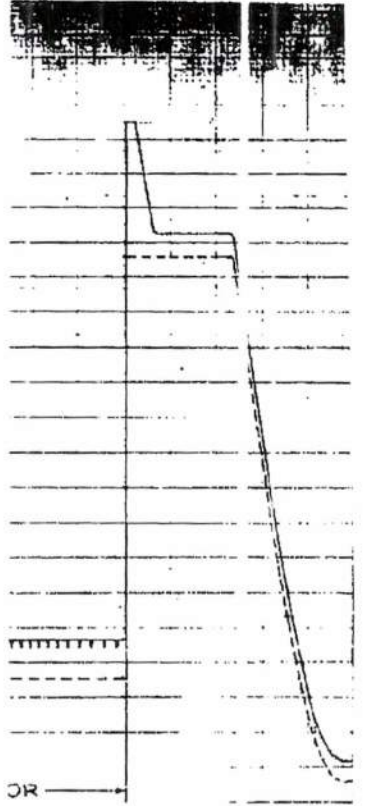
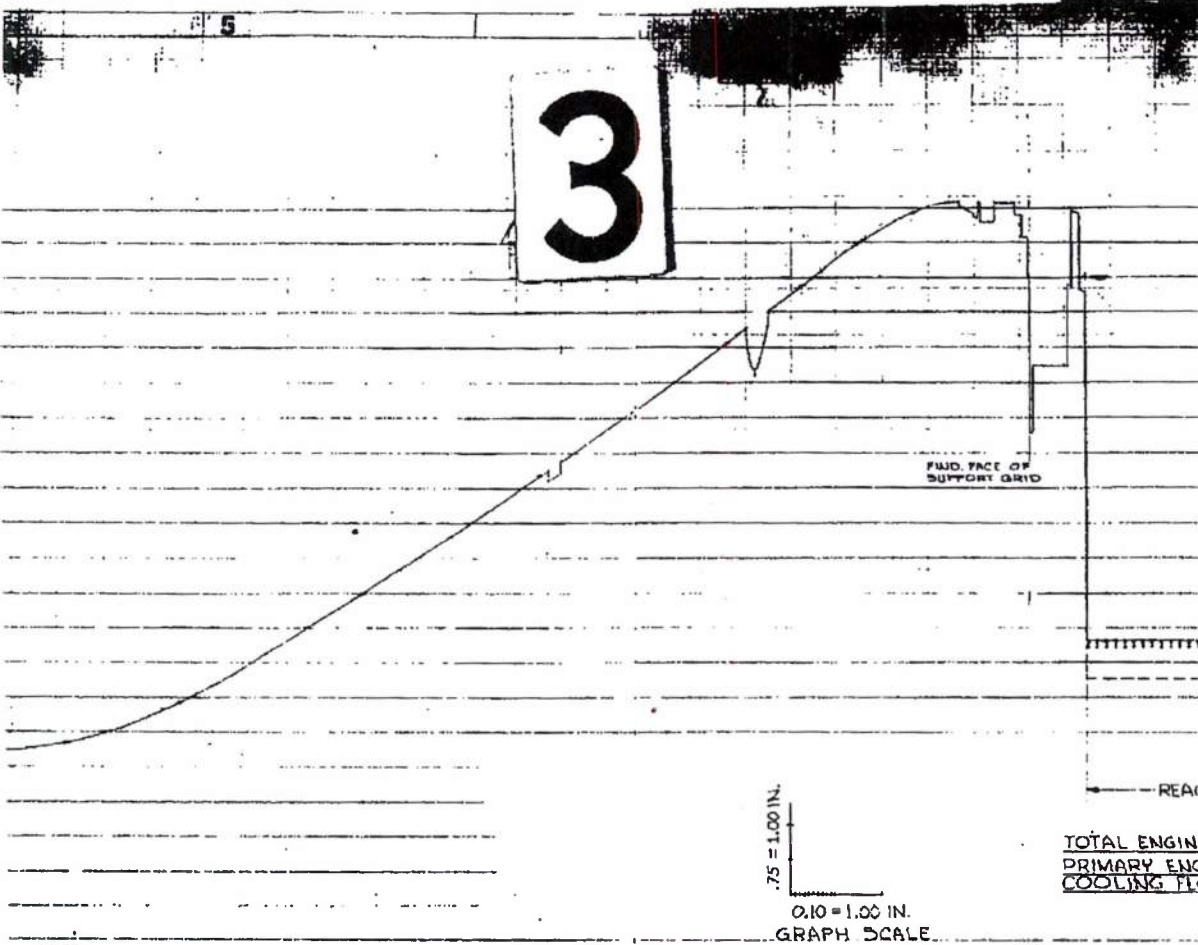
E. D.  
08-734

FLOW AREA ASSUMED NORMAL  
AT INTERSECTION OF CENTER

TO DUCT CENTERLINE  
L.V. STATION

DECLASSIFIED IN FULL  
Authority: EO 13526  
Chief, Records & Declass Div, WHS  
Date: OCT 02 2015

3



TOTAL ENGINE FLOW AREA  
 PRIMARY ENGINE FLOW AREA  
 COOLING FLOW AREA

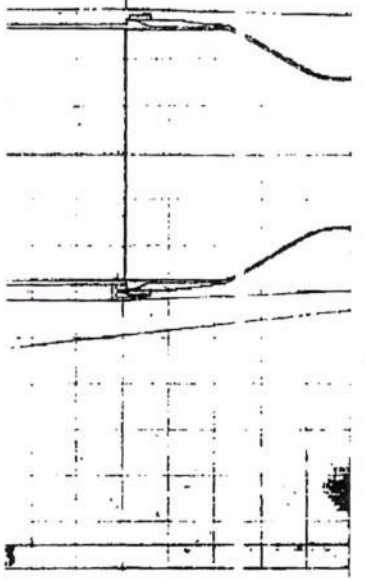
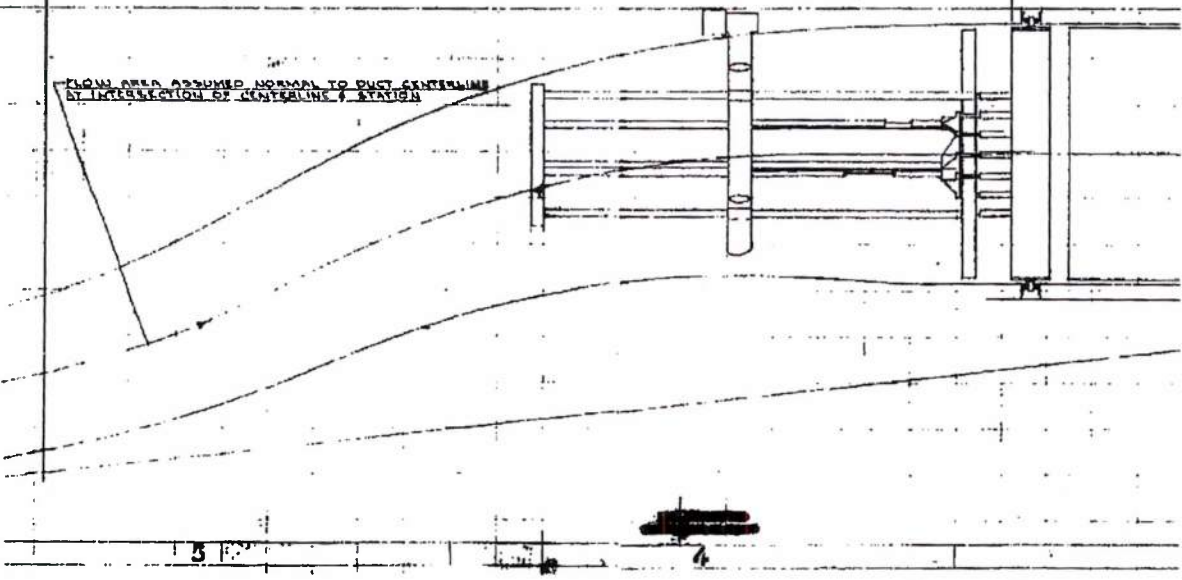
NET FLOW AREA DEFINED BY:  
 THE NET FLOW AREA DEFINED BY  
 THE DIFFERENCE BETWEEN THE

0.75 = 1.00 IN.  
 0.10 = 1.00 IN.  
 GRAPH SCALE

E. S. 476-914

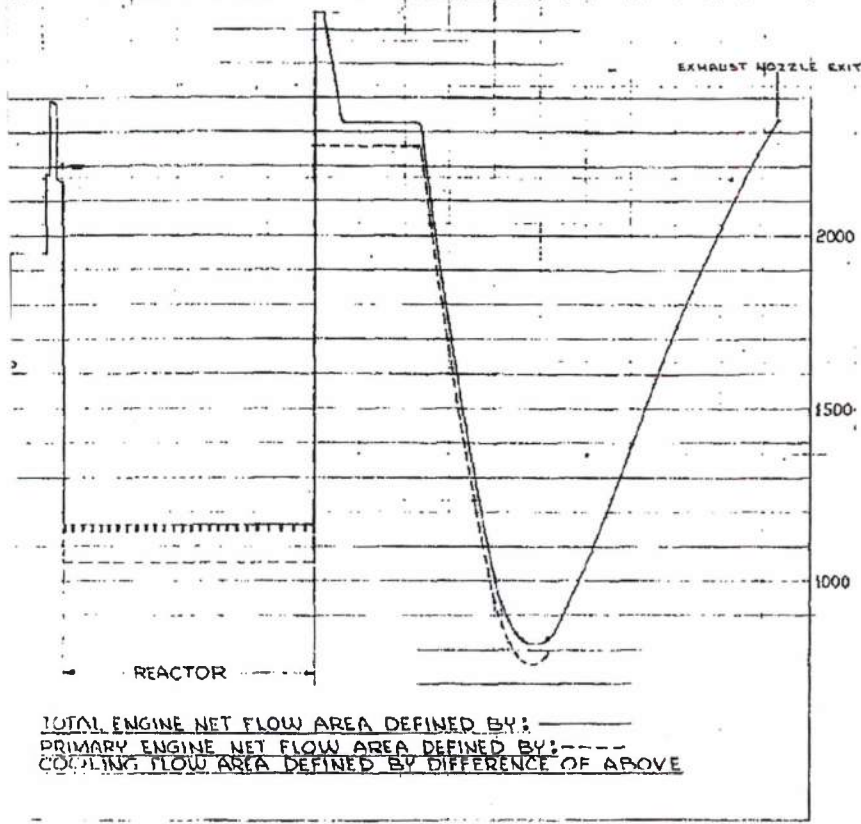
E. S. 476-914

E. S. 476-914



DECLASSIFIED IN FULL  
 Authority: EO 13526  
 Chief, Records & Declass Div, WHS  
 Date: OCT 02 2015

PORT 6003



TOTAL ENGINE NET FLOW AREA DEFINED BY: ———  
 PRIMARY ENGINE NET FLOW AREA DEFINED BY: - - - -  
 COOLING FLOW AREA DEFINED BY DIFFERENCE OF ABOVE

PROPELSION SYSTEM FLOW AREAS - IN<sup>2</sup>

4

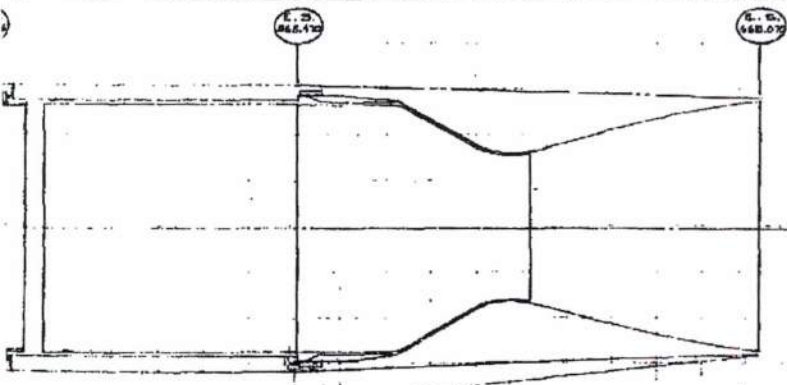


FIGURE 10. MA50-86B Propulsion System Net Flow Areas

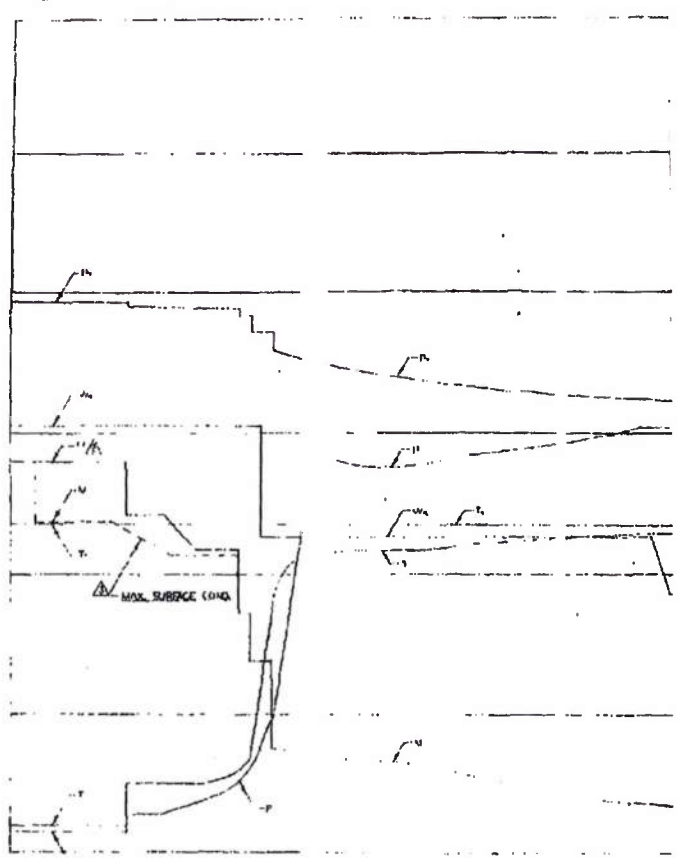
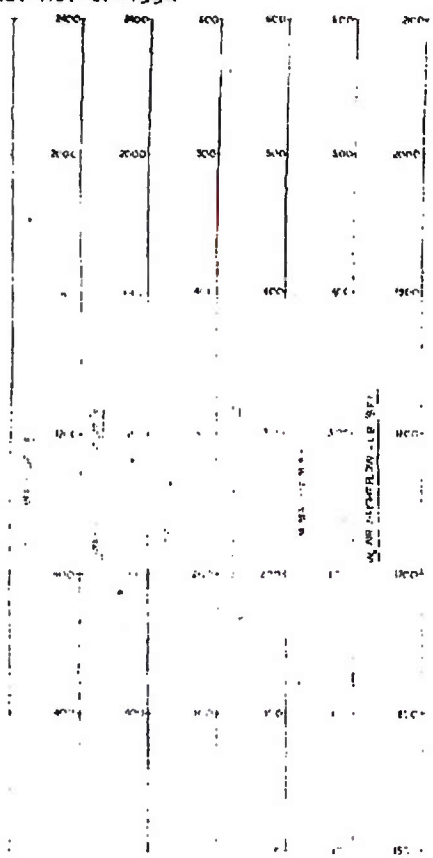


PROJECT NO.	MA50-86B
DATE	1954
DESIGNER	W. J. ...
CHECKED	...
APPROVED	...
MA50-86B PROPELSION SYSTEM NET FLOW	
DEVELOPER	...
Marquardt	
STEM	
EAS 81575	
WORK	R

DECLASSIFIED IN FULL  
 Authority: EO 13526  
 Chief, Records & Declass Div, WHS  
 Date: OCT 02 2015

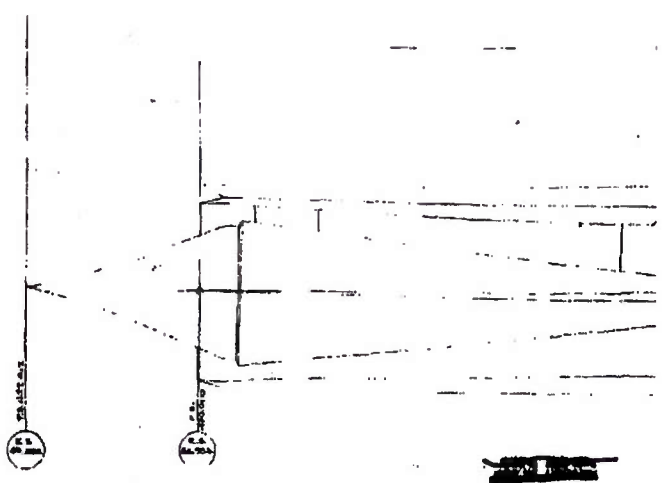
DECLASSIFIED IN FULL  
Authority: EO 13526  
Chief, Records & Declass Div, WHS  
Date: OCT 02 2015

ASB-JDR-63-277, Vol. IV  
~~SECRET RESTRICTED DATA~~  
~~ATOMIC ENERGY ACT OF 1954~~

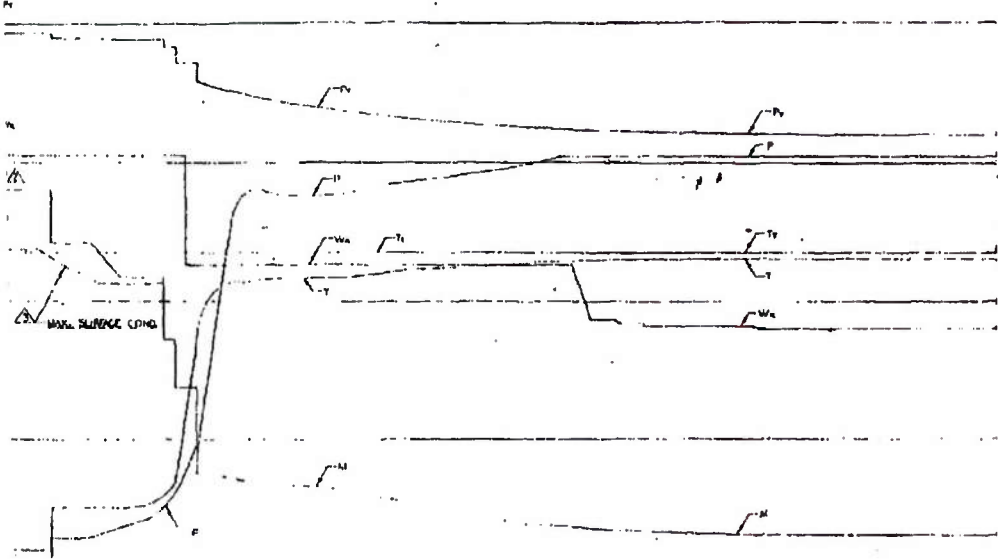


1

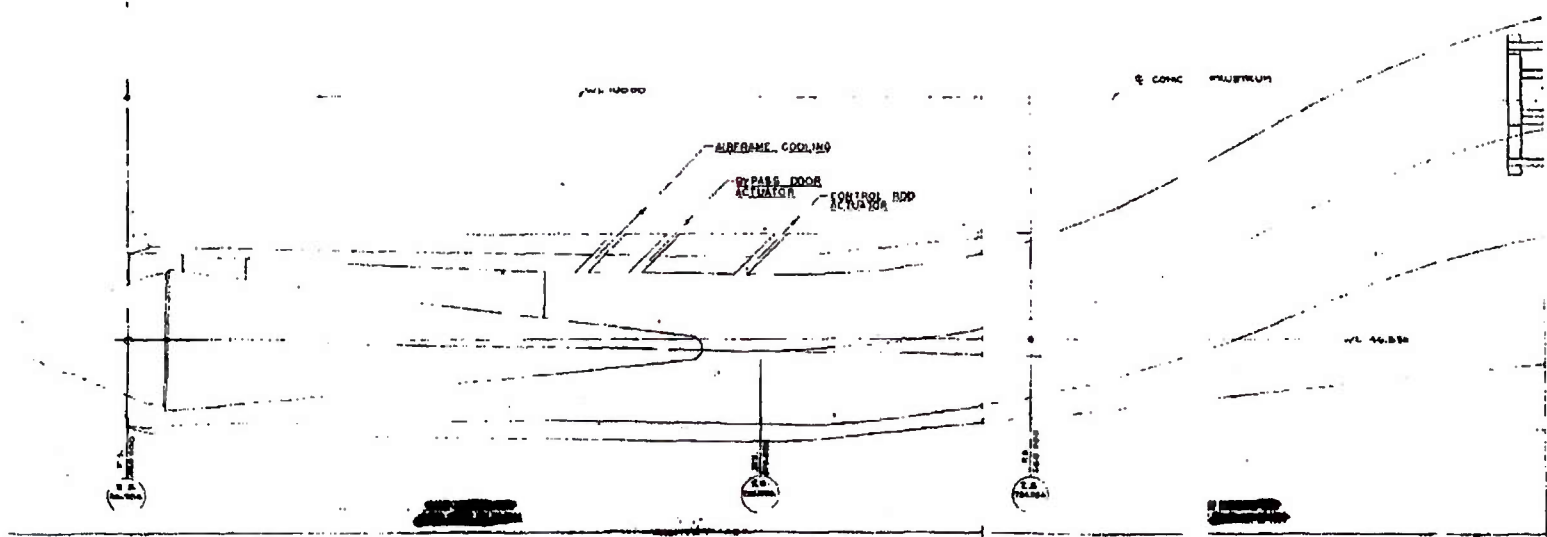
~~SECRET RESTRICTED DATA~~  
~~ATOMIC ENERGY ACT OF 1954~~



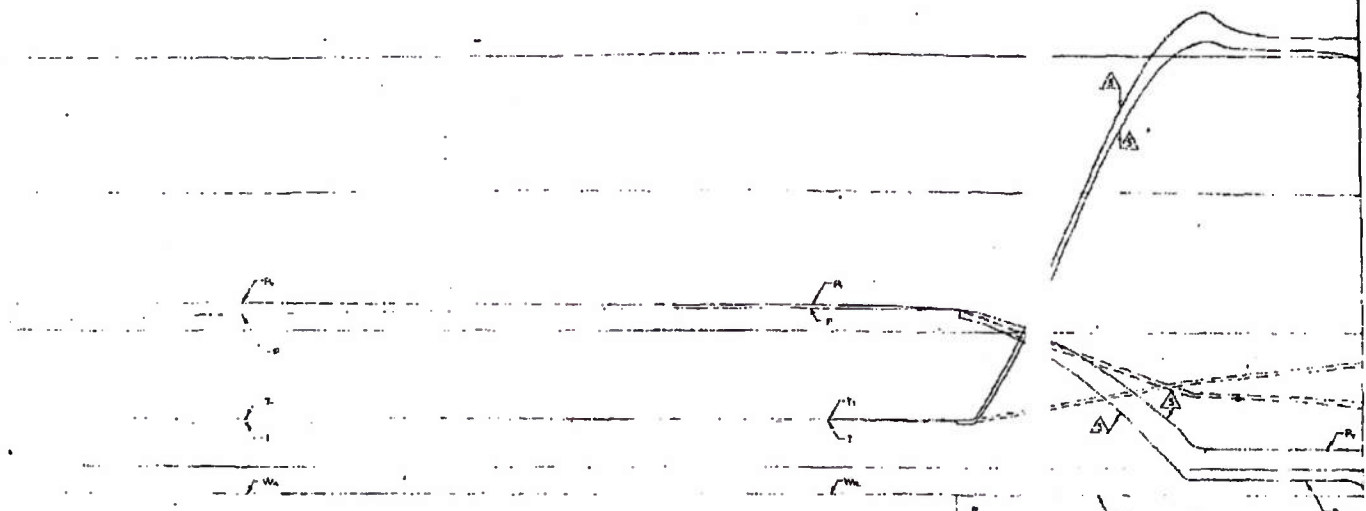
2



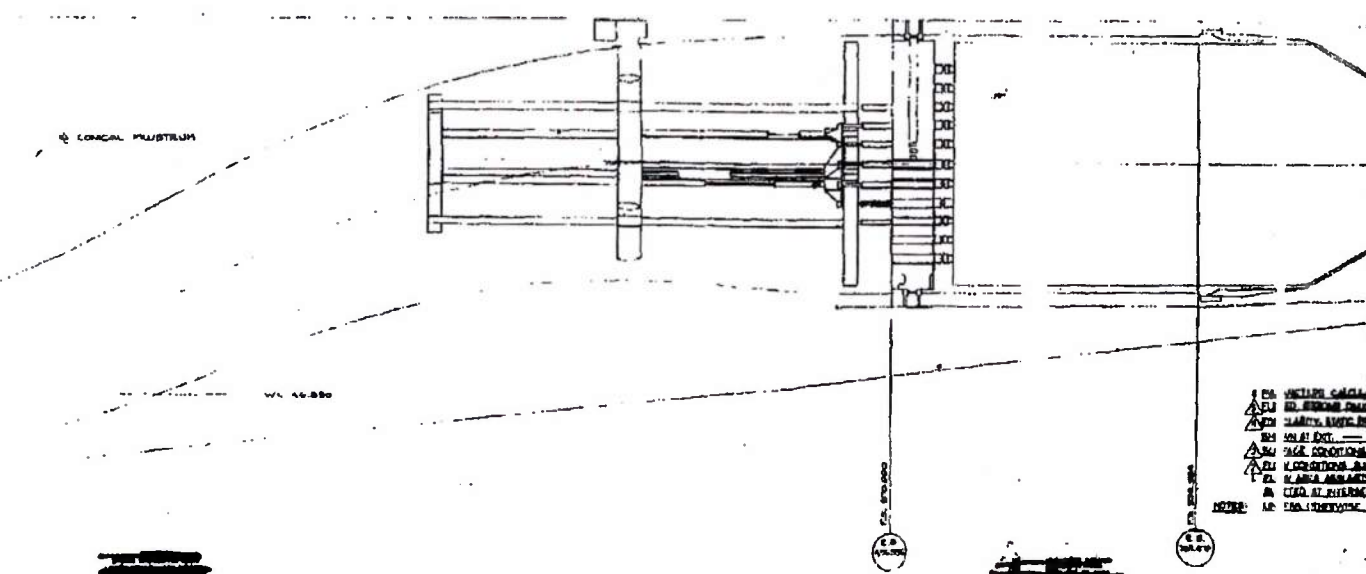
DECLASSIFIED IN FULL  
Authority: EO 13526  
Chief, Records & Declass Div, WHS  
Date: OCT 02 2015



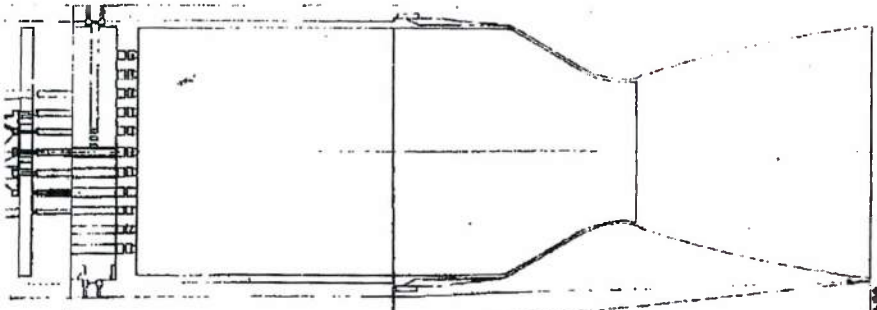
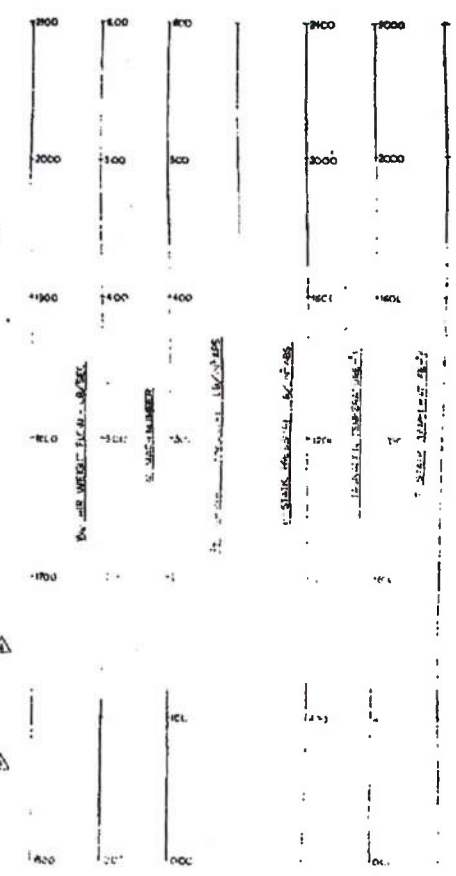
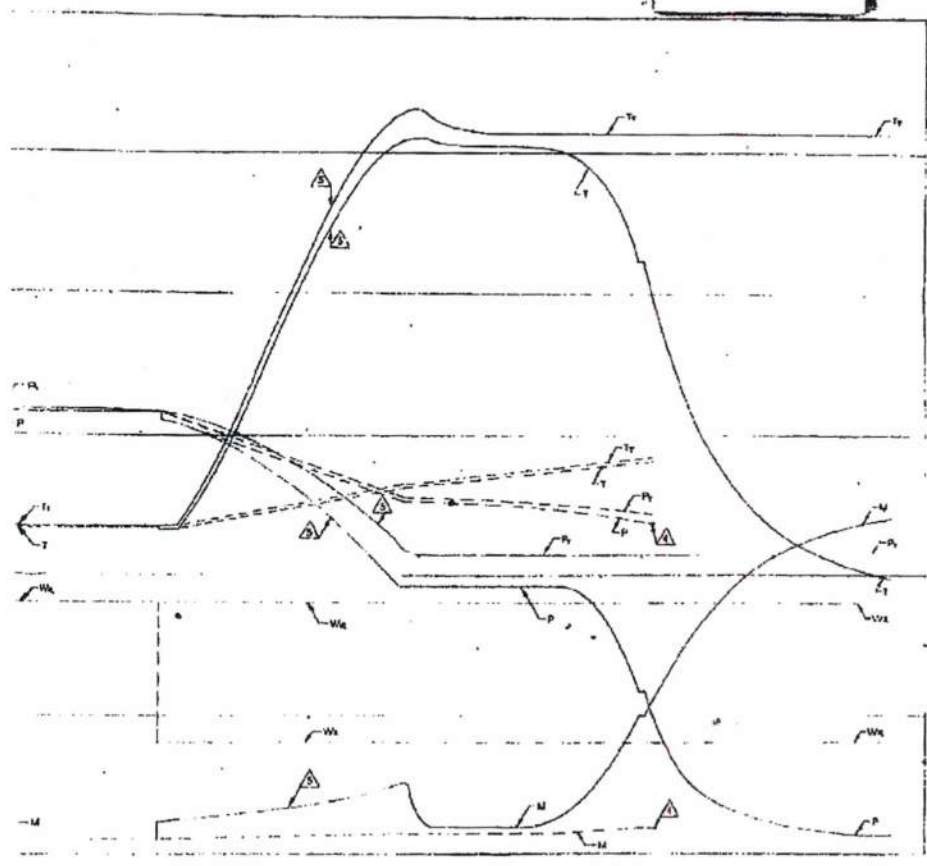
3



DECLASSIFIED IN FULL  
Authority: EO 13526  
Chief, Records & Declass Div, WHS  
Date: OCT 02 2015



1. EN. UNILITE CALCAL  
2. EN. SERVICIO CALCAL  
3. EN. CLAYTON, AMERICA  
4. EN. UNILITE CALCAL  
5. EN. UNILITE CALCAL  
6. EN. UNILITE CALCAL  
7. EN. UNILITE CALCAL  
8. EN. UNILITE CALCAL  
9. EN. UNILITE CALCAL  
10. EN. UNILITE CALCAL  
11. EN. UNILITE CALCAL  
12. EN. UNILITE CALCAL  
13. EN. UNILITE CALCAL  
14. EN. UNILITE CALCAL  
15. EN. UNILITE CALCAL  
16. EN. UNILITE CALCAL  
17. EN. UNILITE CALCAL  
18. EN. UNILITE CALCAL  
19. EN. UNILITE CALCAL  
20. EN. UNILITE CALCAL  
21. EN. UNILITE CALCAL  
22. EN. UNILITE CALCAL  
23. EN. UNILITE CALCAL  
24. EN. UNILITE CALCAL  
25. EN. UNILITE CALCAL  
26. EN. UNILITE CALCAL  
27. EN. UNILITE CALCAL  
28. EN. UNILITE CALCAL  
29. EN. UNILITE CALCAL  
30. EN. UNILITE CALCAL  
31. EN. UNILITE CALCAL  
32. EN. UNILITE CALCAL  
33. EN. UNILITE CALCAL  
34. EN. UNILITE CALCAL  
35. EN. UNILITE CALCAL  
36. EN. UNILITE CALCAL  
37. EN. UNILITE CALCAL  
38. EN. UNILITE CALCAL  
39. EN. UNILITE CALCAL  
40. EN. UNILITE CALCAL  
41. EN. UNILITE CALCAL  
42. EN. UNILITE CALCAL  
43. EN. UNILITE CALCAL  
44. EN. UNILITE CALCAL  
45. EN. UNILITE CALCAL  
46. EN. UNILITE CALCAL  
47. EN. UNILITE CALCAL  
48. EN. UNILITE CALCAL  
49. EN. UNILITE CALCAL  
50. EN. UNILITE CALCAL  
51. EN. UNILITE CALCAL  
52. EN. UNILITE CALCAL  
53. EN. UNILITE CALCAL  
54. EN. UNILITE CALCAL  
55. EN. UNILITE CALCAL  
56. EN. UNILITE CALCAL  
57. EN. UNILITE CALCAL  
58. EN. UNILITE CALCAL  
59. EN. UNILITE CALCAL  
60. EN. UNILITE CALCAL  
61. EN. UNILITE CALCAL  
62. EN. UNILITE CALCAL  
63. EN. UNILITE CALCAL  
64. EN. UNILITE CALCAL  
65. EN. UNILITE CALCAL  
66. EN. UNILITE CALCAL  
67. EN. UNILITE CALCAL  
68. EN. UNILITE CALCAL  
69. EN. UNILITE CALCAL  
70. EN. UNILITE CALCAL  
71. EN. UNILITE CALCAL  
72. EN. UNILITE CALCAL  
73. EN. UNILITE CALCAL  
74. EN. UNILITE CALCAL  
75. EN. UNILITE CALCAL  
76. EN. UNILITE CALCAL  
77. EN. UNILITE CALCAL  
78. EN. UNILITE CALCAL  
79. EN. UNILITE CALCAL  
80. EN. UNILITE CALCAL  
81. EN. UNILITE CALCAL  
82. EN. UNILITE CALCAL  
83. EN. UNILITE CALCAL  
84. EN. UNILITE CALCAL  
85. EN. UNILITE CALCAL  
86. EN. UNILITE CALCAL  
87. EN. UNILITE CALCAL  
88. EN. UNILITE CALCAL  
89. EN. UNILITE CALCAL  
90. EN. UNILITE CALCAL  
91. EN. UNILITE CALCAL  
92. EN. UNILITE CALCAL  
93. EN. UNILITE CALCAL  
94. EN. UNILITE CALCAL  
95. EN. UNILITE CALCAL  
96. EN. UNILITE CALCAL  
97. EN. UNILITE CALCAL  
98. EN. UNILITE CALCAL  
99. EN. UNILITE CALCAL  
100. EN. UNILITE CALCAL



DIMENSIONS CALCULATED FOR MAX. FLOW 1000-1000 FT. ANA. 100 CFS  
 DESIGNED BASED ON  
 FOR CLARITY, STIC. PRESSURE & MOONING CURVES OF SECONDARY FLOW ARE NOT  
 SHOWN IN DET. — WALLS ARE 18" THK. & 150' HIGH  
 SURFACE CONDITIONS DETERMINED BY PRIMARY FLOW  
 FLOW CONDITIONS BASED ON ONE DIMENSIONAL ANALYSIS  
 FLOW AREA ASSUMED NORMAL TO FLOW CENTERLINE & DIMENSIONS  
 NOTED AT INTERSECTION OF CENTERLINE & STREAM  
 UNLESS OTHERWISE SPECIFIED

CODE  
 ITEM NAME  
 — PRIMARY FLOW  
 — SECONDARY FLOW  
 — TOTAL FLOW  
 — PRIMARY FLOW  
 — SECONDARY FLOW

FIGURE 11. Internal Design Parameters for Design Point Operation

MARSHBURY AIRPORT CO.  
 81574  
 DEVELOPMENT DRAWING

DECLASSIFIED IN FULL  
 Authority: EO 13526  
 Chief, Records & Declass Div, WHS  
 Date: OCT 02 2015

REF ID: A66-277, Vol. IV  
~~SECRET RESTRICTED DATA~~  
~~ATOMIC ENERGY ACT OF 1954~~

BOUNDARY LAYER AIR BLEED  
LOCATION: BLEED INLET  
W<sub>0</sub> --- 80  
A --- 65  
T<sub>0</sub> --- 942

COOLING AIRFLOW - INLET INNERBODY  
LOCATION: INSIDE INNERBODY STRUTS  
W<sub>0</sub> --- 80  
A --- 130  
T<sub>0</sub> --- 942

ACTUATING AIRFLOW - BY PASS DOORS MOTOR  
LOCATION: AIR INLET FOR MOTOR  
W<sub>0</sub> --- 5 MAX.  
T<sub>0</sub> --- 942  
P --- 45 TO 350

ACTUATING AIRFLOW - BY PASS DOORS MOTOR  
LOCATION: OVERBOARD EXHAUST  
W<sub>0</sub> --- MAX.

COOLING AIRFLOW - IFRAME  
LOCATION: BLEED EXHAUST FROM IFRAME  
W<sub>0</sub> --- 41  
T<sub>0</sub> --- 942

ACTUATING AIRFLOW - NOSE SPIKE MOTOR  
LOCATION: AIR INLET FOR MOTOR  
W<sub>0</sub> --- 5 MAX.

COOLING AIRFLOW - INLET INNERBODY  
LOCATION: INSIDE INNERBODY STRUTS  
W<sub>0</sub> --- 80  
T<sub>0</sub> --- 942

ACTUATING AIRFLOW - NOSE SPIKE MOTOR  
LOCATION: OVERBOARD EXHAUST  
W<sub>0</sub> --- 5 MAX.

1

~~SECRET RESTRICTED DATA~~  
~~ATOMIC ENERGY ACT OF 1954~~

DECLASSIFIED IN FULL  
Authority: EO 13526  
Chief, Records & Declass Div, WHS  
Date: OCT 02 2015

2

ACTUATING AIRFLOW - BY PASS DOORS MOTOR  
LOCATION: OVERBOARD EXHAUST  
W<sub>0</sub> - 3 MAX.

COOLING AIRFLOW - SHADOW SHIELD  
LOCATION: AVERAGE SECTION THRU SHIELD  
W<sub>0</sub> - 3.0  
T<sub>0</sub> - 34.2  
TEMP OF SHIELD - 1700

AIRFLOW - BY PASS DOORS MOTOR  
INLET, 700 MP/HR  
TO 350

COOLING AIRFLOW - AIRFRAME  
LOCATION: BLEED ENTRANCE FROM MAIN DUCT  
W<sub>0</sub> - 4.1  
T<sub>0</sub> - 34.2

AIR CONDITIONING SYSTEM  
LOCATION: EQUIPMENT COMPARTMENT  
W<sub>0</sub> - 3.5

ACTUATING AIRFLOW  
LOCATION: AIR FLOW FOR MOTOR  
W<sub>0</sub> - 17.04  
T<sub>0</sub> - 34.2  
P<sub>0</sub> - 0.13

CONTROL ROOM MOTOR  
LOCATION: AIRFLOW FOR MOTOR

EXHAUST AIRFLOW - COOLING AIRFLOW  
LOCATION: AIRFLOW FOR MOTOR  
W<sub>0</sub> - 17 MAX.

COOLING AIRFLOW - INLET INNERBODY  
LOCATION: INLET INNERBODY  
W<sub>0</sub> - 8.1  
T<sub>0</sub> - 34.2

COOLING AIRFLOW - INLET INNERBODY  
LOCATION: OVERBOARD EXHAUST  
W<sub>0</sub> - 8.0  
A - 110

DECLASSIFIED IN FULL  
Authority: EO 13526  
Chief, Records & Declass Div, WHS  
Date: OCT 02 2015

COOLING AIRFLOW - AIRFRAME  
LOCATION: AIRFLOW FOR ENGINE  
W<sub>0</sub> - 4.2  
A - VARIABLE  
T<sub>0</sub> - 34.2  
TEMP OF AIR - 1180  
TEMP OF FUEL - 1180  
TEMP OF OIL - 1000

AIRFLOW - NOSE SPIKE MOTOR  
OVERBOARD EXHAUST  
MAX.

DIRTY AIRFLOW DOTTED TO BOTTOM & FOR FWD CLARITY ONLY  
LOWER STRUTS ACTUAL POSITION - NOT AIRFLOW FROM TOP &

[REDACTED]

X 015  
4

# 3

KLING AIRFLOW - SHADOW SHIELD  
 ATION: AVERAGE SECTION THRU SHIELD

--- 34

IR OF SHIELD - 1200

ACTUATING AIRFLOW - CONTROL ROD MOTOR  
 LOCATION: AIR UNITS FOR MOTOR  
 W --- 117 MAX.  
 A --- 843  
 P --- 313

EXHAUST AIRFLOW - CONTROL ROD MOTOR  
 LOCATION: AIRFLOW FROM AIRPUMP  
 W --- 117 MAX.

COOLING AIRFLOW - REACTOR SUPPORT  
 LOCATION: AROUND REACTOR  
 W --- 100  
 A --- 100  
 P --- 313  
 TEMA OF SPRINGS --- 1100  
 TEMP OF PRESSURE SHELL --- 1200

COOLING AIRFLOW  
 LOCATION: ENTIRE  
 W --- 100  
 A --- 72  
 T --- 1088  
 P --- 270  
 V --- 282  
 T<sub>2</sub> --- 1100

OUT NOZZLE  
 TO NOZZLE

COOLING AIRFLOW - EXIT  
 LOCATION: AIR FOR EXIT  
 W --- 100  
 A --- 42  
 T --- 1100  
 P --- 843  
 V --- 248  
 T<sub>2</sub> --- 1210

COOLING AIRFLOW - AIRFRAME  
 LOCATION: AROUND REACTOR  
 W --- 41  
 A --- 600  
 P --- 942  
 TEMP OF SUPPORT --- 1200

COOLING AIRFLOW  
 LOCATION: IC  
 W --- 81  
 A --- 88  
 P --- 101  
 R --- 48  
 V --- 183  
 TEMP OF AIR --- 1200

AIRFRAME  
 MUSCADE FRAME  
 L --- 1200

COOLING AIRFLOW - AIRFRAME  
 LOCATION: AIRFRAME EXIT  
 W --- 78  
 A --- 78  
 T --- 126  
 P --- 3  
 V --- 3

COOLING AIRFLOW - AIRFRAME  
 LOCATION: AIRFRAME ENGINE DUCT  
 W --- 41  
 A --- VARIABLE  
 T --- 942

TEMP OF DUCT --- 1180  
 TEMP OF FRAME --- 1180  
 TEMP OF SKIN --- 1000

NOZZLE

W --- FLOW --- LBS/SEC  
 A --- FLOW AREA --- IN<sup>2</sup>  
 T --- TEMPERATURE --- °F  
 P --- PRESSURE --- LBS/IN<sup>2</sup> ABS.  
 V --- VELOCITY --- FT/SEC  
 T<sub>2</sub> --- TEMPERATURE OF AIRFRAME --- °F  
 T<sub>2</sub> --- TEMPERATURE OF NOZZLE --- °F

**DECLASSIFIED IN FULL**  
 Authority: EO 13526  
 Chief, Records & Declass Div, WHS  
 Date: OCT 02 2015

P. PRELIMINARY DATA SHOWN, ADDITIONAL DATA WILL BE SHOWN WHEN DESIGN POINT OPERATION AT 1000 FT. AND 1000 FT. AND

NOTE:

X 01576

1

5

3

2

4

COOLING AIRFLOW - REACTOR SUPPORT  
LOCATION: AROUND REACTOR

W<sub>1</sub> - 100  
A - 100  
T<sub>1</sub> - 542  
P - 315

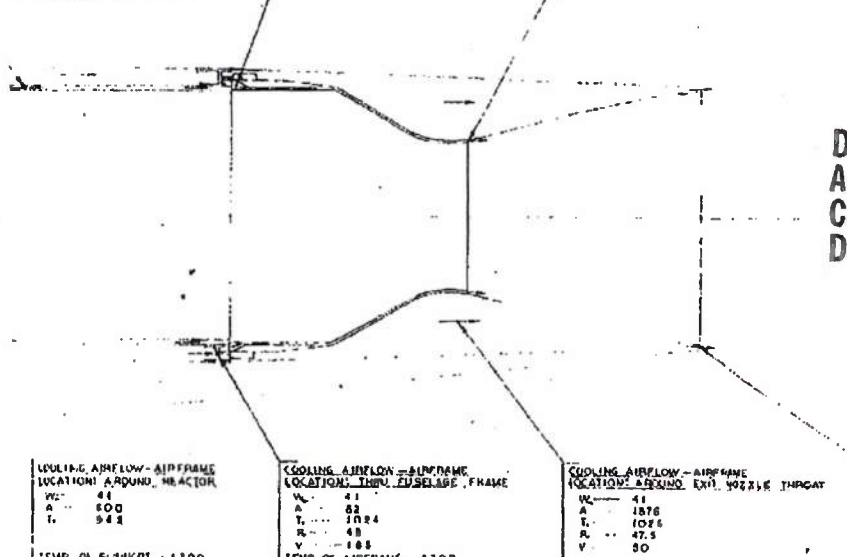
NO. OF SPRINGS - 1400  
TEMP. OF PRESSURE SHELL - 7200

COOLING AIRFLOW - EXIT NOZZLE  
LOCATION: ENTRANCE TO NOZZLE

W<sub>2</sub> - 100  
A - 72  
T<sub>2</sub> - 1062  
P - 270  
V - 865  
T<sub>2</sub> - 1150

COOLING AIRFLOW - EXIT NOZZLE  
LOCATION: EJECTOR EXIT

W<sub>3</sub> - 100  
A - 42  
T<sub>3</sub> - 1130  
P - 665  
V - 2442  
T<sub>3</sub> - 1240



COOLING AIRFLOW - AIRFRAME  
LOCATION: AROUND REACTOR

W<sub>4</sub> - 44  
A - 600  
T<sub>4</sub> - 942

TEMP. OF AIRFRAME - 7200

COOLING AIRFLOW - AIRFRAME  
LOCATION: THRU DISBURSE FRAME

W<sub>5</sub> - 41  
A - 82  
T<sub>5</sub> - 1024  
P - 48  
V - 183

TEMP. OF AIRFRAME - 7200

COOLING AIRFLOW - AIRFRAME  
LOCATION: AROUND EXIT NOZZLE THROAT

W<sub>6</sub> - 41  
A - 1876  
T<sub>6</sub> - 1076  
P - 47.5  
V - 50

COOLING AIRFLOW - AIRFRAME  
LOCATION: AIRFLOW EXIT

W<sub>7</sub> - 41  
A - 82  
T<sub>7</sub> - 1030  
P - 47  
V - 1750

**SYMBOLS**

W<sub>1</sub> AIRFLOW - LBS/SEC  
A AIRFLOW AREA - IN<sup>2</sup>  
T<sub>1</sub> AIR TEMPERATURE - °F  
P AIR PRESSURE - LBS/IN<sup>2</sup> ABS.  
V AIR VELOCITY - FT/SEC  
T<sub>2</sub> TEMPERATURE OF AIRFRAME - °F  
T<sub>3</sub> TEMPERATURE OF NOZZLE - °F

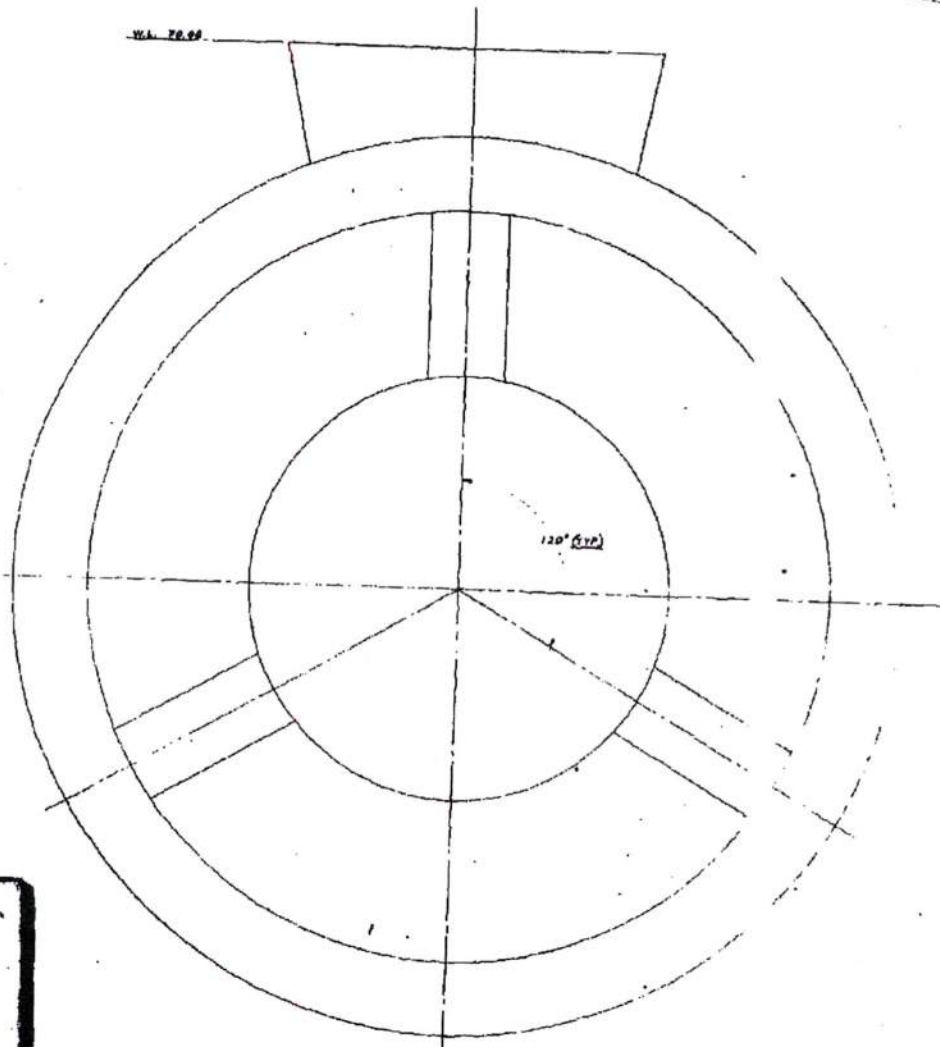
DECLASSIFIED IN FULL  
Authority: EO 13526  
Chief, Records & Declass Div, WHS  
Date: OCT 02 2015

FIGURE 12. MA50-X80-P propulsion System Auxiliary Air Req requirements

1. PRELIMINARY DATA SHOWN, ADDITIONAL DATA WILL BE SHOWN WHEN AVAILABLE.  
2. ALL DATA FOR DESIGN POINT OPERATION AT W<sub>1</sub> 2.4, 1000 FT, AND 101 DAY.

MARQUARDT PROPELLION SYSTEMS AUXILIARY AIR REQUIREMENTS DEPARTMENT OF DEFENSE		X 61576
--	--	---------

ASD-TBR-63-2776 Vol. IV  
~~SECRET RESTRICTED DATA~~  
ATOMIC ENERGY ACT OF 1954

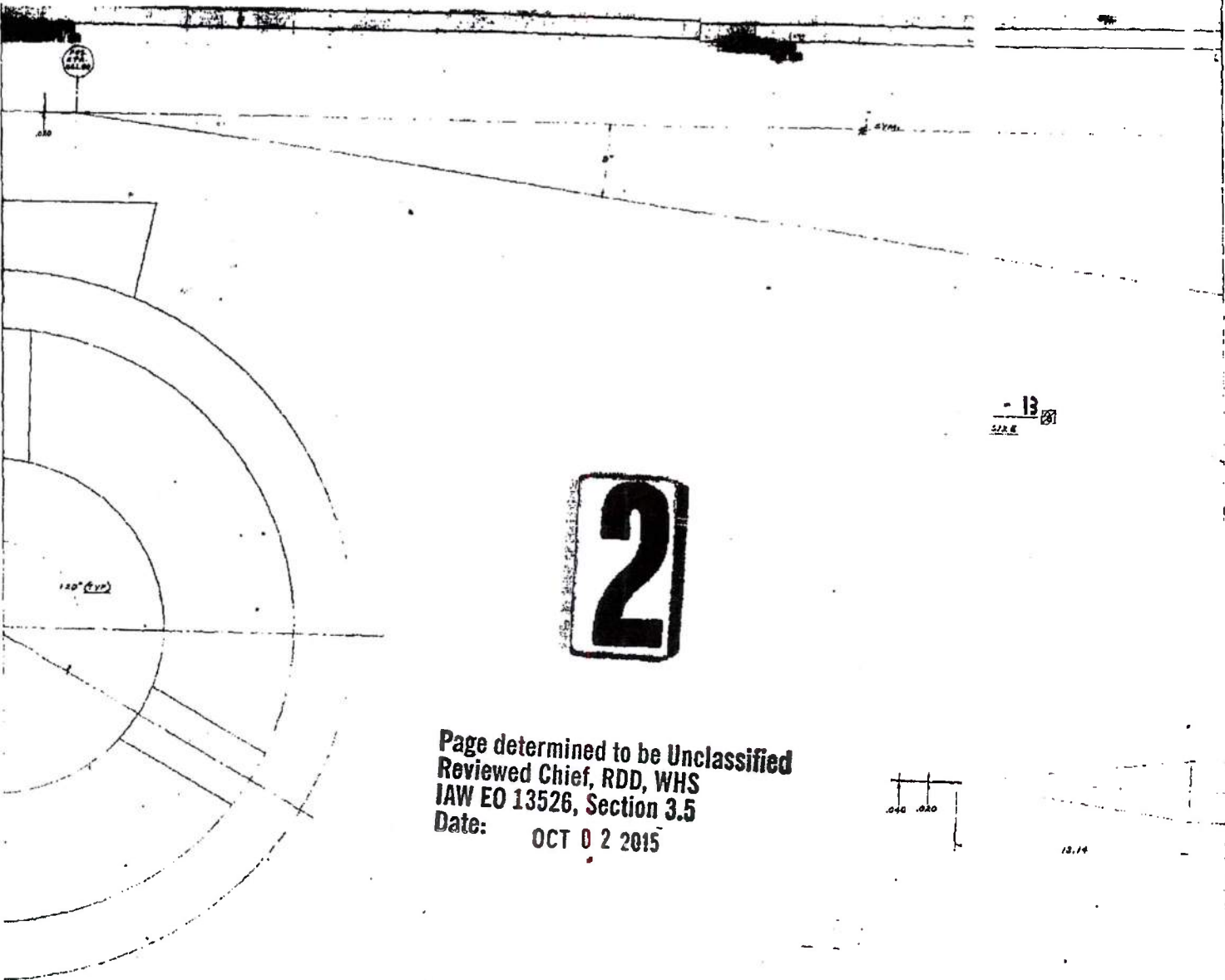


1

~~SECRET RESTRICTED DATA~~  
ATOMIC ENERGY ACT OF 1954

DECLASSIFIED IN FULL  
Authority: EO 13526  
Chief, Records & Declass Div, WHS  
Date: OCT 02 2015

C - C



- 13  
5/22/81

**2**

Page determined to be Unclassified  
Reviewed Chief, RDD, WHS  
IAW EO 13526, Section 3.5  
Date: OCT 02 2015



13.14

X 01418

210

13 - 13  
+ 0.000

3

DECLASSIFIED IN FULL  
Authority: EO 13526  
Chief, Records & Declass Div, WHS  
Date: OCT 02 2015

.048 .020

13.76

A - A

18.76

X 814197

20

19

11



POS	W.L.	0	R.	R.
101-100	101-100			
101-101	101-101			
101-102	101-102			
101-103	101-103			
101-104	101-104			
101-105	101-105			
101-106	101-106			
101-107	101-107			
101-108	101-108			
101-109	101-109			
101-110	101-110			
101-111	101-111			
101-112	101-112			
101-113	101-113			
101-114	101-114			
101-115	101-115			
101-116	101-116			
101-117	101-117			
101-118	101-118			
101-119	101-119			
101-120	101-120			
101-121	101-121			
101-122	101-122			
101-123	101-123			
101-124	101-124			
101-125	101-125			
101-126	101-126			
101-127	101-127			
101-128	101-128			
101-129	101-129			
101-130	101-130			
101-131	101-131			
101-132	101-132			
101-133	101-133			
101-134	101-134			
101-135	101-135			
101-136	101-136			
101-137	101-137			
101-138	101-138			
101-139	101-139			
101-140	101-140			
101-141	101-141			
101-142	101-142			
101-143	101-143			
101-144	101-144			
101-145	101-145			
101-146	101-146			
101-147	101-147			
101-148	101-148			
101-149	101-149			
101-150	101-150			
101-151	101-151			
101-152	101-152			
101-153	101-153			
101-154	101-154			
101-155	101-155			
101-156	101-156			
101-157	101-157			
101-158	101-158			
101-159	101-159			
101-160	101-160			
101-161	101-161			
101-162	101-162			
101-163	101-163			
101-164	101-164			
101-165	101-165			
101-166	101-166			
101-167	101-167			
101-168	101-168			
101-169	101-169			
101-170	101-170			
101-171	101-171			
101-172	101-172			
101-173	101-173			
101-174	101-174			
101-175	101-175			
101-176	101-176			
101-177	101-177			
101-178	101-178			
101-179	101-179			
101-180	101-180			
101-181	101-181			
101-182	101-182			
101-183	101-183			
101-184	101-184			
101-185	101-185			
101-186	101-186			
101-187	101-187			
101-188	101-188			
101-189	101-189			
101-190	101-190			
101-191	101-191			
101-192	101-192			
101-193	101-193			
101-194	101-194			
101-195	101-195			
101-196	101-196			
101-197	101-197			
101-198	101-198			
101-199	101-199			
101-200	101-200			

RECORDED ON FILE OF 101-100

4

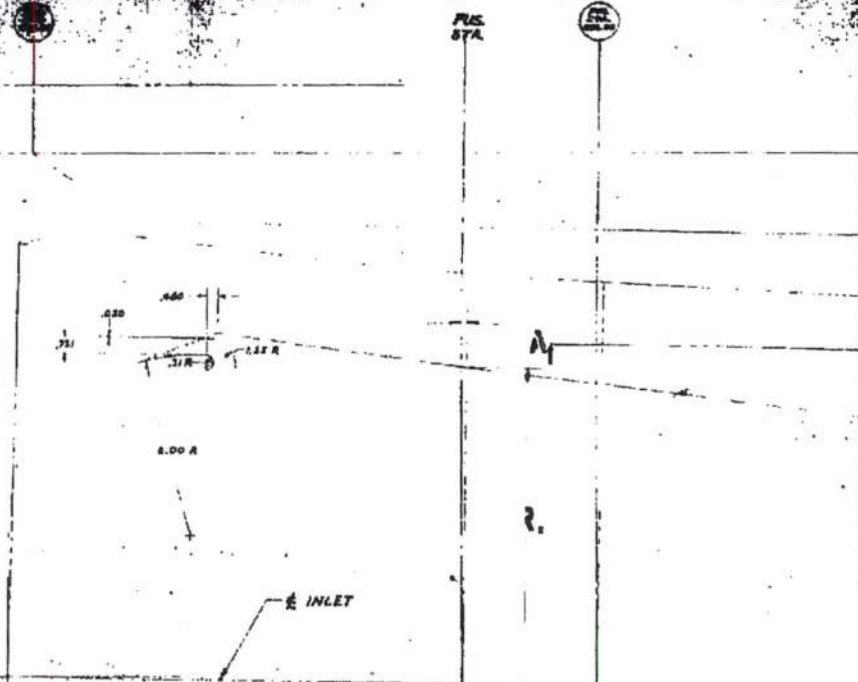
W.L. 44-88

DECLASSIFIED IN FULL  
Authority: EO 13526  
Chief, Records & Declass Div, WHS  
Date: OCT 02 2015



X 8141911

5



Page determined to be Unclassified  
Reviewed Chief, RDD, WHS  
IAW EO 13526, Section 3.5  
Date: OCT 02 2015



6

PUB  
STA



A<sub>1</sub>

R.

20.188 R  
CONSTANT

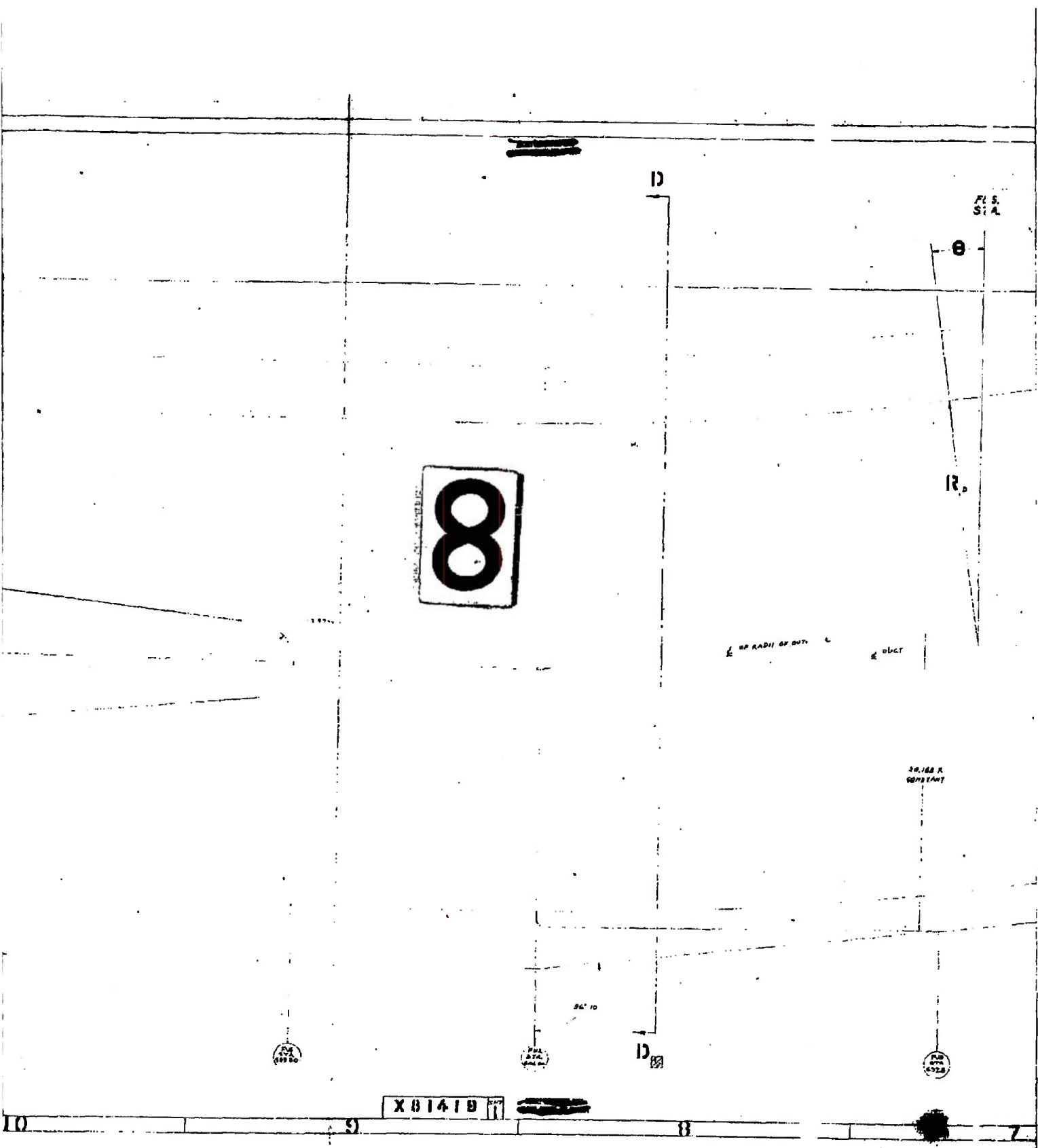
Page determined to be Unclassified  
Reviewed Chief, RDD, WHS  
IAW EO 13526, Section 3.5  
Date: OCT 02 2015

C<sub>10</sub>

7

DECLASSIFIED IN FULL  
Authority: EO 13526  
Chief, Records & Declass Div, WHS  
Date: OCT 02 2015

10



X 01419

DECLASSIFIED IN FULL  
 Authority: EO 13526  
 Chief, Records & Declass Div, WHS  
 Date: OCT 02 2015

FUS.  
STA.

8

13

9

R.

OF RADIUS OF CURVE M.

DUCT

W. L.

20. JAS. R.  
CONSTANT

NOV  
1978

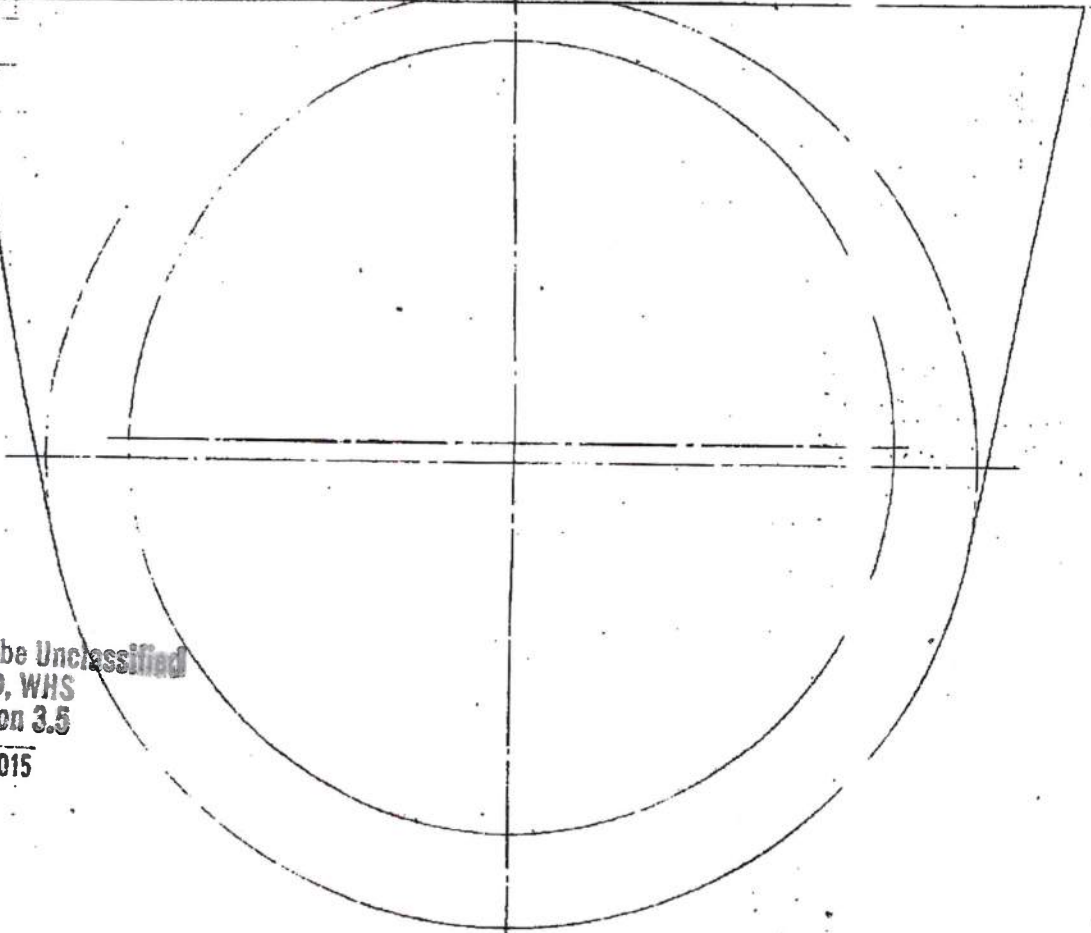
NOV  
1978

F

DECLASSIFIED IN FULL  
Authority: EO 13526  
Chief, Records & Declass Div, WHS  
Date: OCT 02 2015

10

Page determined to be Unclassified  
Reviewed Chief, RDD, WHS  
IAW EO 13526, Section 3.5  
Date: OCT 02 2015



SYM

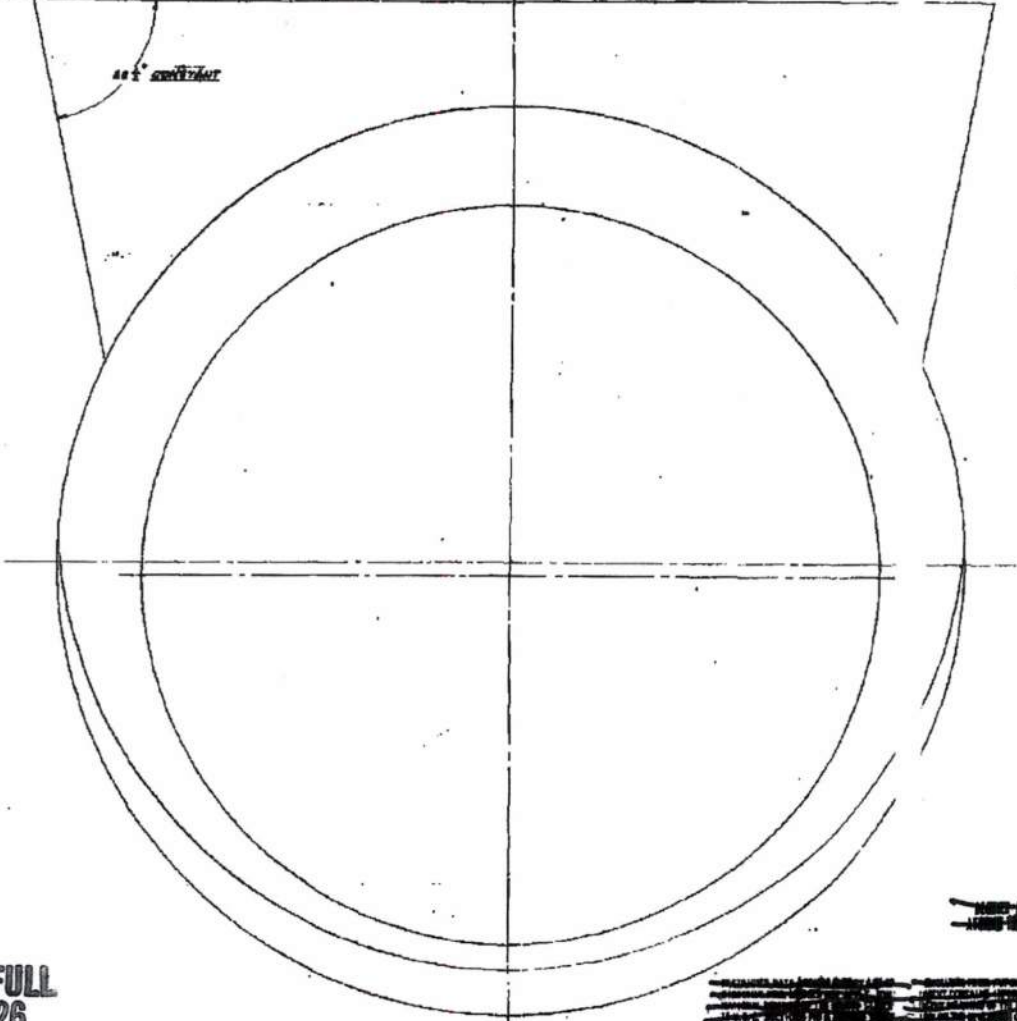
VIEW LOOKING END

11 79.00

71

W.L. 79.00

as + *unintelligible*



**DECLASSIFIED IN FULL**  
 Authority: EO 13526  
 Chief, Records & Declass Div, WBS  
 Date: OCT 02 2015

FIGURE 13  
*unintelligible*

12 - 12.00

159 - 160

**SIGN LAYOUT**  
**OFFICE DIST. LINE**

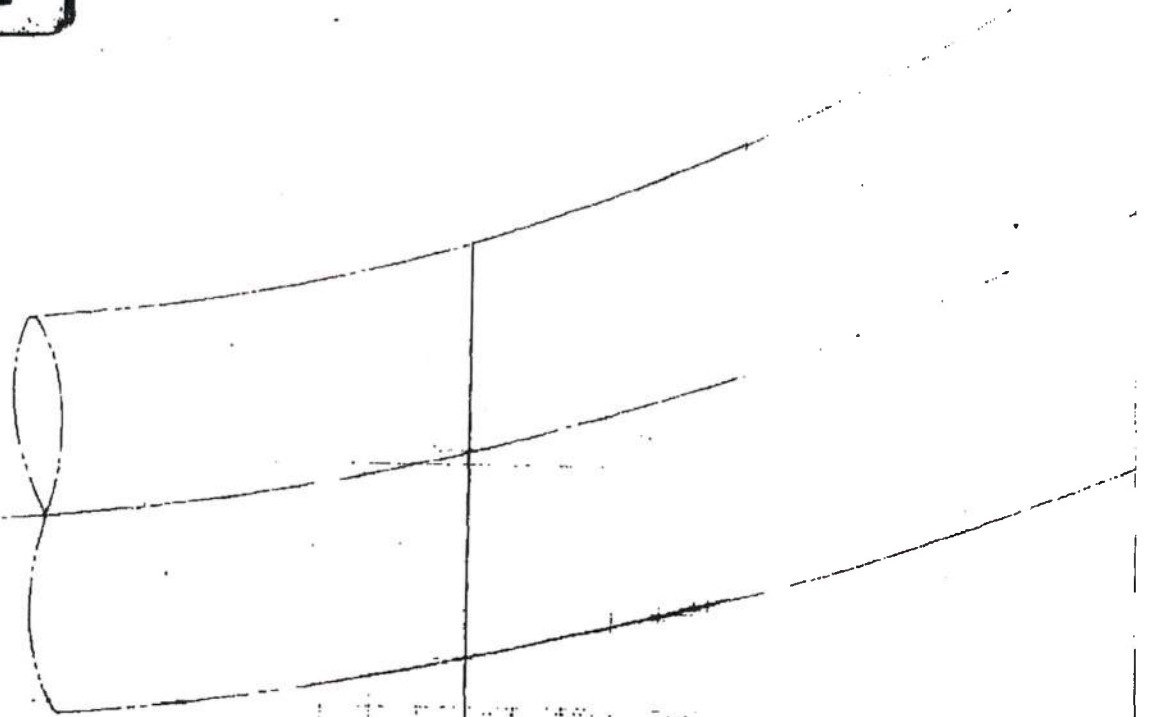
ASD-TDR-63-277, Vol. IV

~~SECRET RESTRICTED DATA~~

~~ATOMIC ENERGY ACT OF 1954~~

DECLASSIFIED IN FULL  
Authority: EO 13526  
Chief, Records & Declass Div, WHS  
Date: OCT 02 2015

1



~~SECRET RESTRICTED DATA~~

~~ATOMIC ENERGY ACT OF 1954~~

X8

2

FUS.  
STA.

⊖

R.

W. L

DECLASSIFIED IN FULL  
Authority: EO 13526  
Chief, Records & Declass Div, WHS  
Date: OCT 02 2015

DUCT FROM PL STA 650.00 TO FUS. S. A. 870.00  
± 3.25

SCALE TO BE USED FOR DIMENSIONS

X61419

2

5

4

3

3

FUS.  
STA.

⊖

R.

W. L.

DECLASSIFIED IN FULL  
Authority: EO 13526  
Chief, Records & Declass Div, WHS  
Date: OCT 02 2015

FIGURE 11. Design

DUCT FROM FUS. STA. 460.00 TO FUS. STA. 870.00

\* SIZE

REFER TO PANEL 1 FOR THICK. OF DIMENSIONS

3

REPT 6003

4

DECLASSIFIED IN FULL  
Authority: EO 13526  
Chief, Records & Declass Div, WHS  
Date: OCT 02 2015

FIGURE 1/4, Design Layout, Inlet and Duct Lines



TO FVS, STA. 870.00

REVISIONS

<table border="1"> <tr><td> </td><td> </td><td> </td><td> </td></tr> <tr><td> </td><td> </td><td> </td><td> </td></tr> <tr><td> </td><td> </td><td> </td><td> </td></tr> <tr><td> </td><td> </td><td> </td><td> </td></tr> </table>																	<table border="1"> <tr><td> </td><td> </td><td> </td><td> </td></tr> <tr><td> </td><td> </td><td> </td><td> </td></tr> <tr><td> </td><td> </td><td> </td><td> </td></tr> <tr><td> </td><td> </td><td> </td><td> </td></tr> </table>																	<table border="1"> <tr><td> </td><td> </td><td> </td><td> </td></tr> <tr><td> </td><td> </td><td> </td><td> </td></tr> <tr><td> </td><td> </td><td> </td><td> </td></tr> <tr><td> </td><td> </td><td> </td><td> </td></tr> </table>																

DESIGN L.  
INLET & DUCT

OUT-  
INRS.

61419

Marquardt

8149

A

C

D

ASD-TDR-63-277, Vol. IV

~~SECRET RESTRICTED DATA~~  
~~ATOMIC ENERGY ACT OF 1954~~

K (SHEET 3 OF 3) SEE

1

DECLASSIFIED IN FULL  
Authority: EO 13526  
Chief, Records & Declass Div, WHS  
Date: OCT 02 2015

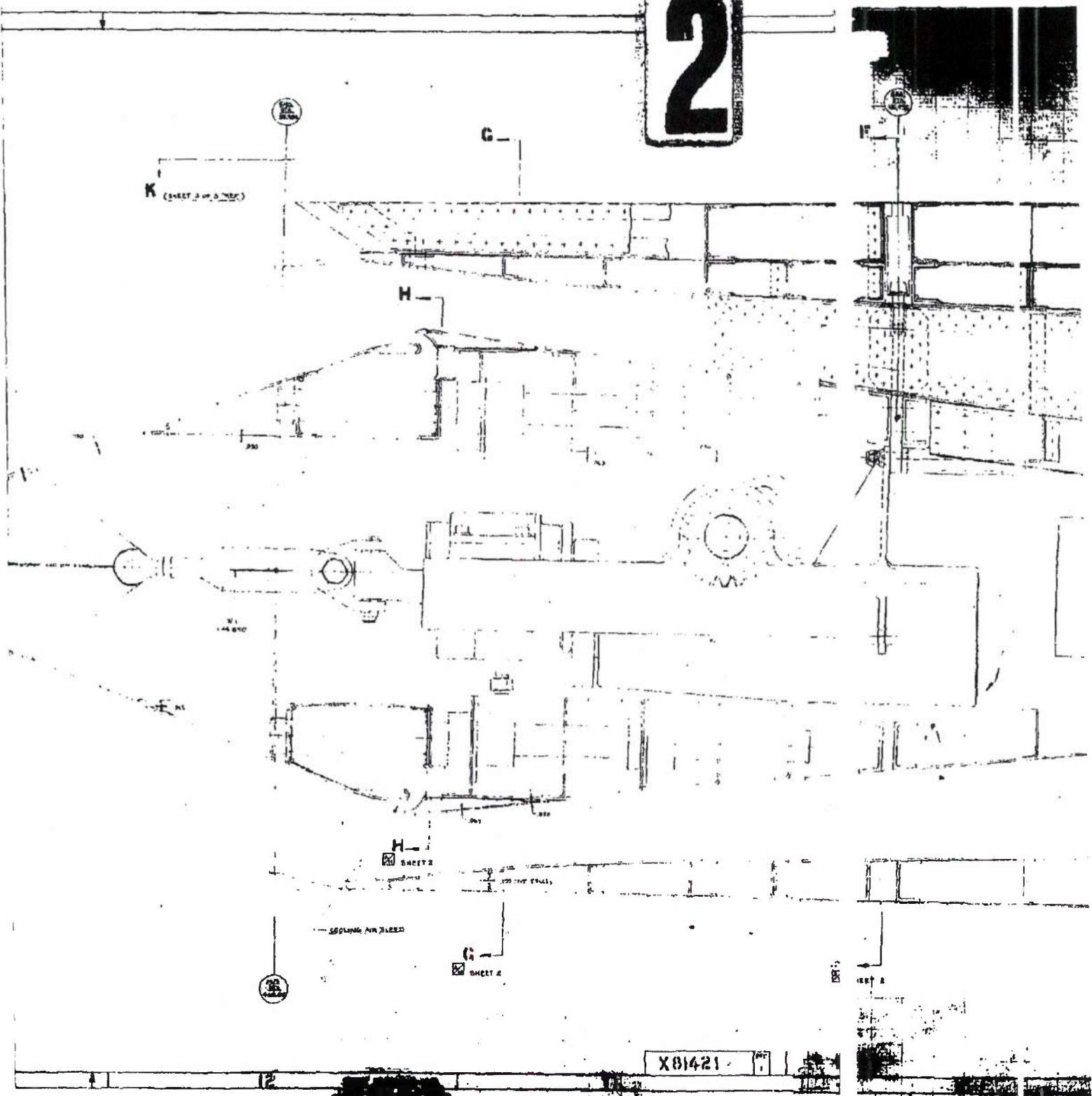
~~SECRET RESTRICTED DATA~~  
~~ATOMIC ENERGY ACT OF 1954~~

14

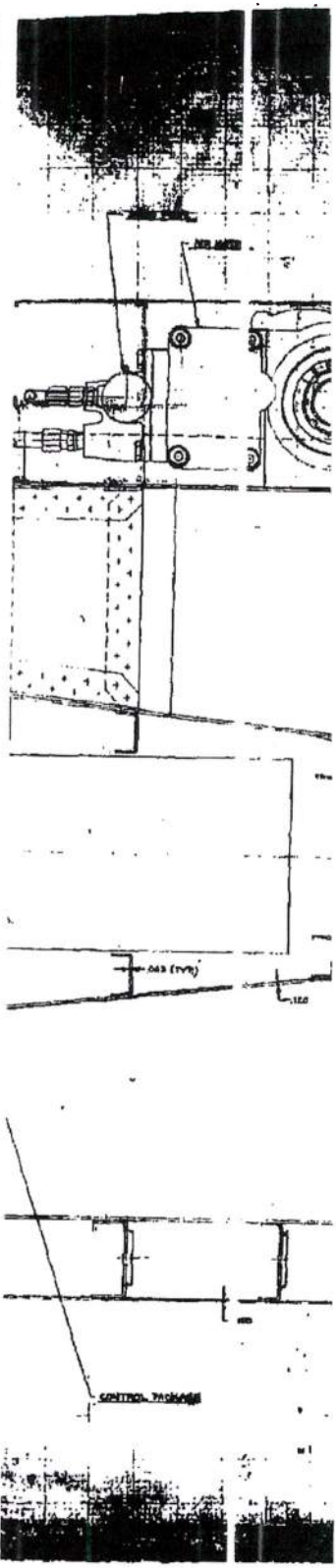
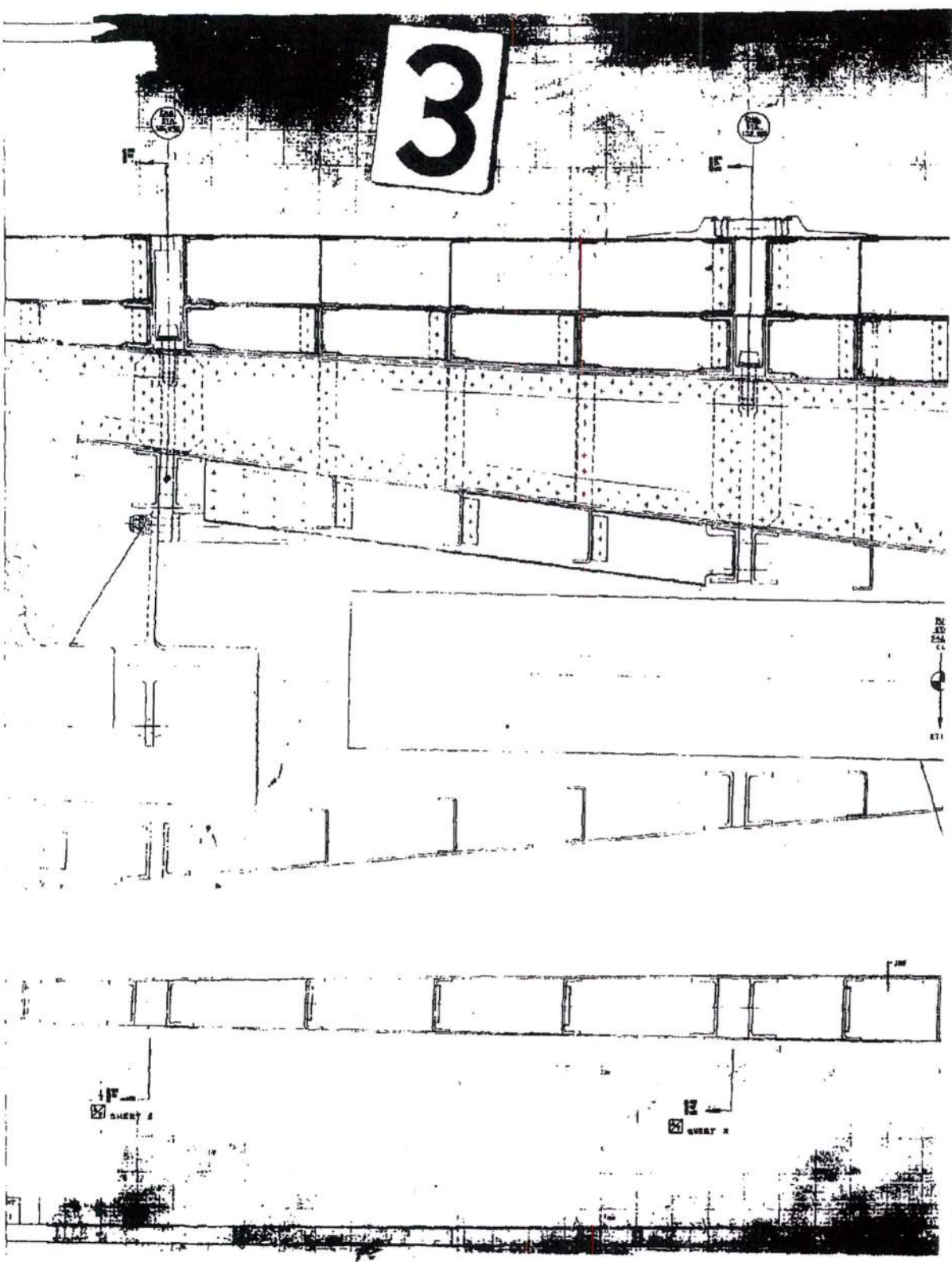
13

12

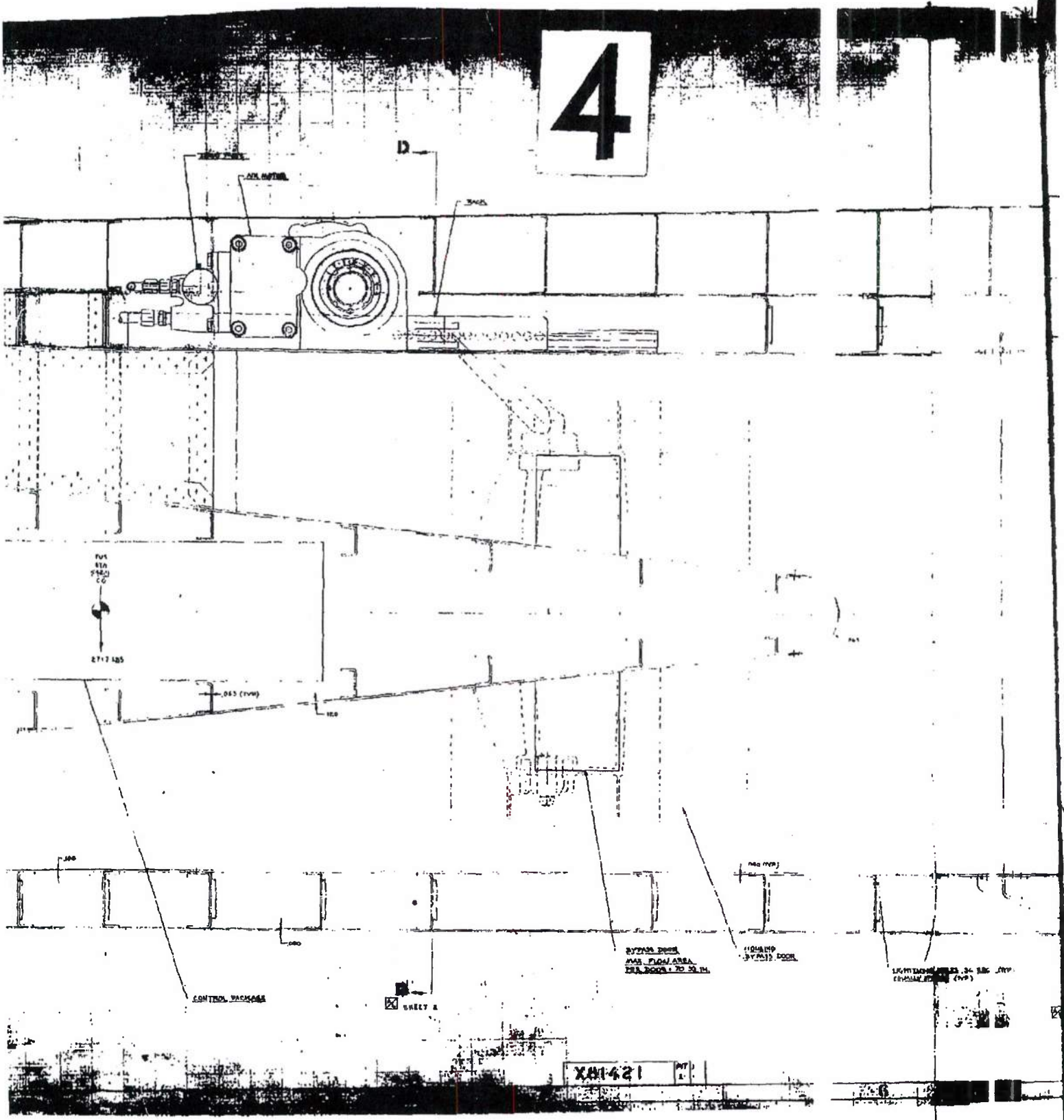
2



DECLASSIFIED IN FULL  
Authority: EO 13526  
Chief, Records & Declass Div, WHS  
Date: OCT 02 2015



4



5

C

B

Page determined to be Unclassified  
Reviewed Chief, RDD, WHS  
IAW EO 13526, Section 3.5  
Date: OCT 02 2015

140 (TP)

HOLDING  
DOOR

INTERIOR WALL (CL. 1400) (TP)

DOOR - BOUNDARY LAYER  
BUILT AIR

C -

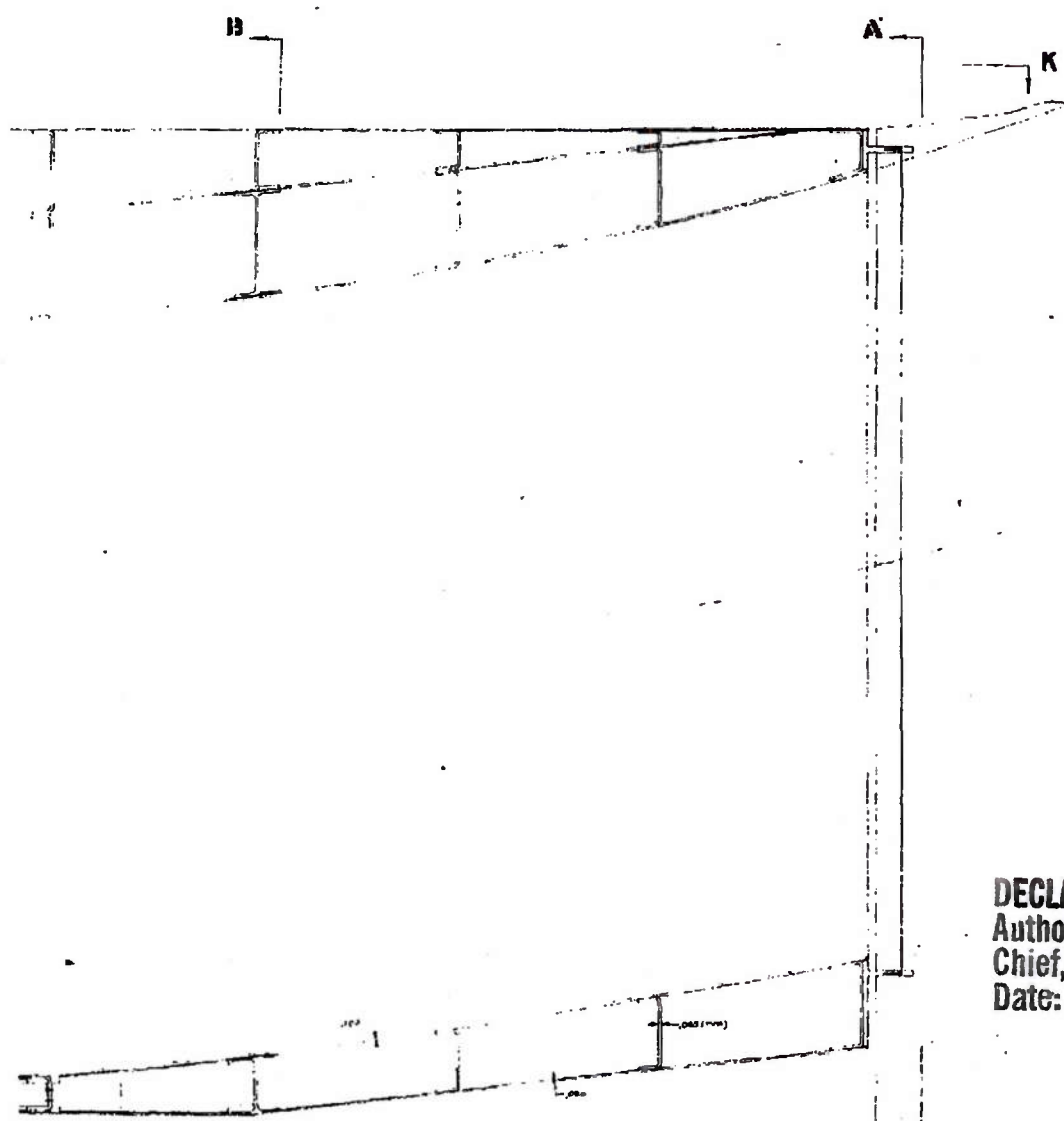
CHIEF



B

5

6



**DECLASSIFIED IN FULL**  
**Authority: EO 13526**  
**Chief, Records & Declass Div, WHS**  
**Date: OCT 02 2015**

FIGURE

**B**  
SHEET A

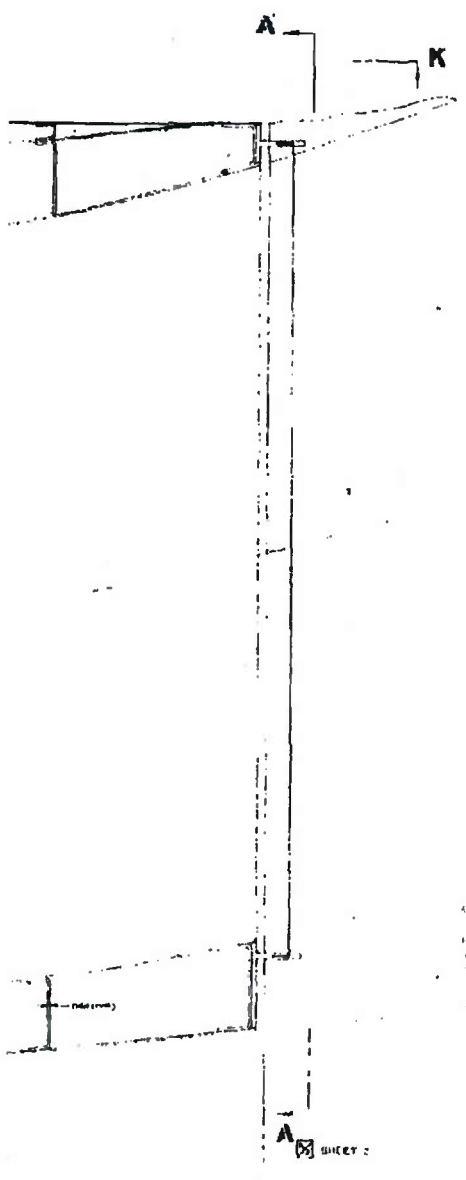
**A**  
SHEET C



3. SHEET B OF 3 FOR BEE A-A TO H-H  
4. AND MUST BE TO BE IN ACCORDANCE  
5. WITH THE TITLES & SHEET LINES  
6. APPROVED BY THE DESIGNER  
7. DATE OF MATERIAL  
8. OTHERWISE SPECIFIED

X81421

7



DECLASSIFIED IN FULL  
 Authority: EO 13526  
 Chief, Records & Declass Div, WHS  
 Date: OCT 02 2015

FIGURE 15. Design Layout, isymmetric Inlet

3 SEE SHEET 4 OF 3 FOR SEC. A-A TO H-H  
 4 INLET AND DUCT SHALL BE IN ACCORDANCE WITH AIRSIDE DRAWING SPECIFICATIONS  
 5 ALL STRUCTURAL PARTS TO BE MADE FROM 2024-T3 ALUMINUM  
 NOTES: 1. ALL DIMENSIONS UNLESS OTHERWISE SPECIFIED

X81421

DESIGN	AXISYMM
LAYOUT	TRIC INLET

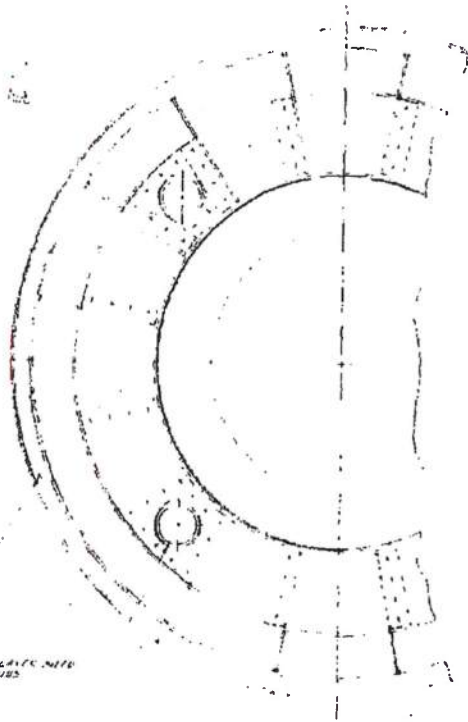
 Thurgood Marshall	X81421
-----------------------	--------

ASD-TDR-63-277, Vol. IV

~~SECRET RESTRICTED DATA~~

~~ATOMIC ENERGY ACT OF 1954~~

1



R44.25000.00000



SECTION H-H SHEET 1

~~SECRET RESTRICTED DATA~~

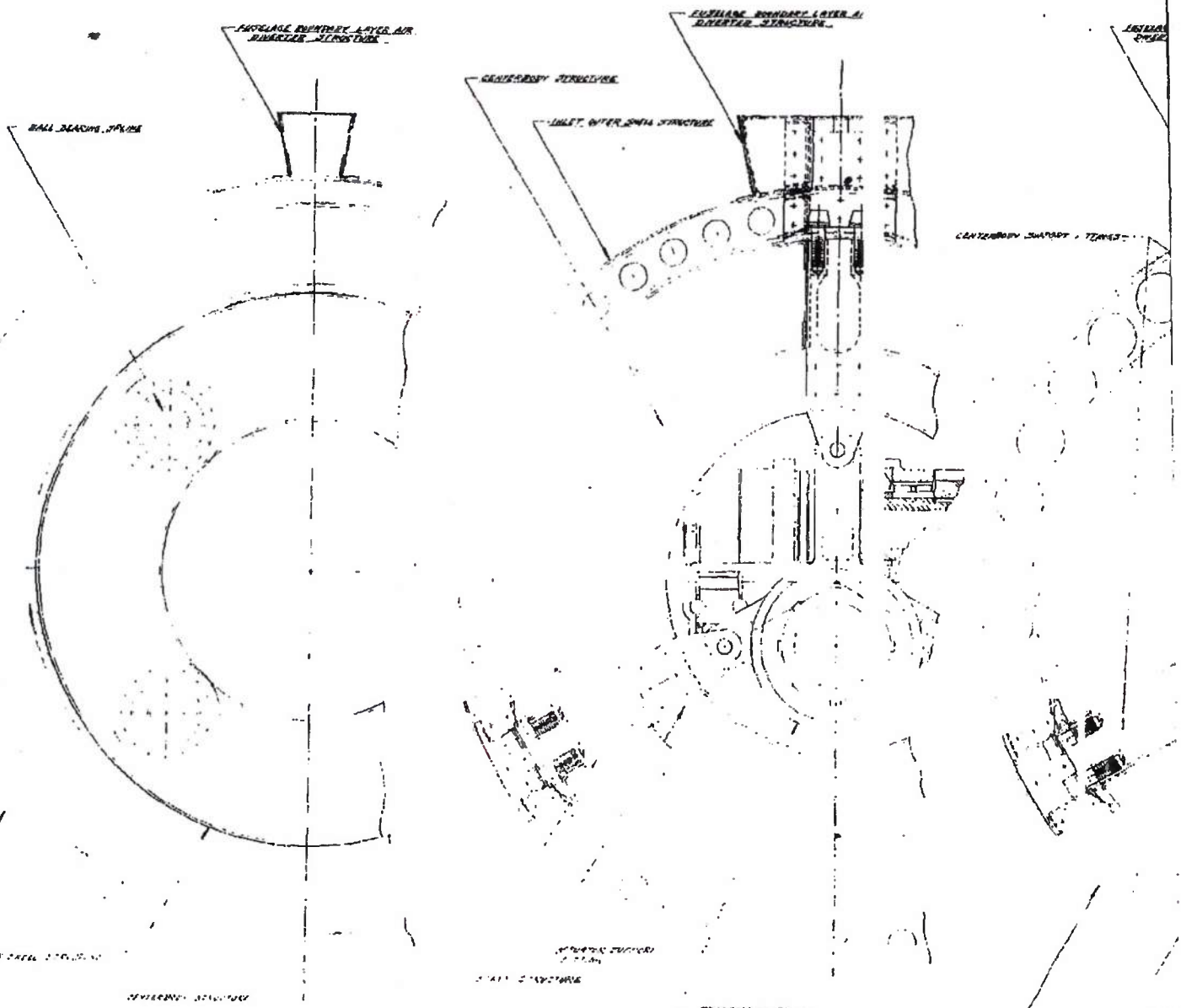
~~ATOMIC ENERGY ACT OF 1954~~

12

11

10

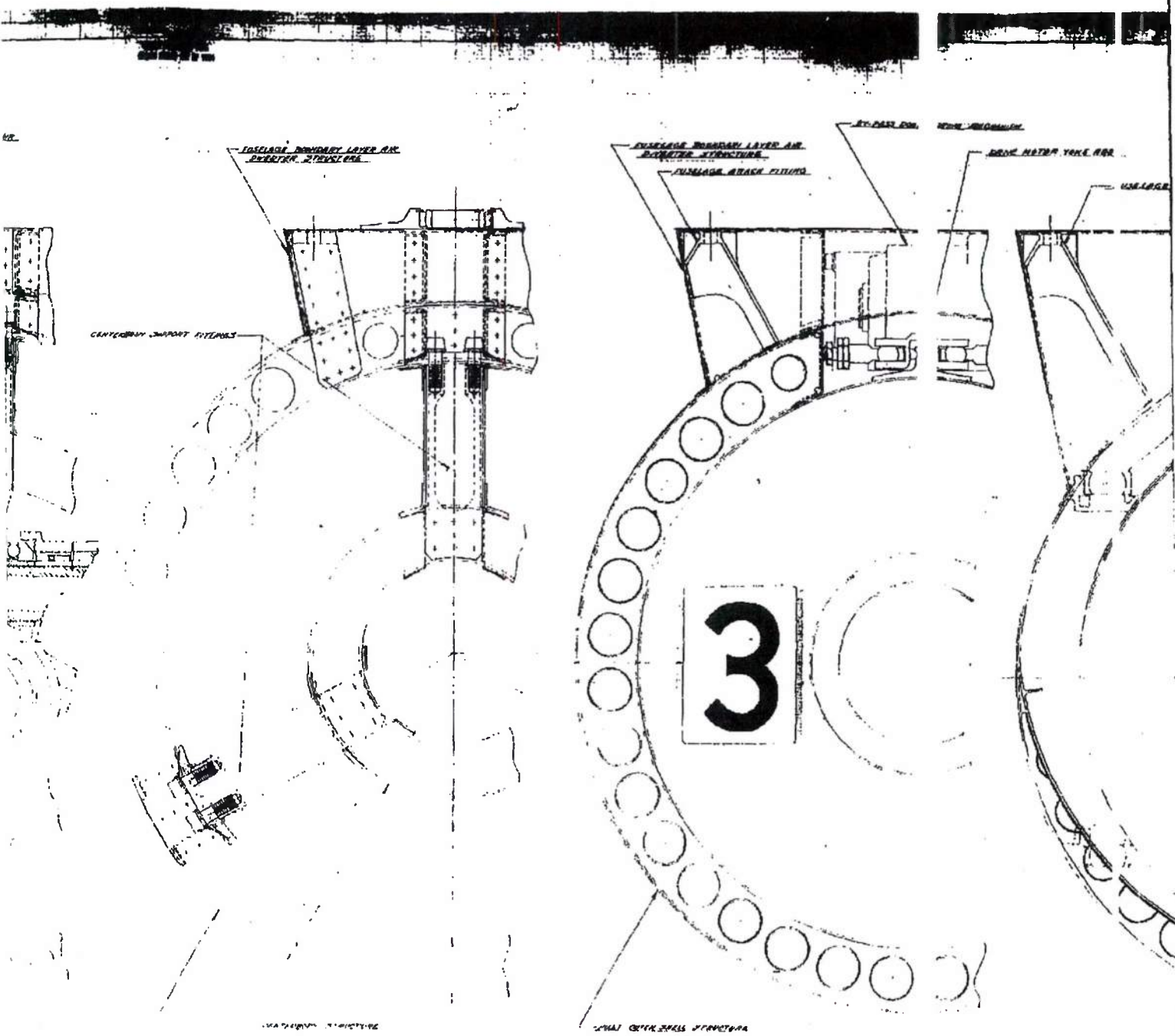
DECLASSIFIED IN FULL  
Authority: EO 13526  
Chief, Records & Declass Div, WHS  
Date: OCT 02 2015



2

X 814 21

DECLASSIFIED IN FULL  
 Authority: EO 13526  
 Chief, Records & Declass Div, WHS  
 Date: OCT 0 2 2015



SHEET 1

SECTION 15-15 SHEET 1

SECTION 13 SHEET 1

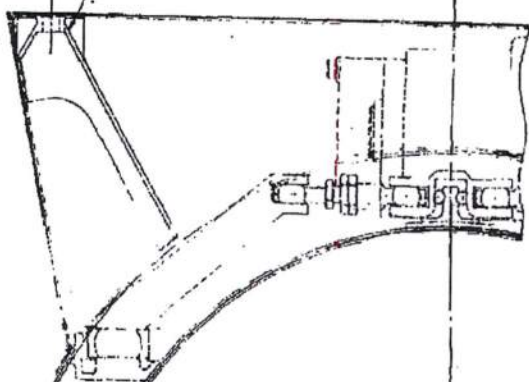
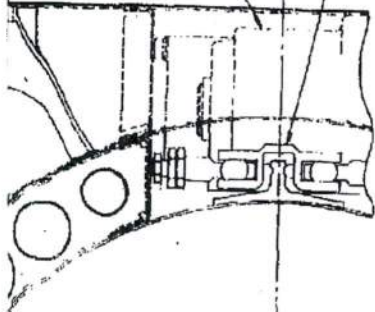
DECLASSIFIED IN FULL  
 Authority: EO 13526  
 Chief, Records & Declass Div, WHS  
 Date: OCT 02 2015

4

DRIVE SHAFT AIR  
DISCONNECT  
W. AIR SEAL PLATING

DRIVE SHAFT YOKER ASSEMBLY

EDGEWELL AIR SEAL PLATING

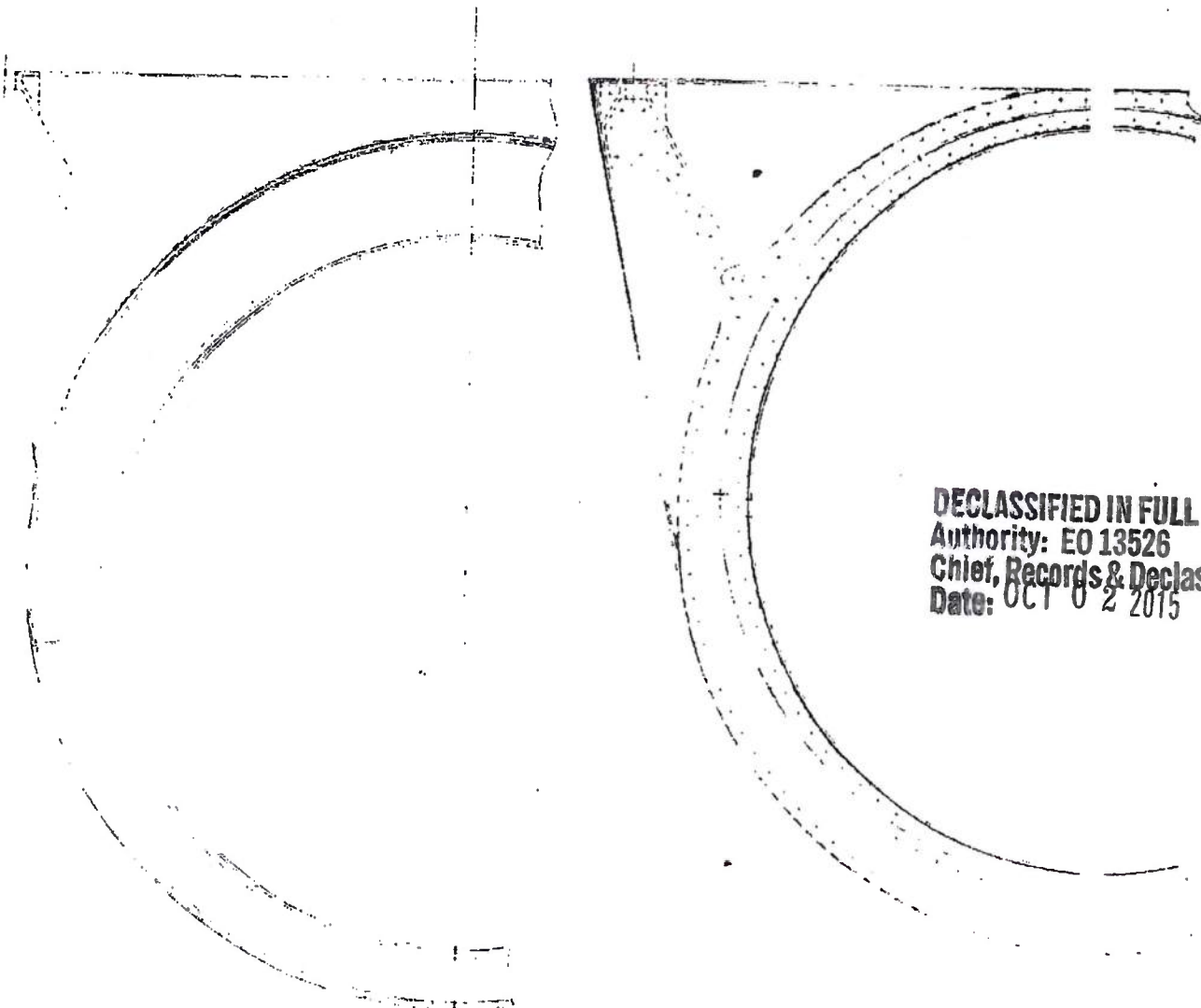


SECTION D-D SHEET 1

SECTION G-G SHEET 1

SECTION H-H SHEET 1

DECLASSIFIED IN FULL  
Authority: EO 13526  
Chief, Records & Declass Div, WHS  
Date: OCT 0 2 2015



DECLASSIFIED IN FULL  
Authority: EO 13526  
Chief, Records & Declass Div, WHS  
Date: OCT 02 2015

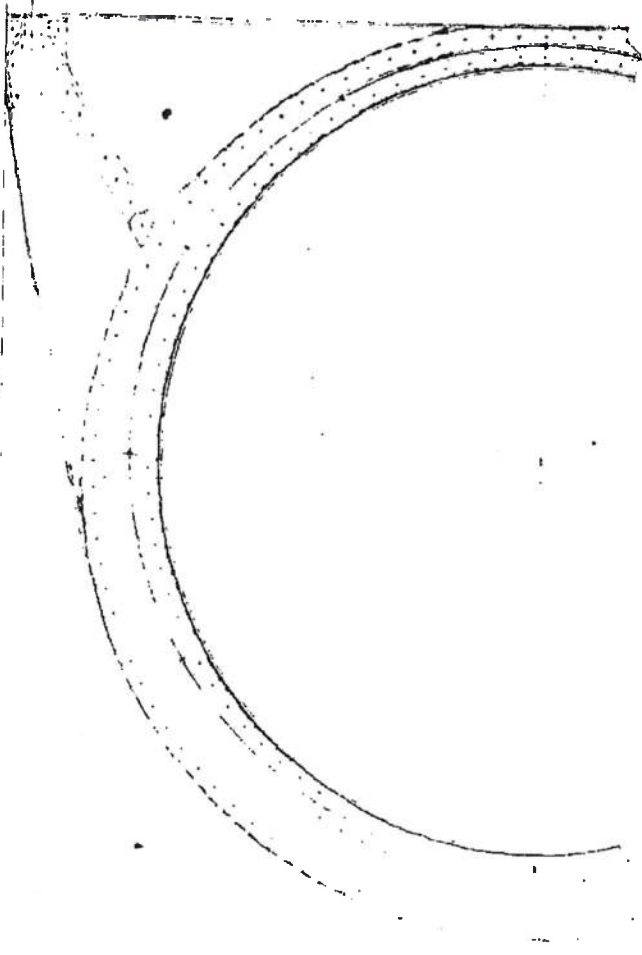
5

FIGU

11-B SHEET 1

11-A SHEET 2

STANDARD SHEET FOR DESIGN AND CONSTRUCTION



DECLASSIFIED IN FULL  
Authority: EO 13526  
Chief, Records & Declass Div, WHS  
Date: OCT 0 2 2015

FIGURE 16. Design Layout, Asymmetric Inlet

SECTION A-A SHEET 2

~~CONFIDENTIAL~~  
~~UNCLASSIFIED~~  
~~EXCLUDED FROM AUTOMATIC DOWNGRADING AND DECLASSIFICATION~~

DESIGN ASYMMETRIC INLET	APPROVED DATE DESIGNED BY CHECKED BY	DRAWN BY DATE PROJECT NO. SHEET NO.	Harquardt x81421
-------------------------------	---	--	---------------------

~~SECRET RESTRICTED DATA~~

~~ATOMIC ENERGY ACT OF 1954~~

CD  
40,340

1

\*SEPARATING INLET STEEL

CONV. LIP STRUCTURE

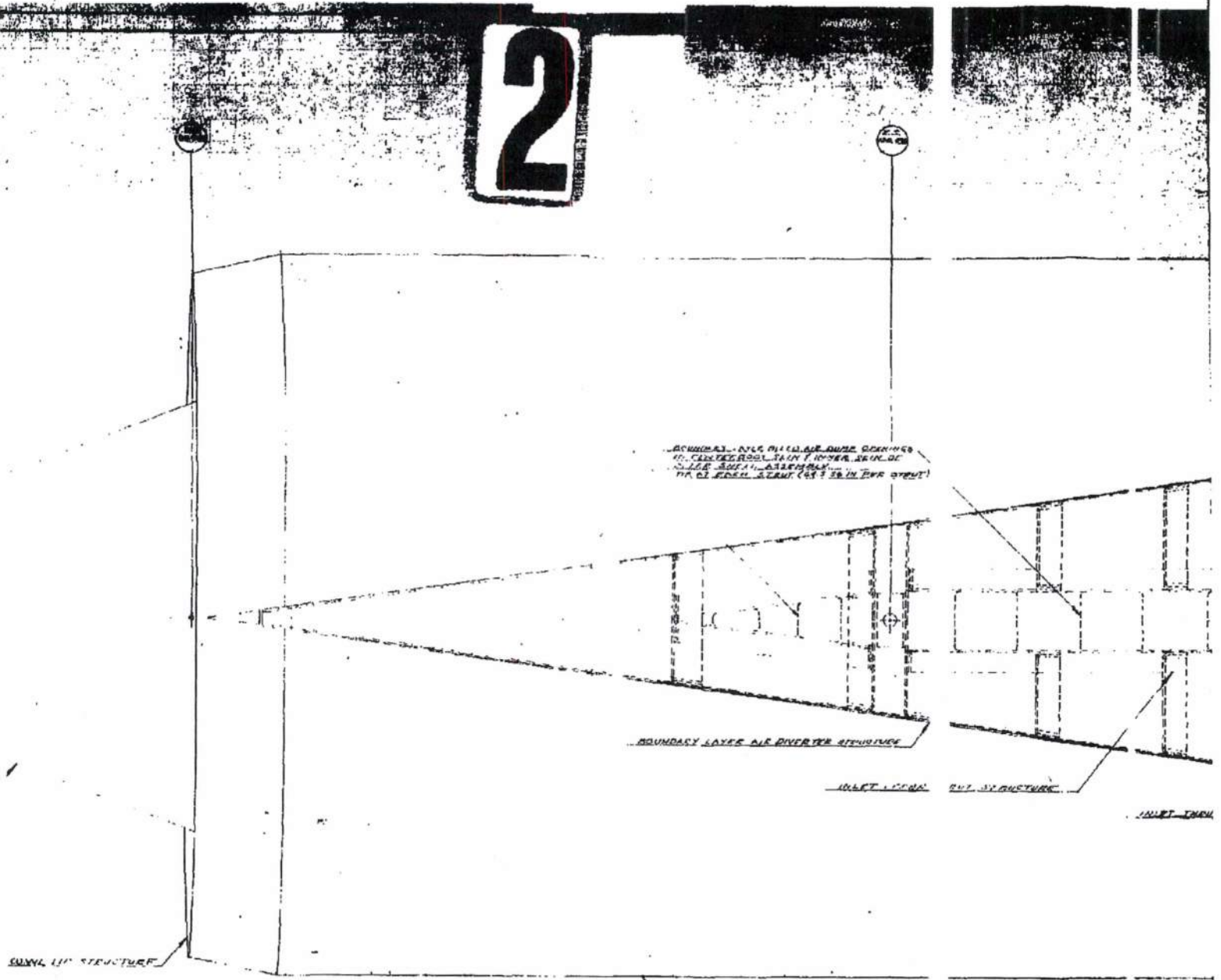
DECLASSIFIED IN FULL  
Authority: EO 13526  
Chief, Records & Declass Div, WHS  
Date: OCT 02 2015

~~SECRET RESTRICTED DATA~~

~~ATOMIC ENERGY ACT OF 1954~~

X81421 3

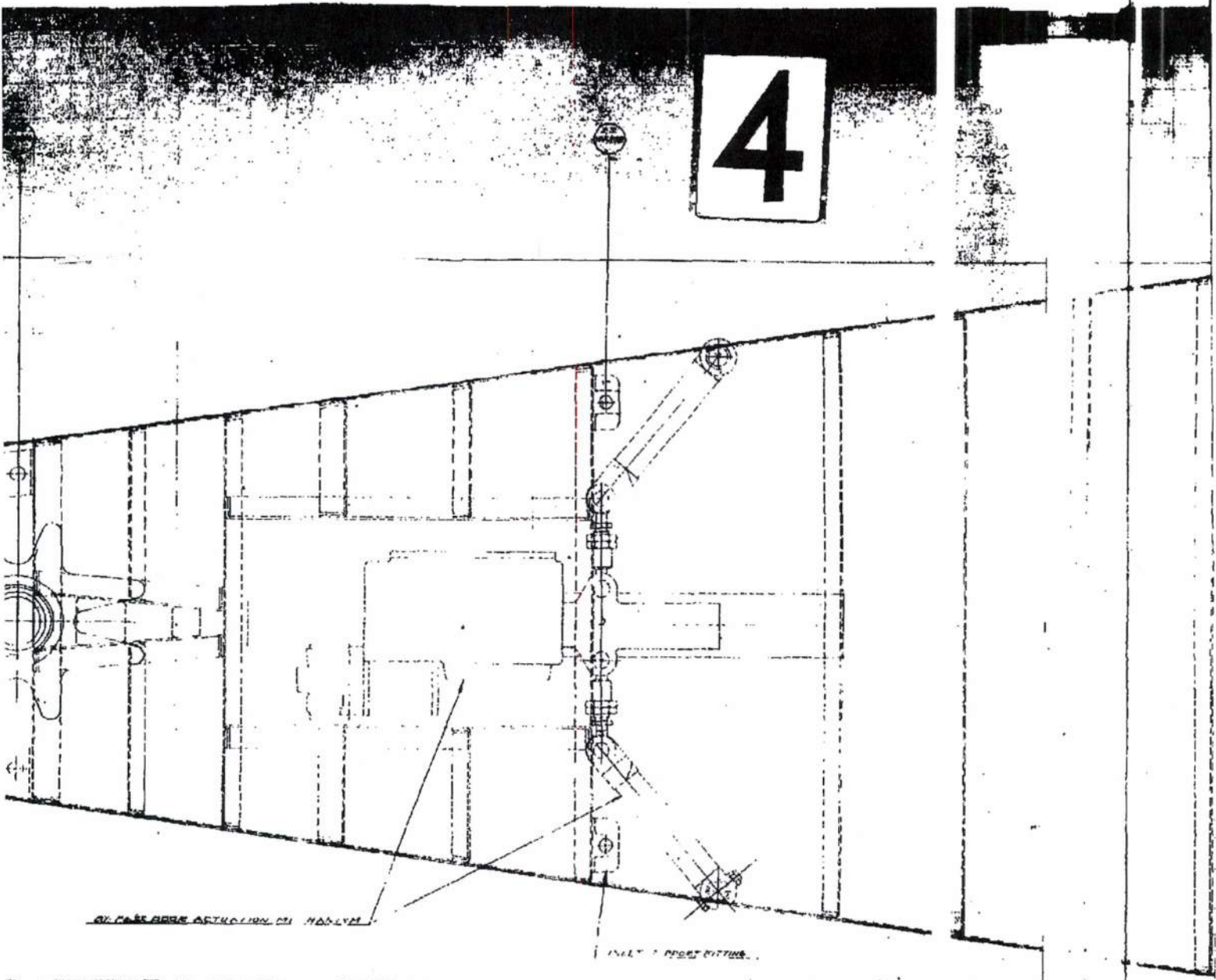
2



Page determined to be Unclassified  
Reviewed Chief, RDD, WHS  
IAW EO 13526, Section 3.5  
Date: OCT 02 2015



4



Page determined to be Unclassified  
Reviewed Chief, RDD, WHS  
LAW EO 13526, Section 3.5  
Date: OCT 02 2015

VIEW K-K

INLET 1 POST CUTTING

X

5

TOP MARKING

⊕

⊕

SMALL SHEET CUTTING

X814213

DECLASSIFIED IN FULL  
Authority: EO 13526  
Chief, Records & Declass Div, WHS  
Date: OCT 02 2015





CONFIDENTIAL

ASD-TDR-63-277, Vol. IV

REPORT 6003

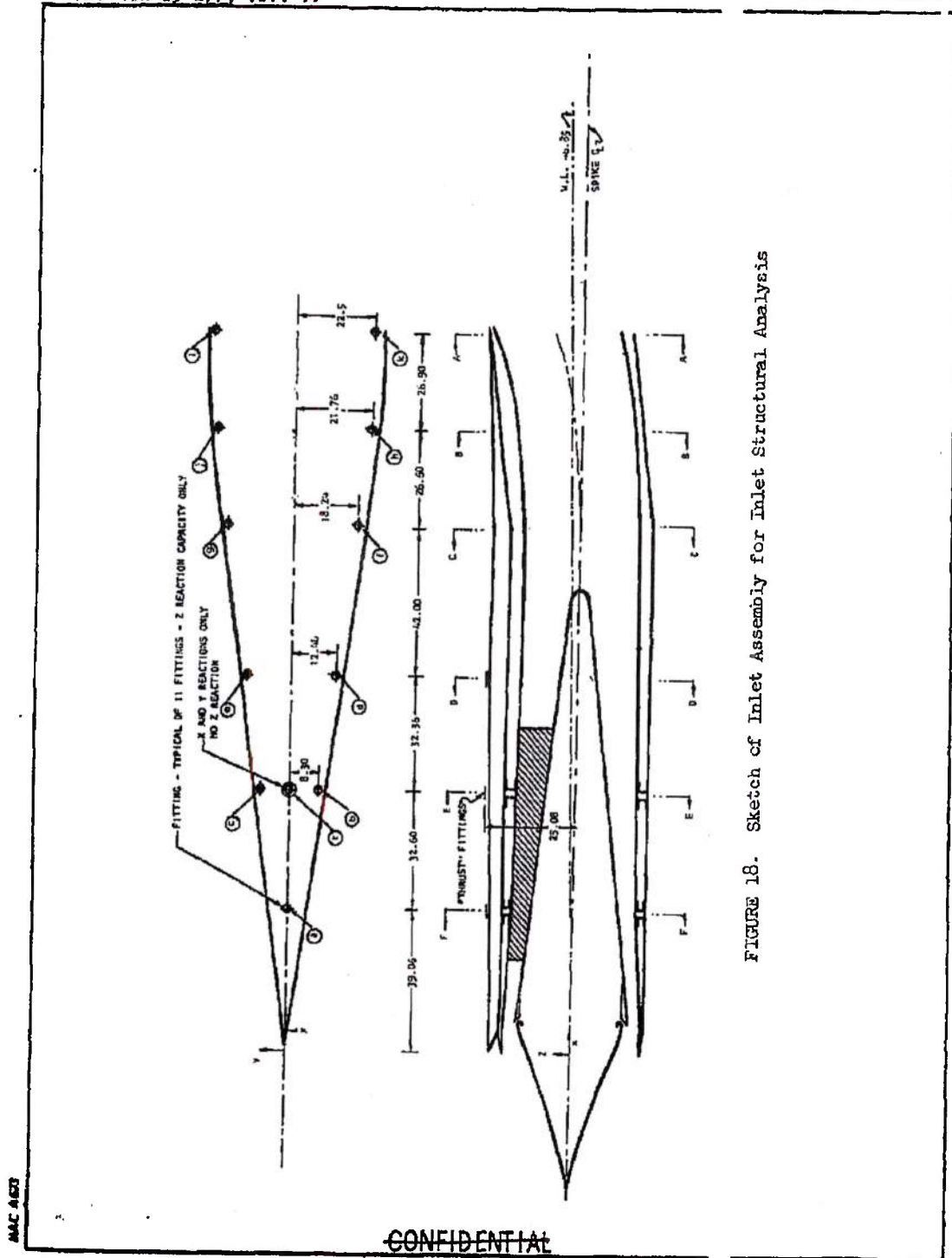


FIGURE 18. Sketch of Inlet Assembly for Inlet Structural Analysis

CONFIDENTIAL

~~CONFIDENTIAL~~

ASD-TDR-63-277, Vol. IV

6003

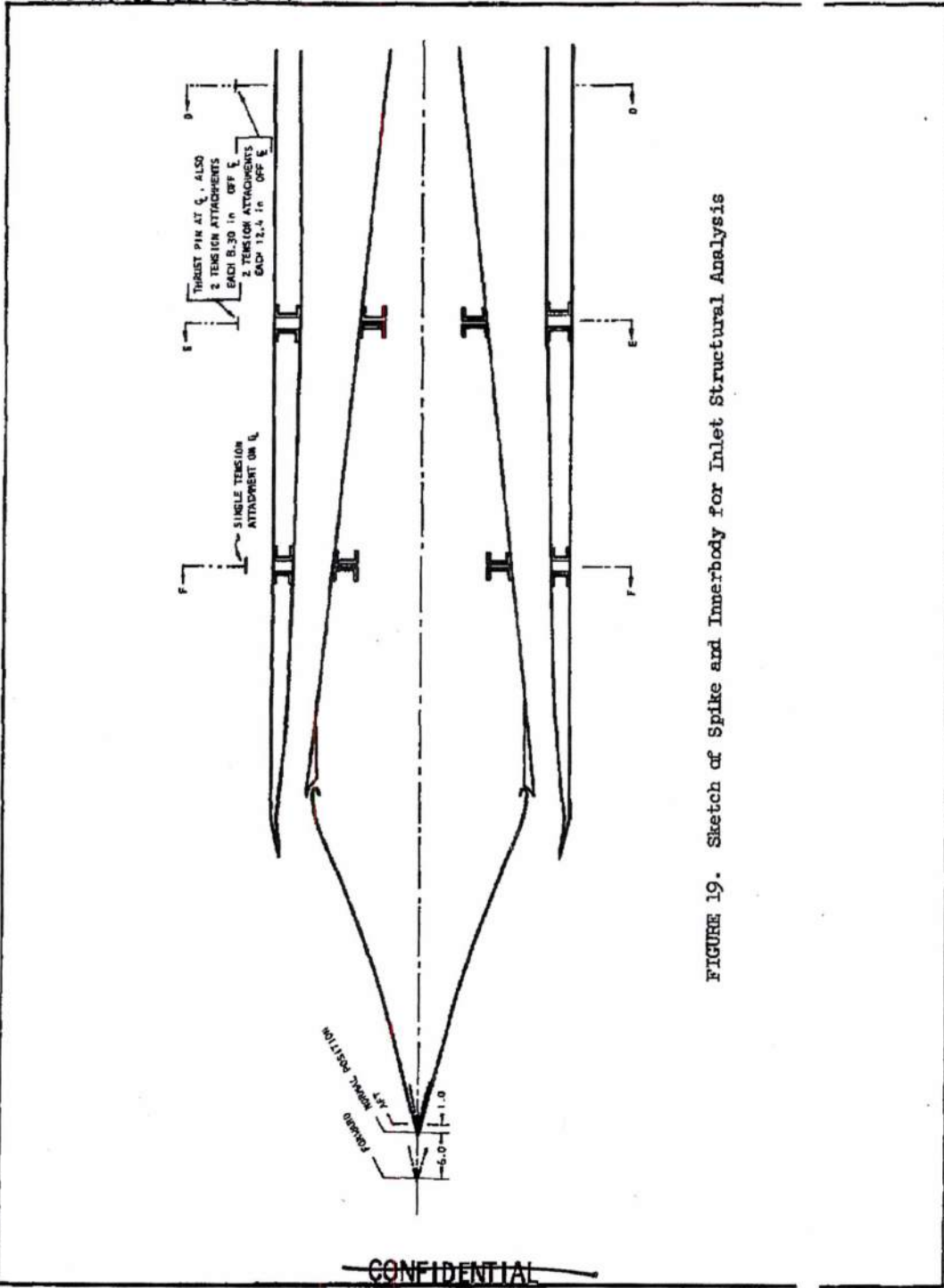


FIGURE 19. Sketch of Spike and Innerbody for Inlet Structural Analysis

~~CONFIDENTIAL~~

DECLASSIFIED IN FULL  
 Authority: EO 13526  
 Chief, Records & Declass Div, WHS  
 Date: OCT 02 2015

~~SECRET RESTRICTED DATA~~  
~~ATOMIC ENERGY ACT OF 1954~~

REPORT 6003

ASD-TDR-63-277, Vol. IV

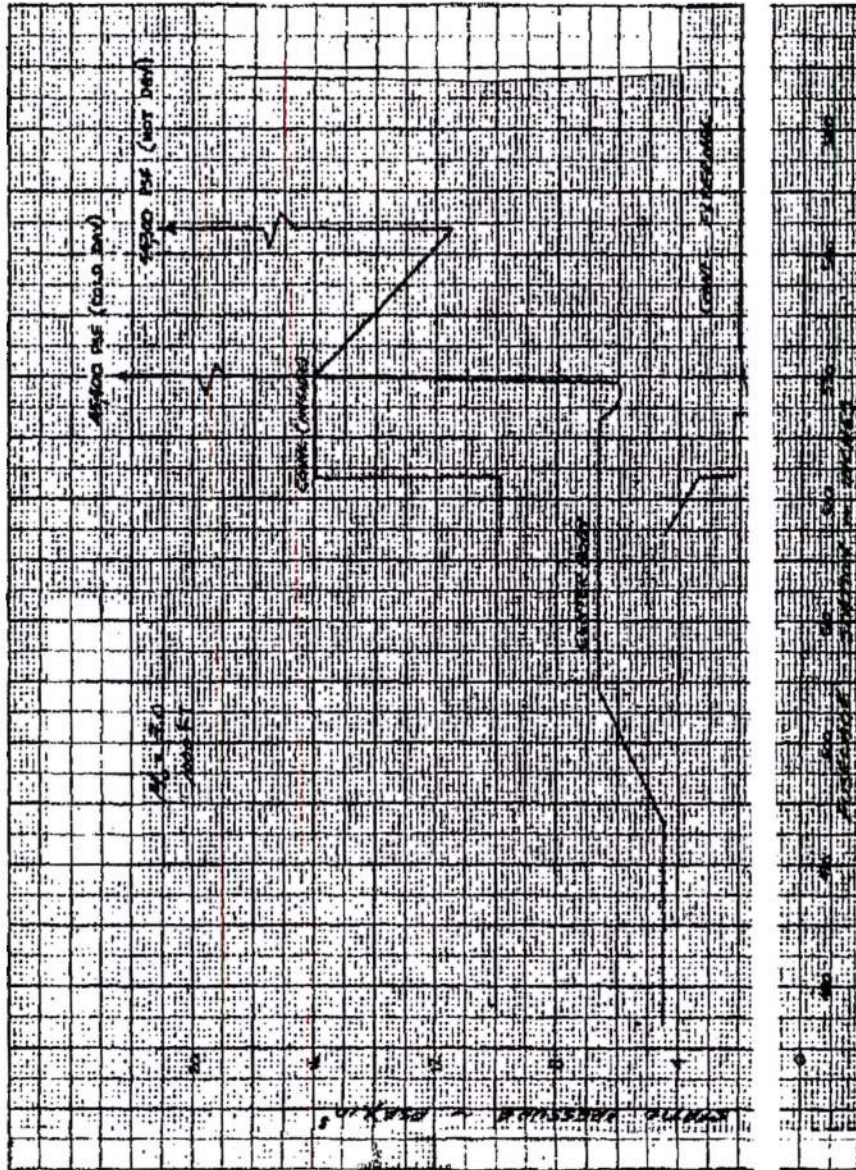


FIGURE 20. MA50-XCA Inlet-Diffuser Static Pressure

MAC AOB

~~SECRET RESTRICTED DATA~~  
~~ATOMIC ENERGY ACT OF 1954~~

N22E615

Page determined to be Unclassified  
Reviewed Chief, RDD, WHS  
IAW EO 13526, Section 3.5  
Date: OCT 02 2015

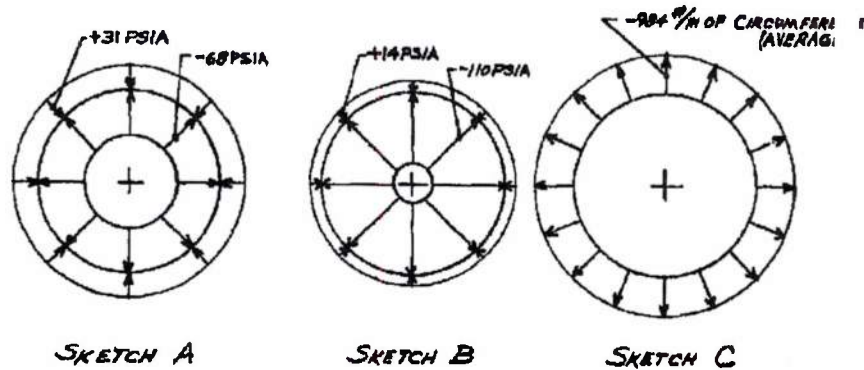


FIGURE 21. Varying Pressures on Inside and Outside Lip and Cowl Surfaces

MAC ACZ

Page determined to be Unclassified  
Reviewed Chief, RDD, WHS  
IAW EO 13526, Section 3.5  
Date:

OCT 02 2015

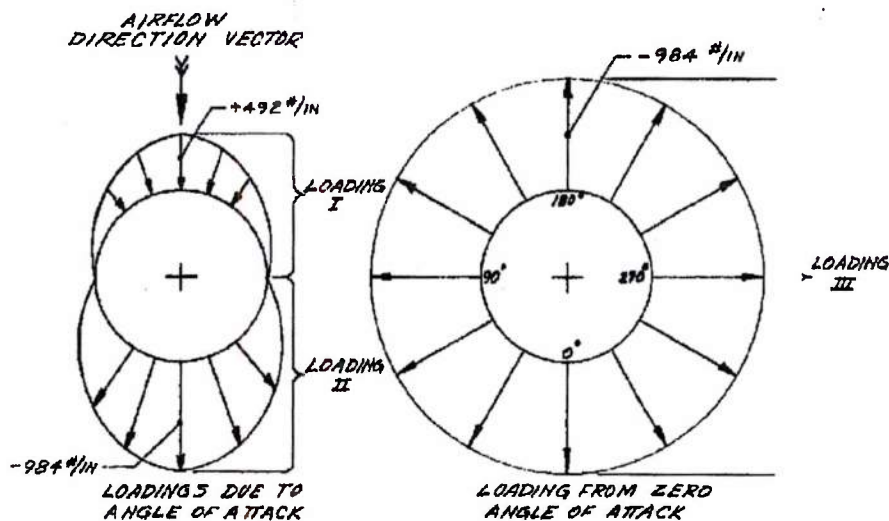


FIGURE 22. Three Loadings for Analysis Structure

MAC A50

~~CONFIDENTIAL~~

ASD-TDR-63-277, Vol. IV

RPC

6003

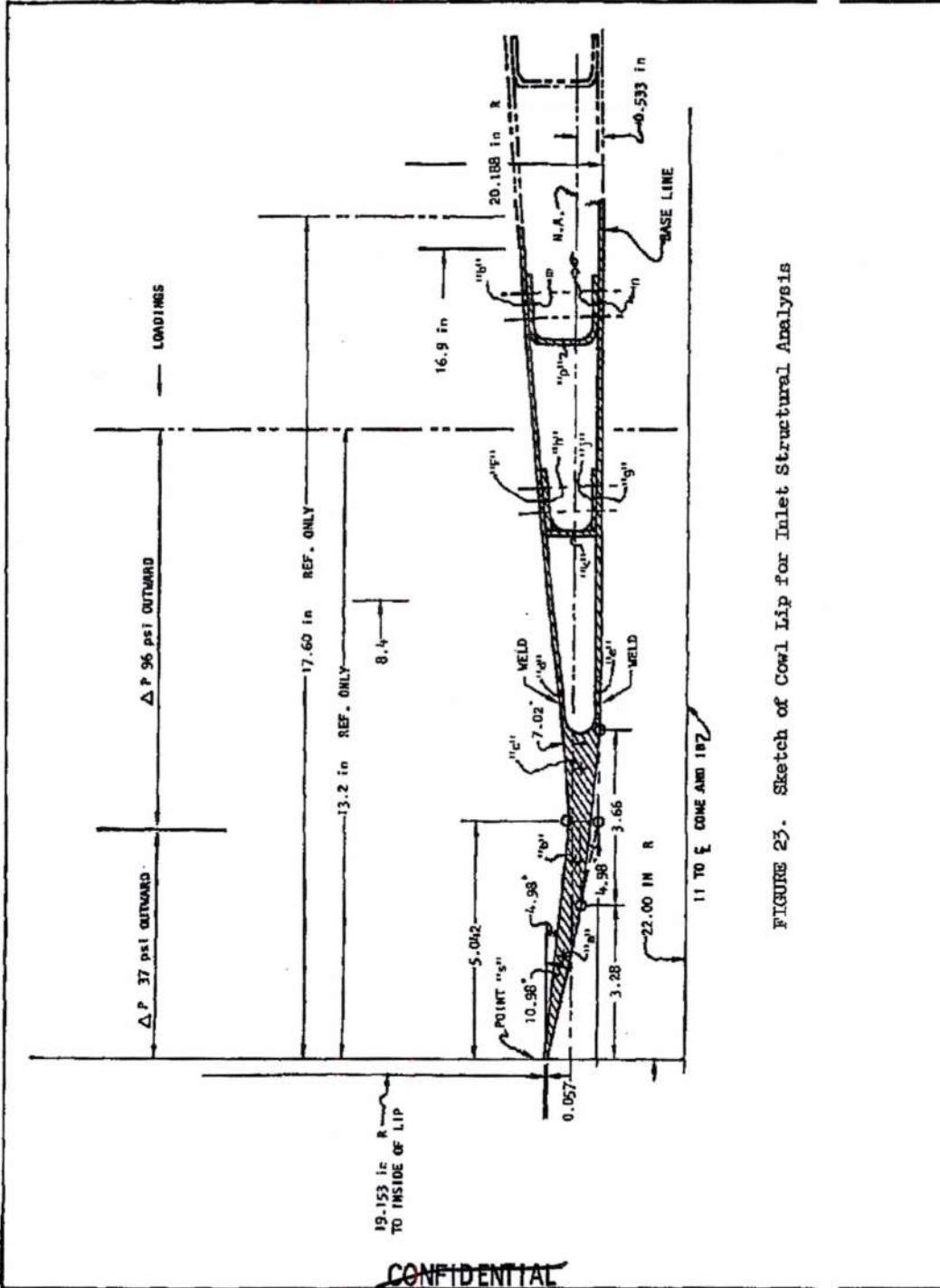


FIGURE 23. Sketch of Cowl Lip for Inlet Structural Analysis

MAC ASD

CONFIDENTIAL

Page determined to be Unclassified  
Reviewed Chief, RDD, WHS  
IAW E.O. 13526, Section 3.5  
Date: OCT 02 2015

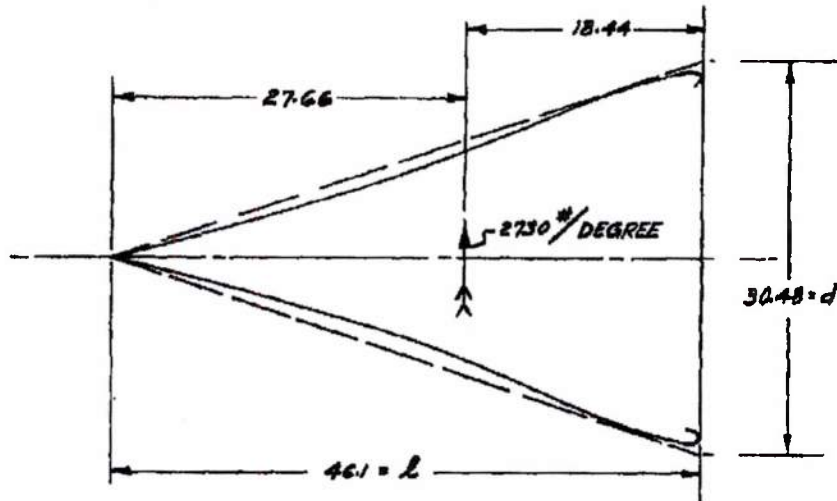


FIGURE 24. Spike Geometry

MAC 1603

UNCLASSIFIED

ASD-TDR-63-277, Vol. IV

DRY 6003

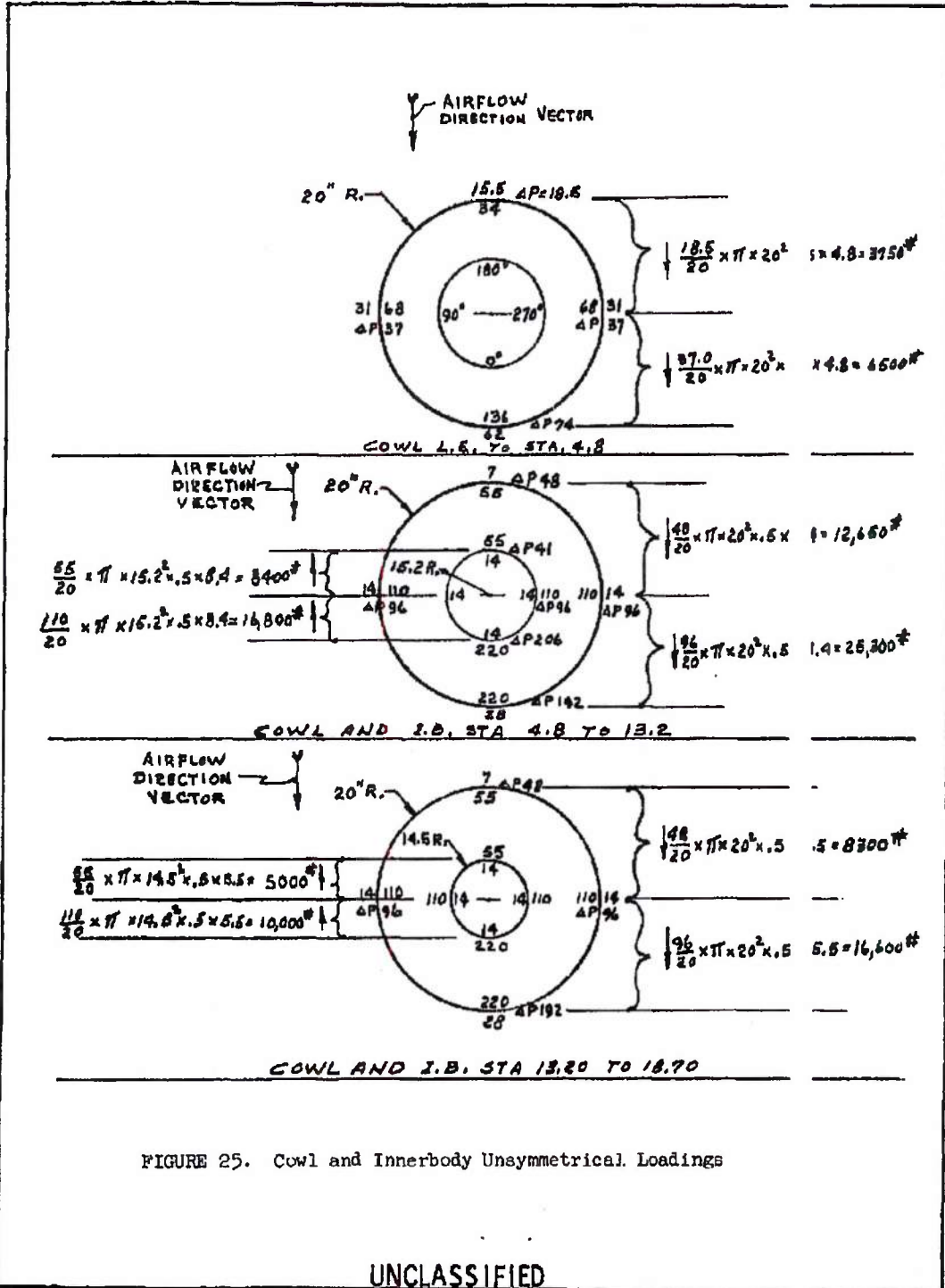


FIGURE 25. Cowl and Innerbody Unsymmetrical Loadings

UNCLASSIFIED

~~CONFIDENTIAL~~

ASD-TDR-63-277, Vol. IV

REPORT 6003

MAC A627

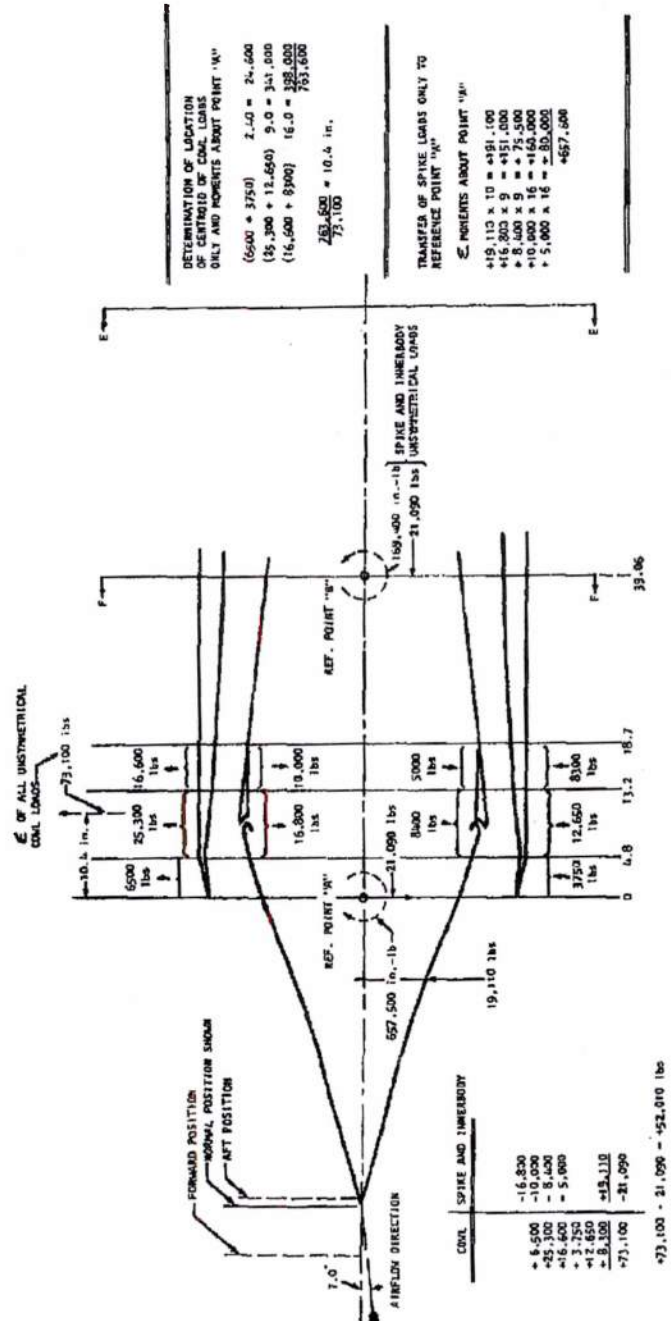


FIGURE 20. CIVIL and Innerbody Load Paths (Unsymmetrical Loadings)

~~CONFIDENTIAL~~

Page determined to be Unclassified  
 Reviewed Chief, RDD, WHS  
 IAW EO 13526, Section 3.5  
 Date: OCT 0 2 2015

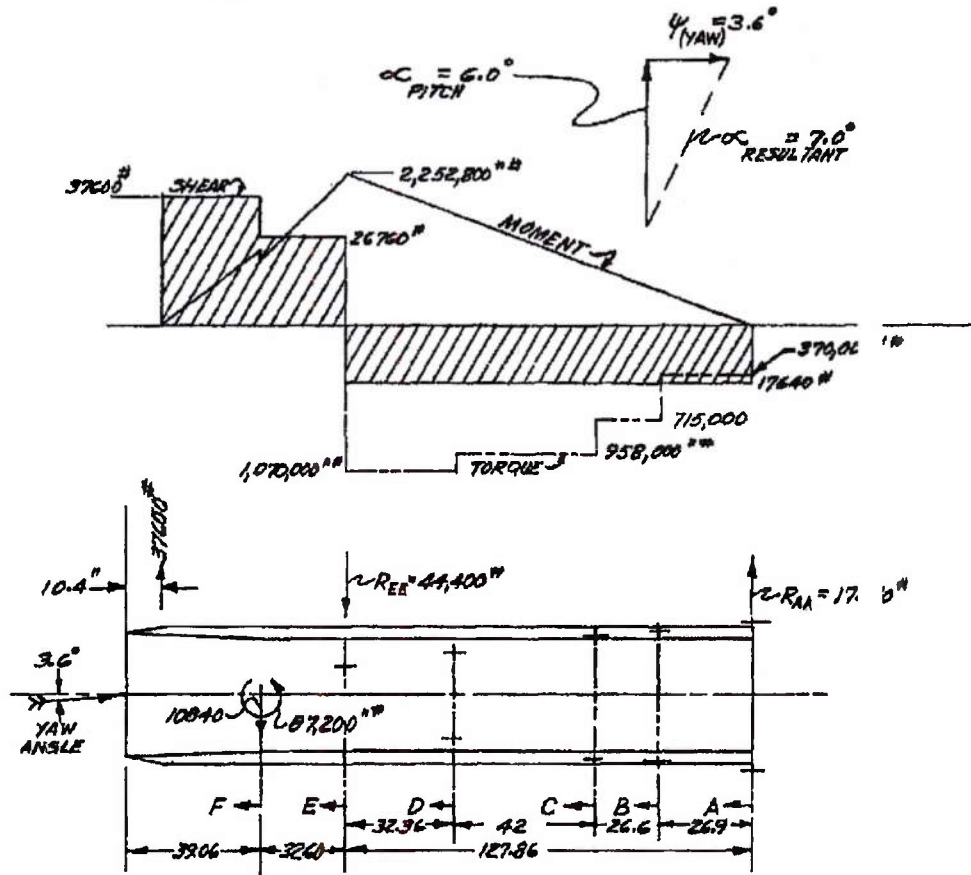


FIGURE 27. Unsymmetrical Air Load Distribution

Page determined to be Unclassified  
Reviewed Chief, RDD, WHS  
IAW EO 13526, Section 3.5  
Date: OCT 02 2015

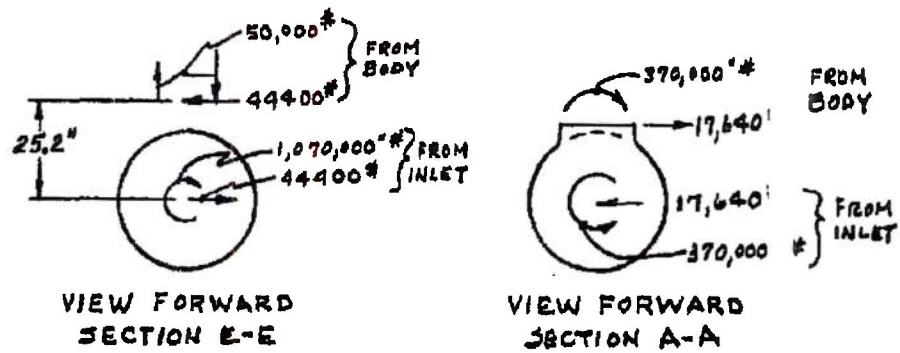


FIGURE 28. Shears, Moments, and Torques from Y Direction

MAC AGO

Page determined to be Unclassified  
Reviewed Chief, RDD, WHS  
IAW E.O. 13526, Section 3.5  
Date: OCT 02 2015

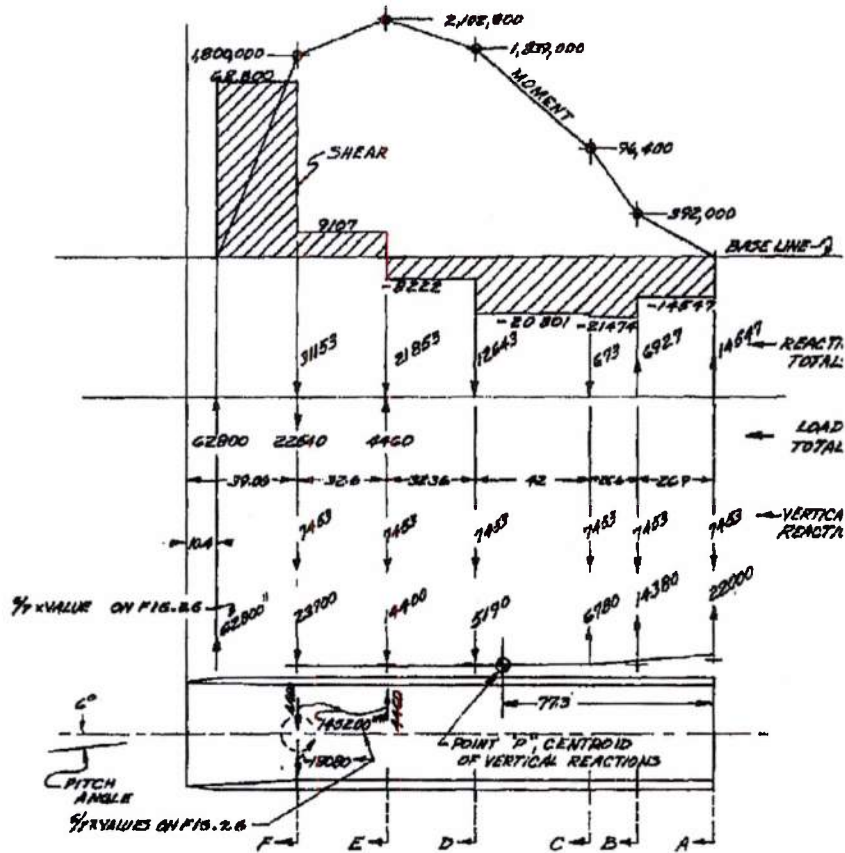


FIGURE 29. Shears and Moments from Z Direction Components

MAC 453

~~CONFIDENTIAL~~

ASD-TDR-63-277, Vol. IV

REPORT 6003

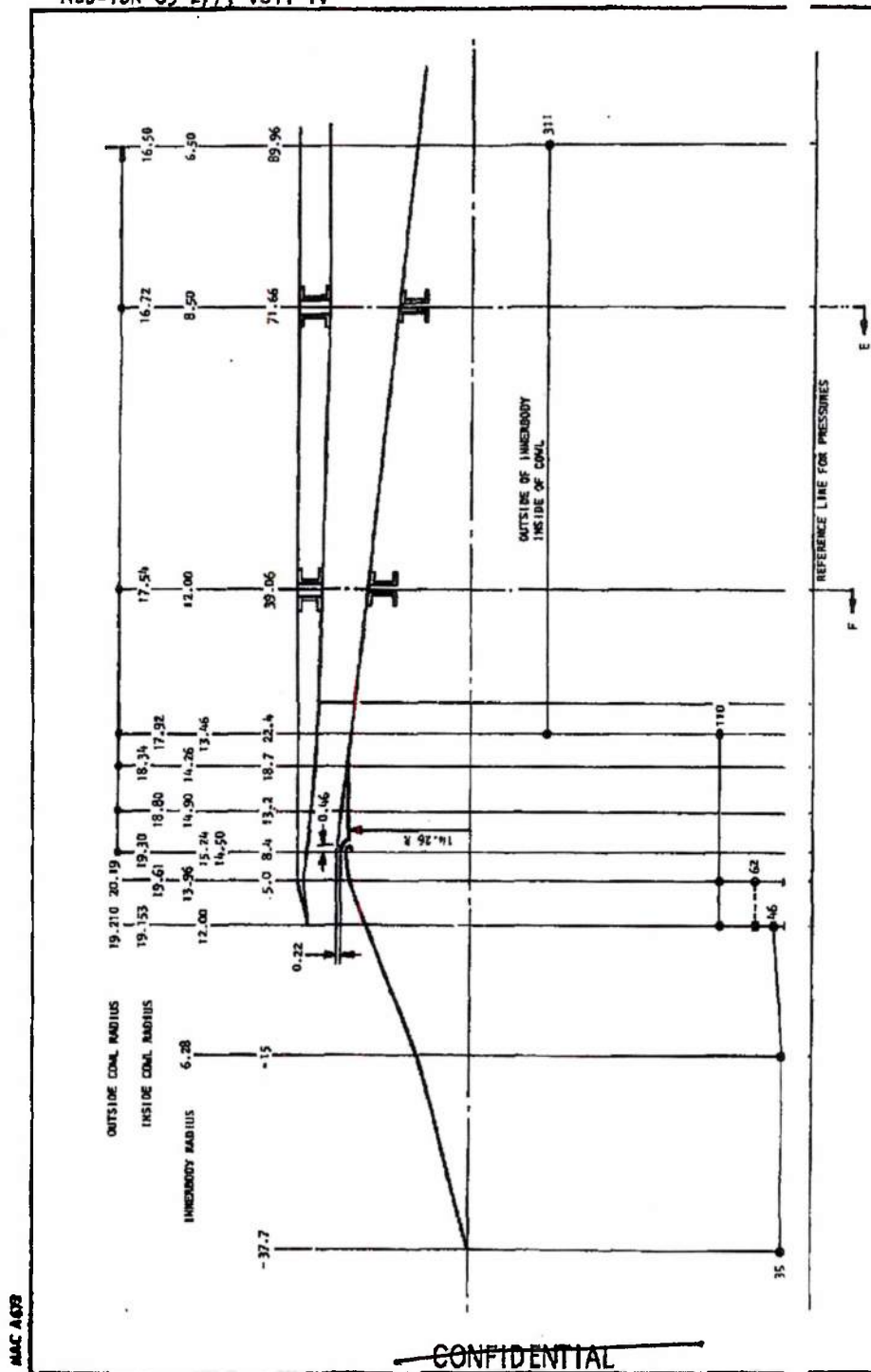


FIGURE 30. Geometry and Pressures for Inlet Structural Analysis

MAC A078

~~CONFIDENTIAL~~

UNCLASSIFIED

ASD-TDR-63-277, Vol. IV

IT 6003

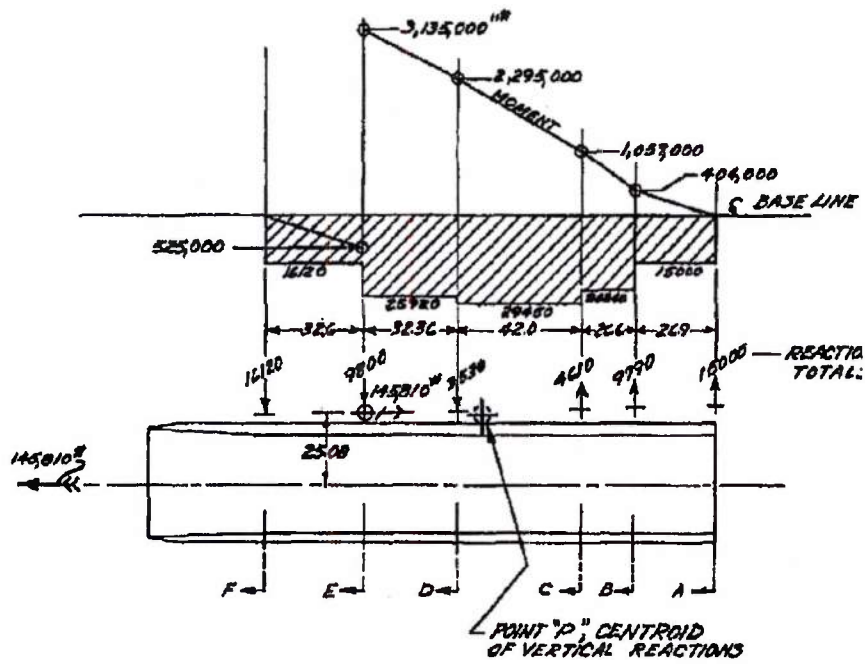


FIGURE 31. Derived Load Distribution on Fittings

MAC ACP

UNCLASSIFIED

Page determined to be unclassified  
Reviewed Chief, RDD, WHS  
IAW EO 13526, Section 3.5  
Date: OCT 0 2 2015

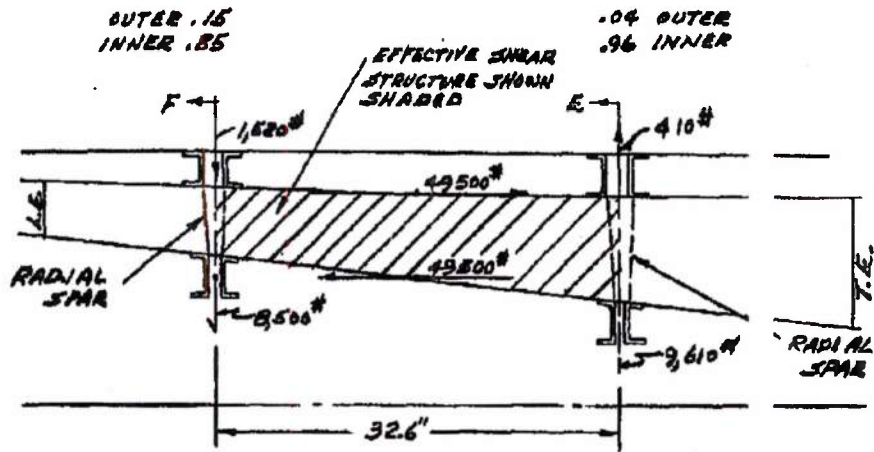


FIGURE 32. Longitudinal Section Through Typical Strut

MAC 443

UNCLASSIFIED

ASD-TDR-63-277, Vol. IV

PORT 6003

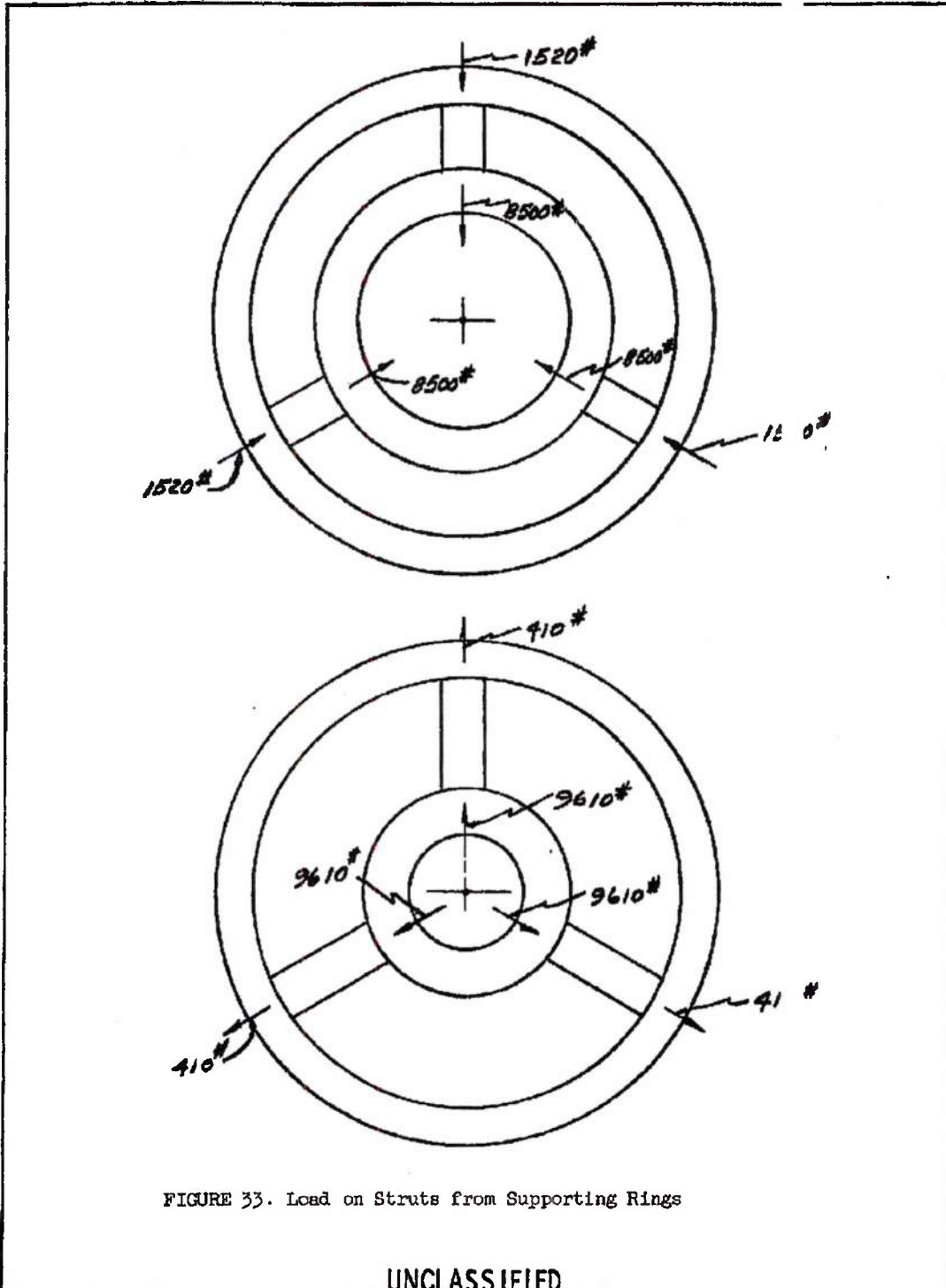


FIGURE 33. Load on Struts from Supporting Rings

UNCLASSIFIED

MAC AGE

UNCLASSIFIED

ASD-TDR-63-277, Vol. IV

REPORT 6003

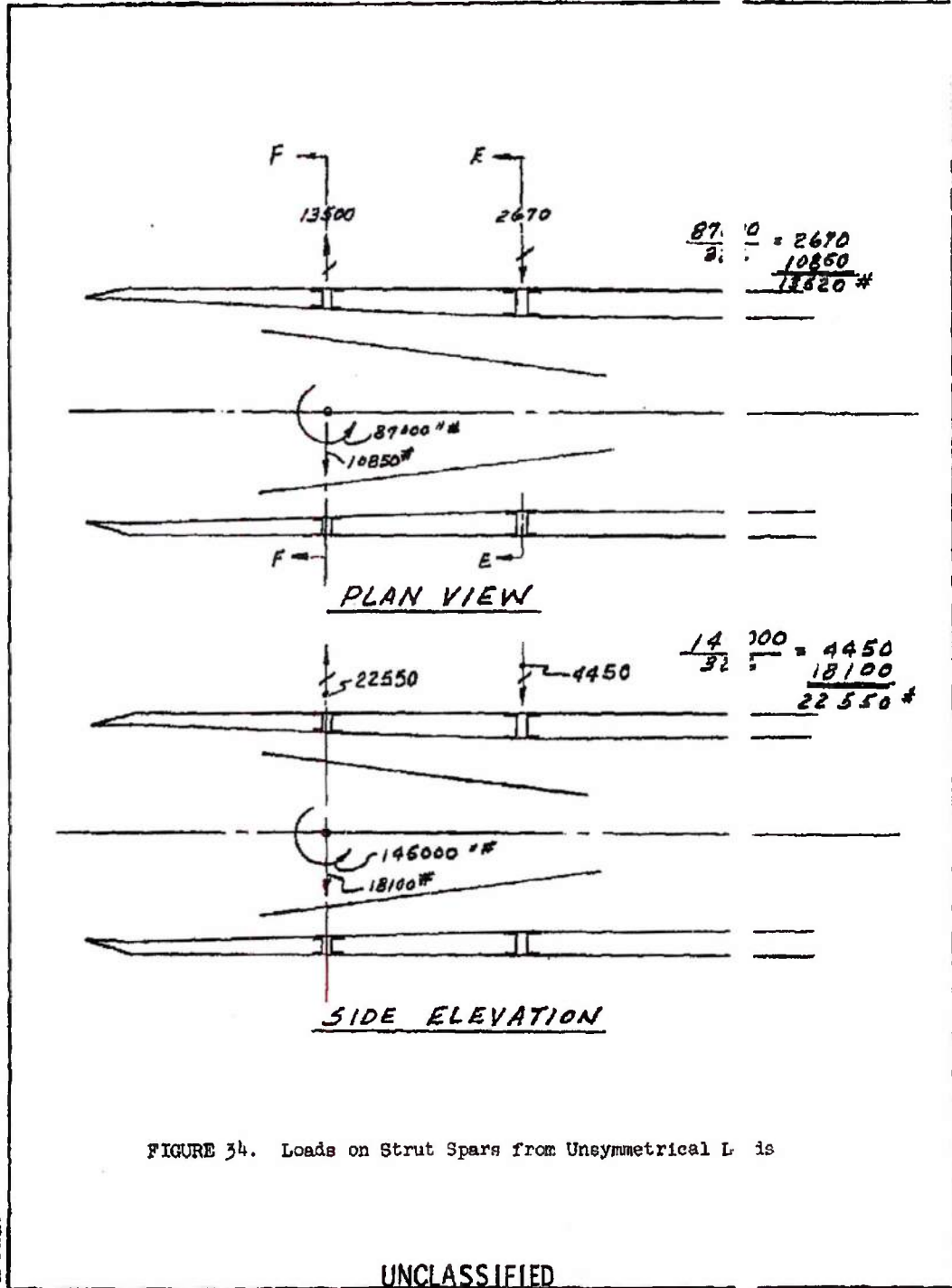


FIGURE 34. Loads on Strut Spars from Unsymmetrical L-1s

UNCLASSIFIED

ASD-TDR-63-277, Vol. IV

REPO 6003

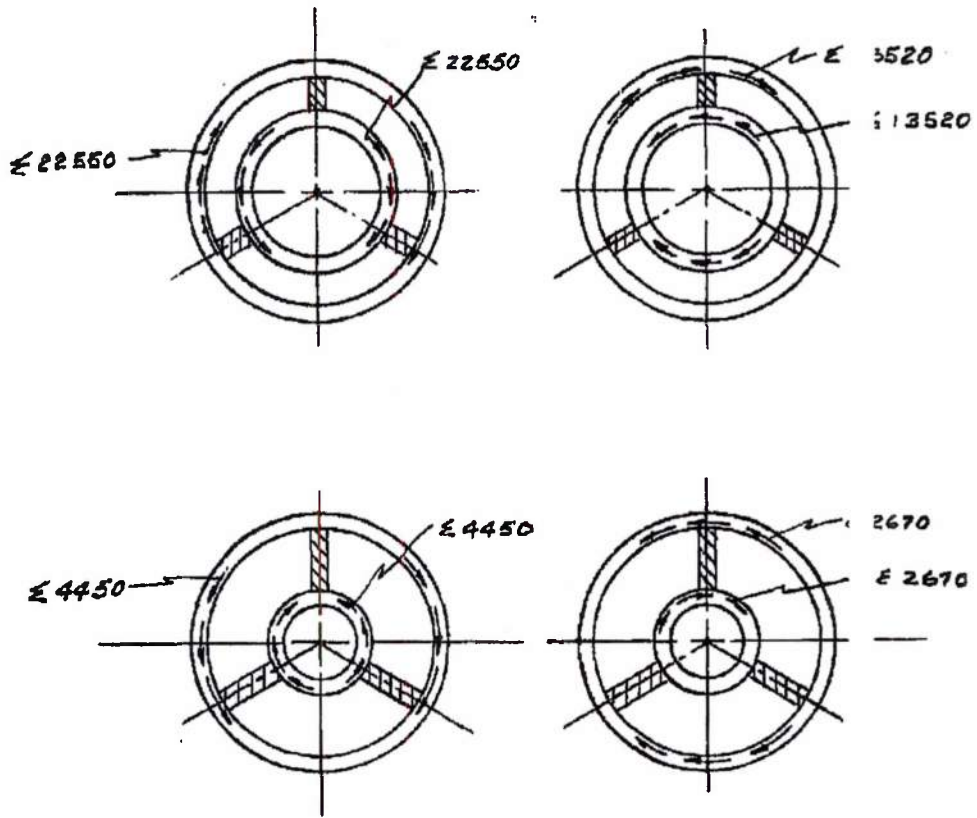


FIGURE 35. Vertical and Horizontal Loads on Strut Spars

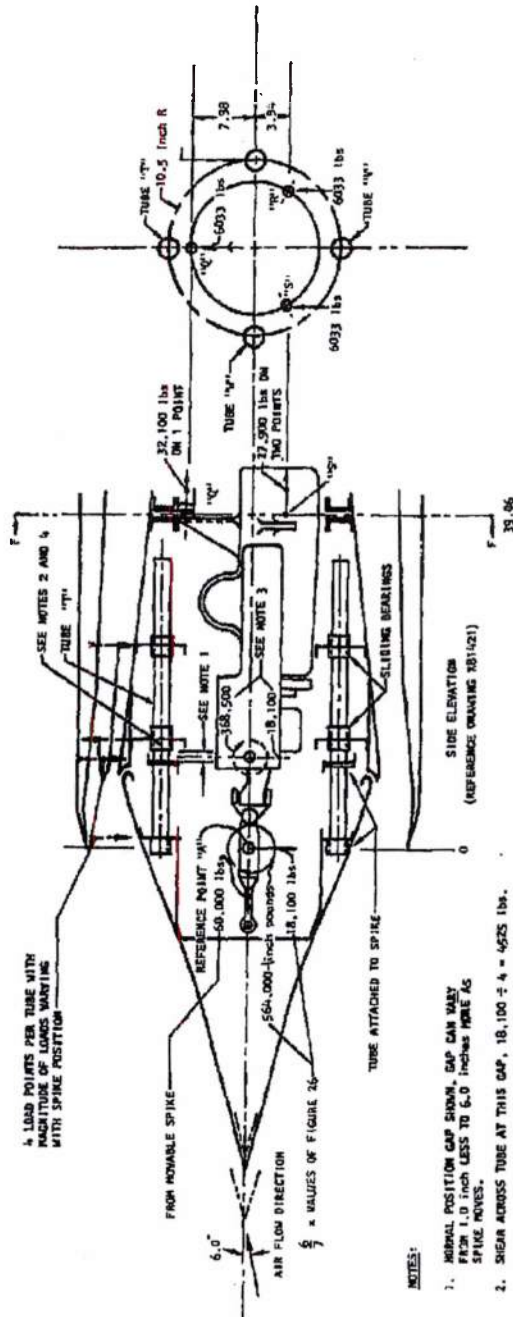
MAC 6073

UNCLASSIFIED

~~CONFIDENTIAL~~

REPORT 6003

ASD-TDR-63-277, Vol. IV



NOTES:

1. NORMAL POSITION GAP SHOWN. GAP CAN VARY FROM 1.0 INCH LESS TO 6.0 INCHES MORE AS SPIKE MOVES.
2. SHEAR ACROSS TUBE AT THIS GAP, 18,100 ± 4 = 4255 LBS.
3. LOADS OF POINT "A" TRANSMITTED FOR REFERENCE PURPOSES.
4. PRIMARY MOMENT OF 168,500 ± 4 MUST BE CARRIED BY EACH TUBE IN ADDITION TO SECONDARY MOMENTS.

MAC AG39

~~CONFIDENTIAL~~

Page determined to be Unclassified  
Reviewed Chief, RDD, WHS  
IAW EO 13526, Section 3.5  
Date: OCT 02 2015

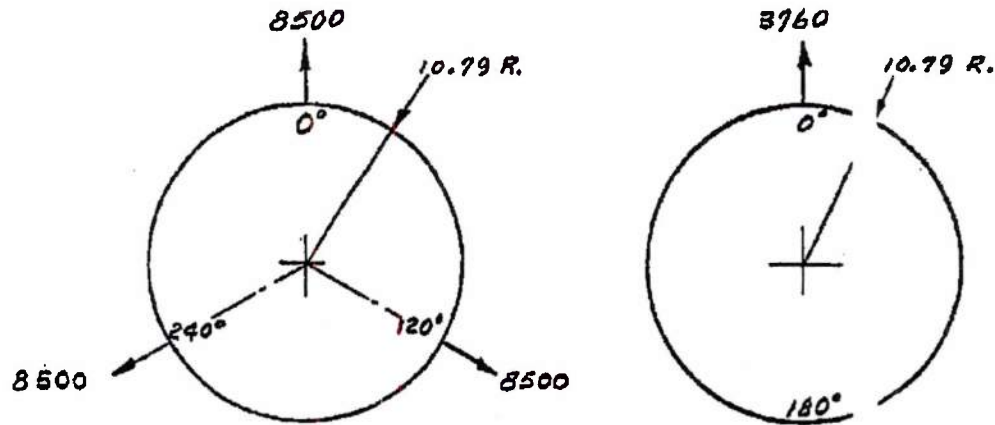


FIGURE 37. Innerbody Ring Loads

MAC A57

Page determined to be Unclassified  
Reviewed Chief, RDD, WHS  
IAW EO 13526, Section 3.5  
Date: OCT 02 2015

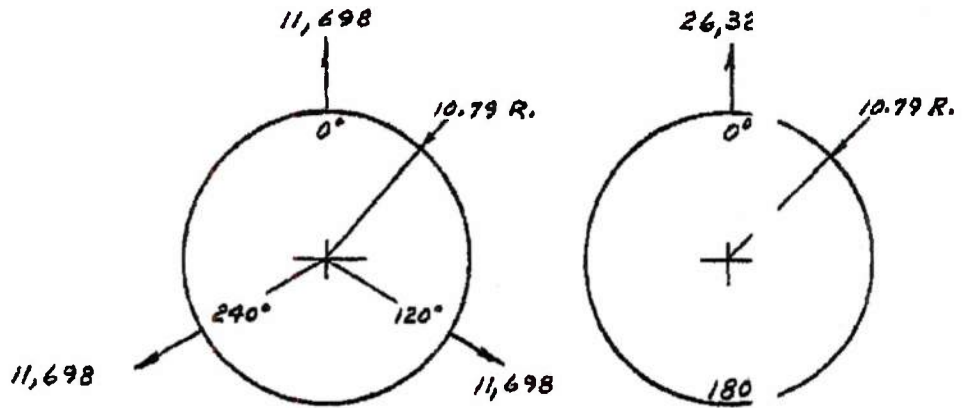


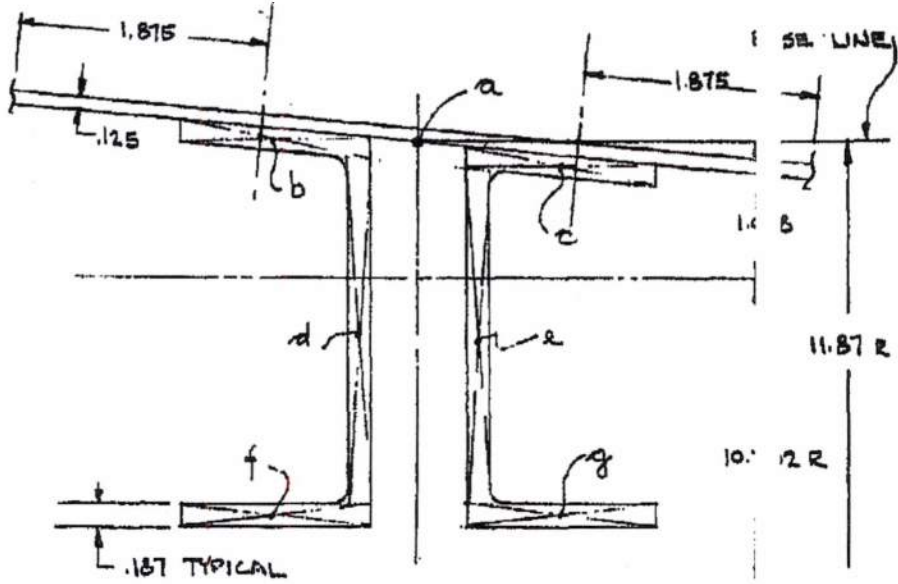
FIGURE 38. Symmetrical and Unsymmetrical Loadings

MAC AEST

UNCLASSIFIED

ASD-TDR-63-277, Vol. IV

RI DT 6003



Item	SIZE & AREA, A In <sup>2</sup>	z	A · z	$\bar{z}$	A · $\bar{z}$	A · $\bar{z}^2$	$I_o$
a	.125 x 6.25 = .7810	-.05	-.0390	-1.128	-.8810	.9990	0
b	.18 x 1.50 = .2700	0	0	-1.078	-.2910	.3140	0
c	.18 x 1.50 = .2700	.20	.0540	-.878	-.2370	.2080	0
d	.18 x 2.70 = .4860	1.50	.7290	+1.422	+2.030	.0865	.294
e	.18 x 2.60 = .4680	1.51	.7060	+1.432	+2.022	.0875	.262
f	.18 x 1.50 = .2700	2.92	.7890	+1.842	+4.975	.9160	0
u	.18 x 1.50 = .2700	2.92	.7890	+1.842	+4.975	.9160	0
	2.8150	1.078	3.0280		-1.4090 +1.4022	3.5230 4.0790	.5560 1.61

I of section with holes is estimated as  $1.80 \times 4.079 = 3.27 \text{ in}^4$

FIGURE 39. Ring Section Properties

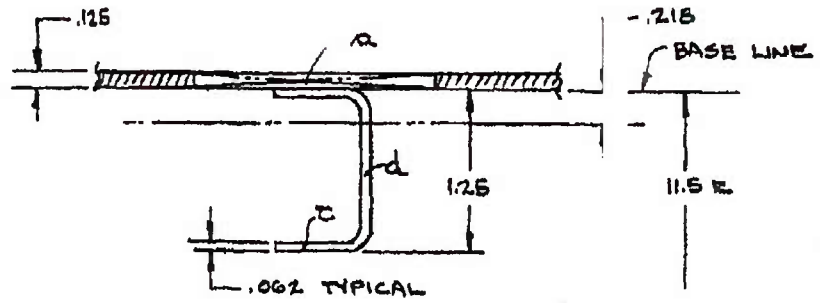
UNCLASSIFIED

MAC 4623

UNCLASSIFIED

ASD-TDR-63-277, Vol. IV

REPORT 6003



ITEM	SIZE	AREA	AREA Z	A·Z	To N.A.	A·Z	A·Z <sup>2</sup>	I <sub>o</sub>
a	.125 x 1.86	.2330	-.0625	-.01460	-.2805	-.0653	.018380	0
b	.062 x .75	.0465	+.0310	+.00144	-.1870	+.0087	.001624	0
c	.062 x .75	.0465	+1.1930	+.03350	+.9750	+.0434	.044206	0
d	.062 x 1.1	.0684	+.6120	+.04180	+.3940	+.02695	.010600	.00693
		.3944	.218	+.08614			.074804	.00693
							.DE	34 in. <sup>4</sup>

FIGURE 40. Ring Section Properties

UNCLASSIFIED

UNCLASSIFIED

ASD-TDR-63-277, Vol. IV

6003

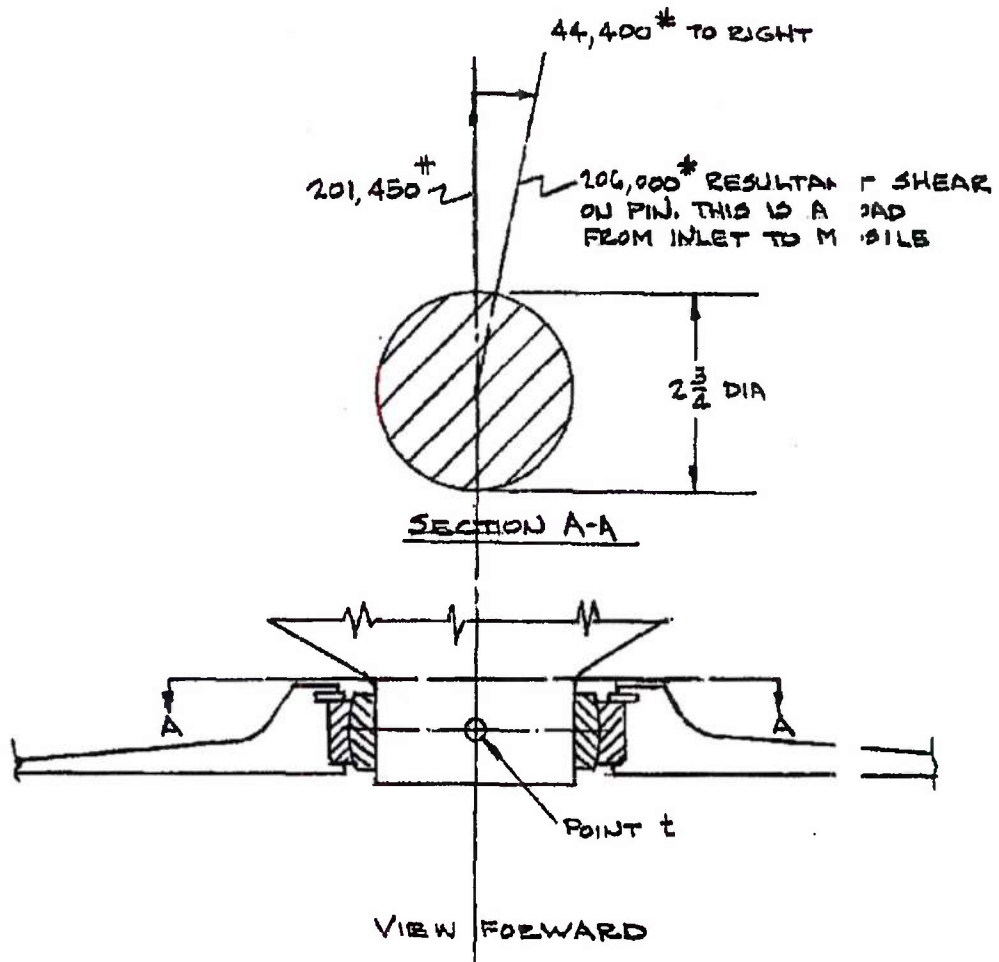


FIGURE 41. Thrust Fitting Loads

MLC AGS

UNCLASSIFIED

UNCLASSIFIED

ASD-TDR-63-277, Vol. IV

REPORT 6003

Page determined to be Unclassified  
Reviewed Chief, RDD, WHS  
IAW EO 13526, Section 3.5  
Date: OCT 02 2015

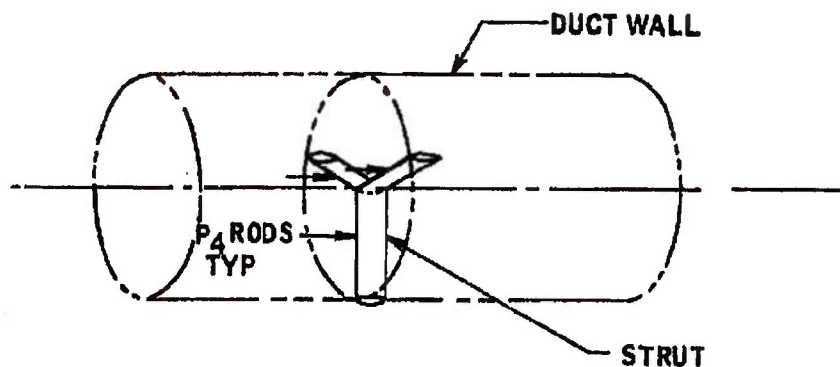


FIGURE 42. Struts

MAC AGR

UNCLASSIFIED

Page determined to be Unclassified  
Reviewed Chief, RDD, WHS  
IAW EO 13526, Section 3.5  
Date: OCT 02 2015

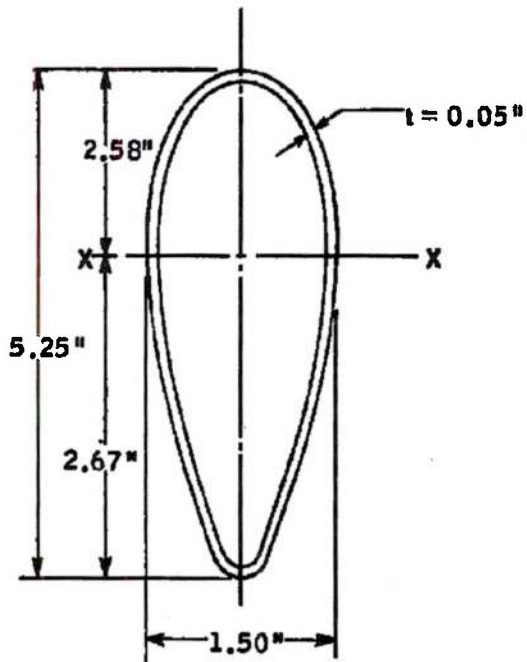


FIGURE 43. Strut Cross Section

MAC ASD

DECLASSIFIED IN FULL  
Authority: EO 13526  
Chief, Records & Declass Div, WHS  
Date: OCT 02 2015

~~SECRET RESTRICTED DATA~~  
~~ATOMIC ENERGY ACT OF 1954~~

ASD-TDR-63-277, Vol. IV

REPORT 6003

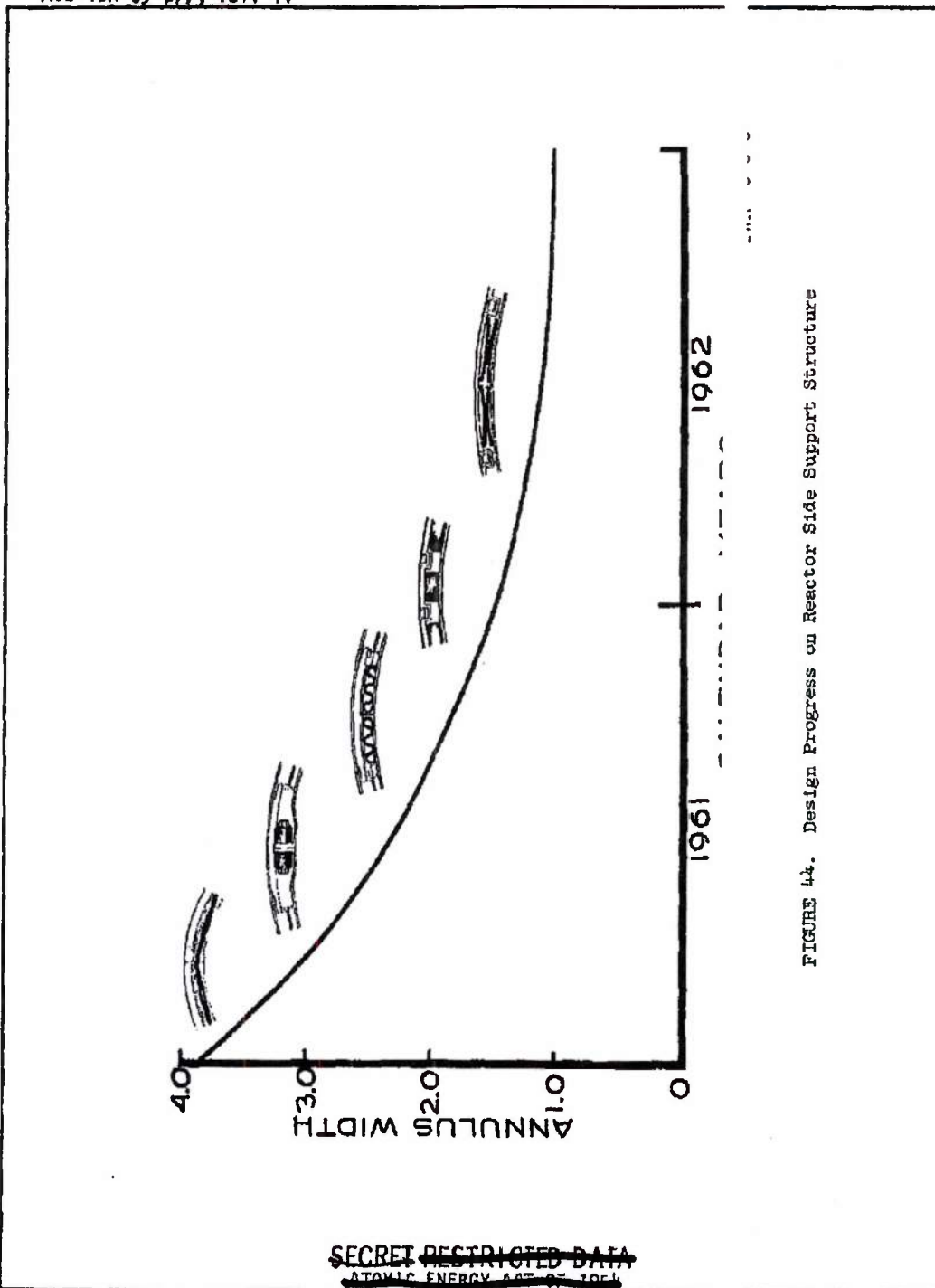


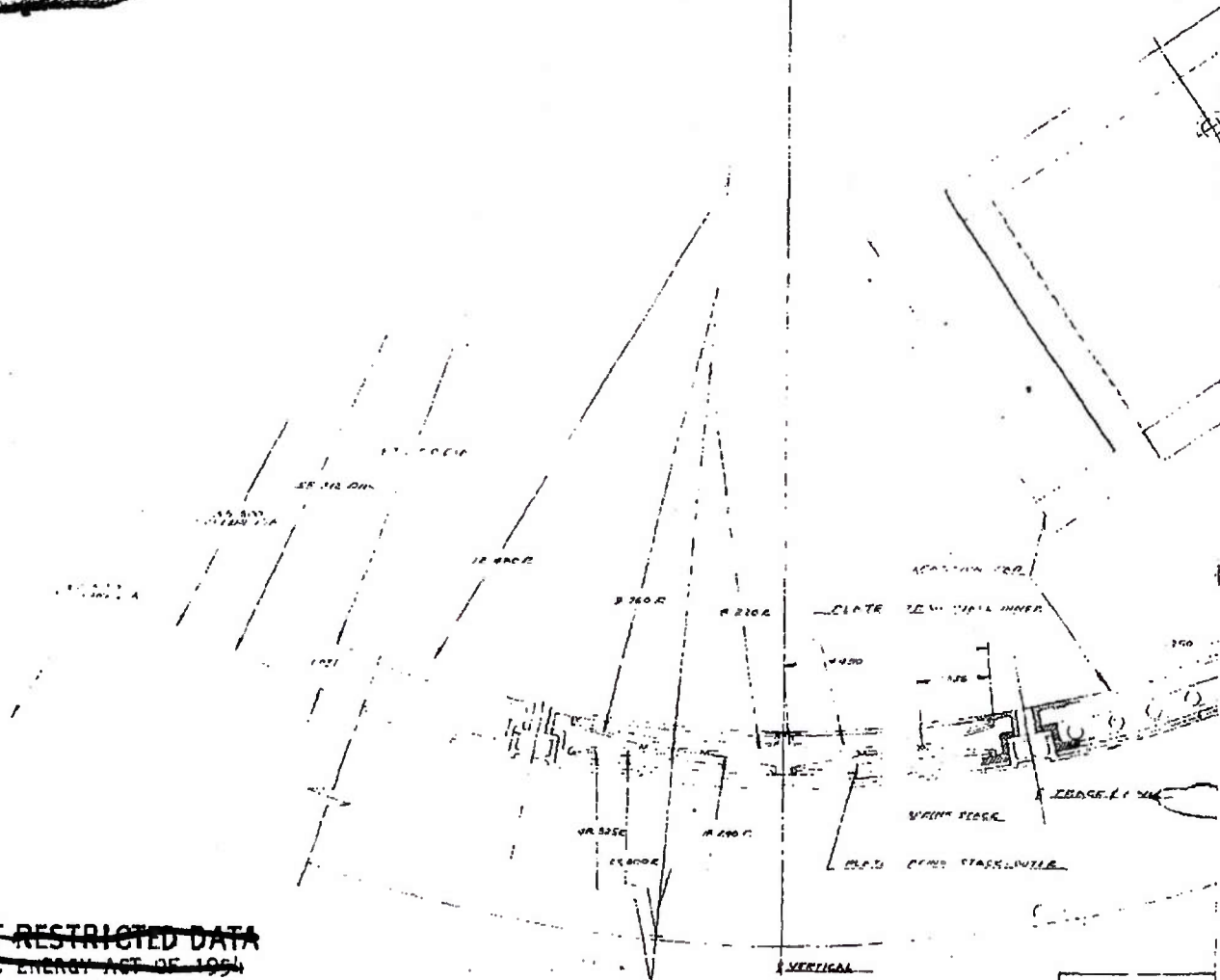
FIGURE 44. Design Progress on Reactor Side Support Structure

~~SECRET RESTRICTED DATA~~  
~~ATOMIC ENERGY ACT OF 1954~~

~~SECRET RESTRICTED DATA~~  
~~ATOMIC ENERGY ACT OF 1954~~

1

DECLASSIFIED IN FULL  
Authority: EO 13526  
Chief, Records & Declass Div, WHS  
Date: OCT 02 2015

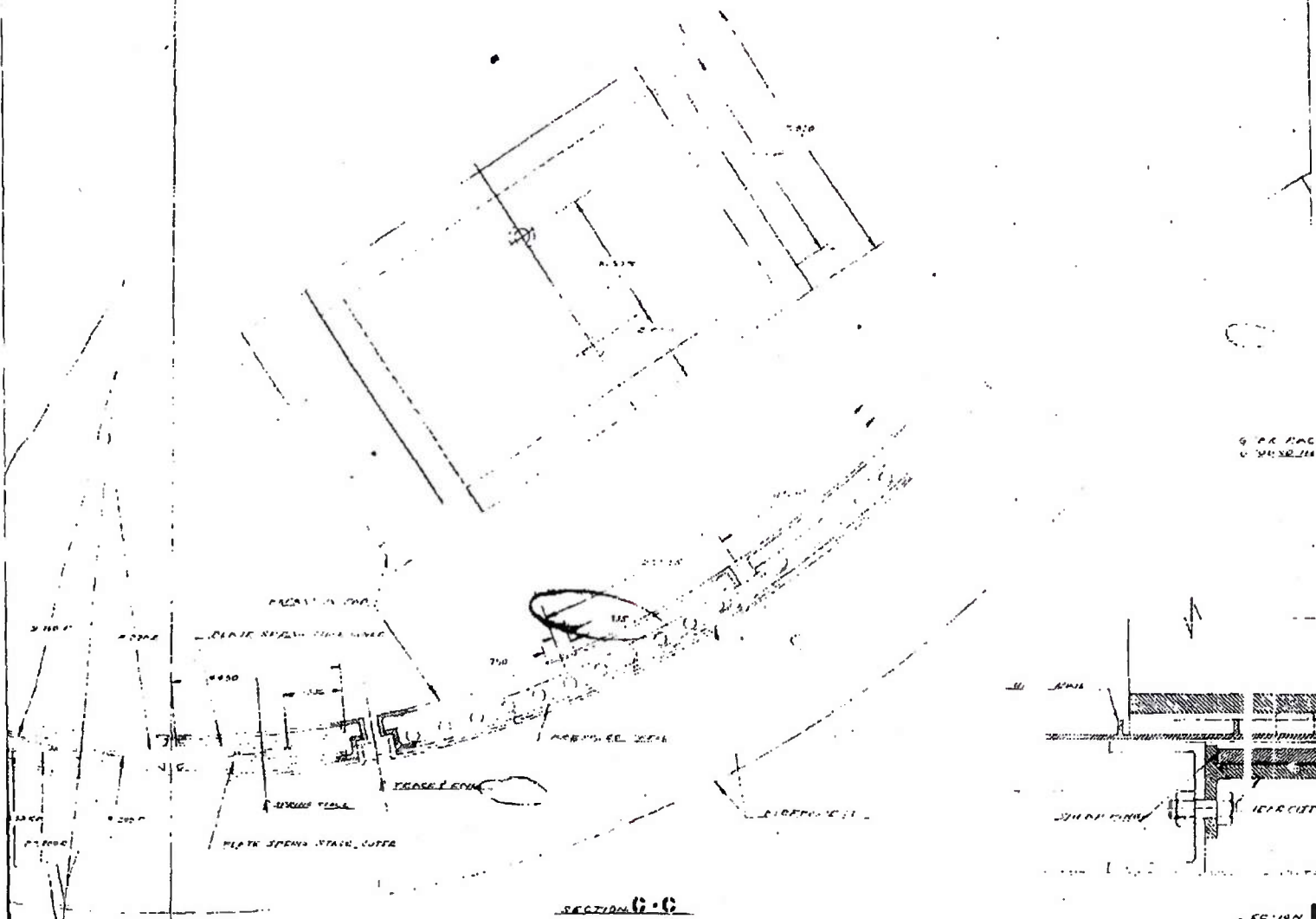


~~SECRET RESTRICTED DATA~~  
~~ATOMIC ENERGY ACT OF 1954~~

X01422  
15

2

DECLASSIFIED IN FULL  
Authority: EO 13526  
Chief, Records & Declass Div, WHS  
Date: OCT 02 2015



X01622 11

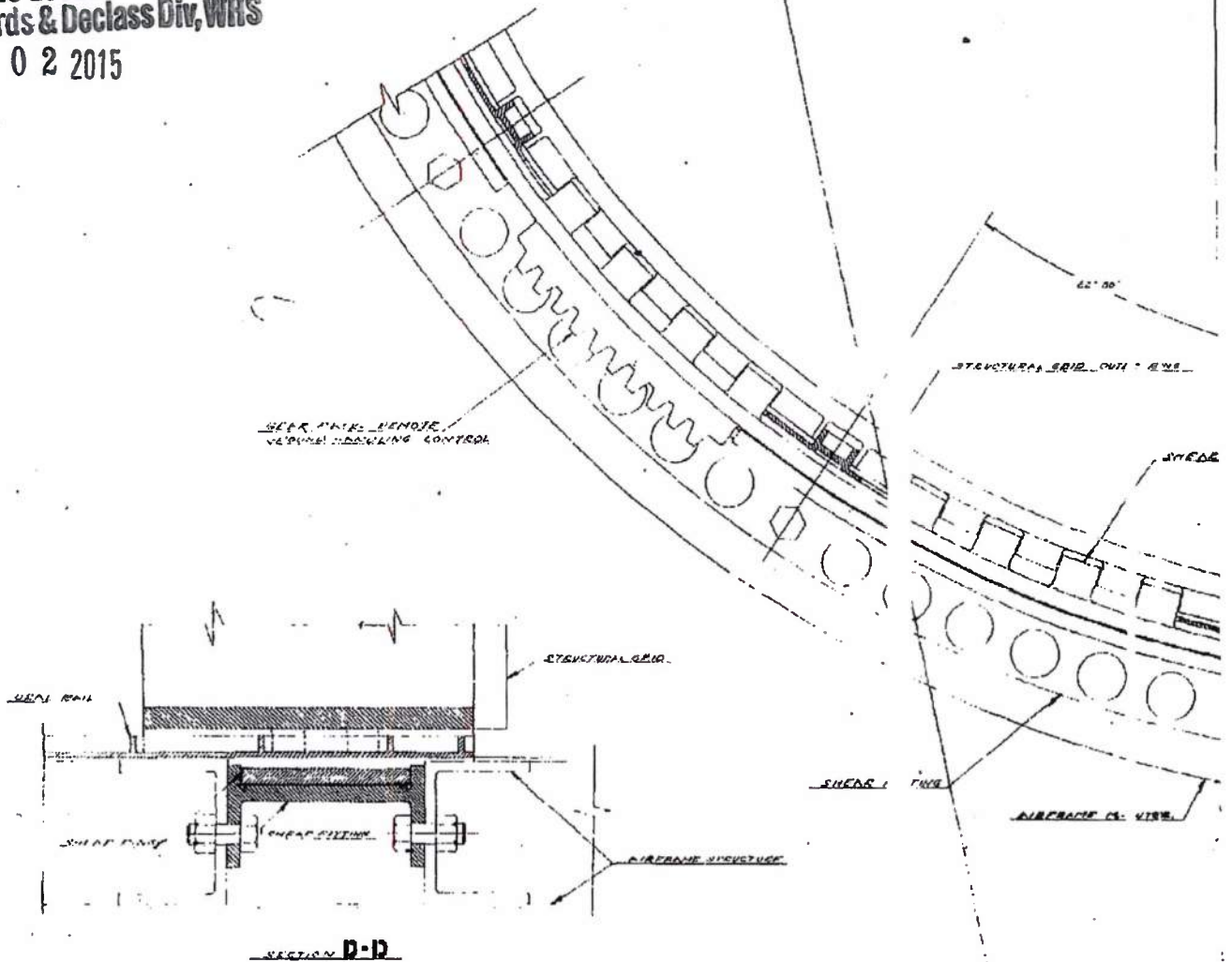
16

15

14

3

DECLASSIFIED IN FULL  
Authority: EO 13526  
Chief, Records & Declass Div, WHS  
Date: OCT 02 2015



14

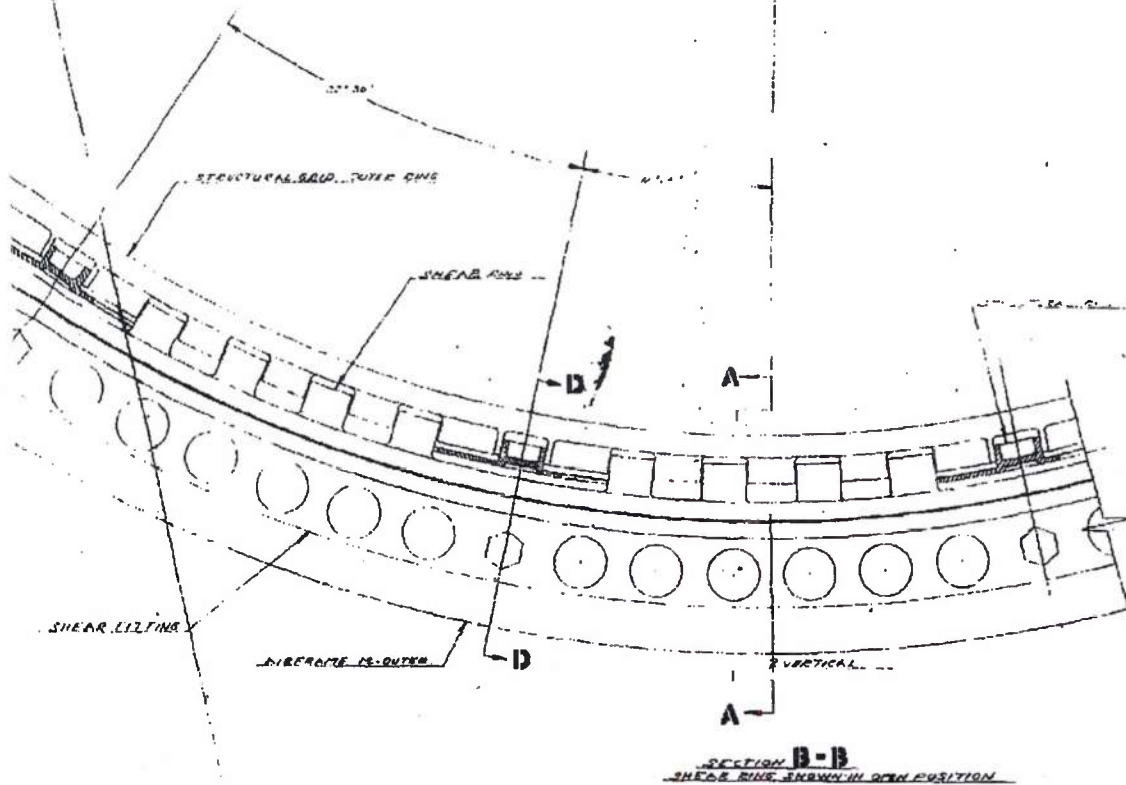
13

12

X

4

Page determined to be Unclassified  
Reviewed Chief, RDD, WHS  
IAW EO 13526, Section 3.5  
Date: OCT 02 2015



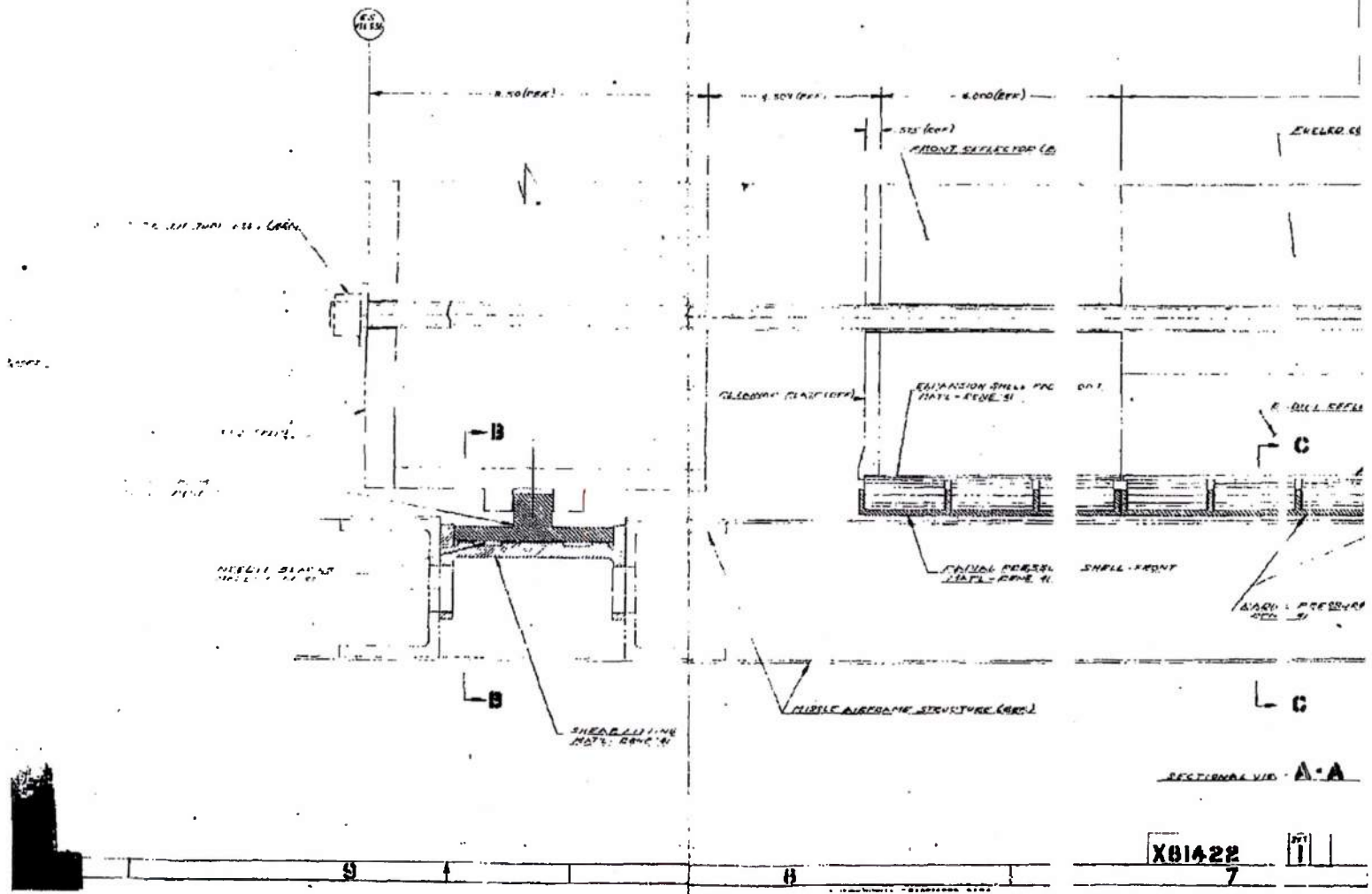
X01422

1

18

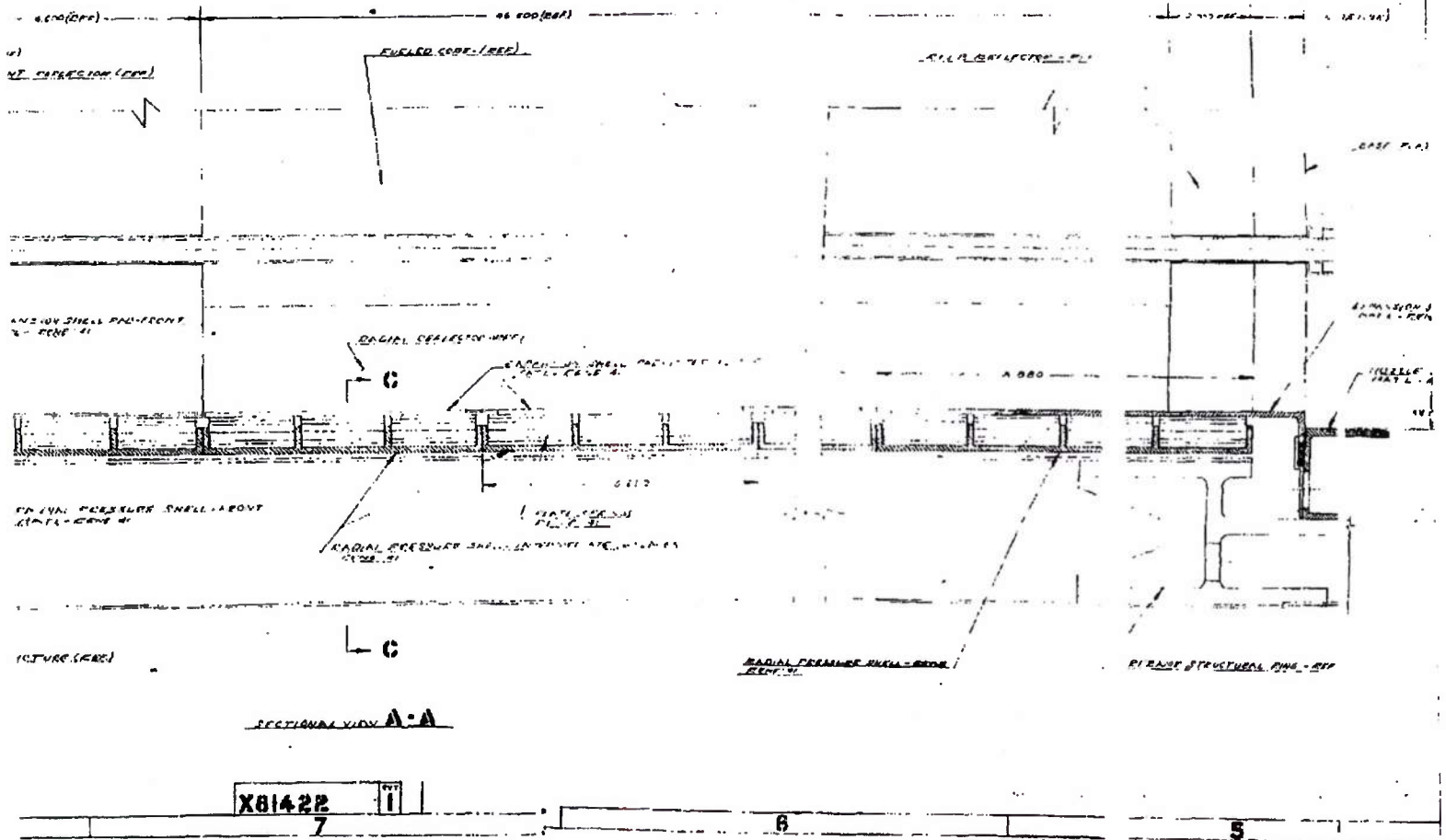
5

DECLASSIFIED IN FULL  
Authority: EO 13526  
Chief, Records & Declass Div, WHS  
Date: OCT 02 2015

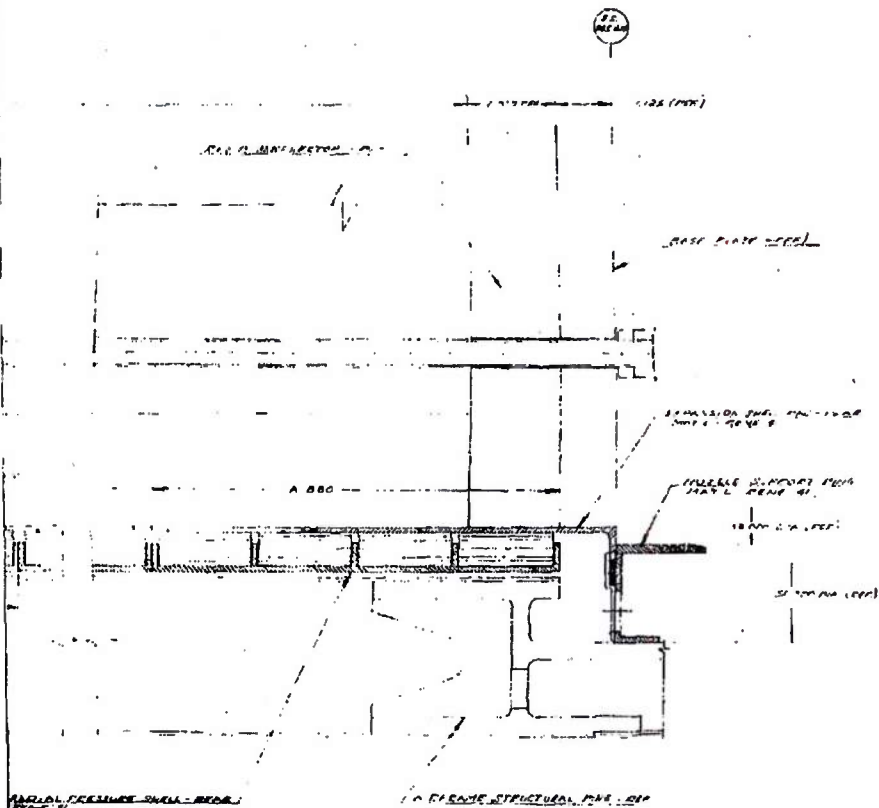


6

DECLASSIFIED IN FULL  
Authority: EO 13526  
Chief, Records & Declass Div, WHS  
Date: OCT 02 2015



7



DECLASSIFIED IN FULL  
Authority: EO 13526  
Chief, Records & Declass Div, WNS  
Date: OCT 02 2015

K81422

6

5

4

4

3

PORT 6003



DECLASSIFIED IN FULL  
Authority: EO 13526  
Chief, Records & Declass Div, WHS  
Date: OCT 02 2015

FIGURE 45. Design Layout,  
Reactor Station

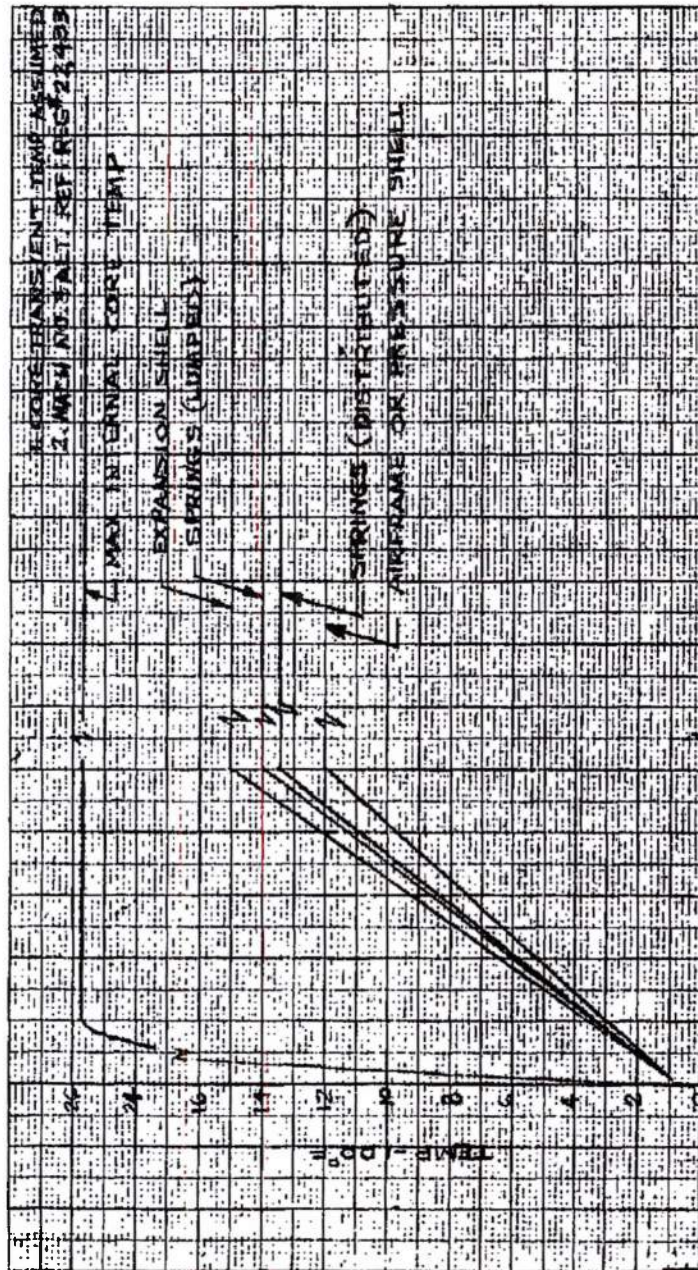
<p>REVISIONS</p> <table border="1"> <tr><th>NO.</th><th>DESCRIPTION</th><th>DATE</th></tr> <tr><td> </td><td> </td><td> </td></tr> <tr><td> </td><td> </td><td> </td></tr> <tr><td> </td><td> </td><td> </td></tr> </table>		NO.	DESCRIPTION	DATE										<p>DATE: 10/2/15</p> <p>BY: [Signature]</p> <p>FOR: [Signature]</p> <p>SCALE: 1/8" = 1'-0"</p> <p>PROJECT: [Redacted]</p> <p>DRAWING NO: X81422</p>
NO.	DESCRIPTION	DATE												

X81422

~~SECRET RESTRICTED DATA~~  
~~ATOMIC ENERGY ACT OF 1954~~

ASD-TDR-63-277, Vol. IV

REPORT 6003



TIME - HRS	TEMP - 100°
0	0
2	1
4	2
6	3
8	4
10	5
12	6
14	7
16	8
18	9
20	10
22	11
24	12

FIGURE 46. Assumed Side Support Temperatures (ANA Hot Day)

MAC 603

~~SECRET RESTRICTED DATA~~  
~~ATOMIC ENERGY ACT OF 1954~~

~~SECRET RESTRICTED DATA~~  
~~ATOMIC ENERGY ACT OF 1954~~

ASD-TDR-63-277, Vol. IV

ORT. 6003

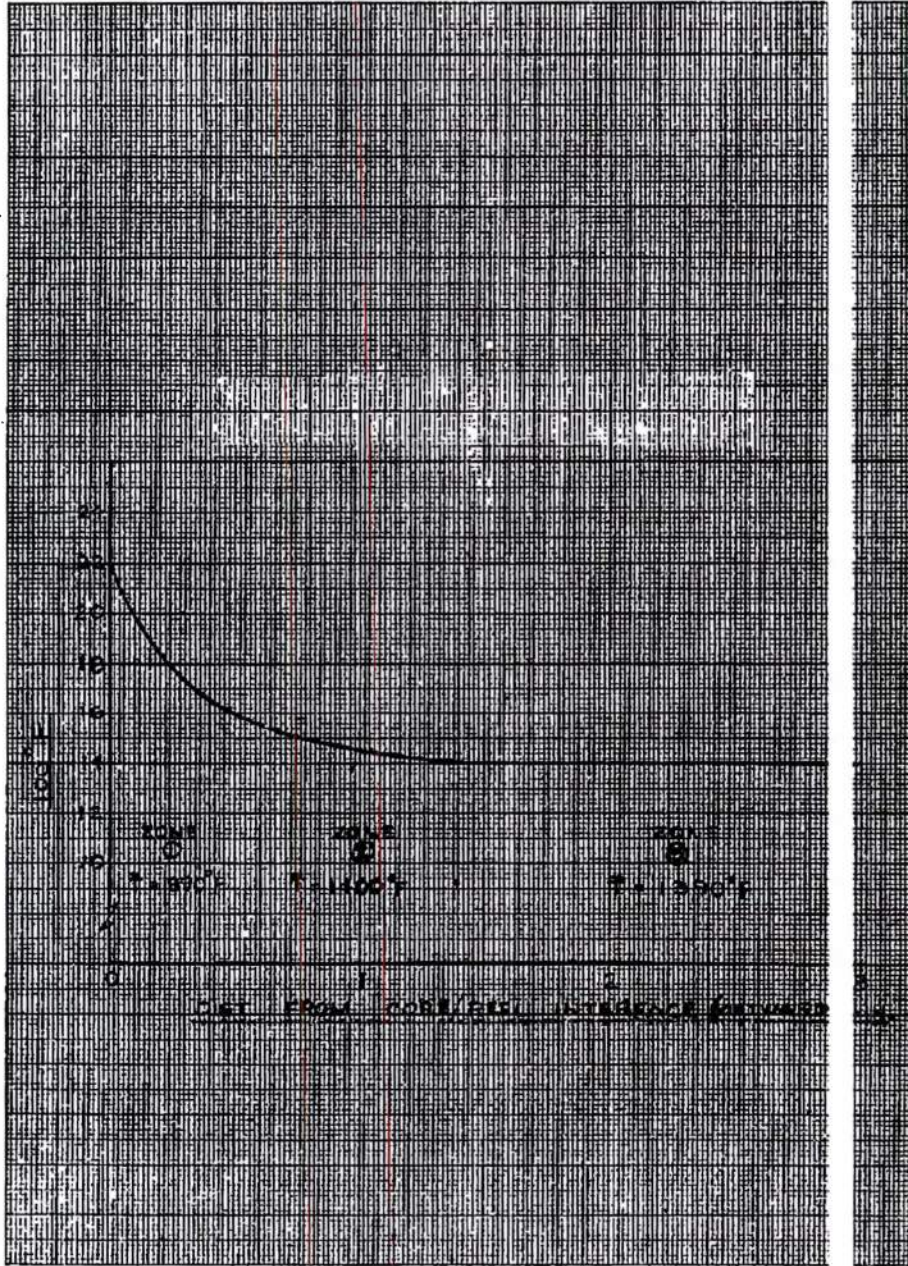


FIGURE 47. Assumed Side Reflector Temperature Distribution

~~SECRET RESTRICTED DATA~~  
~~ATOMIC ENERGY ACT OF 1954~~

MAC 607

N22E958

~~SECRET RESTRICTED DATA~~  
~~ATOMIC ENERGY ACT OF 1954~~

ASD-TDR-63-277, Vol. IV

REPORT 6003

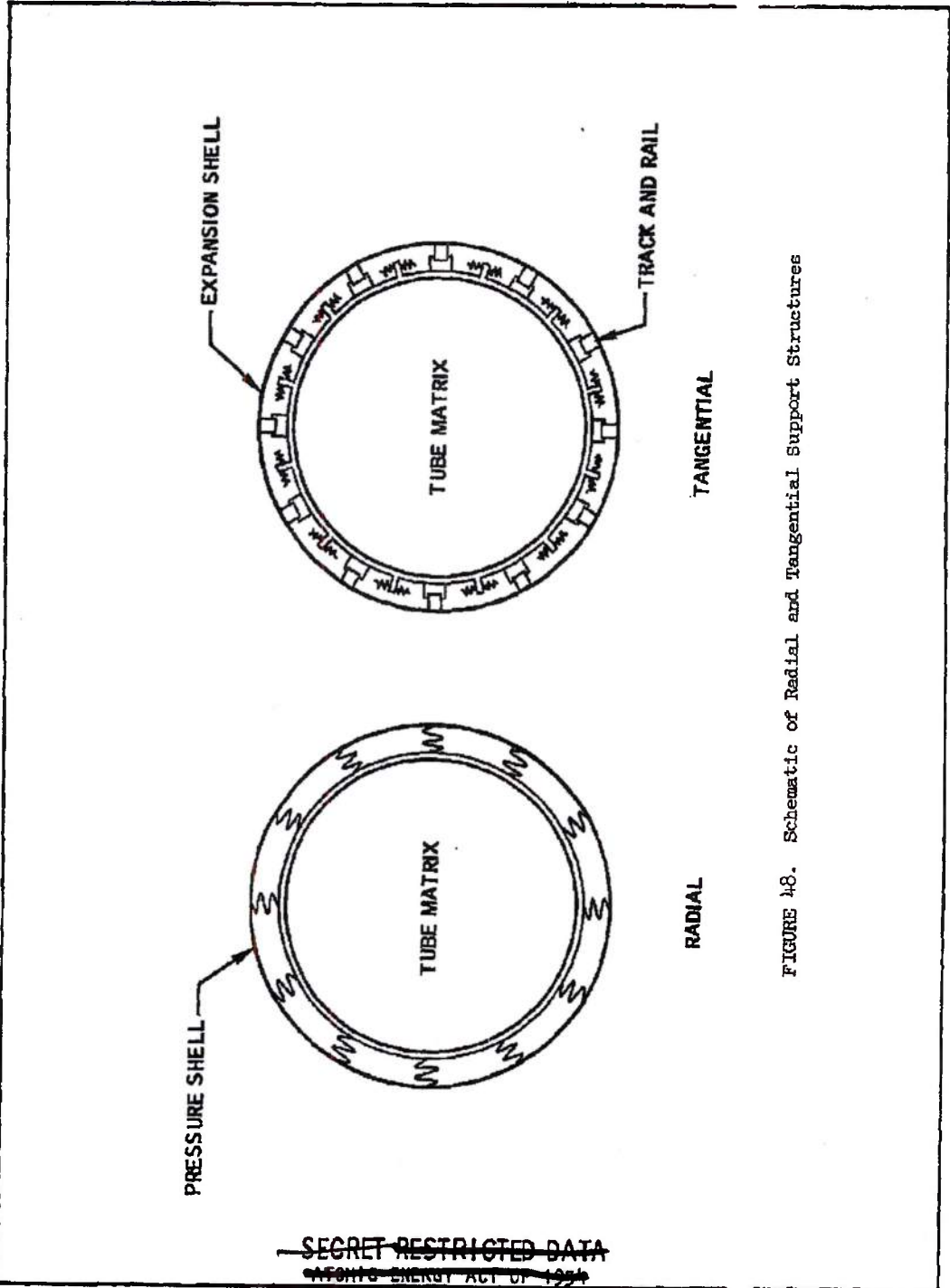


FIGURE 48. Schematic of Radial and Tangential Support Structures

MAC 403

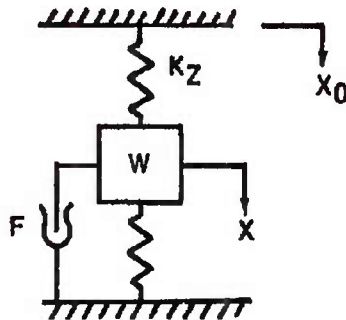
~~SECRET RESTRICTED DATA~~  
~~ATOMIC ENERGY ACT OF 1954~~

N22J90

UNCLASSIFIED

ASD-TDR-63-277, Vol. IV

DRG 6003



$W$  = WEIGHT OF REACTOR, LBS/AXIAL INCH

$K_z$  = EFFECTIVE TRANSVERSE SPRING CONSTANT OF LATERAL SUPPORT,  
LBS/AXIAL INCH/TRANSVERSE INCH

$F$  = FRICTION FORCE EXERTED ON PERIPHERY OF REACTOR, LBS/AXIAL INCH

$x_0$  = PRESCRIBED TRANSVERSE DEFLECTION OF VEHICLE, INCHES

$X$  = RESULTING DEFLECTION OF REACTION, INCHES

FIGURE 49. Dynamic System Model

UNCLASSIFIED

Page determined to be unclassified  
Reviewed Chief, RDD, WHS  
IAW EO 13526, Section 3.5  
Date: OCT 02 2015

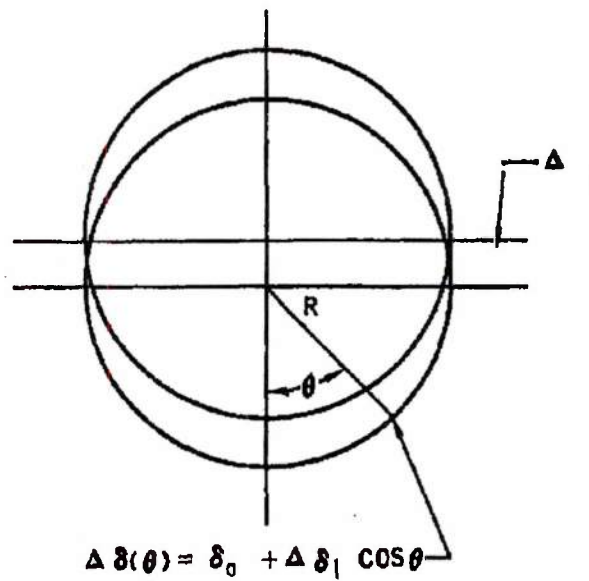


FIGURE 50. Pressure Distribution

MAC A63

DECLASSIFIED IN FULL  
Authority: EO 13526  
Chief, Records & Declass Div, WHS  
Date: OCT 02 2015

~~CONFIDENTIAL RESTRICTED DATA~~  
~~ATOMIC ENERGY ACT OF 1954~~

ASD-TDR-63-277, Vol. IV

6003

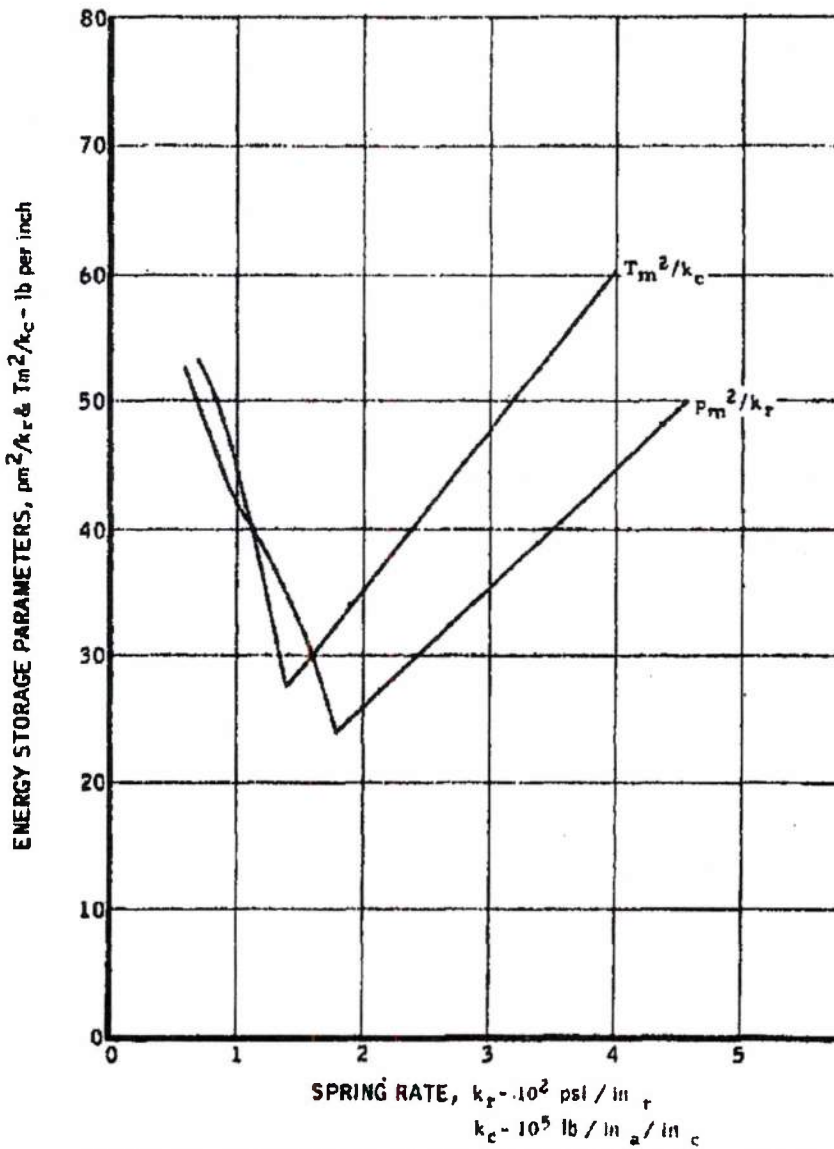


FIGURE 51. Required Energy Storage for Lateral Support System

~~CONFIDENTIAL RESTRICTED DATA~~  
~~ATOMIC ENERGY ACT OF 1954~~

MAC 6271

N22B33

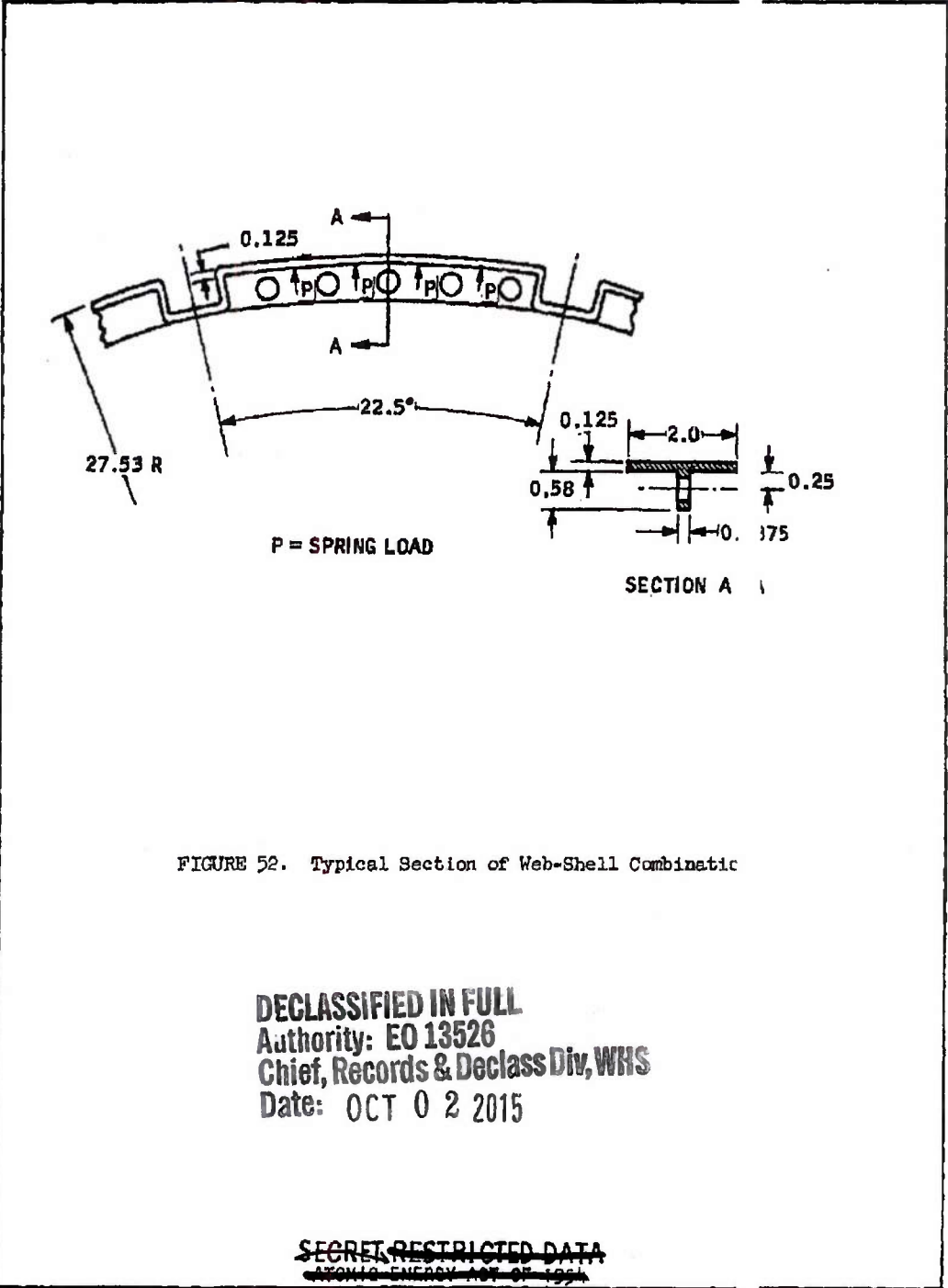


FIGURE 52. Typical Section of Web-Shell Combination

DECLASSIFIED IN FULL  
Authority: EO 13526  
Chief, Records & Declass Div, WHS  
Date: OCT 02 2015

MAC 603

~~SECRET RESTRICTED DATA~~  
~~ATOMIC ENERGY ACT OF 1954~~

ASD-TDR-63-277, Vol. IV

6003

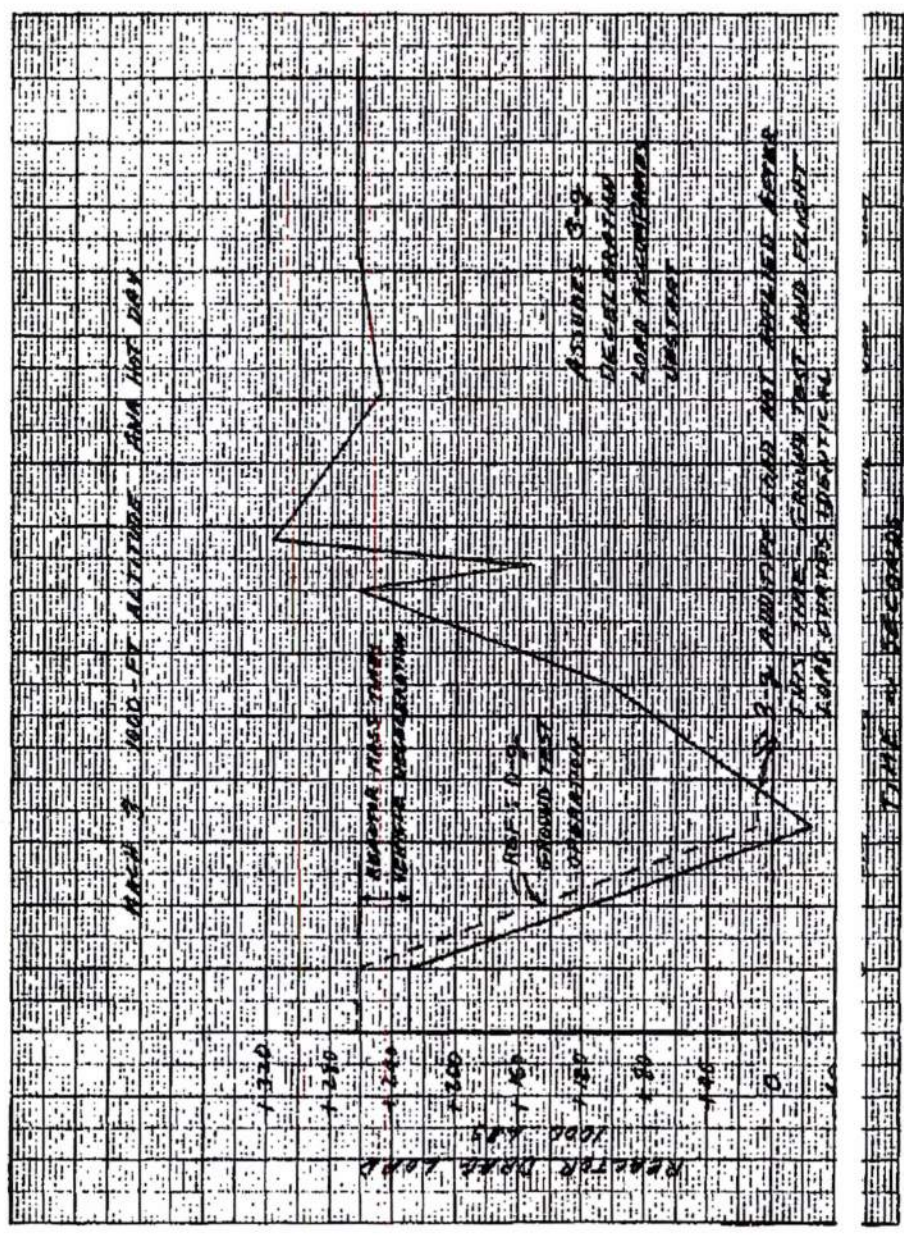


FIGURE 53. Estimated Full Scale Reactor Drag Load Variation During Unstart Transient Flight Operation

MAC 4673

~~SECRET RESTRICTED DATA~~  
~~ATOMIC ENERGY ACT OF 1954~~

~~SECRET RESTRICTED DATA~~  
~~ATOMIC ENERGY ACT OF 1954~~

ASD-TDR-63-277, Vol. IV

REPORT 6003

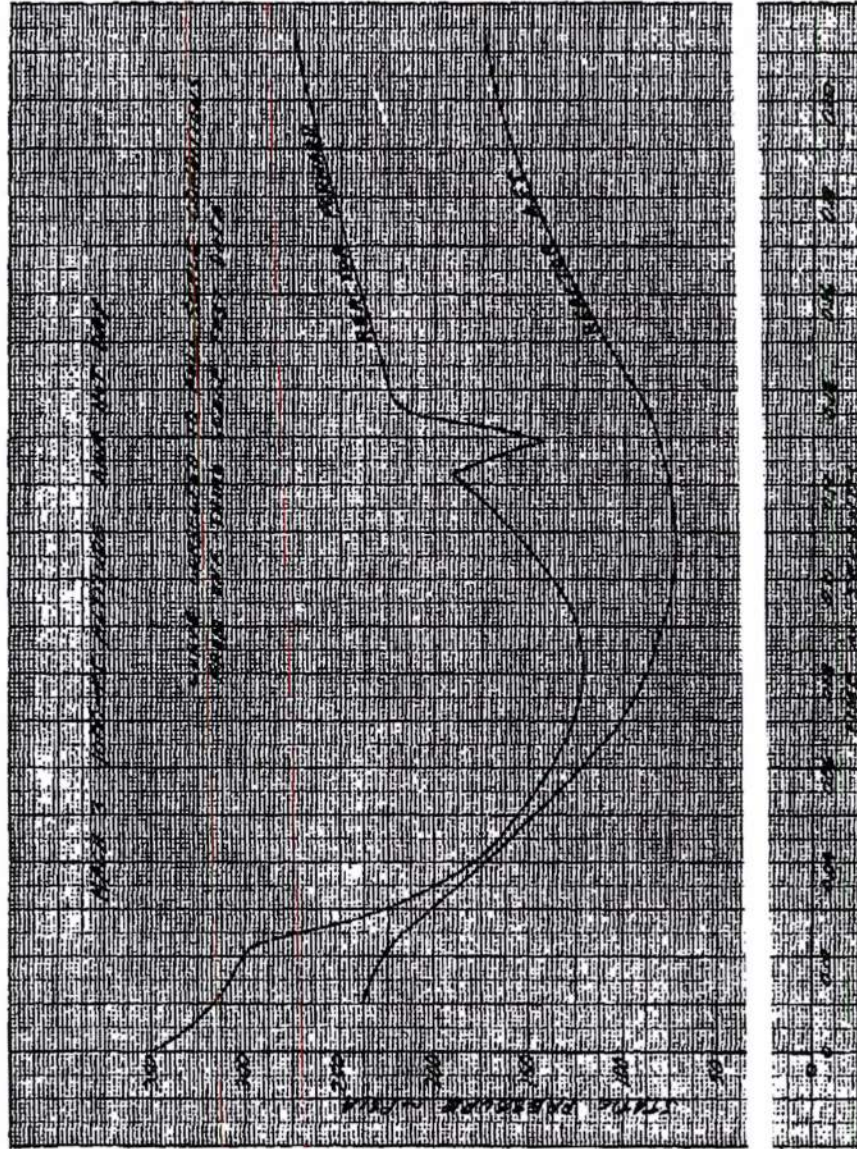


FIGURE 54. Estimated Pressure Transient on Full Scale Reactor During Unstart

MAC ACF

~~SECRET RESTRICTED DATA~~  
~~ATOMIC ENERGY ACT OF 1954~~

N22E723

- 207 -

DECLASSIFIED IN FULL  
Authority: EO 13526  
Chief, Records & Declass Div, WHS  
Date: OCT 02 2015

~~SECRET RESTRICTED DATA~~  
~~ATOMIC ENERGY ACT OF 1954~~

ASD-TDR-63-277, Vol. IV

6003

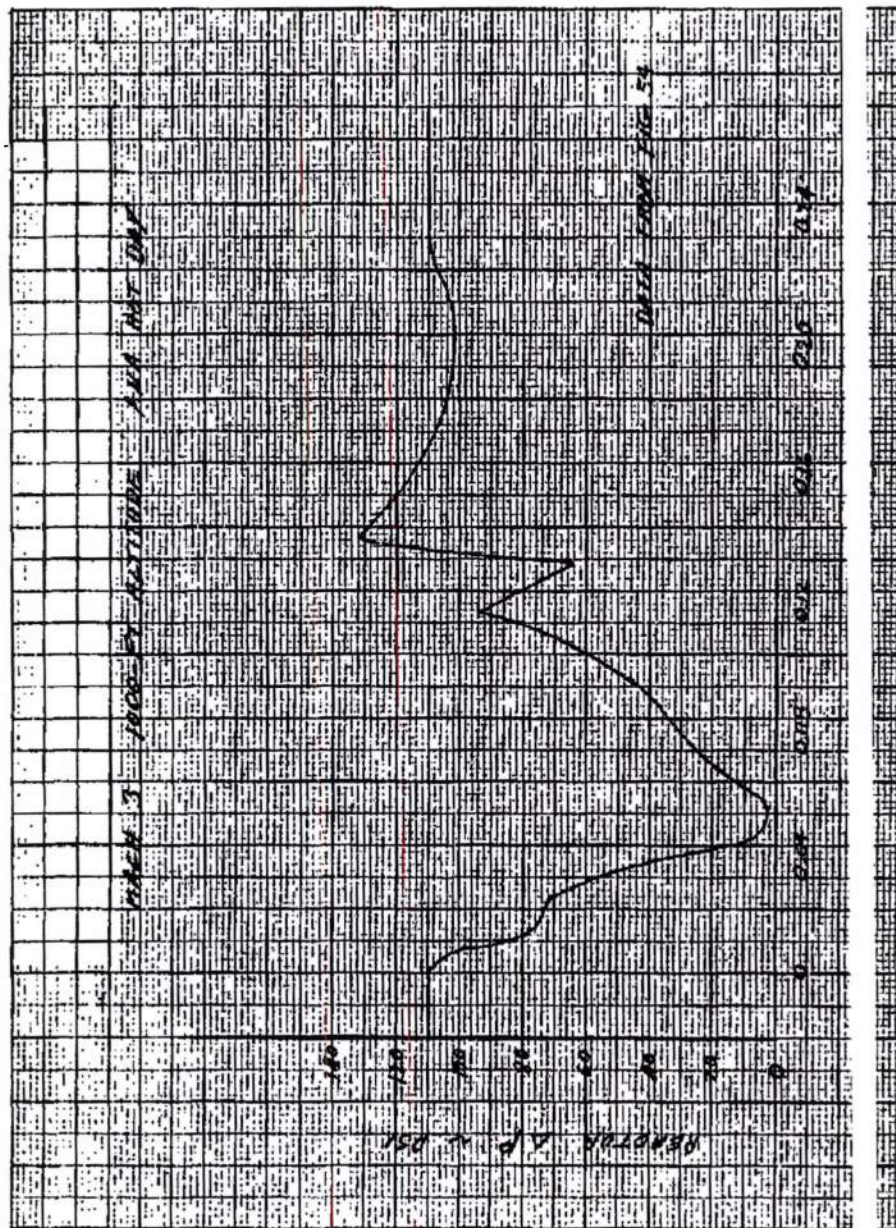


FIGURE 55. Estimated Differential Pressure Variation on Full Scale Reactor During Unstart

MAC 4021

~~SECRET RESTRICTED DATA~~  
~~ATOMIC ENERGY ACT OF 1954~~

N22E724

DECLASSIFIED IN FULL  
Authority: EO 13526  
Chief, Records & Declass Div, WHS  
Date: OCT 02 2015

~~SECRET RESTRICTED DATA~~  
~~ATOMIC ENERGY ACT OF 1954~~

REPORT 6003

ASD-TDR-63-277, Vol. IV

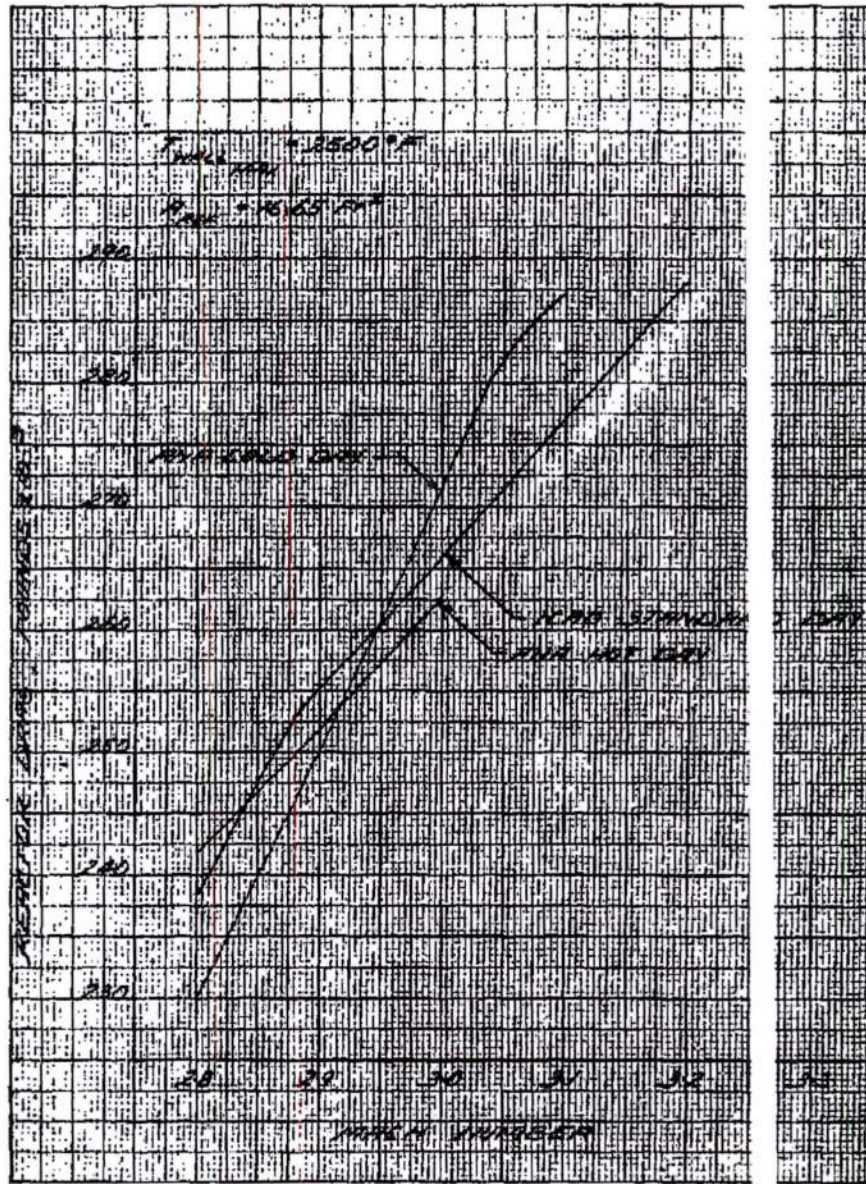


FIGURE 56. Reactor Drag, 1,000-Ft Altitude

~~SECRET RESTRICTED DATA~~  
~~ATOMIC ENERGY ACT OF 1954~~

MAC 400

N22E703

~~SECRET RESTRICTED DATA~~  
~~ATOMIC ENERGY ACT OF 1954~~

ONT 6003

ASD-TDR-63-277, Vol. IV

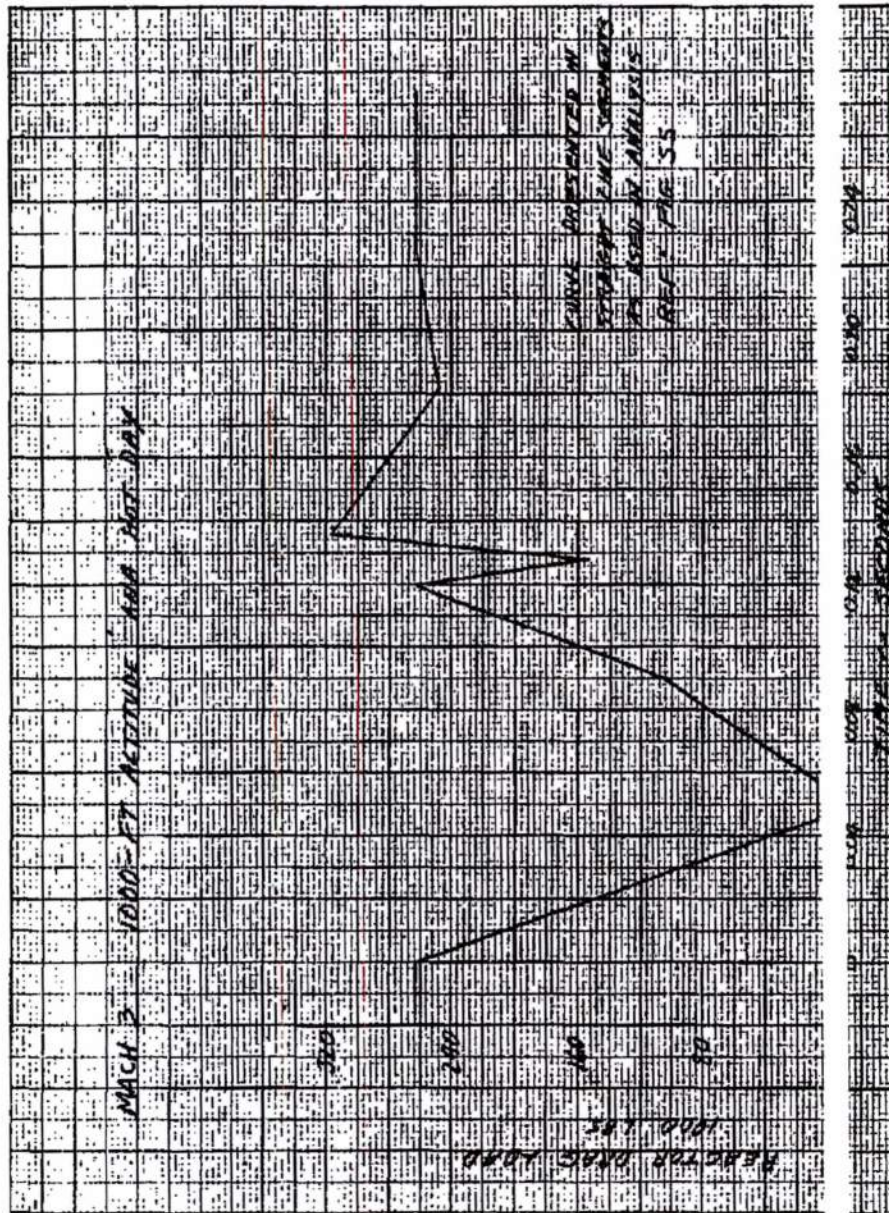


FIGURE 57. Estimated Full Scale Reactor Drag Load Variation During Unstart Transient Ground Test Only

~~SECRET RESTRICTED DATA~~  
~~ATOMIC ENERGY ACT OF 1954~~

~~SECRET RESTRICTED DATA~~  
ATOMIC ENERGY ACT OF 1954

ASD-TDR-63-277, Vol. IV

REPORT 6003

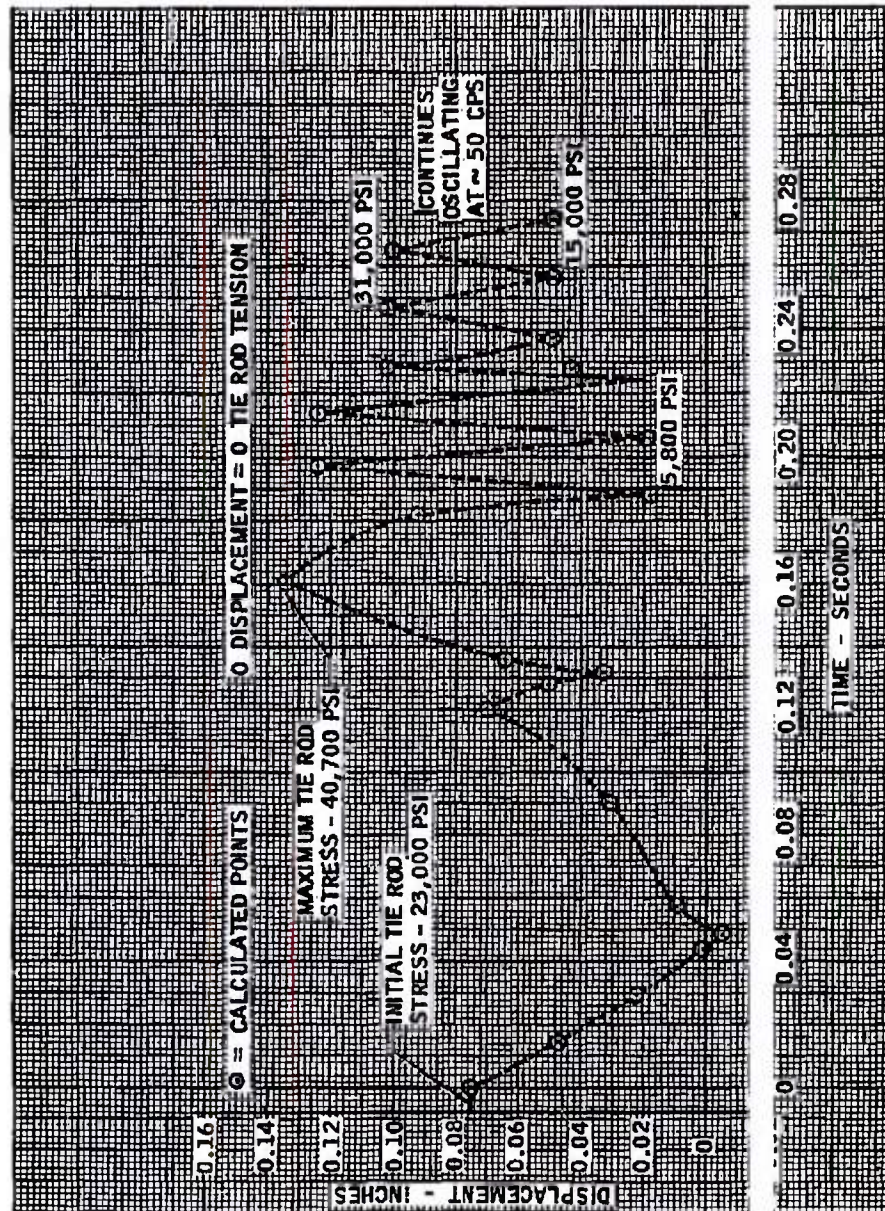


FIGURE 58. Estimated Reactor Displacement During Unstart Transient Ground Test Only--  
Mach 3, 1000-Ft Altitude, ANA Hot Day

MAC 463

~~SECRET RESTRICTED DATA~~  
ATOMIC ENERGY ACT OF 1954

~~SECRET RESTRICTED DATA~~  
~~ATOMIC ENERGY ACT OF 1954~~

ASD-TDR-63-272, Vol. IV

RE # 6003

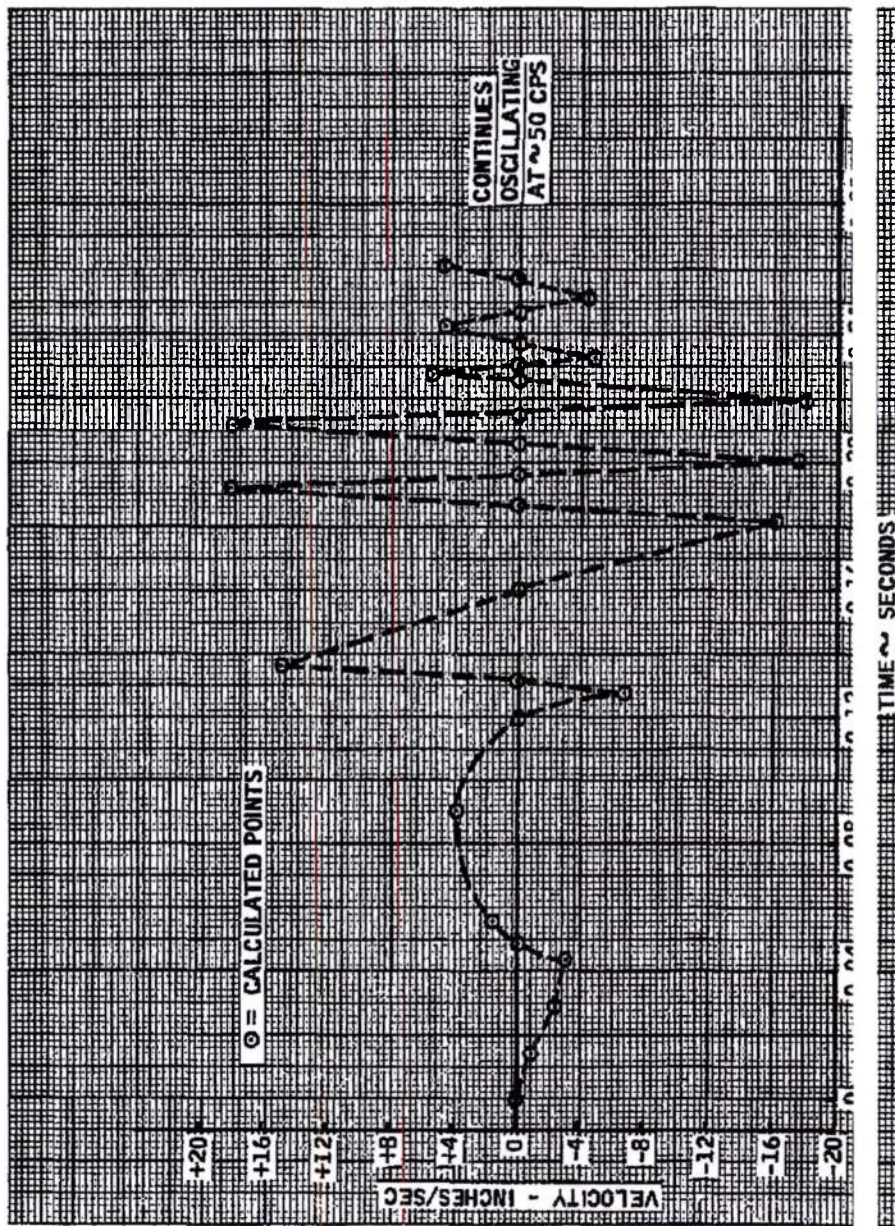


FIGURE 59. Estimated Reactor Velocity During Unstart Transient Ground Test Only--  
Mach 3, 1000-Ft Altitude, AMA Hot Day

MAC 4627

~~SECRET RESTRICTED DATA~~  
~~ATOMIC ENERGY ACT OF 1954~~

N22E727

~~SECRET RESTRICTED DATA~~  
 ATOMIC ENERGY ACT OF 1954

ASD-TDR-63-277, Vol. IV

REPORT 6003

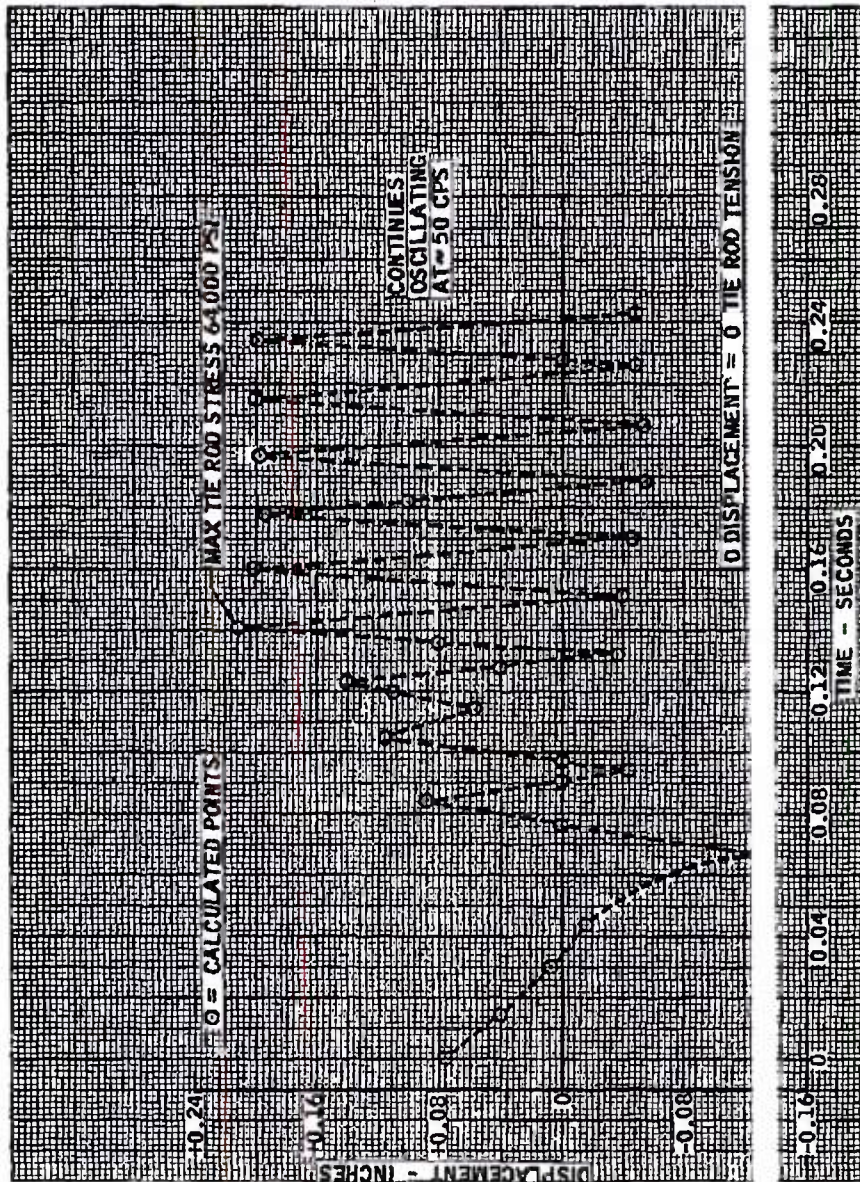


FIGURE 60. Estimated Reactor Displacement During Unstart Transient - Flight Operation  
 With 3 g Vehicle Deceleration--Mach 3, 1000-Ft Altitude, ANA Hot Day

MAC 463

~~SECRET RESTRICTED DATA~~  
 ATOMIC ENERGY ACT OF 1954

DECLASSIFIED IN FULL  
Authority: EO 13526  
Chief, Records & Declass Div, WHS  
Date: OCT 02 2015

~~SECRET RESTRICTED DATA~~  
ATOMIC ENERGY ACT OF 1954

ASD-TDR-63-277, Vol. IV

6003

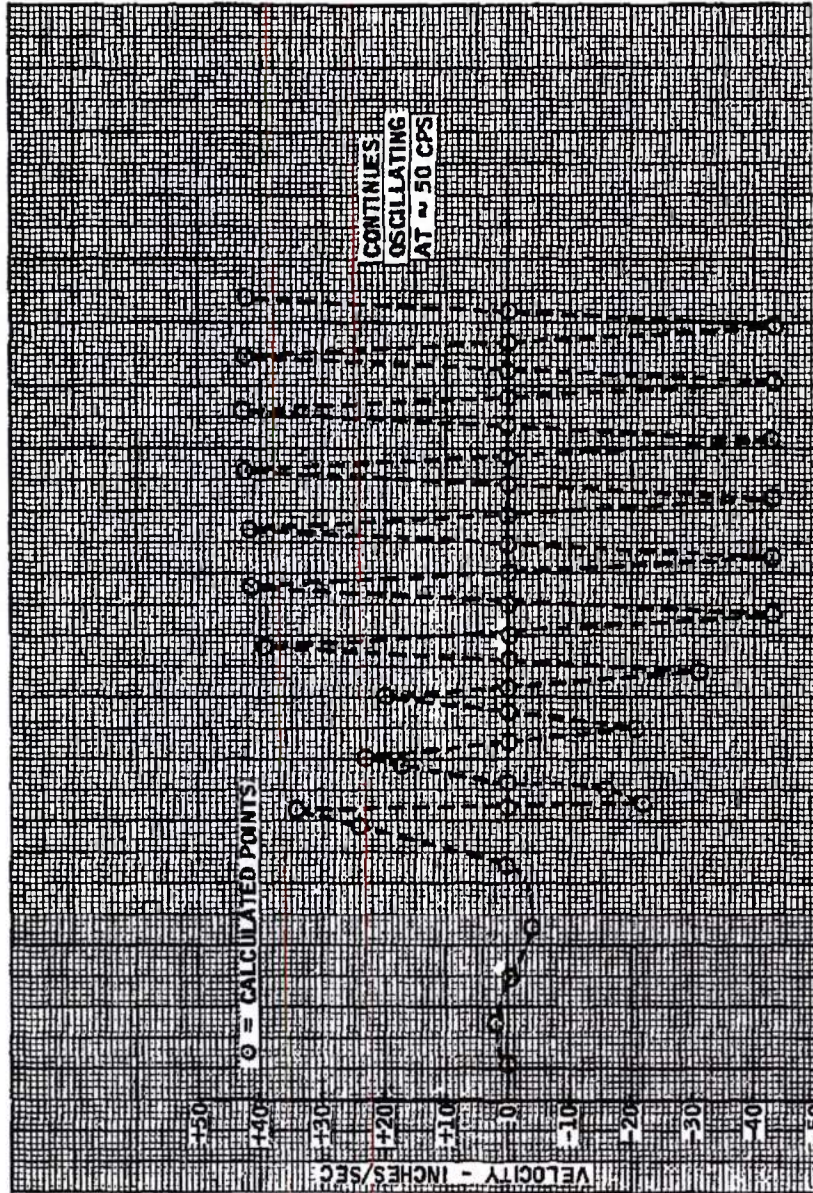


FIGURE 61. Estimated Reactor Velocity During Unstart Transient - Flight Operation  
With 3g Vehicle Deceleration - Mach 3, 10000-Ft Altitude, ANA Hot Day

MAC 4673

~~SECRET RESTRICTED DATA~~  
ATOMIC ENERGY ACT OF 1954

22C58

- 214 -

UNCLASSIFIED

ASD-TDR-63-277, Vol. 11

REPORT 6003

4135-2

MAC ASD

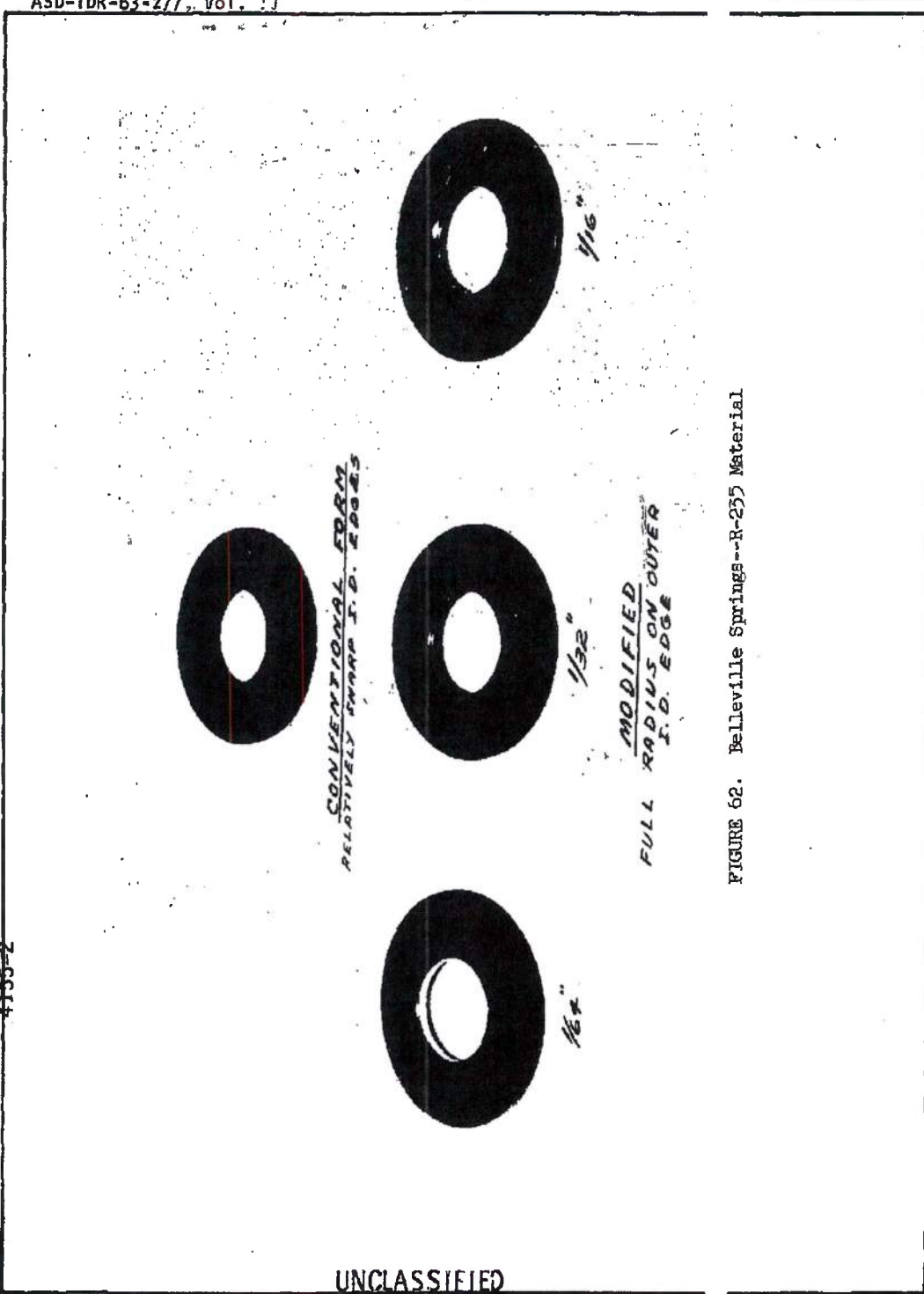


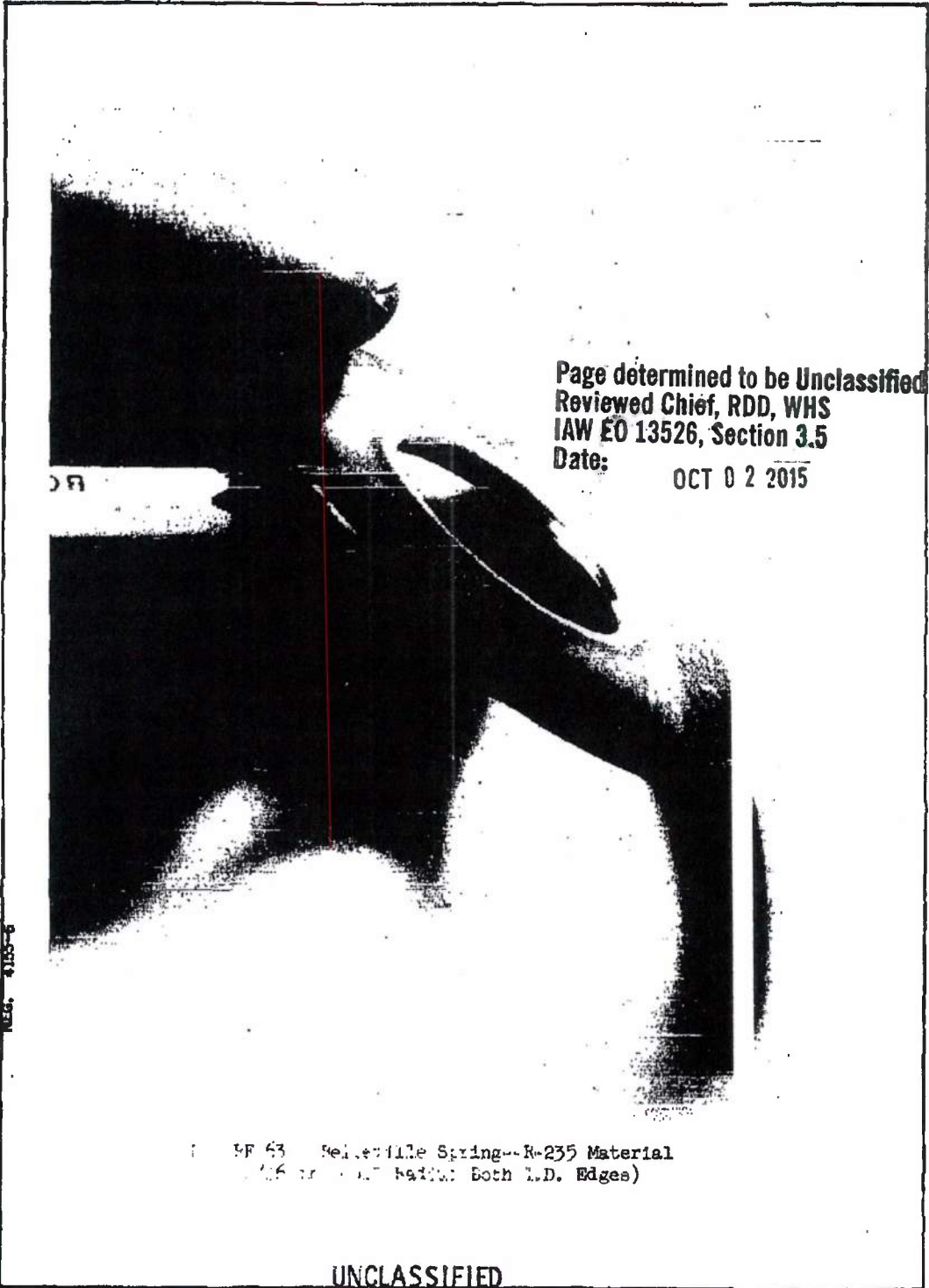
FIGURE 62. Belleville Springs--R-235 Material

UNCLASSIFIED

UNCLASSIFIED

ASD-TPR-63-237

REPORT 6003



Page determined to be Unclassified  
 Reviewed Chief, RDD, WHS  
 IAW EO 13526, Section 3.5  
 Date: OCT 02 2015

OR

NEG. 4155-6

MAC AEB

1 SF 63 Pelletville Spring--R-235 Material  
 (1.6 in. x 1.7 in. Both L.D. Edges)

UNCLASSIFIED

UNCLASSIFIED

ASD-TDR-63-277 - Vol. 11

REPORT 6003

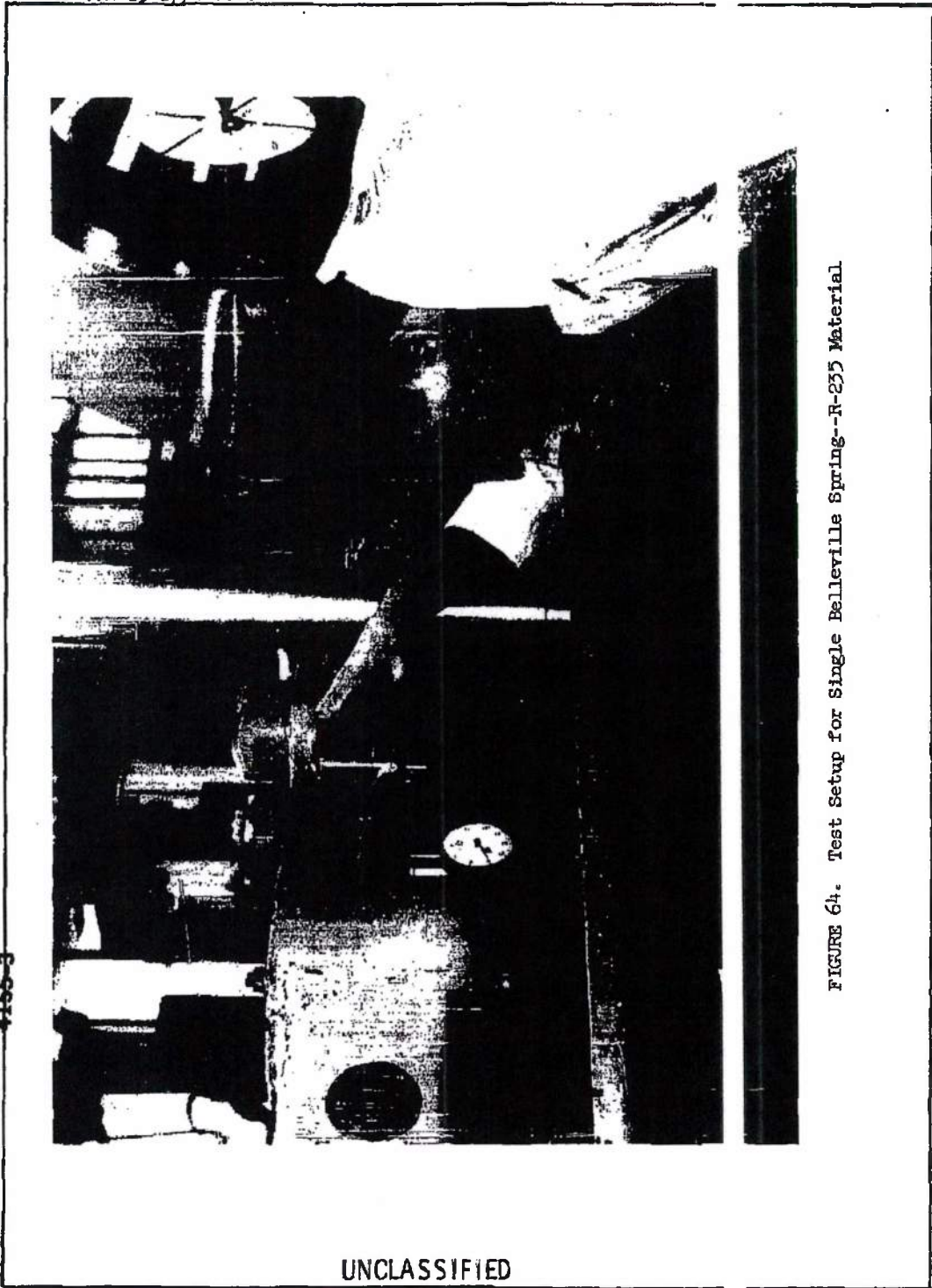


FIGURE 64. Test Setup for Single Belleville Spring--R-235 Material

4155-3

MAC A173

UNCLASSIFIED

UNCLASSIFIED

ASD-TDR-63-277, Vol. 27

REPORT 6003

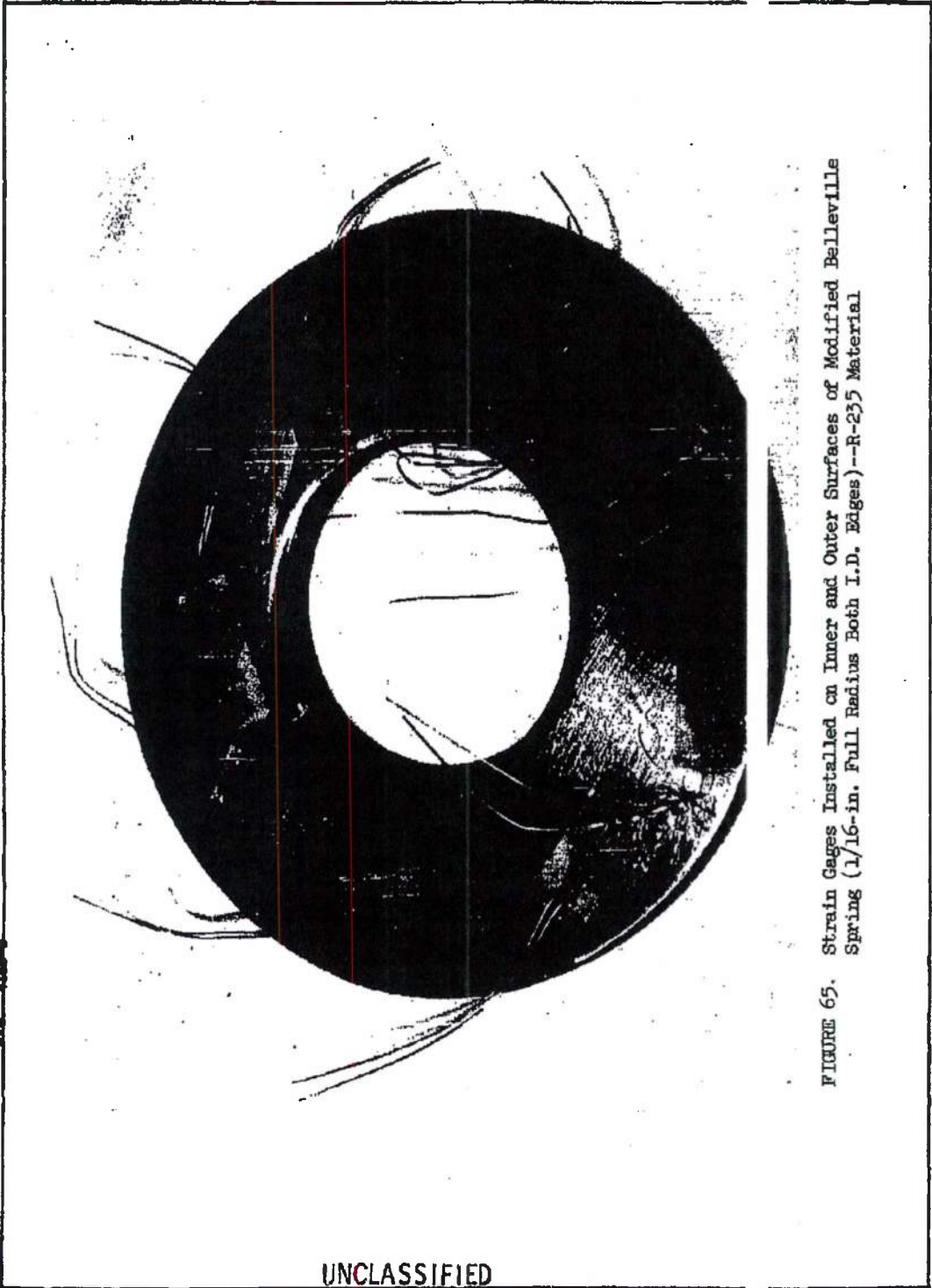


FIGURE 65. Strain Gages Installed on Inner and Outer Surfaces of Modified Belleville Spring (1/16-in. Full Radius Both I.D. Edges)--R-235 Material

MAC A03  
NEG 428-8

UNCLASSIFIED

UNCLASSIFIED

ASD-TDR-63-277, Vol. IV

REPORT 6003

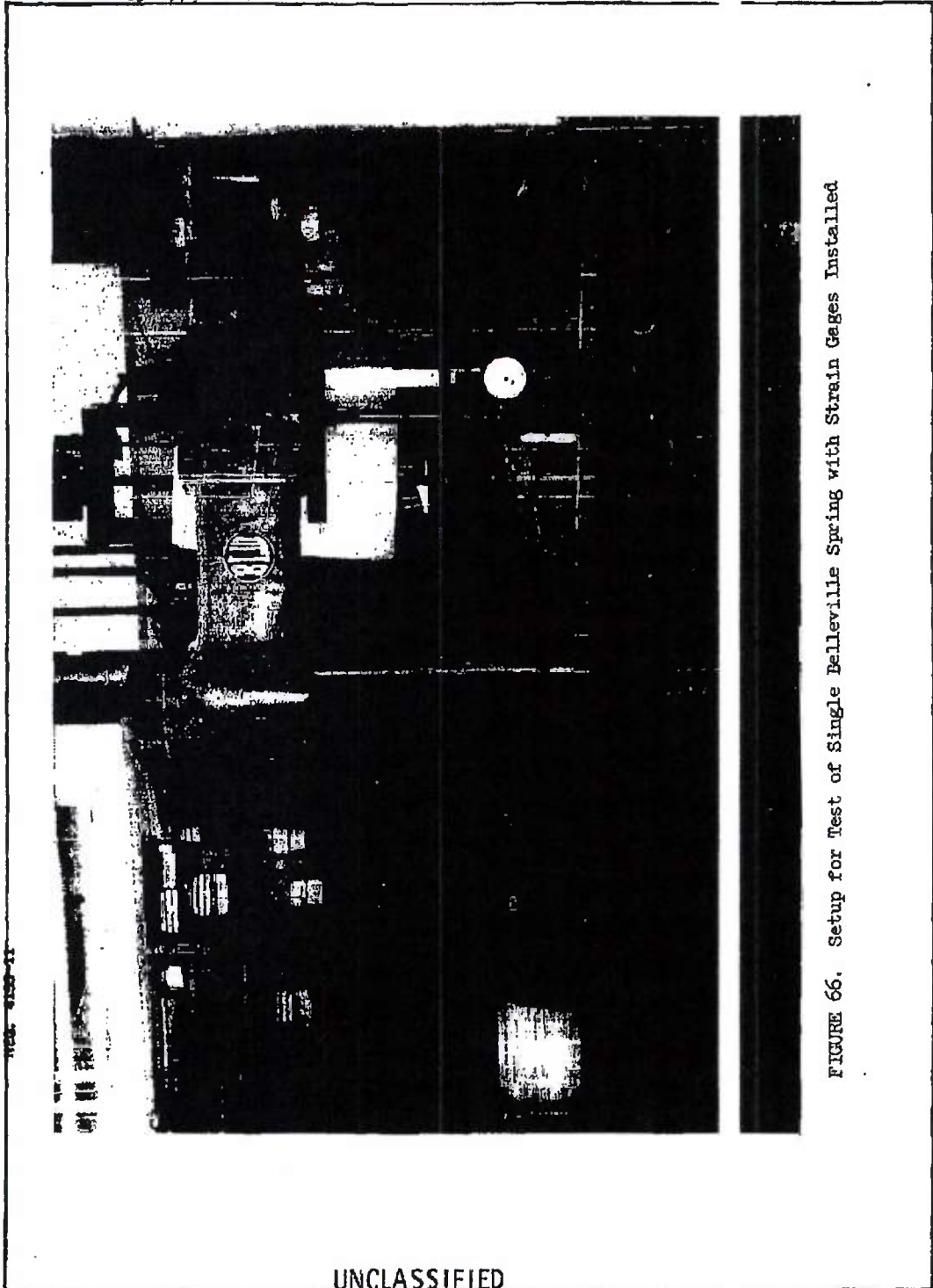


FIGURE 66. Setup for Test of Single Belleville Spring with Strain Gages Installed

MAC 1673

UNCLASSIFIED

UNCLASSIFIED

ASD-TDR-63-277, Vol. IV

REV 6003

(SR-4, A-19 PAPER BACKED, 1/16" x 1/16" STRAIN GAGES)

AMBIENT TEMPERATURE  
 (EFFECTIVE FLAT PLATE LOADING)

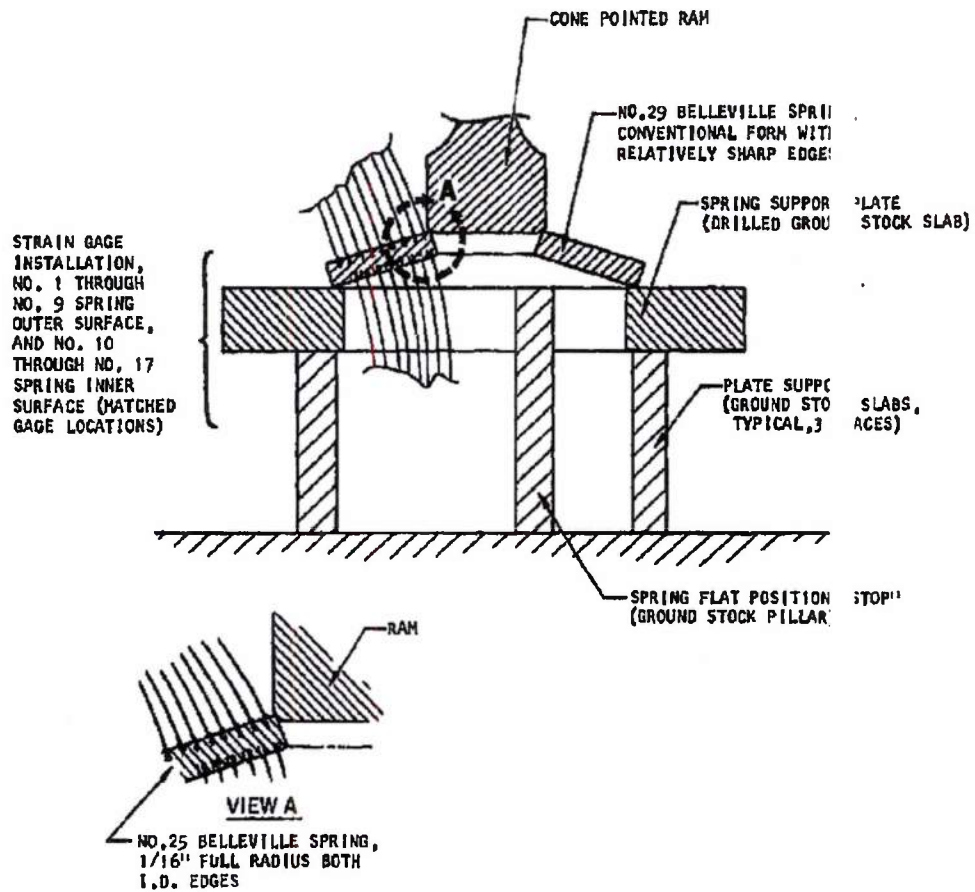


FIGURE 67. Test Setup for Strain Gaged Belleville Springs (R-2351 serial)

REV 6003

UNCLASSIFIED

UNCLASSIFIED

ASD-TER-63-277, Vol. 17

REPORT 6003

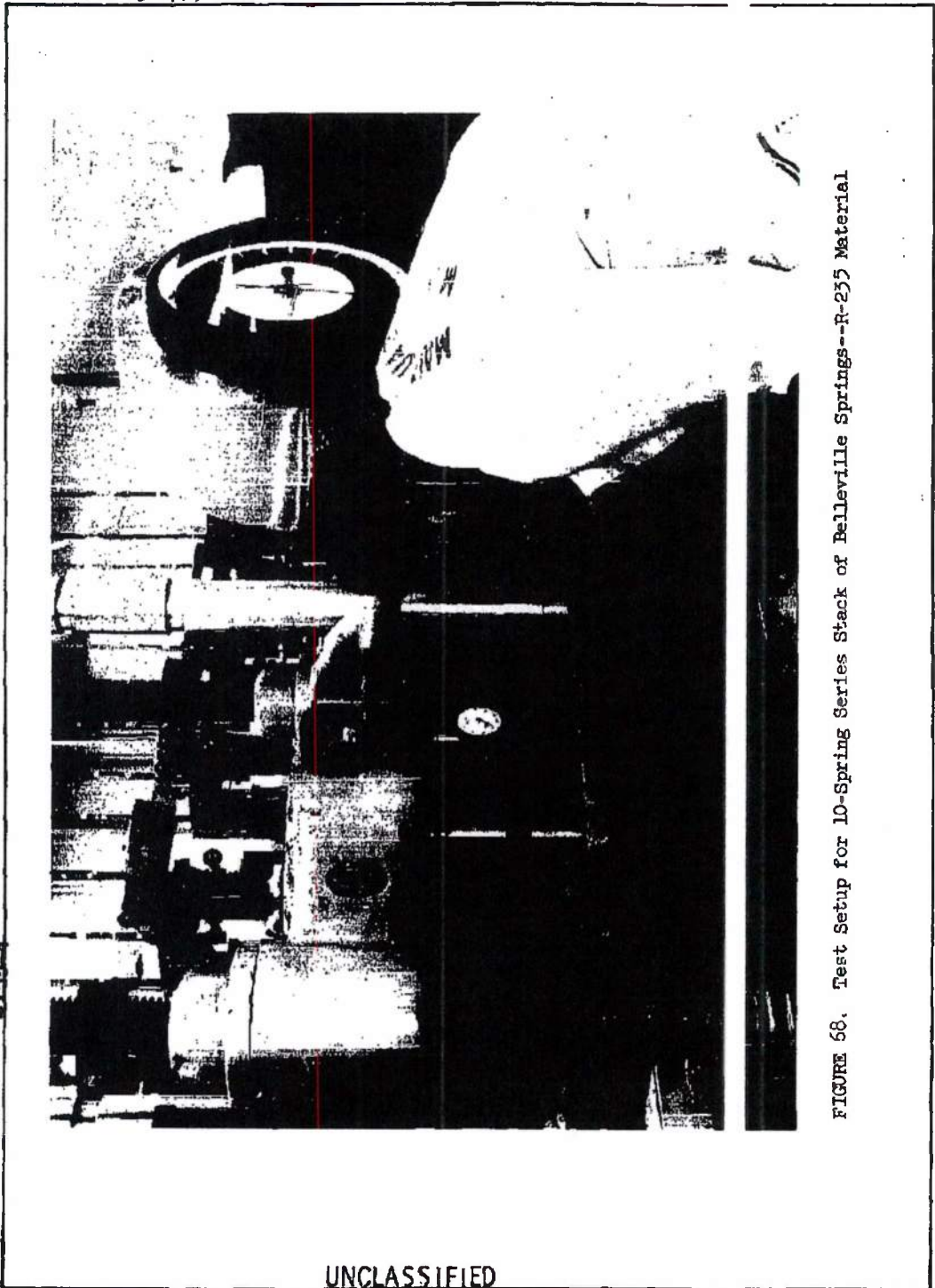


FIGURE 58. Test Setup for 10-Spring Series Stack of Belleville Springs--R-255 Material

UNCLASSIFIED

Page determined to be Unclassified  
Reviewed Chief, RDD, WHS  
IAW EO 13526, Section 3.5  
Date: OCT 02 2015

UNCLASSIFIED

ASD-TDR-63-277, Vol. 17

REPORT 6003

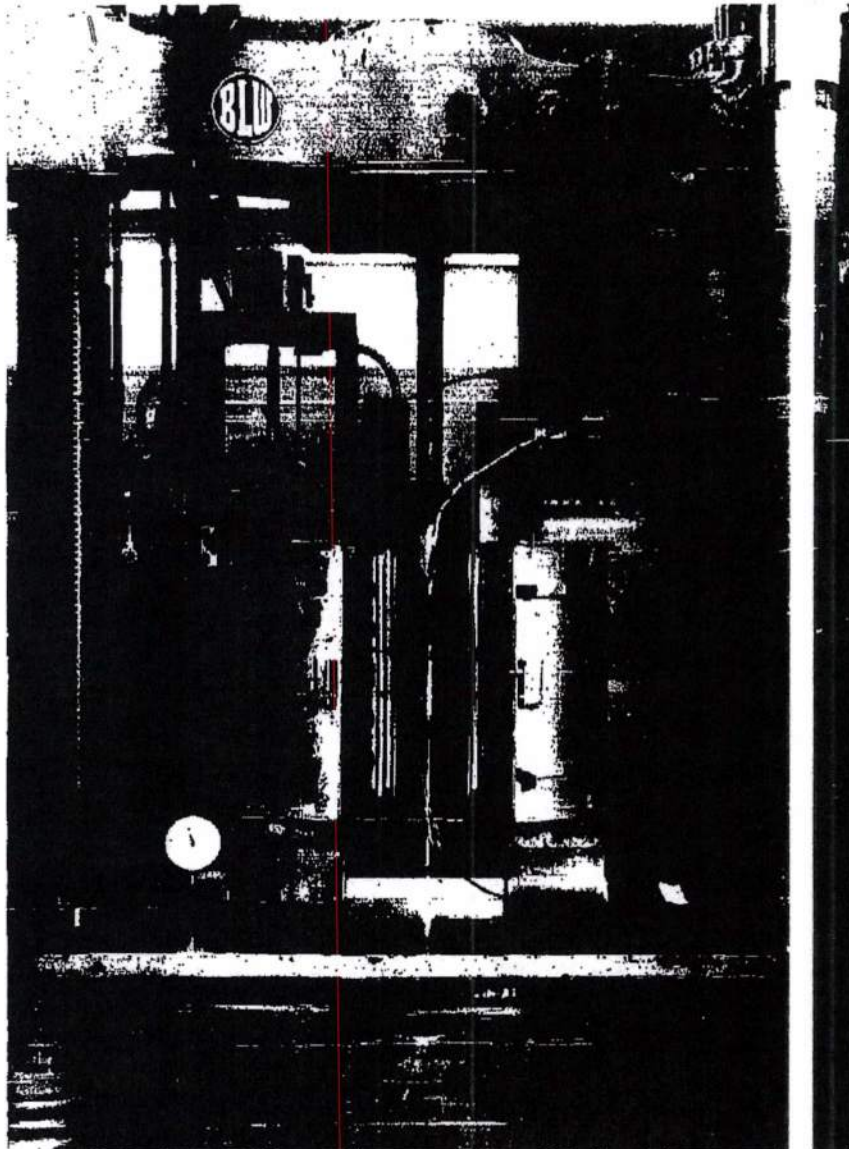


FIGURE 69. Partial Setup for 1400 P Test of 10 Spring  
Series Stack of Belleville Springs--R 235 Material

NEG-1155-5

MAC 472

UNCLASSIFIED

UNCLASSIFIED

ASD-TDR-63-277, Vol. IV

REPORT 6003

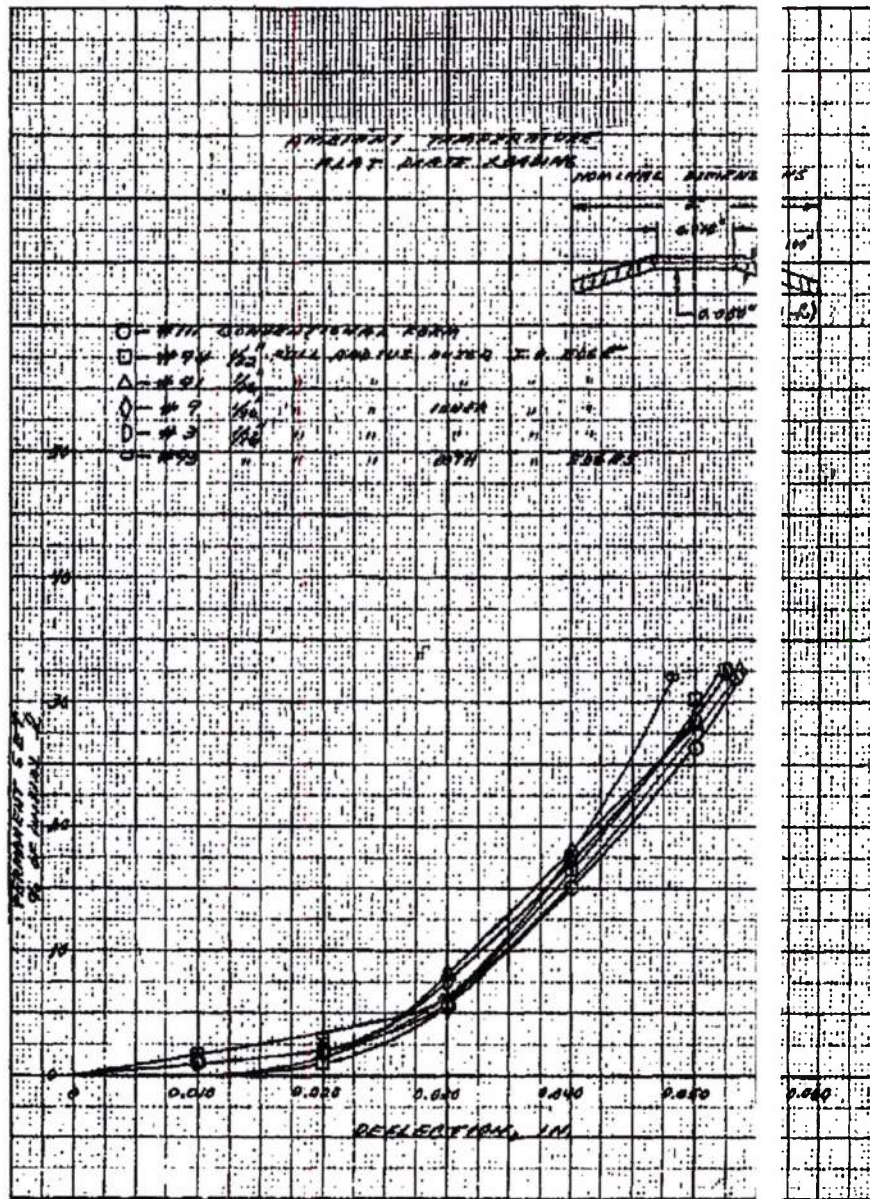


FIGURE 70. Permanent Set vs. Deflection During Presetting of Single Belleville Springs (R-255 Alloy)

UNCLASSIFIED

UNCLASSIFIED

ASD-TDR-63-277, Vol. IV

6003

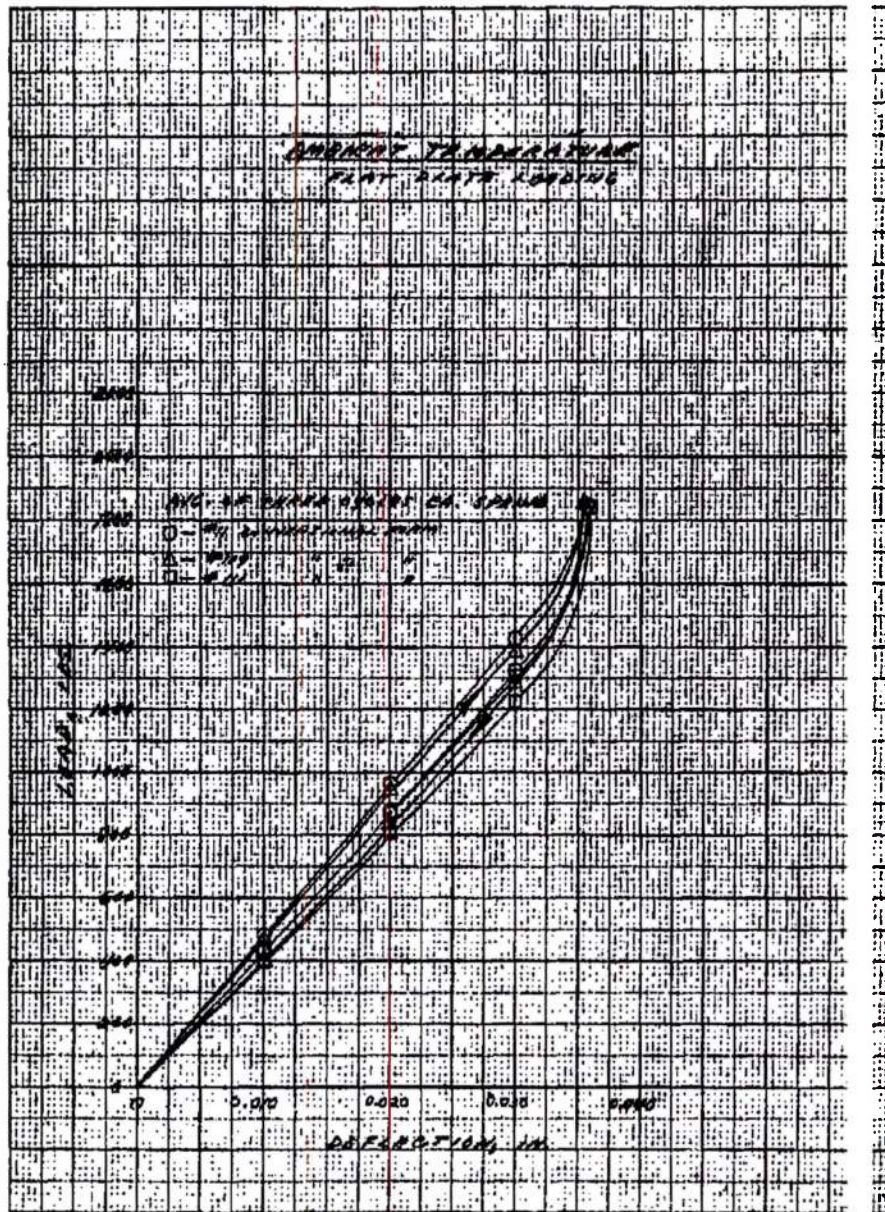


FIGURE 71. Load vs. Deflection: No. 11, No. 109, and No. 111 Single Belleville Springs (R-235 Alloy)

UNCLASSIFIED

UNCLASSIFIED

REPORT 6003

ASD-TDR-63-277, Vol. IV

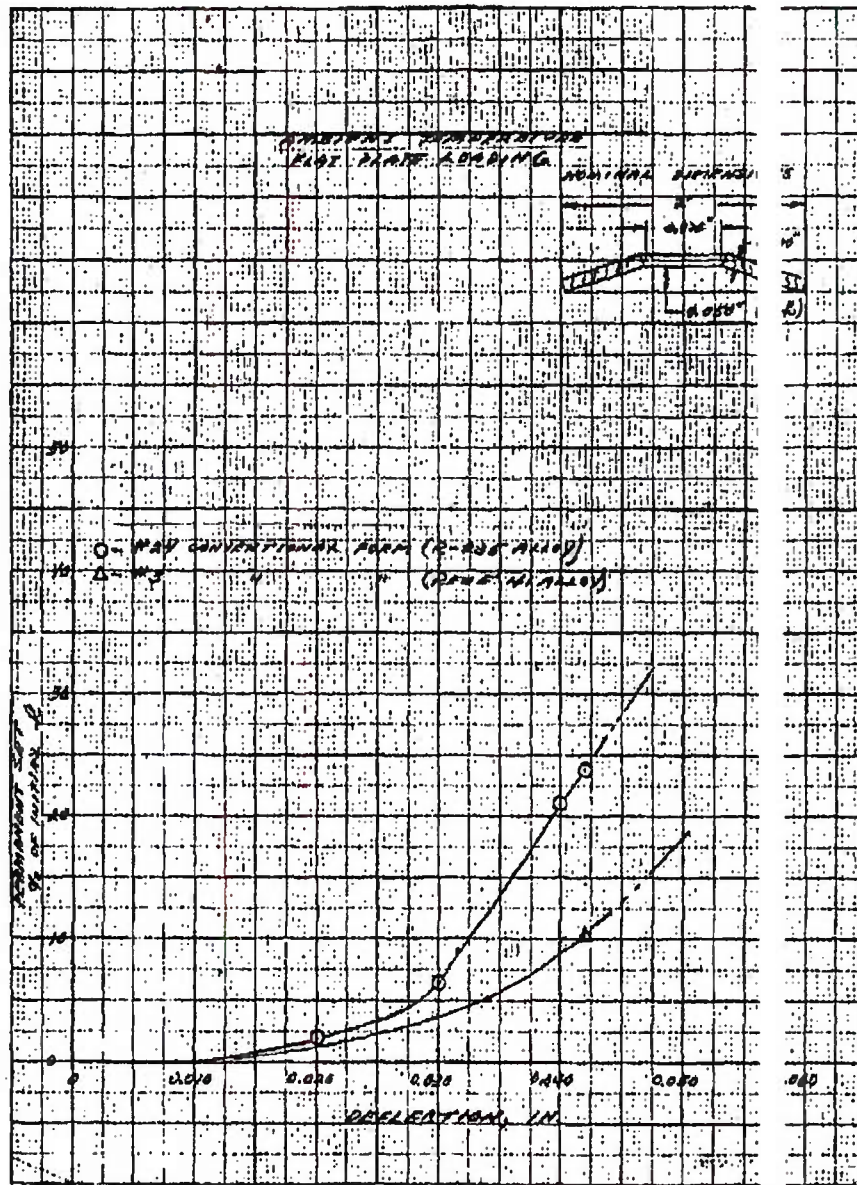


FIGURE 72. Permanent Set vs. Deflection During Preset of Single Belleville Springs

ARCADZ

UNCLASSIFIED

~~SECRET RESTRICTED DATA~~  
~~ATOMIC ENERGY ACT OF 1954~~

REF 6003

ASD-TDR-63-277, Vol. IV

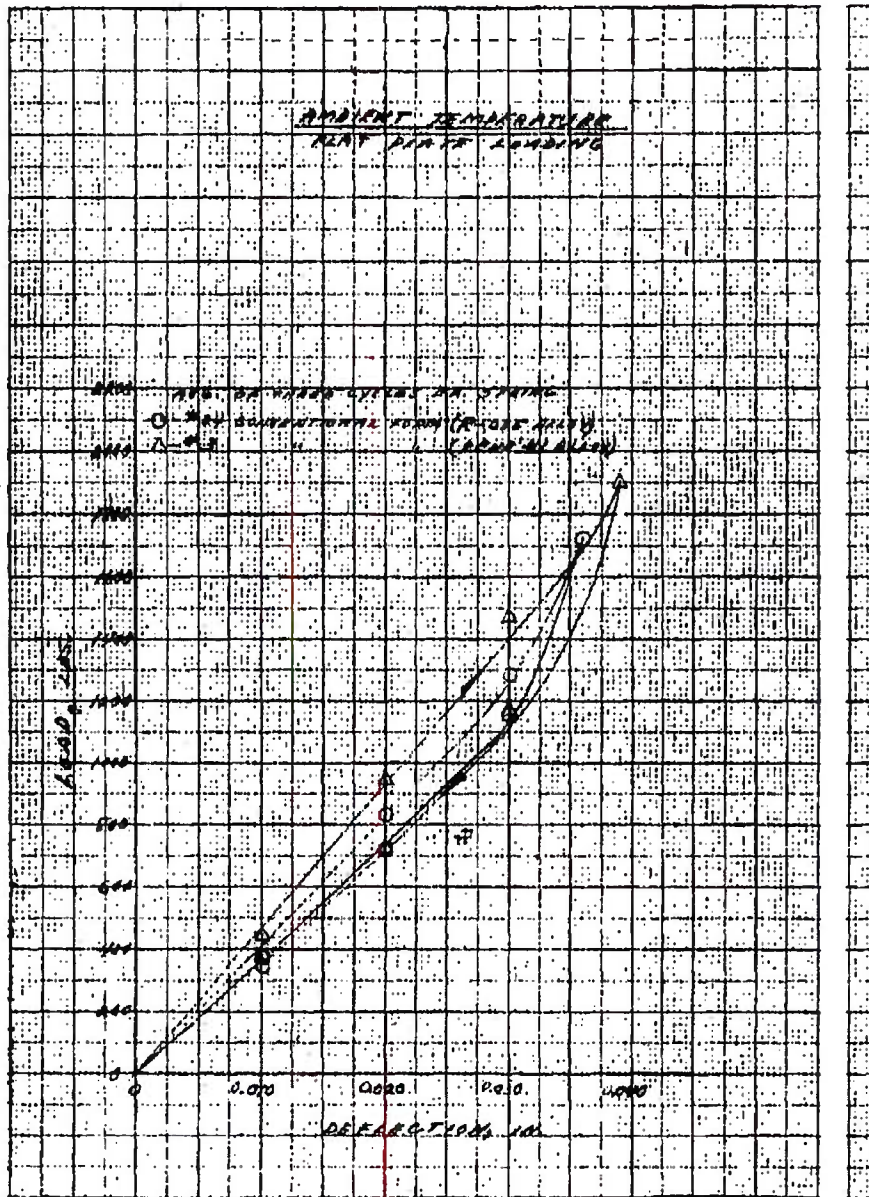


FIGURE 73. Load vs. Deflection for Single Belleville Springs (R-235 Alloy)

~~SECRET RESTRICTED DATA~~  
~~ATOMIC ENERGY ACT OF 1954~~

MAC AEEZ

UNCLASSIFIED

REPORT 6003

ASD-TDR-63-277, Vol. IV

AVERAGE OF THREE TESTS

- #109 CONVENTIONAL FORM
- ▲ 1/32 IN. FULL RADIUS OUTER I.D. EDG
- #92 1/16 IN. FULL RADIUS OUTER I.D. EDGE

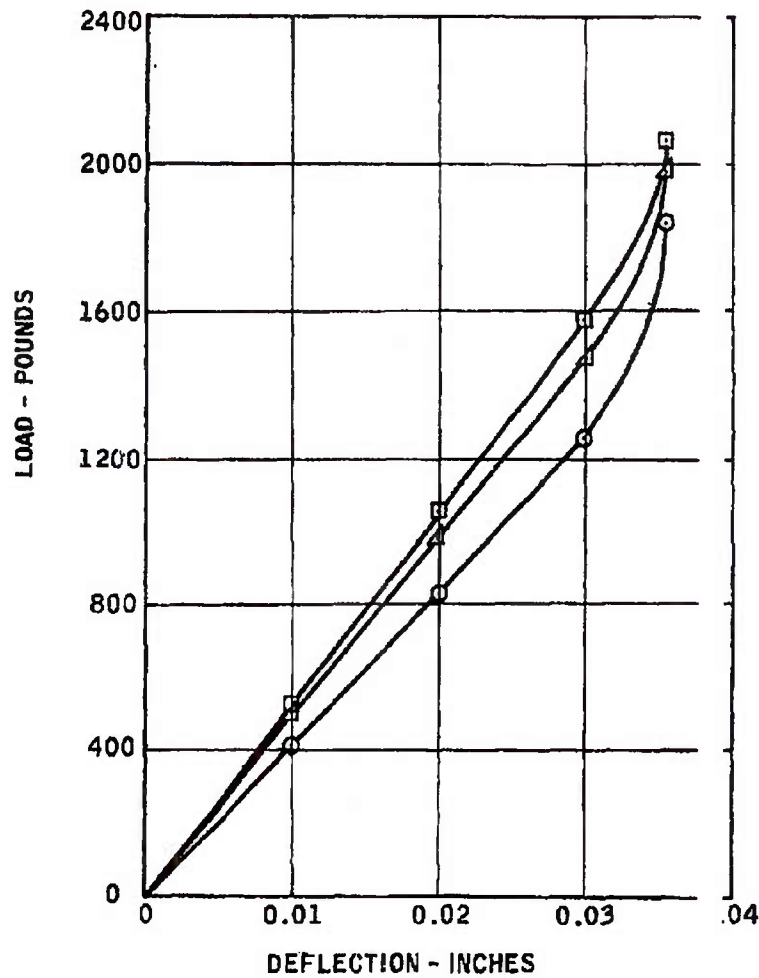


FIGURE 74. Load vs. Deflection for Single Belleville Springs (R-235 Alloy)--Ambient Temperature

UNCLASSIFIED

MAC 4873

UNCLASSIFIED

6003

ASD-TDR-63-277, Vol. IV

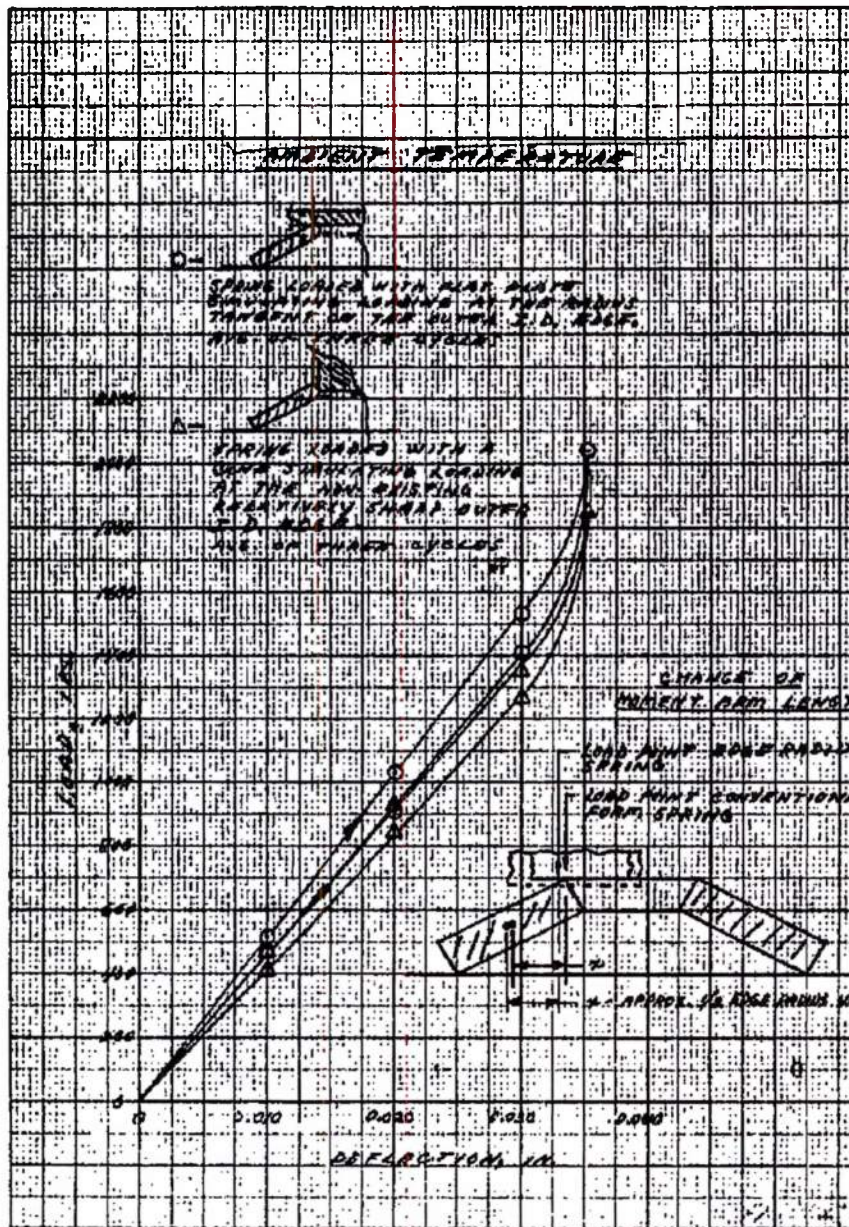


FIGURE 75. Load vs. Deflection: No. 93 Belleville Spring--  
 1/16-in. Full Radius Both I.D. Edges (R-235 Alloy)

UNCLASSIFIED

MAC 462

UNCLASSIFIED

ASD-TDR-63-277, Vol. IV

REPORT 6003

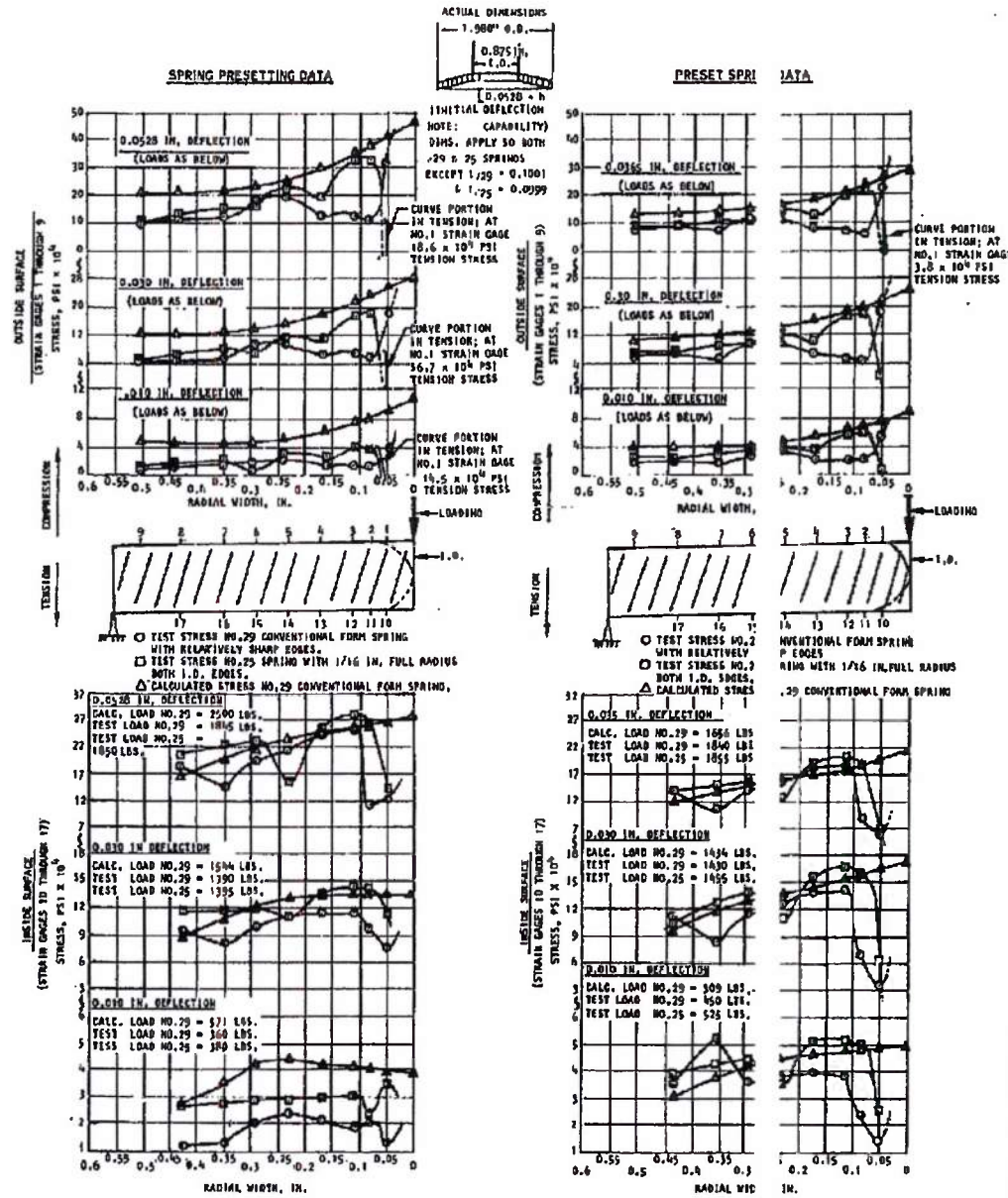


FIGURE 76. Stress vs. Spring Radial Width--Belleville Spring No. 29 and No. 25 (R-235 Material; Ambient Temperature; Flat Plate Loading)

UNCLASSIFIED

MAC 4678

UNCLASSIFIED

om 6003

ASD-TDR-63-277, Vol. IV

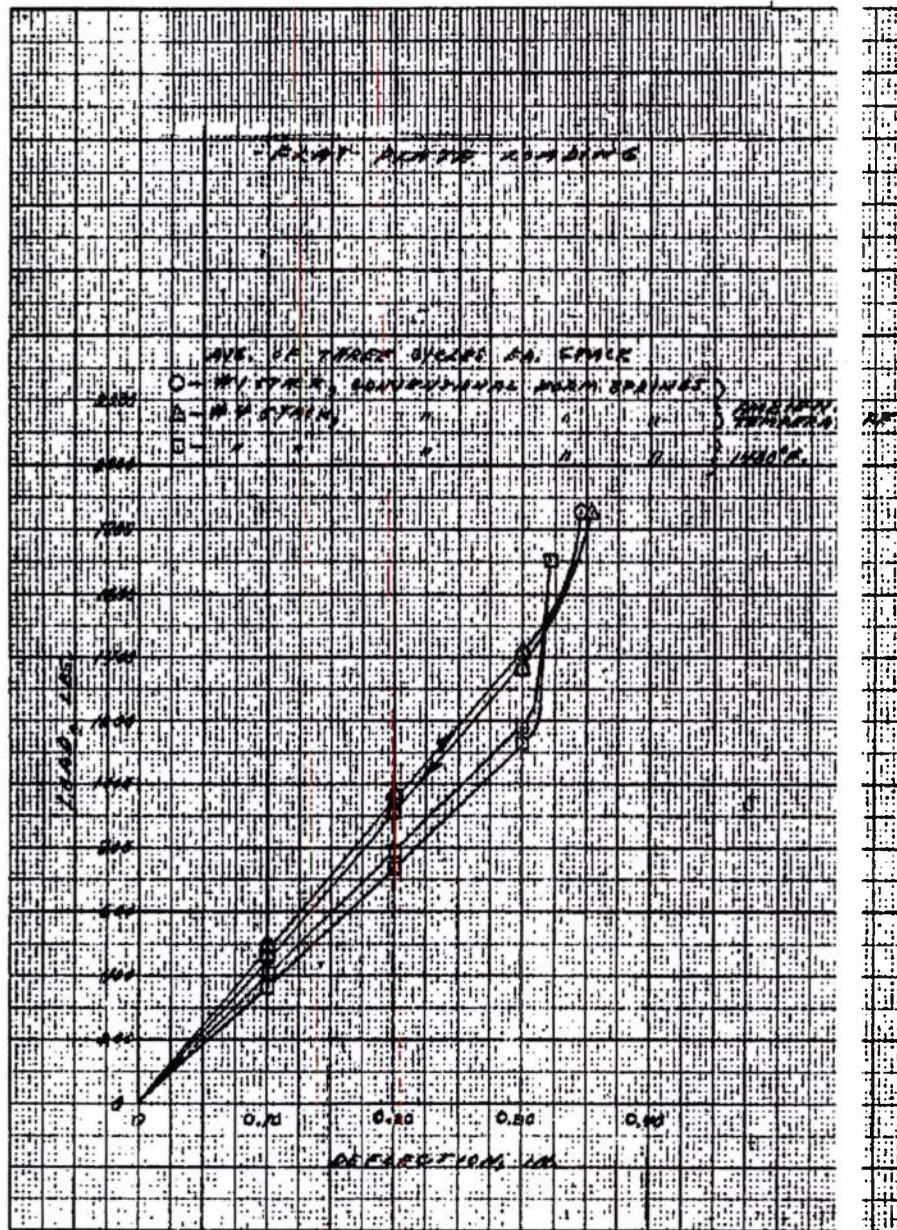


FIGURE 77. Load vs. Deflection: No. 1 and No. 4 10-Spring Series Stack of Belleville Springs (R-235 Alloy)

MAC ACD

UNCLASSIFIED

UNCLASSIFIED

REPORT 6003

ASD-TDR-63-277, Vol. IV

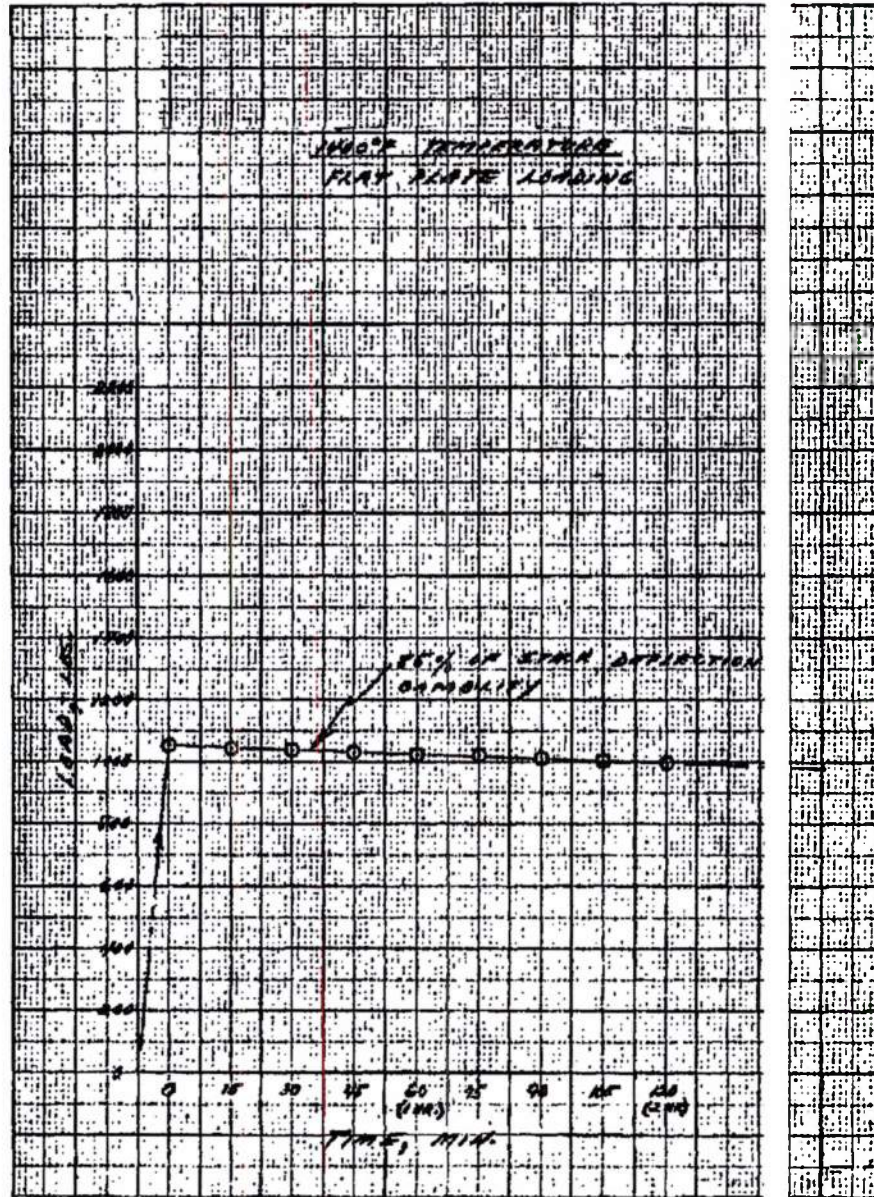


FIGURE 78. Load Loss vs. Time at Constant Spring Deflection:  
10-Spring Series Stack of Belleville Springs (R-235 All )

n. 4

MAC 4873

UNCLASSIFIED

~~CONFIDENTIAL~~

REPORT 6003

ASD-TDR-63-277, Vol. IV

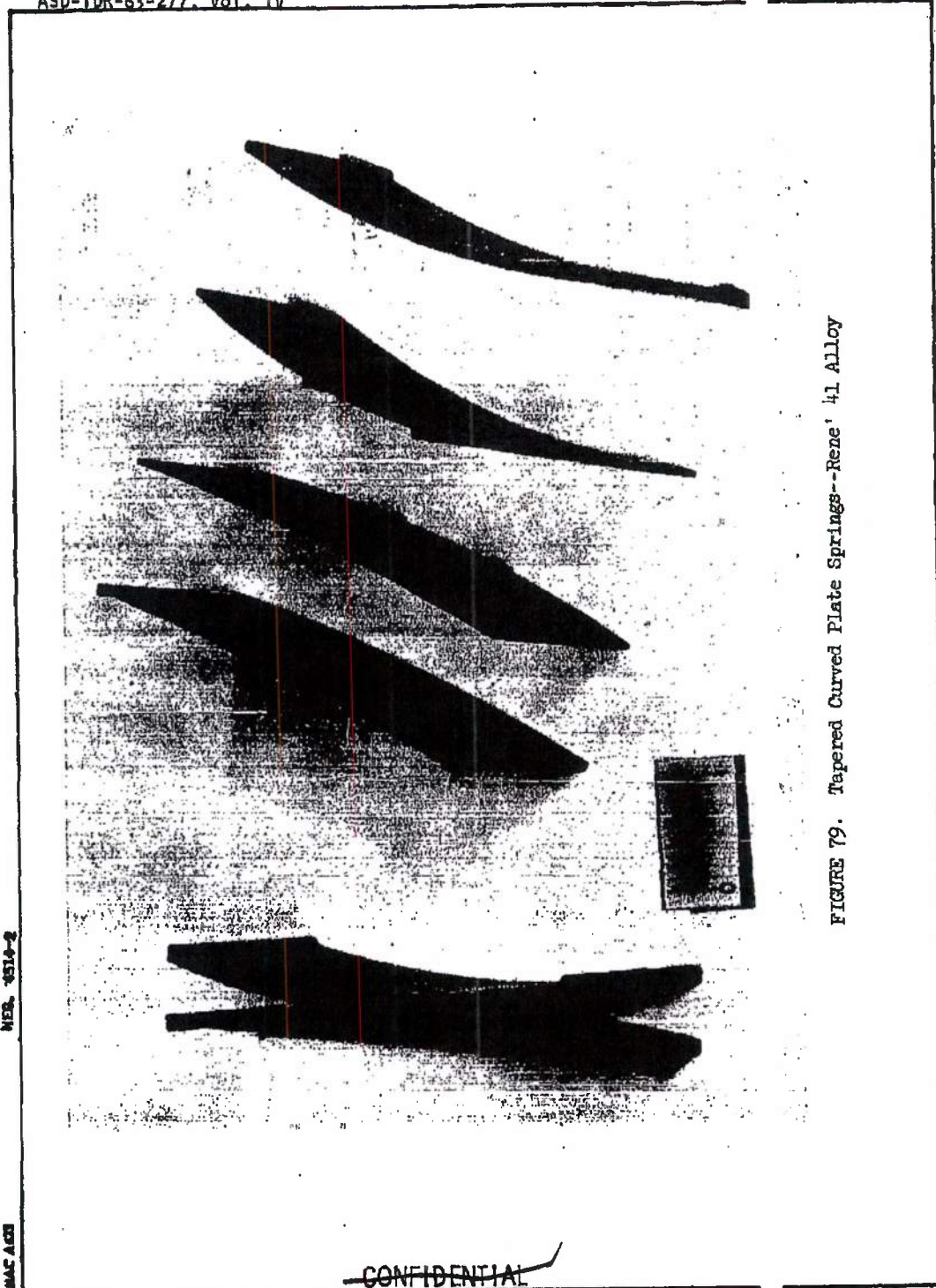


FIGURE 79. Tapered Curved Plate Springs--Rene 41 Alloy

NER. 451A-2

MAC AGC

~~CONFIDENTIAL~~

DECLASSIFIED IN FULL  
Authority: EO 13526  
Chief, Records & Declass Div, WHS  
Date: OCT 02 2015

~~CONFIDENTIAL~~

ASD-TDR-63-277 Vol. 1.

REPORT 6003

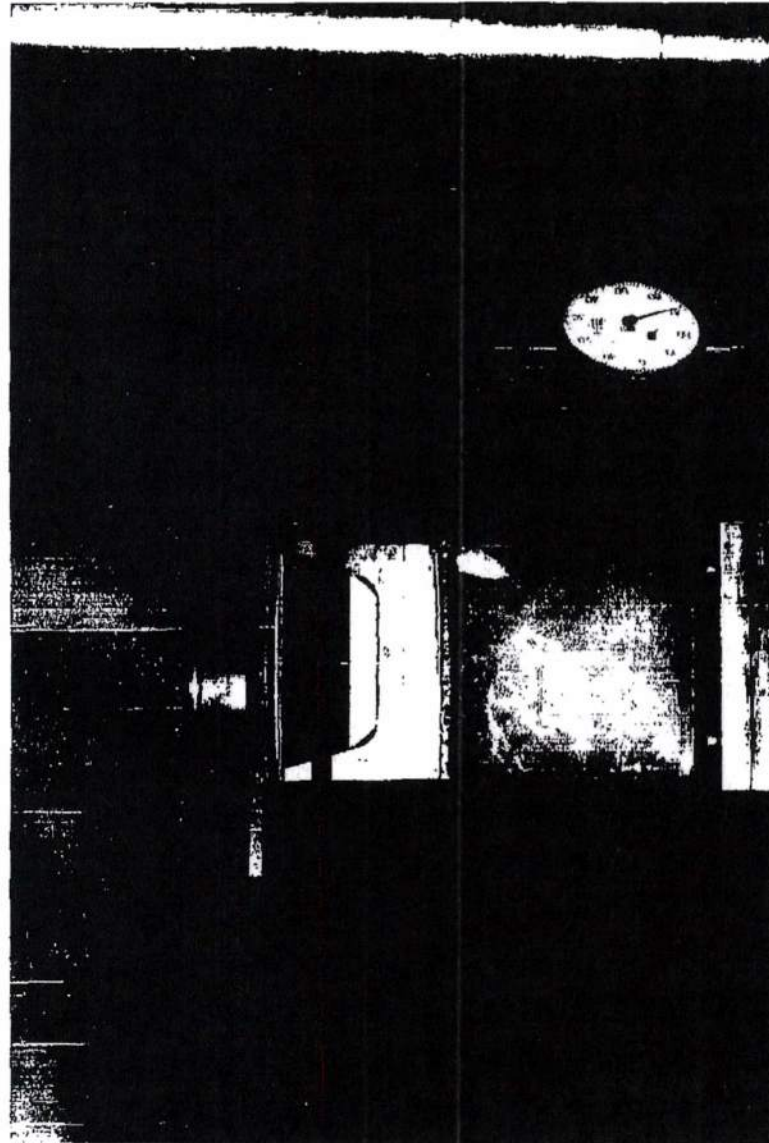


FIGURE 80. Test of Tapered Curved Plate Springs--Spring Stack Profile  
at 0.370-inch Deflection--Ambient Temperature

NER, 451A-4

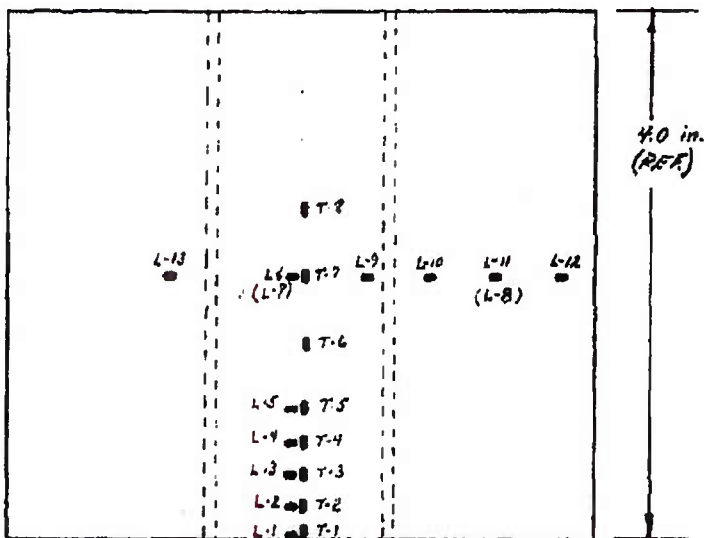
MAC A673

~~CONFIDENTIAL~~

UNCLASSIFIED

6003

ASD-TDR-63-277, Vol. IV



XB1415-503

NOTES -

1. Installed SR-4 type A-18 strain gages as shown on XB1415-503, -501 & -1.
2. L-7 & L-8 on opposite side of spring from L-6 & L-11, respectively.
3. T-5, T-6 & L-5 not used on -501. T-3, T-4, T-5, T-6, T-8, L-3, L-4 & L-5 not used on -1.
4. L - denotes longitudinal orientation  
 T - " " transverse " "

FIGURE 81. Strain Gage Layout for Tapered Curved Plate Spring Test

UNCLASSIFIED

MAC A921

~~CONFIDENTIAL~~

ASD-DR-63277, Vol. 22

REPORT 6003

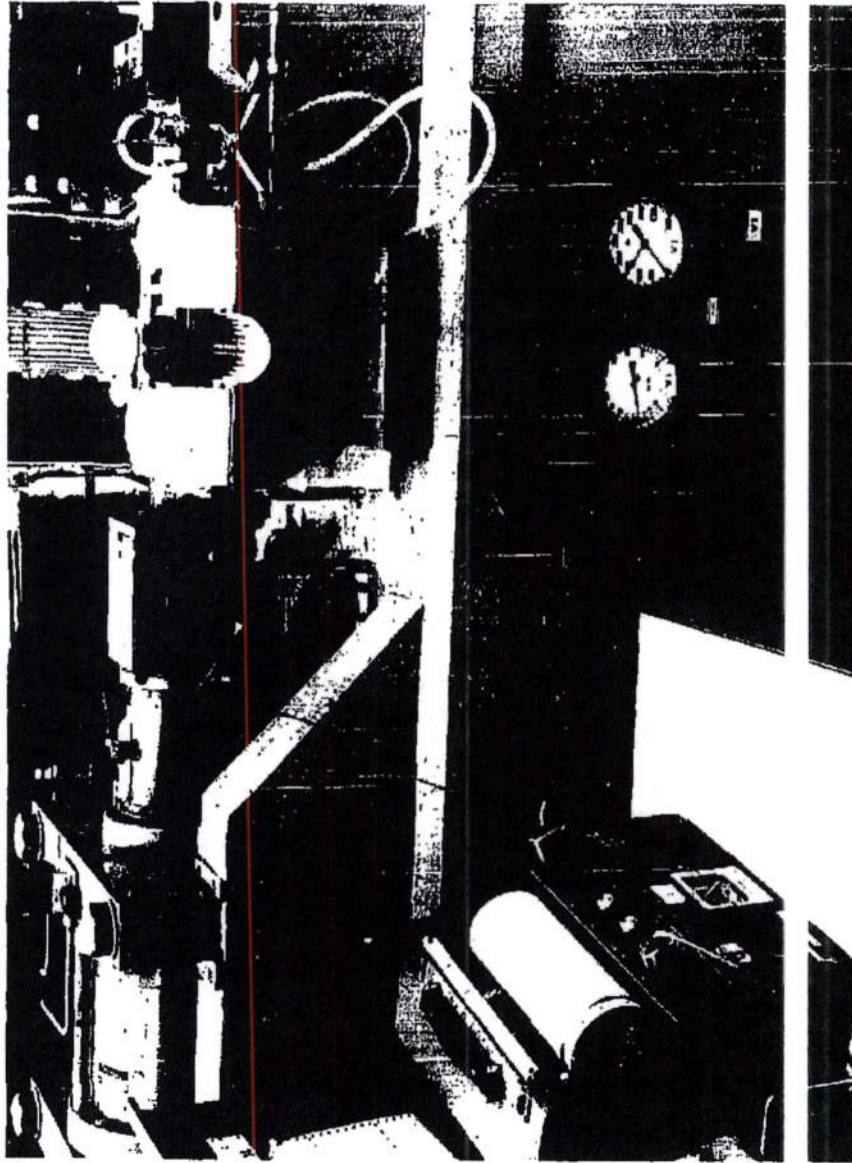


FIGURE 82. Setup for Testing of Tapered Curved Plate Springs  
(1400°F Cyclic Load-Deflection)

NEG. 4514-7

MAC 463

~~CONFIDENTIAL~~

~~CONFIDENTIAL~~

ASD-TDR-63-277, Vol. IV

6003

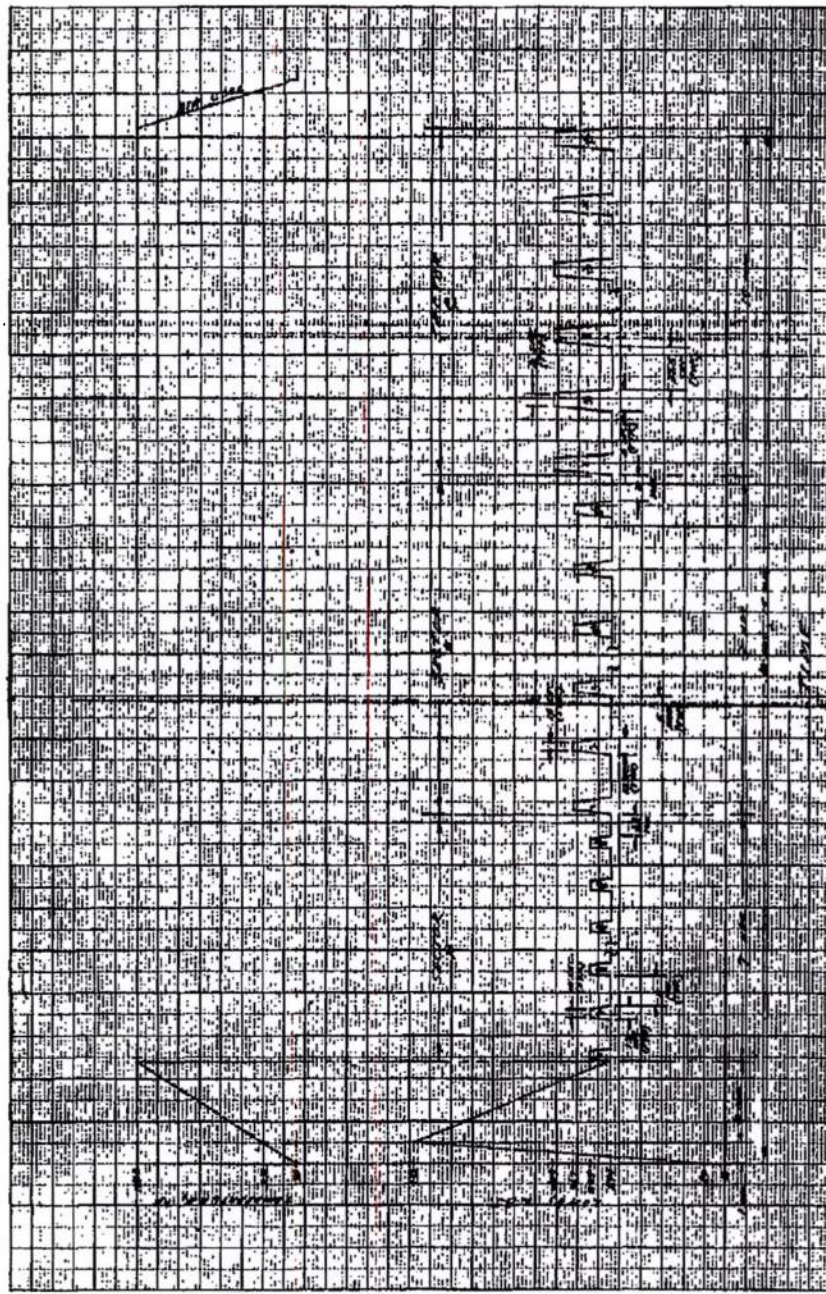


FIGURE 83. Cyclic Load-Deflection for Tapered Curved Plate Springs  
(2-in. Wide Stacks, S/N 2 and 4)

MAC AETD

~~CONFIDENTIAL~~

22J46

~~CONFIDENTIAL~~

ASD-TDR-63-277, Vol. IV

REPORT 6003

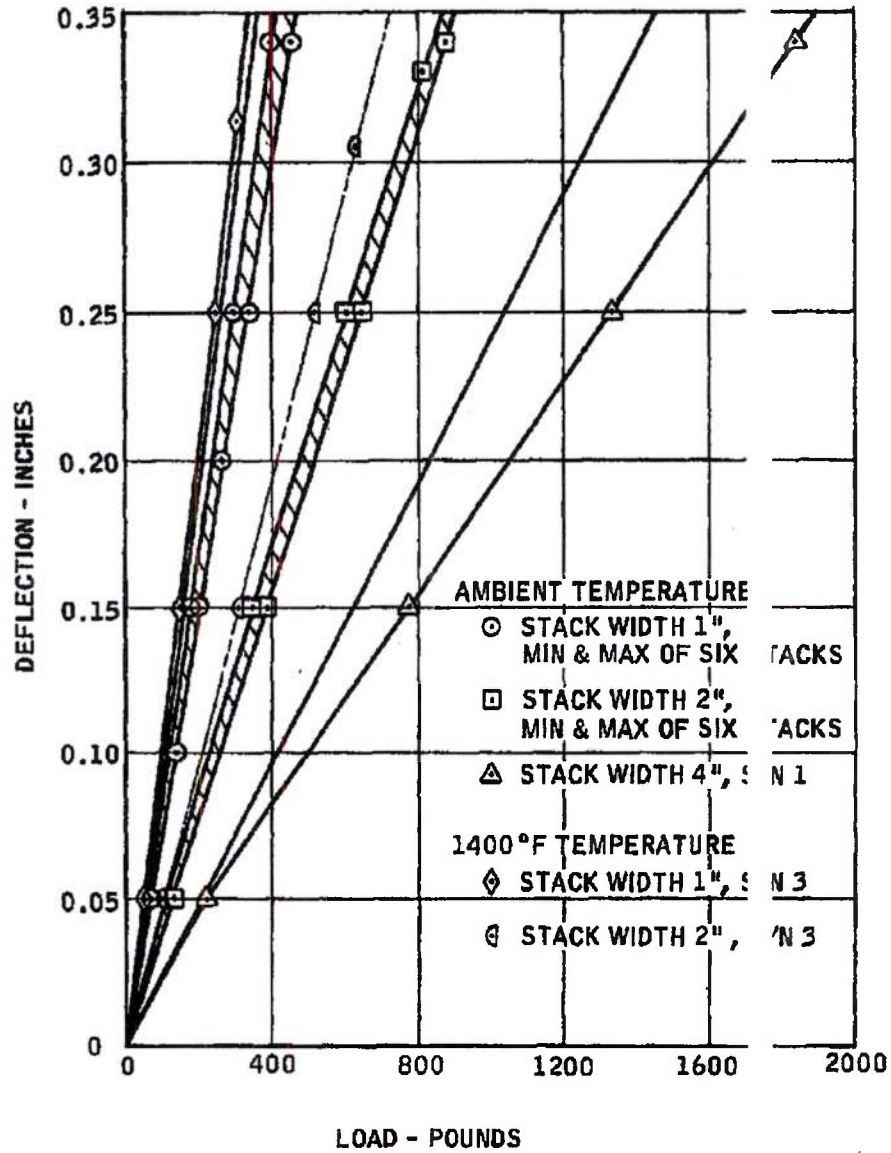


FIGURE 84. Load Deflection Characteristics for Tapered Curved Plate Spring Stack

MAC 603

~~CONFIDENTIAL~~

~~CONFIDENTIAL~~

ASD-TDR-63-277, Vol. IV

DWT 6003

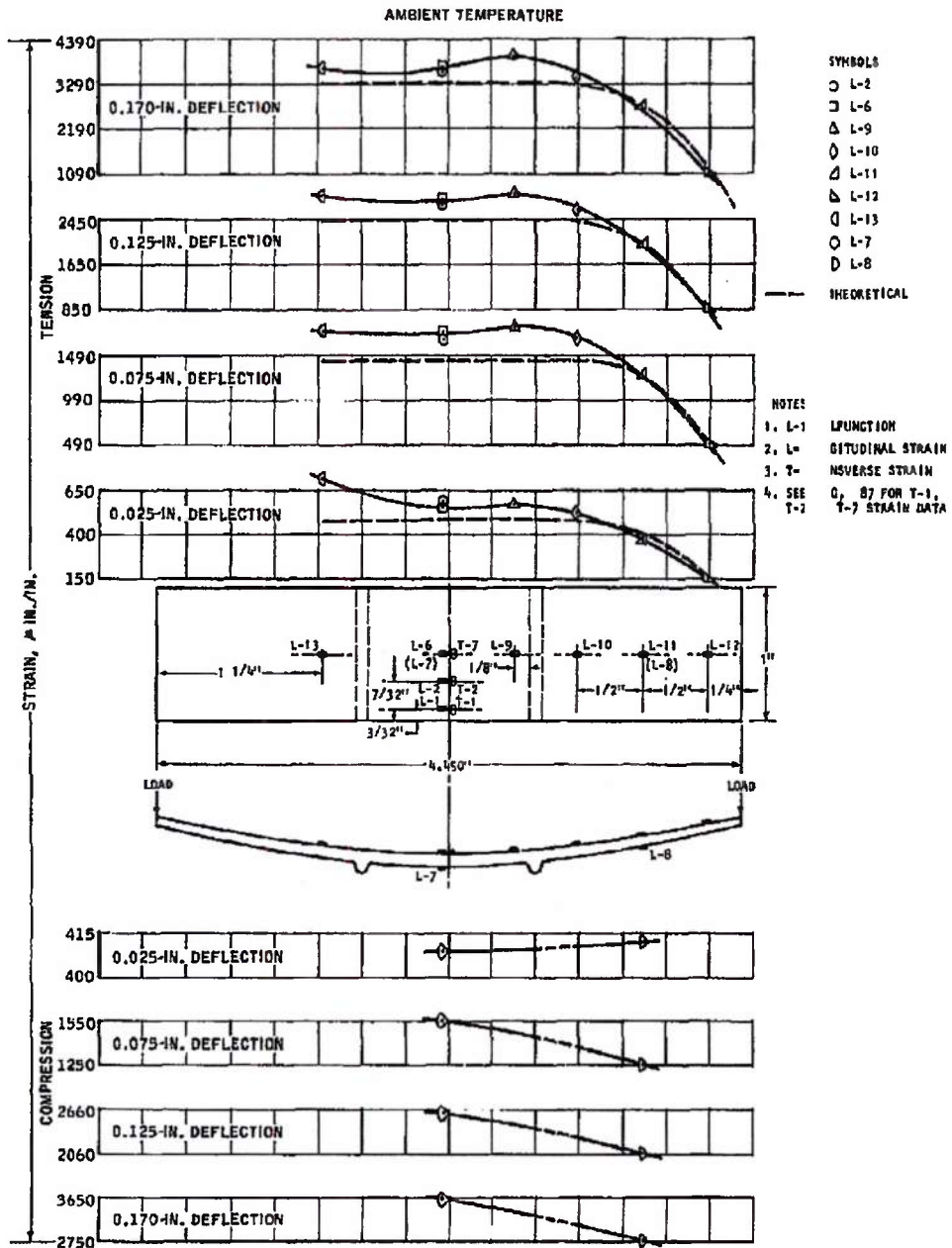


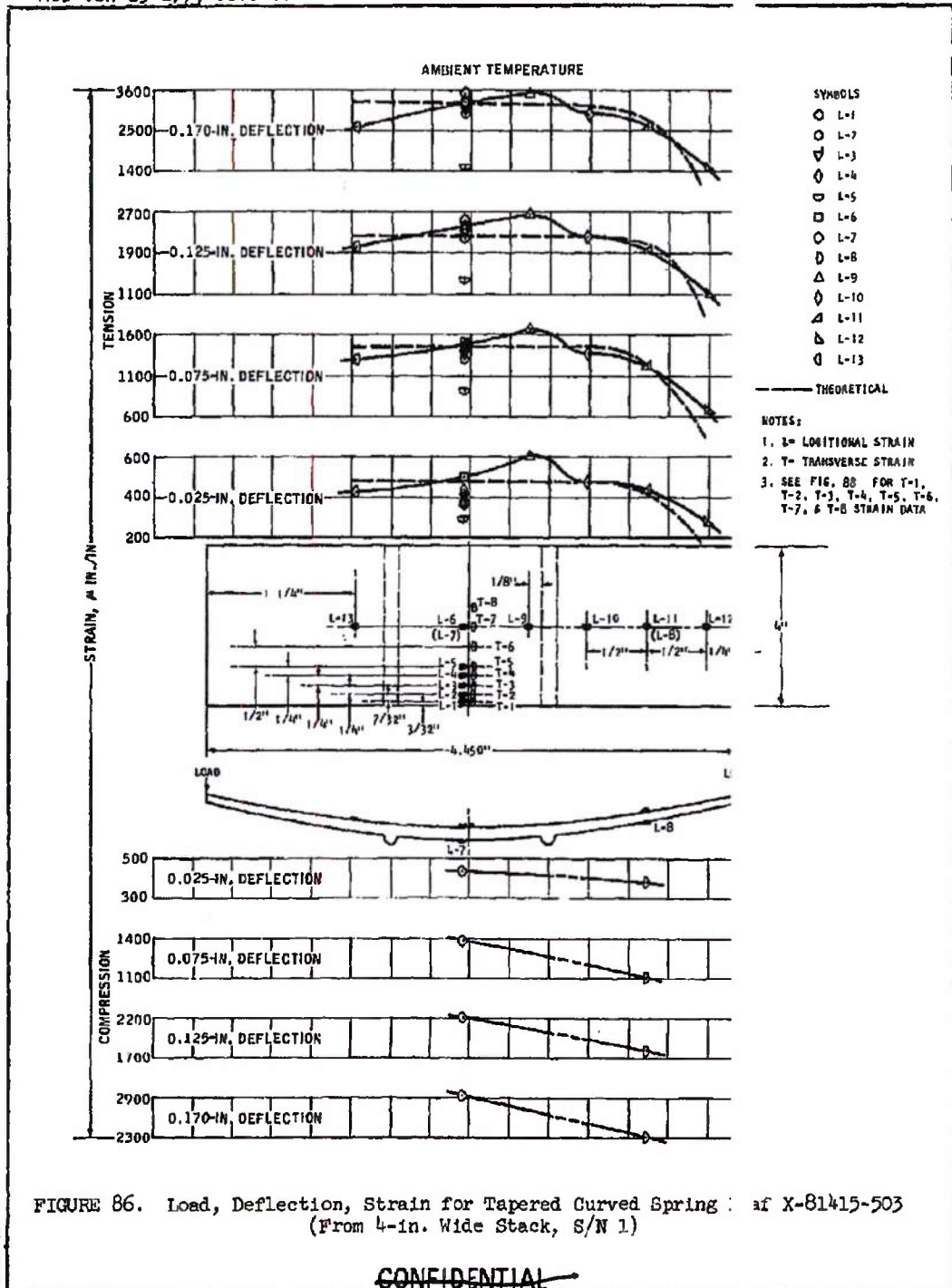
FIGURE 85. Load, Deflection, Strain for Tapered Curved Spring Leaf -18415-1  
 (From 1-in. Wide Stack, S/N 1)

~~CONFIDENTIAL~~

~~CONFIDENTIAL~~

ASD-TDR-63-277, Vol. IV

REPORT 6003



MAC A 03

~~CONFIDENTIAL~~

CONFIDENTIAL

ASD-TDR-63-277, Vol. IV

6003

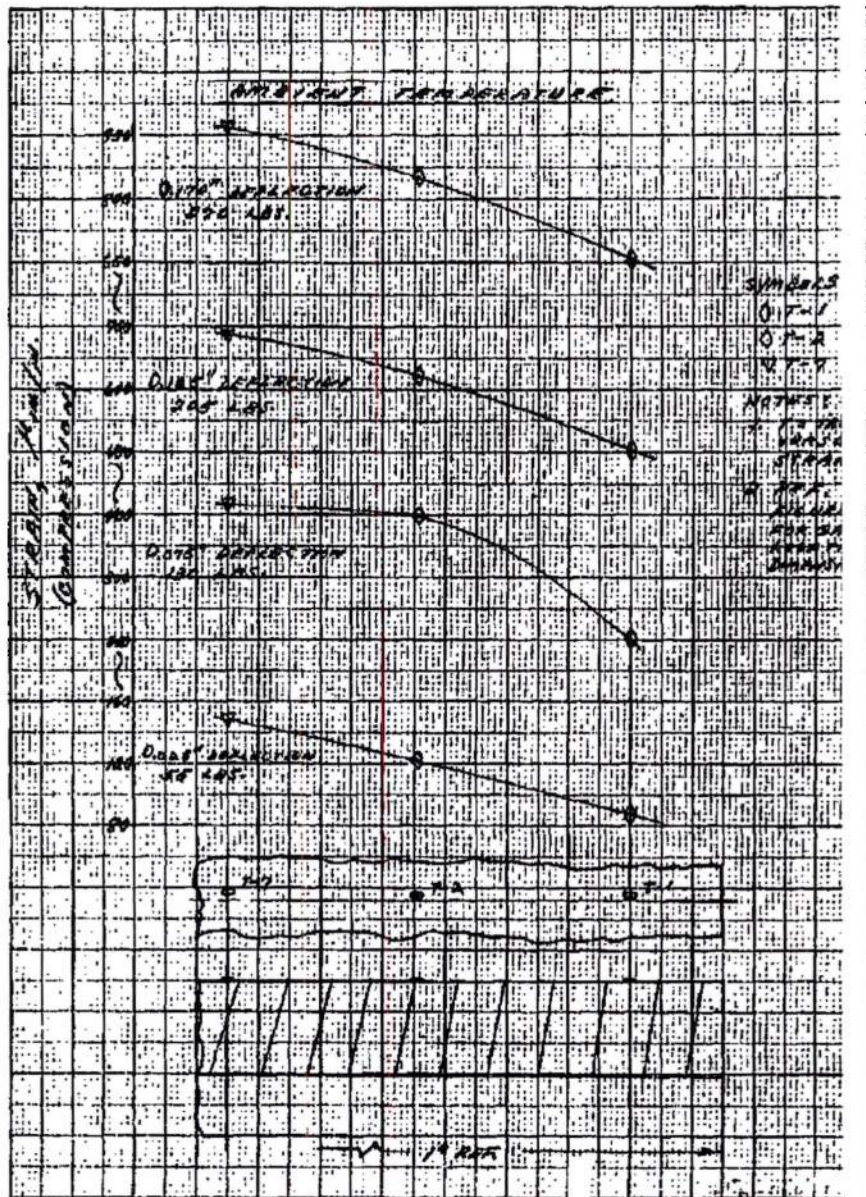


FIGURE 87. Load-Deflection-Strain Data for Tapered Curved Spring Le (X-81415-1) from 1-in. Wide Stack, S/N 1

CONFIDENTIAL

OCT 02 2015

~~CONFIDENTIAL~~

REPORT 6003

ASD-TDR-63-277, Vol. IV

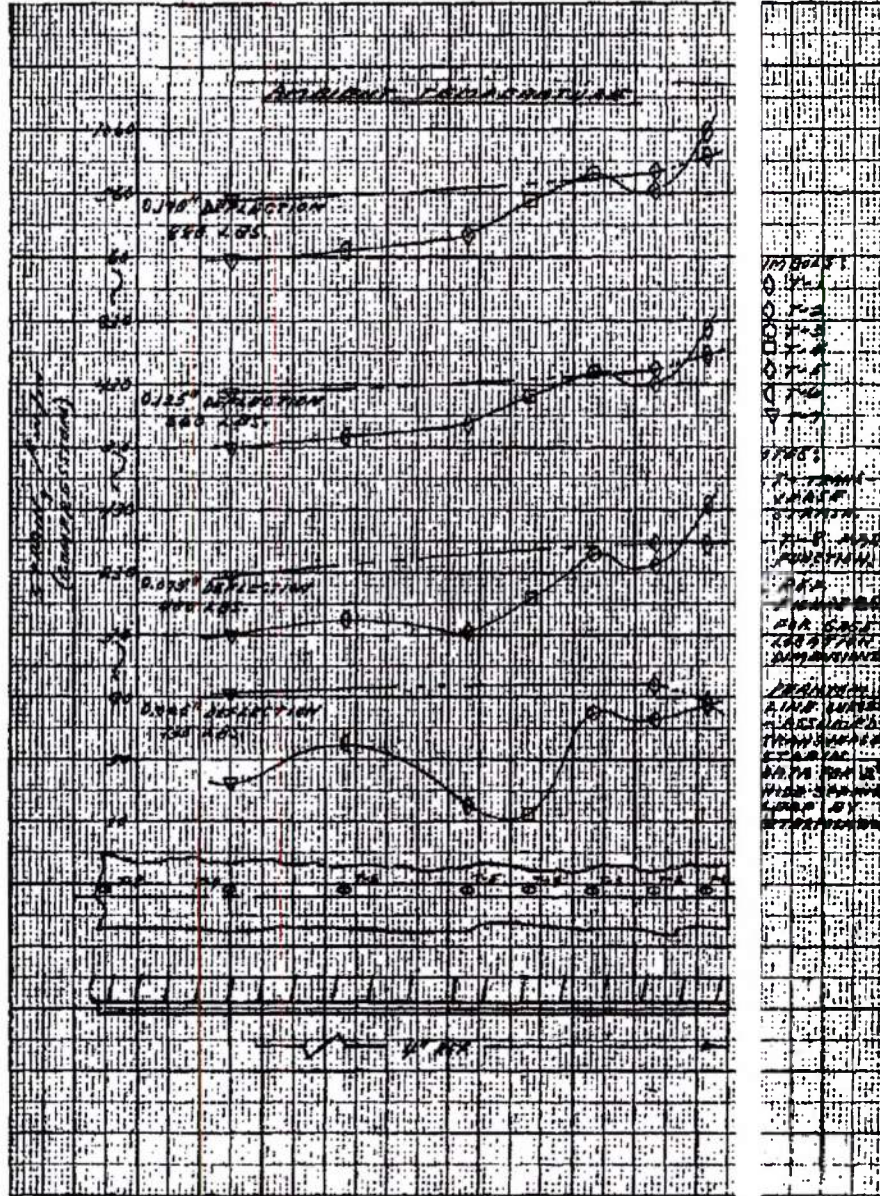


FIGURE 88. Load-Deflection-Strain Data for Tapered Curved Ring Leak (X-181415-503) from 4-in. Wide Stack, S/N

MAC 4603

~~CONFIDENTIAL~~

DECLASSIFIED IN FULL  
Authority: EO 13526  
Chief, Records & Declass Div, WHS  
Date: OCT 02 2015

~~CONFIDENTIAL RESTRICTED DATA~~  
~~ATOMIC ENERGY ACT OF 1954~~

ASD-TDR-63-277, Vol. IV

REPO 6003

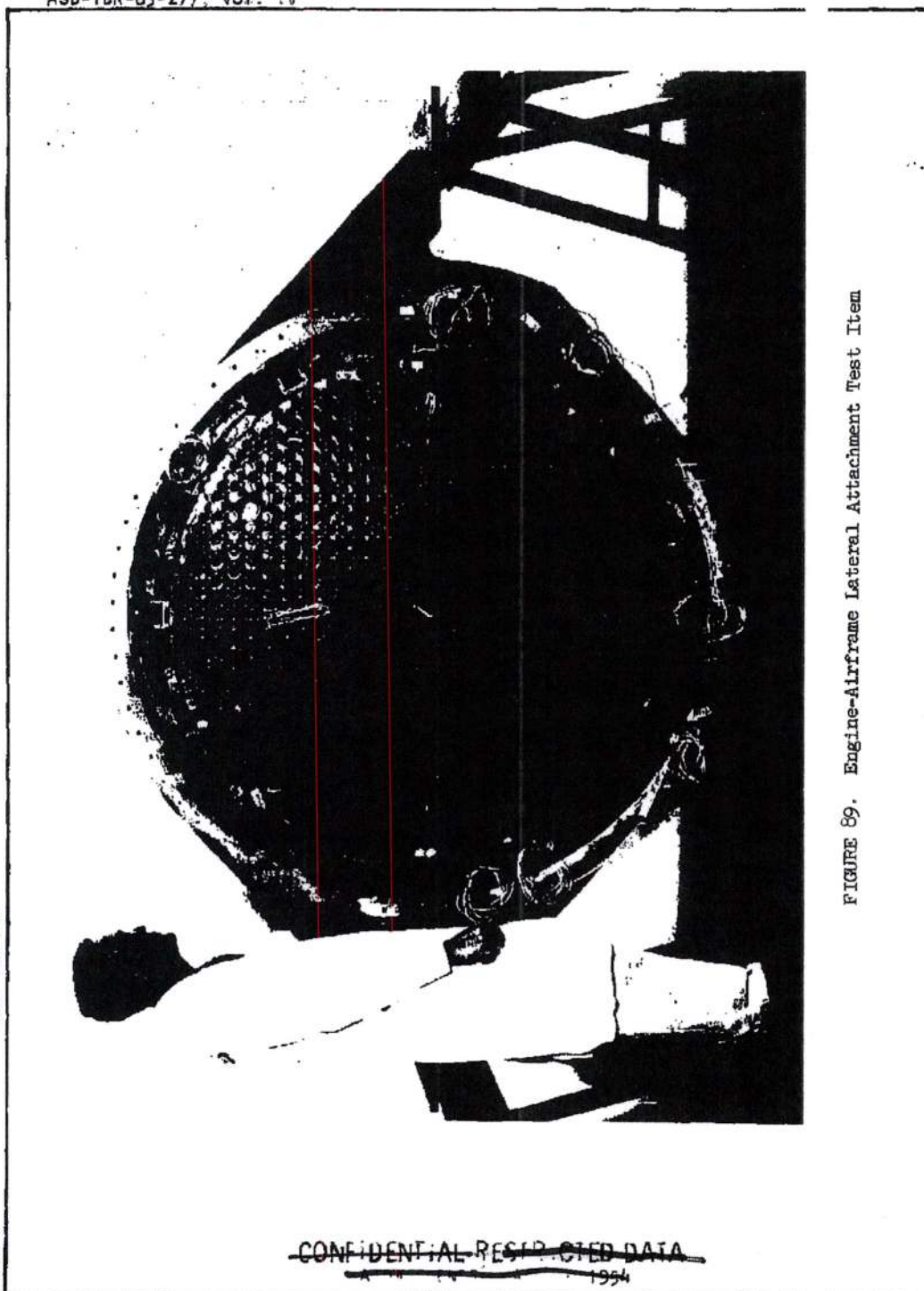


FIGURE 89. Engine-Airframe Lateral Attachment Test Item

~~CONFIDENTIAL RESTRICTED DATA~~  
~~ATOMIC ENERGY ACT OF 1954~~

MEG. 4142-13

MAC 4670

~~CONFIDENTIAL RESTRICTED DATA~~  
~~SECURITY INFORMATION~~

ASD-TDR-63-277, Vol. IV

REPORT 6003

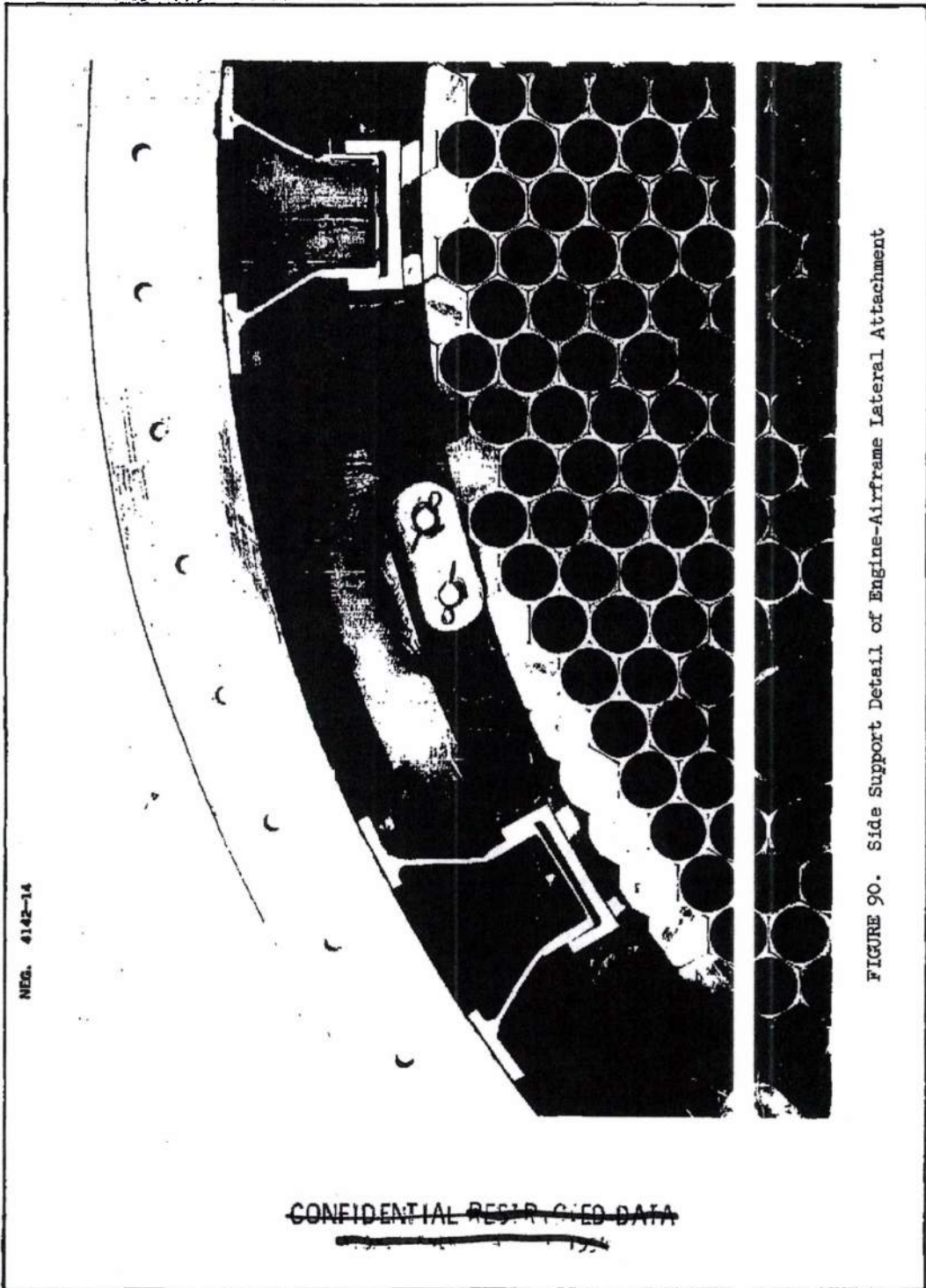


FIGURE 90. Side Support Detail of Engine-Airframe Lateral Attachment

~~CONFIDENTIAL RESTRICTED DATA~~  
~~NO FORN DISSEM 1954~~

ASD-TDR-63-277, Vol. 12

REFC 6003

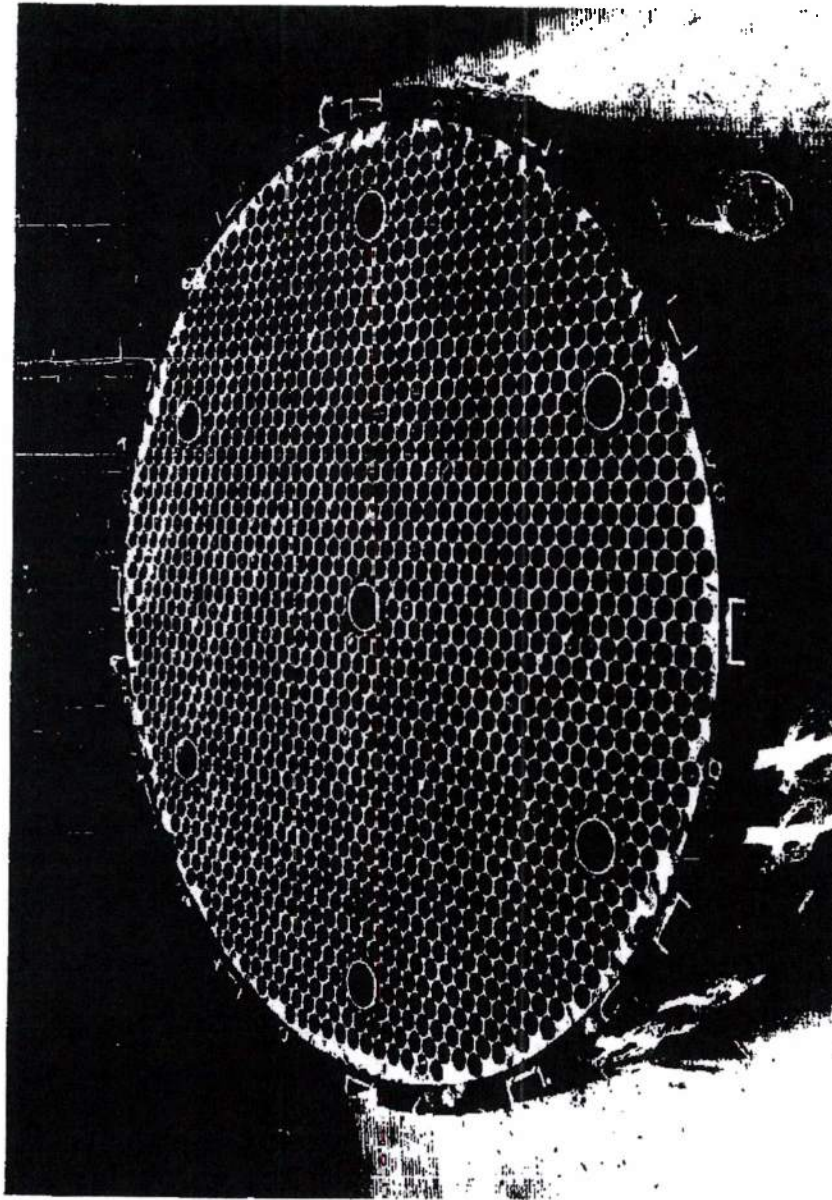


FIGURE 91. Core Matrix and Expansion Shell

4142-9

MAC A677

~~CONFIDENTIAL RESTRICTED DATA~~  
~~NO FORN DISSEM 1954~~

~~CONFIDENTIAL RESTRICTED DATA~~  
1954

ASD-TDR-63-277 Vol. 17

REPORT 6003

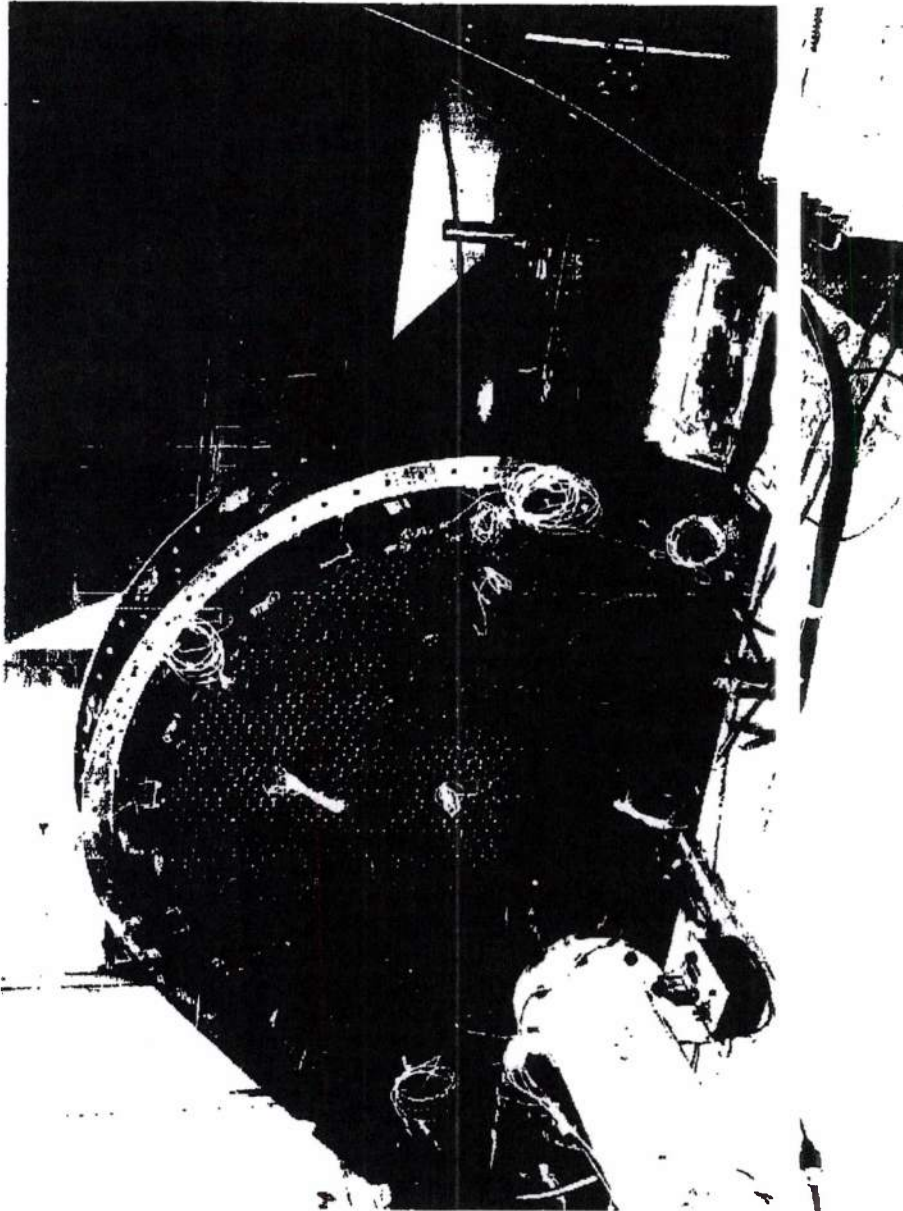


FIGURE 92. Engine-Airframe Lateral Attachment Test Item in Shaker Facility

NEG. 4342-17

MAC 4572

~~CONFIDENTIAL RESTRICTED DATA~~  
1954

DECLASSIFIED IN FULL  
Authority: EO 13526  
Chief, Records & Declass Div, WHS  
Date: OCT 02 2015

~~SECRET RESTRICTED DATA~~  
~~ATOMIC ENERGY ACT OF 1954~~

ASD-TOR-63-277, Vol. IV

NY 6003

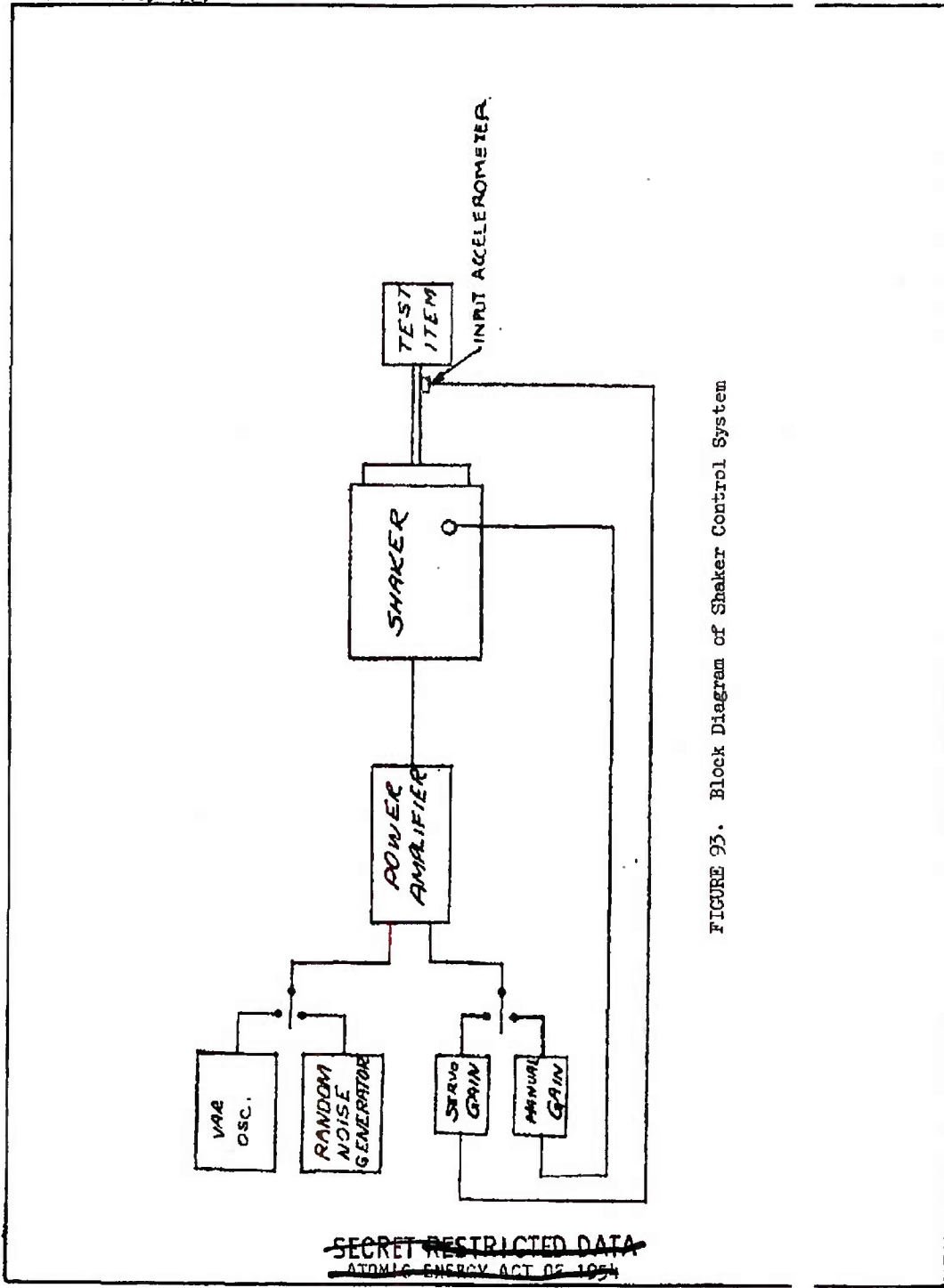


FIGURE 93. Block Diagram of Shaker Control System

~~SECRET RESTRICTED DATA~~  
~~ATOMIC ENERGY ACT OF 1954~~

MAC AGZ

N22K25

Page determined to be Unclassified  
Reviewed Chief, RDD, WHS  
IAW EO 13526, Section 3.5  
Date: OCT 02 2015

MAC A827

NEG-4142-18

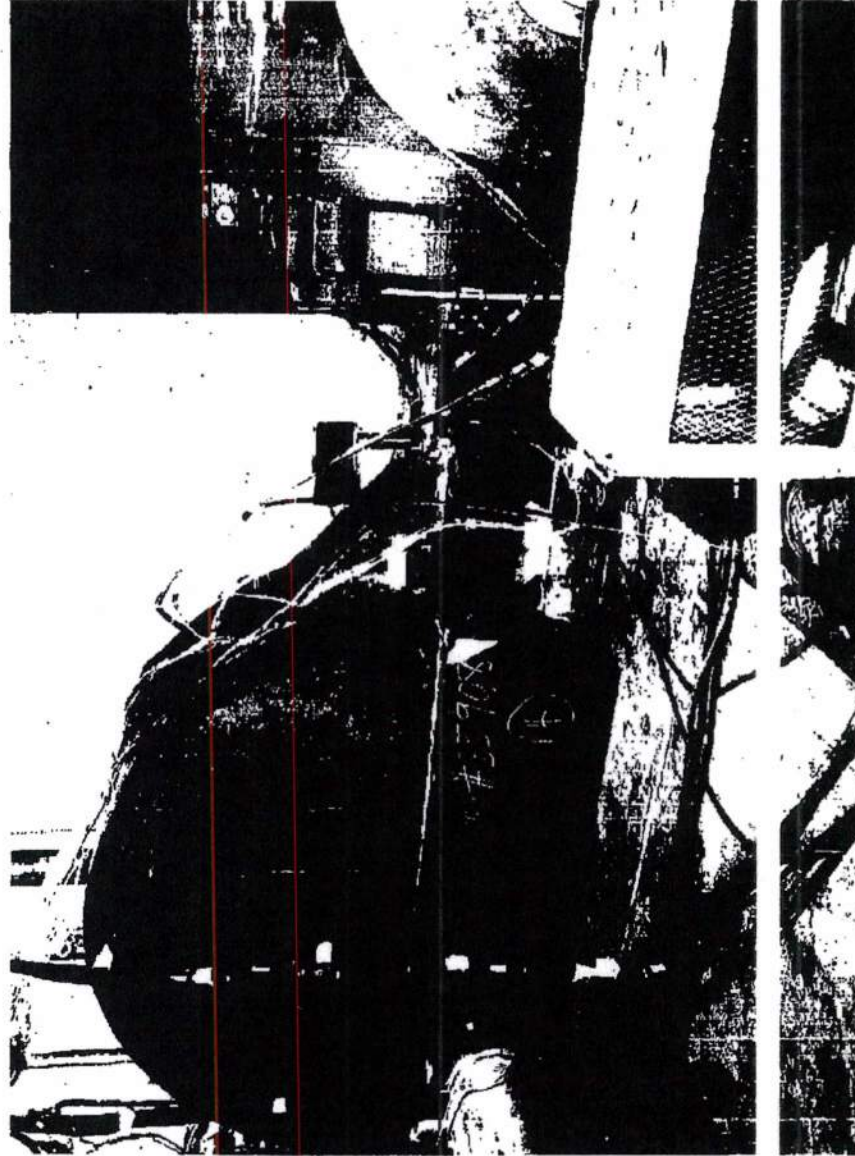


FIGURE 94. Engine-Airframe Lateral Attachment Test Item in Furnace

~~SECRET RESTRICTED DATA~~  
~~ATOMIC ENERGY ACT OF 1954~~

ASD-TDR-63-277, Vol. IV

ORR 6003

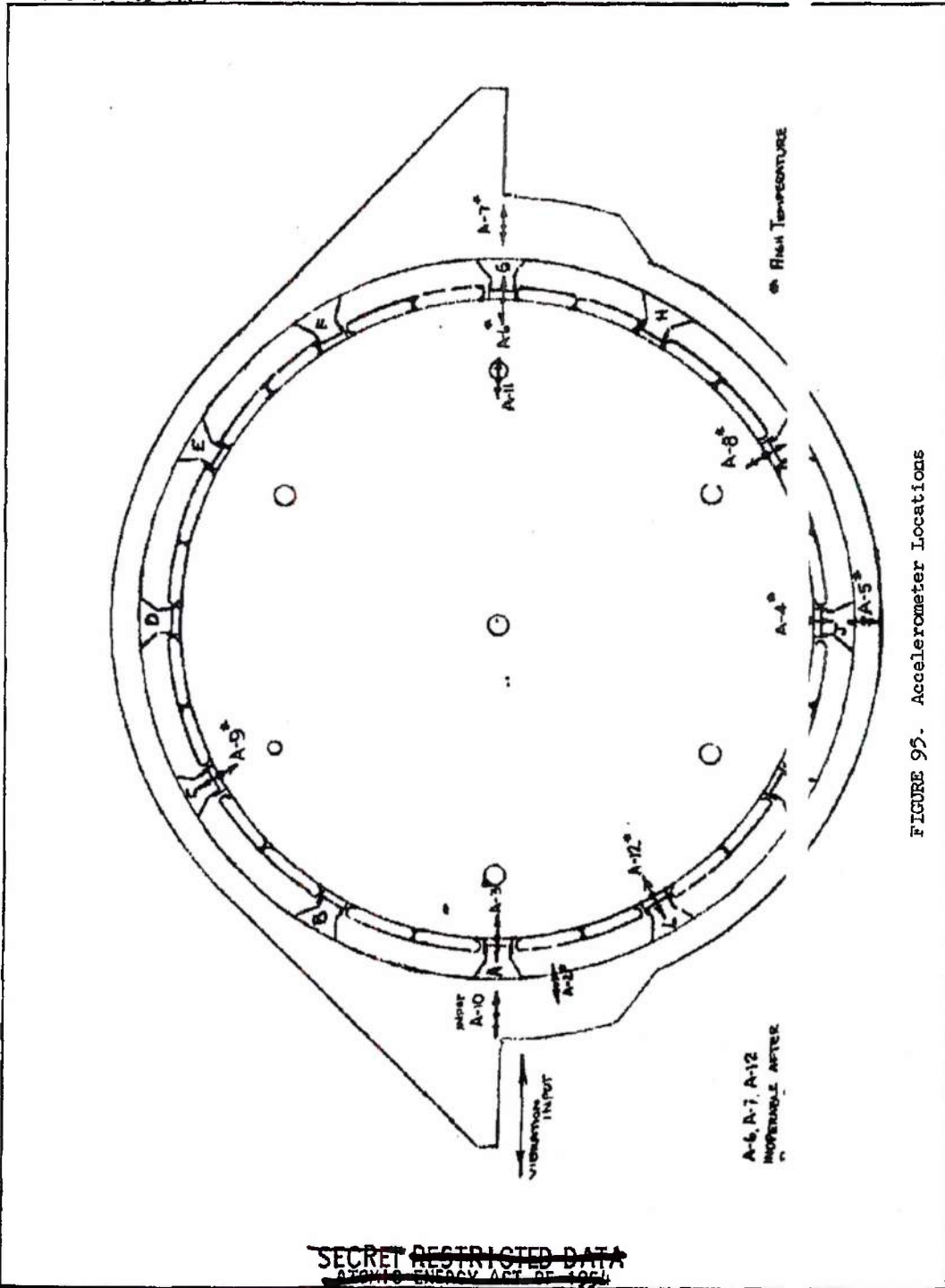


FIGURE 95. Accelerometer Locations

MAC A 63

~~SECRET RESTRICTED DATA~~  
~~ATOMIC ENERGY ACT OF 1954~~

N22B51

~~SECRET RESTRICTED DATA~~  
~~ATOMIC ENERGY ACT OF 1954~~

ASD-TDR-63-277, Vol. IV

REPORT 6003

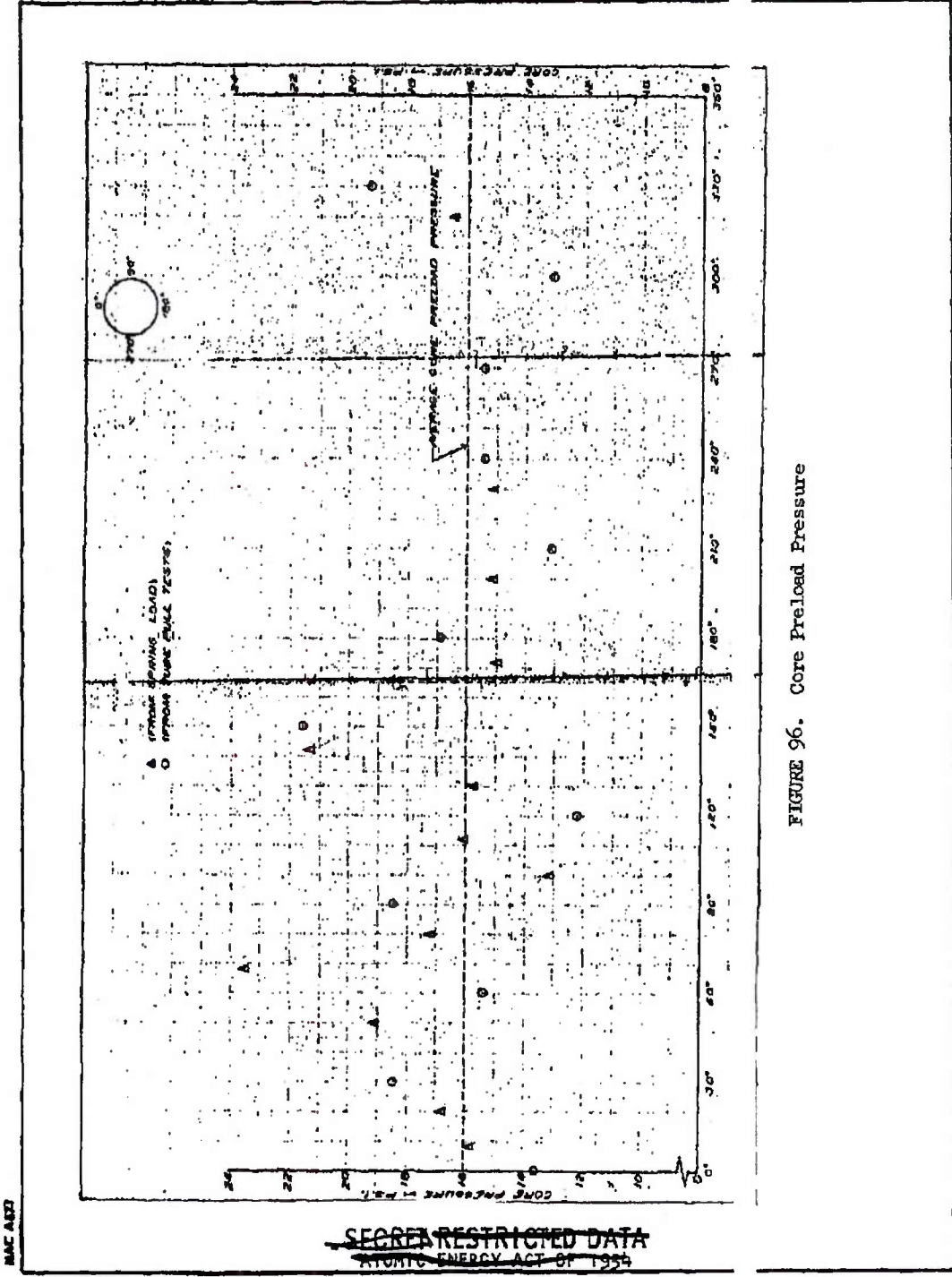


FIGURE 96. Core Preload Pressure

~~SECRET RESTRICTED DATA~~  
~~ATOMIC ENERGY ACT OF 1954~~

ASD-TDR-63-277, Vol. IV

PORT 6003

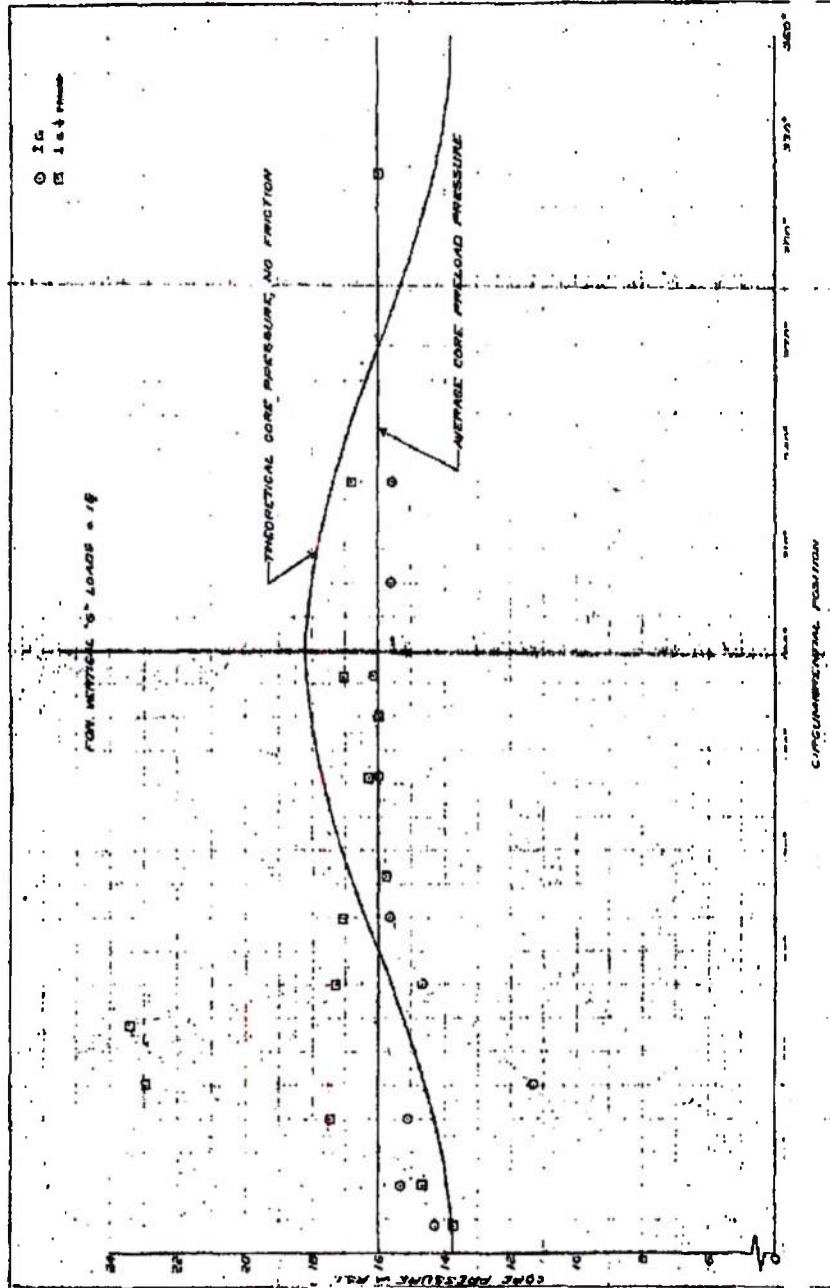


FIGURE 97. Core Pressure (From Spring Loads)

~~SECRET RESTRICTED DATA~~  
~~ATOMIC ENERGY ACT OF 1954~~

22E841

DECLASSIFIED IN FULL  
Authority: EO 13526  
Chief, Records & Declass Div, WHS  
Date: OCT 02 2015

~~SECRET RESTRICTED DATA~~  
~~ATOMIC ENERGY ACT OF 1954~~

REPORT 6003

ASD-TDR-63-277, Vol. IV

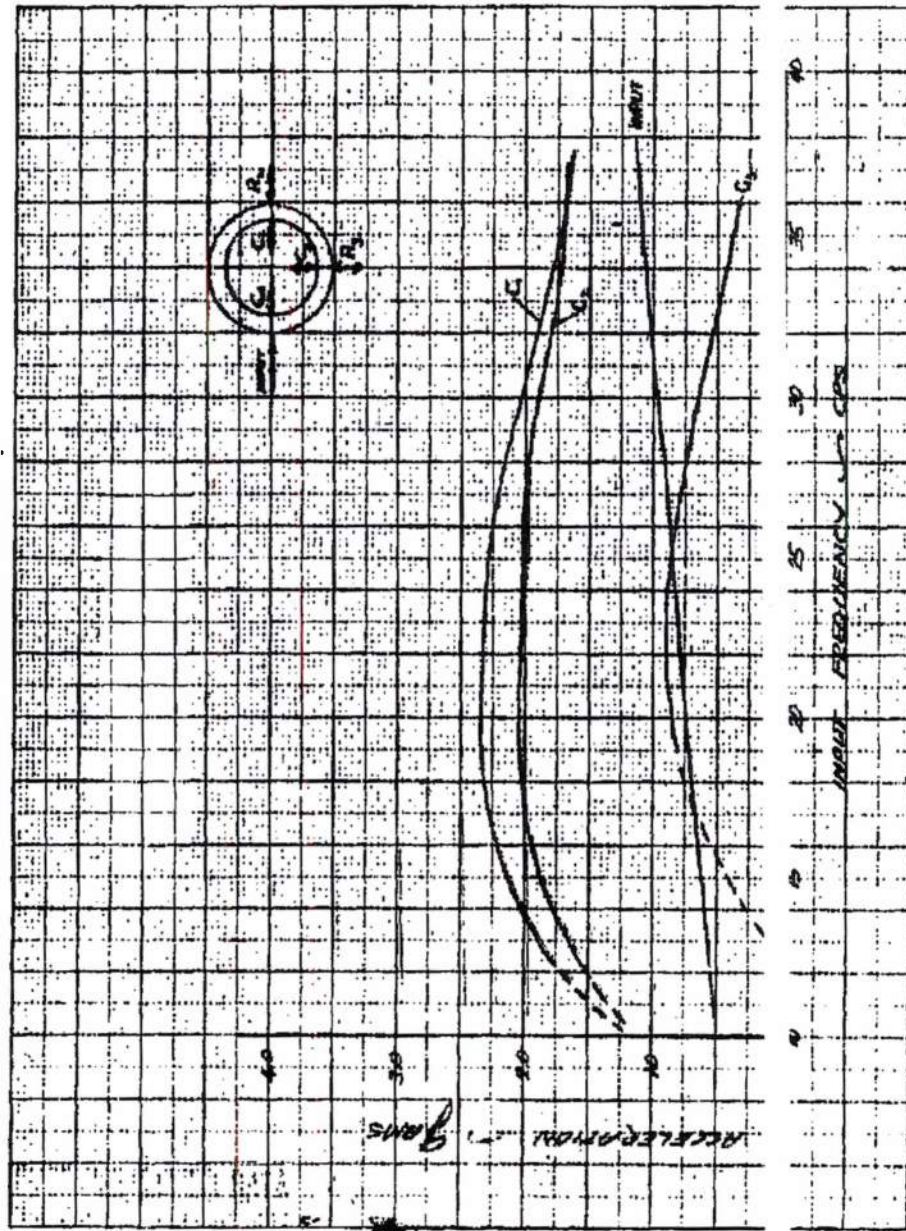


FIGURE 98. Core Dynamic Response (Run No. 4)

~~SECRET RESTRICTED DATA~~  
~~ATOMIC ENERGY ACT OF 1954~~

MAC 603

N22E957

~~SECRET RESTRICTED DATA~~  
~~ATOMIC ENERGY ACT OF 1954~~

ASD-TDR-63-277, Vol. IV

PORT 6003

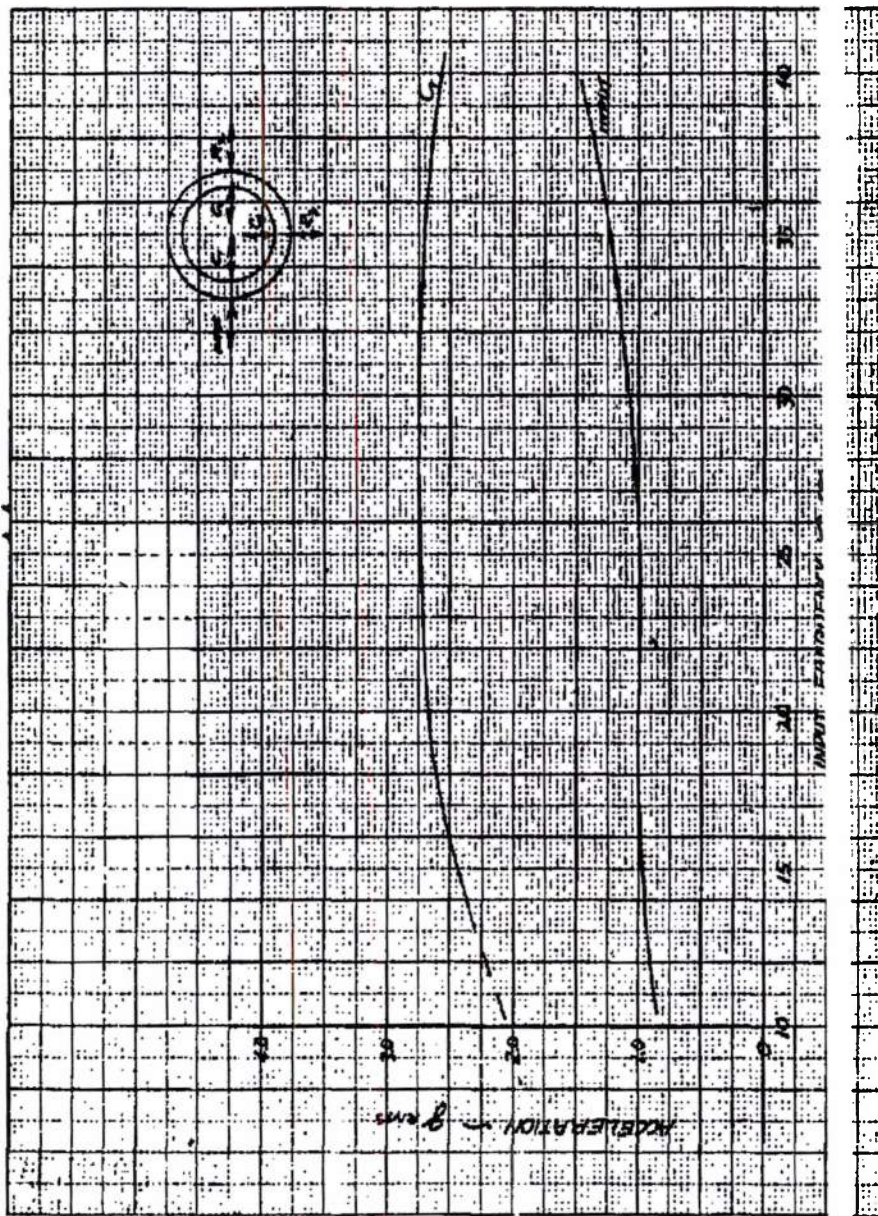


FIGURE 99. Core Dynamic Response (Run No. 10)

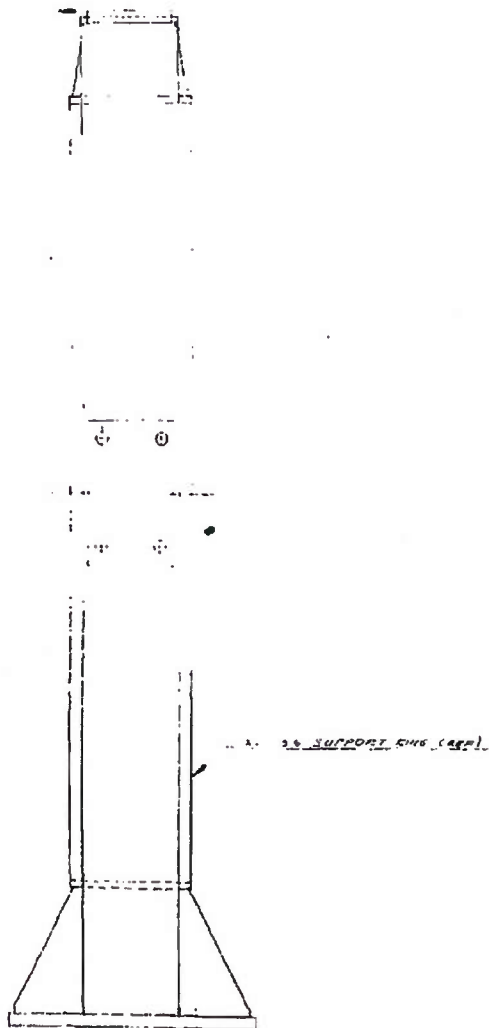
MAC 2 63

~~SECRET RESTRICTED DATA~~  
~~ATOMIC ENERGY ACT OF 1954~~

ASO-TDR-63-277, Vol. IV  
~~SECRET RESTRICTED DATA~~  
~~ATOMIC ENERGY ACT OF 1954~~

DECLASSIFIED IN FULL  
Authority: EO 13526  
Chief, Records & Declass Div, WHS  
Date: OCT 02 2015

1



~~SECRET RESTRICTED DATA~~  
~~ATOMIC ENERGY ACT OF 1954~~

2

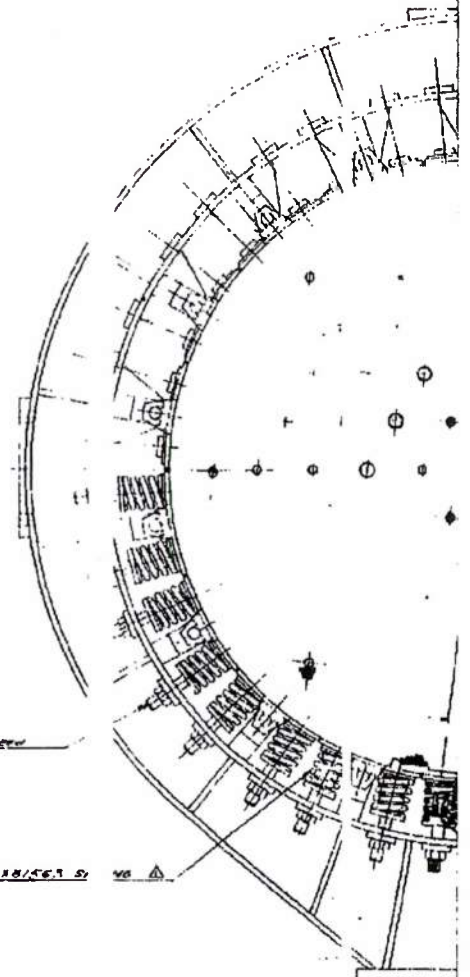
Page determined to be Unclassified  
Reviewed Chief, RDD, WHS  
IAW EO 13526, Section 3.5  
Date: OCT 02 2015



WATER SUPPORT SING (SEMI)

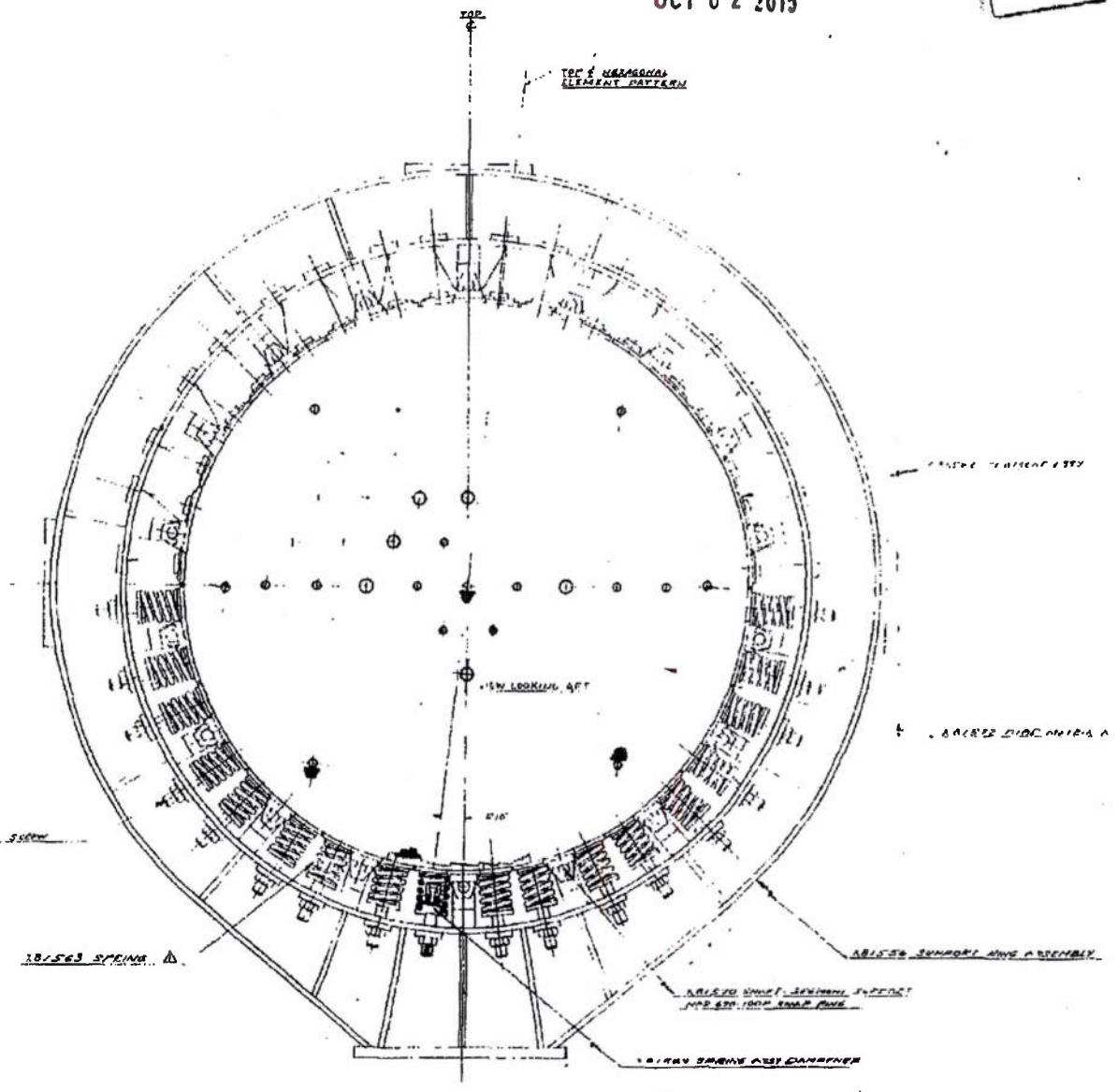
1,000 LB W.A. - 4" Ø - HEX-ROCKET TYPE SET SCREW  
LOAD IN W.A. AREA AS SHOWN

18/06/75



Page determined to be Unclassified  
Reviewed Chief, RDD, WHS  
IAW EO 13526, Section 3.5  
Date: OCT 02 2015

3



REVISED	



**DECLASSIFIED IN FULL**  
 Authority: EO 13526  
 Chief, Records & Declass Div, WHS  
 Date: OCT 02 2015

14-00000-1000

14-00000-1000

14-00000-1000



**FIGURE 100. Lateral Attach Assembly  
 Engine - Airframe**

**Δ SPRING MUST BE INDIVIDUALLY CALIBRATED OR  
 PRELOADED IN FINAL ASSEMBLY AT 200 RPM.**  
 NOTES: UNLESS OTHERWISE SPECIFIED

1	
2	
3	
4	
5	
6	
7	
8	
9	
10	
11	
12	
13	
14	
15	
16	
17	
18	
19	
20	

4

3

2



~~CONFIDENTIAL RESTRICTED DATA~~  
~~ATOMIC ENERGY ACT OF 1954~~

ASD-TDR-63-277, Vol. IV

REPORT 6003

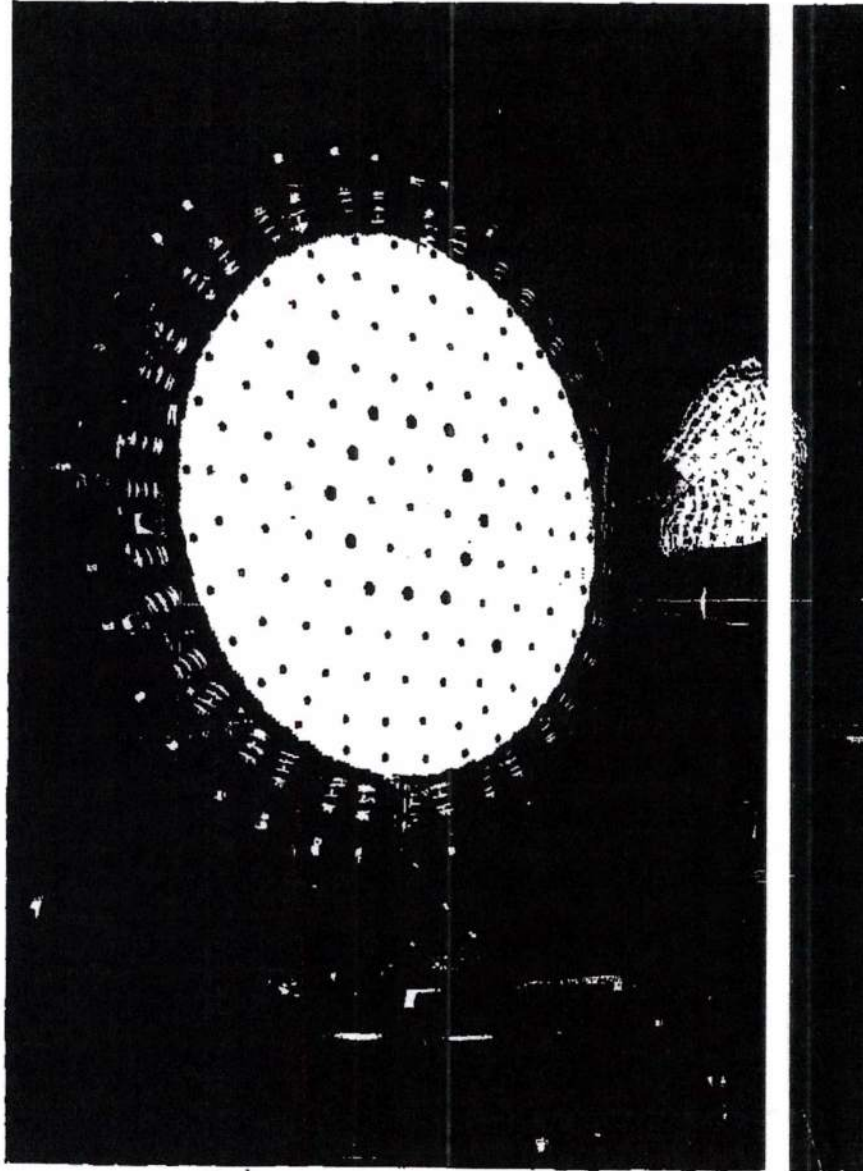


FIGURE 101. Test Item for Engine-Airframe Lateral Attachment Test  
(Phase II)

~~CONFIDENTIAL RESTRICTED DATA~~  
~~ATOMIC ENERGY ACT OF 1954~~

MAC AER  
1108-4012-9

~~CONFIDENTIAL RESTRICTED DATA~~  
~~ATOMIC ENERGY ACT OF 1954~~

ASD-TDR-63-277, Vol. IV

REPORT 6003

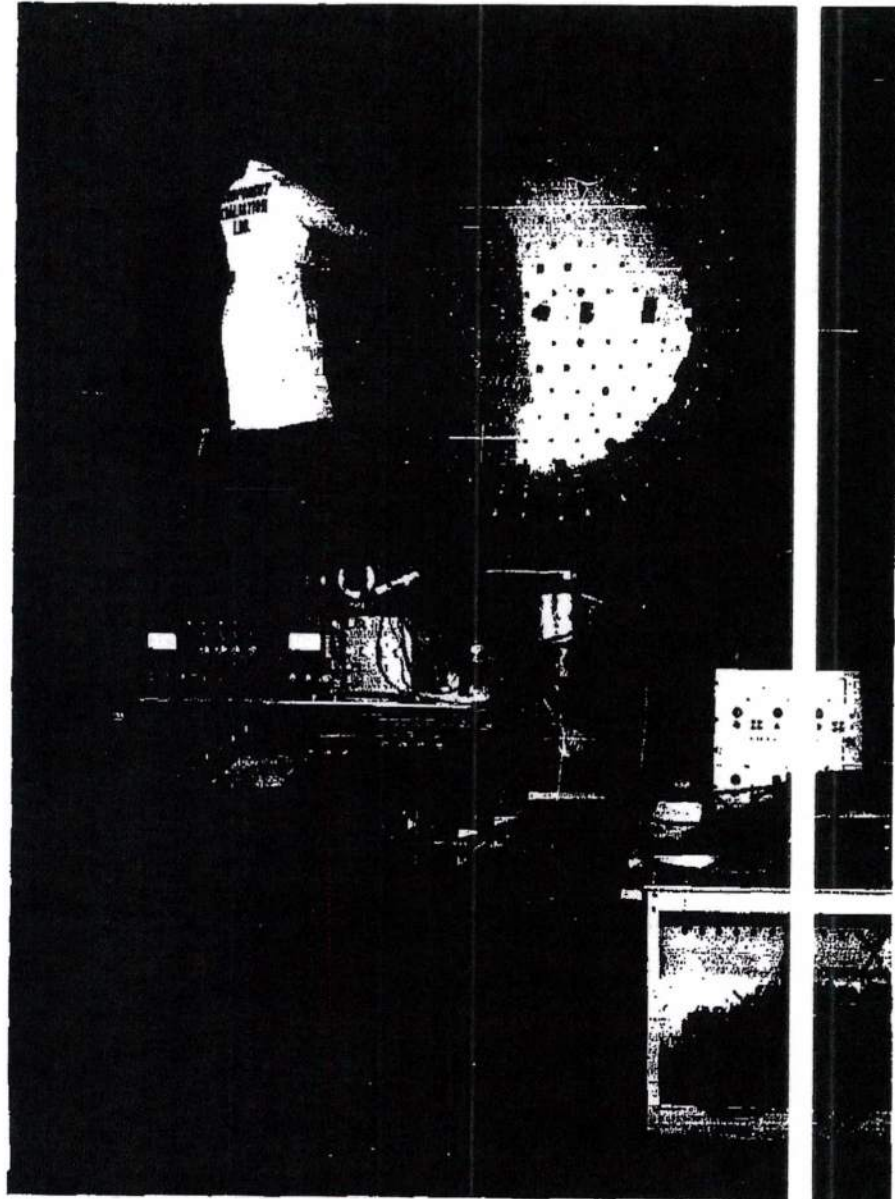


FIGURE 102. Vibration Test Setup for Engine-Airframe  
Lateral Attachment Test (Phase 1).

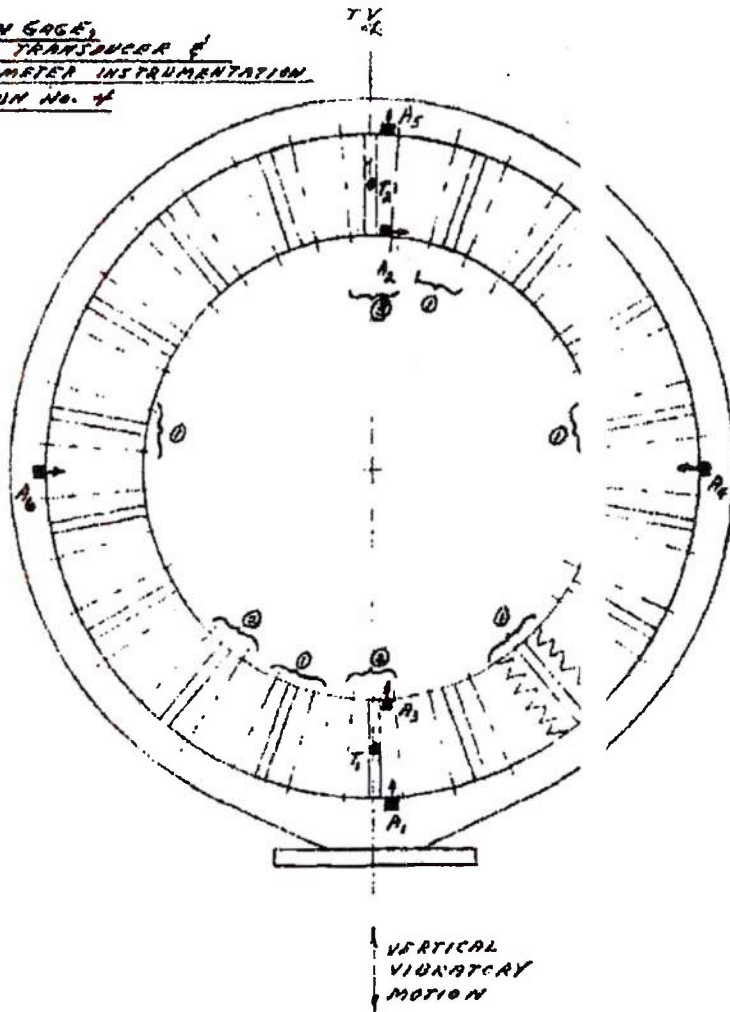
~~CONFIDENTIAL RESTRICTED DATA~~  
~~ATOMIC ENERGY ACT OF 1954~~

NEG. 4512-7

MAC A673

Page determined to be Unclassified  
 Reviewed Chief, RDD, WHS  
 IAW EO 13526, Section 3.5  
 Date: OCT 02 2015

STRAIN GAGE,  
 MOTION TRANSDUCER &  
 ACCELEROMETER INSTRUMENTATION  
 FOR RUN No. 4



NOTES:

1. ● — MOTION TRANSDUCERS (DISPLACEMENT),  
 $T_1$  &  $T_2$ , ACROSS SPRING BAR.
2. ■ — ACCELEROMETERS,  $A_1$  THROUGH  $A_6$ .
3. ~ — LOCATION & NUMBER OF STRAIN  
 GAGED SPRINGS MONITORED.

FIGURE 103. Instrumentation Requirements for Engine-Airframe Lateral Attachment Test (Phase II)

MAC 103

~~SECRET RESTRICTED DATA~~

ASD-TDR-63-277, Vol. IV

IPCI

6003

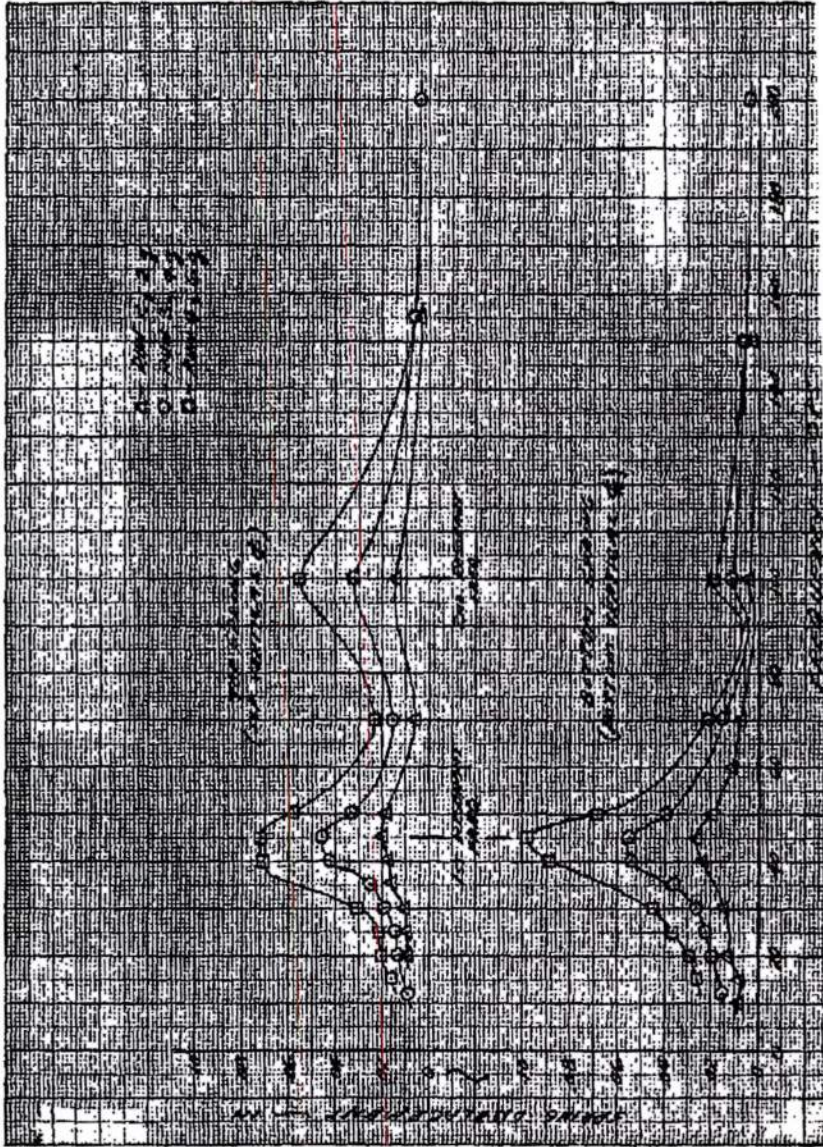


FIGURE 10L. Spring Displacement vs. Frequency (15 psi Core Preload)

~~SECRET RESTRICTED DATA~~

MAC 4072

~~CONFIDENTIAL RESTRICTED DATA~~  
~~ATOMIC ENERGY ACT OF 1954~~

ASD-TDR-63-277, Vol. IV

REPORT 6003

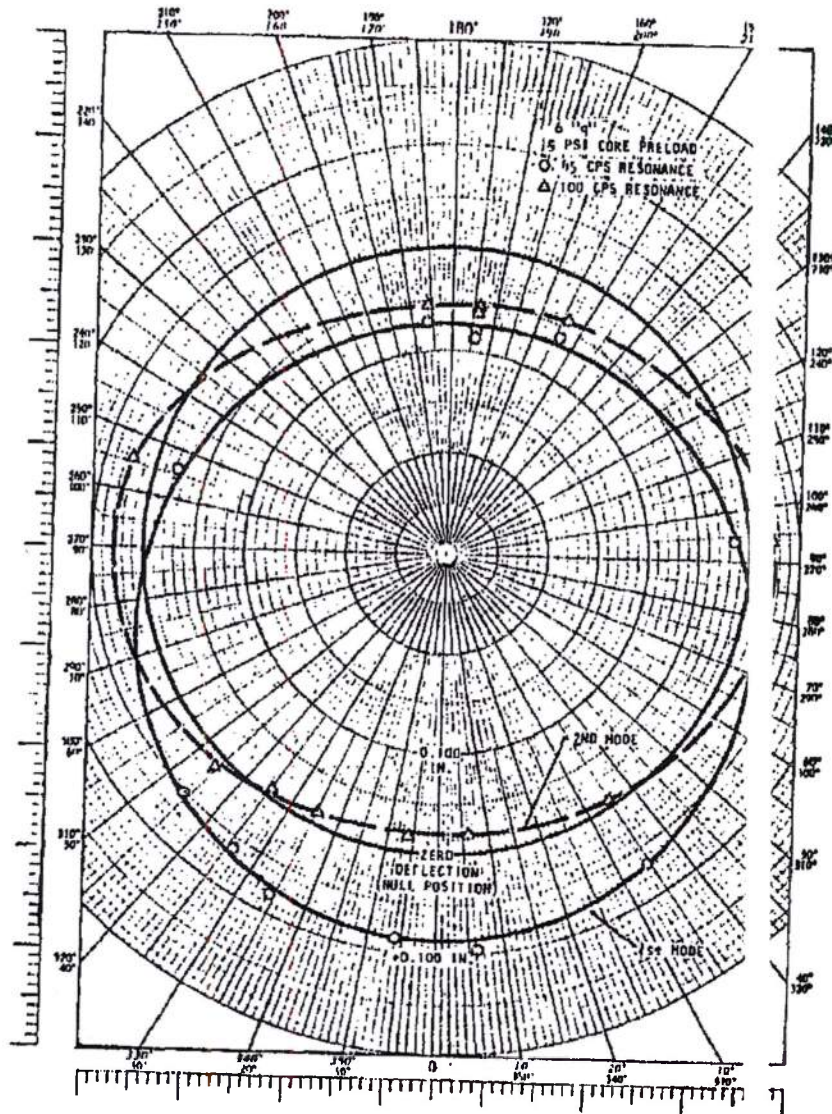


FIGURE 105. Core Deflection Pattern, Run 4

~~CONFIDENTIAL RESTRICTED DATA~~  
~~ATOMIC ENERGY ACT OF 1954~~

MAC 6677

22E782

~~CONFIDENTIAL RESTRICTED DATA~~  
~~ATOMIC ENERGY ACT OF 1954~~

ASD-TCR-63-277, Vol. 17

REPORT 6003

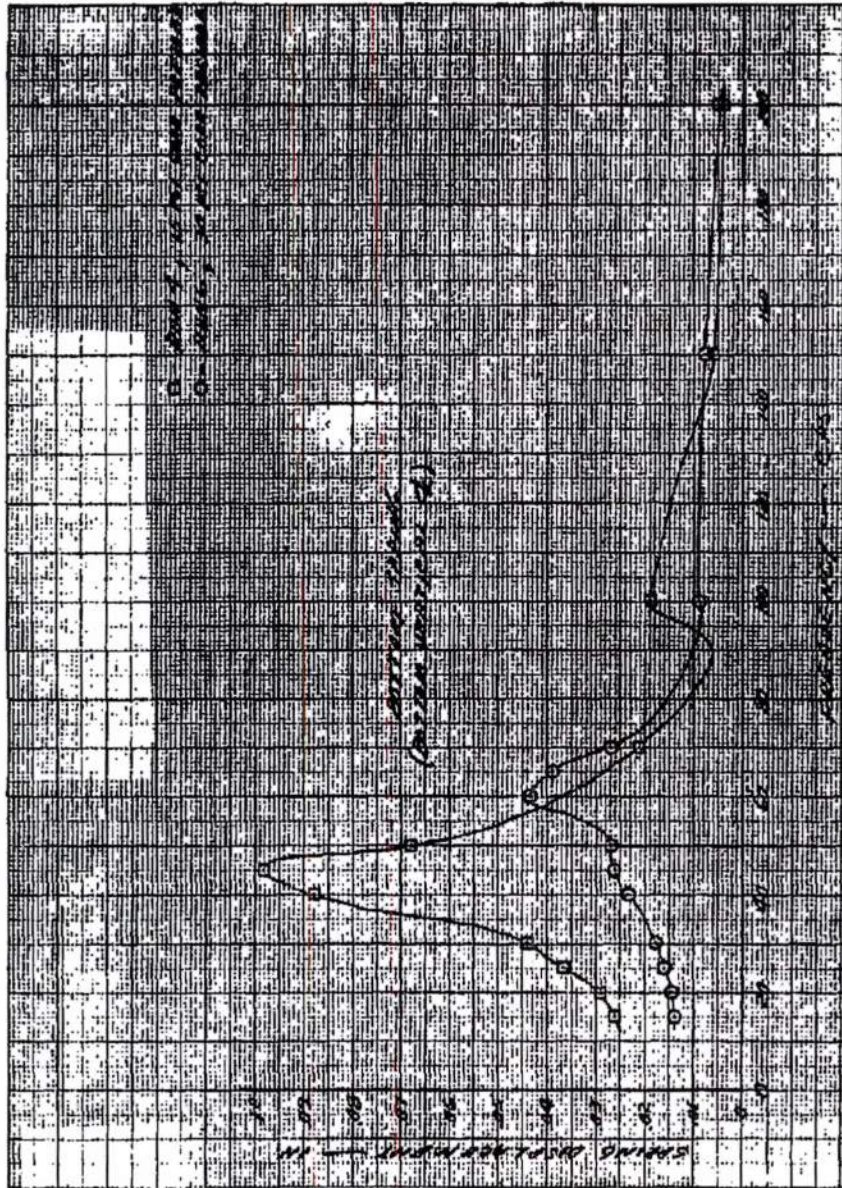


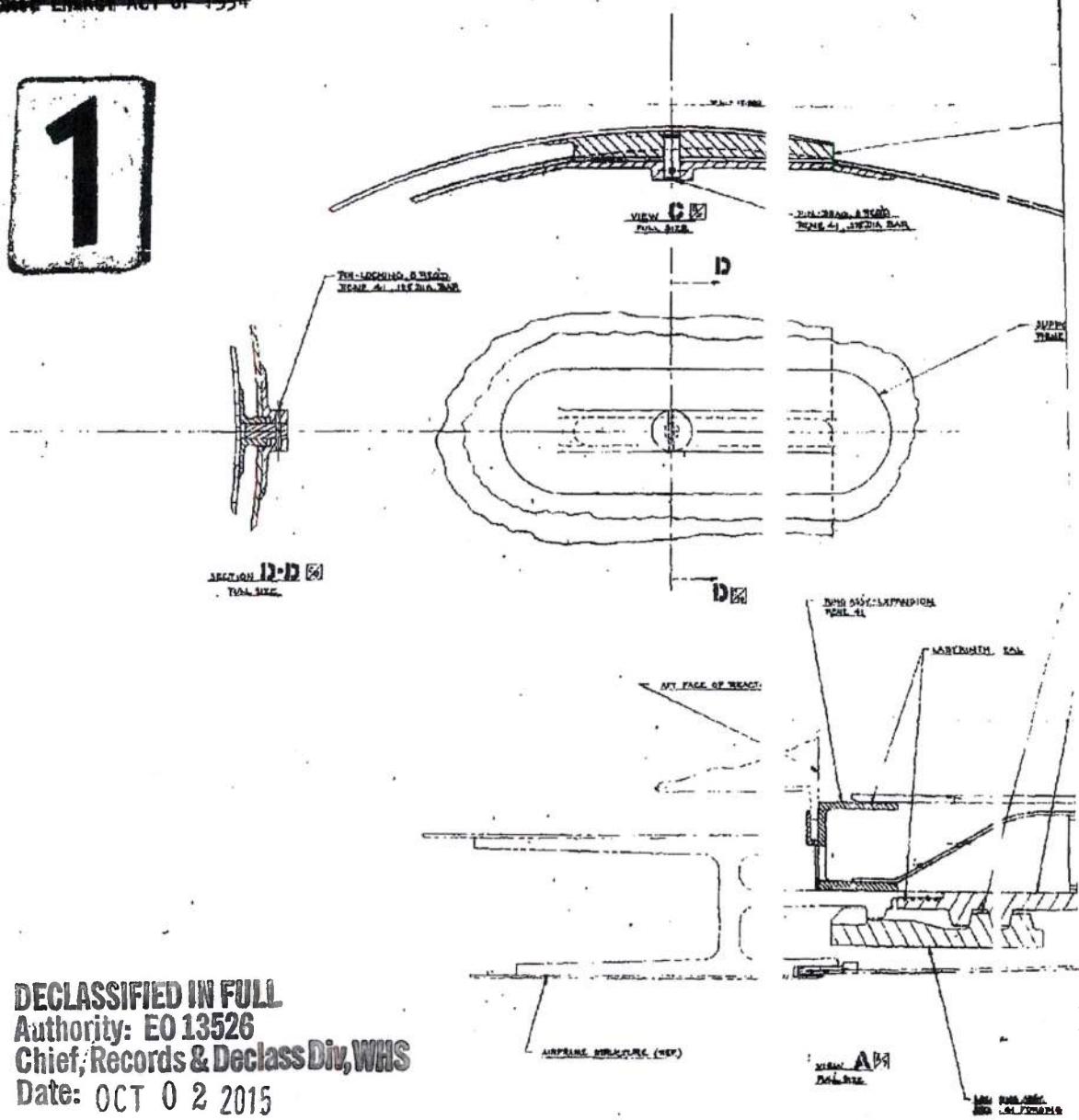
FIGURE 106. Spring Displacement vs. Frequency (6g Force Input)

MAC AGO

~~CONFIDENTIAL RESTRICTED DATA~~  
~~ATOMIC ENERGY ACT OF 1954~~

~~SECRET RESTRICTED DATA~~  
~~ATOMIC ENERGY ACT OF 1954~~

1



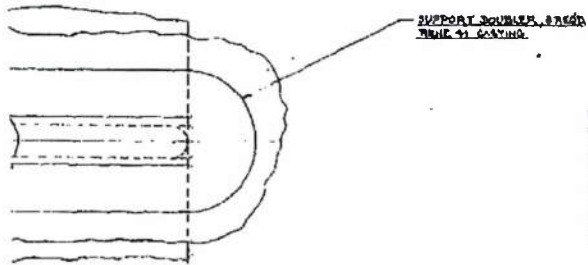
DECLASSIFIED IN FULL  
Authority: EO 13526  
Chief, Records & Declass Div, WHS  
Date: OCT 02 2015

~~SECRET RESTRICTED DATA~~  
~~ATOMIC ENERGY ACT OF 1954~~

2

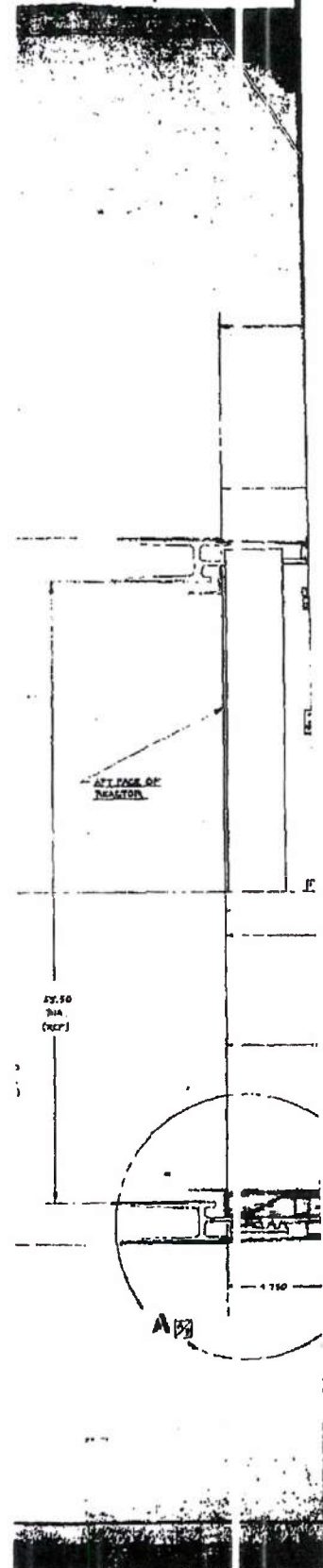
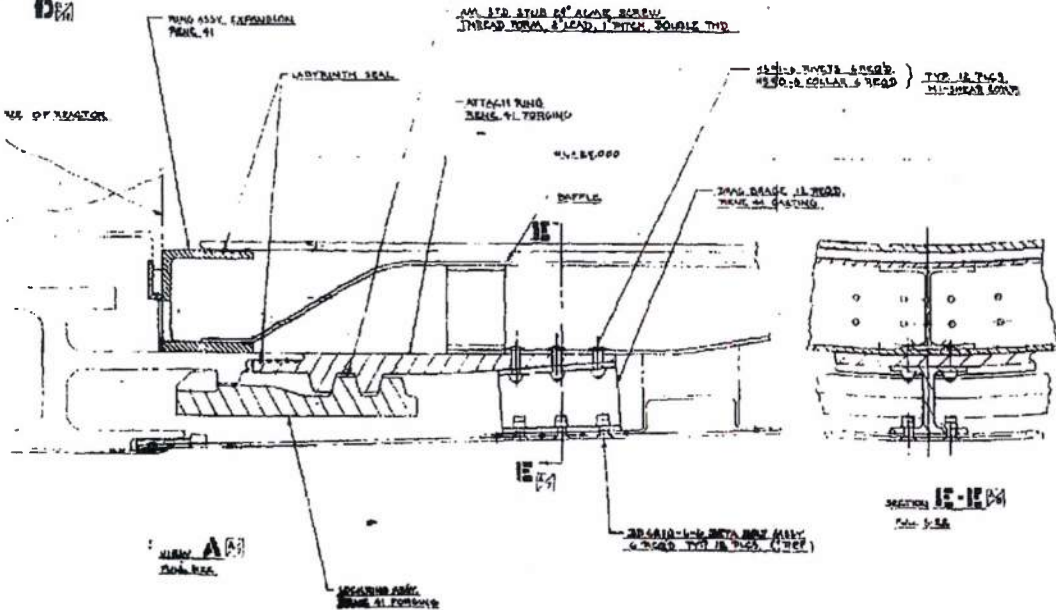


D



DECLASSIFIED IN FULL  
 Authority: EO 13526  
 Chief, Records & Declass Div, WHS  
 Date: OCT 02 2015

D



X81423



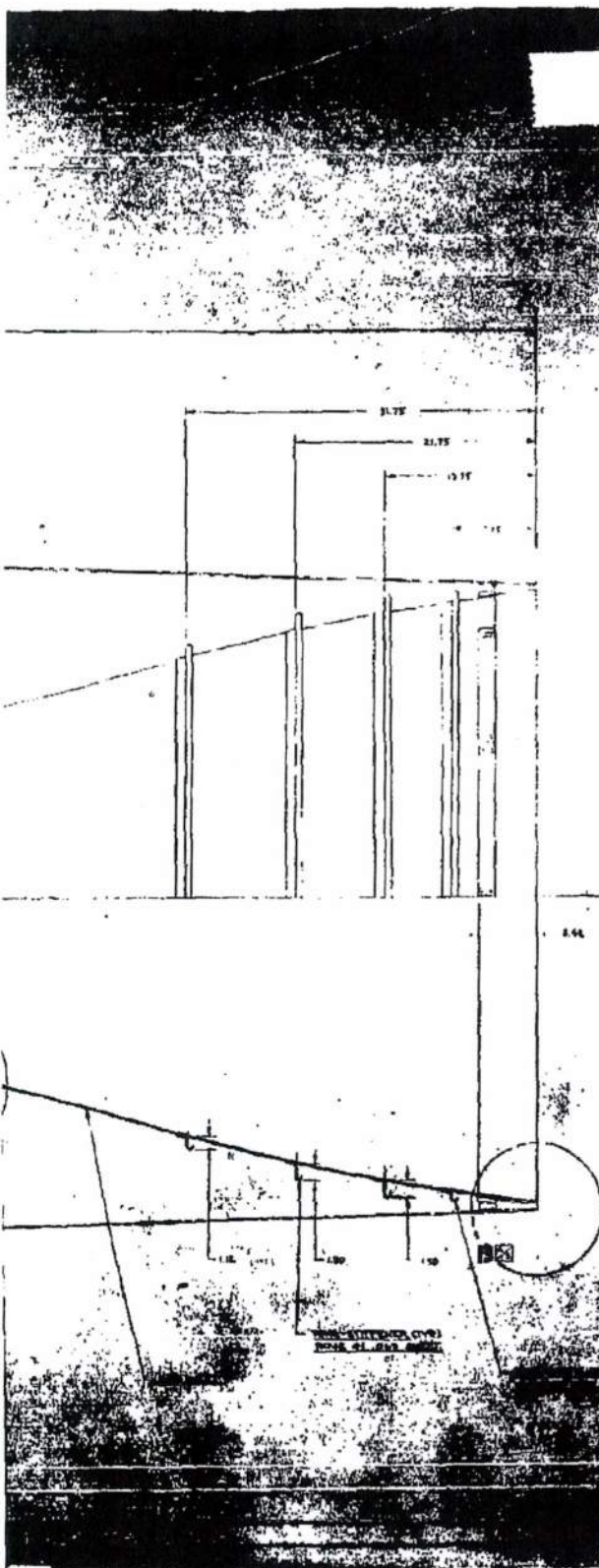
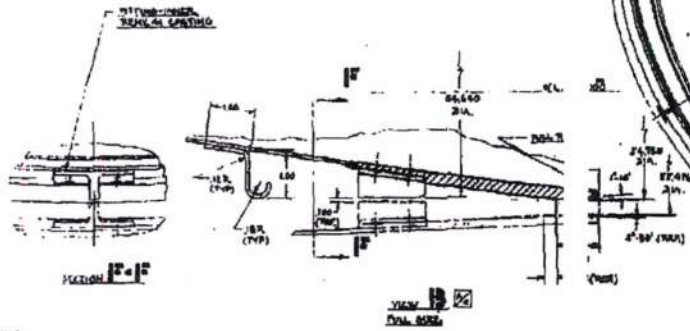


TABLE OF COORDINATES

X	Y	Y'
0.000	10.000	00.000
1.000	10.000	01.000
2.000	10.000	02.000
3.000	10.000	03.000
4.000	10.000	04.000
5.000	10.000	05.000
6.000	10.000	06.000
7.000	10.000	07.000
8.000	10.000	08.000
9.000	10.000	09.000
10.000	10.000	10.000
11.000	10.000	11.000
12.000	10.000	12.000
13.000	10.000	13.000
14.000	10.000	14.000
15.000	10.000	15.000
16.000	10.000	16.000
17.000	10.000	17.000
18.000	10.000	18.000
19.000	10.000	19.000
20.000	10.000	20.000
21.000	10.000	21.000
22.000	10.000	22.000
23.000	10.000	23.000
24.000	10.000	24.000
25.000	10.000	25.000
26.000	10.000	26.000
27.000	10.000	27.000
28.000	10.000	28.000
29.000	10.000	29.000
30.000	10.000	30.000
31.000	10.000	31.000
32.000	10.000	32.000
33.000	10.000	33.000
34.000	10.000	34.000
35.000	10.000	35.000
36.000	10.000	36.000
37.000	10.000	37.000
38.000	10.000	38.000
39.000	10.000	39.000
40.000	10.000	40.000
41.000	10.000	41.000
42.000	10.000	42.000
43.000	10.000	43.000
44.000	10.000	44.000
45.000	10.000	45.000
46.000	10.000	46.000
47.000	10.000	47.000
48.000	10.000	48.000
49.000	10.000	49.000
50.000	10.000	50.000
51.000	10.000	51.000
52.000	10.000	52.000
53.000	10.000	53.000
54.000	10.000	54.000
55.000	10.000	55.000
56.000	10.000	56.000
57.000	10.000	57.000
58.000	10.000	58.000
59.000	10.000	59.000
60.000	10.000	60.000
61.000	10.000	61.000
62.000	10.000	62.000
63.000	10.000	63.000
64.000	10.000	64.000
65.000	10.000	65.000
66.000	10.000	66.000
67.000	10.000	67.000
68.000	10.000	68.000
69.000	10.000	69.000
70.000	10.000	70.000
71.000	10.000	71.000
72.000	10.000	72.000
73.000	10.000	73.000
74.000	10.000	74.000
75.000	10.000	75.000
76.000	10.000	76.000
77.000	10.000	77.000
78.000	10.000	78.000
79.000	10.000	79.000
80.000	10.000	80.000
81.000	10.000	81.000
82.000	10.000	82.000
83.000	10.000	83.000
84.000	10.000	84.000
85.000	10.000	85.000
86.000	10.000	86.000
87.000	10.000	87.000
88.000	10.000	88.000
89.000	10.000	89.000
90.000	10.000	90.000
91.000	10.000	91.000
92.000	10.000	92.000
93.000	10.000	93.000
94.000	10.000	94.000
95.000	10.000	95.000
96.000	10.000	96.000
97.000	10.000	97.000
98.000	10.000	98.000
99.000	10.000	99.000
100.000	10.000	100.000

- ① STREAMLINE
- ② 1.5% SLOPE
- ③ STREAMLINE
- ④ 1.5% SLOPE
- ⑤ STREAMLINE
- ⑥ 1.5% SLOPE

4



X81423



~~SECRET RESTRICTED DATA~~  
 ATOMIC ENERGY ACT OF 1954

ASD-TDR-63-277, Vol. IV

REPORT 6003

MAC 4832

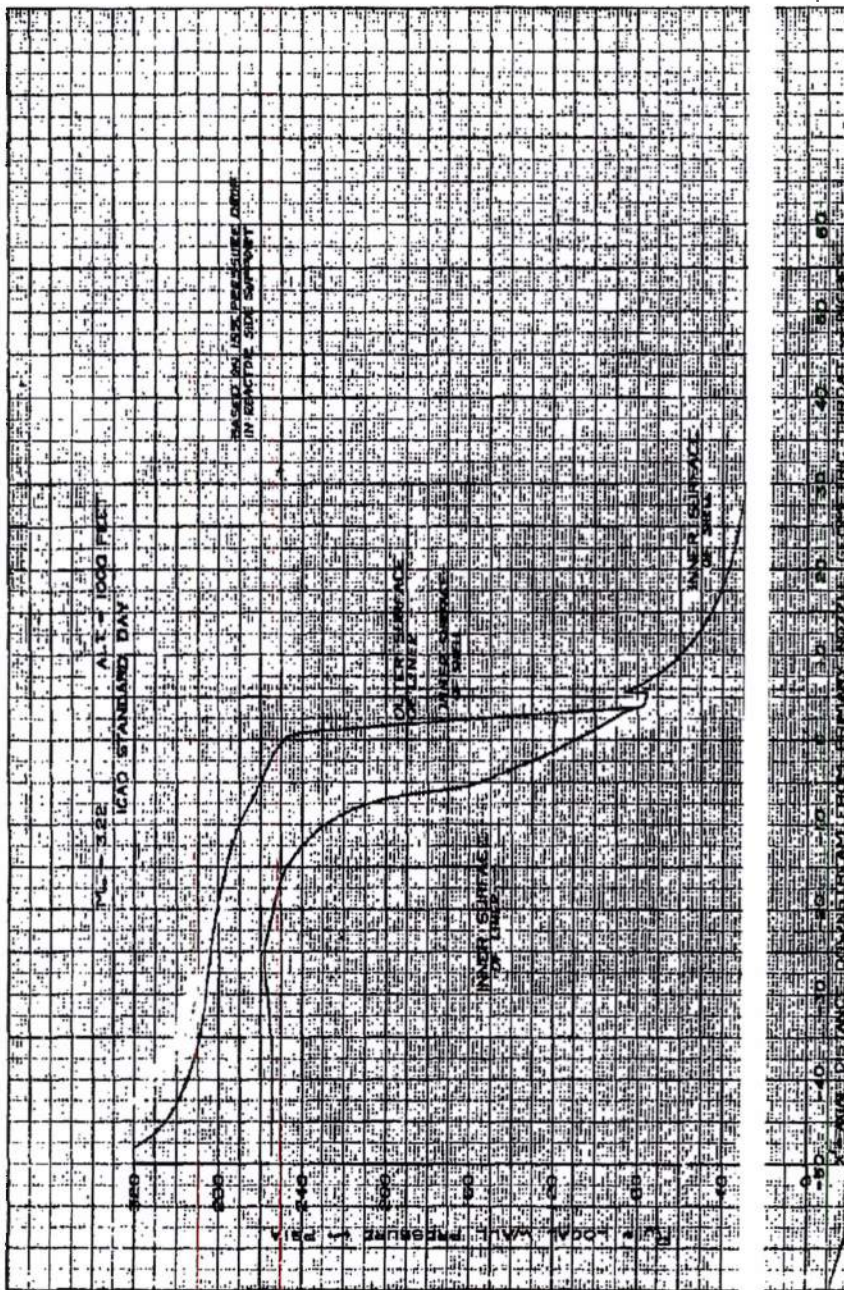


FIGURE 108. Wall Pressure Distribution for MA50-KCB Ejector Nozzle (Altitude = 10,000 Feet)

~~SECRET RESTRICTED DATA~~  
 ATOMIC ENERGY ACT OF 1954

MAC 4827

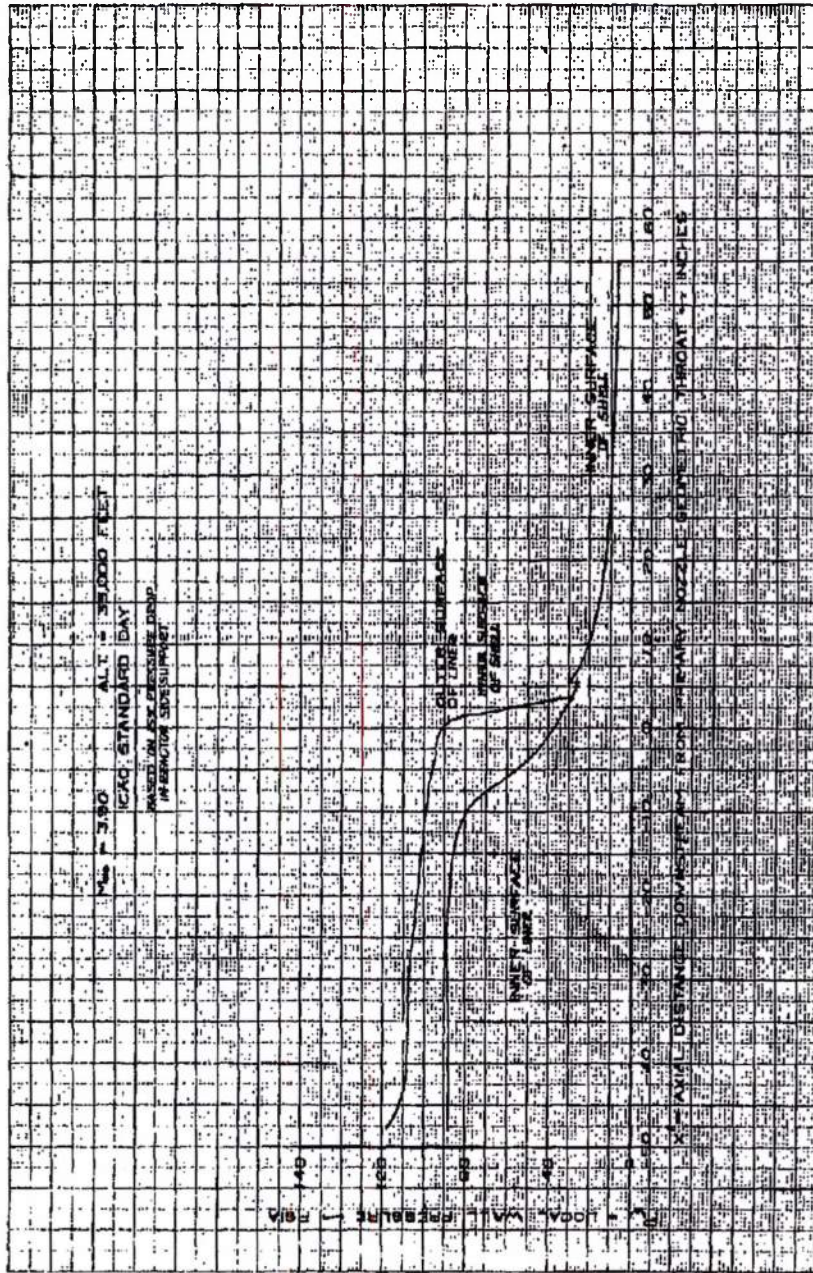


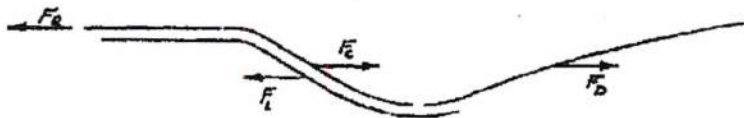
FIGURE 109. Wall Pressure Distribution for MA50-XCB Ejector Nozzle (Altitude = 35,000 Feet)



FIGURE 110. Local Wall Pressure Distribution in Exhaust I Airframe Cooling Flow: MA50-XCB Ejector Nozzle

MAC 4650

MA50-XGB EJECTOR NOZZLE  
 AXIAL LOADS (DRAG)



$F_L$  = AXIAL LOAD ON NOZZLE LINER (LB)  
 $F_C$  = AXIAL LOAD ON SHELL CONVERGENT SECTION (LB)  
 $F_D$  = AXIAL LOAD ON SHELL DIVERGENT SECTION (LB)  
 $F_R$  = AXIAL FORCE REQUIRED TO RETAIN NOZZLE ASSEMBLY IN  
 POSITION ON SIDE SUPPORT SHELL (LB)  
 $M_{\infty}$  = FLIGHT MACH NUMBER  
 $h$  = ALTITUDE (FT)

$M_{\infty}$	$h$	DAY	$F_L$	$F_C$	$F_D$	$F_R$
3.22	1000	STD.	59,961	393,749	33,650	367,481
3.90	35,000	STD.	30,931	144,988	13,712	127,761

FIGURE 111. MA50-XGB Ejector Nozzle Axial Loads (Drag)

DECLASSIFIED IN FULL  
 Authority: EO 13526  
 Chief, Records & Declass Div, WHS  
 Date: OCT 02 2015

MAC 4620

DECLASSIFIED IN FULL  
Authority: EO 13526  
Chief, Records & Declass Div, WHS  
Date: OCT 02 2015

~~SECRET RESTRICTED DATA~~  
~~ASSETS ENERGY ACT OF 1994~~

ASD-TDR-63-277, Vol. IV

REPORT 6003

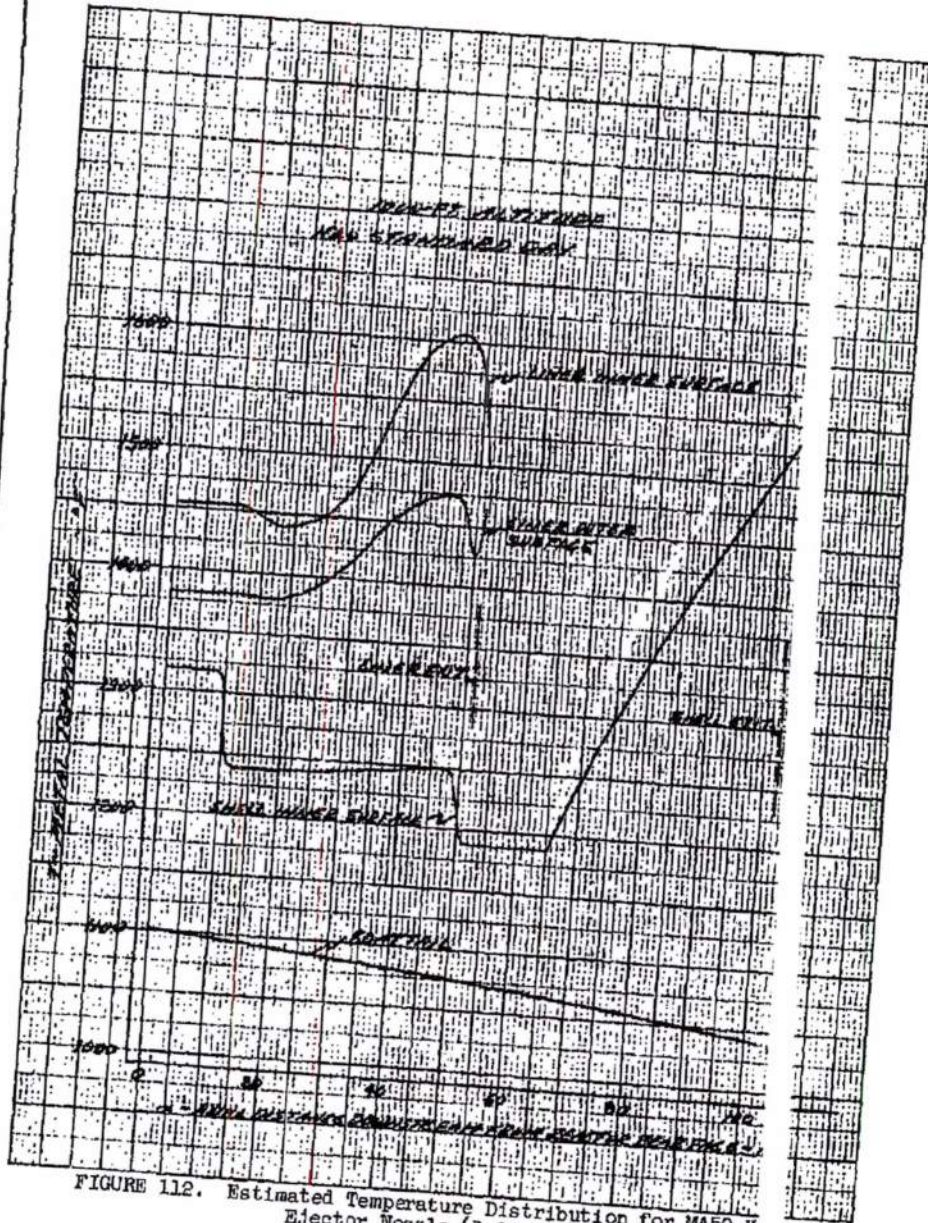


FIGURE 112. Estimated Temperature Distribution for MA50-X Ejector Nozzle (3.22 M<sub>sp</sub>)

~~SECRET RESTRICTED DATA~~  
~~ASSETS ENERGY ACT OF 1994~~

MAC 432

22E776

~~SECRET RESTRICTED DATA~~  
~~ATOMIC ENERGY ACT OF 1954~~

ASD-TDR-63-277, Vol. IV

6003

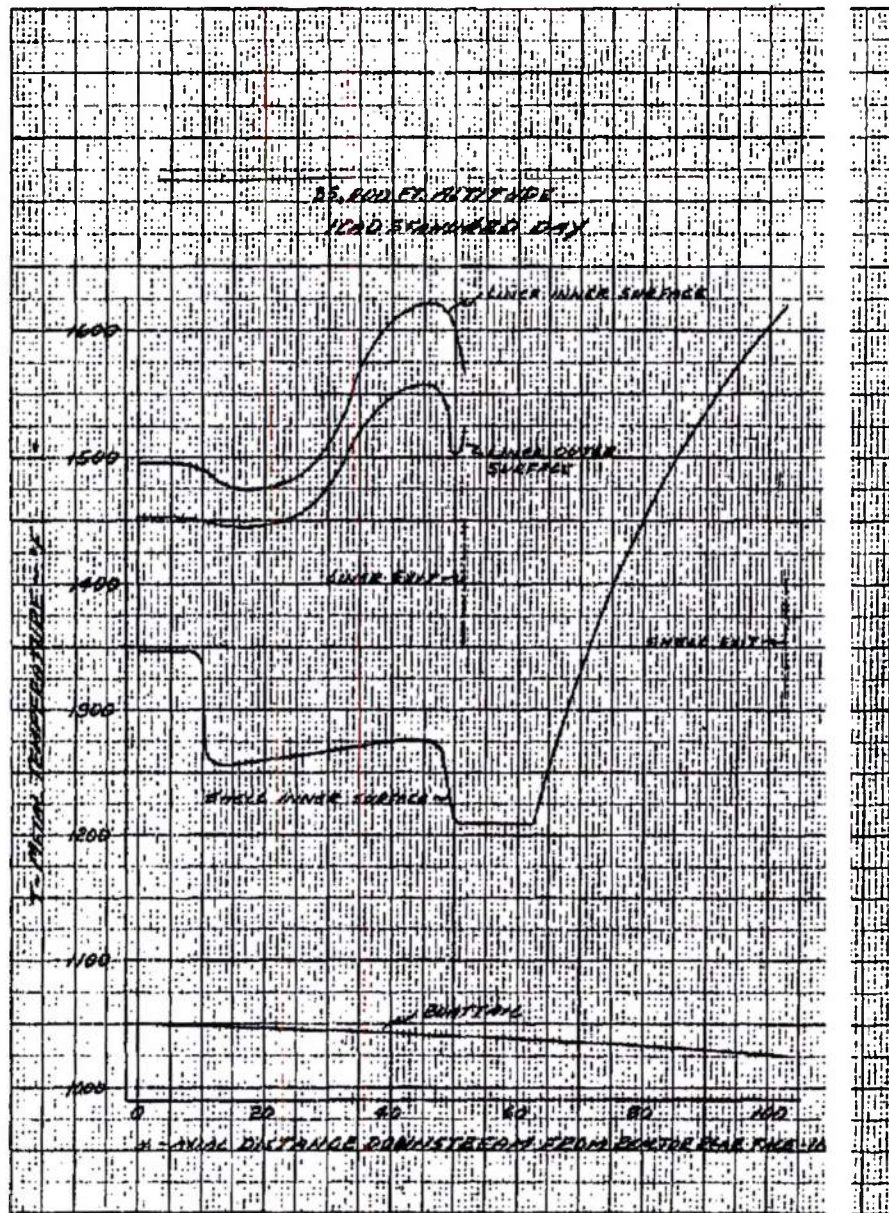


FIGURE 113. Estimated Temperature Distribution for MA50-3 Ejector Nozzle (3.90 M<sub>0</sub>)

~~SECRET RESTRICTED DATA~~  
~~ATOMIC ENERGY ACT OF 1954~~

MAC A03

~~SECRET RESTRICTED DATA~~  
~~ATOMIC ENERGY ACT OF 1954~~

REPORT 6003

ASD-TDR-63-277, Vol. IV

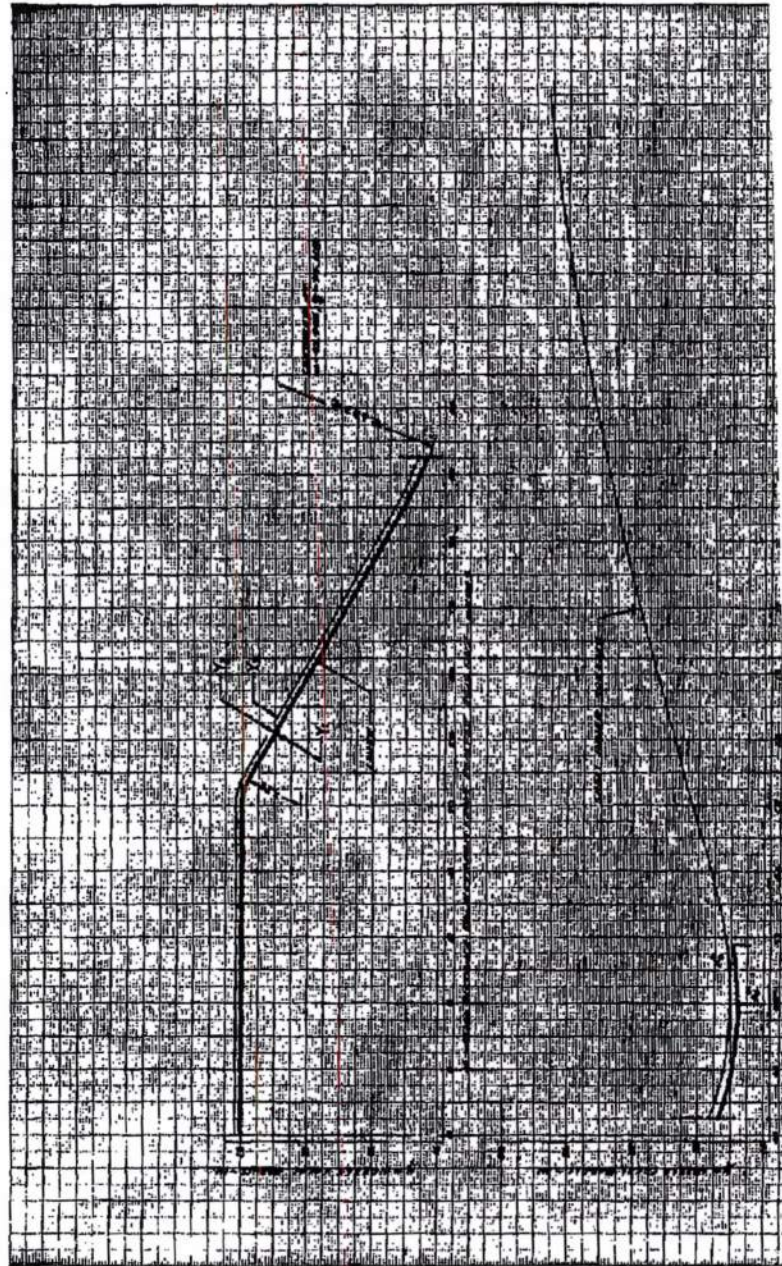


FIGURE 114. MA50-XCB Ejector Nozzle Contours (Based on 0.125 in. Nozzle Liner Thickness)

MAC 460

~~SECRET RESTRICTED DATA~~  
~~ATOMIC ENERGY ACT OF 1954~~

~~SECRET RESTRICTED DATA~~  
 ATOMIC ENERGY ACT OF 1954

ASD-TDR-63-277, Vol. IV

6003

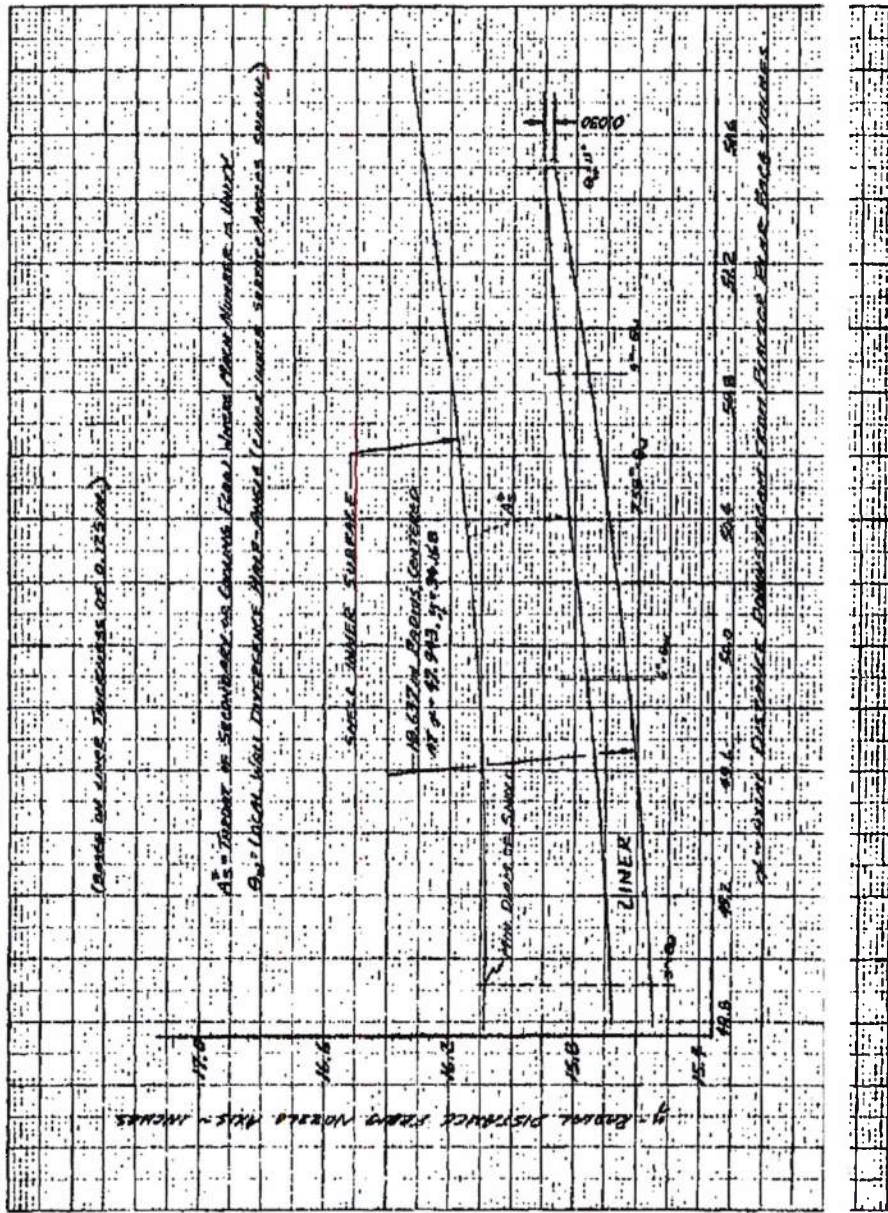


FIGURE 115. MA50-XCB Ejector Nozzle Liner Exit Details

MAC ART

~~SECRET RESTRICTED DATA~~  
 ATOMIC ENERGY ACT OF 1954

~~CONFIDENTIAL~~

REPORT 6003

ASD-TDR-63-277, Vol. IV

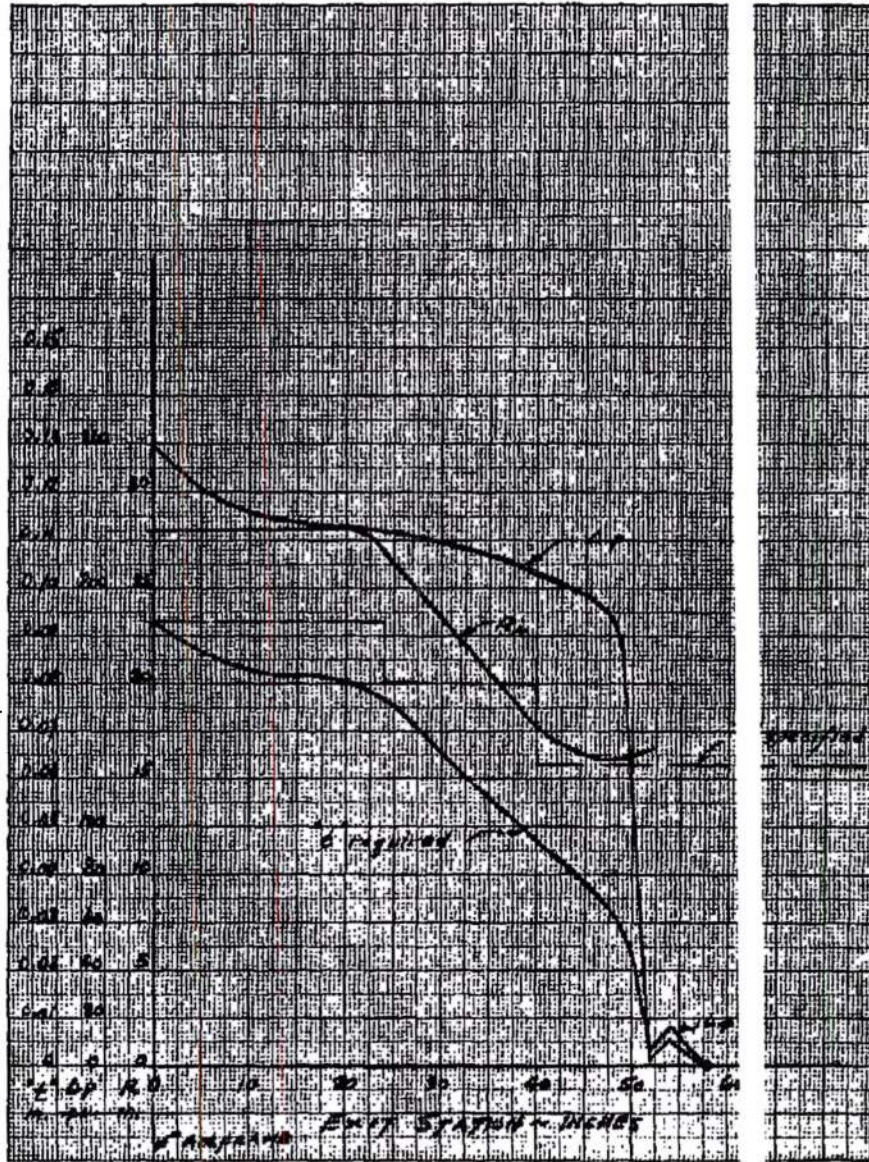


FIGURE 116. Nozzle Load Parameters

~~CONFIDENTIAL~~

22E778

- 271 -

Page determined to be Unclassified  
Reviewed Chief, RDD, WWS  
IAW EO 13526, Section 3.5  
Date: OCT 02 2015

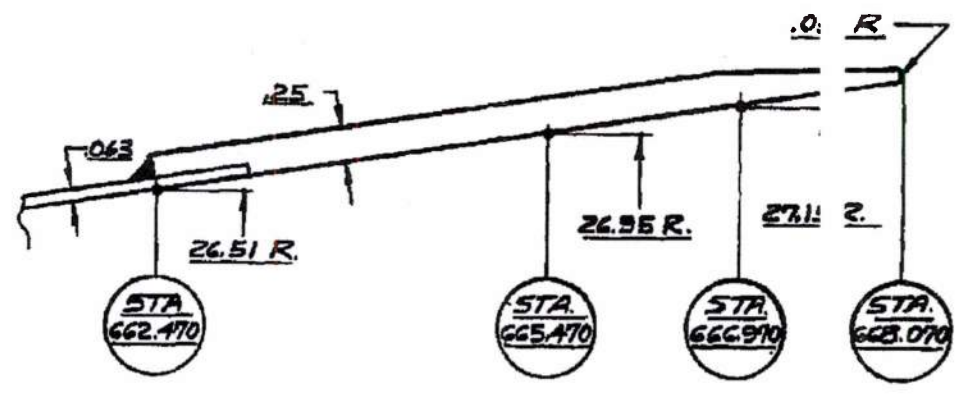


FIGURE 117. Doubler Ring

MAC ACD

CONFIDENTIAL

ASD-TDR-63-277, Vol. IV

REPORT 6003

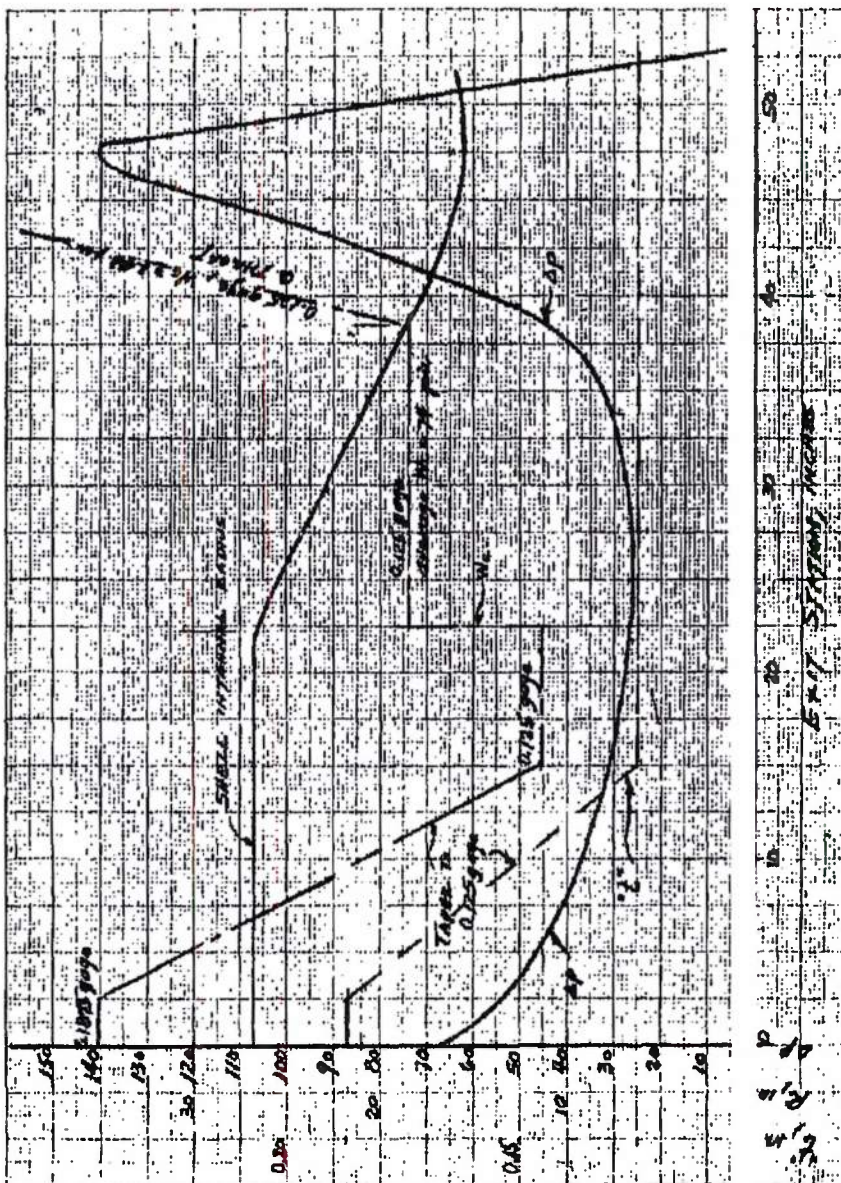


FIGURE 118. Liner Load Parameters

MAC 657

CONFIDENTIAL

Page determined to be Unclassified  
Reviewed Chief, RDD, WIS  
IAW EO 13526, Section 3.5  
Date: OCT 02 2015

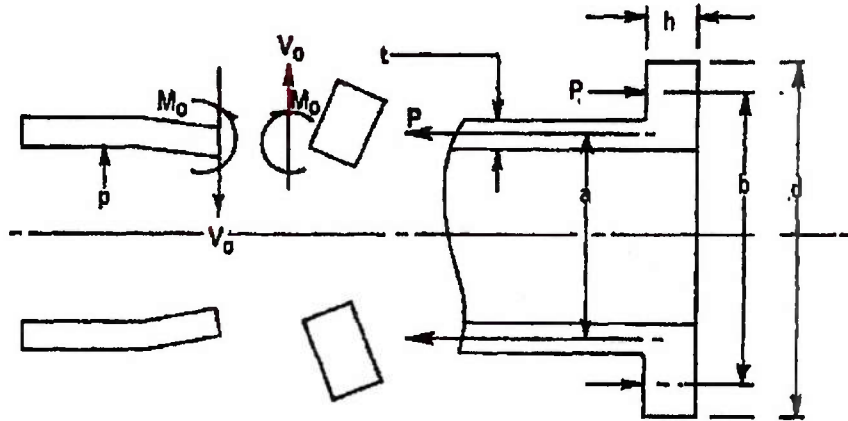


FIGURE 119. Assumed Coupling Geometry

MSC 6003

Page determined to be Unclassified  
Reviewed Chief, RDD, WHS  
IAW EO 13526, Section 3.5  
Date: OCT 02 2015

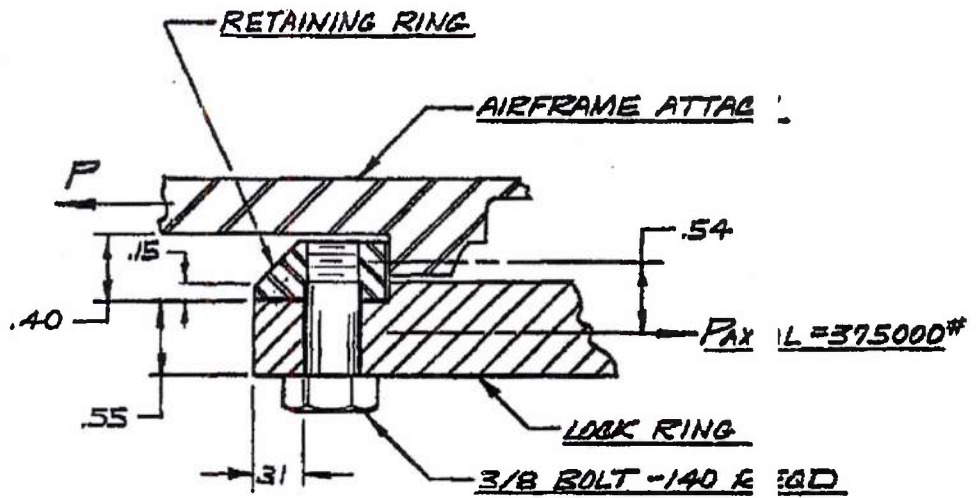


FIGURE 120. Retaining Ring Geometry

MAC AUST

Page determined to be Unclassified  
Reviewed Chief, RDD, WHS  
IAW EO 13526, Section 3.5  
Date: OCT 02 2015

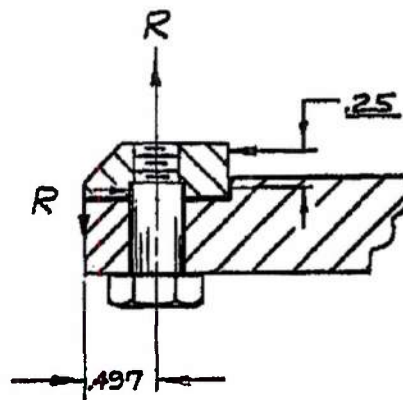


FIGURE 121. Airframe Fitting Shell

MAC A&E

UNCLASSIFIED

ASD-TDR-63-277, Vol. 1V

REPORT 6003

Page determined to be Unclassified  
Reviewed Chief, RDD, WHS  
IAW EO 13526, Section 3.5  
Date: OCT 0 2 2015

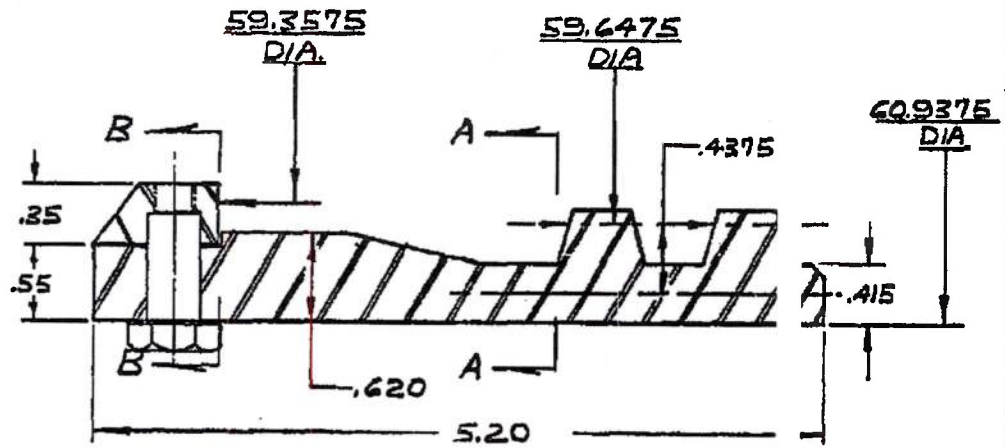


FIGURE 122. Lock Ring

MAC A 573

UNCLASSIFIED

22J88

- 277 -

Page determined to be Unclassified  
Reviewed Chief, RDD, WHS  
IAW EO 13526, Section 3.5  
Date: OCT 02 2015

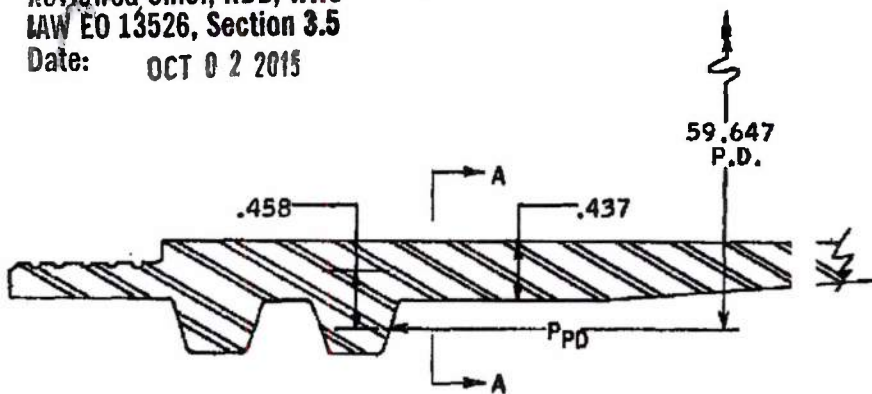


FIGURE 123. Exit Nozzle Attach Ring

MAC A430



DECLASSIFIED IN FULL  
Authority: EO 13526  
Chief, Records & Declass Div, WHS  
Date: OCT 02 2015

~~CONFIDENTIAL RESTRICTED DATA~~  
~~ATOMIC ENERGY ACT OF 1954~~

ASD-TDR-63-277, Vol. IV

POST 6003

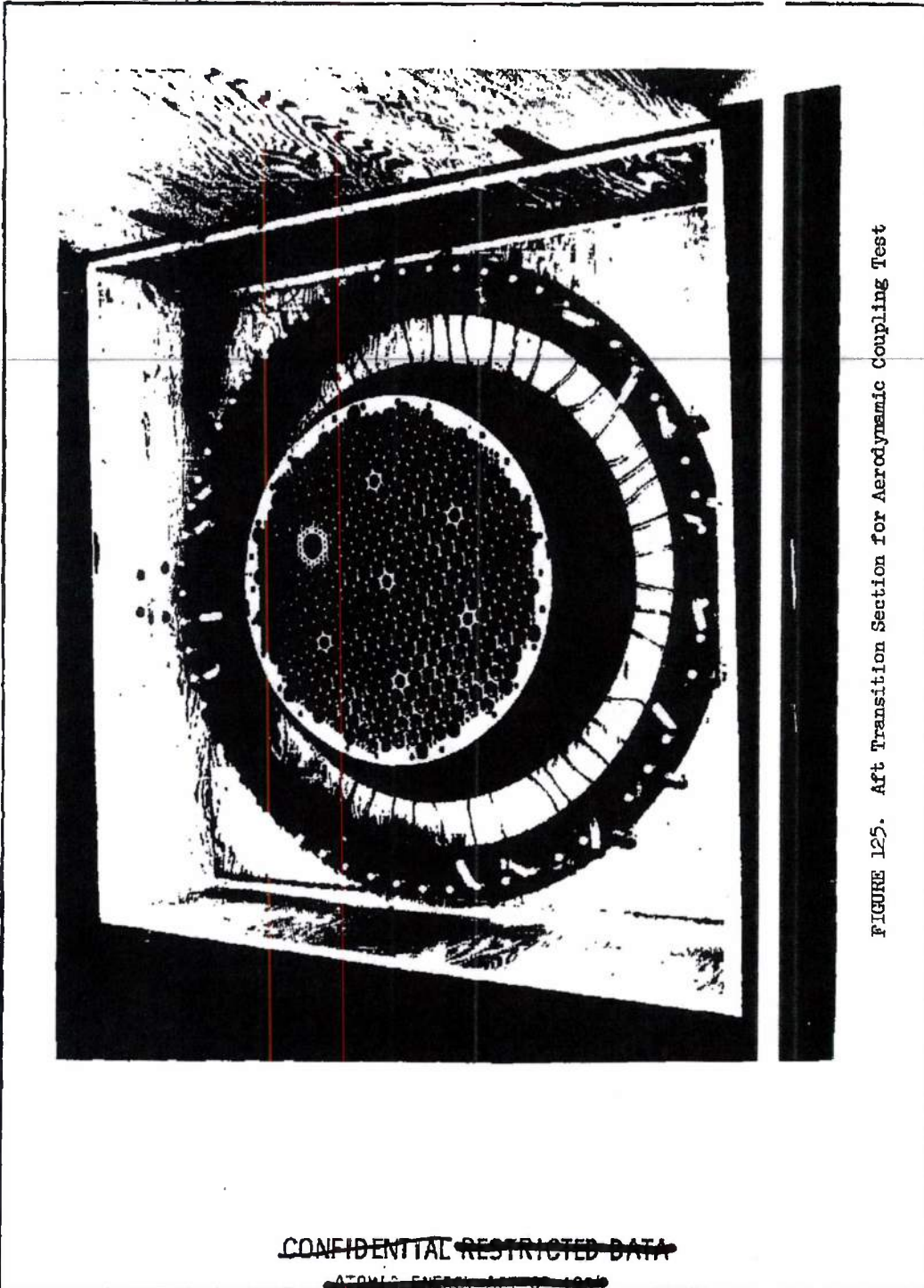


FIGURE 125. Aft Transition Section for Aerodynamic Coupling Test

NER. C 4267-3

MAC 1422

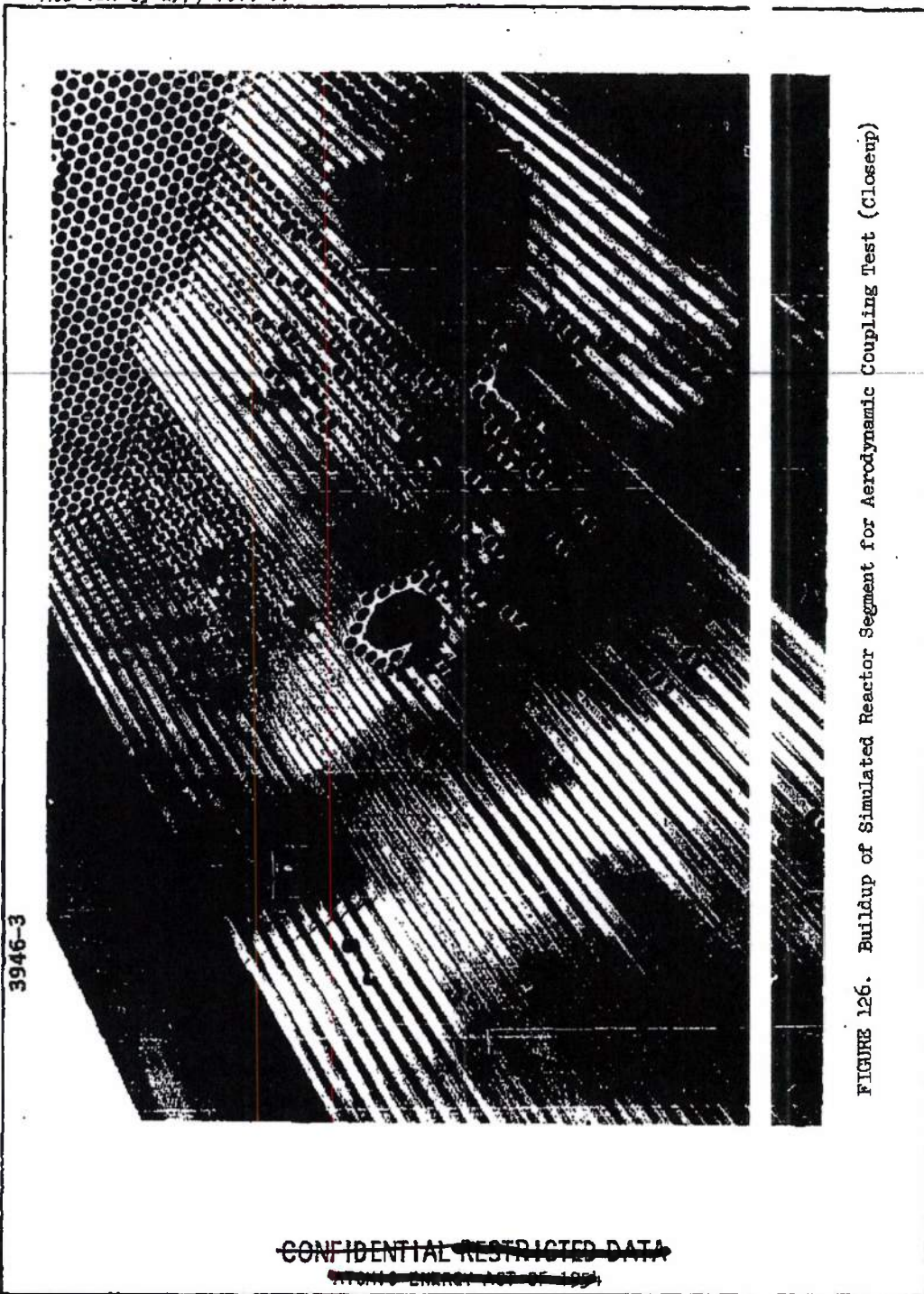
~~CONFIDENTIAL RESTRICTED DATA~~

~~ATOMIC ENERGY ACT OF 1954~~

~~CONFIDENTIAL RESTRICTED DATA~~  
~~ATOMIC ENERGY ACT OF 1954~~

ASD-TDR-63-277, Vol. IV

REPORT 6003



3946-3

FIGURE 126. Buildup of Simulated Reactor Segment for Aerodynamic Coupling Test (Closeup)

MAC 637

~~CONFIDENTIAL RESTRICTED DATA~~  
~~ATOMIC ENERGY ACT OF 1954~~

~~CONFIDENTIAL RESTRICTED DATA~~  
~~APR 1954~~

ASD-TDR-63-277, Vol. 24

REP 6003



FIGURE 127. Front Support Section of Aerodynamic Coupling (Looking Forward)

NEB. C 4037-5

MAC 4072

~~CONFIDENTIAL RESTRICTED DATA~~  
~~APR 1954~~

~~CONFIDENTIAL - RESTRICTED DATA~~  
~~ATOMIC ENERGY ACT OF 1954~~

ASD-TDR-63-277, Vol. 1V

REPORT 6003

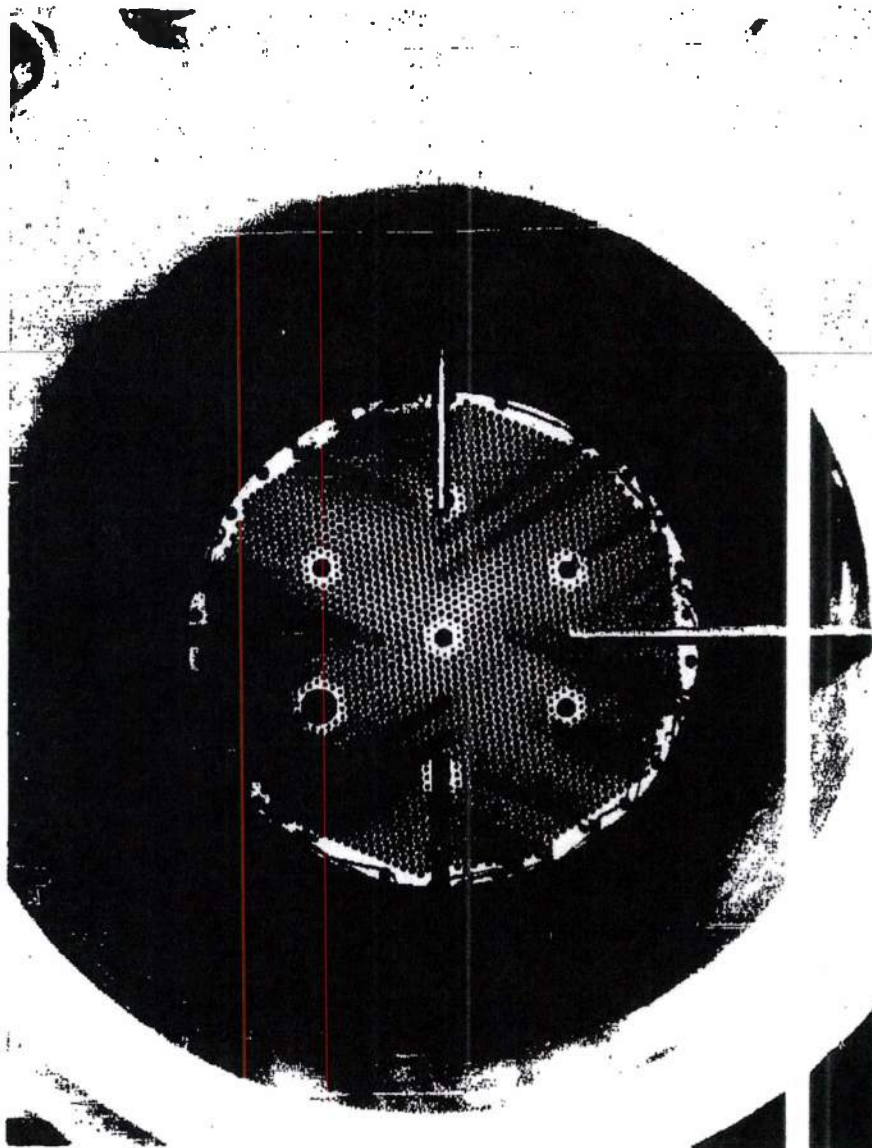
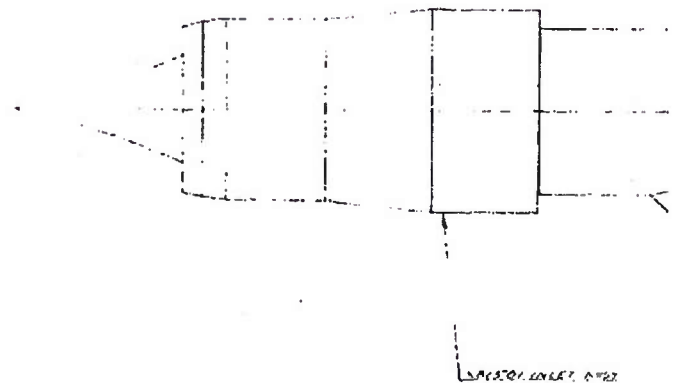


FIGURE 126. Aft End of Simulated Reactor Segment (Viewed Up Exit Nozzle)

REF. C. 127-2  
MAC A67

~~CONFIDENTIAL - RESTRICTED DATA~~  
~~ATOMIC ENERGY ACT OF 1954~~

~~SECRET RESTRICTED DATA~~  
~~ATOMIC ENERGY ACT OF 1954~~

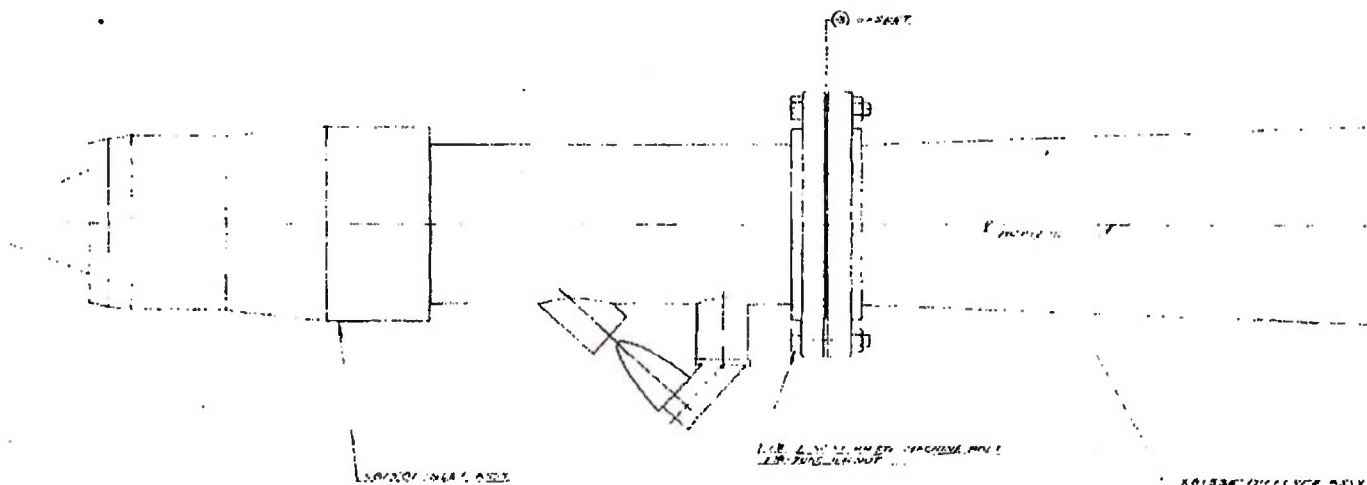


1

DECLASSIFIED IN FULL  
Authority: EO 13526  
Chief, Records & Declass Div, WHS  
Date: OCT 02 2015

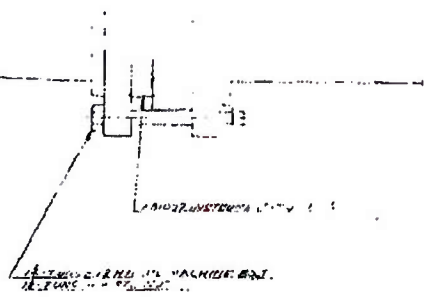
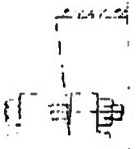
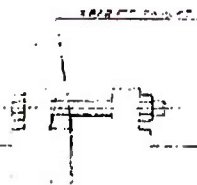
~~SECRET RESTRICTED DATA~~  
~~ATOMIC ENERGY ACT OF 1954~~

2



DECLASSIFIED IN FULL  
Authority: EO 13526  
Chief, Records & Declass Div, WHS  
Date: OCT 02 2015

3

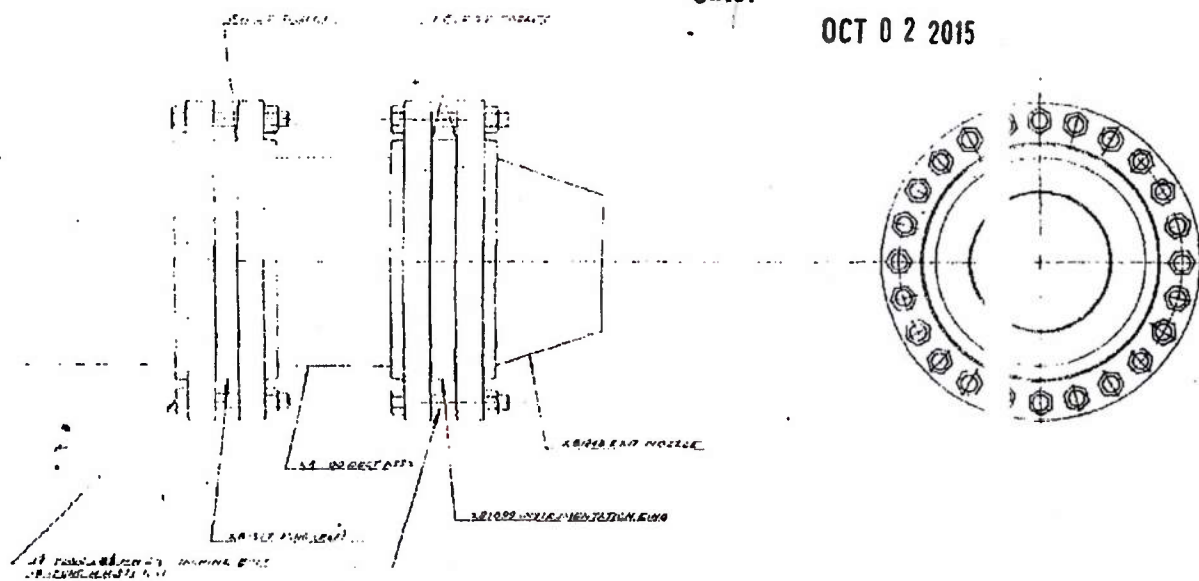


Page determined to be Unclassified  
Reviewed Chief, RDD, WHS  
IAW EO 13526, Section 3.5  
Date: OCT 0 2 2015

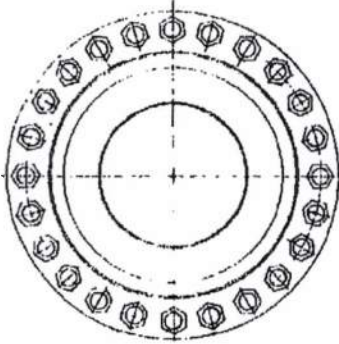
4

DECLASSIFIED IN FULL  
Authority: EO 13526  
Chief, Records & Declass Div, WHS  
Date:

OCT 02 2015



5



DECLASSIFIED IN FULL  
Authority: EO 13526  
Chief, Records & Declass Div, WHS  
Date: OCT 02 2015

FIGURE 129. Engine Assembly  
Aerodynamic Coupling, Free Jet




4 3 2



UNCLASSIFIED

ASD-TDR-63-277, vol. 10

REPORT 6003

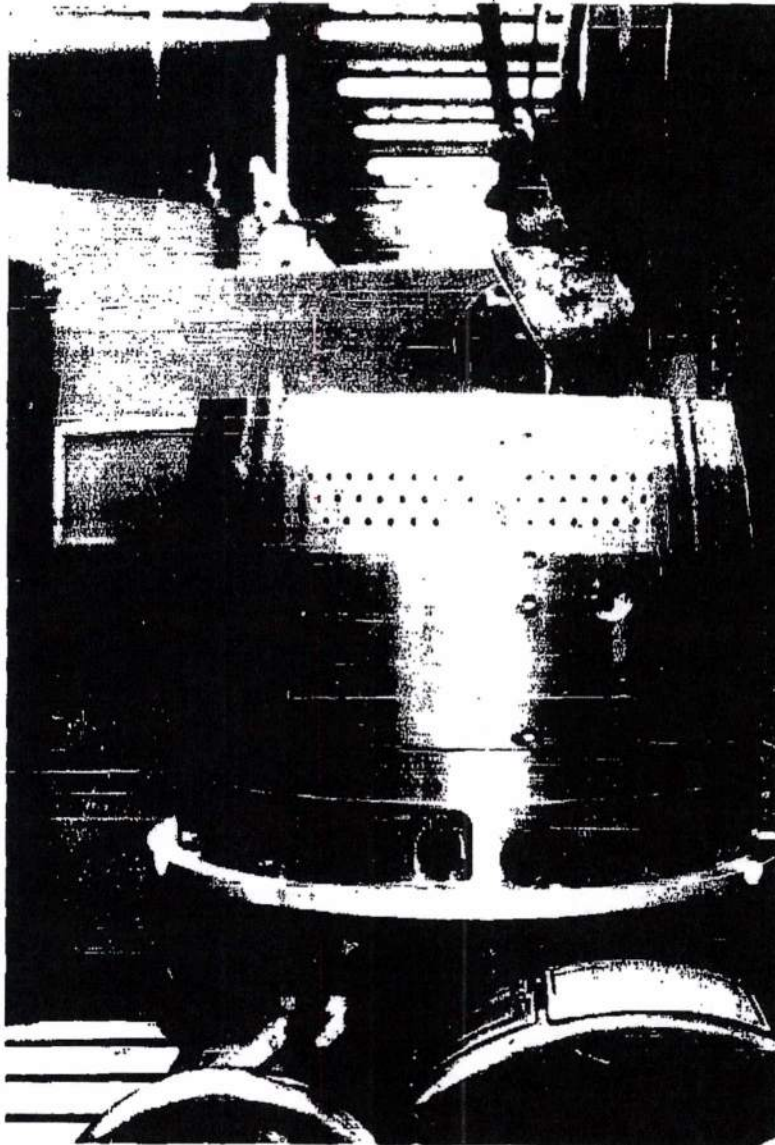


FIGURE 130. Nozzle Assembly for Free Jet Aerodynamic Coupling Test

MAC 4133  
REF: 63-277-9

UNCLASSIFIED

- 29 -

Page determined to be Unclassified  
Reviewed Chief, RDD, WHS  
IAW EO 13526, Section 3.5  
Date: OCT 02 2015

UNCLASSIFIED

ASD-TDR-63-277, Vol. IV

REPORT 6003



FIGURE 131. Spike Adapter for Free Jet Aerodynamic Coupling Test

Page determined to be Unclassified  
Reviewed Chief, RDD, WHS  
IAW EO 13526, Section 3.5  
Date: OCT 02 2015

NEG. 131-3

MAC A07

UNCLASSIFIED

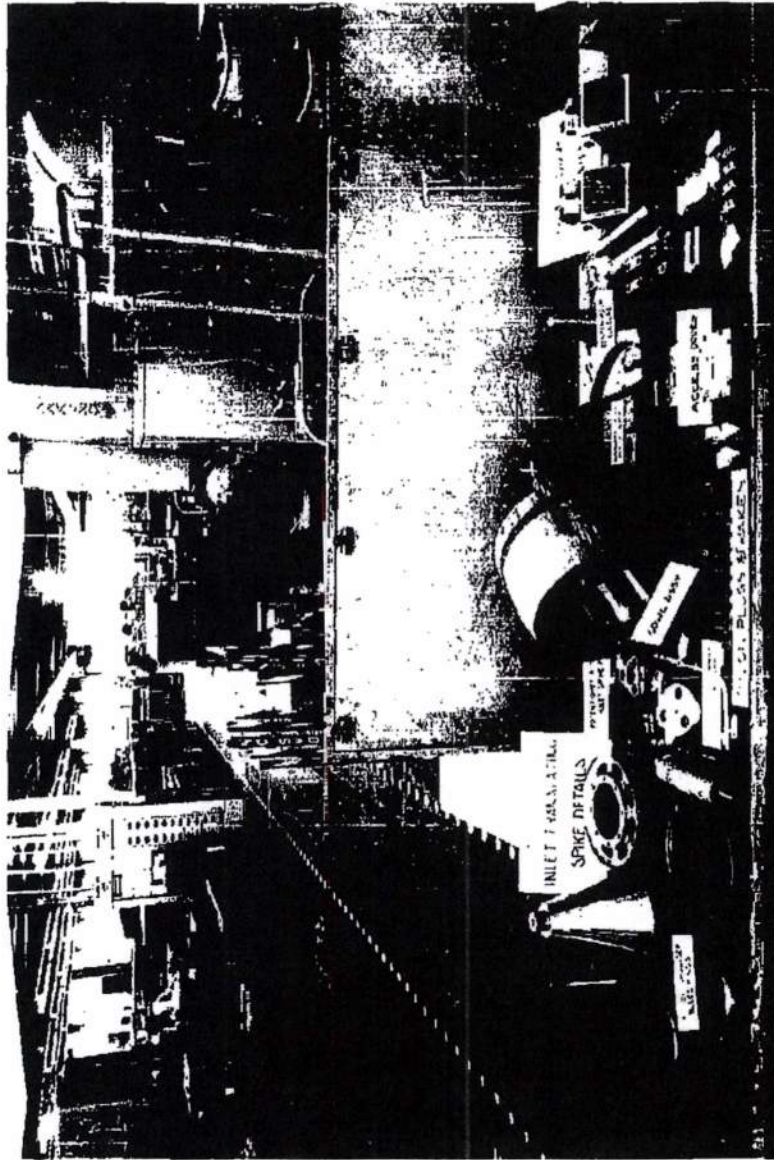


FIGURE 152. Display of Components for Free Jet Aerodynamic Coupling Test

REF 434-11

MAC AXIS

UNCLASSIFIED

ASD-TDR-63-277, Vol. 17

6003

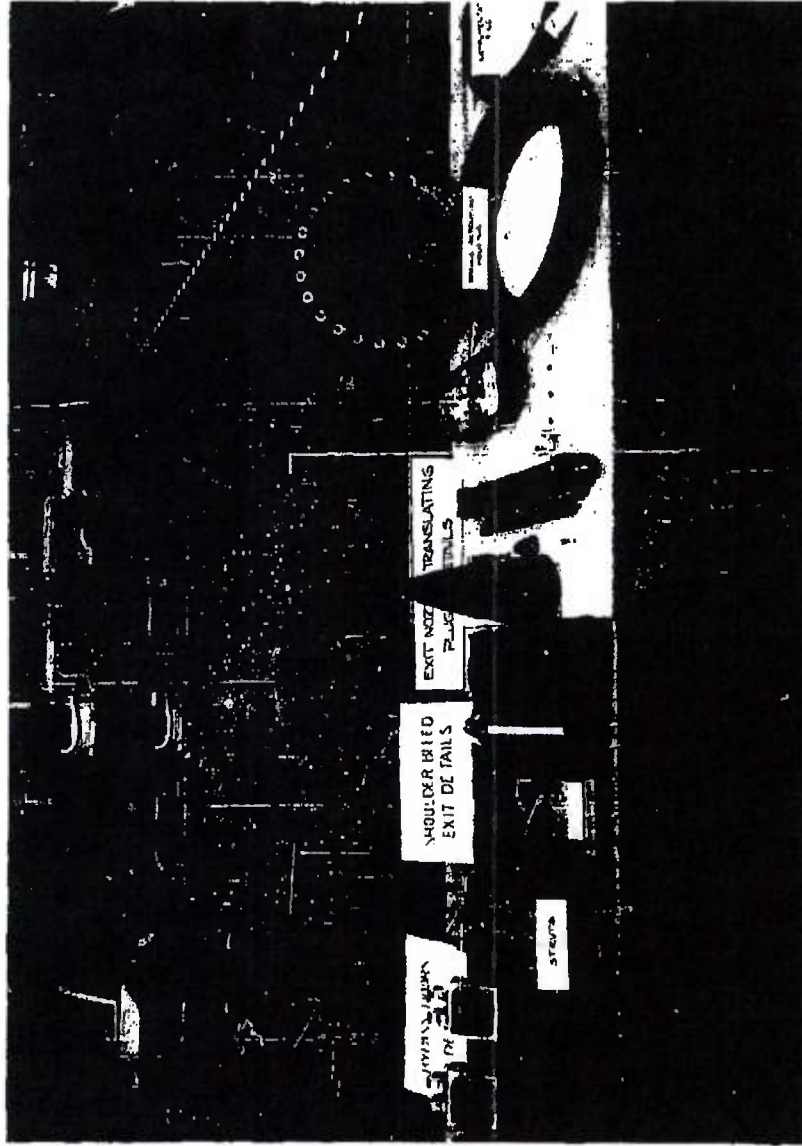


FIGURE 133. Closeup of Components for Free Jet Aerodynamic Coupling Test

MAC A 830

NEG. 4844-12

UNCLASSIFIED

29

Page determined to be Unclassified  
 Reviewed Chief, RDD, WHS  
 IAW EO 13526, Section 3.5  
 Date: OCT 02 2015

UNCLASSIFIED

ASD-TDR-63-277, Vol. IV

REPORT 6003

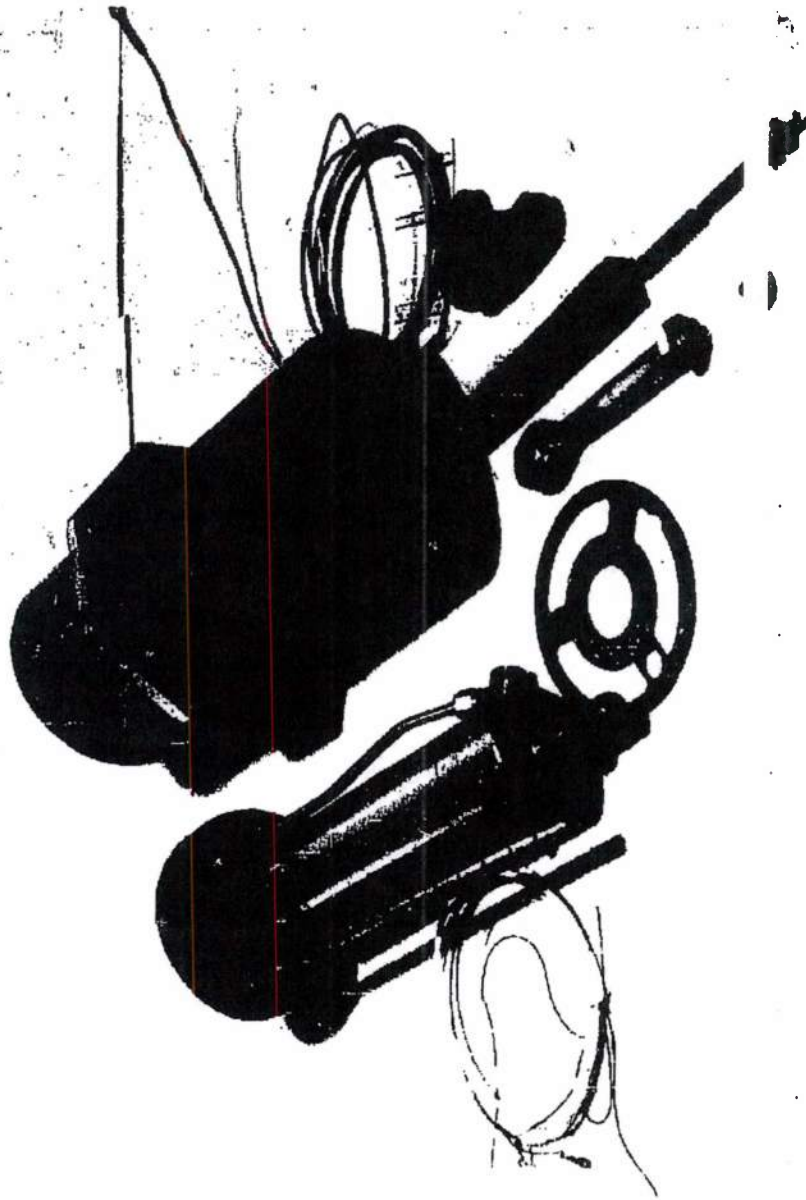


FIGURE 134. Spike Actuator and Housing Details for Free Jet Aerodynamic Coupling Test

MAC 4022  
REF. 4348-15

UNCLASSIFIED

Page determined to be unclassified  
Reviewed Chief, RDD, WWS  
IAW EO 13526, Section 3.5  
Date: OCT 02 2015

UNCLASSIFIED

ASD-TDR-63-277, vol. III

FORM 6003

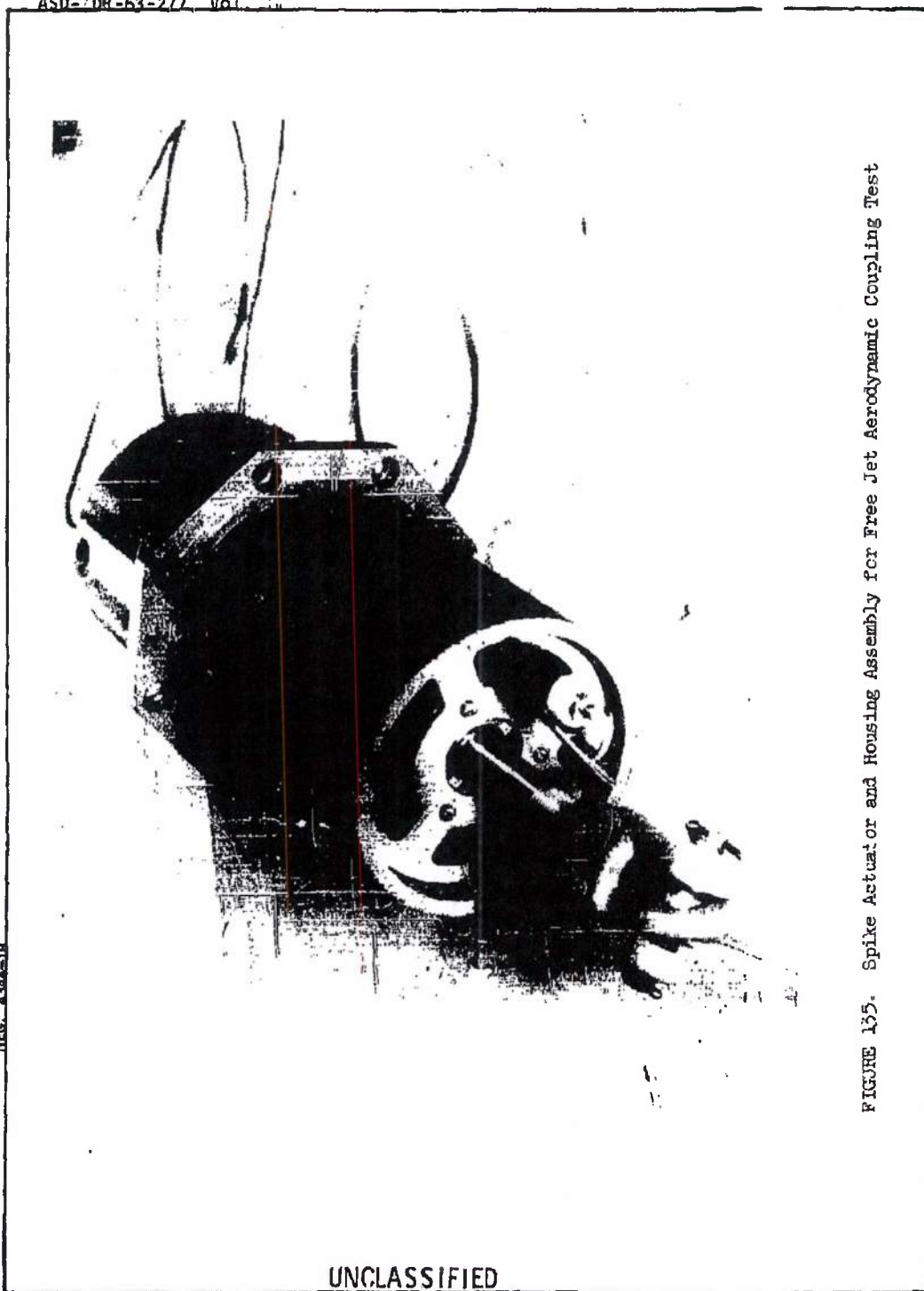


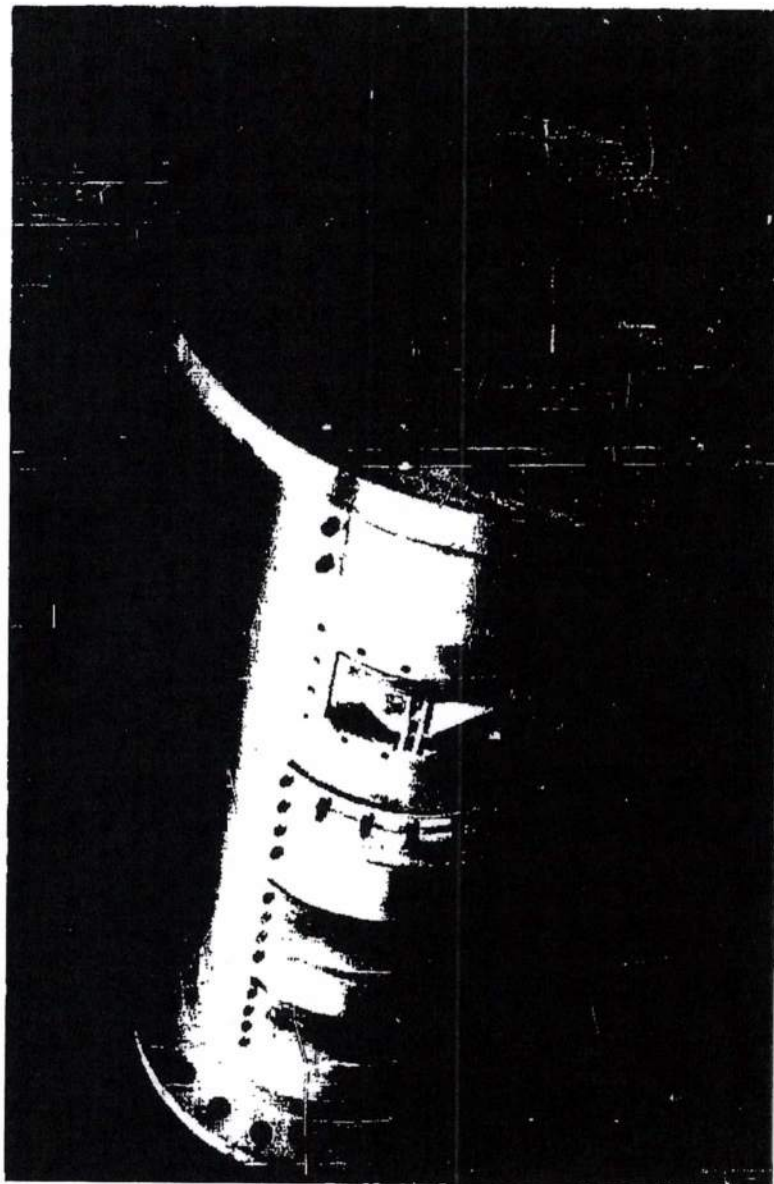
FIGURE 135. Spike Actuator and Housing Assembly for Free Jet Aerodynamic Coupling Test

MAC A 53  
NEG. 43M 518

UNCLASSIFIED

232 -

Page determined to be unclassified  
Reviewed Chief, RDD, WHS  
IAW EO 13526, Section 3.5  
Date: OCT 02 2015



NEG. 4344-19

FIGURE 136. Simulated Reactor and Housing for Free Jet Aerodynamic Coupling Test

MAC 4673

~~SECRET RESTRICTED DATA~~  
~~ATOMIC ENERGY ACT OF 1954~~

ASD-DR-63-277 Vol. 17

PORT 6003



FIGURE 137. Test Item Assembly (Axial Load Spring Retention) for Free Jet Aerodynamic Coupling Test

MEG. 4344-21

MAC 1673

~~SECRET RESTRICTED DATA~~  
~~ATOMIC ENERGY ACT OF 1954~~

~~CONFIDENTIAL~~

ASC-TR-63-277 Vol. 1

REPORT 6003

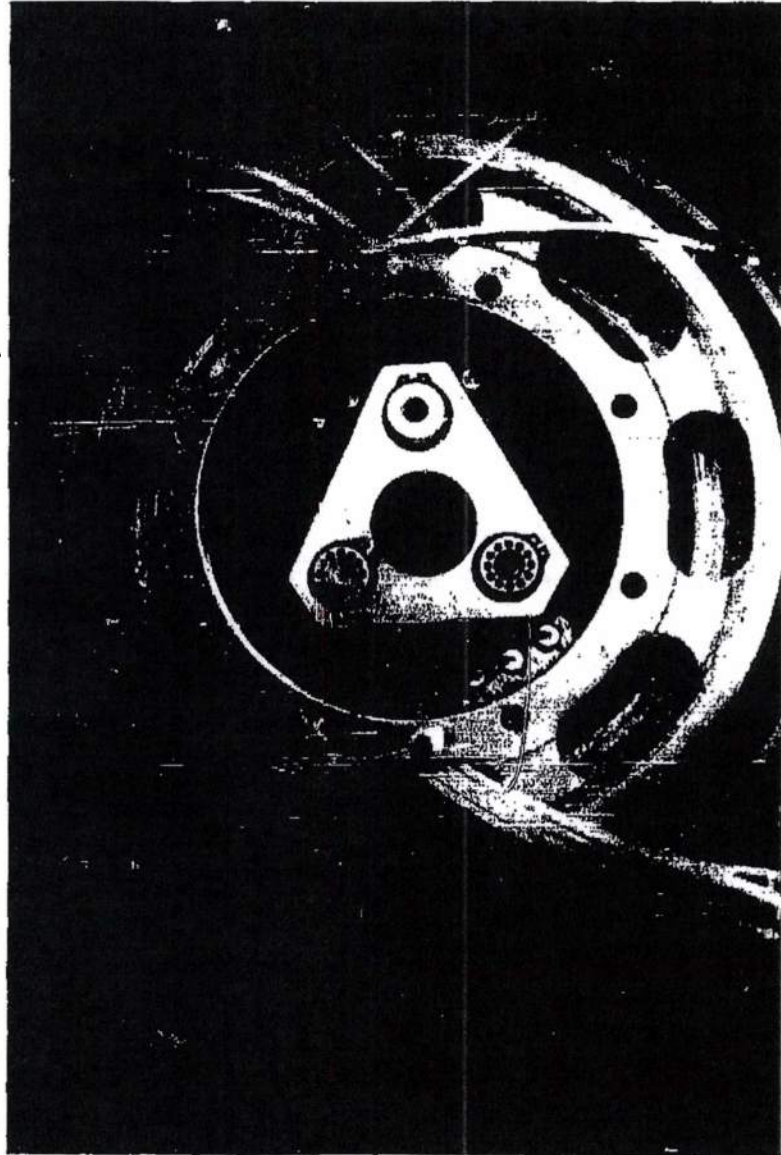


FIGURE 138. Centerbody and Inlet Duct for Free Jet Aerodynamic Coupling Test

NEG. 4344-24

MAC 4153

~~CONFIDENTIAL~~

235

DECLASSIFIED IN FULL  
Authority: EO 13526  
Chief, Records & Declass Div, WHS  
Date: OCT 02 2015

~~CONFIDENTIAL~~

ASD-TDR-63-277 - Vol. 1/1

REPORT 6003

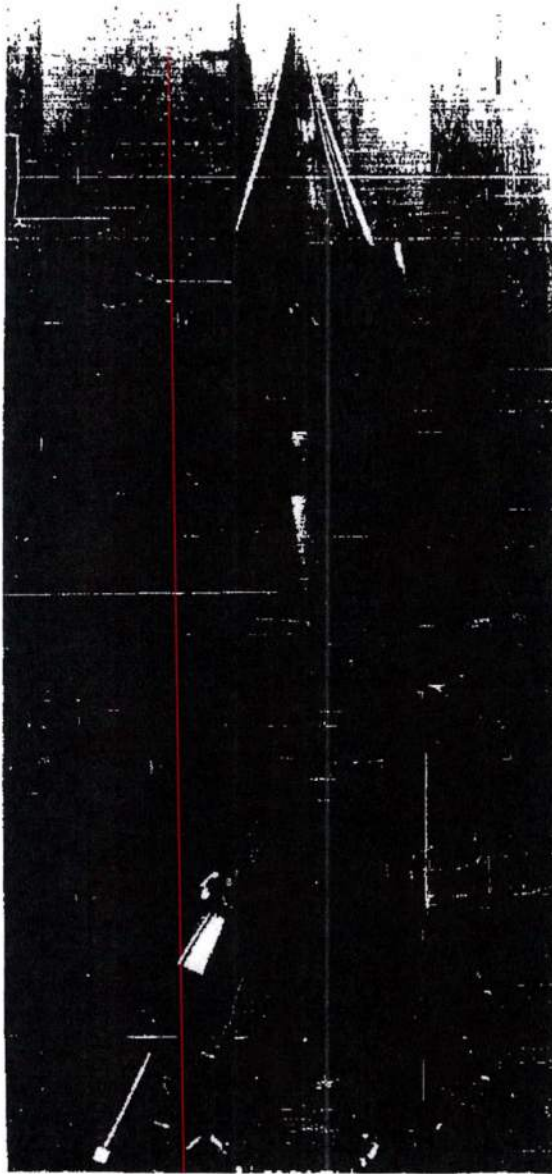


FIGURE 139. Centerbody and Inlet Duct Assembly for Free Jet Aerodynamic Coupling Test

NEG. 4344-26

MAC 8873

~~CONFIDENTIAL~~

~~CONFIDENTIAL~~

ASD-TDR-63-277, Vol. IV

REPORT 6003

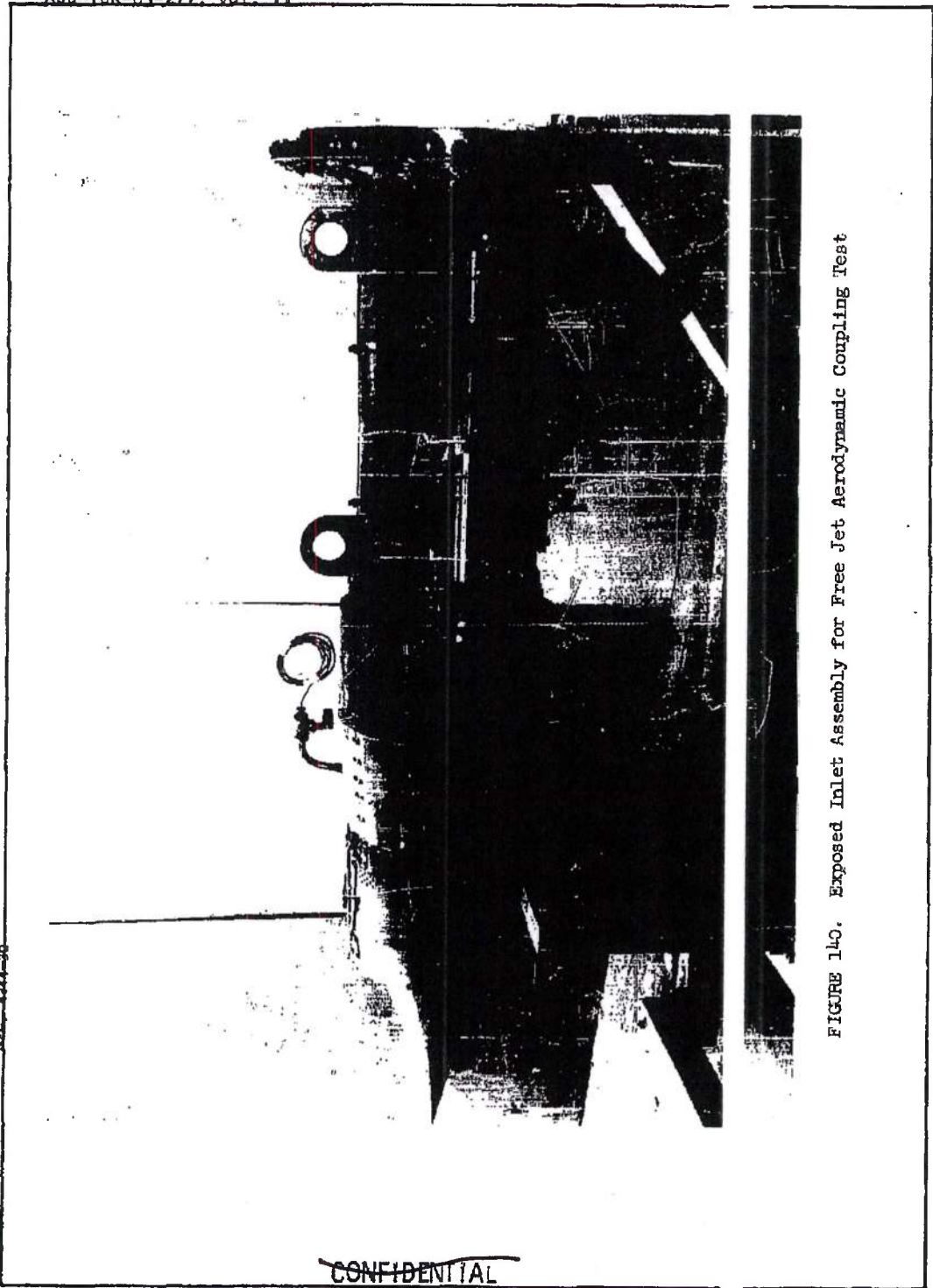


FIGURE 140. Exposed Inlet Assembly for Free Jet Aerodynamic Coupling Test

MAC A673  
REC-4344-90

~~CONFIDENTIAL~~

DECLASSIFIED IN FULL  
Authority: EO 13526  
Chief, Records & Declass Div, WHS  
Date: OCT 02 2015

~~CONFIDENTIAL~~

ASD-TDR-63-277, Vol. 34

6003

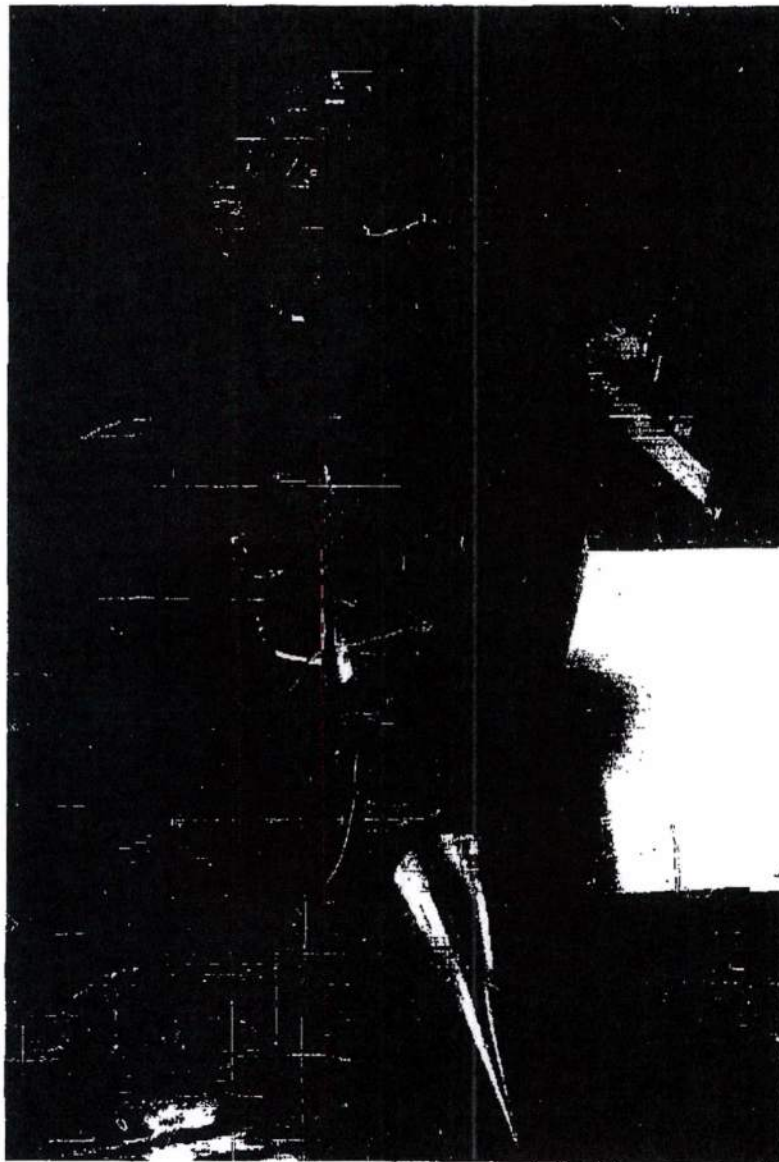


FIGURE 141. Inlet Assembly for Free Jet Aerodynamic Coupling Test  
(Three Quarter View)

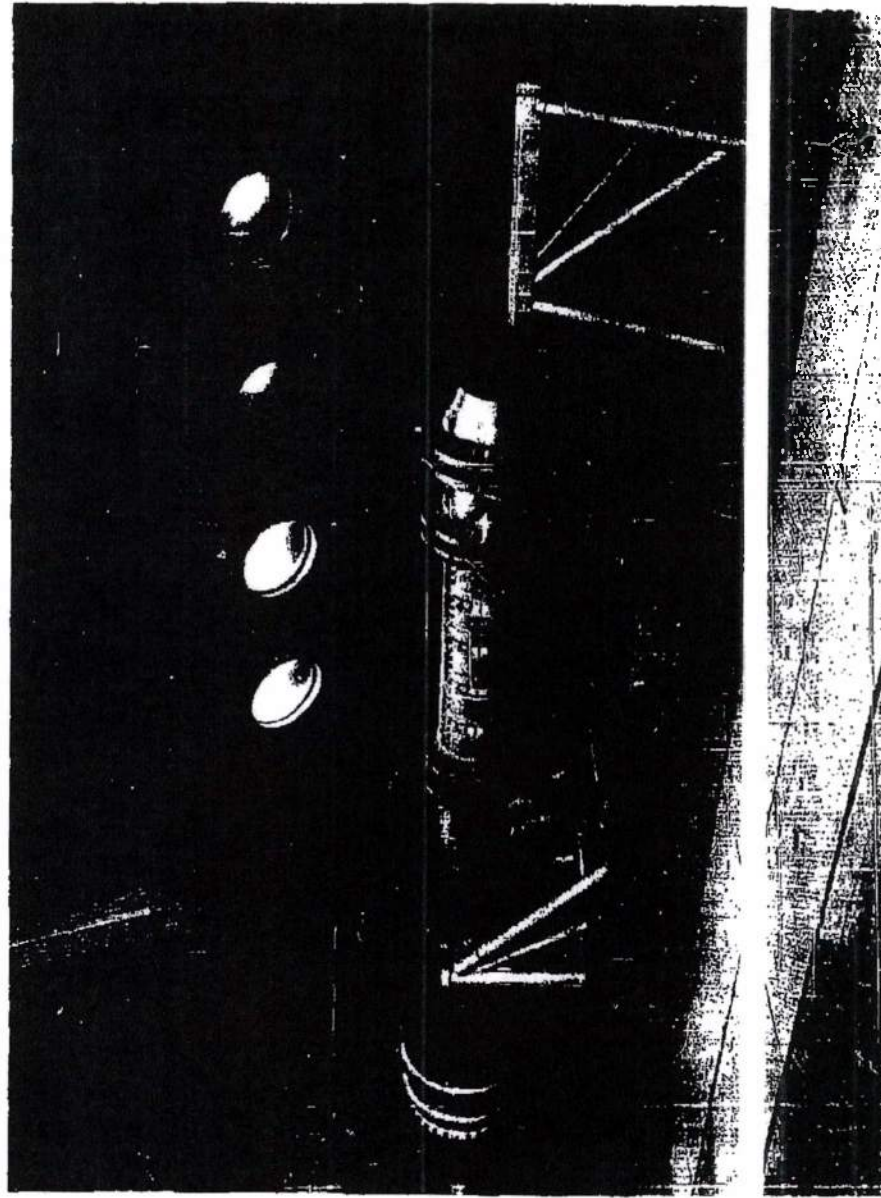
NEG. 4344-31

MAC 4672

~~CONFIDENTIAL~~

293

DECLASSIFIED IN FULL  
Authority: EO 13526  
Chief, Records & Declass Div, WHS  
Date: OCT 02 2015



NEG. T-3066-1

FIGURE 142. Setup of Plute Propulsion System Model for Free Jet Aerodynamic Coupling Test

MAC 403

APPENDIX A

~~CLASSIFIED MATERIALS STUDIES~~

Cyclic Stress Studies on Rene' 41

To evaluate the behavior of Rene' 41 under conditions of cyclic operation, creep specimens of 0.050 in. thick sheet were subjected to cyclic tensile stresses at 1400°F in accordance with the stress-time profile shown in Figure A-1. The results of deformations produced by cyclic loading in comparison with deformations produced on control specimens subjected to a standard creep test at the same temperature, subjected to a constant stress of 52 Ksi and for the same total time are presented in Table A-I. A comparison of results between test and control specimens shows that cyclic specimens elongated less by a factor 1/4 to 1/9, indicating strengthening occurred as a result of this particular cyclic test. Standard tensile tests were also performed at a strain rate of 0.001 in./in./sec at 1400°F, the principle strain rate of cyclic testing. The results of these tensile tests are compared in Table A-II. Cycled specimens show tensile values intermediate to noncycled and creep tested specimens; the creep tested specimens having the highest tensile values.

Table A-III and Figure A-2 present results of creep-rupture tests performed on control specimens at 1400°F under a 52 Ksi stress. The elongation in 10 hours was approximately 0.2% much higher than the cycled specimens. Tensile tests were also performed at 1400°F under stress rates which produced strain rates of 0.001, 0.01, and 0.1 in./in./sec. The results of these tests are presented in Table A-IV and Figures A-3 and A-4. As expected, the short time tensile properties increased with the strain rate.

The strengthening effect shown by these cyclic tests may be due to a combination of additional precipitation and/or solid solution mechanisms stimulated by repeated strains, at the temperature of testing. Considerable additional testing will be needed to resolve the effects to be expected from service cycles. A program of cyclic testing of Rene' 41 and the other alloys should be undertaken to study the effects of temperature and stress cycling on precipitation and nonprecipitation hardening alloys.

**DECLASSIFIED IN FULL**  
**Authority: EO 13526**  
**Chief, Records & Declass Div, WHS**  
**Date: OCT 02 2015**

MAC 4577

TABLE A-I

CREEP OF RENE' 41 DURING CYCLIC TESTING

Specimens - Standard, 0.050 in. thick sheet  
Creep Measurements - Before and after cyclic testing.  
Specimens at room temperature.  
Scribe marks measured with  
Gaertner toolmaker's microscope  
Heating - Resistance

Specimen Number	Length (Inches)		Change in Length In 2 Inches (in.)	Plastic Deformation In 2 Inch Gage Length (%)
	Before Cycling	After Cycling		
G-1	--	1.9978	--	--
G-3	1.9990	2.0008	0.0018	0.09
G-13	1.9988	1.9993	0.0005	0.03
G-14	1.9999	2.0012	0.0013	0.07

CREEP OF RENE' 41 DURING STATIC TESTING

Load, Temperature, and Time - Load - 52,000 psi, constant  
- Same temperature as above  
- time 5 hours

Specimen Number	Length (Inches)		Change in Length In 2 Inches (in.)	Plastic Deformation In 2 Inch Gage Length (%)
	Before Cycling	After Cycling		
G-10	1.9980	2.0068	0.0088	0.44
G-11	1.9990	2.0079	0.0086	0.43

DECLASSIFIED IN FULL  
Authority: EO 13526  
Chief, Records & Declass Div, WHS  
Date: OCT 02 2015

MAC 4638

~~SECRET RESTRICTED DATA~~  
~~ATOMIC ENERGY ACT OF 1954~~

ASD-TDR-63-277, Vol. IV

6003

TABLE A-II  
 TENSILE PROPERTIES OF RENE' 41 SHEET AFTER CYCLIC TESTING

Heat Treatment - 1950°F, 1/2 hr, rapid air cool,  
 Age at 1400°F, 16 hrs  
 Heating - Resistance  
 Hold Time - 5 minutes  
 Specimens - Standard, 0.050 inch thick sheet

Specimen Number	Strain Rate Start to Rupture (in/in/sec)	Test Temperature (°F)	Proportional Limit (ksi)	0.2% Yield Strength (ksi)	Ultimate Tensile Strength (ksi)	Elongation in 2 Inches (%)	Young's Modulus (x 10 <sup>6</sup> psi)
G-1	0.001	1400	97.0	125.0	(127.5)*	(0.9)*	24.0
G-3	0.001	1400	88.0	127.7	141.0	2.4	22.2
G-13	0.001	1400	86.0	126.0	147.0	3.7	23.8
G-14	0.001	1400	90.0	126.0	146.0	3.3	23.1
Average of 3 specimens not cyclic tested.	0.001	Average	90.2	126.2	144.7	3.1	23.3
		1400	77.0	119.7	134.0	2.5	25.3
TENSILE PROPERTIES OF RENE' 41 SHEET AFTER STATIC TESTING SIMULATING CYCLIC TESTING							
G-10	0.001	1400	79.0	133.0	153.8	4.0	24.0
G-11	0.001	1400	81.0	131.8	151.0	4.0	24.0

\* Broke at thermocouple weld, not valid.

~~SECRET RESTRICTED DATA~~  
~~ATOMIC ENERGY ACT OF 1954~~

TABLE A-III

CREEP-RUPTURE OF RENE' 41 SHEET CONTROL SPECIMENS

Test Conditions:

- Rene' 41, 0.050 inch thick sheet
- Heat Treatment - 1950°F 30 minutes
- Age 1400°F, 16 hours
- Heating - Resistance
- Gage Length - 1.5 inches
- Atmosphere - Air
- Specimens - Standard

Specimen Number	Test Temperature (°F)	Creep Stress (ksi)	Time to Produce Indicated Plastic Creep (hours)						Time to Rupture (hours)	Elongation In 1.5 Inches (%)
			0.5%	0.1%	0.2%	0.5%	1.0%	2.0%		
G-18	1400	52	0.3	3.6	13.2	30.1	49.1	63.1	73.35	4.0
G-21	1400	52	2.8	8.6	23.3	48.1	64.5	81.0	87.5	2.3

DECLASSIFIED IN FULL  
 Authority: EO 13526  
 Chief, Records & Declass Div, WHS  
 Date: OCT 02 2015

~~SECRET RESTRICTED DATA~~  
~~ATOMIC ENERGY ACT OF 1954~~

ASD-TDR-63-277, Vol. IV

POST 6003

TABLE A-IV  
 TENSILE PROPERTIES OF REME' 41 SHEET AT SELECTED STRAIN RATES

Test Conditions:

- Heat Treatment - 1950°F, 1/2-hour, rapid air cool
- Age at 1400°F, 16 hours
- Heating - Resistance
- Specimens - 0.050 inch thick sheet, per Dwg. XL4281
- Hold Time - 5 minutes
- Gage Length - 2 inches

Specimen Number	Strain Rate Start to Rupture (in/in/sec)	Test Temperature (°F)	Proportional Limit (ksi)	0.2% Yield Strength (ksi)	Ultimate Tensile Strength (ksi)	Elongation In 2 Inches (%)	Young's Modulus (x 10 <sup>6</sup> psi)
G-2	0.001	1400	78.0	120.0	134.0	2.5	26.3
G-4	0.001	1400	77.0	118.0	134.0	2.5	25.0
G-6	0.001	1400	76.0	121.0	134.0	2.5	25.3
		Average	77.0	119.7	134.0	2.5	25.3
G-7	0.01	1400	80.0	120.0	145.0	4.0	26.6
G-8	0.01	1400	82.0	123.0	148.0	4.0	24.0
G-9	0.01	1400	81.0	123.0	146.0	3.5	22.0
G-28	0.01	1400	78.0	121.0	149.0	4.5	26.7
		Average	80.0	121.8	147.0	4.0	24.8
G-12	0.1	1400	--	--	152.0	8.5	--
G-15	0.1	1400	--	--	160.0	8.5	--
G-5	0.1	1400	--	--	161.0	9.0	--
G-25	0.1	1400	88.0	--	150.0	16.5	24.0
G-33	0.1	1400	98.0	131.5	154.0	7.0	29.0

~~SECRET RESTRICTED DATA~~  
~~ATOMIC ENERGY ACT OF 1954~~

MAC AXE

~~SECRET RESTRICTED DATA~~  
 ATOMIC ENERGY ACT OF 1954

ASD-TDR-63-277, Vol. IV

REPORT 6003

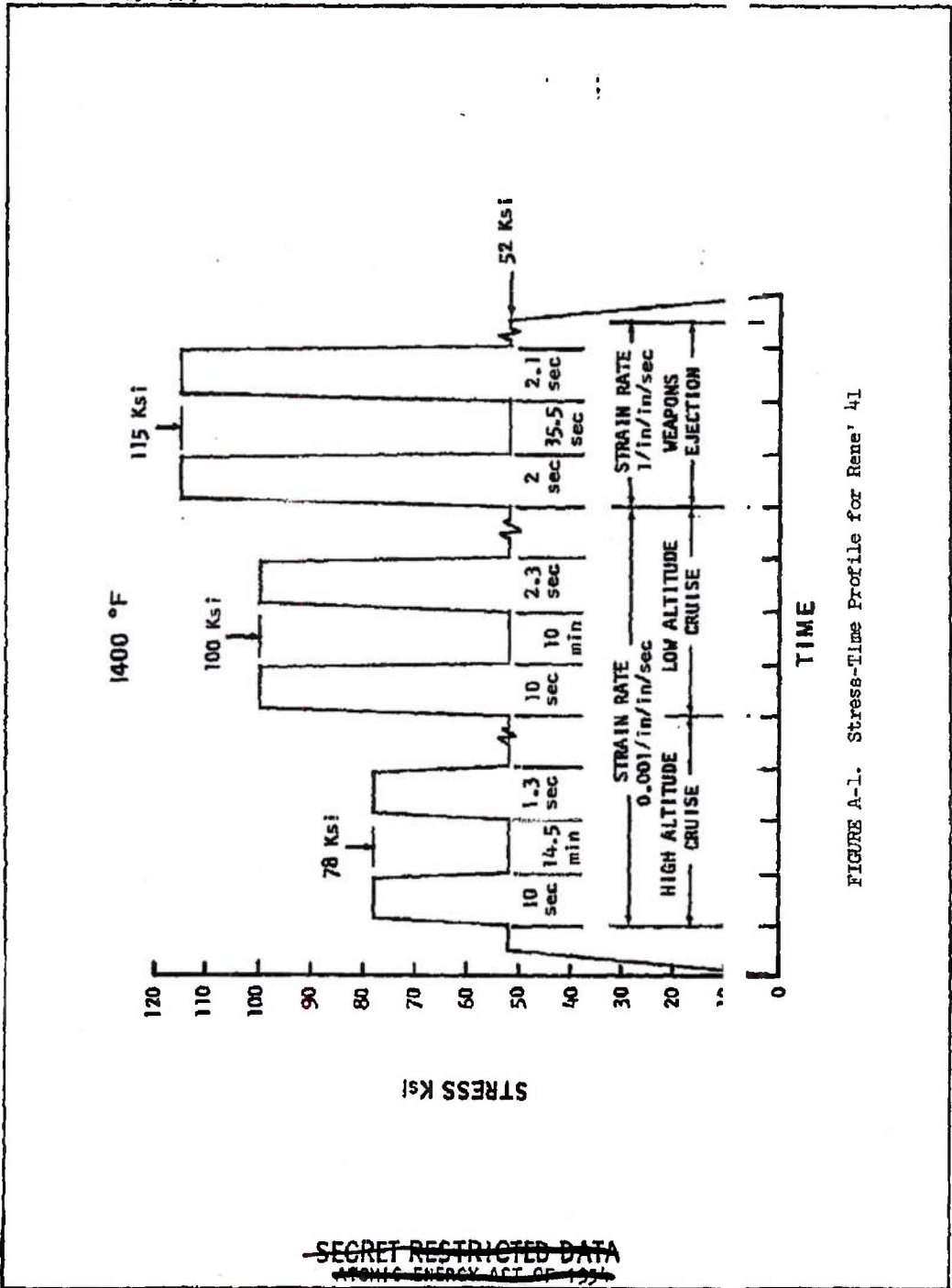


FIGURE A-1. Stress-Time Profile for Rene' 41

MAC 4600

~~SECRET RESTRICTED DATA~~  
 ATOMIC ENERGY ACT OF 1954

UNCLASSIFIED

ASD-TDR-63-277, Vol. IV

MI 6003

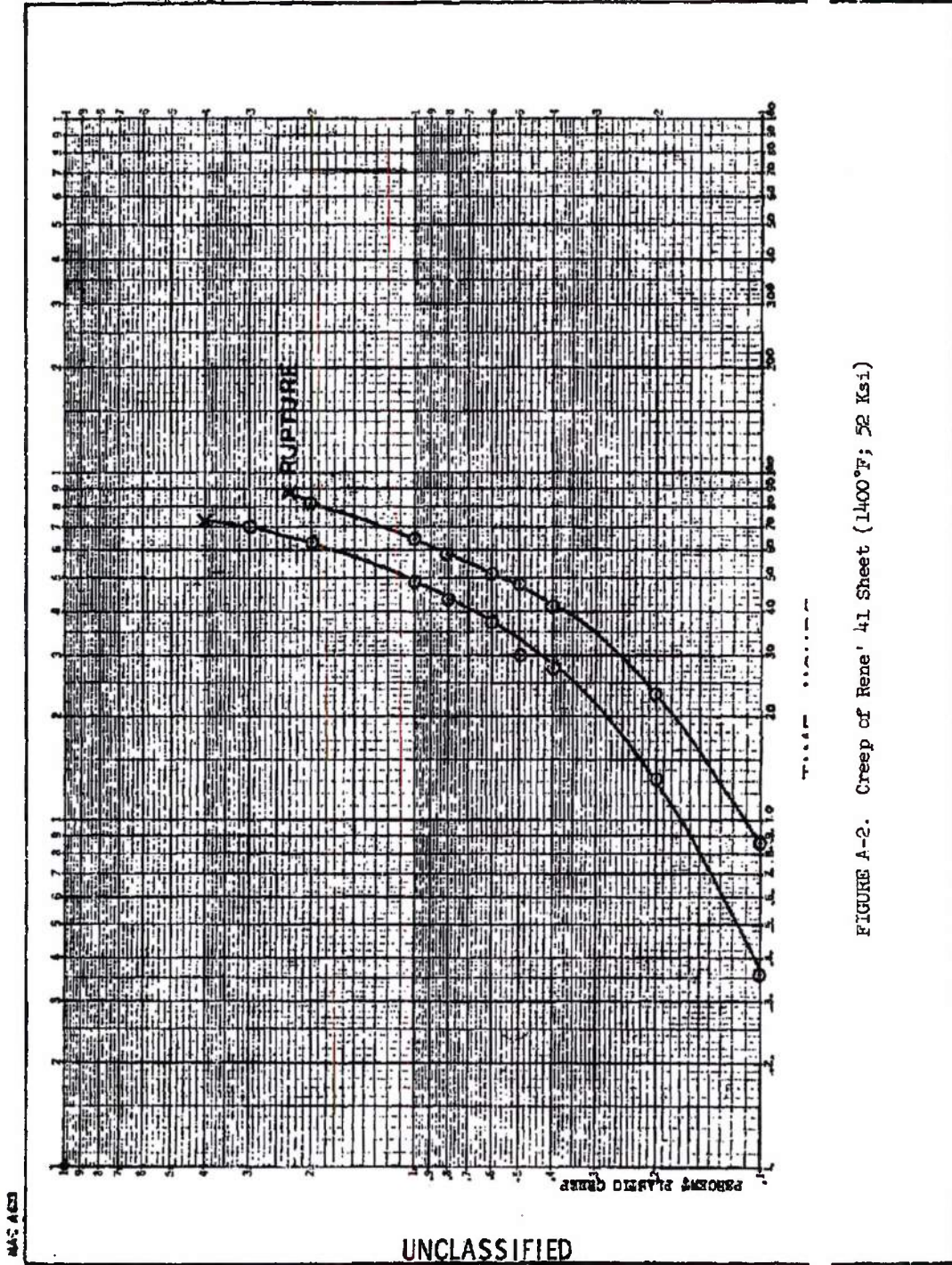


FIGURE A-2. Creep of Rene 41 Sheet (1400°F; 52 Ksi)

MAC A23

UNCLASSIFIED

28B364

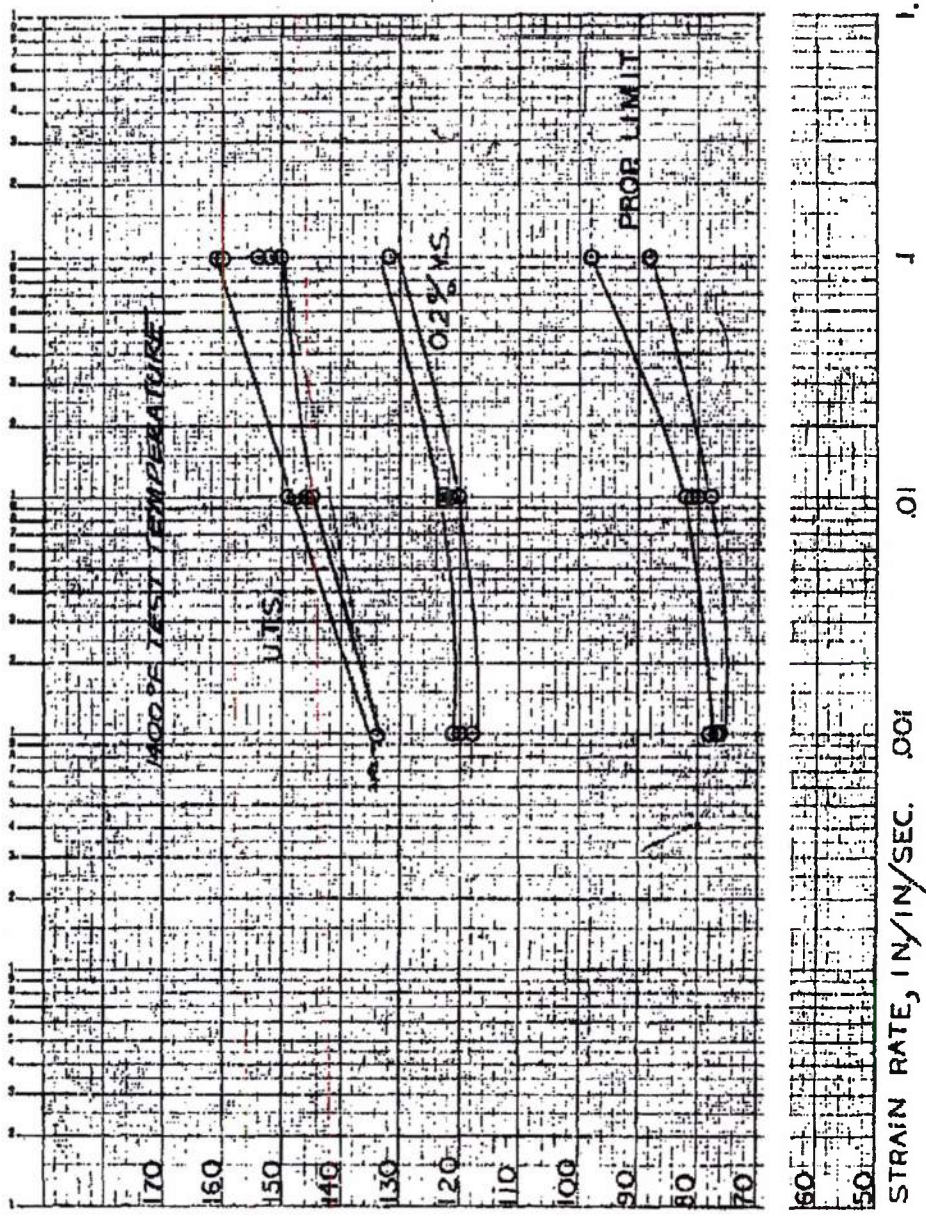


FIGURE A-3. Ultimate Tensile Strength and Yield Strength of Rene' 41 Sheet at Selected Strain Rates

BAC A-3

Page determined to be Unclassified  
Reviewed Chief, RDD, WHS  
IAW EO 13526, Section 3.5  
Date: OCT 02 2015

UNCLASSIFIED

ASD-TDR-63-277, Vol. IV

6003

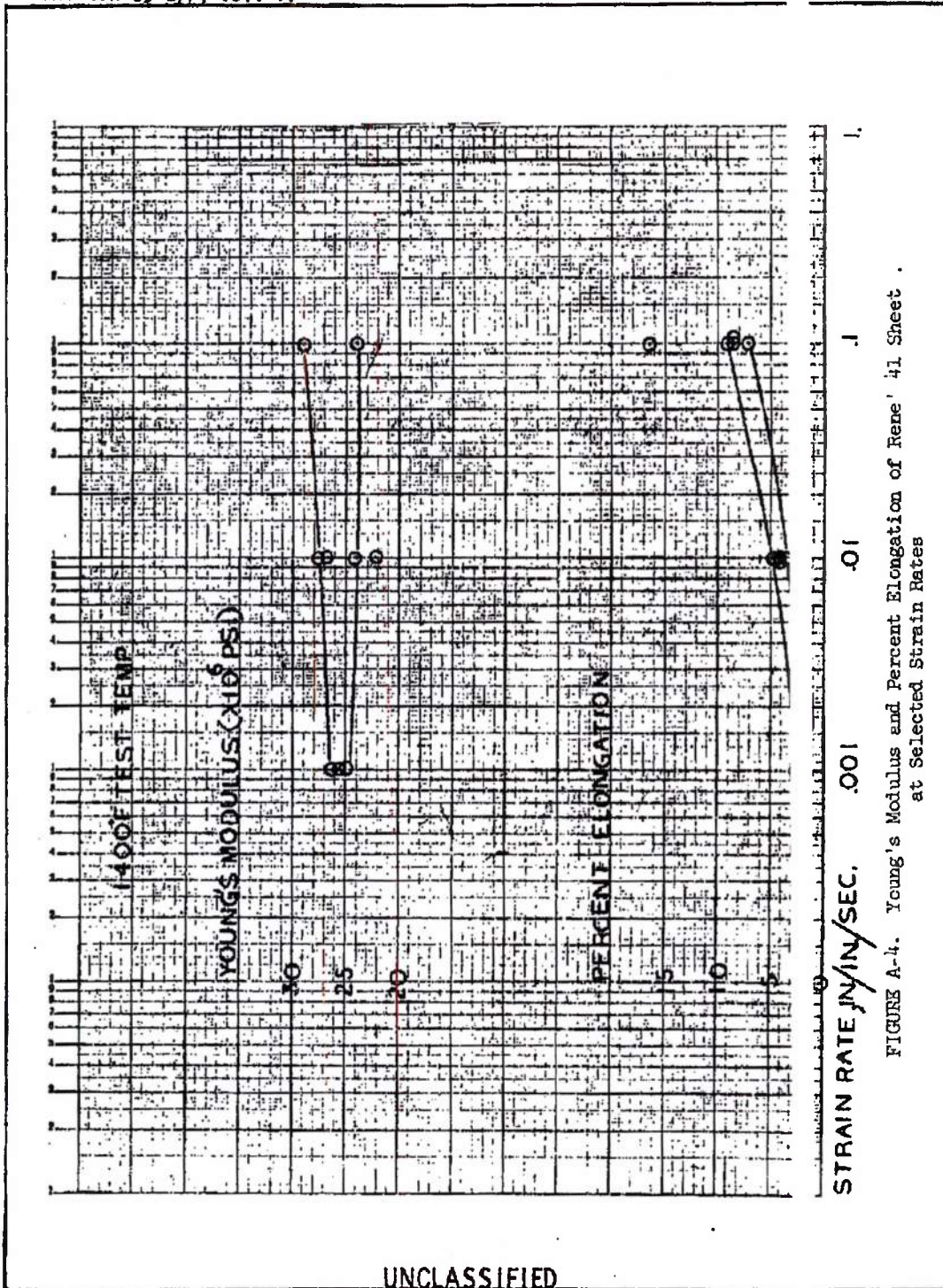


FIGURE A-4. Young's Modulus and Percent Elongation of Rene 41 Sheet .  
at Selected Strain Rates

MAC 4673

28A527

UNCLASSIFIED

Page determined to be Unclassified  
 Reviewed Chief, RDD, WHS  
 IAW EO 13526, Section 3.5  
 Date: OCT 02 2016

<p>UNCLASSIFIED</p> <ol style="list-style-type: none"> <li>1. Nuclear ramjet propulsion systems</li> <li>2. Propulsion systems</li> <li>3. Aircraft nuclear power propulsion</li> <li>4. Nuclear powerplants</li> <li>5. Ramjet engines</li> </ol> <p>I. AFSC Project 655A, Task 1 and 5        II. Contract AF 33(657)-8123        III. The Marquardt Corp., Van Nuys, Calif.        IV. R. D. Grossman        V. TMC Report 6003        VI. Not eval fr OPS</p> <p>UNCLASSIFIED</p>	<p>UNCLASSIFIED</p> <ol style="list-style-type: none"> <li>1. Nuclear ramjet propulsion systems</li> <li>2. Propulsion systems</li> <li>3. Aircraft nuclear power propulsion</li> <li>4. Nuclear powerplants</li> <li>5. Ramjet engines</li> </ol> <p>I. AFSC Project 655A, Task 1 and 5        II. Contract AF 33(657)-8123        III. The Marquardt Corp., Van Nuys, Calif.        IV. R. D. Grossman        V. TMC Report 6003</p> <p>UNCLASSIFIED</p>
---	--

<p>Aeronautical Systems Division, Dir/Aeromechanics, Propulsion Lab, Wright-Patterson AFB, Ohio Rpt Nr ASD-TDR-63-277, vol IV. NUCLEAR RAMJET PROPELLION SYSTEM APPLIED RESEARCH AND TECHNOLOGY (1962 TECHNICAL SUMMARY): VOL. IV. Propulsion System Design and Structural Analysis Summary, Annual Summary Report, 15 Feb 63. P Incl. illus., tables, 25 refs.</p> <p>Volume contains results of design, material studies, and structures component testing of a nuclear propulsion system for the Pluto reactor program. Design concepts, structural analysis of steady state and dynamic loads, material evaluation, and recommended dynamic and structural test programs are studied. Methods of analysis are outlined.</p> <p>Unclassified Abstract</p>	<p>Aeronautical Systems Division, Dir/Aeromechanics, Propulsion Lab, Wright-Patterson AFB, Ohio Rpt Nr ASD-TDR-63-277, vol IV. NUCLEAR RAMJET PROPELLION SYSTEM APPLIED RESEARCH AND TECHNOLOGY (1962 TECHNICAL SUMMARY): VOL. IV. Propulsion System Design and Structural Analysis Summary, Annual Summary Report, 15 Feb 63. P Incl. illus., tables, 25 refs.</p> <p>Volume contains results of design, material studies, and structures component testing of a nuclear propulsion system for the Pluto reactor program. Design concepts, structural analysis of steady state and dynamic loads, material evaluation, and recommended dynamic and structural test programs are studied.</p> <p>Unclassified Abstract</p>
--	--

<p>UNCLASSIFIED</p> <ol style="list-style-type: none"> <li>1. Nuclear ramjet propulsion systems</li> <li>2. Propulsion systems</li> <li>3. Aircraft nuclear power propulsion</li> <li>4. Nuclear powerplants</li> <li>5. Ramjet engines</li> </ol> <p>I. AFSC Project 655A, Task 1 and 5        II. Contract AF 33(657)-8123        III. The Marquardt Corp., Van Nuys, Calif.        IV. R. D. Grossman        V. TMC Report 6003        VI. Not eval fr OPS</p> <p>UNCLASSIFIED</p>	<p>UNCLASSIFIED</p> <ol style="list-style-type: none"> <li>1. Nuclear ramjet propulsion systems</li> <li>2. Propulsion systems</li> <li>3. Aircraft nuclear power propulsion</li> <li>4. Nuclear powerplants</li> <li>5. Ramjet engines</li> </ol> <p>I. AFSC Project 655A, Task 1 and 5        II. Contract AF 33(657)-8123        III. The Marquardt Corp., Van Nuys, Calif.        IV. R. D. Grossman        V. TMC Report 6003</p> <p>UNCLASSIFIED</p>
---	--

<p>Aeronautical Systems Division, Dir/Aeromechanics, Propulsion Lab, Wright-Patterson AFB, Ohio Rpt Nr ASD-TDR-63-277, vol IV. NUCLEAR RAMJET PROPELLION SYSTEM APPLIED RESEARCH AND TECHNOLOGY (1962 TECHNICAL SUMMARY): VOL. IV. Propulsion System Design and Structural Analysis Summary, Annual Summary Report, 15 Feb 63. P Incl. illus., tables, 25 refs.</p> <p>Volume contains results of design, material studies, and structures component testing of a nuclear propulsion system for the Pluto reactor program. Design concepts, structural analysis of steady state and dynamic loads, material evaluation, and recommended dynamic and structural test programs are studied. Methods of analysis are outlined.</p> <p>Unclassified Abstract</p>	<p>Aeronautical Systems Division, Dir/Aeromechanics, Propulsion Lab, Wright-Patterson AFB, Ohio Rpt Nr ASD-TDR-63-277, vol IV. NUCLEAR RAMJET PROPELLION SYSTEM APPLIED RESEARCH AND TECHNOLOGY (1962 TECHNICAL SUMMARY): VOL. IV. Propulsion System Design and Structural Analysis Summary, Annual Summary Report, 15 Feb 63. P Incl. illus., tables, 25 refs.</p> <p>Volume contains results of design, material studies, and structures component testing of a nuclear propulsion system for the Pluto reactor program. Design concepts, structural analysis of steady state and dynamic loads, material evaluation, and recommended dynamic and structural test programs are studied.</p> <p>Unclassified Abstract</p>
--	--

Page determined to be Unclassified  
 Reviewed Chief, RDD, WHS  
 IAW EO 13526, Section 3.5  
 Date: OCT 0 2 2015

<p>UNCLASSIFIED</p> <ol style="list-style-type: none"> <li>1. Nuclear ramjet propulsion systems</li> <li>2. Propulsion systems</li> <li>3. Aircraft nuclear power propulsion</li> <li>4. Nuclear powerplants</li> <li>5. Ramjet engines</li> <li>I. AFSC Project 655A, Task 1 and 5</li> <li>II. Contract AF 33(657)-8123</li> <li>III. The Marquardt Corp., Van Nuys, Calif.</li> <li>IV. R. D. Grossman</li> <li>V. TMC Report 6005</li> <li>VI. Not avail fr OTS</li> </ol>	<p>Aeronautical Systems Division, Dlr/Aeromechanics, Propulsion Lab, Wright-Patterson AFB, Ohio Rpt Nr ASD-TDR-63-277, vol IV. NUCLEAR RAMJET PROPULSION SYSTEM APPLIED RESEARCH AND TECHNOLOGY (1962 TECHNICAL SUMMARY): VOL. IV. Propulsion System Design and Structural Analysis <del>Summary</del>, Annual Summary Report, 15 Feb 63. p Incl. illus., tables, 25 refs.</p> <p>Volume contains results of design, material studies, and structures component testing of a nuclear propulsion system for the Pluto reactor program. Design concepts, structural analysis of steady state and dynamic loads, material evaluation, and recommended dynamic and structural test programs are studied. Methods of analysis are outlined.</p> <p>Unclassified Abstract</p>	<p>UNCLASSIFIED</p> <ol style="list-style-type: none"> <li>1. Nuclear ramjet propulsion systems</li> <li>2. Propulsion systems</li> <li>3. Aircraft nuclear power propulsion</li> <li>4. Nuclear powerplants</li> <li>5. Ramjet engines</li> <li>I. AFSC Project 655A, Task 1 and 5</li> <li>II. Contract AF 33(657)-8123</li> <li>III. The Marquardt Corp., Van Nuys, Calif.</li> <li>IV. R. D. Grossman</li> <li>V. TMC Report 6005</li> <li>VI. Not avail fr OTS</li> </ol>
<p>UNCLASSIFIED</p> <ol style="list-style-type: none"> <li>1. Nuclear ramjet propulsion systems</li> <li>2. Propulsion systems</li> <li>3. Aircraft nuclear power propulsion</li> <li>4. Nuclear powerplants</li> <li>5. Ramjet engines</li> <li>I. AFSC Project 655A, Task 1 and 5</li> <li>II. Contract AF 33(657)-8123</li> <li>III. The Marquardt Corp., Van Nuys, Calif.</li> <li>IV. R. D. Grossman</li> <li>VI. Not avail fr OTS</li> </ol>	<p>Aeronautical Systems Division, Dlr/Aeromechanics, Propulsion Lab, Wright-Patterson AFB, Ohio Rpt Nr ASD-TDR-63-277, vol IV. NUCLEAR RAMJET PROPULSION SYSTEM APPLIED RESEARCH AND TECHNOLOGY (1962 TECHNICAL SUMMARY): VOL. IV. Propulsion System Design and Structural Analysis <del>Summary</del>, Annual Summary Report, 15 Feb 63. p Incl. illus., tables, 25 refs.</p> <p>Volume contains results of design, material studies, and structures component testing of a nuclear propulsion system for the Pluto reactor program. Design concepts, structural analysis of steady state and dynamic loads, material evaluation, and recommended dynamic and structural test programs are outlined.</p> <p>Unclassified Abstract</p>	<p>UNCLASSIFIED</p> <ol style="list-style-type: none"> <li>1. Nuclear ramjet propulsion systems</li> <li>2. Propulsion systems</li> <li>3. Aircraft nuclear power propulsion</li> <li>4. Nuclear powerplants</li> <li>5. Ramjet engines</li> <li>I. AFSC Project 655A, Task 1 and 5</li> <li>II. Contract AF 33(657)-8123</li> <li>III. The Marquardt Corp., Van Nuys, Calif.</li> <li>IV. R. D. Grossman</li> <li>VI. Not avail fr OTS</li> </ol>